Basic Principles

of

Membrane

Technology

second edition

Marcel Mulder
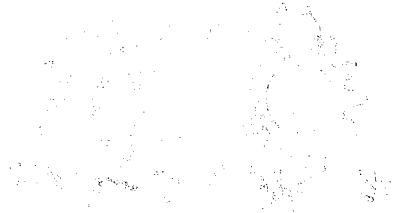
Basic Principles of Membrane Technology

by

Marcel Mulder

Center for Membrane Science and Technology,
University of Twente,
Enschede, The Netherlands

Printed on acid-free paper

Printed in the Netherlands

CONTENTS

I Introduction

II Materials and material properties

III Preparation of synthetic membranes

VI   Membrane processes

Membranes play a central role in our daily life, or as indicated by one of my foreign colleagues, Richard Bowen, 'If you are tired of membranes, you are tired of life'. Biological membranes are hardly used in industrial applications, but separations with synthetic membranes have become increasingly important. Today, membrane processes are used in a wide range of applications and their numbers will certainly increase. Therefore, there is a need for well educated and qualified engineers, chemists, scientists and technicians who have been taught the basic principles of membrane technology. However, despite the growing importance of membrane processes, there are only a few universities that include membrane technology in their regular curricula. One of the reasons for this may be the lack of a comprehensive textbook. For me, this was one of the driving forces for writing a textbook on the basic principles of membrane technology which provides a broad view on the various aspects of membrane technology. I realise that membrane technology covers a broad field but nevertheless I have tried to describe the basic principles of the various disciplines. Although the book was written with the student in mind it can also serve as a first introduction for engineers, chemists, and technicians in all kind of industries who wish to learn the basics of membrane technology.

The book is divided into eight chapters, each covering a basic topic:

Chapter 1 is an introduction to the field and gives some definitions and the historical development. Chapter 2 is a survey of polymers used as membrane material and describes the factors that determine the material properties. Chapter 3 gives an overview of various preparation techniques. Most of the commercial available membranes are prepared by phase-inversion and this technique will be described in detail. Chapter 4 describes all kind of characterisation techniques, both for porous membranes as well as for nonporous membranes. Transport across a membrane occurs when a driving force is applied. Different types of driving forces can be applied and are described in chapter 5. Also membrane transport is described in this chapter. Chapter 6 gives a survey of various technical membrane processes. These processes are classified according to their driving forces. Concentration polarisation is a phenomenon which is inherently related to membrane separation. Description of this phenomenon and of fouling are given in chapter 7. Finally, in chapter 8 the basic aspects of module and process design are described. At the end of this chapter some process calculations are given.

Let me conclude by acknowledging the many who helped me writing this book. I am pleased to say that they are all (former) members of our membrane research group at the University of Twente. My first experience with membrane technology was in 1974 when I entered this university. Membrane research had just started at that time initiated by the promising expectations from the activities of the Office of Saline Water in the USA. Since then, the research activities have grown and at this moment membrane technology is one of the main research topics in our faculty, with more than 70 researchers being active in various fields.

In 1980, we started a graduate course on membrane technology for chemical engineering students. Since then, the course has been extended and improved. All my colleagues who contributed to the course also contributed directly or indirectly to helping me write this book. I am specially indebted to Kees Smolders, the driving force behind membrane research at our

University, who is always very dynamic, enthusiastic and stimulating. Other colleagues of the beginning period were Frank Altena and Maarten van der Waal. Since then a number of people have been involved in the membrane course: Hans Wijmans, Hans van den Berg, Hans Wesselingh, Matthias Wessling, Heiner Strathmann, Thonie van den Boomgaard, and Gert van den Berg. I would like to thank all these colleagues who added substantially to this book. Furthermore, I wish to thank Zandrie Borneman who made a number of the scanning electron micrographs and Ingo Blume, who has critically read the manuscript and suggested corrections. Errors that remain are my fault. It was also Ingo Blume who designed the cover and Willem Puper who drew the Maxwell demon. Especially, I wish to acknowledge my wife Jos for her patience and understanding during the many hours in the evenings when I was writing the book. Finally, I wish to express my warm feelings to my sons Ivo and Joris for just being there.

Marcel Mulder, April 1991

Preface to second edition

Membrane technology is increasingly expanding and the number of people dealing with membranes is growing rapidly. Most applications refer to concentration, purification and fractionation. However, in the last decade much research has been devoted to membrane reactors (and membrane bioreactors), the combination of a chemical reaction with a membrane separation process to shift the equilibrium or to provide in a better way the reactants that a higher productivity is obtained. New materials and membranes are required in which catalytic activity has been incorporated but there is still a long way to go. Some aspects of membrane reactors are described in chapter VI. Also membrane contactors, in which the membrane acts as an interphase, are described now, at least some basic principles. The major difference with the first edition is the incorporation of problems. It was said in one of the book reviews, 'problems should be a part of a (any) textbook' and I agree with that.
I want to thank all the people from all places around the world for their comments, considerations and positive reactions. This makes it worth to put so many hours in writing and up-dating the book and it helped me to finalize the second edition.

Marcel Mulder, May 1996

I   INTRODUCTION

I.1.   Separation processes

In 1861, at about the time that Graham reported his first dialysis experiments using synthetic membranes [1], Maxwell created the 'sorting demon', "a being whose faculties are so sharpened that he can follow every molecule in its course and would be able to what is at present impossible to us" [2]. In other words, the demon is able to discriminate between molecules. Suppose that a vessel is divided into two parts A and B by a division in which there is a small hole and that Maxwell's demon sits at the hole which he can open and close at will (see figure I - 1).
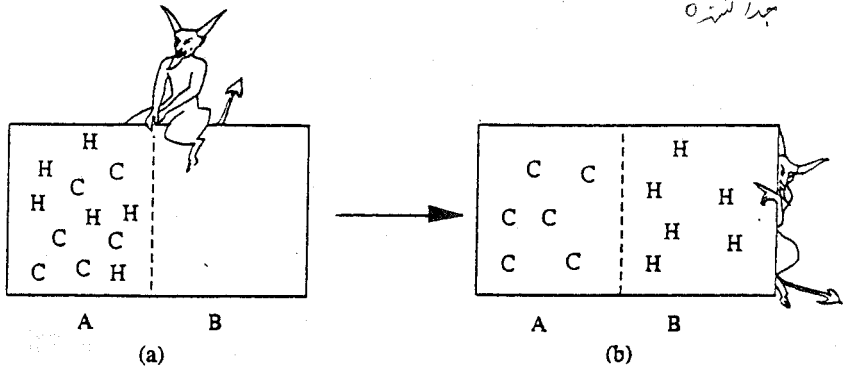
Figure I - 1.   The 'sorting demon' has ensured that a random situation (a) has been transformed into an ordered one (b).

Part A is filled with a gas consisting of hot (H) and cold (C) molecules (i.e. H and C differ in average speed) and the demon allows only the hot molecules (H) to pass. After he has been doing this for a while, the hot (H) and cold (C) molecules will be separated completely (figure 1b). Hence, starting from a random situation, an ordered one is attained which is against the second law of thermodynamics. This law states that a system tends to maximise its entropy, i.e. when left alone, the system tries to reach a situation of maximum disorder. Suppose now we have a membrane that separates the two parts of the vessel, with part A being filled with an isomeric mixture. Now, instead of employing a demon, we exert a driving force on both isomers. The membrane may discriminate between the two types of molecules because of differences in size, shape or chemical structure, and again separation will be achieved, but only to a limited extent: the membrane will never do the job as well as the demon, i.e. the membrane will not be able to separate the mixture completely. Of

course, these two examples are not quite comparable, irrespective of the fact that such a demon does not exist, for in the case of the membrane we put energy (work or heat) into the system while the demon is assumed to do the job without the expenditure of work.

The separation of substances which mix spontaneously can be accomplished either via a demon or some device which consumes energy supplied in the form of heat or mechanical work. The basic principle of any separation process is that a certain amount of energy is required to accomplish the separation. Hence, two substances A and B will mix spontaneously when the free enthalpy of the product (the mixture) is smaller than the sum of the free enthalpies of the pure substances. The minimum amount of energy (W_{min}), necessary to accomplish complete separation is at least equal to or larger than the free enthalpy of mixing.

$$W_{min} \geq \Delta G_m = \Delta H_m - T\Delta S_m \tag{I - 1}$$

In practice, the energy requirement for separation will be many times greater than this minimum value W_{min}. Different types of separation processes exist and each requires a different amount of energy. Thus, the production of fresh water from the sea, which is a very practical problem, can be performed by several commercially available separation processes:

i) distillation: heat is supplied to the solution in such a way that water distils off;
ii) freezing: the solution is cooled and pure ice is obtained;
iii) reverse osmosis : the solution is pressurised allowing water molecules to pass through the membrane while salt molecules are retained;
iv) electrodialysis: an electric field is applied to a salt solution between a number of charged membranes, and ions are forced into certain compartments leaving water molecules in other compartments; and
v) membrane distillation: heat is supplied to a salt solution causing the transport of water vapour through non-wetted the membrane.

The minimum amount of energy necessary for the desalination of sea water can be obtained by simple thermodynamic calculations. When 1 mol of solvent (in this case water) passes through the membrane, the minimum work done when the process is carried out reversibly is:

$$W_{min} = \pi . V_w = 25. 10^5 \ (N \ m^{-2}). \ 18. \ 10^{-6} \ (m^3 \ mol^{-1}) = 45 \ J \ mol^{-1} = 2.5 \ MJ \ m^{-3}$$

where π is the osmotic pressure of seawater ($\approx$ 25 bar) and V_w is the molar volume of water (0.018 l mol^{-1}). However, separation processes consume more energy than this minimum amount, with reverse osmosis having the lowest energy consumption of those mentioned above. Also the mechanisms necessary to achieve separation are quite different among these processes, with distillation and membrane distillation being based on differences in (partial) vapour pressure, the freezing or crystallisation process on differences in freezing tendencies, reverse osmosis on differences in solubility and on the diffusivity of water and

salt in the membrane and electrodialysis on ion transport in charge selective ion-exchange membranes. Freezing and distillation involve a phase transition, which means that a heat of vaporisation has to be supplied. Membrane processes such as reverse osmosis and electrodialysis occur without a phase transition, and involve a lower energy consumption. Membrane distillation, which is also a membrane process, involves no net phase transition although two transitions, vaporisation (on the feed side) and condensation (on the permeate side) occur in fact.

Desalination of (sea)water is an illustrative example of a separation problem for which competitive separation processes, based on different separation principles and consuming different amounts of energy, can be used.

A classification of some separation processes in terms of the physical or chemical properties of the components to be separated is given in table I.1. This table is far from complete and a more detailed description of separation processes can be found in a number of excellent textbooks (see e.g.[3]).

Table I.1 Separation processes based on physical/chemical properties

physical/chemical property	separation process
size	filtration, microfiltration, ultrafiltration, dialysis, gas separation, gel permeation chromatography
vapour pressure	distillation, membrane distillation
freezing point	crystallisation
affinity	extraction, adsorption, absorption, reverse osmosis, gas separation, pervaporation, affinity chromatography
charge	ion exchange, electrodialysis, electrophoresis, diffusion dialysis
density	centrifugation
chemical nature	complexation, carrier mediated transport

It can be seen from table I.1 that differences in the size, vapour pressure, affinity, charge or chemical nature of molecules facilitate membrane separation. The number of possible separation principles, some of which are used in combination, distinguish this technique from other separation processes and also provide an indication of the number of situations in which membrane processes can be applied. It should be noted that competitive separation processes are not necessarily based on the same separation mechanism. This has already been demonstrated in the example given above on water desalination. However, this example did not indicate which of the separation processes mentioned is to be preferred.

How can a separation process be selected to solve a given problem? Since several factors influence the choice of the separation process but are not generally applicable specific criteria often have to be met. However, two general criteria apply to all separation

processes:

i) the separation must be feasible technically; and

ii) the separation must be feasible economically.

The first criterion is not surprising since the separation process must be capable of accomplishing the desired separation and achieve a quality product. Sometimes a combination of two or more separation processes is necessary to attain these requirements. However, economical feasibility depends strongly on the value of the products isolated. This is often related to the concentration of the raw material. A decreasing concentration generally leads to an enhanced price for the pure product, as expressed by a so-called 'Sherwood-plot' [4,5].

Costs can be reduced by improving the technique employed for separation. In this respect, the high-value products of biotechnology are interesting since these bioproducts must be recovered from very dilute aqueous solutions. However, other factors also determine the price besides the degree of dilution. The bioproducts are usually very fragile and hence require specific separation conditions. Furthermore, the medium from which the bioproduct are isolated usually contains a large number of low and high molecular weight materials as well as many with similar properties. To obtain high-value products the energy costs must constitute only a small fraction of the product value, whereas with low-value products the energy costs may contribute appreciably to the overall price.
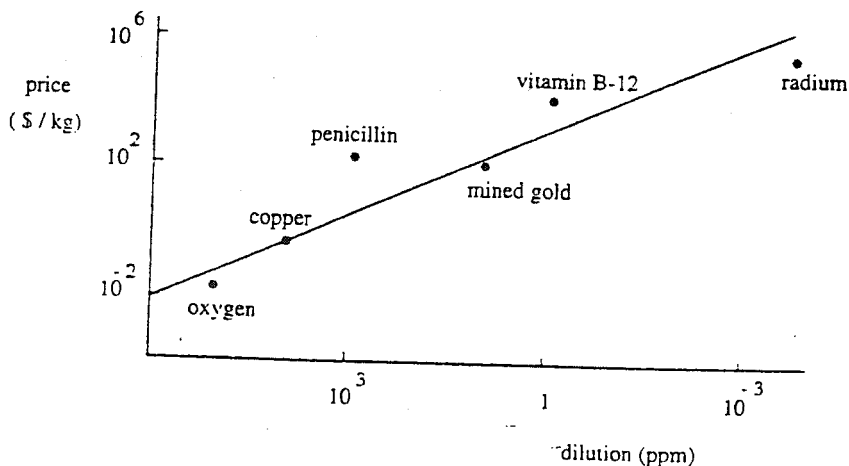
Figure I - 2.   Sale price as related to the degree of dilution (expressed in parts per million) of the raw material [4,5].

Other factors can be mentioned that determine the price of low-value products. Water is a very cheap product but its price changes from location to location. Hence, potable water is a cheap product in the western world whilst energy is relative expensive. However,

in the Middle East water is much more expensive whilst energy is cheap. This implies that, because of geographic differences, different criteria are involved in selecting separation processes. Energy and investment costs become more important with decreasing product values. Other factors which can be mentioned are politics and the environment.

From an economical point of view worthless waste streams are hardly worthy of treatment, but environmental considerations and governmental regulations often determine that the separation must be carried out. In addition, political considerations often insist that a certain process be used which may not be the most advantageous from an economical point of view.

Finally, the economics of a separation process may be governed by product loss and damage. Damage to the product can occur particularly when heat-sensitive components are produced, e.g. in the pharmaceutical industry (enzymes, antibiotics, vitamins). Product loss will be especially important in the case of high-value products.

In order to achieve a given separation, a number of different processes can be used. The objectives of separation can be classified roughly as follows:

- concentration: the desired component is present in a low concentration and solvent has to be removed;
- purification: undesirable impurities have to be removed; and
- fractionation: a mixture must be separated into two or more desired components.
- reaction mediation: combination of a chemical or biochemical reaction with a contineous removal of products will increase the the reaction rate.

The membrane processes necessary to undertake these basic functions will be described in more detail in chapter VI.

Membrane processes are characterized by the fact that the feed stream is divided into two streams, i.e. into the retentate or concentrate stream and the permeate stream (figure I - 3), which implies that either the concentrate or permeate stream is the product.
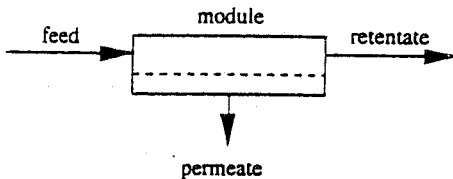
Figure I - 3. Schematic representation of a membrane process where the feed stream has been separated into a retentate and a permeate stream.

If the aim is concentration, the retentate will usually be the product stream. However, in the case of purification, both the retentate or the permeate can yield the desired product depending on the impurities that have to be removed. For example, if potable water is required from surface water containing traces of volatile organic contaminants, both reverse osmosis and pervaporation can be used for separation. With reverse osmosis the solute is

retained and the permeate (potable water) is the product, whereas with pervaporation the trace organics are selectively removed and the retentate, being pure water, is the product. With fractionation, either the retentate or the permeate can be the product. Membrane processes can be used as well in combination with a chemical or a biochemical reaction. In this way the chemical equilibrium will be shifted by removing one of the products by a suitable membrane process. For instance in a dehydrogenation process catalytically active membranes are used to remove the hydrogen while in an alcohol fermentation process the membranes are employed to remove the ethanol. This concept of membrane reactors and membrane bioreactors is rather new and only some basic aspects will be described in chapter VI.

· Membrane technology is an emerging technology and because of its multi-disciplinary character it can be used in a large number of separation processes. However, comparison between the different separation processes is difficult. The benefits of membrane technology can be summarised as follows:
- separation can be carried out continuously;
- energy consumption is generally low;
- membrane processes can easily be combined with other separation processes (hybrid processing);
- separation can be carried out under mild conditions;
- up-scaling is easy;
- membrane properties are variable and can be adjusted;
- no additives are required.

The following drawbacks should be mentioned:
- concentration polarisation/membrane fouling;
- low membrane lifetime;
- low selectivity or flux;
- up-scaling factor is more or less linear .

It should be noted that the specific features of membrane technology described here have only been considered very qualitatively and differ from process to process and from application to application. In addition, membrane fouling and concentration polarization should in fact not be considered as a disadvantage since these phenomena are inherently part of the separation process. Measures should be taken to reduce these phenomena as much as possible and this requires sufficient basic and application know-how. Furthermore, the market is very heterogeneous which makes it very difficult to give a general outline. Nowadays, membrane technology can be found in all industrial areas such as food and beverages, metallurgy, pulp and paper, textile, pharmaceutical, automotive, dairy, biotechnology, chemical industry. Also in water treatment for domestic and industrial water supply, membrane processes become more and more important. Finally, a very promising market are environmental applications where membrane technology can be applied in *clean* technology and *cleaning* technology [6,7].

I.2.   Introduction to membrane processes

As a method of separation membrane processes are rather new. Thus membrane filtration was not considered a technically important separation process until 25 years ago. Today membrane processes are used in a wide range of applications and the number of such applications is still growing. From an economic point of view, the present time is intermediate between the development of first generation membrane processes such as microfiltration (MF), ultrafiltration (UF), nanofiltration (NF), reverse osmosis (RO), electrodialysis (ED), membrane electrolysis (ME), diffusion dialysis (DD), and dialysis and second generation membrane processes such as gas separation (GS), vapour permeation (VP), pervaporation (PV), membrane distillation (MD), membrane contactors (MC) and carrier mediated processes.

Since membrane technology is a rapidly emerging technology, a state-of-the-art review is beyond the scope of this book. Many excellent review articles on specific fields in membrane technology are published regularly to keep the interested reader informed. The aim of this book is to describe the principles of membrane filtration providing definitions and simple descriptions, as well as more extended theoretical considerations.

There are many membrane processes, based on different separation principles or mechanisms and specific problems can cover the broad size range from particles to molecules. In spite of these various differences, all membrane processes have one thing in common, the membrane.

The membrane is at the heart of every membrane process and can be considered as a permselective barrier or interfase between two phases. A schematic representation of membrane separation is given in figure I - 4.
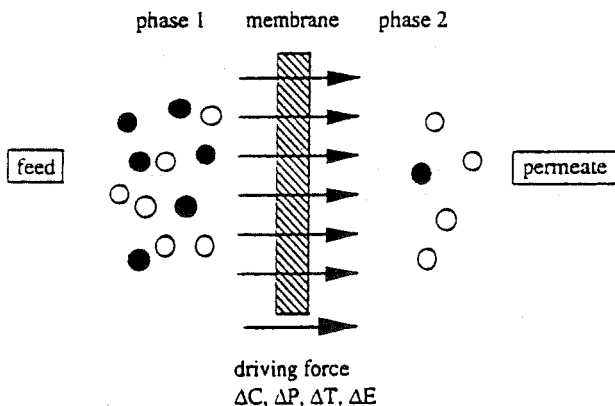
Figure I - 4.   Schematic representation of a two-phase system separated by a membrane.

Phase 1 is usually considered as the feed or upstream side phase while phase 2 is considered the permeate or downstream side. Separation is achieved because the membrane

has the ability to transport one component from the feed mixture more readily than any other component or components. This may occur through various mechanism as will be discussed later.

The performance or efficiency of a given membrane is determined by two parameters; its _selectivity_ and the _flow_ through the membrane. The latter, often denoted as the flux or permeation rate, is defined as the volume flowing through the membrane per unit area and time. Although SI units are recommended, several other units are used in the literature to represent the flux. If the flux is considered to be a volume flux, the following units are used: 1 m^{-2} hr^{-1}, 1 m^{-2} day^{-1}, gal ft^{-2} day^{-1} and cm^3 cm^{-2} hr^{-1}. The respective conversion factors are given in table I.2.

Table   I.2   Conversion table for volume fluxes

	m^3 m^{-2} s^{-1}	cm^3 cm^{-2} hr^{-1}	gal ft^{-2} day^{-1}	1 m^{-2} hr^{-1}	1 m^{-2} day^{-1}
m^3 m^{-2} s^{-1}	1	$3.6\ 10^5$	$2.1\ 10^6$	$3.6\ 10^6$	$8.6\ 10^7$
cm^3 cm^{-2} hr^{-1}	$2.8\ 10^{-6}$	1	5.9	10	240
gal ft^{-2} day^{-1}	$4.7\ 10^{-7}$	$1.7\ 10^{-1}$	1	1.7	41
1 m^{-2} hr^{-1}	$2.8\ 10^{-7}$	0.1	0.59	1	24
1 m^{-2} day^{-1}	$1.2\ 10^{-8}$	$4.2\ 10^{-3}$	$2.5\ 10^{-2}$	$4.2\ 10^{-2}$	1

Volume flux may be readily converted to mass flux or mole flux by using the density and molecular weight. This is shown in table I.3.

Table I.3   Conversion table for fluxes

1 1 m^{-2} hr^{-1}	=	ρ kg m^{-2} hr^{-1}	=	ρ/M mole m^{-2} hr^{-1}
(volume flux)		(mass flux)		(mole flux)

In the case of transport of gases and vapours the same units may be applied but with a different meaning. This is due that gases behave different from liquids, i.e. the volume of a gas is strongly dependent on pressure and temperature while liquids are not. In order to compare gas fluxes with each other the volume is always given under standard conditions (STP) which is at $0°C$ and 1 atmosphere (= 1.0013 bar). In this case 1 mole of ideal gas has a volume of $V/n = RT/P = (8.31 * 273)/1.013\ 10^5 = 22.4\ 10^{-3}$ $m^3 = 22.4$ litre.

The selectivity of a membrane towards a mixture is generally expressed by one of two parameters; the retention (R) or the separation factor (α). For dilute aqueous mixtures, consisting of a solvent (mostly water) and a solute, it is more convenient to express the selectivity in terms of the retention towards the solute. The solute is partly or completely retained while the solvent (water) molecules pass freely through the membrane. The retention is given by

$$R = \frac{c_f - c_p}{c_f} = 1 - \frac{c_p}{c_f}$$

(I - 2)

where c_f is the solute concentration in the feed and c_p is the solute concentration in the permeate. Since R is a dimensionless parameter, it does not depend on the units in which the concentration is expressed. The value of R varies between 100% (complete retention of the solute; in this case we have an 'ideal' semipermeable membrane) and 0% (solute and solvent pass through the membrane freely).

$$\alpha_{A/B} = \frac{y_A / y_B}{x_A / x_B}$$

(I - 3)

Membrane selectivity towards gas mixtures and mixtures of organic liquids is usually expressed in terms of the separation factor α. For a mixture consisting of components A and B the selectivity factor $\alpha_{A/B}$ is given by eq. I . 3, where y_A and y_B are the concentrations of components A and B in the permeate and x_A and x_B are the concentrations of the components in the feed. The SI unit for the amount of substance is the mole but the kilogram (kg) is frequently used as well. Hence, the concentrations can be expressed either as a mass concentration (c_i) or a molar concentration (n_i). The composition of a solution or a mixture can also be described by means of mole fractions, weight fractions or volume fractions. The units used to describe the composition of solutions or mixtures are summarised in table I.4.

Table I.4　　　`　Concentration units

mass concentration	$kg\ m^{-3}$
mole concentration	$mol\ m^{-3}$
mole fraction (mol/mol)	dimensionless
weight fraction (w/w)	dimensionless
volume fraction (v/v)	dimensionless

The selectivity α is chosen in such a way that its value is greater than unity. Then if the permeation rate of component A through the membrane is larger than that of component B, the separation factor is denoted as $\alpha_{A/B}$; if component B permeates preferentially, then the separation factor is given by $\alpha_{B/A}$. If $\alpha_{A/B} = \alpha_{B/A} = 1$, no separation is achieved.

I.3.　　　History

Two developments can be distinguished as far as the history of membrane technology is concerned; scientific development and commercial development. Even towards the middle

of the eighteenth century membrane phenomena were observed and studied, primarily to elucidate the barrier properties and related phenomena rather than to develop membranes for technical and industrial applications. Traditionally, research on membranes has not been carried out solely by chemists and physicists, but also others such as biologists, biochemists, biophysics and zoologists. Some scientific milestones worthy of mention are listed in table I.5. A number of the authentic contributions listed in table I.5 have been published recently in a special issue of the Journal of Membrane Science to celebrate the publication of volume 100 [24].

Table I.6 lists the development of some membrane processes. The first commercial membranes for practical applications were manufactured by Sartorius in Germany after World War I, the know-how necessary to prepare these membranes originating from the early work of Zsigmondy [25]. However, these porous cellulose nitrate or cellulose nitrate-cellulose acetate membranes were only used on a laboratory scale and the same applied to the more dense ultrafiltration membranes developed at the same

Table   I.5   Scientific milestones

observations:	osmosis: Nollet 1748 [8]
	electroosmosis: Reuss 1803 [9], Porret 1816 [10]
	dialysis: Graham 1861 [1]
relations:	diffusion: Fick 1855 [11]
	osmotic pressure: Van 't Hoff 1887 [12]
	electrolyte transport: Nernst-Planck 1889 [13]
theoretical considerations:	osmotic pressure: Einstein 1905 [14]
	membrane potentials: Henderson 1907 [16]
	membrane equilibrium: Donnan 1911 [15]
	anomalous osmosis: Sollner 1930 [17]
	irreversible thermodynamics: Kedem, Katchalsky 1964 [18]
transport models:	ionic membranes: Teorell 1937 [19], Meyer, Sievers 1936 [20]
	pore model: Schmid 1950 [22], Meares 1956 [23]
	solution-diffusion model: Lonsdale 1965 [21]

time. Early work on microfiltration and ultrafiltration membranes has been reviewed by Ferry [26].

Although the phenomenon of dialysis had already been known for a long time, the first practical membrane application on hemodialysis was demonstrated by Kolff [27] in the 1940s.

Table I.6.   Development of (technical) membrane processes

membrane process	country	year	application
microfiltration[†]	Germany	1920	laboratory use (bacteria filter)
ultrafiltration[†]	Germany	1930	laboratory use
hemodialysis[†]	Netherlands	1950	artificial kidney
electrodialysis[#]	USA	1955	desalination
reverse osmosis[#]	USA	1960	sea water desalination
ultrafiltration[#]	USA	1960	conc. of macromolecules
gas separation[#]	USA	1979	hydrogen recovery
membrane distillation[†]	Germany	1981	concentration of aqueous solutions
pervaporation[#]	Germany / Netherlands	1982	dehydration of organic solvents

† small scale
# industrial scale

A breakthrough as far as industrial membrane applications were concerned was achieved by the development of asymmetric membranes (Loeb and Sourirajan [28]). These membranes consist of a very thin dense toplayer (thickness < 0.5 μm) supported by a porous sublayer (thickness 50-200 μm). The toplayer or skin determines the transport rate while the porous sublayer only acts as a support. The permeation rate is inversely proportional to the thickness of the actual barrier layer and thus asymmetric membranes show a much higher permeation rate (water flux) than (homogeneous) symmetric membranes of a comparable thickness.

The work of Henis and Tripodi [29] made industrial gas separation economically feasible. They placed a very thin homogeneous layer of a polymer with high gas permeability on top of an asymmetric membrane, ensuring that the pores in the toplayer were filled and that a leak-free composite membrane suitable for gas separation was obtained.

Although membranes for membrane distillation (hydrophobic porous membranes) have been in existence for a time, this process has only been applied on a pilot-plant scale recently [27]. This is an example of a membrane process that makes use of existing membranes, developed initially for other purposes (microfiltration)

Pervaporation is another membrane process that has been developed recently. Binning and coworkers tried to commercialise the pervaporation process for industrial use in the late fifties, but despite intensive investigations [31] they were not very successful. This process became competitive with other methods of separation [32] due to the development of process-specific composite membranes for the dehydration of organic solvents.

The examples listed in table I.6 only relate to the beginning of the development of technical membrane processes. The search for new and better membranes is still

continuing, not only for membrane processes yet to reach the stage of commercialisation, but also for already existing membrane processes.

I.4.   Definition of a membrane

Although it is difficult to give an exact definition of a membrane, a general definition could be: *a selective barrier between two phases, the term 'selective' being inherent to a membrane or a membrane process.* It should be noted that this is a macroscopic definition while separation should be considered at the microscopic level. The definition says nothing about membrane structure nor membrane function.

A membrane can be thick or thin, its structure can be homogeneous or heterogeneous, transport can be active or passive, passive transport can be driven by a pressure, concentration or a temperature difference. In addition, membranes can be natural or synthetic, neutral or charged. To obtain a more informative understanding, membranes can be classified according to different view points. The first classification is by nature, i.e. biological or synthetic membranes. This is the clearest distinction possible. It is also an essential first distinction since the two types of membranes differ completely in structure and functionality. Although this book emphasises synthetic membranes, a section in chapter II is also devoted to biological membranes. The latter can be subdivided into living and non-living membranes, and although living membranes are essential for life on earth they are not included here because this would increase the scope of this book to too great an extent. On the other hand, non-living biological membranes (liposomes and vesicles from phospholipids) are increasingly important in actual separation processes, especially in medicine and biomedicine. Synthetic membranes can be subdivided into organic (polymeric or liquid) and inorganic (ceramic, metal) membranes. Both types will be discussed in more detail in chapter III.

Another means of classifying membranes is by morphology or structure. This is also a very illustrative route because the membrane structure determines the separation mechanism and hence the application. If we confine ourselves to solid synthetic membranes, two types of membrane may be distinguished, i.e. symmetric or asymmetric membranes. The two classes can be subdivided further as shown schematically in figure I - 5. The thicknesses of symmetric membranes (porous or nonporous) range roughly from 10 to 200 μm, the resistance to mass transfer being determined by the total membrane thickness. A decrease in membrane thickness results in an increased permeation rate.

A breakthrough to industrial applications was the development of asymmetric membranes [25]. These consist of a very dense toplayer or skin with a thickness of 0.1 to 0.5 μm supported by a porous sublayer with a thickness of about 50 to 150 μm. These membranes combine the high selectivity of a dense membrane with the high permeation rate of a very thin membrane. Figure I - 6 depicts the cross-section of an asymmetric membrane in which the structural asymmetry is clearly visible. The resistance to mass transfer is

symmetric

cylindrical
porous

porous

homogeneous
(nonporous)

asymmetric

porous

porous
with toplayer
(integrally skinned)

toplayer

dense toplayer

porous membrane
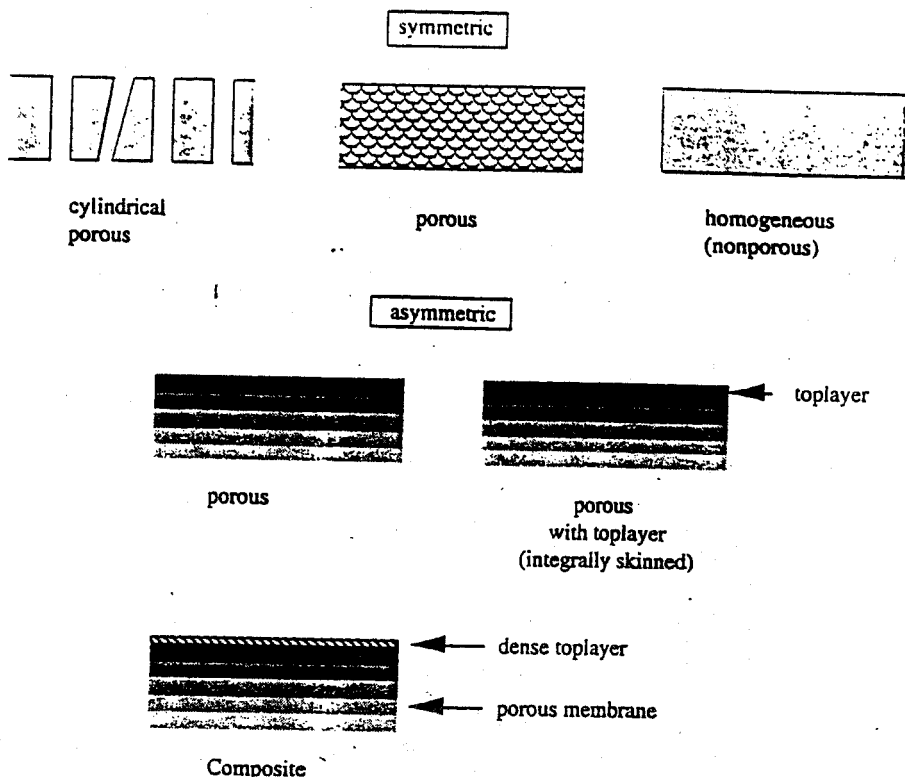
Composite

Figure I - 5.   Schematic representation of various membrane cross-sections.

determined largely or completely by the thin toplayer.

It is also possible to employ composite membranes which are skinned asymmetric membranes. However, in composite membranes, the toplayer and sublayer originate from different polymeric materials; each layer can be optimised independently. Generally the support layer is already an asymmetric membrane on which a thin dense layer is deposited. Several methods have been developed to achieve this such as dip-coating, interfacial polymerisation, in-situ polymerisation and plasma polymerisation.

Differences in membranes and membrane structures will be explained in greater detail in chapters II, III, IV, V and VI, respectively where materials, membrane formation, membrane characterisation, membrane transport and membrane processes are described.
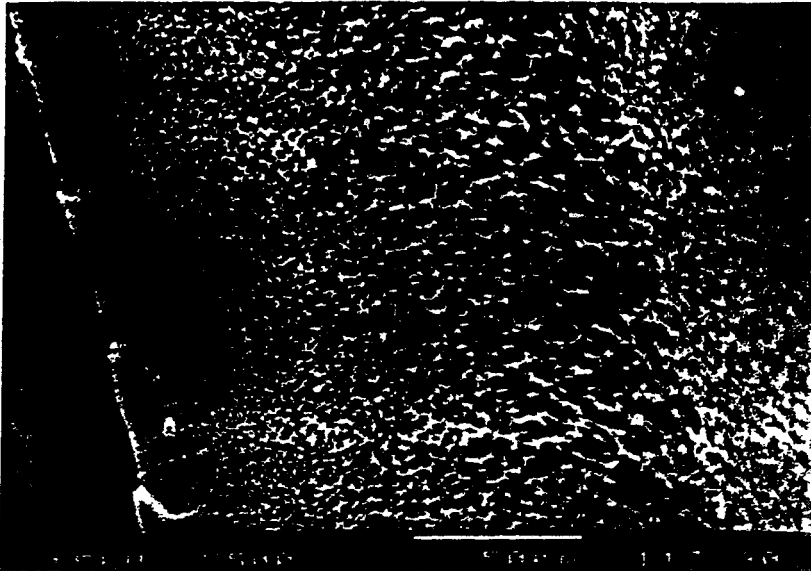
Figure I - 6.   Cross-section of an asymmetric polysulfone ultrafiltration membrane

I.5.   Membrane processes

Every membrane separation process is characterised by the use of a membrane to accomplish a particular separation. The membrane has the ability to transport one component more readily than other because of differences in physical and/or chemical properties between the membrane and the permeating components. Transport through the membrane takes place as a result of a driving force acting on the components in the feed (phase 1 in figure I - 2). In many cases the permeation rate through the membrane is proportional to the driving force, i.e. the flux-force relationship can be described by a linear phenomenological equation. Proportionality between the flux (J) and the driving force is given by

$$J = - A \frac{dX}{dx} \qquad\qquad\qquad (I - 4)$$

where A is called the phenomenological coefficient and (dX/dx) is the driving force, expressed as the gradient of X (temperature, concentration, pressure) along a coordinate x perpendicular to the transport barrier. Phenomenological equations are not confined to describing mass transport but can also be used to describe heat flux, volume flux, momentum flux and electrical flux.

Phenomenological coefficients relating flux and force are the diffusion coefficient (D. Fick's law). permeability coefficient (L_p, Darcy's law), thermal diffusivity (λ, Fourier's law). kinematic viscosity ($\upsilon = (\eta/\rho)$, Newton's law), and electrical conductivity (1/R. Ohm's law). Phenomenological equations are summarised in table I.7.

Table I. 7 Phenomenological equations

mass flux	J_m	$=$	$- D\ dc/dx$	(Fick)
volume flux	J_v	$=$	$- L_p\ dP/dx$	(Darcy)
heat flux	J_h	$=$	$- \lambda\ dT/dx$	(Fourier)
momentum flux	J_n	$=$	$- \upsilon\ dv/dx$	(Newton)
electrical flux	J_i	$=$	$- 1/R\ dE/dx$	(Ohm)

In using such equations, the transport process is considered as being macroscopic and the membrane as a black box. The factor 'membrane structure' can be considered as an interphase in which a permeating molecule or particle experience a friction or resistance.
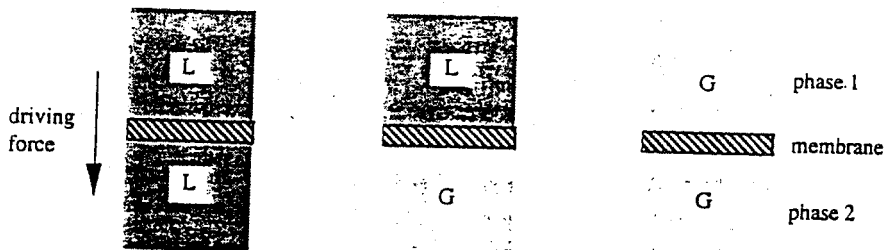
Figure I - 7. Schematic representation of phases divided by a membrane.

Driving forces can be gradients in pressure, concentration, electrical potential or temperature. An overview of various membrane processes and driving forces is given in table I. 8.

For a pure component permeating through a membrane, it is possible to employ linear relations to describe transport. However, when two or more components permeate simultaneously, such relations cannot be generally employed since coupling phenomena may occur in the fluxes and forces. These coupling phenomena can be described in terms of the formalism of non-equilibrium thermodynamics.

♦ Other than the driving force, the membrane itself is the principal factor determining the selectivity and flux. In fact the nature of the membrane (its structure and material) determines the type of application, ranging from the separation of microscopic particles to the separation of molecules of an identical size or shape.

Table 1. 8   Some membrane processes and driving forces

membrane process	phase 1	phase 2	driving force
microfiltration	L	L	ΔP
ultrafiltration	L	L	ΔP
nanofiltration	L	L	ΔP
reverse osmosis	L	L	ΔP
piezodialysis	L	L	ΔP
gas separation	G	G	Δp
vapour permeation	G	G	Δp
pervaporation	L	G	Δp
electrodialysis	L	L	ΔE
membrane electrolysis	L	L	ΔE
dialysis	L	L	Δc
diffusion dialysis	L	L	Δc
membrane contactors	L	L	Δc
	G	L	$\Delta c/\Delta p$
	L	G	$\Delta c/\Delta p$
thermo-osmosis	L	L	$\Delta T/\Delta p$
membrane distillation	L	L	$\Delta T/\Delta p$

When particles of diameter > 100 nm have to be retained, it is possible to use a rather open membrane structure. The hydrodynamic resistance of such membranes is low and small driving forces (low hydrostatic pressures) are sufficient to obtain high fluxes. The membrane process is then called microfiltration.

To separate macromolecules (with molecular weights ranging from about 10^4 to more than 10^6) from an aqueous solution, the membrane structure must be more dense and hence its hydrodynamic resistance also increases. The applied pressure is now greater than in microfiltration: this separation process is called ultrafiltration.

It is also possible to separate low molecular weight components of approximately equal size from each other. In this case a very dense (asymmetric) membrane is used, resulting in a very high hydrodynamic resistance: this process is called reverse osmosis. Going from microfiltration through ultrafiltration and nanofiltration to reverse osmosis, the hydrodynamic resistance increases and consequently higher driving forces are needed. On the other hand the product flux through the membrane and the size of the molecules (particles) being retained decreases.

The product flux obtained is determined by the applied pressure and the membrane resistance (or permeability). Typical values for applied pressures and fluxes are given in table I.9. Present day industrial membrane processes involve microfiltration, ultrafiltration, nanofiltration and reverse osmosis. Other commercial membrane processes are electrodialysis, membrane electrolysis, diffusion dialysis, pervaporation, vapour

Table I.9   Flux range and pressures in various pressure driven membrane processes.

membrane process	pressure range (bar)	flux range ($l.m^{-2}.h^{-1}.bar^{-1}$)
microfiltration	0.1 - 2.0	> 50
ultrafiltration	1.0 - 5.0	10 - 50
nanofiltration	5.0 - 20	1.4 - 12
reverse osmosis	10 - 100	0.05 - 1.4

permeation and gas separation. Electrodialysis and membrane electrolysis are membrane processes in which the driving force for (ionic) transport is supplied by an electrical potential difference. These processes can be employed only when charged molecules are present using ionic or charged membranes.

In gas separation two completely different types of membranes can be used in this process (although in different regimes of application): a dense membrane where transport takes place via diffusion, and a porous membrane where Knudsen flow occurs. A commercial application of gas separation membranes occurs in hydrogen recovery, the separation of air (oxygen/nitrogen) and of methane and carbon dioxide provide other examples. Pervaporation and vapour permeation make use of a dense separating layer.

As can be seen from table I.8, pervaporation is the only membrane process where a phase transition occurs with the feed being a liquid and the permeate a vapour. This means that at least the heat of vaporisation of the permeated product has to be supplied. Pervaporation is mainly used to dehydrate organic mixtures. It seems that in the case of membrane contactors the feed (phase 1) can be a gas and phase 2 a liquid. However, phase two is the extractant in this case and in fact the gaseous component which has been removed from the feed ans is dissolved in this liquid extractant must be removed as well (e.g. by distillation) which again results in a gaseous phase.

Two compensating phase transitions occur in membrane distillation. In this case, two aqueous solutions at different temperatures are separated by a porous hydrophobic membrane and because of a difference in partial pressure (i.e. temperature difference) vapour transport takes place through the pores of the membrane from the hot to the cold side. The solutions may not wet the membrane. Evaporation of the liquid occurs at the high temperature side while the vapour condenses at the low temperature side. Membrane distillation can be used in the concentration and purification of aqueous (inorganic) solutions.

If a dense homogeneous membrane is used instead of a microporous one the process is called thermo-osmosis. In comparison to membrane distillation no phase transition occurs, and the separation characteristics and mechanism are completely different. When a concentration difference is applied across a homogeneous membrane, the process is called dialysis. The most important application of dialysis is in the medical field for the treatment of patients with kidney failure. Transport takes place by diffusion and separation is obtained through differences in diffusion rates because of differences in molecular weight.

Calculate the toluene flux. What assumption do you have to make ? The viscosities of ethanol and toluene are 1.13 10^{-3} and 0.58 10^{-3} Pa.s, respectively

7.   A support layer for a composite membrane has a nitrogen flux of 5.10^{-2} $cm^3(STP)/cm^2.s.cmHg$. What is the flux in $m^3(STP)/m^2.h.bar$ and $mol/m^2.s.Pa$?

8a.   Describe which membrane processes you can apply to isolate a volatile componen. (e.g. ethanol) from a fermentation broth ?

b.   Describe which membrane processes you can apply to isolate a non-volatile componen (e.g. γ-interferon) from a fermentation broth ?

c.   Describe which membrane processes you can apply to isolate an ionic component (e.g sodium citrate) from a fermentation broth ?

9.   In a pervaporation experiment at room temperature a mixture of ethanol/water (60/40 by weight) is separated by a homogeneous cellulosic membrane. The total flux is $J = 2.2$ 10^{-2} cm/hr (!) and the selectivity is $\alpha = 10$. Calculate the water flux and ethanol flux ir. $l/m^2.hr.$

I.8.   Literature

1.   Graham, T.. *Phil. Trans. Roy. Soc.*, **151** (1861) 183.
2.   see e.g., Din, F, *Thermodynamic functions of gases*, Butterworth, 1962.
3.   Judson King, C., *Separation Processes*, McGraw Hill, 1971.
4.   Sherwood, T.K., 'Mass transfer between phases', Phi Lambda Upsilon
     Univ. Press, Pa, Pennsylvania State University, 1959.
5.   *Separation & Purification, Critical needs and opportunities*, National Academy
     Press, Washington, 1987.
6.   Mulder, M.H.V., 'The use of Membrane Processes in Environmental Problems. An
     Introduction., in Crespo, J.G. and Böddeker, K.W. (Eds.), *Membrane Processes
     in Separation and Purification, NATO ASI Series, Vol. 272*, Kluwer Academic
     Publishers. 1994, p. 229.
7.   Mulder, M.H.V., 'Energy Requirements in Membrane Separation Processes, in
     Crespo, J.G. and Böddeker, K.W. (Eds.), *Membrane Processes in Separation and
     Purification. NATO ASI Series, Vol. 272*, Kluwer Academic Publishers, 1994, p.
     445.
8.   Nollet, A.. *Leçons de physique-experimentale*, Hippolyte-Louis Guerin,
     Paris, 1748.
9.   Reuss, *Mem. de la Soc. imper. de naturalistes de Moscou*, **2** (1803) 327.
10. Porret, T., *Ann. Phil.*, **8** (1816) 74.
11. Fick, A., *Pogg. Ann.*, **94** (1855) 59.
12. van 't Hoff, J.H., *Z. Phys. Chem.*, **1** (1887) 481.
13. Nernst, W.. *Z. Phys. Chem.*, **4** (1889) 129.
     Planck, M.. *Ann. Phys. u. Chem.*, **39** (1890) 161.

14. Einstein, A., *Ann. Phys.*, **17** (1905) 549.
15. Donnan, F.G., *Z.Elektrochem.* **17** (1911) 572.
16. Henderson, P., *Z. Phys. Chem.*, **59** (1907) 118.
17. Sollner, K., *Z. Elektrochem.*, **36** (1930) 234.
18. Kedem, O., and Katchalsky, A., *J. Gen. Physiol.*, **45** (1961) 143.
19. Teorell, T., *Trans. Far. Soc.*, **33** (1937) 1035, 1086.
20. Meyer, K.H., and Sievers, J.F., *Helv. Chim. Acta.*, **19** (1936) 665.
21. Lonsdale, H.K., Merten, U., Riley, R.L., *J. Appl. Polym. Sci.*, **9** (1965) 1341.
22. Schmid, G., *Z. Elektrochem.*, **54** (1950) 424.
23. Meares, P., *J. Polym. Sci.*, **20** (1956) 507.
24. Special Issue of the Journal of Membrane Science, Volume 100, 1995
25. Zsigmondy, R., and Bachmann, W., *Z. Anorg. Chem.*, **103** (1918) 119.
26. Ferry, J.D., *Chem. Rev.*, **18** (1936) 373.
27. Kolff, W.J., Berk, H.T.,ter Welle, M., van der Leg, J.W., van Dijk, E.C., and van Noordwijk, J., *Acta. Med. Scand.*, **117** (1944) 121.
28. Loeb, S., and Sourirajan, S., *Adv. Chem. Ser.*, **38** (1962) 117.
29. Henis, J.M.S., and Tripodi, M.K., *J. Membr. Sci.*, **8** (1981) 233.
30. Schneider, K., and v. Gassel, T.J., *Chem. Ing. Tech.*, **56** (1984) 514.
31. Binning, R.C., Lee, R.J., Jennings, J.F., and Martin, E.C., *Ind. Eng. Chem.*, **53** (1961) 45.
32. Brüschke, H.E.A., Schneider, W.H., and Tusel, G.F., Lecture presented at the European Workshop on Pervaporation, Nancy, 1982.

II   MATERIALS AND MATERIAL PROPERTIES

II.1.   Introduction

Membranes can be made from a large number of different materials. As mentioned in chapter I, a first classification can be made into two groups, i.e. biological and synthetic membranes. Biological membranes are essential for life on earth. Every living cell is surrounded by a membrane, but these membranes differ fundamentally in structure, functionality etc. from synthetic organic and inorganic membranes. A detailed description is beyond the scope of this book but a short survey will be given at the end of this chapter.
      Synthetic membranes can be divided further into organic (polymeric) and inorganic membranes, the most important class of membrane materials being organic, i.e. polymers or macromolecules. The choice of a given polymer as a membrane material is not arbitrary but based on very specific properties, originating from structural factors. In order to understand the properties of a polymeric material some basic knowledge of polymer chemistry is required. This chapter will describe the structural factors that determine the thermal, chemical and mechanical properties of polymers. Such factors also determine the permeability, which is more or less an intrinsic property. Initially, a description of how polymers are built will be given. Then various structural factors such as molecular weight, chain flexibility and chain interaction will be described and the relation between the properties of these materials and membrane properties discussed. For a more detiled description of this subject, the reader is referred to a number of textbooks on polymer science (e.g. ref [1 - 4]). Finally, since inorganic materials such as glasses and ceramics are frequently used as membrane materials, some properties of these materials will be described briefly.

II.2.   Polymers

Polymers are high molecular weight components built up from a number of basic units, the monomers. The number of structural units linked together to form the 'long chain molecule' is defined as the degree of polymerisation. Consequently, the molecular weight of a long chain molecule is dependent on the degree of polymerisation and on the molecular weight of the basic unit, the monomer. The simplest polymer is polyethylene, which is obtained from ethene, $CH_2=CH_2$. On polymerisation, the double bond of ethene is opened and a large number of C_2H_4 molecules are coupled together to form a chain, which in the case of polyethylene is linear with two ends (figure II - 1). The four valences of a carbon atom form a tetrahedron, the angle between the C - C bonds being 109.5°. A polymer chain has an infinite number of different conformations, ranging from completely coiled to completely uncoiled. A schematic drawing of its most extended conformation is also given in figure II - 1.
      The -CH_2-CH_2- unit is called a segment. With increasing number of segments the

physical, chemical and mechanical properties of the polymer changes as well.

$$n\ CH_2 = CH_2 \quad \Rightarrow \quad [-\ CH_2 - CH_2 -]_n$$

109.5°
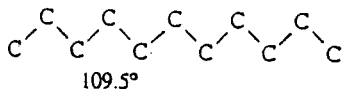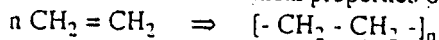
Figure II - 1. Polymerisation of ethene to polyethylene.

Table II.1 demonstrates the relation between molecular weight and molecular character for different degrees of polymerisation (i.e. for different chain lengths). Since all the repeating

Table II.1   Character of polyethylene in relation to molecular weight [4]

number of units of $-C_2H_4-$	molecular weight	character at 25°C
1	28	gas
6	170	liquid
200	5600	wax
750	21000	plastic
5000	140000	plastic

units, the segments, are the same in polyethylene this polymer is called a *homopolymer*. However, it is not necessary that a single monomer is used. Certain polyamides, for example, are prepared from two different monomers, a diacid and a diamine, but the repeating unit is the same throughout so that the resulting polymer is also a homopolymer. With *copolymers* the repeating units are different, i.e. two monomers A and B are coupled together in various ways and a number of different structures can be distinguished. When the sequence of the structural units is completely irregular, the copolymer is said to be random. The properties of random copolymers are strongly dependent on the molar ratios of A and B. Many synthetic rubbers such as NBR (nitrile-butadiene-rubber), SBR (styrene-butadiene-rubber), EPDM (ethene-propene-diene rubber), ABS (acrylonitrile-butadiene-styrene rubber), EVA (ethylene-vinyl acetate copolymer) and EVAL (ethylene-vinyl alcohol copolymer) are *random copolymers*. However, in a *block copolymer* the chain is built up by linking blocks of each of the monomers. An example of a block copolymer is SIS (styrene-isoprene-styrene). Often one part (the minor fraction) is dispersed in the other part, the continuous phase, and a type of domain structure is thereby obtained. These structural differences, random relative to domain, also have a large influence on the physical properties. Finally, in *graft copolymers* the irregularities occur in the side chains rather than the main chain. The second monomer can be attached to the main chain by chemical means (peroxides) or by radiation (see also chapter III).

The polymers mentioned so far are either linear or branched. It is also possible to connect two or more chains to each other by means of crosslinks. Crosslinking often

occurs via chemical reaction, the chains being connected together by covalent bonding. Crosslinking has an enormous effect on the physical, mechanical and thermal properties of the resulting polymer.

....AAAAAABBBBBBBBBBBBBBBBBBBBBAAAAAAAAAA....   block copolymer

....AABABBABABABABAABAAABABBABAABBABBAB....   random copolymer

....AAAAAAAAAAAAAAAAAAAAAAAAAAAAAAAAAA....   graft copolymer
    B   B
    B   B
    B   B
    B   B
    B
    B
    B
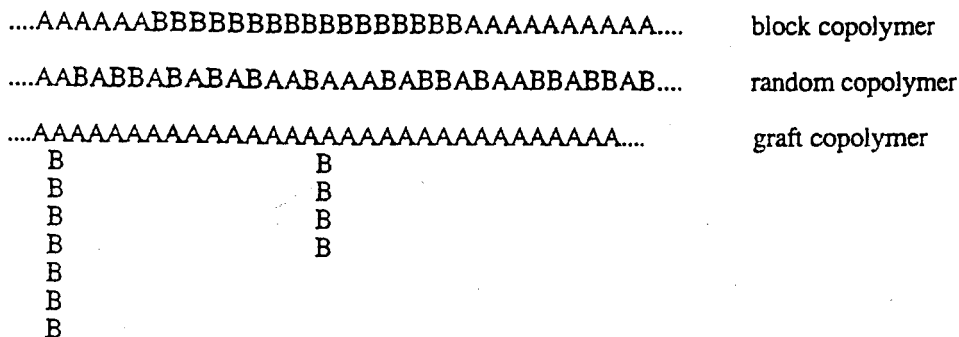
Figure II - 2.   Schematic representation of various copolymers.

One characteristic is that the polymer becomes insoluble. In addition to chemical crosslinks, physical crosslinks may exist, for example in (semi)-crystalline polymers where the crystallites act as crosslinks or in block copolymers where the domains of the dispersed phases act as physical crosslinks.
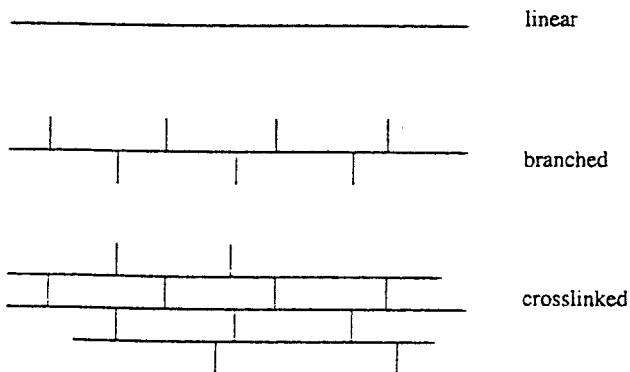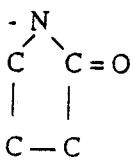
Figure II - 3.   Schematic drawing of various methods of building up macromolecules.

II.3.   Stereoisomerism

A very important class of polymers are the vinyl polymers, which are obtained by polymerisation of vinyl compounds $H_2C = CHR$. The most simple one is polyethylene where only hydrogen atoms are attached to the carbon main chain ($R = H$).

Vinyl polymers are characterised by $—CH_2—CHR—$ repeating units, where the side group $—R$ is different for different polymers. Table II.2 summarises some important vinyl polymers.

Table II.2   Some important vinyl polymers

name	- R
polypropylene	$- CH_3$
polybutylene	$- C_2H_5$
polystyrene	$- C_6H_5$
polyvinylalcohol	$- OH$
polyacrylonitrile	$- CN$
polyvinylchloride	$- Cl$
polymethacrylate	$- C = O$ $O - CH_3$
polyvinylpyrrolidone	$- N$ $C \quad C = O$ $C - C$

The side group R can be attached to the carbon atom in two different ways (the so-called D and L form), which implies that three different arrangements may be distinguished in the polymer (see figure II - 4).
- isotactic, where all the side groups R lie on the same side along the main chain.
- atactic, where the side groups R are arranged randomly along the main chain.
- syndiotactic, where the side groups R are placed on alternate sides of the main chain.

The position of the side group R has a very important influence on the polymer properties. Since crystallinity depends on the regularity of the structure, isotactic polymers may be very crystalline whereas atactic polymers are non-crystalline. Thus, atactic polystyrene and polypropylene are completely amorphous, whereas isotactic polystyrene and polypropylene are partially crystalline. Crystallinity not only affects the mechanical properties of the polymer but also its permeability.
Polymers containing a double bond in the main chain exhibit cis-trans isomerism. The polymerisation of 1,3-isoprene, for example, gives two possible products, i.e. cis-1,4-polyisoprene or trans-1,4-polyisoprene (see figure II - 5), both with different properties. The cis-isomer is natural rubber and it can be used as a membrane material whereas the trans-isomer is a stiff leathery material exhibiting thermoplastic properties. Other polymers containing a double-bond, such as chloroprene (neoprene) or butadiene rubber, also exhibit cis-trans isomerism.
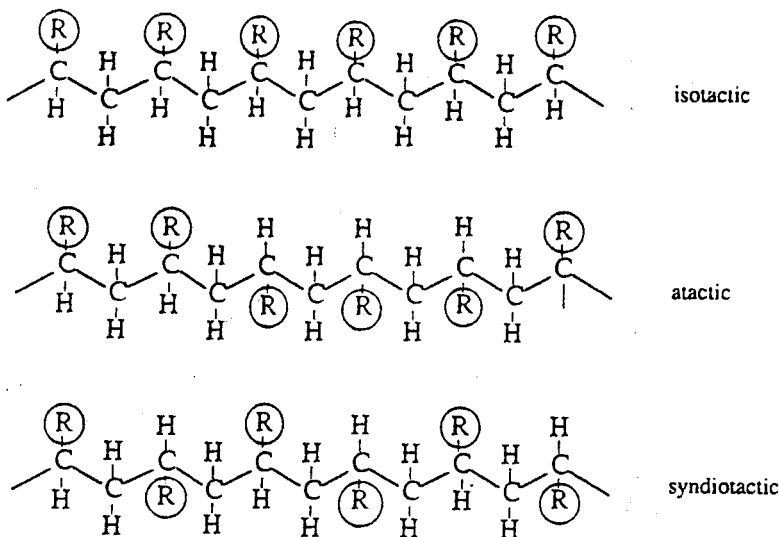
Figure II - 4.   Isotactic, atactic and syndiotactic polymers.

II.4.   Chain flexibility

One of the main structural characteristics, i.e. chain flexibility, is determined by two factors: *i)* the character of the main chain and *ii)* the presence and nature of the side chains or side groups. In many polymers (e.g. vinyl polymers) the main chain consists entirely of —C—C— bonds. Rotation around each —C—C— bond is possible, which makes the chain rather flexible. However, when the main chain is completely unsaturated, i.e. constructed of —C=C— bonds, no rotation is possible and a very rigid chain is obtained. In the case of a chain containing both saturated and unsaturated bonds as in polybutadiene [—C—C=C—C—]. rotation around the single —C—C— bond is still possible and this chain is also very flexible. Introduction of heterocyclic and aromatic groups into the main chain leads to a substantial decrease in flexibility. These types of polymers often show excellent chemical and thermal stability. Other elements, in addition to carbon may also be present in the main chain, such as oxygen in polyesters and polyethers and nitrogen in polyamides. Generally, the presence of oxygen and nitrogen in the main chain linked to a carbon atom increases the flexibility but often aromatic or heterocyclic groups are also present in the main chain and these tend to dominate the structure giving the chain a rigid character. For this reason the properties of aliphatic and aromatic polyamides differ quite considerably.

A further class of polymer does not contain carbon atoms in the main chain; such polymers are called inorganic polymers. The most important of these polymers are the silicone rubbers containing silicium rather than carbon. These polymers are often built up through a sequence of — Si—O— units. Another group of inorganic polymers are the polyphosphazenes which contain phosphorus in the main chain ([—P=N—]). Whereas the —Si—O— chain is very flexible the —P=N— chain is quite rigid.

$$H_2C=CH_2 \text{---} CH=CH_2$$
$$| \quad CH_3$$

methyl-butadiene
(isoprene)

$$\left[CH_2 \text{---} CH=C \text{---} CH_2 \right]$$
$$| \quad CH_3$$

polyisoprene

$$H \diagdown \quad \diagup CH_3$$
$$C=C$$
$$\text{---} H_2C \diagup \quad \diagdown CH_2 \text{---}$$

cis-1.4-polyisoprene

$$H \diagdown \quad \diagup CH_2 \text{---}$$
$$C=C$$
$$\text{---} H_2C \diagup \quad \diagdown CH_3$$

trans-1,4-polyisoprene
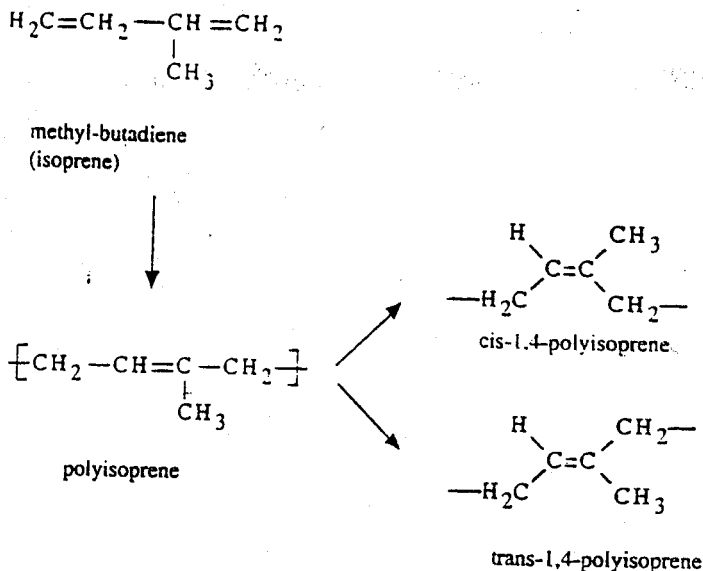
Figure II - 5. An example of cis-trans isomerism.

Chain flexibility is also determined by the character of the side groups, which determine to some extent whether rotation around the main chain can take place readily or whether steric hindrance occurs. In addition, the character of the side group has a strong effect on inter-chain interaction. The smallest possible side group is the hydrogen atom (—H). This has no influence on the rotational freedom of the bonds in the main chain and its affect on inter-chain distance and interaction is also minimal. On the other hand a side group such as the phenyl group (—C_6H_5) reduces rotational freedom in the main chain while the distance between the various chains is also increased.

II.5. Molecular weight

The chain length is an important parameter in determining the properties of a polymer. Polymers generally consist of a large number of chains and these do not necessarily have the same chain length. Hence there is a distribution in molecular weight. The length of the chain can often be expressed quite adequately by means of the molecular weight. The consequence of the existence of different chain lengths in a polymer is that a uniform molecular weight does not exist but rather a molecular weight average. Figure II - 6 shows a histogram of a polymer exhibiting a particular molecular weight distribution. This figure illustrates the number or fraction of molecules (n_i) with a particular molecular weight (M_i). The molecular weight distribution is an important property relative to membrane preparation (see chapter III) and particularly to membrane characterisation (see chapter V).

There are various definitions of the molecular weight of a polymer. By multiplying

the number of chains of a certain length with their molecular weight and adding this to the number of a second class of chain multiplied by their molecular weight, and so on, and then dividing by the total number of chains, the number average molecular weight (M_n) may be obtained (see eq. II - 1)
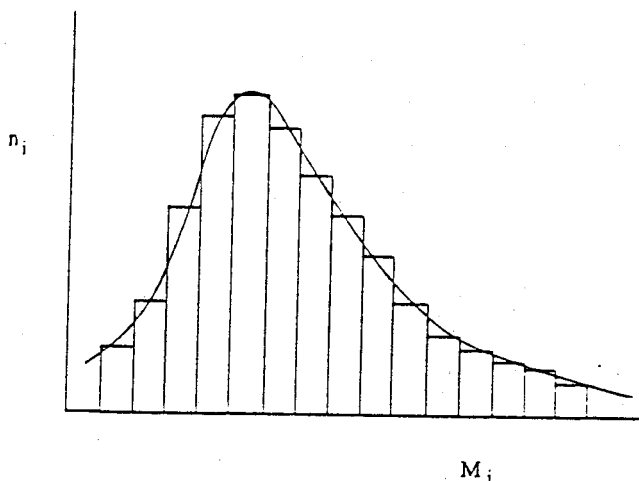
Figure II - 6.   Histogram demonstrating a possible molecular weight distribution in a polymer.

$$M_n = \frac{\sum_i n_i M_i}{\sum_i n_i}$$

(number average molecular weight)   (II - 1)

If instead of the number of molecules n_i with a molecular weight M_i, the weight of the fraction w_i is used, then the weight average molecular weight (M_w) is obtained.

$$M_w = \frac{\sum_i w_i M_i}{\sum_i w_i}$$

(weight average molecular weight)   (II - 2)

When a relatively small amount of very long chains is present in the polymer, M_w may differ quite considerably from M_n. A small amount of long chains has a great effect upon M_w but hardly influences M_n.

The difference between M_n and M_w can be illustrated by the following example. When 1 gram of long molecules with a molecular weight equal to 10,000 g/mol is mixed with 1 gram of smaller molecules having a molecular weight equal to 1000 g/mol, the weight average molecular weight is 5500. However, since there are now ten times as many as small molecules as there are long molecules this implies that the number average molecular weight is (10 * 1000 + 1 * 10000) / 11 ≈ 2000. The broad distribution depicted

in figure II - 6 has a considerable influence on M_w and less on M_n. Such a broad distribution can be expressed in terms of the *polydispersity* p which is the ratio of M_w to M_n. For most commercially available polymers the polydispersity is greater than 2.

With increasing chain length the number of interaction sites between the various chains increases and consequently the chemical, physical and mechanical properties of the polymer vary. In addition, the coiled polymer chains are not situated separately from each other but are entangled. The number of entanglements increases with increasing chain length. A schematic drawing of such an entanglement is given in figure II - 7.
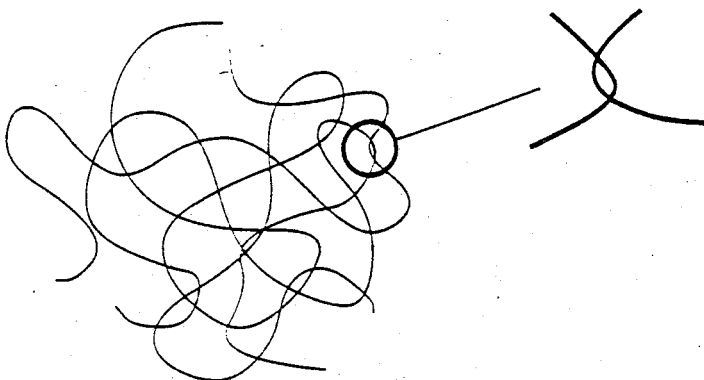
Figure II - 7. Schematic drawing of an entanglement.

II.6. Chain interactions

In linear and branched polymers only secondary interaction forces act between the different chains, whereas in network polymers the various chains are bound to each other covalently. Secondary intermolecular forces are considerably weaker than primary covalent bonds. Nevertheless they have a strong effect on the physical properties of the polymer (and consequently on its permeability) because of the large number of interactions possible. Three different types of secondary force can be considered:

- dipole forces (Debye forces)

Table II.3   Average values of strength of primary and secondary forces

type of force	kJ/mole
covalent	≈ 400
ionic	≈ 400
hydrogen bonding	≈ 40
dipole	≈ 20
dispersion	≈ 2

- dispersion forces (or London forces)
- hydrogen bonding forces

The relative strengths of these secondary forces, the ionic forces and the covalent bonds are listed in table II.3. Some polymers contain groups or atoms in which the charge is not distributed homogeneously. The effect of the charge distribution (dipole) is only apparent at short distances. Such dipoles exert a strong attraction on other permanent dipoles and dipole-dipole interaction takes place. Permanent dipoles can also influence neutral groups in which they can induce a dipole. This dipole-induced dipole interaction is weaker than the dipole-dipole interaction. Examples of some groups with permanent dipoles are hydroxyl (— OH), carbonyl (— C = O) or halide (—I, —Br, —Cl, or —F). Although many polymers do not contain groups or atoms with a permanent dipole, interaction forces, known as dispersion forces, can still exist between the chains. In this case, because of fluctuations in the electron density, a varying dipole is formed. Dispersion forces are the weakest, but also the most common, forces capable of inducing chain interaction.

The strongest secondary forces are hydrogen bonds. These appear when a hydrogen atom, attached to an electronegative atom such as oxygen (hydroxyl), is attracted by an electronegative group in another chain. In particular the following types of attraction are very strong: —O...H...O—, —N...H...O— and —N...H...N—. The forces in these cases can be so strong that the polymer can hardly be dissolved, as demonstrated by polyamides and cellulose, for example. Hydrogen bonding has also a positive effect on crystallisation. Hydrogen bonding ability can be subdivided into proton donor and proton acceptor character. Some groups are of the proton donor type, others of the proton acceptor type, some have both characteristics and some are unable to form hydrogen bonds. Table II.4 presents a summary.

Table II.4   Groups with proton donor and /or proton acceptor character

group	proton donor	proton acceptor
- OH	x	x
- NH_2	x	x
- NRH	x	x
- NR_2		x
- C=O		x
- X (halide)		x
- C_6H_5		x
- C≡N		x
- CH_3	x	
- CRH_2	x	
- CR_2H	x	

All the parameters discussed above such as molecular conformation, molecular configuration, chain interaction and chain length are important in determining the overall state of the polymer and will be further discussed in the next section.

II.7.   State of the polymer

The state of the polymer is very important relative to its mechanical, chemical, thermal and permeation properties. The state of a polymer is defined as the phase in which the polymer appears. Compared to low molecular weight compounds this is more complex with polymers. For instance, the solid phase may be rubbery or glassy, but the properties differ drastically.

The selection of a material for a certain application involves different criteria. The choice of the polymer is not that important when porous membranes (micro/ultrafiltration) are considered in terms of separation (a similar pore size distribution should give the same water flux), but definitely affects the chemical and thermal stability and surface effects such as adsorption and wettability. In addition, the choice of cleaning agent is determined by the choice of the polymer, e.g. polyamides are strongly attacked by chlorine-containing cleaning agents.

In contrast, when dense nonporous membranes are considered, the polymeric material chosen directly influences the membrane performance and especially the glass transition temperature T_g and the crystallinity which are very important parameters. These parameters are determined by structural factors such as chain flexibility, chain interaction and molecular weight, as discussed in the previous section.

When a non-crystalline (amorphous) polymer is heated, a temperature exists at which the polymer changes from a glassy to a rubbery state. Figure II - 8 shows the variation in the tensile modulus E of a completely amorphous polymer as a function of the temperature.
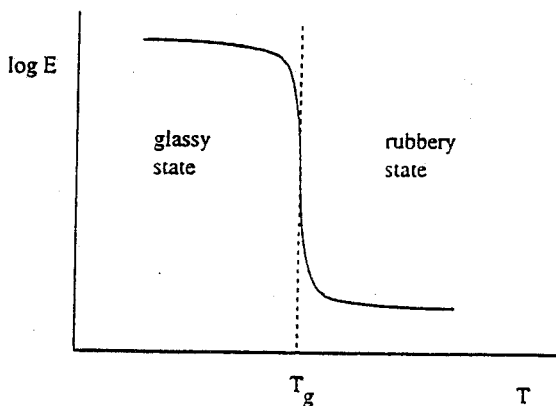
Figure II - 8.   Tensile modulus E as a function of the temperature for an amorphous polymer.

The tensile modulus E is a characteristic parameter for a given polymer and may be defined as the force F applied across an area A ('stress') necessary to obtain a given deformation

('strain'). The unit of E is N.m^{-2} or Pascal (Pa).

Two regions can be distinguished in figure II - 8: the glassy state with a high modulus and the rubbery state with a modulus, which is often three to four orders of magnitude lower. The mobility of the polymeric chains is very restricted in the glassy state, since the segments cannot rotate freely around the main chain bonds. On increasing the temperature, some motions can occur in the side chains or in a few segments of the main chain. However, these are only marginal changes with the density of the polymer decreasing to a limited extent (or conversely the specific volume increasing a little). The temperature at which transition from the glassy to the rubbery state occurs is defined as the glass transition temperature (T_g). At this temperature the thermal energy is just sufficient to overcome the restriction in rotation due to bulky side groups or to overcome the interactions between the chains. For this reason, the important parameters which determine the glass transition are chain flexibility and chain interaction. In the rubbery state the segments can rotate freely along the main chain bonds, implying a high degree of chain mobility. The change in physical behaviour of the polymer from the glassy to the rubbery state is discontinuous. In addition to the modulus, all kind of physical properties change at the glass transition temperature such as specific volume, specific heat, refractive index and permeability. Figure II - 9 represents the specific volume and the free volume of a polymer as a function of temperature.
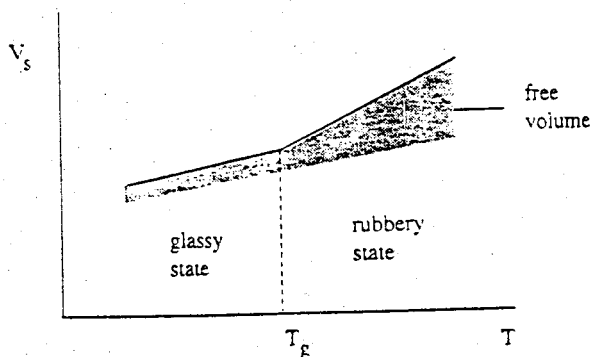
Figure II - 9.   Specific volume and free volume as a function of temperature.

The free volume can be defined simply as the volume unoccupied by the macromolecules (the occupied volume contains both the van der Waals volume of the atoms and the excluded volume, see also chapter V). In the glassy state ($T < T_g$) the free volume fraction v_f is virtually constant. However, above the glass transition temperature the free volume increases linearly according to

$$v_f = v_{f,T_g} + \Delta\alpha \, (T - T_g)$$

(II - 3)

where $\Delta\alpha$ is the difference between the value of the thermal expansion coefficient (the thermal expansion coefficient being defined as $\alpha = V^{-1}((\partial V/\partial T)_P)$ above and below T_g. The concept of free volume is very important in the transport of non-interacting permeants, such as nitrogen, helium and oxygen. For interacting permeants, such as organic vapours and liquids, segmental motions are a function of permeant concentration. It is possible to base the transport of penetrants through nonporous membranes on the free volume concept (see chapter V).

II.8. Effect of polymeric structure on Tg

The physical properties of a polymer are determined to a large extent by the chemical structure. The thermal motion of the polymer chains is dependent on the ability to rotate around the main chain. This is mainly determined by two factors :

i) chain flexibility
ii) chain interaction

flexible

$-C-C-$ polyethylene

$-C-O-$ polyoxymethylene

$-C-N-$ polyamide

$-C-C=C-C-$ polybutadiene

rigid

$-C=C-C=C-$ polyacetylene

polyether

polyoxadiazole

polyimide

polybenzimidazoles

polypyrrone (ladder polymer, very rigid)
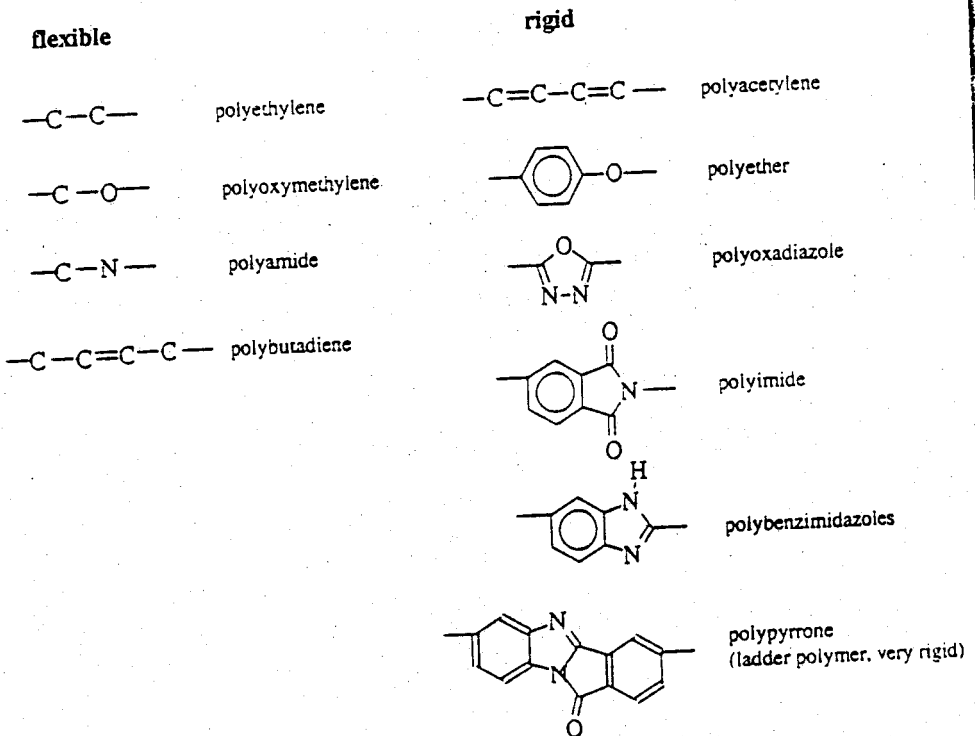
Figure II - 10. Relative stiffnesses of the main chain

The chain flexibility is mainly determined by the flexibility of the main chain. The presence of aromatic and heterocyclic groups in the main chain reduces the rotation dramatically whereas a saturated main chain is very flexible. In the latter case the type of side groups can become very important. Figure II - 10 gives a qualitative indication of the chemical structure on the main chain stiffness. A main chain based on —C—C— bonds (as in vinyl polymers) is very flexible as are those based on —C—O— or —Si—O— linkages and hence T_g is low (especially for the Si — O bond which has a very low rotational energy). When aromatic groups or heterocyclic groups are present in the main chain, T_g increases dramatically. For example, an aliphatic polyamide has a much lower T_g value than an aromatic one (Nylon - 6) has a T_g value of 50°C while poly(m-phenylene isophthalamide) or Nomex has a T_g value of 273°C; the structures of these polymers are depicted in figure II - 26.
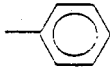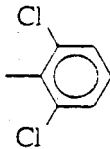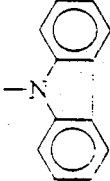
$$\text{+CH}_2\text{—CH+}$$
$$|$$
$$\text{R}$$ Vinyl polymers

— R	T_g (°C)	— R	T_g (°C)
—H	- 120	—CH$_3$	- 15
—CH$_3$	- 15	—Cl	87
phenyl	100	—CN	120
dichlorophenyl (Cl, Cl)	167		
carbazolyl (N)	208		

Figure II - 11 .   Glass transition temperature for various vinyl polymers containing different side groups [4].

Some well-known polymers containing aromatic groups in the main chain have high glass transition temperatures, examples being polysulfone (T_g = 190°C), polyether sulfone (T_g = 230°C) and polyphenylene oxide (T_g = 214°C). Rotation around the unsaturated —C=C— and —C≡C— bond is not possible. However, where the chain contains alternating saturated (—C—C—) and unsaturated (—C=C—) bonds the T_g value is not enhanced significantly since the increased rotation around the —C—C— bonds compensates for the stiffness of the —C=C— bond. Thus, the T_g value for polybutadiene (—C—C=C—C—), for example, of - 73°C is not much higher than that for polyethylene (—C—C—), i.e. a value of - 120°C. When the main chain becomes completely unsaturated such as in polyacetylenes (—C=C—C=C—) the T_g value increases dramatically.

Chain flexibility is not solely determined by the groups present in the main chain; the side chain (or side groups) can also be quite important. However, the influence of the side chain or side groups on T_g is mainly confined to polymers containing flexible main chains. In case of a polymer with a rigid main chain the influence of side groups is less dramatic. Most of the polymers with flexible —C—C— bonds in the main chain are vinyl polymers. In figure II - 11 the T_g value is listed for polyethylene, polypropylene, polystyrene, poly-2,6-dichlorostyrene, and poly(vinyl carbazole) [4]. As the size of the side group increases, rotation around the main chain is hindered sterically and the T_g value increases. In the case where a flexible main chain exists the nature of the side group can have a dominant effect, the difference between a hydrogen atom (polyethylene) and a carbazole group poly(vinyl) carbazole amounting to a difference of more than 300°C in the T_g value. Interaction between the chains is increased when polar side groups are introduced. On comparing polypropylene, poly(vinyl chloride), and polyacrylonitrile, which have side groups of about the same size the polarity increases and consequently the inter-chain interaction and T_g values increase. This is also depicted in figure II - 11.

Flexible side groups (e.g. alkyl groups) have no effect on the mobility of the main chain. However, they increase the inter-chain distance and cause a decrease in T_g because the inter-chain interactions decrease. Table II.5 summarises the glass transition temperatures of a number of polymers. In addition to the glass transition temperature, another important parameter, the degree of crystallinity, also determines the state of the polymer. Some polymers have very regular structural units and are therefore able to crystallise because the chains can be packed in a regular pattern. Atactic vinyl polymers are generally too irregular to allow crystallisation. Only when strong intermolecular interactions, such as hydrogen bonding, occur between the various chains crystallisation may occur. Thus although poly(vinyl alcohol) is an atactic polymer, because of hydrogen bonding it still exhibits semi-crystalline character. On the other hand isotactic and syndiotactic polymers generally crystallise. With unsaturated polymers, crystallisation occurs when all the chains have the same conformation, i.e. are either cis or trans. Cis-1,4-polybutadiene or cis-1,4-polyisoprene, for example, are semi-crystalline elastomers. Since various kinds of irregularities can disturb the crystallisation process, copolymers do not generally crystallise. Some polymers are not completely crystalline, the degree of crystallinity being far less than 100%. These polymers are called semi-crystalline and consist of an amorphous and a crystalline fraction. A large number of semi-crystalline

Table II.5   Glass transition temperature of various polymers [4]

Polymer	Tg (°C)
polydimethylsiloxane	- 123
polyethylene	- 120
poly-(cis-1,4-butadiene)	- 90
poly-(cis-1,4-methylbutadiene)	- 73
natural rubber	- 72
butyl rubber	- 65
polychloroprene	- 50
poly(vinylidene fluoride)	- 40
poly-(cis-1,4-propylene)	- 15
poly(methylacryate)	10
poly(vinyl acetate)	29
polymethylpentene	30
ethylcelulose	43
Nylon-6 (alif. polyamide)	50
cellulose nitrate	53
polyethyleneterephtalate	69
cellulose diacetate	80
poly(vinyl alcohol)	85
poly(phenylene sulfide)	85
poly(vinyl chloride)	87
polystyrene	100
polymethylmethacrylate	110
polyacrylonitrile	120
polytetrafluoroethylene	126
polyetheretherketone	143
polycarbonate	150
polyvinyltrimethylsilane	170
polysulfone	190
polytrimethylsilylpropyne ≈	200
poly(ether imide)	210
poly-(2,6-dimethylphenylene oxide)	210
poly(ether sulfone)	230
polyimide (Kapton)	300
polyoxadiazole (POD)# >	450

Polymer degrades prior to the glass transition temperature

polymers exist such as polyethylene, polypropylene, various polyamides and polyesters.

The degree of crystallinity provides no information about the size and the shape of the crystallites. Two types of crystallites often found are the 'fringed micelles' and the spherulites (figure II - 12). In the fringed micelles sections of adjacent linear polymeric chains are located in a crystal lattice. Ordering here is intermolecular, with a number of segments of various chains being arranged parallel to each other. Spherulites can be obtained by the slow crystallisation of dilute polymer solutions. Here crystallisation is intramolecular and occurs in the form of lamellae.

fringed - micelle
(inter - molecular)

spherulites
(intra - molecular)
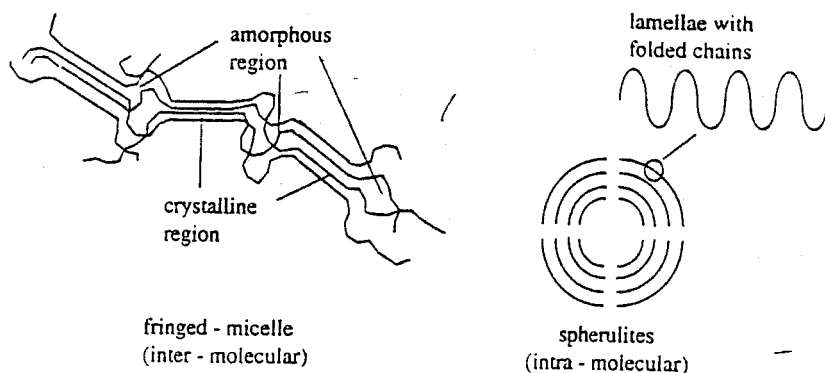
Figure II - 12. Schematic drawing of two types of crystallites: (a) fringed micelles and (b) spherulites.

Crystallites have a large influence not only on the mechanical properties of a polymer but also on its transport properties. The influence of crystallinity on the tensile modulus E is depicted in figure II - 13. In the glassy state the mechanical properties are little influenced by the presence of crystallites. On passing through the glass transition temperature the amorphous glassy state is transformed into the rubbery state but the crystalline phase remains unchanged, i.e. the chains remain in the crystal lattice which maintains its rigidity until the melting temperature has been reached. Hence, for a perfect crystalline polymer (100% crystallinity) changes in the modulus are most likely at the melting temperature (T_m) rather than the glass transition temperature (T_g). In semi-crystalline polymers the glassy phase exhibits the same mechanical properties as for a completely amorphous polymer. However, in the rubbery state the mechanical properties will depend on the crystalline content of the polymer. Generally the tensile modulus of a semi-crystalline polymer decreases as a function of temperature (curve b, figure II - 13). This figure also depicts the tensile modulus of a completely crystalline polymer (curve a) indicating that no rubbery state is observed in this case and that the modulus only decreases drastically at the melting point.

In order to correlate the structural parameters of a polymer to its permeability

some examples will be given. Table II.6 lists the permeabilities of nitrogen and oxygen together with the ideal separation factor ($\alpha_{ideal} = P_{O2}/P_{N2}$) for a number of polymers, and indicating a number of remarkable features. The gas (oxygen or nitrogen) permeabilities through polymers can differ by as much as seven orders of magnitude. Elastomers (low T_g) are very permeable and listed at the top of the table with polydimethylsiloxane ($T_g = -123°C$) as the highest permeable one. In contrast, glassy polymers (high T_g) are located in the lower part of the table.

Another very striking point is that the selectivities for O_2/N_2 do not increase automatically as the permeability decreases. Most polymers exhibit selectivities within the range from 2 to 6. Although the glass transition temperatures are not given, no unique relationship exists between permeability and T_g, merely a rough trend. Elastomers generally exhibit high permeabilities and glassy polymers low permeabilities, but, there are a number of striking exceptions. Polyphenylene oxide, for example, with a very high T_g value ($T_g = 220°C$!) also has a high permeability towards nitrogen and oxygen. Indeed the highest permeability is found for polytrimethylsilylpropyne (PTMSP), a glassy polymer. Another glassy polymer, polyvinyltrimethylsilane (PVTMS), also shows a very high permeability. The structures of these two polymers are given in figure II - 14. The gas permeability coefficient of PTMSP is one order of magnitude higher than that of the very permeable elastomer, polydimethylsiloxane (PDMS). PTMSP and PVTMS both contain the same side group, $Si(CH_3)_3$, but PTMSP has a very rigid main chain in contrast to PVTMS which has a more flexible (vinyl) main chain. The high permeability of PTMSP originates from its high (thermal) free volume, which in turn is determined by the large pendant side group in combination with a rigid main chain. Because of its very high free
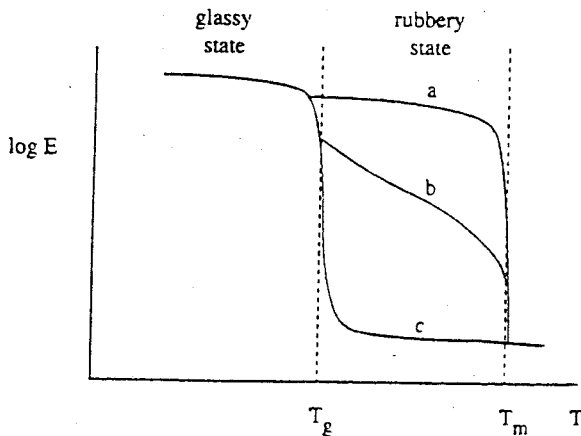
Figure II - 13.   Tensile modulus of a semi-crystalline polymer as a function of the temperature.
a) (completely) crystalline polymer; b) semi-crystalline polymer; c) amorphous polymer.

volume, PTMSP can in fact be considered as an interconnecting porous network, with pores sizes within the range of 5 Å [5]. Poly-(t-butyl acetylene) (TBA), another polymer in

Table II.6   Permeabilities of nitrogen and oxygen in various polymers [5-10]

Polymer	P_{O_2} (Barrer)	P_{N_2} (Barrer)	α_{ideal} (P_{O_2}/P_{N_2})
polytrimethylsilylpropyne	10040.0	6745.0	1.5
polydimethylsiloxane	600.0	280.0	2.2
poly-(t-butyl acetylene)	200.0	118.0	1.7
polymethylpentene	37.2	8.9	4.2
polyvinyltrimethylsilane	36.0	8.0	4.5
polyisoprene	23.7	8.7	2.7
poly(phenylene oxide)	16.8	3.8	4.4
ethyl cellulose	11.2	3.3	3.4
polystyrene	7.5	2.5	2.9
polyethylene	6.6	2.1	3.2
polypropylene	1.6	0.30	5.4
polycarbonate	1.4	0.30	4.7
butyl rubber	1.3	0.30	4.3
polytriazole	1.1	0.13	8.4
cellulose acetate	0.7	0.25	3.0
poly(vinylidene fluoride)	0.24	0.055	4.4
polyamide (nylon 6)	0.093	0.025	2.8
poly(vinyl alcohol)	0.0019	0.00057	3.2
polyimide (Kapton)	0.001	0.00012	8.0

1 Barrer = 10^{-10} cm^3(STP).cm.cm^{-2}.s^{-1}.cmHg^{-1} = 27.4 m^3(STP).m.m^{-2}.h^{-1}.bar^{-1}
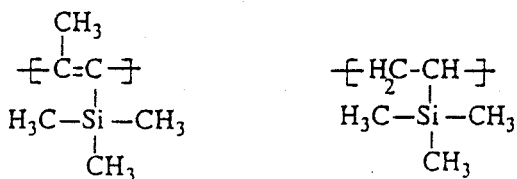
PTMSP   PVTMS

Figure II - 14.   The chemical structures of polytrimethylsilylpropyne (PTMSP) and polyvinyltrimethylsilane (PVTMS).

the polyacetylene group, also exhibits very high permeabilities. The influence of the crystallinity is also apparent in this table. The glass transition temperatures of nylon-6 and cellulose acetate are little different but because of its much higher crystallinity the permeability of nylon-6 is lower. Poly(vinyl alcohol) (PVA) also has a very low permeability because of its high crystallinity. In addition to the permeability, the chemical and thermal stability of polymers and/or membranes are also determined by the same structural factors, i.e. chain flexibility, chain interactions and crystallinity. The chemical stability can be expressed in terms of the hydrolytic stability, solvent resistance, pH resistance and chlorine resistance. So-called 'weak-spots' such as unsaturated groups, -NH groups, ester groups, must be avoided if highly resistant membranes are required.

II.9. Glass transition temperature depression

The glass transition temperature is a very important parameter for polymers since the mechanical and physical properties change drastically over a relatively small temperature interval. The glassy state of a polymer can be considered as a frozen state with a highly restricted chain mobility. However, in the presence of a diluent or penetrant, which is generally the case during membrane transport and membrane formation, depression of the glass transition may occur. This process is similar to the melting point depression. Several relationships have been proposed to described this T_g depression and here we will use the Kelley-Bueche equation which is based on the free volume concept [11]. Here it is assumed that the free volume of polymer and diluent are additionally, then eq. II - 3 becomes

$$v_f = v_{f,T_g} + \Delta\alpha_2 (T - T_{g,2}) \phi_2 + \Delta\alpha_1 (T - T_{g,1}) \phi_1 \qquad (II - 4)$$

in which subscripts 1 and 2 refer to polymer and diluent respectively. ϕ gives the volume fraction and the other parameters are equivalent to the ones given in eq. II - 3. At $T = T_g$ then $v_f = v_{f,T_g}$ and eq. II - 4 becomes

$$T_g = \frac{\Delta\alpha_2 T_{g,2} \phi_2 + \Delta\alpha_1 T_{g,1} \phi_1}{\Delta\alpha_2 \phi_2 + \Delta\alpha_1 \phi_1} \qquad (II - 5)$$

R is the ratio of the difference in thermal expansion coefficients of both components (R $\Delta\alpha_1/\Delta\alpha_2$) then eq. II - 5 becomes

$$T_g = \frac{R T_{g,2} \phi_2 + T_{g,1} \phi_1}{R \phi_2 + \phi_1} \qquad (II - 6)$$

The glass transition temperature of the system can now be determined if the T_g's of both

pure components are known. R is generally assumed to be an empirical constant and often a value has been found between 2 and 3. For ternary systems a similar equation has been derived by Burghardt [12]. Data on polymers are available in literature but information on low molecular weight components is hardly available. A compilation of the Tg of various solvents is given by Fedors [13]. In addition equation II - 7 has been proposed [10] to estimate Tg of the solvent. T_m and T_b are melting point and boiling point of the solvent and the constant γ has been estimated to be 1.15.

$$\gamma = \frac{T_m + T_b}{T_g + T_b}$$

(II - 7)

Table II.7 summarizes the Tg of various organic solvents and then the glass transition temperature of the swollen or plasticised polymer can then be calculated from eq. II - 6 for each polymer-penetrant system if the volume fraction of penetrant is known. The Tg depression is important as well to determine the moment of vitrification in phase inversion processes as will be discussed in chapter III.

Table II.7   Glass transition temperature of various solvents [13]

Polymer	Tg (K)
water	136 - 139
methanol	102 - 110
ethanol	97 - 100
DMAc	150
DMF	129
toluene	115 - 117
methylene chloride	99 - 103
chloroform	106 - 114
acetone	93 - 100

II.10.   Thermal and chemical stability

Ceramics have become of increasing interest as membrane materials because of their outstanding thermal and chemical stability in comparison to polymers. However many separation problems do not require that high temperatures, i.e. generally a temperature below 200°C covers most problems. High resistant polymers can be applied up to a temperature of 400°C and some even to 600°C [14]. The definition of thermal and chemical stability is not exact and a distinguish should be made between i) change or loss of properties which is a reversible process and often referred to as softening and ii)

decomposition or degradation which is an irreversible process. The latter process generally involves cleavage of the covalent bonds in the main chain and/or side chain. On increasing the temperature the physical and chemical properties of polymers change and they finally degrade. The extent of such change depends on the type of polymer with roughly speaking the glass transition temperature T_g being an important parameter for amorphous polymers and the melting point T_m for crystalline polymers. Above these respective temperatures the properties of the polymer change drastically.

In general, the following factors which lead to an increase in the thermal stability also increase the chemical stability: i) those that increase T_g and T_m and ii) those that increase the crystallinity. The principal factor favouring crystallinity is a symmetrical structure with the absence of random side groups. In the case of aromatic ring structures these should be para-substituted. Chain interactions, especially induced by hydrogen bonding, also increase the crystallinity. Atactic polymers (see figure II - 4) are non-crystalline. In contrast, a factor that has a particular influence on T_g increase is a rigid main chain consisting of aromatic and/or heterocyclic groups without any flexible ($-C-C-$)

polybenzimidazole

polyoxadiazole
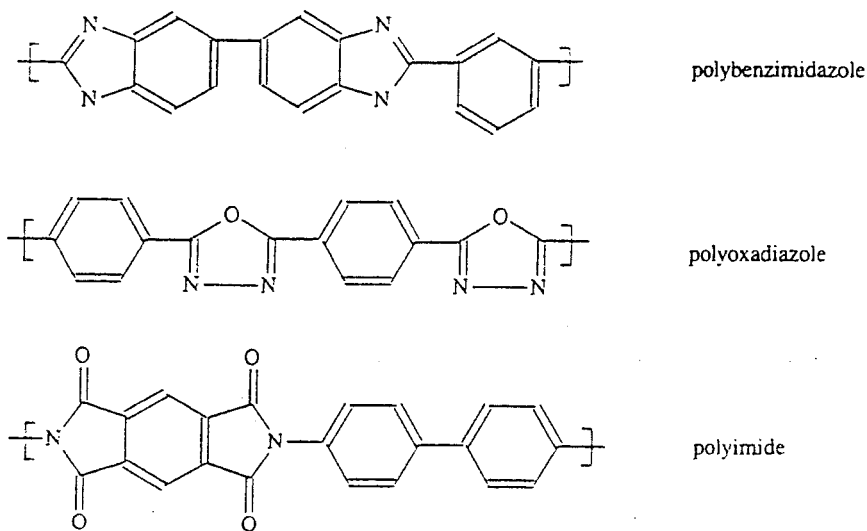
polyimide

Figure II - 15.   Resonance structures in polyimide, polyoxadiazole and polybenzimidazole.

groups. In some cases it is possible for the T_g to be so high that the degradation temperature is lower than the glass transition temperature, as for example in polyphenylene or polyoxadiazole both of which contain only aromatic and heterocyclic groups. Bulky side groups also increase the T_g value because of the reduction of rotational freedom around the main chain. Furthermore, the presence of resonance structures, as in polybenzimidazoles,

polyoxadiazoles and ladder polymers, increases the thermal stability. Figure II - 15 gives some examples of resonance structures found in thermally stable polymers used as membrane materials. As the stability of a polymer increases it generally becomes more difficult to process. The two effects, stability and processability, oppose each other. Thus

Fluoro polymers
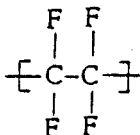
polytetrafluoroethylene

Aromatic polymers
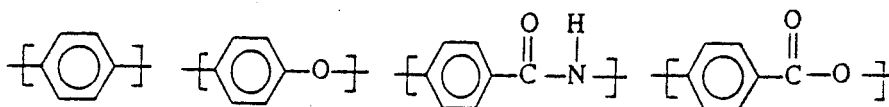
polyphenylene   polyether   polyamide   polyester

Heterocyclic polymers
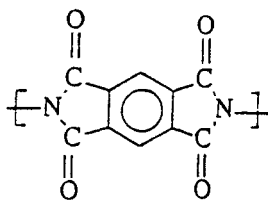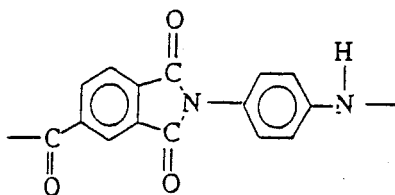
polyimide   polyamideimide

Inorganic polymers
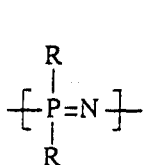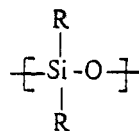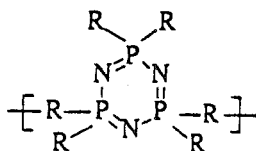
polyphosphasenes   polysiloxanes

Figure II - 16. An overview of a number of thermally and chemically stable polymers.

very stable ladder polymers are not soluble and cannot be processed from the melt as are a number of other thermally stable polymers. In terms of membrane preparation, this means that the polymer must be soluble in a more or less normal solvent (other than concentrated inorganic acids) in order to apply appropriate preparation techniques. An overview of a number of thermally stable polymers is given in figure II - 16.

II.11 . Mechanical properties

Mechanical behaviour involves the deformation of a material under the influence of an applied force. Generally, mechanical properties are not very important in membrane processes because the membrane is held by a supporting material. However, hollow fibers and capillary membranes are self-supporting and in these cases the mechanical properties may become important, especially when high pressures are applied such as in gas separation. For example, when a high pressure (e.g. more than 10 bar) is applied to a capillary of a low tensile modulus material (e.g. silicone rubber), the capillary will break. However, a material with a high tensile modulus (e.g. polyimide) can easily withstand such a pressure and indeed much higher pressures with a proper choice of fiber diameter and wall thickness. The tensile modulus E has already been discussed in section II - 5, but the brittleness (or toughness) is also an important parameter in addition to the modulus. Information on the tensile modulus and on the toughness of a material can be obtained from a stress-strain diagram where the force per unit area (stress) is measured when the material has been deformed at a constant rate.
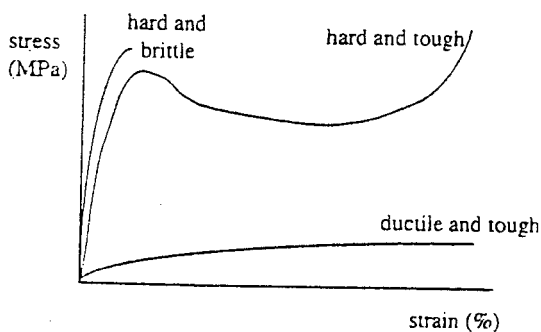
Figure II - 17.   Stress-strain diagrams for different types of polymer.

The tensile modulus E has been obtained from the initial slopes of the stress-strain curves as shown in figure II - 17 and II - 18. A relatively large force has to be applied to obtain a small deformation for a glassy polymer whereas for elastomers a small force is sufficient to obtain a large deformation. At a certain stress the material may break or may show

permanent or plastic deformation. Figure II - 17 gives a schematic drawing of the stress-strain diagrams for various characteristic polymers. If the material breaks under a small deformation (about 1 to 2%) the material is said to be brittle and typical stresses in the order of 50 MPa can be found for a number of glassy polymers. The material is said to be tough when it breaks under a large deformation, as with cellulose esters and polycarbonate, for example. After a linear stress-strain curve an extensive elongation can be observed at a constant stress. This is a plastic flow region of nonlinear viscoelasticity. Elastomers exhibit behaviours which are both ductile and tough. The area under the curves is a measure of the toughness (or brittleness) of a material. Factors which influence the brittleness are molecular weight, crystallinity and intermolecular forces.
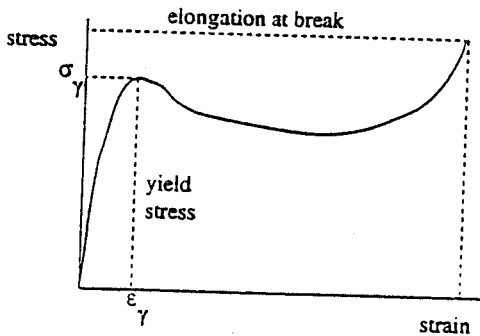
Figure II - 18.   Generalized stress-strain diagram

The tensile modulus or Young's modulus E is given by the initial slope of the stress-strain curve,

$$E = d\sigma/d\varepsilon \text{ at } \varepsilon = 0$$

(II - 8)

in which the strain ε has been defined as $\varepsilon = (L - L_o)/L_o = \Delta L/L_o$ and the stress σ the force F per cross-sectional area. The maximum in the stress-strain curve defines the stress at yield, σ_γ and the elongation at yield ε_γ (yield-stress). It can be seen that when the yield stress has been reached further deformation does not result in a stress increase anymore, in fact it decreases. At this point the material has lost its mechanical properties.

II.12.   Elastomers

Elastomers are a very important class of materials and some well-known elastomers are listed in table II.8, together with their corresponding glass transition temperatures. The chemical structure of some of these are given in figure II - 19. Most of the polymers listed in table II - 8 have an unsaturated —C=C— bond in their main chain adjacent to a saturated

Table II.8   Some elastomers with their corresponding T_g value

polymer	Tg (°C)
polydimethylsiloxane	- 123
polyethylene (HDPE and LDPE)	- 120
polybutadiene	- 85
polyisoprene	- 73
natural rubber	- 72
polyisobutylene	- 70
butyl rubber	- 65
polychloroprene	- 50
polyoxymethylene	- 50
polyvinylidenefluoride	- 40

polydimethylsiloxane (silicone rubber)

polyisobutene (butyl rubber)

polybutadiene

polychloroprene

polyisoprene
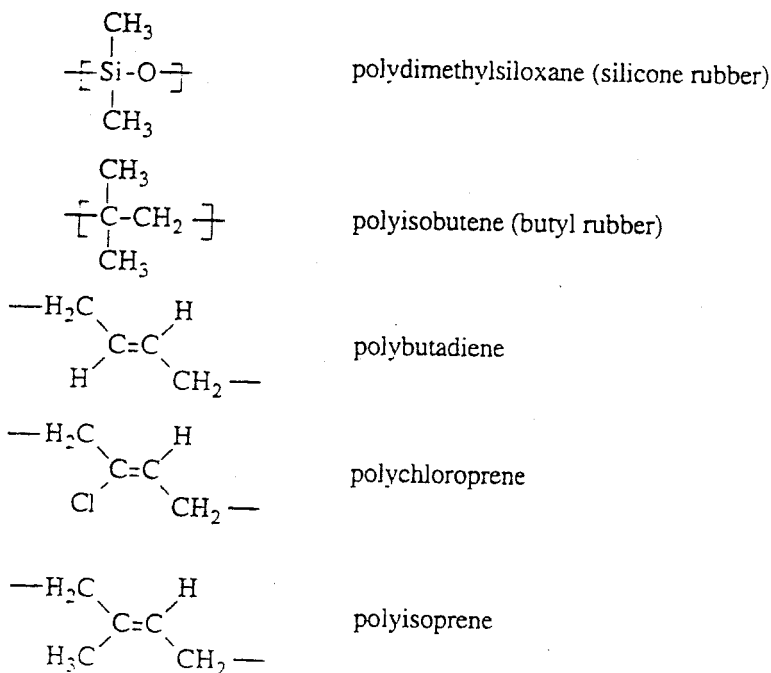
Figure II - 19.   The chemical structures of some elastomers.

—C—C— bond. This results in a decreased flexibility relative to a completely saturated
—C—C— backbone. With copolymers such as styrene-butadiene-rubber (SBR),

acrylonitrile-butadiene-rubber (NBR), ethene-propene-diene-rubber (EPDM), acrylonitrile-butadiene-styrene (ABS), the glass transition temperature depends on the relative content of the corresponding monomers in the polymer. Often two glass transition temperatures are observed dependent on the size of the domains.

II.13.   Thermoplastic elastomers

The thermoplastic elastomers (TPE) are a very special class of materials which are characterised by the fact that the two blocks are not miscible with each other which results in phase separation in which one block constitutes the continuous phase whereas the other block exist as micro-domains within this continuous phase. Often the dispersed phase is a glassy or crystalline polymer and they form the thermo-reversible physical crosslinks. For instance, in polystyrene - block - polybutadiene - block - polystyrene, a triblock copolymer, polybutadiene constitute the soft continuous phase (T_g = - 95°C) with polystyrene as the hard segment (T_g = 95°C). These hard domains act as physical cross-links and heating above the glass transition temperature of this hard block, makes the polymer soft. Other materials are polyurethanes and polyester-polyether block forming a multiblock copolymer of the type - $(AB)_n$ -. The block arrangements in these latter type is shown schematically in figure II - 20.

soft block
flexible
amorphous
low Tg

hard block
rigid
crystalline/glassy
high Tg
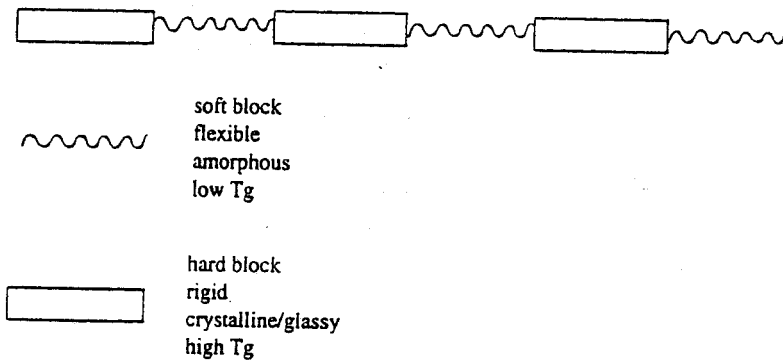
Figure II - 20.   Schematic drawing of a so-called -$(AB)_n$- block copolymer.

The morphology and properties of the TEP are mainly determined by the A/B ratio and the size of the blocks.

II.14.   Polyelectrolytes

Up to this point only neutral polymers have been considered. However, there is a class of

polymer, the polyelectrolytes, which contain ionic groups. Because of the presence of fixed charges strong interactions exist in such polymers and counterions are attracted to the fixed charges. In water or other strongly polar solvents polyelectrolytes are ionised. Such polymers are used mainly as membrane materials in processes where an electrical potential difference is employed as a driving force such as in electrodialysis. They can also be used in other membrane processes such as microfiltration, ultrafiltration, reverse osmosis, diffusion dialysis, gas separation or pervaporation. Polyelectrolytes that contain a fixed negatively charged group are called cation-exchange membranes because they are capable of exchanging positively charged counterions. When the fixed charged group is positive, the membrane (or polymer) can exchange negatively charged anions; such membranes are called anion-exchange membranes. A schematic representation of both types of membrane is given in figure II - 21. The properties of the polyelectrolytes are completely determined by the presence of the ionic groups. Due to a high affinity to water the polymer swells quite strongly in aqueous solutions or even becomes soluble (polyelectrolytes are usually soluble in aqueous solution). To prevent extensive swelling the polymer should therefore be crosslinked. Even very hydrophobic polymers such as polysulfone can be made water-soluble by introducing a large number of sulfonic groups. A very interesting polymer for

cation-exchange   anion-exchange

$$-CH_2-CH-CH_2-CH-\qquad\qquad -CH_2-CH-CH_2-CH-$$
$$\quad\ \ \ |\qquad\qquad |\qquad\qquad\qquad\qquad\quad |\qquad\qquad |$$
$$\quad\ \ \ R^-\,A^+\qquad\ \ R^-\,A^+\qquad\qquad\qquad R^+\,A^-\qquad\ R^+\,A^-$$

$$R=\ \ -SO_3^-\qquad\qquad\qquad\qquad R=\ \ -NR_3^+$$
$$\qquad\ \ -COO^-$$
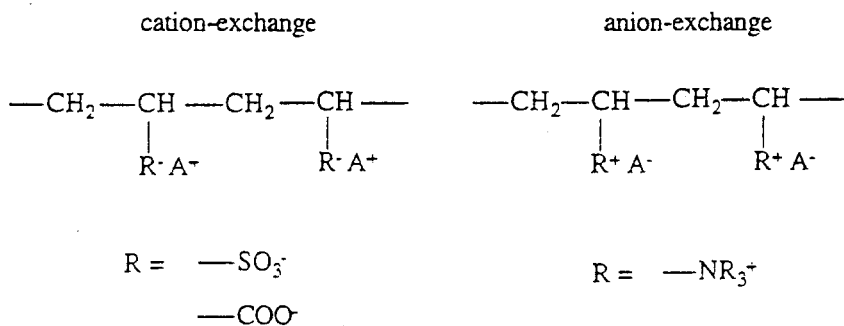
Figure II - 21.   Schematic representation of ion-exchange membranes.

preparing ionic membranes is polytetrafluoroethylene. This polymer is very stable with respect to chemicals, pH and temperature. Ionic groups can be introduced into this polymer to yield a very stable polyelectrolyte based on a teflon matrix. One such polymer obtained on this basis is Nafion (see figure II - 22). Other ion-exchange membranes are also depicted in this figure. A schematic drawing of an ion exchange polymer, in this case a anion exchange polymer, is shown in figure II - 23. The negative charges (negative charged ions) have been fixed to the polymeric chains. The positively charged cations, the counter ions, can move freely within in the limits of the Coulomb forces and electro-neutralitality. Due to the fixed negative charge there will be an excess of positive charge at the interface and a so- called electrical double layer is formed (see chapter IV).

$$\begin{array}{c} -\!\!\!\left[CF_2-CF_2\right]\!CF_2-CF- \\ \left[O-CF_2-CF\right]\!O-CF_2-SO_3^-Na^+ \\ CF_3 \end{array}$$

Nafion®

$$-\!\!\!\left[\begin{array}{cc} CH-CH_2 & CH-CH_2 \\ SO_3^-Na^+ & SO_3^-Na^+ \end{array}\right]\!\!-$$

sulfonated polyethylene

$$-\!\!\!\left[O-\bigcirc-\overset{\overset{\displaystyle CH_3}{|}}{\underset{\underset{\displaystyle CH_3}{|}}{C}}-\bigcirc-O-\bigcirc-SO_2-\bigcirc\right]\!\!-$$
$$SO_3^-Na^+$$

sulfonated polysulfone
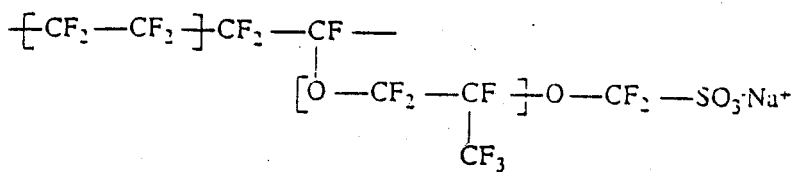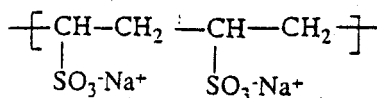
Figure II - 22. The chemical structures of Nafion, sulfonated polyethylene, sulfonated polysulfone.

The specific properties of the charged membranes and charged particles will be further discussed in chapters IV, V, and VI.

II.15.   Polymer blends

Homopolymers consist of only one type of repeating unit whereas copolymers are composed of two (or more) different monomers which after polymerisation give either a random distribution or block- or graft structures. It is also possible to mix two different (homo- or co-) polymers with each other on a molecular level although only a few such polymers are really miscible. As will be discussed in chapter III, two components are miscible if this causes a decrease in free enthalpy. In the case of two polymers the entropy of mixing is very small and hence a negative (exothermic) heat of mixing is necessary to ensure compatibility. Specific interactions, such as hydrogen bonding, are often necessary. When the two polymers are miscible on a molecular level the material is said to be a homogeneous blend, in contrast to a heterogeneous blend, where one polymer is dispersed in another. In this latter system, the polymers are not in fact compatible. The properties of a
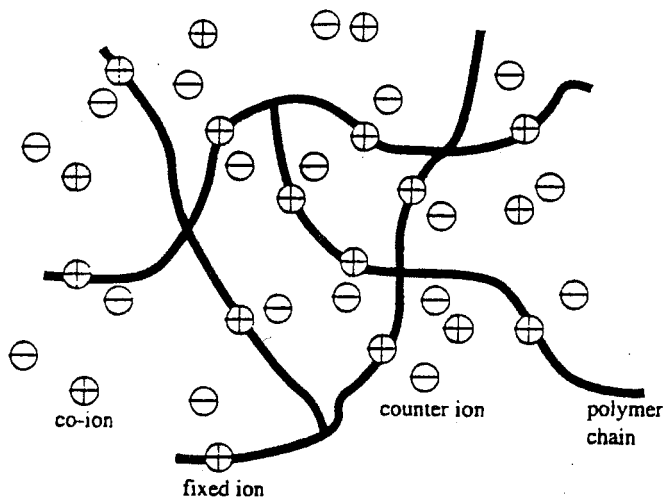
Figure II - 23.   Schematic drawing of an anion exchange membrane

homogeneous blend differ substantially from those of a heterogeneous blend. The properties of the individual polymers disappear in a homogeneous blend and often the properties of the blend lie between those of the two polymers. Thus such a blend has one glass transition temperature which indicates that it is homogeneous. The properties of both materials are still present in a heterogeneous blend and two glass transition temperatures can be observed. Figure II - 24 shows a schematic drawing of a Differential Scanning Calorimeter plot of a heterogeneous blend exhibiting two glass transition temperatures and a homogeneous blend with one glass transition temperature. In chapter III the preparation of membranes by a phase inversion technique using three components, a solvent, a nonsolvent and a polymer, will be discussed. In practice, a number of additives of both high and low molecular weight are used in membrane formation. These additives are used to give the membrane the desired properties with respect to performance and macrostructure. High molecular weight additives such as poly(vinyl pyrrolidone) are frequently used. This polymer is water soluble and compatible with a large number of membrane-forming polymers e.g. poly(ether imide), poly(ether sulfone), and polyimide. Table II.9 lists the glass transition temperatures of these polymers and of their blends with poly(vinyl pyrrolidone). Besides the polymers mentioned here there is a large number of other polymers which are compatible with each other [16].
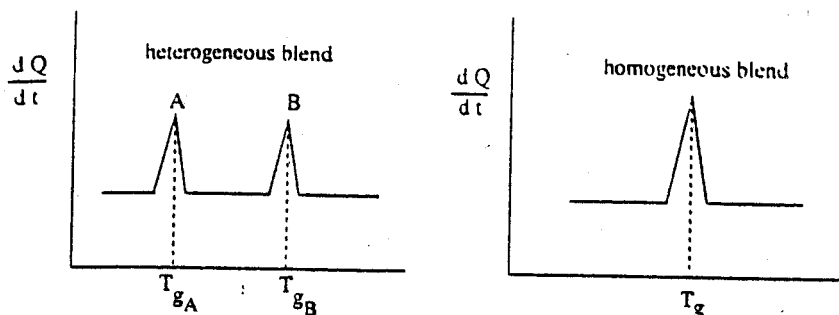
Figure II - 24. A DSC-plot (first derivative) exhibiting two T_g values in the case of a heterogeneous blend (left) and one T_g for a homogeneous blend (right).

Table II.9 Glass transition temperatures of some homopolymers and blends with PVP 360,000 (containing 25% PVP) [15]

Polymer	Tg (°C)	Blend	Tg(°C)
PEI	217	PEI/PVP	215
PES	225	PES/PVP	201
PI	321	PI/PVP	317
PVP 360,000	177		

II.16. Membrane polymers

So far quite a number of polymers have been mentioned and the structural parameters determining the physical state of the polymer have also been described. Basically, all polymers can be used as barrier or membrane material but the chemical and physical properties differ so much that only a limited number will be used in practice. It is beyond the scope of this book to describe the properties of all polymers in detail (the reader is referred to a number of good handbooks in this field); only some important polymers or classes of polymer related to membrane applications will be considered [17 - 19].

A classification will be made between the open porous membranes, which are applied in microfiltration and ultrafiltration and the dense nonporous membranes, applied in gas separation and pervaporation. The reason for this classification is the different

requirements when the polymeric materials are used as membranes. For the porous microfiltration/ultrafiltration membranes the choice of the material is mainly determined by the processing requirements (membrane manufacture), fouling tendency and chemical and thermal stability of the membrane. For the second class of polymers which are used for gas separation/pervaporation, the choice of the material directly determines the membrane performance (selectivity and flux).

II.16.1   Porous membranes

Porous membranes contain fixed pores, in the range of 0.1 - 10 μm for microfiltration and 2 - 100 nm for ultrafiltration. The selectivity is mainly determined by the dimensions of the pores but the choice of the material affects phenomena such as adsorption and chemical stability under condition of actual application and membrane cleaning. This implies that the requirements for the polymeric material are not primarily determined by the flux and selectivity but also by the chemical and thermal properties of the material. The main problem in ultrafiltration/microfiltration is flux decline because of concentration polarisation and fouling (see chapter VII). Therefore the choice of the material is primarily based on preventing fouling and how to clean the membranes after fouling. Also, in the case of applications in non-aqueous mixtures or at high temperatures, chemical and thermal resistance of the polymeric material are the most important factors.

As will be described in chapter III, quite a number of techniques exist for preparing microfiltration membranes, i.e. sintering, stretching, track-etching and phase inversion. These techniques are not generally used to prepare ultrafiltration membranes, because the pore sizes obtained are only in

Table II.10   Polymers for microfiltration membranes

polycarbonate
poly(vinylidene-fluoride)
polytetrafluoroethyiene
polypropylene
polyamide
cellulose-esters
polysulfone
poly(ether-imide)
poiyetheretherketone

the microfiltration range, except for the case of phase inversion. Hence, polymers for microfiltration membranes are not 'a priori' the same as those used for ultrafiltration

membranes. Table II.10 lists polymers which are frequently used for microfiltration membranes.

A special type of microfiltration membrane may be prepared by track-etching various polymeric films (see chapter III). Polycarbonate is often used for this purpose because of its outstanding mechanical properties (see figure II - 25).
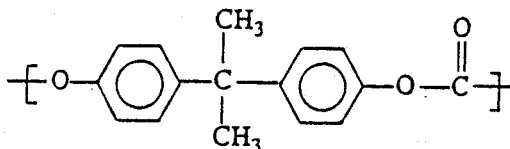
Figure II - 25. The chemical structure of polycarbonate.

Hydrophobic materials such as polytetrafluoroethylene (PTFE), poly(vinylidene fluoride) (PVDF) and isotactic polypropylene (PP) (see figure II - 26) are often used for microfiltration membranes. PTFE is highly crystalline and exhibits excellent thermal stability. It is not soluble in any common solvent and hence also shows high chemical resistance. Poly(vinylidene fluoride) (PVDF) also shows good thermal and chemical resistance although not quite as good as PTFE. PVDF is soluble in aprotic solvents such as dimethylformamide (DMF), dimethylacetamide (DMAc) and in triethylphosphate (TEP). Microfiltration membranes from PTFE may be prepared by sintering and stretching (see chapter III) whereas PVDF membranes are made by phase inversion.

Polypropylene (PP) is also an excellent solvent resistant polymer when it is in the isotactic configuration. This isotactic configuration is highly crystalline in contrast to the atactic form which is amorphous. Polypropylene

polytetrafluoroethylene   polyvinylidenefluoride   polypropylene
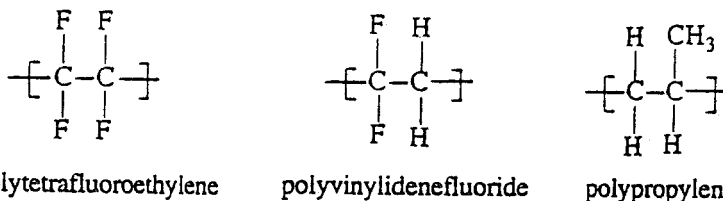
Figure II - 26.   Some hydrophobic polymers used as membrane material for microfiltration.

membranes may be prepared by stretching and phase inversion (see chapter III). Indeed, the three polymers PTFE, PVDF and PP have some properties which are similar. They all

xhibit good to excellent chemical and thermal stability. Because of their hydrophobic
atures, water cannot wet these membranes spontaneously, i.e. when used in aqueous
iixtures they have to be pre-wetted (e.g. by the use of ethanol). Furthermore they can be
sed in membrane distillation, simply because they are not wetted by water or other
quids with a high surface tension (see chapter VI - 5).

Despite the excellent chemical and thermal stability of these hydrophobic
olymers, stable hydrophilic polymers are more interesting as membrane materials
ecause of their reduced adsorption tendencies. The adsorption of solutes has a negative
ifluence on the flux because the adsorbed layer presents an extra resistance towards mass
ransfer and consequently contributes to a decline in flux (see chapter VII). In addition,
dsorption layers are difficult to remove by cleaning methods. A number of hydrophilic
olymers exist capable of being used as membrane materials. The best known class of
uch polymer is cellulose and its derivatives such as cellulose esters. These include
ellulose acetate, cellulose triacetate, cellulose tripropionate, ethyl cellulose, cellulose
trate and mixed esters such as cellulose acetate-butyrate. Not only are cellulose and its
erivatives used in microfiltration and ultrafiltration but also in reverse osmosis, gas
eparation and dialysis. They provide a very important class of basic materials for
embranes.

Cellulose is a polysaccharide that can be obtained from plants. Its molecular weight
aries from 500,000 to 1,500,000 implying that the number of segments is roughly
etween 3000 and 9000. The glucose segment contains three hydroxyl groups which are
ry susceptible towards chemical reaction, forming esters (cellulose acetate and cellulose
trate) and ethers (ethyl cellulose). The glucose repeating units in cellulose are connected
b-1,4-glucosidic linkages (see figure II - 27). Because of its regular linear chain
ructure, cellulose is quite crystalline, and although the polymer is very hydrophilic it is
ot water-soluble. This is because of the crystallinity and intermolecular hydrogen
nding between the hydroxyl groups.
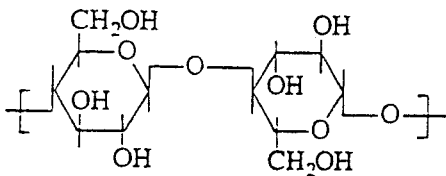
ure II - 27. The chemical structure of cellulose.

lulose (or regenerated cellulose) is mainly used as a material for dialysis membranes.
lulose derivatives such as cellulose nitrate and cellulose acetate are used for
rofiltration/ultrafiltration applications, whereas cellulose triacetate exhibit good

properties as a reverse osmosis membrane in desalination applications.

Despite their outstanding membrane properties, cellulose esters are very sensitive to thermal, chemical and biological degradation. To avoid such degradation, the pH must be maintained between 4 and 6.5 at ambient temperature. In alkaline conditions hydrolysis occurs very rapidly. In addition, the polymer is also very sensitive to biological degradation.

Another class of membrane polymers are the polyamides. These polymers are characterised by the amide group (—CO — NH —). Although aliphatic polyamides comprise a very large class of polymers, the aromatic polyamides are to be preferred as membrane materials because of their outstanding mechanical, thermal, chemical and hydrolytic stability, as well as their permselective properties, particularly in reverse osmosis. However, the aliphatic polyamides also show good chemical stability and may be used in microfiltration/ultrafiltration applications.

$$\left[N\!-\!(CH_2)_5\!-\!C \right]$$

Nylon-6

$$\left[N\!-\!\bigcirc\!-\!N\!-\!C\!-\!\bigcirc\!-\!C \right]$$
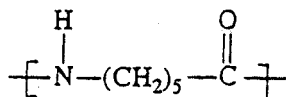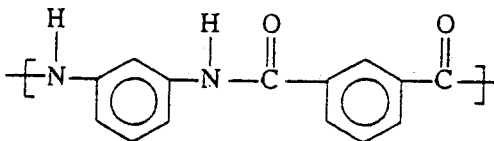
poly(m-phenylene isophtalamide) (Nomex)

Figure II - 28.   The chemical structure of an aliphatic polyamide (Nylon-6) and and aromatic polyamide (Nomex).

The properties of the aromatic polyamides are determined by the aromatic groups in the main chain which considerably reduce the chain flexibility. As a result, aromatic polyamides have glass transition temperatures of 280°C and higher, compared to values of less than 100°C for the aliphatic polyamides. Table II.11 lists some properties of an aliphatic polyamide (nylon-6) and an aromatic polyamide (Nomex); their chemical structures are depicted in figure II - 28. The aromatic polyamide contains meta-substituted rings. However, the chemical and thermal stability can be increased further through the use of a para-substituted ring. Under these circumstances the crystallinity also increases. These para-substituted polybenzamides (Kevlar® and Twaron®) can be produced as so-

called super-fibers because of their very high tensile strength, obtained after chain orientation in the fiber direction. However, as membrane materials these polymers are of little interest. Aliphatic polyamides such as nylon-6, nylon 6-6 and recently nylon 4-6, are of greater interest as microfiltration membranes.

Table II.11   Some properties of Nylon-6 and Nomex [4,20]

polyamide	T_g (°C)	T_m (°C)	water sorption (%)
Nylon-6	50	215	10.5
Nomex	273	380	17.0

Ultrafiltration membranes are also porous, and it is therefore surprising at first sight that polymeric materials of a different type are used to that employed in microfiltration. A number of microfiltration membranes are prepared by techniques such as sintering, track-etching and stretching which lead to pores with a minimum size of about 0.05 - 0.1 µm. Smaller pores, i.e.

Table II.12   Polymers for ultrafiltration membranes

polysulfone/poly(ether sulfone)
polyacrylonitrile
cellulose esters
polyimide/poly(ether imide)
polyamide (aliphatic)
poly(vinylidene fluoride)
polyetheretherketone

ultrafiltration membranes with pores in the nanometer range, cannot be prepared with these techniques. Most ultrafiltration membranes are prepared by phase inversion (for a detailed description see chapter III). Table II.12 gives a list of polymers frequently used as materials for ultrafiltration
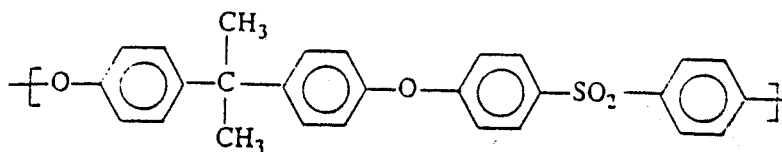
Polysulfone (PSf)
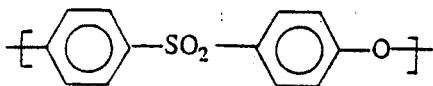
Polyethersulfone (PES)

Figure II - 29. The chemical structures of polysulfone (PSf) and poly(ether sulfone) (PES)

membranes. A very important class of polymers are the polysulfones (PSf) and poly(ether sulfones) (PES) (see figure II - 29).
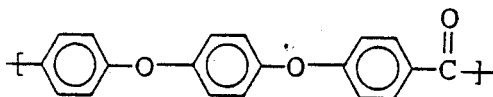
Polyetheretherketone (PEEK)
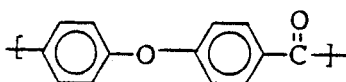
Polyetherketone (PEK)

Figure II - 30. The chemical structure of polyetheretherketone (PEEK) and polyetherketone (PEK).

The chemical structure of two of the polymers from this class are given below. The polysulfones possess very good chemical and thermal stability as indicated by their T_g values (PSf: T_g =190°C; PES: T_g = 230°C). These polymers are widely used as basic materials for ultrafiltration membranes and as support materials for composite membranes. Polyetherketones is a new group of chemically and thermally resistant

polymers. Due to their chemical resistancy they are difficult to process and e.g. polyetheretherketone (PEEK) is only soluble   at room temperature in concentrated inorganic acids such as sulfuric acid or chlorosulfonic acid. The chemical structure is given in figure II - 30. Polyimides are a group of polymers with an excellent thermal stability combined with good chemical stability. The chemical structure of two types of this class of polymer are given in figure II - 31.

polyimide (PI)
(Kapton)

polyetherimide (PEI)
(Ultem)
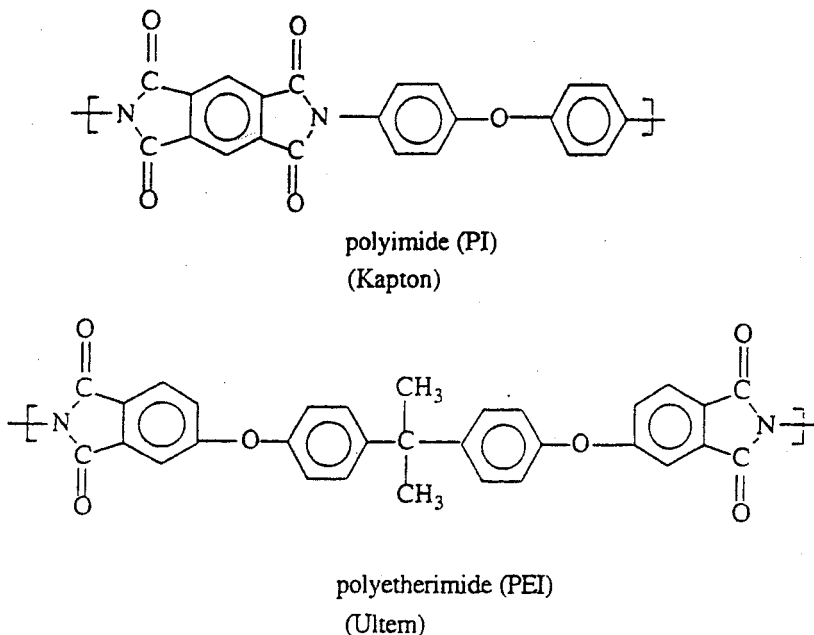
Figure II - 31.   The chemical structure of a polyimide (PI) and a poly(ether imide) (PEI).

Polyacrylonitrile (PAN) is a polymer which is commonly used for ultrafiltration membranes (see table II.2). Despite the nitrile group being a very strongly polar group, the polymer is not very hydrophilic. A comonomer (e.g. vinyl acetate or methylmethacrylate) is often added to increase chain flexibility and hydrophilicity and to improve processability.

II .16.2   Nonporous membranes
Nonporous membranes are used in gas and vapour separation and pervaporation. For these processes either composite or asymmetric membranes are used. In this type of membrane the performance (permeability and selectivity) is determined by the intrinsic

properties of the material. The choice of material is determined by the type of application, and the polymer type can range from an elastomer to a glassy material.
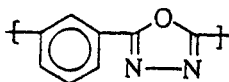
poly(m-phenylene)-1,3,4-oxadiazole
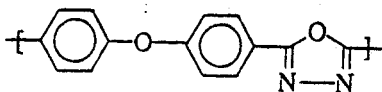
poly(4,4'-diphenylether)-1,3,4-oxadiazole
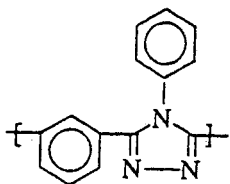
poly(m-phenylene)-1,2,4-triazole

Figure II - 32.   Chemical structure of some polyoxadiazoles and a polytriazole

Various tabulations of some of the more important materials employed in relation to their application can be found in chapters V and VI. In gas separation frequently glassy polymers are used with a high T_g showing high selectvities. An example is the class of polyoxadiazoles and polytriazoles. These polymers show an extremely high thermal stability, e.g. polyoxadiazole has a glass transition temperatures above the degradation temperature. Figure II - 32 shows the chemical structure of three polymers out of this class and it can be observed that these polymers combine a heterocyclic moiety with an aromatic one. Due to their high stability they are difficult to process and introduction of a pendant group as for instance in polytriazole does increase the solubility properties.

II.17.   Inorganic membranes

Inorganic materials generally possess superior chemical and thermal stability relative to polymeric materials. Nevertheless their use as membrane material has been limited

although a growing interest can now be observed. The only application in the past was the enrichment of uranium hexafluoride (^{235}U) by Knudsen flow through porous ceramic membranes. Nowadays all kind of applications are found in the field of microfiltration and ultrafiltration.

Four different types of inorganic materials frequently used may be distinguished: ceramic membranes; glass membranes; and metallic membranes (including carbon) and zeolitic membranes.

Metallic membranes, mainly obtained via the sintering of metal powders (e.g. stainless steel, tungsten or molybdenum), have only received limited attention to date.

Ceramics are formed by the combination of a metal (e.g. aluminium, titanium, silicium or zirconium) with a non-metal in the form of an oxide, nitride, or carbide. Ceramic membranes prepared from such materials form the main class of inorganic membranes, with aluminium oxide or alumina (γ-Al_2O_3) and zirconium oxide or zirconia (ZrO_2) as the most important representatives. These membranes are usually prepared by sintering or by sol-gel processes. Glass can be considered as well as a ceramic material. Glass membranes (silicon oxide or silica, SiO_2) are mainly prepared by techniques involving leaching on demixed glasses. These preparation techniques will be described briefly in chapter III. Recently, a new class of materials are studied and developed, the zeolite membranes. These materials have very narrow pore sizes and can be applied in gas separation and pervaporation. Only ceramics will be considered here and the following material properties are discussed briefly:
-   thermal stability
-   chemical stability
-   mechanical stability

II .17.1   Thermal stability

Thermally stable polymers were discussed in section II - 10. These polymers can be applied over temperatures ranging from 100 - 300 °C. The very specific properties of the ceramics originate from their electronic behaviour. The valence electrons of the metal part are retained by the nonmetal atoms resulting in a highly stable bond and consequently

Table   II.13   Melting points of ceramics [21]

ceramics		melting point (°C)
Alumina	Al_2O_3	2050
Zirconia	ZrO_2	2770
Titania	TiO_2	1605
Silicon carbide	SiC	2500

these materials are highly thermally and chemically resistant. The melting points are very high and can reach values above 4000 °C. Some melting points are given in table II.13. The high temperature resistant make these materials very attractive for gas separation at high temperatures, especially in combination with a chemical reaction where the membrane is used as catalyst as well as a selective barrier to remove one of the components which has been formed. The application in membrane reactors, the combination of a membrane separation process and a chemical reaction will be further discussed in chapter VI.

II .17.2   Chemical stability

The chemical stability of existing polymeric membrane materials is limited with respect to pH and organic liquids. The chemical stability of inorganic materials is superior and they can generally be applied at any pH and in any organic solvent. Thus, in the field of ultrafiltration and microfiltration the number of applications can be expected to increase, especially in harsh environments. Another important factor is the ease of cleaning, especially in high fouling applications involving ultrafiltration and microfiltration. Fouling leads to a drastic decrease of flux through the membranes and periodic cleaning is necessary. For inorganic membranes all kinds of cleaning agents can be used, allowing strong acid and alkali treatment. Another point to consider is that the lifetime of inorganic membranes is greater than that of organic polymeric membranes.

II .17.3   Mechanical stability

Mechanical stability is not a very high priority in membrane separations and only in some applications, for instance those involving high pressures or self-supporting materials, this parameter must be considered. Ceramics are characterized as hard and brittle materials with a high E-modulus. Figure II - 33 gives the stress-strain curve of alumina and of polymethylmethacrylate, indicating clearly the difference in mechanical behaviour between the two materials.
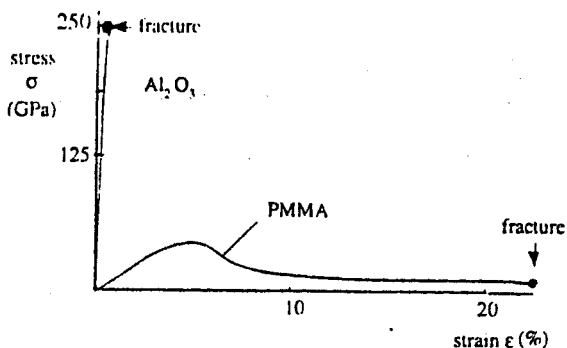
Figure   II - 33.   Stress - strain curve of polymethylmethacrylate (PMMA) (T_g = 110 °C) and of
alumina (Al_2O_3) [22].

II.18.   Biological membranes

The structure and functionality of a biological membrane (in this context the plasma or cell
membrane) differs fundamentally from that of a synthetic membrane. A short introduction
into the field of biological membranes will be given here in order to first illustrate the
considerable difference between these two classes of membrane and secondly because
interest in so-called synthetic biological membranes is growing rapidly. For those who
are more interested in this field, a number of excellent books and articles may be
consulted [see e.g. ref. 23].

Biological membranes or cell membranes have very complex structures because
they must be able to accomplish specific functions. However, a characteristic of various
cell membranes is that they contain a basic lipid bilayer structure. Each lipid molecule
possess a hydrophobic and a hydrophilic part. A schematic drawing of such a lipid bilayer
is given in figure II - 34. This structure exists in different types of cell membrane. the
polar part being situated at the water/membrane interface with the hydrophobic part being
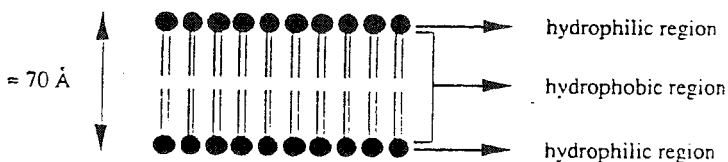
Figure II - 34.   Schematic drawing of a lipid bilayer.

located in between. One of the most common class of lipids are the phospholipids whose basic chemical structure is given in figure II - 35. Two hydroxyl groups of glycerol are attached to two long fatty acid chains. These long fatty acid chains, generally consisting of 16 to 21 carbon atoms, form the hydrophobic part of the lipid molecule. The fatty acid can be completely saturated, as for instance in palmitic acid (see figure II - 35), but it can also contain one or more double bond. The phosphate group is attached to the third hydroxyl group of glycerol. Another polar group, often a quaternary ammonium salt, as for instance in choline, is attached to this phosphate group.

These lipid bilayers are not very permeable towards a variety of molecules. Nevertheless, for cell metabolism and growth to occur, molecules such as sugars and amino acids must enter the cell. Specific transport of this type is accomplished by proteins which are incorporated within the bilayer membrane. The protein serves as a carrier and the type of transport can be defined as carrier-mediated transport. The cell membrane consists of two main components: the lipid bilayer which is the backbone, whereas the proteins take care of the specific transport functions. Some of the proteins are located on the outside of the lipid bilayer (the extrinsic proteins), whereas other proteins (the intrinsic proteins), completely penetrate through the lipid bilayer. The intrinsic proteins especially

phospholipid

— R_1 R_2 : fatty acid

— R_3 : polar group (serine, ethanolamine)
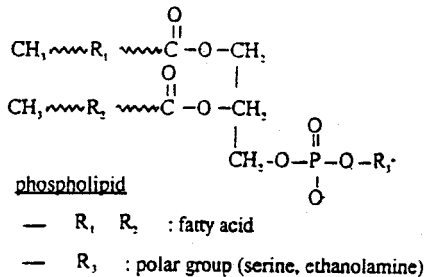
Example of a phospholipid : dipalmitoylphosphatidylcholine
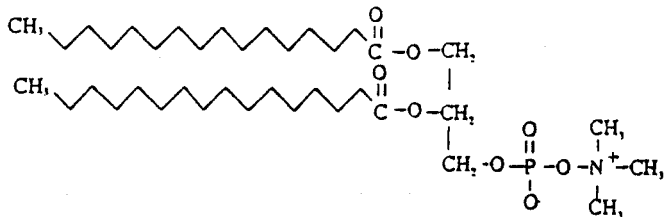
Figure II - 35.   General chemical structure of a phospholipid (upper drawing) and an example of a very common type of phospholipid, dipalmitoylphosphatidylcholine (lecithine).

have an important role in transport functions. Two types of carrier-mediated transport can occur: active and passive transport. In passive transport, permeation of a solute occurs because of a concentration gradient across the membrane. Normally the lipid bilayer is impermeable towards most solutes, but the presence of a specific protein allows the transport of a specific solute by means of a special carrier-mediated transport system. Although transport occurs because of an activity gradient, it cannot be considered as simple diffusion because of the complex function of the carrier. Furthermore, this kind of transport exhibits a kind of saturation kinetics (comparable to Michaelis-Menten kinetics for enzymatic reactions, see e.g. [24]) which means that the transport rate decreases as the concentration increases. This exerts a kind of control mechanism within the cell.

Another characteristic feature of transport is that the carrier can be very specific. For example, the carrier in the membrane of the red blood cell (erythrocyte) that controls the transport of glucose does not allow the passage of fructose.

Three different types of passive carrier-mediated transport mechanism may be distinguished similar to transport in liquid membranes (see chapter VI):
i) facilitated diffusion; ii) co-transport; and iii) counter-transport.
A schematic drawing of these three types of transport is given in figure II - 36. The simplest type of carrier-mediated transport is 'diffusion' or 'facilitated diffusion', because the protein carrier allows the solute to diffuse through the membrane.
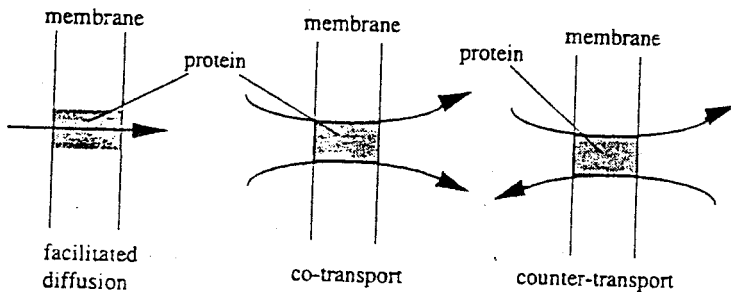
Figure II - 36.   Schematic drawing of three different types of passive carrier-mediated transport.

Transport occurs because of the activity gradient or concentration gradient and proceeds from the high concentration side to the low concentration side.

The second type of carrier-mediated transport is 'cotransport'. Here a solute A is transported through the membrane together with a solute B. Both solutes are located on the same side of the membrane and the driving force is the concentration gradient of one of the solutes, for example of B. This means that solute A can be transported even against its own concentration gradient.

The third type of carrier-mediated transport is 'counter transport'. Here two solutes are transported in opposite directions. The driving force in this process is the concentration gradient of one of the solutes, hence the second solute may be transported against its own concentration gradient.
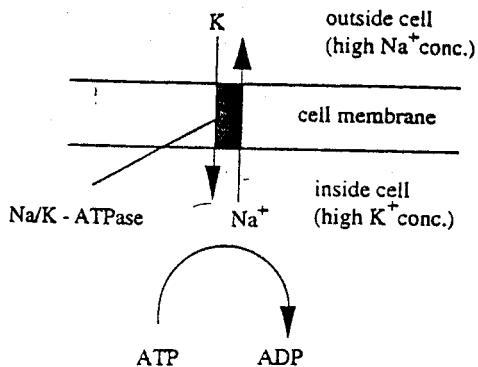
Figure II - 37.   Schematic representation of Na/K transport.

In active facilitated transport, the solute can permeate against its concentration gradient, i.e. from a low concentration to a high concentration, by using cellular energy. This energy is mostly obtained from the hydrolysis of adenosine triphosphate (ATP) to adenosine diphosphate (ADP). An example of active transport is the sodium-potassium pump across the cell membrane. The potassium concentration is high within a cell and the sodium concentration low, whereas outside the cell in the tissues the reverse is the case, i.e. a high sodium concentration and a low potassium concentration. Energy is necessary to maintain the desired Na and K concentrations. One ATP molecule allows two potassium ions to enter the cell whereas three sodium ions are pumped outside the cell. A schematic drawing is given in figure II - 37. Although a number of transport mechanisms have been discussed briefly above, they are generally quite complex and much can be learned from these systems with respect to liquid membranes. The 'more simple' transport mechanisms of liquid membranes will be discussed in greater detail in chapter VI.

liposome (MLV)

vesicle (ULV)

lipid bilayer
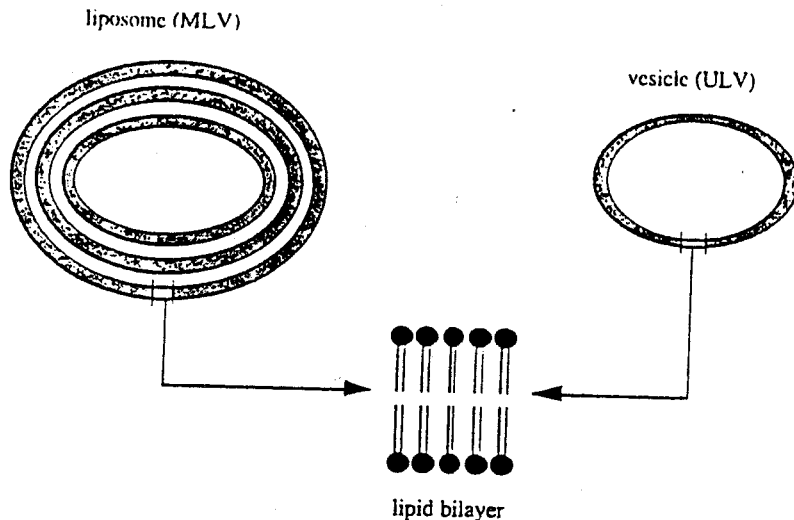
Figure II · 38.   Schematic representation of a multilamellar vesicle (MLV) or liposome   and an unilamellar vesicle (ULV).

II .18.1   Synthetic biological membranes

Because of the heterogeneity of cell membranes, their specific functions are very difficult to study directly. However, from one component, i.e. the lipids, it is possible to construct model systems which can be related to the biological membranes.

When lipids are brought into contact with an electrolyte solution, multilamellar vesicles (MLV) or liposomes are formed spontaneously. These liposomes are spherical aggregates of concentric lipid bilayers. By sonication, these multilamellar vesicles can be transformed into unilamellar vesicles (ULV) which contains one lipid bilayer (see figure II - 38). The stability of these vesicles can be further improved by means of polymerisation. If double bonds are present, this can be achieved either in the hydrophobic part or in the polar head. Polymerisation can be accomplished by UV-radiation or by adding free-radical initiators such as azobisisobutyronitrile (AIBN). Other types of polymerisation reactions are also possible, for instance by a condensation reaction. A schematic representation of such double bond crosslinking is shown in figure II - 39. The increased stability of polymerised vesicles relative to unpolymerised ones can be demonstrated by means of surfactants, for example sodium dodecylsulphate. These surfactants destroy the spherical unpolymerised vesicles while the polymerised vesicles remain intact. The polymerised and unpolymerised liposomes and vesicles can be used as drug delivery systems because of their very good biocompatibility. All kinds of materials

can be encapsulated such as enzymes and adsorbents, for example.
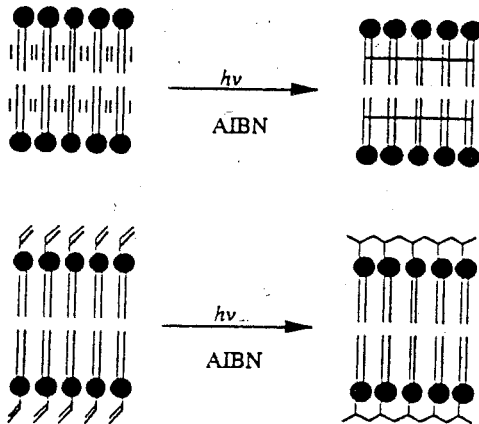
Figure II - 39. Polymerisation of vesicles by means of UV-radiation or AIBN.

II.19.   Solved problems

1. The glass transition temperature of polystyrene is 100°C at 1 bar. What is the glass temperature at 100 bar (the difference in thermal expansion coefficient at Tg is $\Delta\alpha = 4.8 \ 10^{-4} \ K^{-1}$ and the difference in isobaric compressibility is $\Delta\kappa = 3.3 \ 10^{-5} \ bar^{-1}$) ?

II.20.   Unsolved problems

1a. Poly(methyl acrylate) and poly(methyl methacrylate) are similar polymers. Draw the chemical structures and explain which of the two polymers will have the higher glass transition temperature ?
A number of poly(alkyl methacrylates) are available. Explain how the glass transition temperature will change with increasing alkyl chain length?

2. Polyetherketone (PEK) and poly(ether etherketone) (PEEK) are two engineering polymers which are highly chemical resistant.
Which of the two has a higher glass transition temperature T_g, PEK or PEEK ? Why do you think that these materials are highly chemical resistant ?
PEEK has a T_g ; 144°C and a T_m ; 335°C, respectively. How does the mechanical

behaviour (e.g. the E-modulus) change between 25 to 335°C ? Draw a stress-strain curve of PEEK at 35°C .

3. The chemical structure of the polymer main chain is very important for the properties of a polymer. Set the following polymers in a sequence with increasing T_g.

$$— CH_2—CH_2—$$

$$—\langle O \rangle—CH_2—CH_2—$$

$$—\langle O \rangle—O—$$

$$—CH_2—CH_2—O—$$

$$—\langle O \rangle—O—\langle O \rangle—SO_2$$

$$—CH_2—CH=CH—CH_2—$$

$$
\begin{array}{c}
CH_3 \\
| \\
—Si—O— \\
| \\
CH_3
\end{array}
$$
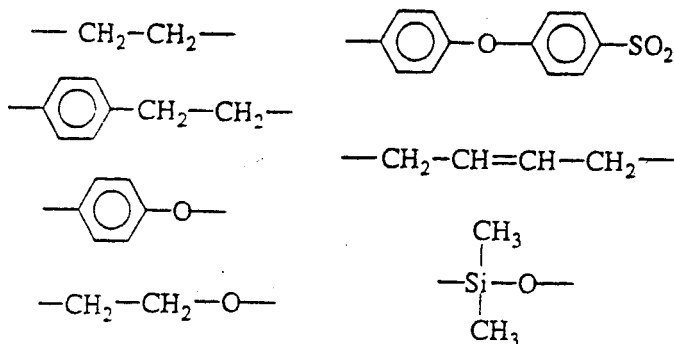
4. Give qualitatively the difference in various physical properties of high density polyethylene (HDPE) versus low density polyethylene (LDPE): glass transition temperature, melt temperature, E-modulus at 25°C, helium permeability, water vapour permeability.

5.
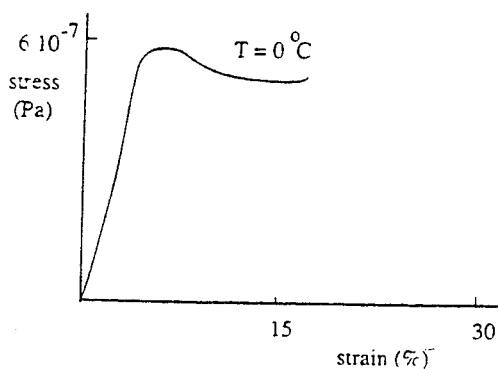
The stress-strain curve of cellulose acetate at 0°C is shown above. Draw the curves at 25°C and 60°C.

6. EVA (ethylene vinyl acetate) is a copolymer which is available in various compositions of ethylene and vinyl acetate. At a content of 50% vinyl acetate or more the crystallinity has been vanished completely. Give qualitatively the nitrogen permeability at room temperature for a copolymer with 10%, 50% and 90% vinyl acetate respectively and indicate the character of the polymer in terms of rubbery and glassy, crystalline and amorphous (The glass transition temperatures of the pure polymers polyethylene and polyvinyl acetate are given in table II - 5).

7. A polymer P is made up of two monodisperse fractions; fraction A with molecular weight of 1000 g/mole and fraction B with a molecular weight of 100,000 g/mole. The batch contains an equal mole fraction of each fraction. Calculate the number average and the weight average of polymer P.

8. At 35°C, the permeability of helium in silicone rubber is 561 Barrer and in polycarbonate 14 Barrer, respectively. The ratio of permeabilities of helium over methane (P_{He}/P_{CH4}) is 0.41 in silicone rubber and 50 in polycarbonate. Explain these values.

9a. Draw the chemical structure of the block copolymer of poly(butylene terephtalate) and polyethylene oxide.
 b. Indicate which is the rigid block and which the flexible block
 c. Indicate how the water-permeable properties can be adjusted.

II.21. Literature

1. Billmeyer, F.W., *Textbook of Polymer Science*, Wiley - Interscience, New York, USA, 1962
2. Hiemenz, P.C., *Polymer Chemistry. The Basic Concepts*, Marcel Dekker, New York, USA, 1984
3. Sperling, L.H., *Introduction to Physical Plymer Science*, Wiley - Interscience, New York, USA, 1986
4. Schouten, A.E. and van der Vegt, A.K., *Plastics*, Delta Press, The Netherlands, 1987
5. Auvil, S.R. , Srinivasan, R., and Burban, P.M., *Int. Symposium on Membranes for Gas and Vapour Separation*, Suzdal, USSR, Febr. 1989
6. Paul, D.R. and Barlow, J.W. *J. Macromol. Sci. Rev. Macromol. Chem.*, C18 (1980) 109
7. Stannet, V.T., Koros, W.J., Paul, D.R., Lonsdale, H.K., and Baker, R.W., *Adv. Pol. Sci.*, 32 (1979) 69
8. Proceedings of the 4th Priestley Conference, *Membranes in gas separation*,

Leeds, England, Sept. 1987.

9.   Nitto Denko, Technical Report, The 70 th Anniversary Special Issue, 1989

10. Gebben, B., Mulder, M.H.V., Smolders, C.A., *J.Membr.Sci.,* 46 (1989) 29

11. Kelley, F.N., and Bueche F.J., *J. Pol. Sci.,* 50 (1961) 549

12. Burghardt, W.R., Yilmaz, L., and McHugh, A.J., *Polymer,* 28 (1987) 2085

13. Fedors, R.F., *J.Pol.Sci.Polym.Lett.Ed.,* 17 (1979) 719

14. Cassidy, P.E., *Thermally stable polymers,* Marcel dekker, New York, 1980

15. Roesink, H.D.W., *PhD Thesis,* University of Twente, 1989

16. Krause, S., in *Polymer Blends* , Paul, D.R., and Newman, S., eds., vol. I, Ch. 2. Academic Press, New York, 1978

17. Cabasso, I., *Encyclopedia of Polymer Science and Engineering,* Vol. 9, p. 509.

18. Mulder, M.H.V., 'Nature of Membranes', in Howell, J.A., Sanchez, V., and R.W. Field (eds.), *Membranes in Bioprocessing. Theory and applications,* Chapman & Hall, London, 1993

19. Dutch Membrane Guide, Tholen, J., Maaskant. W., and Mulder, M.H.V., Eds., Haskoning, Nijmegen, The Netherlands, 1996

20. Strathmann, H. and Michaels, A.S., *Desalination,* 21 (1977) 195

21. Wyatt, O.H, and Dew-Hughes, D., *Metals, Ceramics and Polymers,* Cambridge University Press, London, 1974

22. Guy, A.G., Introduction to Material Science, McGraw-Hill, New York, 1971

23. Fendler, J.H., *Membrane Mimetic Chemistry,* John Wiley, New York, 1982

24. Lehninger, A.L., *Biochemistry,* Worth Publishers Inc., New York, 1976

III PREPARATION OF SYNTHETIC MEMBRANES

III.1.   Introduction

In chapter II it was shown that a large number of materials can be used as the basis for membrane preparation. A number of preparation techniques exist which enable a membrane to be constructed from a given material. The kind of technique employed depends mainly on the material used and on the desired membrane structure (which in turn is dependent on the separation problem). Three basic types of membrane can be distinguished based on structure and separation principles:
- porous membranes (microfiltration, ultrafiltration)
- nonporous membranes (gas separation, pervaporation, dialysis)
- carrier membranes

A schematic drawing of these various types of membrane is given in figure III - 1. Although the division shown is rather rough, it is very informative because it clearly shows the basic differences in structure (morphology), transport and application.

porous membrane
microfiltration/
ultrafiltration

nonporous membrane
gas separation/
pervaporation

carrier membrane
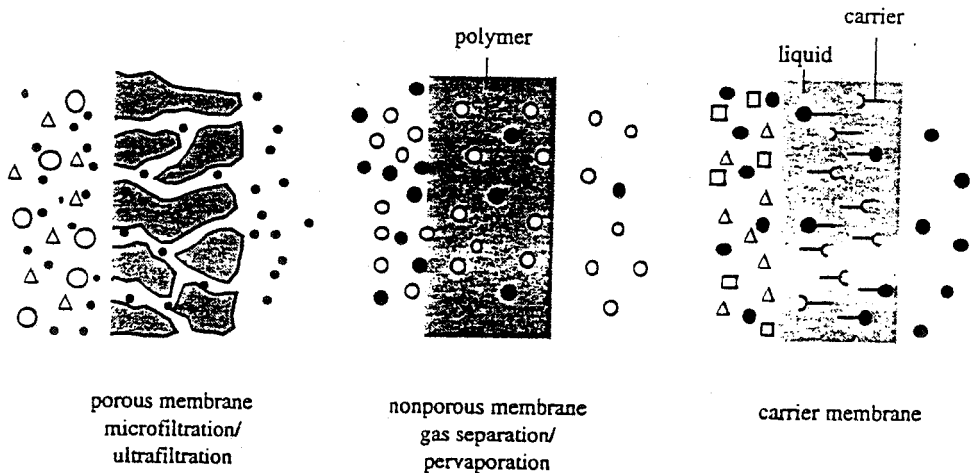
Figure III - 1.   Schematic drawing of the three basic types of membrane.

This subdivision is used throughout this book, but the emphasis in this chapter is mainly on porous and nonporous membranes.

Not all membranes and membrane structures are covered by the classification given in figure III - 1. This approach is used for the sake of simplicity so that the basic principles can be understood more readily. There is no distinct transition from one type to the other. Reverse osmosis membranes, for example, can be considered as being intermediate between porous and nonporous membranes.

For the porous membranes the dimension of the pore mainly determines the separation characteristics, the type of membrane material being of crucial importance for chemical, thermal and mechanical stability but not for flux and rejection. On the other hand, for nonporous membranes, the intrinsic properties of the material are mainly responsible for the separation. Some major characteristics of the three basic types are given below:

i) porous membranes
Membranes of this class induce separation by discriminating between particle size. Such membranes are used in microfiltration and ultrafiltration. High selectivities can be obtained when the solute size or particle size is large relative to the pore size in the membrane. Nowadays a number of different types of membranes are employed and these are described in chapters II and VI.

ii) nonporous membranes
Membranes from this class are capable of separating molecules of approximately the same size from each other. Separation takes place through differences in solubility and/or differences in diffusivity. This means that the intrinsic properties of the polymeric material determine the extent of selectivity and permeability. Such membranes are used in pervaporation, vapour permeation, gas separation and dialysis.

iii) carrier mediated transport
With membranes of this class transport is not determined in any way by the membrane (or membrane material) but by a very specific carrier-molecule which facilitates specific transport. Two different concepts can be distinguished, the carrier is fixed to the membrane matrix or the carrier is mobile when it is dissolved in a liquid. In the latter case the carrier containing liquid is located inside the pores of a porous membrane. The permselectivity towards a component depends mainly on the specificity of the carrier molecule. Through the use of specially tailored carriers, extremely high selectivities can be obtained. The component to be removed can be gaseous or liquid, ionic or non-ionic. To some extent the functionality of this kind of membrane approaches that of a cell membrane.

II.2.   Preparation of synthetic membranes

All kinds of different synthetic materials can be used for preparing membranes. Thus the material can either be inorganic such as a ceramic, glass, metal or organic including all kinds of polymers. The aim is to modify the material by means of an appropriate technique to obtain a membrane structure with a morphology suitable for a specific separation. The material limits the preparation techniques employed, the membrane morphology obtained and the separation principle applied. In other words, not every separation problem can be accomplished with every kind of material.

A number of different techniques are available to prepare synthetic membranes. Some of these techniques can be used to prepare polymeric as well as inorganic membranes. The most important techniques are sintering, stretching, track-etching, phase inversion, sol-gel process, vapour deposition and solution coating.

- *Sintering*

Sintering is quite a simple technique allowing porous membranes to be obtained from organic as well as from inorganic materials. The method involves compressing a powder consisting of particles of a given size and sintering at elevated temperatures. The required temperature depends on the material used. During sintering the 'interfaces' between the contacting particles disappears. A schematic preparation procedure is depicted in figure III - 2.
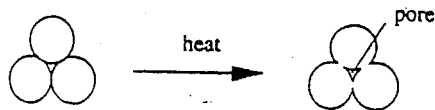
Figure III - 2.   Schematic drawing illustrating the sintering process.

A wide range of different materials can be used such as powders of polymers (polyethylene, polytetrafluoroethylene, polypropylene), metals (stainless steel, tungsten), ceramics (aluminium oxide, zirconium oxide), graphite (carbon) and glass (silicates). The pore size of the resulting membrane is determined by the particle size and particle size distribution of the powder. The narrower the particle size distribution the narrower the pore size distribution in the resulting membrane. This technique allows pore sizes of about 0.1 to 10 μm to be obtained, the lower limit being determined by the minimum particle size.

Sintering is a very suitable technique for preparing membranes from polytetrafluoroethylene because this very chemically and thermally resistant polymer is not soluble. In fact, all the materials mentioned here as basic materials for the sintering process, have the common feature of outstanding chemical, thermal and mechanical stability, particularly the inorganic materials.

Only microfiltration membranes can be prepared via sintering, however. The porosity of porous polymeric membranes is generally low, normally in the range of 10 to 20% or sometimes a little higher.

- *Stretching*

In this method an extruded film or foil made from a partially crystalline polymeric material (polytetrafluoroethylene, polypropylene, polyethylene) is stretched perpendicular to the direction of the extrusion, so that the crystalline regions are located parallel to the extrusion direction. When a mechanical stress is applied small ruptures occur and a porous structure is obtained with pore sizes of about 0.1 μm minimum to a maximum of about 3 μm maximum. Only (semi) crystalline polymeric materials can be used for this technique. The porosity of these membranes is much higher than that of the membranes obtained by sintering, and values up to 90% can be obtained.

- *Track-etching*

The simplest pore geometry in a membrane is an assembly of parallel cylindrically shaped pores of uniform dimension. Such structures can be obtained by track-etching.

In this method a film or foil (often a polycarbonate) is subjected to high energy particle radiation applied perpendicular to the film. The particles damage the polymer matrix and create tracks. The film is then immersed in an acid or alkaline bath and the polymeric material is etched away along these tracks to form uniform cylindrical pores with a narrow pore size distribution. Pore sizes can range from 0.02 to 10 μm but the surface porosity is low (about 10% at a maximum). The choice of the material depends mainly on the thickness of the film and on the energy of the particles being applied (usually about 1 MeV). The maximum penetration thickness of particles with this energy is about 20 μm. When the energy of the particles is increased the film thickness can also be increased and even inorganic materials (e.g. mica) can be used. The porosity is mainly determined by the radiation time whereas the pore diameter is determined by the etching time. A schematic drawing of this technique is given in figure III - 3.
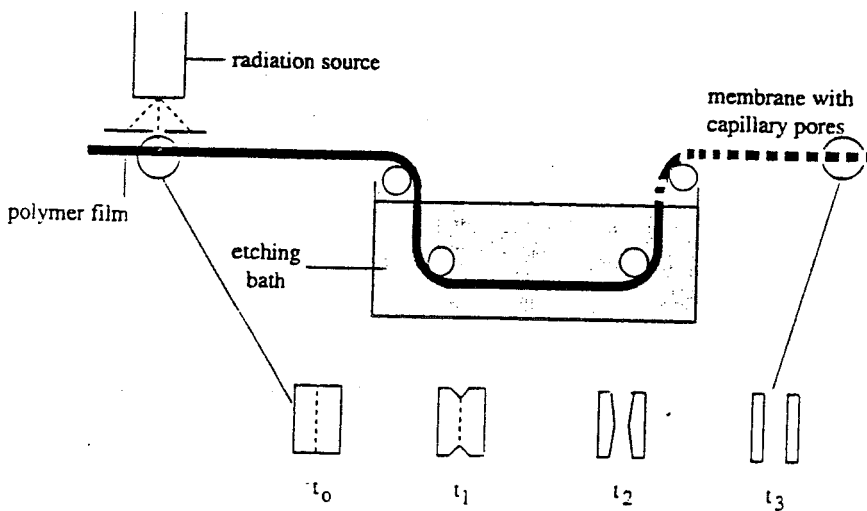
Figure III - 3.   Schematic drawing of the preparation of porous membranes by track-etching.

- *Template leaching*

Another technique for preparing porous membranes is by leaching out one of the components from a film. Porous glass membranes can be prepared by this technique [1]. A homogeneous melt (1000 - 1500 °C) of a three component system (e.g. Na_2O-B_2O_3-SiO_2) is cooled and as a consequence the system separates into two phases, one phase consisting mainly of SiO_2 which is not soluble whereas the other phase is soluble. This second phase is leached out by an acid or base and a wide range of pore diameters can be obtained with a minimum size of about 0.005 μm (5 nm) (see also section III.8).

- *Phase inversion*

Most commercially available membranes are obtained by phase inversion. This is a very versatile technique allowing all kind of morphologies to be obtained. This preparation technique will be described in detail later in this chapter.

- *Coating*

Dense polymeric membranes in which transport takes place by diffusion generally show low fluxes. To increase the flux through these membranes the effective membrane thickness must be reduced as much as possible. This may be achieved by preparing composite membranes.

Such composite membranes consist of two different materials, with a very selective membrane material being deposited as a thin layer upon a more or less porous sublayer (see figure III - 4). The actual selectivity is determined by the thin toplayer, whereas the porous sublayer merely serves as a support. Several coating procedures can be used such as dip coating, plasma polymerisation, interfacial polymerisation, and in-situ polymerisation to achieve these membranes. These techniques will be described in more detail later in this chapter. Another type of coating technique is also possible, where the coating layer plugs the pores in the sublayer. In this case, the (intrinsic) properties of the sublayer rather than those of the coating layer mainly determine the overall properties.
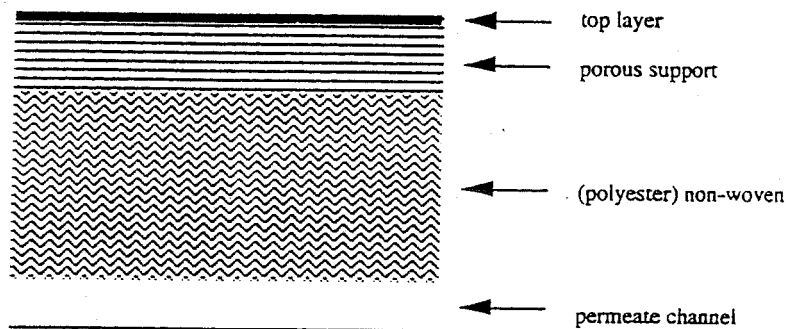
Figure III - 4. Schematic drawing of a composite membrane.

With sintering, stretching, leaching out and track-etching techniques only porous membranes are obtained. These membranes can also be used as sublayer for composite membranes, so that their application can be extended to other areas. Through the use of phase inversion techniques it is possible to obtain open as well as dense structures. Coating techniques are normally used to prepare thin but dense structures, possessing a high (intrinsic) selectivity and a relatively high flux. The basic support material for a composite membrane is often an asymmetric membrane obtained by phase inversion. Preparation techniques for both phase inversion membranes and for composite membranes will now be described in greater detail.

III.3. Phase inversion membranes

Phase inversion is a process whereby a polymer is transformed in a controlled manner from a liquid to a solid state. The process of solidification is very often initiated by the transition from one liquid state into two liquids (liquid-liquid demixing). At a certain stage during demixing, one of the liquid phases (the high polymer concentration phase) will

solidify so that a solid matrix is formed. By controlling the initial stage of phase transition the membrane morphology can be controlled, i.e. porous as well as nonporous membranes can be prepared.

The concept of phase inversion covers a range of different techniques such as solvent evaporation, precipitation by controlled evaporation, thermal precipitation, precipitation from the vapour phase and immersion precipitation. The majority of the phase inversion membranes are prepared by immersion precipitation.

III.3.1 *Precipitation by solvent evaporation*

The most simple technique for preparing phase inversion membranes is precipitation by solvent evaporation. In this method a polymer is dissolved in a solvent and the polymer solution is cast on a suitable support, e.g. a glass plate or another kind of support, which may be porous (e.g. nonwoven polyester) or nonporous (metal, glass or polymer such as polymethylmethacrylate or teflon). The solvent is allowed to evaporate in an inert (e.g. nitrogen) atmosphere, in order to exclude water vapour, allowing a dense homogeneous membrane to be obtained. Instead of casting it is also possible to deposit the polymer solution on a substrate by dip coating (see figure III - 10) or by spraying, followed by evaporation.

III.3.2 *Precipitation from the vapour phase [1,2].*

This method was used as early as 1918 by Zsigmondy. A cast film, consisting of a polymer and a solvent, is placed in a vapour atmosphere where the vapour phase consists of a nonsolvent saturated with the same solvent. The high solvent concentration in the vapour phase prevents the evaporation of solvent from the cast film. Membrane formation occurs because of the penetration (diffusion) of nonsolvent into the cast film. This leads to a porous membrane without toplayer. With immersion precipitation an evaporation step in air is sometimes introduced and if the solvent is miscible with water precipitation from the vapour will start at this stage. An evaporation stage is often introduced in the case of hollow fiber preparation by immersion precipitation ('wet-dry spinning') exchange between the solvent and nonsolvent from the vapour phase leading to precipitation.

III.3.3 *Precipitation by controlled evaporation [3 - 5].*

Precipitation by controlled evaporation was already used in the early years of this century. In this case the polymer is dissolved in a mixture of solvent and nonsolvent (the mixture acts as a solvent for the polymer). Since the solvent is more volatile than the nonsolvent, the composition shifts during evaporation to a higher nonsolvent and polymer content. This leads eventually to the polymer precipitation leading to the formation of a skinned membrane.

III.3.4 *Thermal precipitation [6].*

A solution of polymer in a mixed or single solvent is cooled to enable phase separation to occur. Evaporation of the solvent often allows the formation of a skinned membrane. This

method is frequently used to prepare microfiltration membranes as will be discussed later.

III.3.5   Immersion precipitation [7 - 11].

Most commercially available membranes are prepared by immersion precipitation: a polymer solution (polymer plus solvent) is cast on a suitable support and immersed in a coagulation bath containing a nonsolvent. Precipitation occurs because of the exchange of solvent and nonsolvent. The membrane structure ultimately obtained results from a combination of mass transfer and phase separation.

All phase inversion processes are based on the same thermodynamic principles as will be described in section III - 6.

III.4.   Preparation techniques for immersion precipitation

Most of the membranes in use today are phase inversion membranes obtained by immersion precipitation. Phase inversion membranes can be prepared from a wide variety of polymers. The only requirement is that the polymer must be soluble in a solvent or a solvent mixture. In general the choice of polymer does not limit the preparation technique.

The various techniques will be described very schematically here so that their characteristics may be understood. Pretreatment and post-treatment will not be considered because they are very specific and depend on the polymer used and on the type of application. Basically, the membranes can be prepared in two configurations: flat or tubular.

III.4.1   Flat membranes

Flat membranes are used in plate-and-frame and spiral-wound systems whereas tubular membranes are used in hollow fiber, capillary and tubular systems. These module designs are described in greater detail in chapter VIII. The same flat membranes can be used for both flat membrane configurations (plate-and-frame and spiral wound). The preparation of flat membranes on a semi-technical or technical scale is shown schematically in figure III - 5.
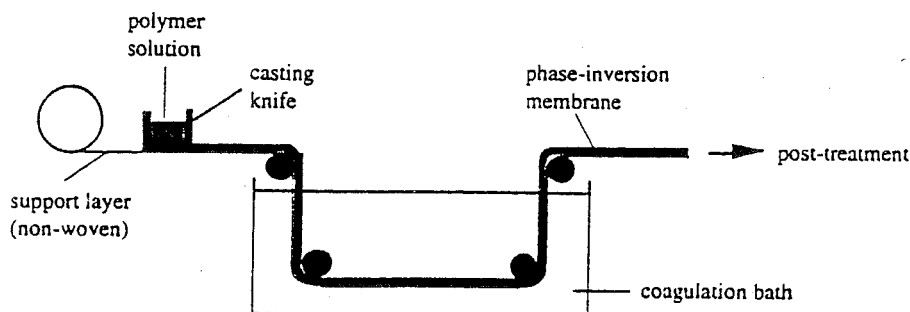
Figure III - 5.   Schematic drawing depicting the preparation of flat membranes.

The polymer is dissolved in a suitable solvent or solvent mixture (which may include additives). The viscosity of the solution depends on the molecular weight of the polymer, its concentration, the kind of solvent (mixture) and the various additives. In figure III - 5 the polymer solution (often referred to as the casting solution) is cast directly upon a supporting layer, for example a non-woven polyester, by means of a casting knife. The casting thickness can vary roughly from 50 to 500 µm. The cast film is then immersed in a nonsolvent bath where exchange occurs between the solvent and nonsolvent and eventually the polymer precipitates. Water is often used (and from an environmental point of view also preferred) as a nonsolvent but organic solvents (e.g. methanol) can be used as well. Since the solvent/nonsolvent pair is a very important parameter in obtaining the desired structure the nonsolvent can not be chosen at will (see section III.7.1)

Other preparation parameters are: polymer concentration, evaporation time, humidity, temperature, and the composition of the casting solution (e.g. additives). These parameters are mainly determining the ultimate membrane performance (flux and selectivity) and hence for its application. The relation between these parameters and membrane structure will be described in greater detail in section III - 6. The membranes obtained after precipitation can be used directly or a post treatment (e.g. heat treatment) can be applied.

Free flat membranes can be obtained by casting the polymer solution upon a metal or polymer belt. After coagulation (and thorough washing!) the free flat-sheet can be collected.

Since flat membranes are relatively simple to prepare, they are very useful for testing on a laboratory scale. For very small membrane surface areas (less than 1000 cm^2), the membranes are cast mostly by hand or semi-automatically, not on a non-woven polyester but often on a glass plate (other materials can also be used, e. g. metals, and polymers such as polytetrafluoroethylene, polymethylmethacrylate etc.). The same procedure is followed as that depicted in figure III - 5.

III.4.2   Tubular membranes

The tubular form is the alternative geometry for a membrane. On the basis of differences in dimensions, the following types may be distinguished:
a) hollow fiber membranes (diameter: < 0.5 mm)
b) capillary membranes (diameter: 0.5 - 5 mm)
c) tubular membranes (diameter: > 5 mm)

The dimensions of the tubular membranes are so large that they have to be supported whereas the hollow fibers and capillaries are self-supporting. Hollow fibers and capillaries can be prepared via three different methods:
-   wet spinning (or dry-wet spinning)
-   melt spinning
-   dry spinning

Although both flat membranes and hollow fiber membranes can exhibit similar performances, the procedures for their preparation are not the same. Since hollow fibers are self-supporting, the fiber dimensions are very important. Furthermore, demixing takes place from the bore side or lumen and from the shell side or outside, whereas in the

preparation of flat membrane demixing occurs from only one side. Spinning parameters are also important with respect to membrane performance during the preparation of hollow fiber. A schematic drawing of the dry-wet spinning process in shown in figure III - 6.

A viscous polymer solution containing a polymer, solvent and sometimes additives (e.g. a second polymer or a nonsolvent) is pumped through a spinneret, the polymer solution being filtered before it enters the spinneret. The viscosity of the polymer solution must be high (in general more than 100 Poise). The bore injection fluid is pumped
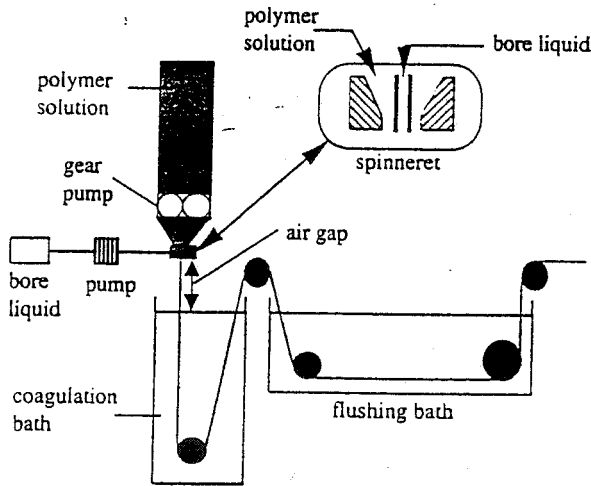
Figure III - 6.   Schematic drawing of a dry-wet spinning process.
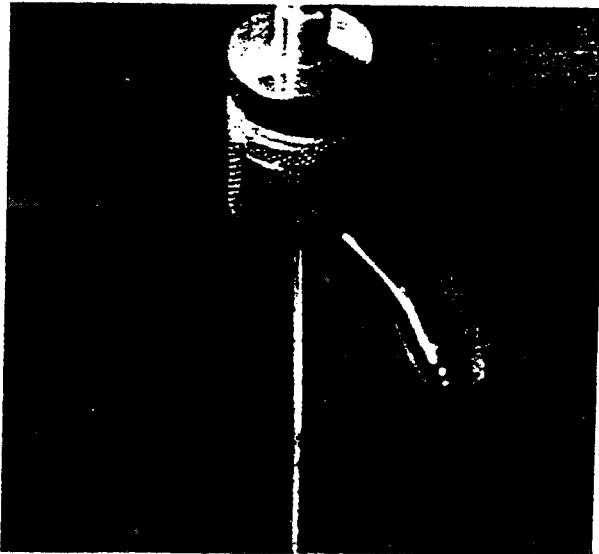
Figure III - 7.   Photograph of a fiber in the air gap.

through the inner tube of the spinneret. After a short residence time in the air or a controlled atmosphere (the term dry originates from this step) the fiber is immersed in a nonsolvent bath where coagulation occurs. The fiber is then collected upon a godet.

The main spinning parameters are: the extrusion rate of the polymer solution; the bore fluid rate; the 'tearing-rate'; the residence time in the air-gap; and the dimensions of the spinneret. These parameters interfere with the membrane-forming parameters such as the composition of the polymer solution, the composition of the coagulation bath, and its temperature. Figure III - 7 shows a spun fiber in the air gap.

The cross-sections of two types of spinnerets are given in figure III - 8. In dry-wet spinning the dimensions of the spinneret are very important since the fiber dimensions are mainly determined by these. The fiber dimensions are more or less fixed after immersion in the coagulation bath.
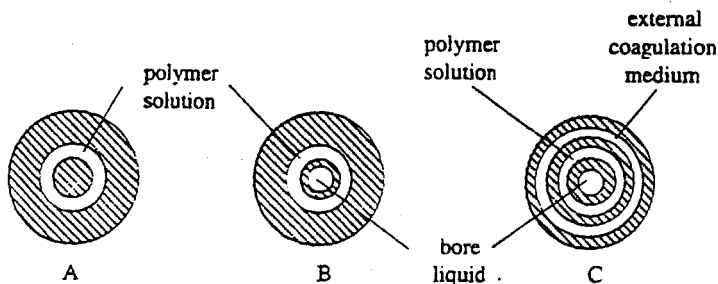
Figure III - 8.   Cross-section of three types of spinnerets; (A) used for melt spinning and dry-spinning, (B) used for wet spinning and dry-wet spinning; and (C) triple spinneret used for wet spinning.

In melt spinning and dry-spinning the dimensions of the spinneret are less crucial because the fiber dimensions are mainly determined by the ratio of the extrusion rate and tearing-rate'. The spinning rate in melt spinning (thousands of meters per minute) is much higher than that used in the dry-wet spin process (meters per minute).

Another typical membrane configuration is the tubular membrane. Although this may seem to be similar to the hollow fiber concept (both are tubular!) some distinct differences exist (see chapter VIII). The preparation techniques are also completely different.

Polymeric tubular membranes are not self-supporting and casting of the polymer solution is carried out on a supporting tubular material, for example a non-woven polyester or a porous carbon tube.

A schematic drawing illustrating the preparation of tubular membranes is given in figure III - 9. Pressure is applied to a reservoir filled with a polymer solution so that the solution is forced through a hollow pipe. At the end of the pipe is a 'casting bob' with small holes through which the polymer solution is forced (see figure III - 9a). The porous tube is moving vertically, either mechanically or by gravity, and a film is cast upon its inner wall (figure III - 9b). The pipe is then immersed in a coagulation bath where precipitation of the cast polymer solution leads to the formation of a tubular membrane

(figure III - 9c).
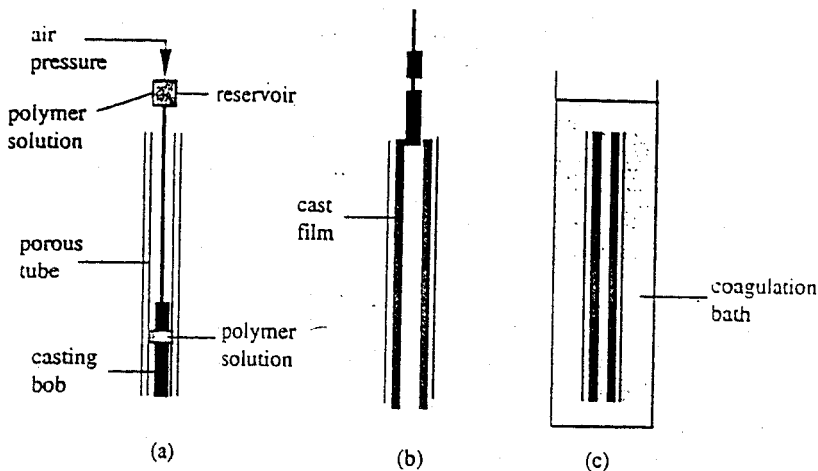
Figure III - 9.   Laboratory set-up for tubular membrane preparation.

III.5.   Preparation techniques for composite membranes

Dense homogeneous polymer films can separate various gaseous or liquid mixtures very effectively. However, normal thicknesses (20 - 200 μm) lead to very low permeation rates. Such membranes cannot be made thin enough (of the order of 0.1 to 1 μm) to improve permeation because they are very difficult to handle (no mechanical strength), and also because such thin layers need to be supported.

A major breakthrough in the history of membrane technology was the development of 'asymmetric' membranes, where a very thin selective layer (of the order of 0.1 to 1 μm) is supported by a porous sublayer of the same material. These asymmetric membranes are prepared by a phase inversion technique. Another breakthrough was the development of composite membranes with an asymmetric structure, where a thin dense toplayer is supported by a porous sublayer. In this case the two layers originate from different (polymeric) materials. The advantage of composite membranes is that each layer can be optimised independently to obtain optimal membrane performance with respect to selectivity, permeation rate, and chemical and thermal stability. In general the porous support layer is again obtained by phase inversion. Furthermore, the toplayer in composite membranes can be made from a material (such as an elastomer) which is difficult to use in phase inversion techniques, e.g. immersion precipitation. The first types of composite membrane were made by spreading a thin layer of a very dilute polymer solution on a liquid (water, mercury). The solvent was allowed to evaporate and a very thin polymeric film was formed. A porous substrate was then carefully placed below this thin polymeric film as a support. The mechanical stability of such composite membranes was however poor, and this technique is not very suitable for large-scale production.

Several techniques can be used to apply an (ultra)thin toplayer upon a support :
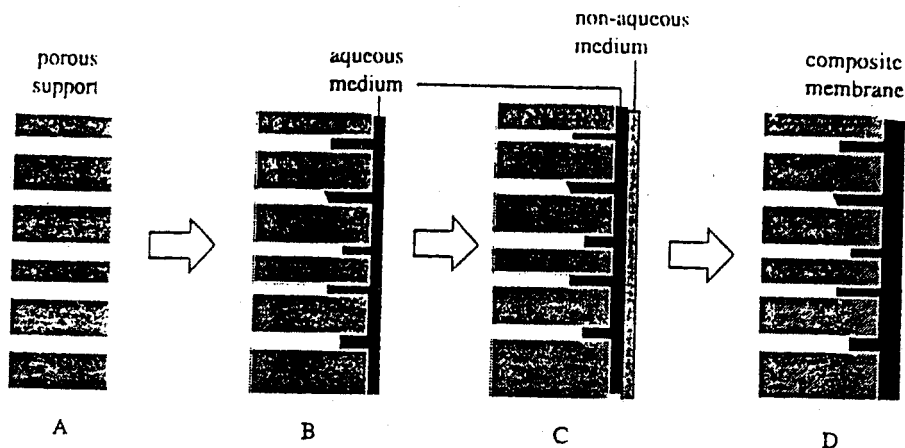
Figure III - 10. Schematic drawing of the formation of a composite membrane via interfacial polymerisation.

- dip-coating
- spray coating
- spin coating
- interfacial polymerisation
- in-situ polymerisation
- plasma polymerisation
- grafting

Except for solution coating (dip-coating, spin coating and spray coating), all these techniques involve polymerisation reactions which generate new polymers as a very thin layer.

III.5.1   *Interfacial polymerisation*

Interfacial polymerisation provides another method for depositing a thin layer upon a porous support. In this case, a polymerisation reaction occurs between two very reactive monomers (or one pre-polymer) at the interface of two immiscible solvents. This is shown schematically in figure III - 10. The support layer, which is generally an ultrafiltration or microfiltration membrane (figure III - 10A), is immersed in an aqueous solution (figure III - 10B) containing a reactive monomer or a pre-polymer, frequently of the amine-type. The film (or fiber) is then immersed in a second bath containing a water-immiscible solvent (figure III - 10C) in which another reactive monomer, often an acid chloride, has been dissolved. These two reactive monomers (i.e. amine and acid chloride) react with each other to form a dense polymeric toplayer (fig. III - 10D). Heat treatment is often applied to complete the interfacial reaction and to crosslink the water-soluble monomer or pre-polymer. The advantage of interfacial polymerisation is that the reaction is self-inhibiting through passage of a limited supply of reactants through the already formed layer, resulting in an extremely thin film of thickness within the 50 nm range. Table III.1 provides a number of examples of the several types of monomers and pre-polymer that can be used. The amine is in the aqueous phase while the acid chloride or isocyanate is in the organic

Table III.1   Some examples of the preparation of composite membranes by interfacial polymerisation. The amine is in the aqueous phase while the acid chloride or isocyanate is in the organic phase.

| aqueous phase | organic phase | product |
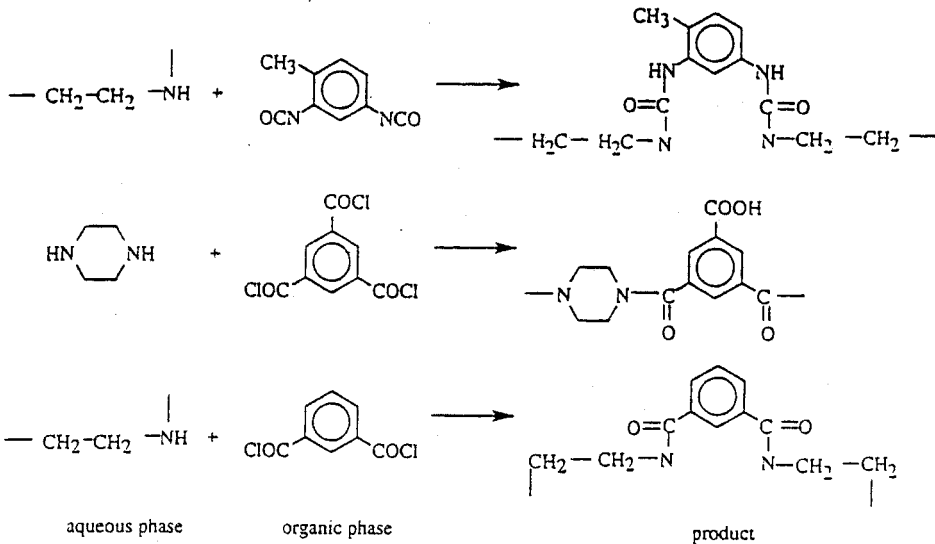
phase. The resulting products of the specific interfacial polymerisation reactions involved. are also given in this table.

III.5.2   Dip-coating

Dip-coating is a very simple and useful technique for preparing composite membranes with a very thin but dense toplayer. Membranes obtained by this method are used in reverse osmosis, gas separation and pervaporation. The principle of this technique is shown schematically in figure III - 11.
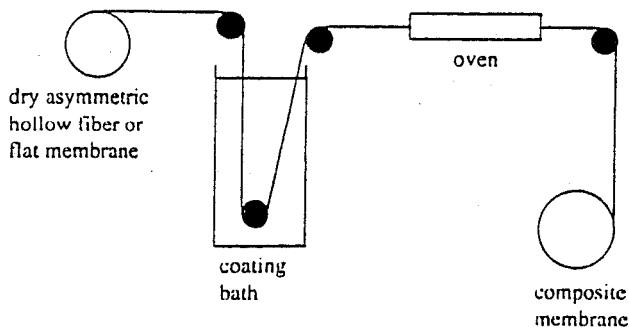
Figure III - 11.   Schematic illustration of dip-coating.
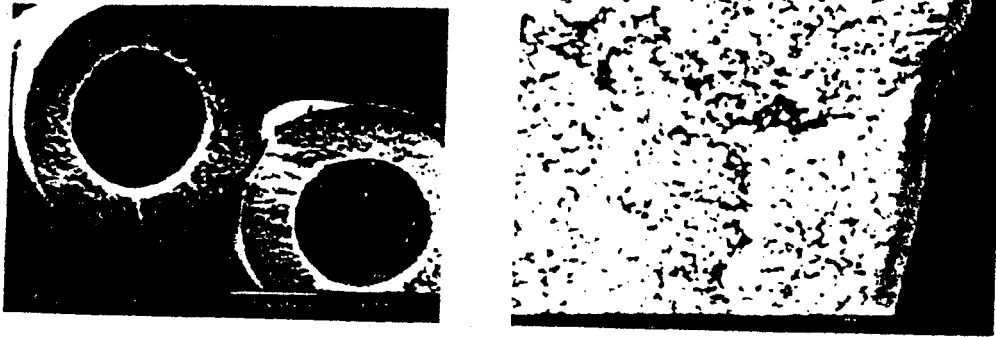
Figure   III - 12. Two scanning electron micrographs of a composite hollow fiber with a poly(ether
imide) sublayer and a polydimethylsiloxane toplayer. The picture on the left provides
an overall view of the cross-section (magnification 500x); the picture on the right
gives a view of the outside of the fiber with the silicone rubber toplayer
(magnification 10,000 x) [12].

In this case, an asymmetric membrane (hollow fiber or flat sheet), often of the type used in
ultrafiltration, is immersed in the coating solution containing the polymer, prepolymer or
monomer, the concentration of the solute in the solution being low (often less than 1%).
When the asymmetric membrane is removed from the bath containing the coating material
and the solvent, a thin layer of solution adheres to it. This film is then put in an oven where
the solvent evaporates and where crosslinking also occurs. Such crosslinking leads to the
thin layer becoming fixed to the porous sublayer. Crosslinking is often also necessary
because the coated layer has no mechanical or chemical stability itself or its separation
performance is not sufficiently high in the uncrosslinked state. Figure III - 12 illustrates a
composite hollow fiber with the toplayer on the outside of the fiber. The sublayer here is a
hollow fiber of poly(ether imide) obtained by immersion precipitation in which a thin layer
of polydimethylsiloxane was deposited by a dip-coating procedure. Crosslinking of the
dimethylsiloxane was achieved by heat treatment. It can be seen that a very thin toplayer of
about 1 μm can be applied via this technique. The ultimate thickness of the coating
thickness can be described by solution hyrodynamics. As can be seen in figure III - 13, an
equilibrium thickness is obtained after a certain period of the withdrawal of the fiber or
sheet from the solution in which the gravity forces and drag forces are balanced. The final
thickness is the result of various forces that are acting, i.e., viscous forces, capillary forces
and inertial forces. The coating process can be described by the Navier-Stokes equation
which may finally result in an equation for the final thickness of the coating layer [13]).

$$n_\infty = \frac{2}{3}\sqrt{\frac{\eta\,v}{\rho\,g}}$$

(III-1)

in which h_∞ is the equilibrium thickness, v the coating velocity and ρ the viscosity. After evaporation of the solvent a thin polymer film is formed at the surface with a thickness proportional to volume fraction of polymer in the solution. Although the method itself is experimentally rather simple to carry out, there are a number of points that should be emphasized and these will be discussed briefly.
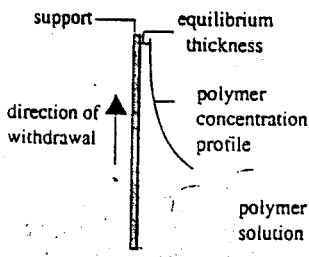
Figure III - 13. Schematic drawing of the concentration profile in a dip-coating process

i) State of the polymer

One of the most important features in the solution coating process is the state of the polymer, glassy or rubbery. If the polymer is an elastomer a thin defect-free layer can be mostly obtained but if the polymer is glassy then the glass transition temperature is passed at a certain moment during the evaporation process. Upon further evaporation large forces may be generated and this may result in defects and consequently in leakages.

ii) Pore penetration

If a porous support is used pore penetration will occur during the dip-coating process due to capillary forces. Especially in the case of glassy polymers, the support may then exhibit an extremely high resistance to mass transfer although the layer that may have been penetrated into the pores reaches a thickness one or a few micrometers. This may already be dimentrial. Pore penetration may be avoided or reduced by various methods. The most versatile method is the pre-filling of the pores which prevents the coating solution to penetrate. Other methods that can be apply are a high molecular weight and the employment of a good solvent since both parameters do increase the hydrodynamic radius of the polymer coil in solution. A high molecular weight does increase the viscosity as well. Another important factor in this respect is the pore size distribution of the substrate which should be as narrow as possible. On the other hand, the surface porosity must be high. A well performed characterization of the support layers is essential for the proper selection.

iii) non-wetting liquids

If the solvent of the coating solution does not wet the porous substrate, no pore penetration will occur. This method can be applied to coat porous hydrophobic polymers such as polyethylene, polypropylene, polytetrafluoroethylene or polyvinylidene fluoride with a water soluble polymer. Since water does not wet the membrane (at least if the Laplace pressure is not exceeded) the polymer will definitely not penetrate. The solution properties are very important and this is determined by four parameters

- type of polymer
- type of solvent
- polymer concentration
- molecular weight

The polymer, which is assumed to be linearly and amorphous, occurs in solution as a random coil. The dimensions of the coil depend on the type of solvent, in good solvents the coil dimensions are large whereas in poor solvents the coil dimensions are much smaller. If the solvent is very poor then the coils aggregate and precipitation may occur. The quality of the solvent can be expressed by the Flory-Huggins interaction parameter χ. An increase of the molecular weight will also result in an increase in coil dimension. If the polymer concentration increases then the coils will overlap. This process always occurs in dipcoating where the solvent is being evaporating. At a certain moment the coils will overlap and will form an entangled network. The formation and morphology of this network strongly depend then on the solvent and polymer. An important property is the state of the polymer, i.e. the polymer can be either glassy or elastomeric at room temperature. Elastomers are good film formers and during the coating process the polymer remains in the rubbery state. On the other hand, glassy polymers pass at a certain concentration the transition from rubbery state to glassy state (see chapter II and later this chapter). At that moment the mobility of the polymeric chains have been reduced drastically. Often the material is not able to compensate the stress built up due to evaporation and this may results in failure (defects). The tensile strength of the polymer may be increased by increasing the molecular weight and especially for intrinsically brittle polymers this is even a requirement.

III.5.3   Plasma polymerisation

Another method of applying a very thin dense layer upon a (porous) sublayer is via plasma polymerisation, the plasma being obtained by the ionisation of a gas by means of an electrical discharge at high frequencies up to 10 MHz. Two types of plasma reactors are used: i) the electrodes are located inside the reactor and ii) the coil is located outside the reactor. In figure III - 14 an apparatus is depicted where plasma polymerisation can occur with the discharge coil outside the reactor, the so-called electrodeless glow discharge. The pressure in the reactor is maintained between 10 to 10^3 Pascal (10^{-4} to 10^{-1} mbar). On entering the reactor the gas is ionised and by ensuring that the reactants are supplied separately to the reactor all kinds of radicals will be formed through collisions with the ionised gas which are capable of reacting with each other. The resulting product will precipitate (e.g. on a membrane) when their molecular weight becomes too high. The flow control of gas as well as that of the monomer is very crucial in the plasma polymerisation apparatus given in figure III - 14. A very thin layer of thickness in the range of 50 nm can be obtained provided that the concentration of the monomer in the reactor (the partial pressure) is carefully monitored to control the thickness. Other factors important in controlling the thickness of the layer are the polymerisation time, vacuum pressure, gas flow, gas pressure and frequency. The structure of the resulting polymer is generally difficult to control and is often highly crosslinked.
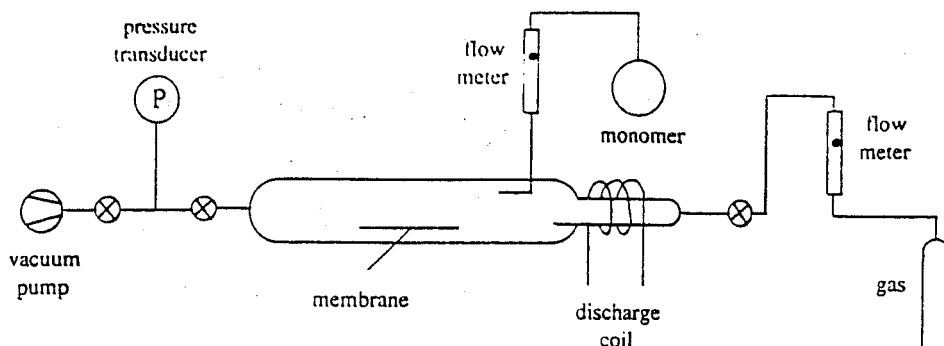
Figure III - 14. Plasma polymerisation apparatus.

III.5.4   Modification of homogeneous dense membranes

Chemical or physical modification of homogeneous membranes can drastically change their intrinsic properties, especially when ionic groups are introduced. Such charged membranes can be applied in electrodialysis, where ionic groups are necessary. Ionic membranes also show remarkable results in other processes.

We shall describe two examples of modification of homogeneous dense films here, one by chemical and the other by physical means. The first example concerns polyethylene, which, although a very important bulk plastic, is only in limited use as

$$-CH_2-CH_2-CH_2- \quad + \quad SO_2 \quad + \quad Cl_2 \quad \longrightarrow \quad -\underset{\underset{SO_2Cl}{|}}{CH}-CH_2-CH_2-$$

$$-\underset{\underset{SO_2Cl}{|}}{CH}-CH_2- \quad + \quad NaOH \quad \longrightarrow \quad -\underset{\underset{SO_3Na^+}{|}}{CH}-CH_2-$$

and

$$-\underset{\underset{SO_2Cl}{|}}{CH}-CH_2- \quad + \quad NH_2-CH_2-NR_2 \quad \longrightarrow \quad -\underset{\underset{SO_2-NH-CH_2-NR_2}{|}}{CH}-CH_2-$$

$$-\underset{\underset{SO_2-NH-CH_2-NR_2}{|}}{CH}-CH_2- \quad + \quad RBr \quad \longrightarrow \quad -\underset{\underset{SO_2-NH-CH_2-NR_3^+Br^-}{|}}{CH}-CH_2-$$
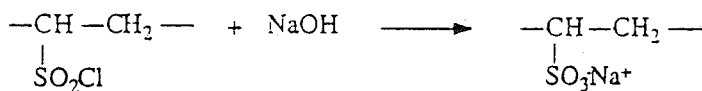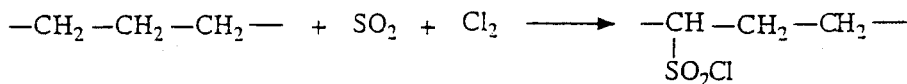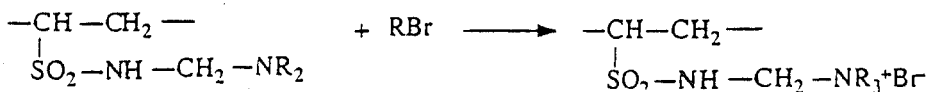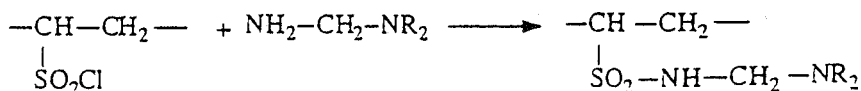
Figure III - 15.   Introduction of sulfonic acid groups and quarternary amine groups into polyethylene.

membrane material. As shown in figure III - 15, cation-exchange as well as anion-exchange groups can be introduced quite easily into this material. Such ionic groups can cause the polymer to change from hydrophobic to hydrophilic behaviour. In addition to polyethylene it is also possible to modify other polymers such as polytetrafluoroethylene or polysulfone chemically and once again the membrane performance is changed considerably while the chemical and thermal stability remain the same. Chemical modification offers the possibility of modifying the intrinsic properties of all kinds of bulk polymer. It is beyond the scope of this book to describe such modifications in detail.
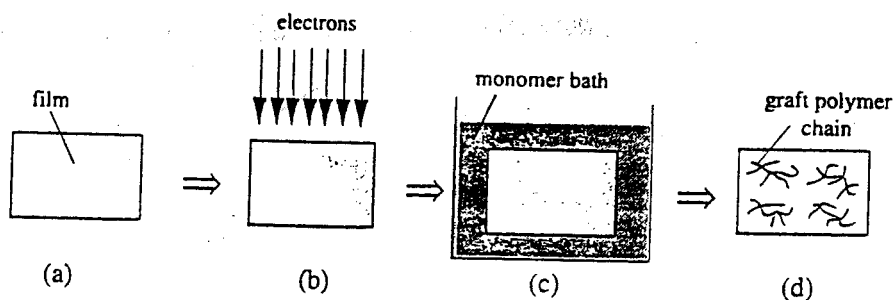
Figure III - 16.   Schematic representation of grafting by radiation [14].

Another method of modifying dense membranes is by means of grafting (e.g. radiation-induced grafting, see chapter II). This method allows a number of different kinds of groups to be introduced into the polymer, resulting in membranes with completely different properties [14]. A representation of this technique is given in figure III - 16.

Table III.2   Some monomers useful for radiation induced-grafting [14]

neutral	basic	acid
$CH=CH_2$	$CH=CH_2$	$CH=CH_2$
		$COOH$
		acrylic acid
N-vinyl pyrrolidone	N-vinyl pyridine	
$CH=CH_2$		CH_3
$O-C-CH_3$		$C=CH_2$
O		$COOH$
vinyl acetate		methacrylic acid

A polymer film (III - 16a) is irradiated with electrons (≈ 200 keV) which leads to the generation of radicals (III - 16b). The film is now immersed in a monomer bath where the monomers diffuse into the film (III - 16c). Polymerisation is initiated at the radical sites in the polymeric substrate and a graft polymer is covalently bound to the basic polymer.

Not all kinds of low molecular weight monomers can be used for these polymerisations, since for example an unsaturated group $RHC = CH_2$, must be present. However, this technique will allow ionic groups (both acidic and basic) and neutral groups to be introduced. Table III.2 gives some examples of monomers which can be used. Very specific membranes can be developed by this technique because of the large number of possible variations.

III.6.   Phase separation in polymer systems

III.6.1   Introduction
In this section the basic principles of membrane formation by phase inversion will be described in greater detail. All phase inversion processes are based on the same thermodynamic principles, since the starting point in all cases is a thermodynamically stable solution which is subjected to demixing. Special attention will be paid to the immersion precipitation process with the basic characteristic that at least three components are used: a polymer, a solvent and a nonsolvent where the solvent and nonsolvent must be miscible with each other. In fact, most of the commercial phase inversion membranes are prepared from multi-component mixtures, but in order to understand the basic principles only three component systems will be considered. An introduction to the thermodynamics of polymer solutions is first given, a qualitatively useful approach for describing polymer solubility or polymer-penetrant interaction is the solubility parameter theory. A more quantitative description is provided by the Flory-Huggins theory. Other more sophisticated theories have been developed but they will not be considered here.

III.6.1.1   Thermodynamics
The state of any system, open, closed or isolated are described by state functions; internal energy (U), enthalpy (H), entropy (S) and free enthalpy (G). These state functions determine whether a process is in equilibrium or may be changed spontaneously. The criterion of equilibrium at constant temperature and pressure is given by the free enthalpy, expressed by the symbol G and is defined as

$$G = H - TS \qquad\qquad\qquad\qquad (III - 2)$$

For a closed system, i.e. a system in which exchange of heat may occur but where no transport of matter occurs the change in free enthalpy for a reversible process is given by

$$dG = - S\, dT + V\, dP \qquad\qquad\qquad\qquad (III - 3)$$

Similar equations can be derived for the enthalpy (H), the internal energy (U) or the

Helmholtz free energy (A) and these can be find in any thermodynamic textbook. Since process conditions are conveniently described and measured as a function of pressure P and temperature T, this energy parameter G is used as a criterion of equilibrium at constant temperature and pressure.

For a spontaneous irreversible process at constant T and P the free enthalpy decreases, $(dG)_{T,P} < 0$. On the other hand $dG = 0$ at constant T and P for an equilibrium process.

For a process at constant temperature the free enthalpy change ΔG is given by

$$\Delta G = \Delta H - T \Delta S$$

(III - 4)

Whether or not a certain process, i.e. chemical reaction, mixing of components etc, is spontaneous depends upon ΔH and $T \Delta S$. For the mixing of two or more components the free enthalpy of mixing (ΔG_m) with the subscript m for mixing, is given by.

$$\Delta G_m = \Delta H_m - T \Delta S_m$$

(III - 5)

where ΔH_m is the enthalpy of mixing and ΔS_m is the entropy of mixing. Two components (polymer/solvent or polymer/polymer) will mix spontaneously if the free enthalpy of mixing is negative ($\Delta G_m < 0$). For polymeric systems (polymer/solvent) the entropy of mixing ΔS_m is small (as will be described later). This means that the solubility is determined by the sign and the magnitude of ΔH_m. For small apolar solvents Hildebrand [15] derived the following expression for ΔH_m

$$\Delta H_m = V_m \left[\left(\frac{\Delta E_1}{V_1} \right)^{0.5} - \left(\frac{\Delta E_2}{V_2} \right)^{0.5} \right]^2 v_1 v_2$$

(III - 6)

where v_1 and v_2 are the volume fraction of both components, V_m, V_1, V_2 are the molar volumes of the solution and the components, and ΔE the energy of vaporisation. The term $\Delta E/V$ is called the cohesive energy density (CED) and the square root of the CED is the solubility parameter δ.

$$\delta \equiv [CED]^{1/2}$$

(III - 7)

The cohesive energy per unit volume is the energy necessary to remove a molecule from its neighbouring molecules, as in the case of evaporation. The intermolecular forces are determined by the sum of the secondary forces, dispersion forces, polar forces and hydrogen bonding.

Combination of eqs. III - 6 and III - 7 gives

$$\Delta H_m = V_m (\delta_1 - \delta_2)^2 v_1 v_2$$

(III - 8)

As can be seen from eq. III - 8, when $\delta_1 = \delta_2$, the value of ΔH_m approaches zero and

polymer and solvent are miscible (because ΔS_m is always positive). When the affinity between the polymer and solvent (penetrant) decreases, the difference between δ_1 and δ_2 becomes larger. Hansen [16] divided the solubility parameter into three contributions

$$\delta^2 = \delta_d^2 + \delta_p^2 + \delta_h^2 \tag{III - 9}$$

where
δ_d : solubility parameter due to dispersion forces
δ_p : solubility parameter due to polar forces
δ_h : solubility parameter due to hydrogen bonding

These three dimensional solubility parameters may be considered as three vectors along othogonal axes where the solubility parameter is given as the end-point of the radius vector. This is shown schematically in figure III - 17 where each component, solvent or polymer, can be located in a three-dimensional $(\delta_d, \delta_p, \delta_h)$ space. The distance between the endpoints of two vectors is given by [17].

$$\Delta = [(\delta_{d,p} - \delta_{d,s})^2 + (\delta_{p,p} - \delta_{p,s})^2 + (\delta_{h,p} - \delta_{h,s})^2] \tag{III - 10}$$

The affinity between polymer and solvent or in general between two components increase with decreasing value of Δ, with a limit value of $\Delta \Rightarrow 0$.
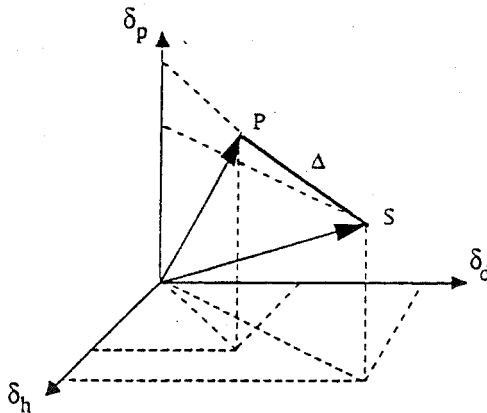
Figure III - 17. Schematic drawing of polymer (P) and solvent (S) in a three dimensional $\delta_p, \delta_d, \delta_h$-space. Δ is the distance between the endpoint of the polymer and solvent vectors.

Large compilations exist of solubility parameter data of solvents and polymers [18]. Table III.3 summarises data for some of the polymers frequently used as membrane materials. However, solubility behaviour can be better described by changes in the free enthalpy of

mixing than via the solubility parameter approach. The change in Gibbs free enthalpy of mixing for a two-component system i and j and number of moles n_i and n_j respectively, is

Table III.3   Solubility parameter data for some polymers

polymer	δ_d	δ_p	δ_h	$\delta^{\#}$	ref.
polyethylene	8.6	0	0	8.6	19
Nylon 66	9.1	2.5	6.0	11.6	19
polysulfone	9.0	2.3	2.7	9.6	20
polyacrylonitrile	8.9	7.9	3.3	12.3	19
cellulose acetate	7.9	3.5	6.3	10.7	21
poly(phenylene oxide)	9.4	1.3	2.4	9.8	19

$\#$ the δ parameters are expressed in $(cal/cm^3)^{0.5}$

given by

$$dG = V\,dP - S\,dT + \left(\frac{dG}{dn_i}\right)_{T,P,n_i} dn_i + \left(\frac{dG}{dn_j}\right)_{T,P,n_i} dn_j \qquad (III - 11)$$

This equation is similar to equation III - 3, only two terms have been added which describe the change in number of moles of both components. The chemical potential of a component i, which is the partial molar free enthalpy, is defined as

$$\mu_i = \left(\frac{\partial G}{\partial n_i}\right)_{P,T,n_j,n_k,\ldots} \qquad (III - 12)$$

where μ_i is equal to the change in free enthalpy of a system containing n_i moles when the pressure, temperature and the number of moles of all the other components are held constant. For a multi-component system eq. III - 11 becomes

$$dG = V\,dP - S\,dT + \Sigma\,\mu_i\,dn_i \qquad (III - 13)$$

The chemical potential μ_i is defined at temperature T, pressure P, and composition x_i. For the pure component ($x_i = 1$), the chemical potential may be written as μ_i°.

The free enthalpy of a mixture G_m of a mixture consisting of two components is given by the sum of the chemical potentials (the partial free enthalpy). If G_m is expressed per mole then

$$G_m = x_1 \mu_1 + x_2 \mu_2 \hspace{6cm} (III - 14)$$

The dependence of the free enthalpy on the composition of the mixture is shown schematically in figure III - 18. The value of the G_m at the y-axis represent the chemical potential of the pure components, $\mu_1°$ and $\mu_2°$ respectively.
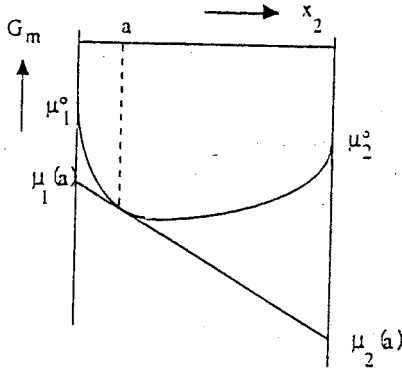
Figure III - 18. Schematic drawing of the free enthalpy of a mixture at temperature T as a function of the composition.

The change in the free enthalpy of mixing ΔG_m which occurs on mixing n_1 mol of component 1 with n_2 mol of component 2 at constant P and T is now given by

$$\Delta G_m = n_1 \mu_1 + n_2 \mu_2 - n_1 \mu_1° - n_2 \mu_2° \hspace{4cm} (III - 15)$$

When, $\Delta \mu_i = \mu_i - \mu_i°$, eq. III - 15 becomes

$$\Delta G_m = n_1 \Delta \mu_1 + n_2 \Delta \mu_2 \hspace{5cm} (III - 16)$$

If the chemical potential difference is known, ΔG_m can then be calculated. For ideal solutions ($a_i = x_i$)

$$\mu_i = \mu_i° + RT \ln x_i \hspace{5cm} (III - 17)$$

or

$$\Delta \mu_i = \mu_i - \mu_i° = RT \ln x_i \hspace{4cm} (III - 18)$$

The number of moles may be replaced by mole fraction and this lead to the general expression for the free enthalpy of mixing per mole for an ideal solution.

$$\Delta G_m = RT (x_1 \ln x_1 + x_2 \ln x_2)$$

(III - 19)

Since $\ln x_1$ and $\ln x_2$ are always negative, ΔG_m is negative and ideal solutions always mix spontaneously. For ideal solutions, $\Delta H_m = 0$, i.e. ΔG_m is solely determined by ΔS_m. For ideal solutions consisting of two components, ΔS_m is given by the combination of eqs. III - 5 and III - 19.

$$\Delta S_m = - R (x_1 . \ln x_1 + x_2 . \ln x_2)$$

(III - 20)

The solubility behaviour of polymer solutions differs completely from that of a solution containing low molecular weight components because the entropy of mixing of the long polymeric chains is much lower. Flory and Huggins [22] used a lattice model to describe the entropy of mixing of (polymer) solutions. In the case of low molecular weight components every molecule occupies one lattice site (fig III - 19a).

(a)

(b)

(c)
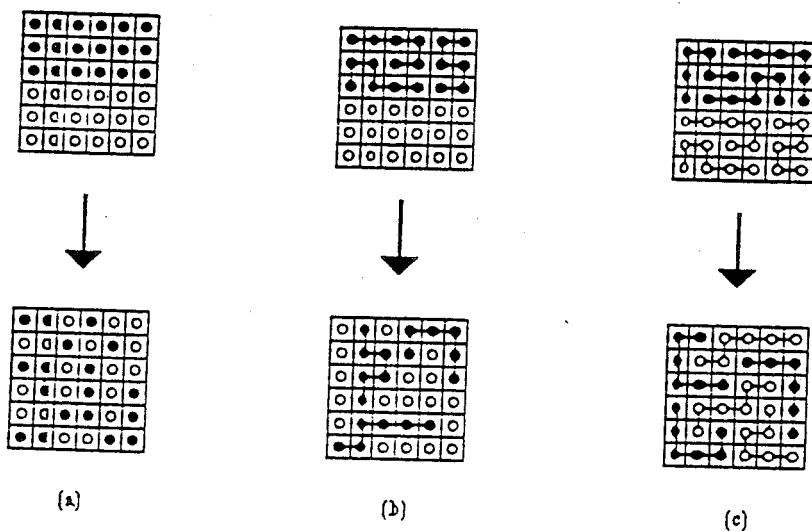
Figure III - 19.   Schematic representation of mixing: (a) binary low molecular weight components; (b) polymer solution; (c) binary polymer mixture.

The total number of molecules $n_t = n_1 + n_2$. With macromolecules, a lattice site is not occupied by a complete molecule (or chain) but rather by a segment. It is assumed that segment and solvent molecules are identical in size. Now the total numbers of sites occupied is $n_1 + N.n_2$ where N is the number of segments in a polymer chain. When two polymers are mixed the total number of occupied sites is $N_1.n_1 + N_2.n_2$, where N_1 is the number of segments in the chain of polymer 1 and N_2 is the number of segments in the chain of polymer 2. The number of combinations to arrange all the molecules in a lattice is

considerably reduced in going from two low molecular weight solvents (fig. III - 19a) to a solvent and a polymer (fig. III - 19b), and then to two polymers (fig. III - 19c).

Expressed in volume fractions, the entropy of mixing is given by

$$\Delta S_m = - R (n_1 . \ln\phi_1 + n_2 . \ln\phi_2) \qquad\qquad (III - 21)$$

When the two components are solvents with the same molar volume, the volume fraction and mole fraction are equal. When component 1 is a solvent and component 2 a polymer, the volume fractions are:

$$\phi_1 = \frac{n_1}{n_1 + N\ n_2} \qquad\qquad \phi_2 = \frac{N\ n_2}{n_1 + N\ n_2} \qquad\qquad (III - 22)$$

or if n_t is the total numbers of sites ($n_t = n_1 + N . n_2$)

$$n_1 = \phi_1\ n_t \qquad\qquad n_2 = \left(\frac{\phi_2}{N}\right)\ n_t \qquad\qquad (III - 23)$$

With $\Delta H_m = 0$, then

$$\frac{\Delta\ G_m}{R\ T} = - \frac{\Delta S_m}{R} \qquad\qquad (III - 24)$$

Substitution of eq. III - 23 into eqs. III - 21 and III - 24 gives

$$\frac{\Delta G_m}{n_t\ RT} = \phi_1 \ln \phi_1 + \left(\frac{\phi_2}{N}\right) \ln \phi_2 \qquad\qquad (III - 25)$$

When two polymers are mixed with each other, eq. III - 23 becomes

$$n_1 = \left(\frac{\phi_1}{N_1}\right)\ n_t \qquad\qquad n_2 = \left(\frac{\phi_2}{N_2}\right)\ n_t \qquad\qquad (III - 26)$$

Substitution of eq. III - 26 into eqs. III - 21 and III - 24 gives

$$\frac{\Delta G_m}{n_t\ RT} = \left(\frac{\phi_1}{N_1}\right) \ln \phi_1 + \left(\frac{\phi_2}{N_2}\right) \ln \phi_2 \qquad\qquad (III - 27)$$

For ideal low molecular weight mixtures $N_1 = 1$ and $N_2 = 1$, and for a polymer solution containing a solvent and a polymer, $N_1 = 1$ (solvent) and $N_2 > 1$ (polymer). In the case of two polymers, both $N_1 > 1$ and $N_2 > 1$. Figure III - 20 shows the free enthalpy of mixing (ΔG_m) of these three systems as a function of the volume fraction of component 2, calculated from eq. III - 20. The effect of the chain length (N) on ΔG_m is demonstrated
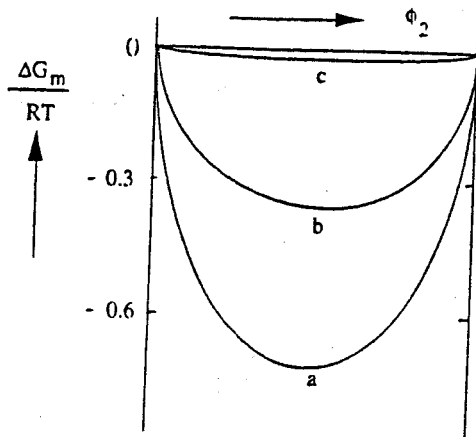
Figure III - 20. Free enthalpy of mixing as a function of the volume fraction ϕ for different combinations of N_1 and N_2: curve a: $N_1/N_2 = 1/1$; curve b: $N_1/N_2 = 1/1000$ and curve c: $N_1/N_2 = 100/1000$ [16].

very clearly. The decrease in ΔG_m is a maximum for low molecular components (curve a), whereas in the case of two polymeric components (curve c) the decrease in ΔG_m is minimal. In addition, these figures show that for the systems in question the components are miscible in all proportions. This means that ideal low molecular mixtures and athermal (polymer) solutions ($\Delta H_m = 0$) cannot demix. Demixing can occur only because of the existence of a positive interaction (enthalpy) term ($\Delta H_m > 0$). In the case of two polymers a very small positive enthalpy is sufficient to cause demixing because the entropy contribution is very small (see fig. III - 20, curve c). This explains why polymers are not miscible generally with each other. Again, for a polymer and a solvent, the entropy of mixing is not so high and a small positive enthalpy of mixing ($\Delta H_m > 0$) can once more cause demixing. In deriving eq. III - 27 it was assumed that $\Delta H_m = 0$, which is only the case for athermal solutions. In general for a binary system ΔG_m is given by

$$\Delta G_m = RT \, (n_1 \, \ln\phi_1 \, + \, n_2 \, \ln\phi_2 \, + \, n_1 \, \phi_2 \, \chi) \tag{III - 28}$$

in which an additional term has been added which originally has been derived as an enthalpic contribution [19] which contains the Flory-Huggins interaction parameter χ. In the original Flory theory χ was considered to be constant but for many systems it has been proven that this is not the case. In addition, χ is rather considered to be an excess parameter containing all non-ideality (see further at ternary systems, eq. III - 36). Differentiation with respect to n_1 and n_2 respectively, gives the partial molar free enthalpy difference of component 1 ($\Delta\mu_1$) and ($\Delta\mu_2$) upon mixing.

$$\Delta\mu_1 = \mu_1 - \mu_1^0 = \left(\frac{\partial\Delta G_m}{\partial n_1}\right)_{P,T,n_2} = RT\left(\ln\phi_1 - (1 - \frac{V_1}{V_2})\phi_2 + \chi\,\phi_2^2\right)$$

(III - 29)

and

$$\Delta\mu_2 = \mu_2 - \mu_2^0 = \left(\frac{\partial\Delta G_m}{\partial n_2}\right)_{P,T,n_1} = RT\left(\ln\phi_2 - (1 - \frac{V_2}{V_1})\phi_1 + \chi\frac{V_2}{V_1}\,\phi_1^2\right)$$

(III - 30)

In figure III - 20 it has been shown that the entropy of mixing is always positive and therefore components which mix without heat effect (ΔH_m = 0) are always miscible. In the case polymers the entropy term is very small and a positive enthalpy of mixing will cause demixing. Decreasing the temperature often causes an increase in the enthalpy of mixing.
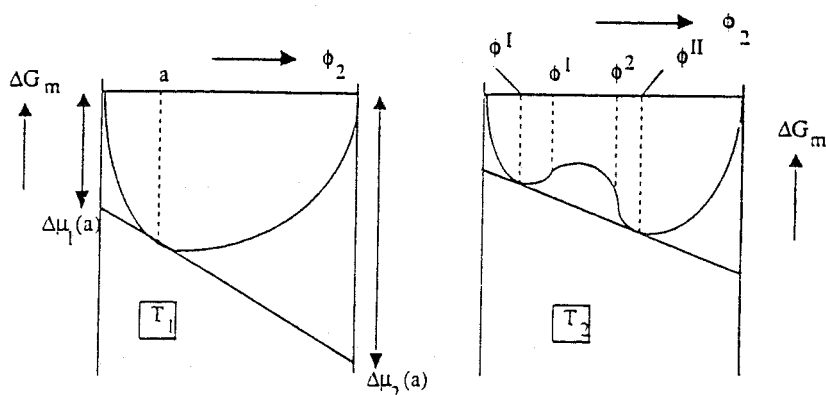
Figure III - 21. Free energy of mixing as a function of composition for a binary mixture. $T_2 < T_1$ ($H_m > 0$).

Figure III - 21 shows two plots of ΔG_m versus ϕ for two different temperatures. At the temperature T_1, (figure III - 21 left), the system is completely miscible over the whole composition range. This is indicated by the tangent to the ΔG_m curve which can be drawn at any composition. For example, at composition a the intercept at ϕ_2=0 gives $\mu_1(a)$ (the chemical potential of component 1 in the mixture of composition a) and the intercept at ϕ_2 = 1 gives $\mu_2(a)$. This means that the chemical potentials of both components 1 and 2 decrease (or $\Delta\mu_i < 0$). At the temperature T_2 (figure III - 21 right), the curve of ΔG_m exhibits an upward bend between ϕ^I and ϕ^{II}. These two points lie on the same tangent and are thus in equilibrium with each other. All the points on the tangent have the same derivative ($= \partial\Delta G_m/\partial n_i = \Delta\mu_i$), i.e. the chemical potentials are the same. In general, increasing the temperature leads to an increase in miscibility, which means that the enthalpy term becomes smaller. The two points on the tangent will approach each other and eventually they will coincide at the so-called critical point. This critical point is characterised by $(\partial^2\Delta G_m/\partial\phi^2_i) = 0$ and $(\partial^3\Delta G_m/\partial\phi^3_i) = 0$. Two points of inflection are also observed in figure III - 21 (right), i.e. ϕ^1 and ϕ^2. A point of inflection is the point at
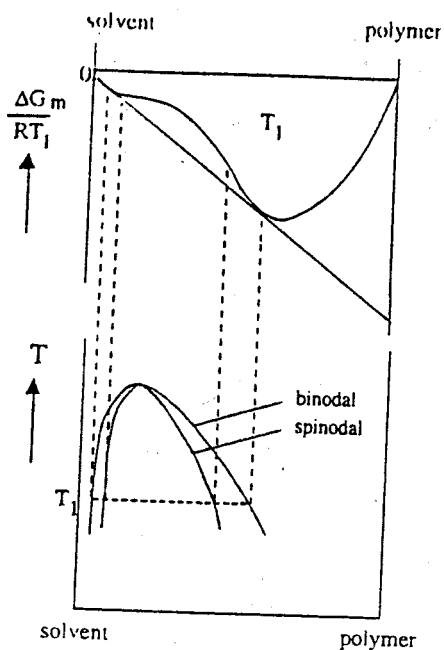
Figure III - 22. Temperature-composition phase diagram for a binary polymer-solvent system.

which a curve changes from being concave to convex or vice versa. These points are characterised by $(\partial^2\Delta G_m/\partial\phi^2_i = 0)$. Plotting the locus of the minima in a ΔG_m versus ϕ diagram leads to the binodal curve. The locus of the inflection points is called the spinodal. A typical temperature-composition diagram is depicted in figure III - 22.
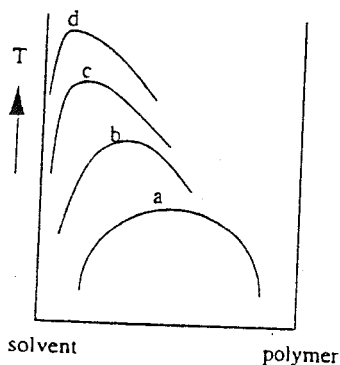
Figure III - 23. Schematic drawing of a binary mixture with a region of immiscibility. Binodal a: mixture of two low molecular weight components; binodals b, c, d: mixtures of a low molecular weight solvent and a polymer with increasing molecular weight.

The location of the miscibility gap for a given binary polymer/solvent system depends principally on the chain length of the polymer (see figure III - 23). As the chain lengthincreases the miscibility gap shifts towards the solvent axis as well as to higher temperatures. The critical point shifts towards the solvent axis, while the asymmetry of the binodal curve increases.

III.6.2   Demixing processes

III.6.2.1   Binary mixtures

In order to understand the mechanism of liquid-liquid demixing more easily, a binary system consisting of a polymer and a solvent will be considered. The starting point for preparing phase inversion membranes is a thermodynamically stable solution, for example one with the composition A at a temperature T_1 (with $T_1 > T_c$). All compositions with a temperature $T > T_c$ are thermodynamically stable in figure III - 24. As the temperature decreases demixing of the solution will occur when the binodal is reached. The solution demixes into two liquid phases and this is referred to as liquid-liquid (L - L) demixing.
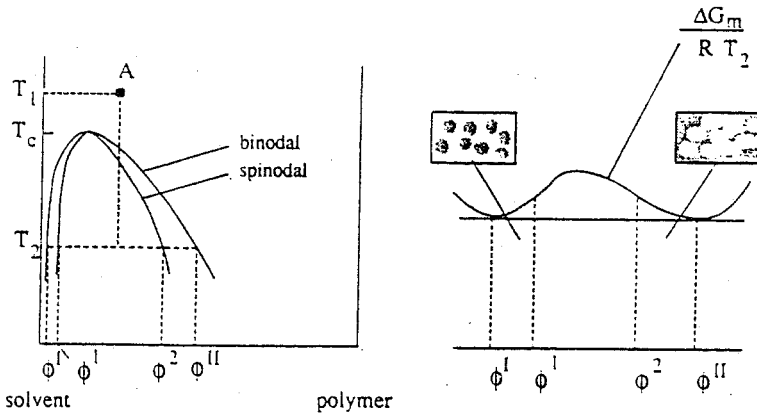
Figure III - 24. Demixing of a binary polymer solution by deceasing the temperature. T_c is the critical temperature.

Suppose that the temperature is decreased from T_1 to T_2. The composition A at temperature T_2 lies inside the demixing gap and is not stable thermodynamically. The curve of ΔG_m at temperature T_2 is also given in figure III - 24. At temperature T_2 all compositions between ϕ^I and ϕ^{II} can reduce their free enthalpies of mixing by demixing into two phases with of compositions ϕ^I and ϕ^{II} respectively (see figure III - 22). These two phases are in equilibrium with each other since they lie on the same tangent to the ΔG_m curve, i.e., the chemical potential in phase ϕ^I must be equal to that of phase ϕ^{II}.

Figure III - 25 again gives the curve of ΔG_m plotted versus composition at a given temperature (e.g. T_2), together with the first and second derivative. Two regions can clearly be observed from the second derivative (the lowest figure). Over the interval $\phi^1 < \phi < \phi^2$ the second derivative of ΔG_m with respect to ϕ is negative

$$\frac{\partial^2 \Delta G_m}{\partial \phi^2} < 0 \qquad \left(\phi^1 < \phi < \phi^2\right)$$

(III - 31)

implying that the solution is thermodynamically unstable and will demix spontaneously into very small interconnected regions of compositions ϕ^1 and ϕ^{II}.

The amplitude of small fluctuations in the local concentration increases in time as shown schematically in figure III - 26. In this way a lacy structure of a membrane is obtained, and the type of demixing observed is called spinodal demixing [23].
Over the intervals $\phi^I < \phi < \phi^1$ and $\phi^2 < \phi < \phi^{II}$, the second derivative of ΔG_m with respect to ϕ is positive and the solution is metastable. This means that there is no driving force for
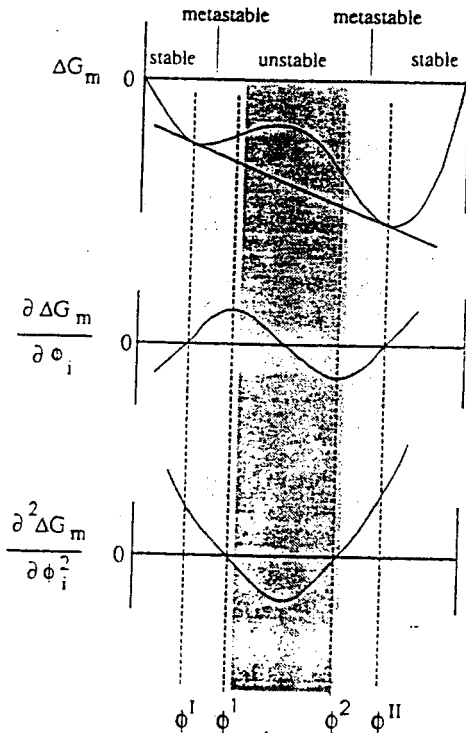
Figure III - 25. Plots of ΔG_m, the first derivative of ΔG_m and the second derivative of ΔG_m versus ϕ.

spontaneous demixing and the solution is stable towards small fluctuations in composition. Demixing can commence only when a stable nucleus has been formed. A nucleus is stable when it lowers the free enthalpy of the system; hence over the interval $\phi^I < \phi < \phi^I$ the nucleus must have a composition near ϕ^{II}, and over the interval $\phi^2 < \phi < \phi^{II}$ it must have a composition near ϕ^I.

$$\frac{\partial^2 \Delta G_m}{\partial \phi^2} > 0 \qquad \left(\phi^I < \phi < \phi^I\right) \quad \text{and} \quad \left(\phi^2 < \phi < \phi^{II}\right)$$

$$(III - 32)$$

After nucleation, these nuclei grow further in size by downhill diffusion whereas the composition of the continuous phase moves gradually towards that of the other equilibrium phase. The type of structure obtained after liquid-liquid demixing by nucleation and growth depends on the initial concentration.

Starting with a very dilute polymer solution (see figure III - 24), the critical point will be passed on the left hand side of the diagram and liquid-liquid demixing will start when the binodal is reached and a nucleus is formed with a composition near ϕ^{II}. The nuclei formed will grow further until thermodynamic equilibrium is reached (Nucleation and growth of the polymer-rich phase). A two-phase system has been formed now consisting of concentrated polymer droplets of composition ϕ^{II} dispersed in a dilute polymer solution with composition ϕ^I. In this way a latex type of structure is obtained which has little mechanical strength. When the starting point is a more concentrated solution (composition A in figure III - 23), demixing will occur by nucleation and growth of the polymer-lean phase (composition ϕ^I). Droplets with a very low polymer concentration will now grow further until equilibrium has been reached.
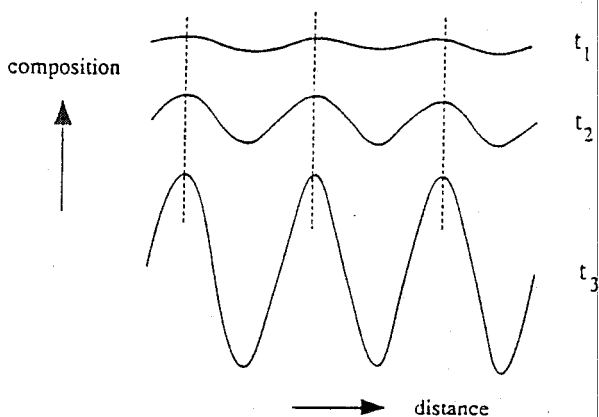
Figure III - 26. Spinodal demixing; increase in amplitude with increasing time ($t_3 > t_2 > t_1$).

As can be seen from figure III - 24, the location of the critical point is close to the solvent axis. Hence the binodal for a polymer/solvent system will be reached on the right-hand side of the critical point indicating that liquid-liquid demixing will occur by nucleation of the polymer-lean phase. These tiny droplets will grow further until the polymer-rich phase solidifies. If these droplets have the opportunity to coalesce before the polymer-rich phase has solidified, an open porous system will result.

III.6.2.2   Ternary systems

In addition to temperature changes, changes in composition brought about by the addition of a third component, a nonsolvent, can also cause demixing. Under these circumstances
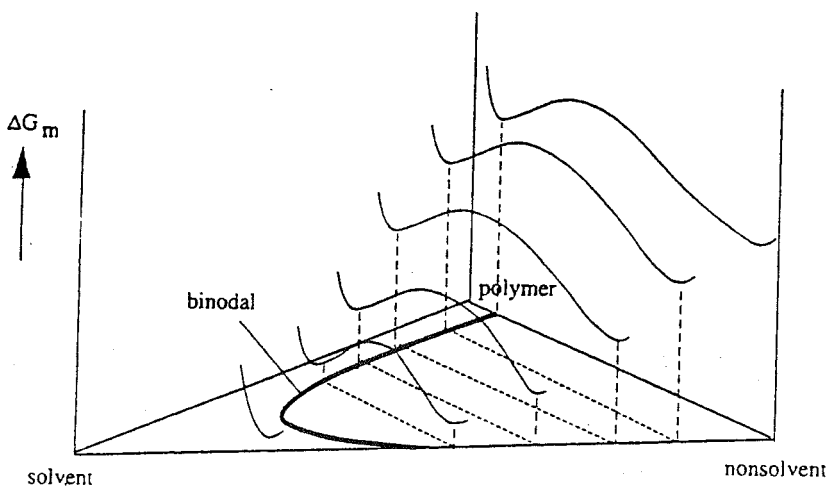
Figure III - 27.   Schematic drawing of the free enthalpy of mixing (ΔG_m) as a function of the composition for a ternary system consisting of polymer, solvent and nonsolvent.

we have a ternary system consisting of a solvent, a nonsolvent and a polymer. The liquid-liquid demixing area must now be represented as a three-dimensional surface. The free enthalpy of mixing is a function of the composition as can be seen from figure III - 27 where some drawings from the ΔG_m surface has been given at a certain temperature. All pairs of compositions with a common tangent plane to the ΔG_m surface consitute the solid line projected in the phase diagram, the binodal. Figure III - 28 shows a schematic illustration of the temperature dependency of such a three dimensional L - L demixing surface for a ternary system. The demixing area takes the form of a part of a beehive. As the temperature increases the demixing area decreases. and if the temperature is sufficiently high the components are miscible in all proportions. From this figure an isothermal cross-section can be obtained at any temperatureas shown in figure III - 29.
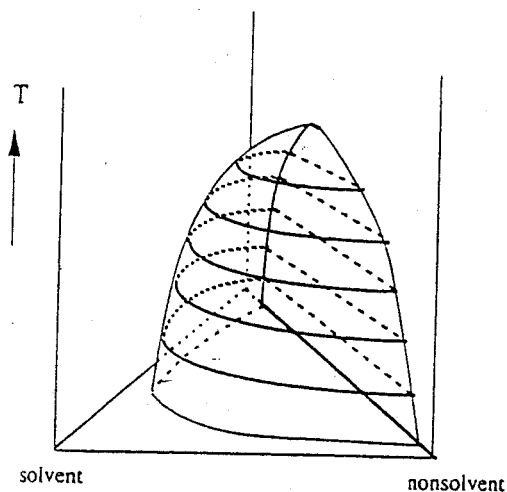
Figure III - 28. Three-dimensional representation of the binodial surface at various temperatures for a ternary system consisting of polymer, solvent and a nonsolvent.

The corners of the triangle represent the pure components polymer, solvent and nonsolvent. A point located on one of the sides of the triangle represents a mixture consisting of the two corner components. Any point within the triangle represents a mixture of the three components. In this region a spinodal curve and a binodal curve can be observed. The tie lines connect points on the binodal that are in equilibrium. A composition within this two-phase region always lies on a tie line and splits into two phases represented by the two intersections between the tieline and the binodal. As in the binary system, one end point of the tieline is rich in polymer and the other end point is poor in polymer. The binodal may be calculated numerically [24]. The tielines connect the two co-existing phases which are in equilibrium with each other, and these have the same chemical potential. By minimizing the following function the compositions of the end points may be obtained

$$F = \sum_i f_i^2 \qquad\qquad\qquad (III - 33)$$

with $f_i = (\Delta\mu_i' - \Delta\mu_i'')$, and i = 1, 2, 3. Furthermore, ' is the polymer lean phase and " is the polymer rich phase.

     The initial procedure for membrane formation from such ternary systems is always to prepare a homogeneous (thermodynamically stable) polymer solution. This will often correspond to a point on the polymer/solvent axis. However, it is also possible to add nonsolvent to such an extent that all the components are still miscible. Demixing will occur by the addition of such an amount of nonsolvent that the solution becomes thermodynamically unstable.
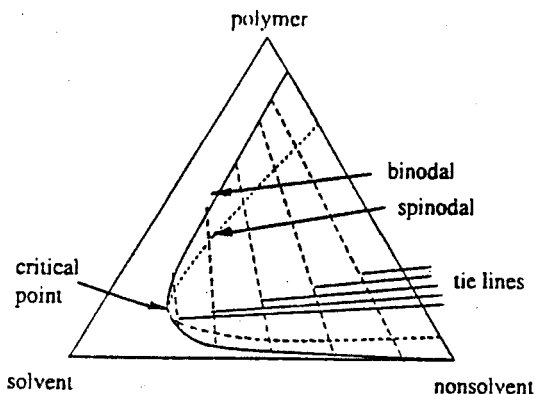
Figure III - 29. Schematic representation of a ternary system with a liquid-liquid demixing gap.

When the binodal is reached liquid-liquid demixing will occur. As in the binary system, the side from which the critical point is approached is important. In general, the critical point is situated at low to very low polymer concentrations (see figure III - 29). When the metastable miscibility gap is entered at compositions above the critical point, nucleation of the polymer-lean phase occurs. The tiny droplets formed consist of a mixture of solvent and nonsolvent with very little polymer dispersed in the polymer-rich phase, as described in the binary example (see figure III - 24). These droplets can grow further until the surrounding continuous phase solidifies via crystallisation, gelation or when the glass transition temperature has been passed (only in the case of glassy polymers !). Coalescence of the droplets before solidification leads to the formation of an open porous structure.

III.6.3   Crystallisation

Many polymers are partially crystalline. They consist of an amorphous phase without any ordering and an ordered crystalline phase. Crystallization may occur if the temperature of the solution is below the melting point of the polymer. Figure III - 30 shows the free enthalpy of mixing (ΔG_m) for a binary system polymer and solvent (or diluent) that shows no liquid-liquid demixing. However, below the melting point the chemical potential of the polymer in the solid state will be smaller than that in the solution. Therefore, the solution can lower its free enthalpy by phase separation in a pure crystalline solid state (ϕ_2) and a liquid state $(\phi_a$ in figure III - 30) which are in equilibrium with each other $(\Delta\mu_{2,L} = \Delta\mu_{2,S})$. The corresponding melting temperature for this mixture ϕ_a is T_1. This is shown schematically in figure III - 30 (right). $T_m{}^o$ is the melting point of the pure polymer and the melting point depression for a binary polymer-solvent system which has been derived by Flory [22] is given below.
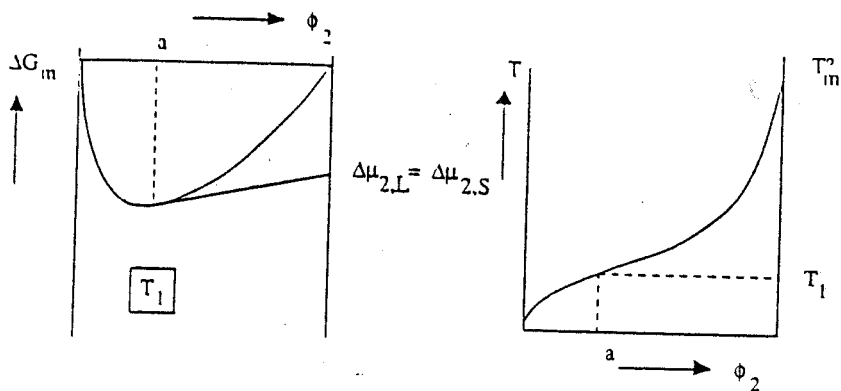
Figure III - 30. Schematic drawing of the free enthalpy of mixing for a binary system in which component 2 is able to crystallize (left) and the melting point curve as a function of the composition (right).

$$\frac{1}{T_m} - \frac{1}{T_m^0} = \frac{R}{\Delta H_f}\frac{V_2}{V_1}\left(\phi_1 - \chi\,\phi_1^2\right)$$

<div align="right">(III - 34)</div>

Here ϕ_1 is the volume fraction solvent and χ is the polymer-solvent interaction parameter. T_m is the melting temperature of the diluted polymer and ΔH_f is the heat of fusion per mole of repeating units, V_1 and V_2 are the molar volume of the solvent and of the polymer repeating unit respectively.

For a ternary system a similar ternary diagram can be constructed as shown in figure III - 31 only it is somewhat more complex since solid-liquid (S - L) demixing occurs in addition to liquid-liquid (L - L) demixing. A schematic ternary phase diagram with a semi-crystalline polymer is shown in figure III - 31. Except for the homogeneous region (I) where all components are miscible with each other and a region where L - L demixing occurs (II) other phases can be observed. The curve PQ is the crystallization curve and a composition somewhere in the region P-Q-polymer will contain crystalline pure polymer which is in equilibrium with a composition somewhere on the crystallization line PQ. The morphology of a semi-crystalline polymer is shown schematically in figure III - 32 (see also chapter II). In fact, many morphologies are possible extending between a completely crystalline and a completely amorphous conformation. The formation of crystalline regions in a given polymer depends on the time allowed for crystallisation from the solution. In very dilute solutions the polymer chains can form single crystals of the lamellar type, whereas in medium and concentrated solutions more complex morphologies occur, e.g. dendrites and spherulites.
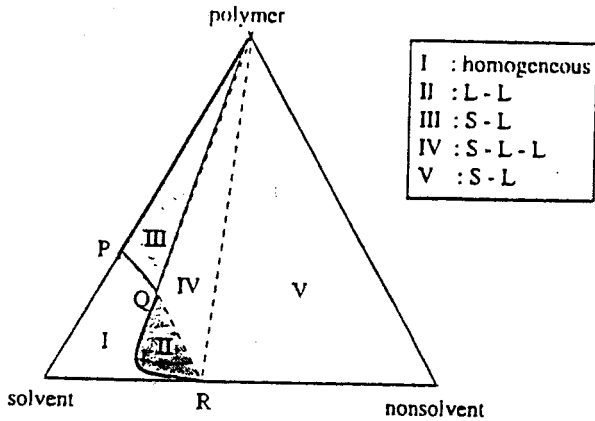
Figure III - 31. Ternary system of a semi-crystalline polymer, solvent and nonsolvent.

Membrane formation is generally a fast process and only polymers that are capable of crystallising rapidly (e.g.polyethylene, polypropylene, aliphatic polyamides) will exhibit an appreciable amount of crystallinity. Other semi-crystalline polymers contain a low to very low crystalline content after membrane formation. For example, PPO (2,6-dimethylphenylene oxide) shows a broad melting endotherm at 245°C [24]. Ultrafiltration membranes derived from this polymer, prepared by phase inversion, hardly contain any crystalline material indicating that membrane formation was too fast to allow crystallisation.
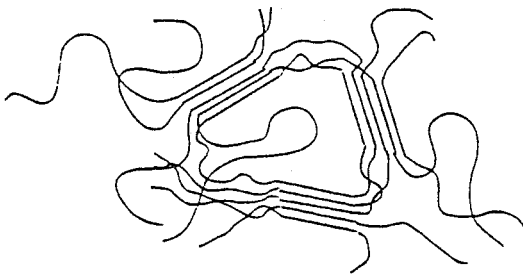
Figure III - 32. Morphology of a semi-crystalline polymer (fringed micelle structure).

III.6.4   Gelation

Gelation is a phenomenon of considerable importance during membrane formation, especially for the formation of the top layer. It was mentioned in the previous section that a large number of semi-crystalline polymers exhibit a low crystalline content in the final membrane because membrane formation is too fast. However, these polymers generally

undergo another solidification process, i.e. gelation. Gelation can be defined as the formation of a three-dimensional network by chemical or physical crosslinking. Chemical crosslinking, the covalent bonding of polymer chains by means of a chemical reaction, will not be considered here.

When gelation occurs, a dilute or more viscous polymer solution is converted into a system of infinite viscosity, i.e. a gel. A gel may be considered as a highly elastic, rubberlike solid. A gelled solution does not demonstrate any flow when a tube containing the solution is tilted. Gelation is, in fact, not a phase separation process and it may take place in a homogeneous system as well, consisting of a polymer and a solvent. Many polymers used as membrane materials exhibit gelation behaviour, e.g. cellulose acetate, poly(phenylene oxide), polyacrylonitrile, polymethylmethacrylate, poly(vinyl chloride) and poly(vinyl alcohol). Physical gelation may occur by various mechanisms dependent on the type of polymer and solvent or solvent/nonsolvent mixture used. In the case of semi-crystalline polymers especially, gelation is often initiated by the formation of microcrystallites. These microcrystallites, which are small ordered regions, are in fact the nuclei for the crystallisation process but without the ability to grow further. However, if these microcrystallites can connect various polymeric chains together, a three dimensional network will be formed. Because of their crystalline nature these gels are thermo-reversible, i.e. upon heating the crystallites melt and the solution can flow. Upon cooling, the solution again gels. The formation of helices often occurs during the gelation process. Gelation may also occur by other mechanisms, e.g. the addition of complexing ions (Cr^{3+}) or by hydrogen bonding.
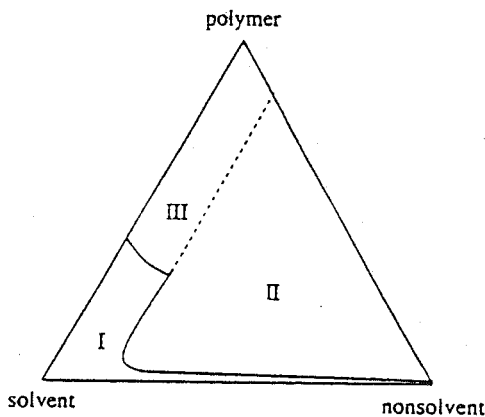
Figure III - 33. Isothermal cross-section of a ternary system containing a one-phase region (I), a two-phase region (II) and a gel region (III).

Gelation is also possible in completely amorphous polymers (e.g. atactic polystyrene [25]). In a number of systems the involvement of gelation in the membrane formation process often involves a sol-gel transition. This is shown schematically in figure III - 33. As can be

seen from this figure, a sol-gel transition occurs where the solution gels. The addition of a nonsolvent induces the formation of polymer-polymer bonds and gelation occurs at a lower polymer concentration. These sol-gel transitions have been observed in a number of systems, e.g. cellulose acetate/acetone/water [26], cellulose acetate/dioxan/water [26], poly(phenylene oxide)/trichloroethylene/octanol [26,27], poly(phenylene oxide)/ trichloroethylene /methanol [26,27].

III.6.5 *Vitrification*

There are polymers that neither show crystallization nor gelation behaviour. Nevertheless these polymers finally solidify during a phase inversion process. This solidification process may be defined as vitrification and may be defined as the stage where the polymer chains are frozen in a glassy state, i.e. it is a phase where the glass transition temperature has been passed and the mobility of the polymer chains have been reduced drastically. In the absence of gelation or crystallization, vitrification is the mechanism of solidification in any membrane forming system with an amorphous glassy polymer.
The glass transition of a polymer is reduced by the presence of an additive, i.e. a solvent or nonsolvent. This glass transition depression can been described by various theories from which the one of Kelley-Bueche is widely used [28] (see chapter II, eq. II - 6). A schematic phase diagram of the system PPO/trichloroethylene/methanol is shown in figure III - 34. Four regions can be observed;
i. a one-phase regions were all the components are miscible with each other
ii. a gel region where the polymer is able to form a three dimensional network, providing that certain conditions have been established. Gaides et al. [29] have determined a sol-gel transition for the system PPO-DMAc. However, a minimum time of 1 hour was necessary for gel formation whereas in immersion precipitation the time scale is much shorter.
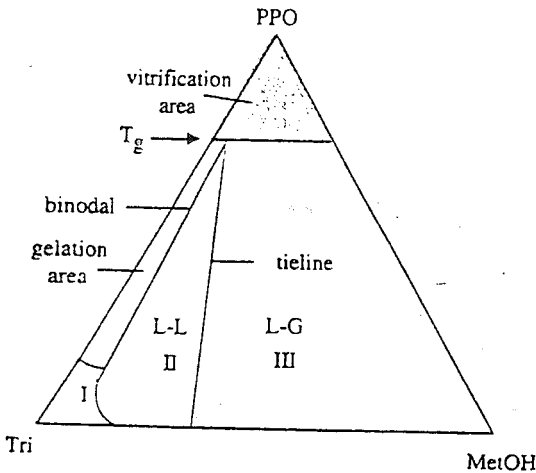
igure III - 34.   Schematic phase diagram of the quasi ternary system PPO/trichloroethylene/methanol

iii . a glassy region or vitrification region where the glass transition of the polymer has been passed. During immersion precipitation the diffusion of solvent and nonsolvent proceed according to their corresponding driving forces independent whether gelation occurs. The final solidification may be a combined gelation/vitrification process or in absence of gelation vitrification will be the dominant process.

iv. a two-phase region where liquid-liquid demixing occurs. In the figure only one tieline is given in which the polymer rich phase has entered the vitrification area. On the left side of this tieline (II) the (equilibrium) system is still a liquid whereas at the right side (III) vitrification of the polymer rich phase has been occurred.

III.6.6 Thermal precipitation.

Before describing immersion precipitation in detail, a short description of thermal precipitation or 'thermally-induced phase separation' (TIPS) will be given.

Table III.4   Some examples of thermally induced phase separation systems

polymer	solvent	ref.
polypropylene	mineral oil (nujol)	6
polyethylene	mineral oil (nujol)	6
polyethylene	dihydroxy tallow amine	30
polymethylmethacrylate	sulfolane	31
cellulose acetate/PEG	sulfolane	32
cellulose acetate/PEG	dioctyl phthalate	33
nylon-6	triethylene glycol	34
nylon-12	triethylene glycol	34
poly(4-methyl pentene)	mineral oil (nujol)	34

This process allows the ready preparation of porous membranes from a binary system consisting of a polymer and a solvent. Generally, the solvent has a high boiling point , e.g. sulfolane (tetramethylene sulfone, bp: 287 °C) or oil (e.g. nujol). The starting point is a homogeneous solution, for example composition A at temperature T_1 (see figure III - 24). This solution is cooled slowly to the temperature T_2. When the binodal is attained liquid-liquid demixing occurs and the solution separates into two phases, one rich in polymer and the other poor in polymer. When the temperature is decreased further to T_2, the composition of the two phases follow the binodal and eventually the compositions ϕ^I and ϕ^{II} are obtained. At a certain temperature the polymer-rich phase solidifies by crystallisation (polyethylene), gelation (cellulose acetate) or on passing the glass transition temperature (atactic polymethylmethacrylate).   Frequently, semi-crystalline polymers are used (polyethylene, polypropylene, aliphatic polyamides) which crystallise relatively fast, and hence a solid-liquid phase transition should be included.
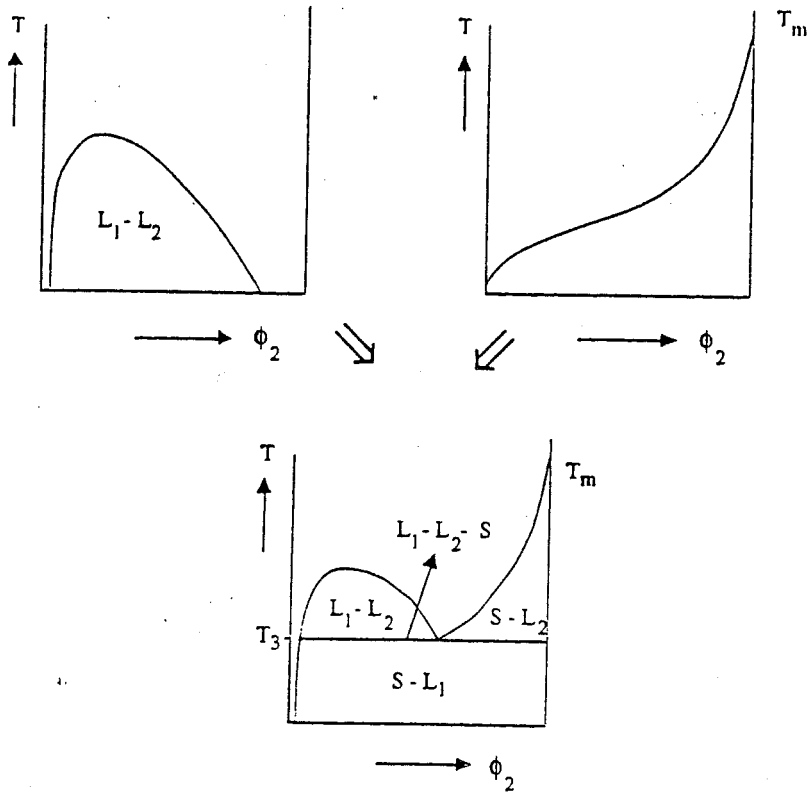
Figure III - 35.   Construction of a T - φ diagram for a binary system polymer-solvent. The
solidification line is the glass transition temperature line.

Figure III - 35 shows how the liquid-liquid (L - L) demixing area and the solid-liquid (S - L) demixing area can be combined. and now three areas can be observed, one where two liquids are in equilibrium (L_1 - L_2), one where solid phase and liquid phase are in equilibrium (S - L_2) and the last where liquid phase 1 is in equilibrium with the solid phase (S - L_1). Furthermore, there is a temperature T_3 where three phases are in equilibrium with each other.

In case of glassy amorphous polymers the melting line may be replaced by a vitrification line. This concept may be applied to various systems and table III - 4 summarises some examples of this thermally induced phase separation (TIPS) process.

III.6.7   Immersion precipitation

An interesting question remains after all these theoretical considerations: what factors are important in order to obtain the desired (asymmetric) morphology after immersion of a

polymer/solvent mixture in a nonsolvent coagulation bath? Other interesting questions are: why a more open (porous) top layer is obtained in some cases whereas in other cases a very dense (nonporous) top layer supported by an (open) sponge-like structure develops? To answer these questions and to promote an understanding of the basic principles leading to membrane formation via immersion precipitation a qualitative description will be given. For the sake of simplicity, the concept of membrane formation will be described in terms of three components: nonsolvent (1), solvent (2), and polymer (3). The effect of additives such as a second polymer or low molecular weight material will not be considered because the number of possibilities would then become so large and every (quarternary) or multi-component system has its own complex thermodynamic and kinetic descriptions.

Immersion precipitation membranes in their most simple form are prepared in the following way. A polymer solution consisting of a polymer (3) and a solvent (2) is cast as a thin film upon a support (e.g. a glass plate) and then immersed in a nonsolvent (1) bath. The solvent diffuses into the coagulation bath (J_2) whereas the nonsolvent will diffuse into the cast film (J_1). After a given period of time the exchange of solvent and nonsolvent has proceeded so far that the solution becomes thermodynamically unstable and demixing takes place. Finally a solid polymeric film is obtained with an asymmetric structure. A schematic representation of the film/bath interface during immersion is shown in figure III - 36.
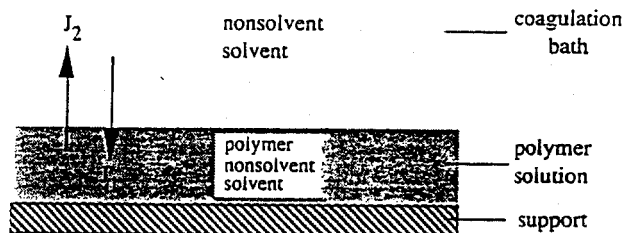
Figure   III - 36. Schematic representation of a film/bath interface. Components: nonsolvent (1), solvent (2) and polymer (3). J_1 is the nonsolvent flux and J_2 the solvent flux.

The local composition at any point in the cast film depends on the time. However, it is not possible to measure composition changes very accurately with time because the thickness of the film is only of the order of a few micrometers. Furthermore, sometimes membrane formation can occur instantaneously, i.e. all the compositional changes must be measured as a function of place and time within a very small time interval. Nevertheless, these composition changes can be calculated. Such calculations provide a good insight into the influence of various parameters upon membrane structure and performance.

Different factors have a major effect upon membrane structure. These are:

- choice of polymer
- choice of solvent and nonsolvent
- composition of casting solution
- composition of coagulation bath
- gelation and crystallisation behaviour of the polymer
- location of the liquid-liquid demixing gap
- temperature of the casting solution and the coagulation bath
- evaporation time

By varying one or more of these parameters, which are not independent of each other (!), the membrane structure can be changed from a very open porous form to a very dense nonporous variety.

Let us take polysulfone as an example. This is a polymer which is frequently used as a membrane material, both for microfiltration/ultrafiltration as well as a sublayer in composite membranes. These applications require an open porous structure, but in addition also asymmetric membranes with a dense nonporous top layer can also be obtained which are useful for pervaporation or gas separation applications. Some examples are given in table III.5 which clearly demonstrate the influence of various parameters on the membrane structure when the same system, DMAc/polysulfone (PSf), is employed in each case. How is it possible to obtain such different structures with one and the same system ? To understand this it is necessary to consider how each of the variables affects the phase inversion process. The ultimate structure arises through two mechanisms: i) diffusion

Table III.5   Influence of preparation procedure on membrane structure

evaporation PSf/DMAc $\Rightarrow$ pervaporation /gas separation
precipitation of 35% PSf/DMAc in water $\Rightarrow$ pervaporation/gas separation[a]
precipitation of 15% PSf/DMAc in water $\Rightarrow$ ultrafiltration
precipitation of 15% PSf/DMAc in water/DMAc $\Rightarrow$ microfiltration[b]

a) It will be shown later that integrally skinned asymmetric membranes can be prepared with completely defect-free toplayers

b) In order to obtain an open (interconnected) porous membrane an additive, e.g. poly(vinyl pyrrolidone) must be added to the polymer solution,.

processes involving solvent and nonsolvent occurring during membrane formation; and ii) demixing processes.

Demixing processes will first be considered. Two types of demixing are possible: i) liquid-liquid demixing; and ii) gelation, vitrification or crystallisation. In order to determine the composition or temperature at which the solution is no longer thermodynamically stable, turbidity or cloud points must be determined. Cloud points are defined as the moment when the solution changes from clear to turbid. They can be determined by a variety of techniques:

i) titration

In this case, the nonsolvent or a mixture of the solvent and nonsolvent is added slowly to a solution of the polymer and solvent. The turbidity point is determined visually.

ii) cooling

With this technique a tube is filled with either a binary mixture of polymer/solvent or a ternary mixture of polymer/solvent/nonsolvent and then sealed. The solution is homogenised at elevated temperature and the temperature of the thermostat bath is then decreased slowly at a constant cooling rate. At a certain temperature the solution is not thermodynamically stable anymore and demixing occurs which causes turbidity. This technique is easy to operate automatically by means of light transmission measurements [35], but can also be performed visually.

The latter technique, i.e. cooling, is preferred over the simple titration technique because it can discriminate as to what type of demixing process is occurring, liquid-liquid demixing or gelation/vitrification/crystallisation. The fact that gelation affects turbidity is often overlooked. Liquid-liquid demixing is a fast process and the rate of demixing is independent of the cooling rate, whereas the cooling rate is a very important parameter in the case of gelation/vitrification/crystallisation. Thus, by measuring the cloud point curves at different cooling rates it is possible to distinguish both processes. This is shown in figure III - 37 for cellulose acetate (CA)/water systems employing acetone, dioxan and tetrahydrofuran as the solvent [35]. System CA/THF/water, is independent of the cooling rate which means that the turbidity arises from liquid-liquid demixing. The same is true for the system CA/dioxan/water, in that the cloud points are independent of the cooling rate up to a certain polymer concentration. Above this concentration, however, gelation occurs at slower cooling rates, and liquid-liquid demixing at higher cooling rates. Finally in the system CA/acetone/water, the cloud point curves at both high and slow cooling rates are caused by gelation. This latter behaviour is also observed in the system poly(phenylene oxide)/trichloroethylene/octanol.
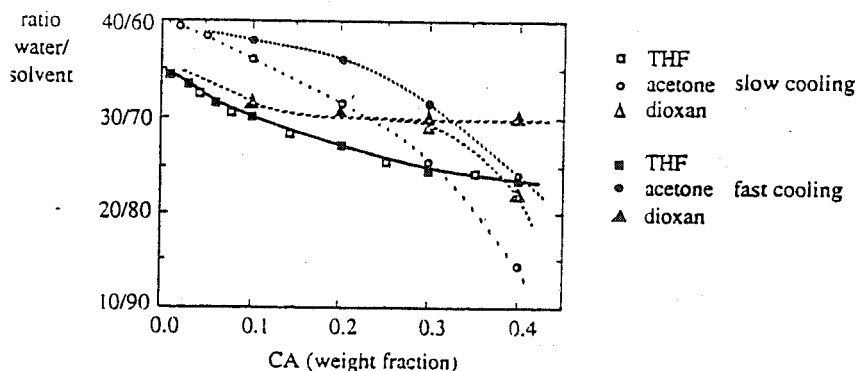
Figure III - 37.   Cloud point curves as a function of the polymer concentration measured at slow and fast cooling rates [35].

III.6.8 *Diffusional aspects*

Membrane formation by phase inversion techniques, e.g. immersion precipitation, is a non-equilibrium process which cannot be described by thermodynamics alone since kinetics have also to be considered. The composition of any point in the cast film is a function of place and time. In order to know what type of demixing process occurs and how it occurs, it is necessary to know the exact local composition at a given instant. However, this composition cannot be determined very accurately experimentally because the change in composition occurs extremely quickly (in often less than 1 second) and the film is very thin (less than 200 μm). However it can be described theoretically.

The change in composition may be considered as determined by the diffusion of the solvent (J_2) and of the nonsolvent (J_1) (see figure III - 36) in a polymer fixed frame of reference. The fluxes J_1 and J_2 at any point in the cast film can be represented by a phenomenological relationship:

$$J_i = - \sum_{j=1}^{2} L_{ij}(\phi_i, \phi_j) \frac{\partial \mu_j}{\partial x} \qquad (i = 1,2) \qquad \text{(III - 35)}$$

where $- \partial\mu/\partial x$, the gradient in the chemical potential, is the driving force for mass transfer of component i at any point in the film and L_{ij} is the permeability coefficient. From equation III - 35 the following relations may be obtained for the nonsolvent flux (J_1) and the solvent flux (J_2).

$$J_1 = - L_{11} \frac{d\mu_1}{dx} - L_{12} \frac{d\mu_2}{dx} \qquad \text{(III - 36)}$$

$$J_2 = - L_{21} \frac{d\mu_1}{dx} - L_{22} \frac{d\mu_2}{dx}$$

$$\text{(III - 37)}$$

As can be seen from the above equations, the fluxes in a given polymer/solvent/nonsolvent system are determined by the gradient in the chemical potential as driving force while they appear as well in the phenomenological coefficients. This implies that a knowledge of the chemical potentials, or better the factors that determine the chemical potential, is of great importance. An expression for the free enthalpy of mixing has been given by Flory and Huggins [22]. For a three component system (polymer/solvent/nonsolvent), the Gibbs free energy of mixing (ΔG_m) is given by:

$$\Delta G_m = RT \ (n_1 \ln\phi_1 + n_2 \ln\phi_2 + n_3 \ln\phi_3 + \chi_{12}n_1\phi_2 + \chi_{13}n_1\phi_3 + \chi_{23}n_2\phi_3) \qquad \text{(III - 38)}$$

where R is the gas constant and T the temperature in kelvin. The subscripts refer to

nonsolvent (1), solvent (2) and polymer (3). The number of moles and the volume fraction of component i are n_i and ϕ_i, respectively. χ_{ij} is called the Flory-Huggins interaction parameter. In a ternary system there are three interaction parameters: χ_{13} (nonsolvent/polymer), χ_{23} (solvent/polymer) and χ_{12} (solvent/nonsolvent). χ_{12} can be obtained from data on excess free energy of mixing which have been compiled recently [36] or from vapour-liquid equilibria. χ_{13} can be obtained from swelling measurements and χ_{23} can be obtained from vapour pressure or membrane osmometry [37]. The interaction parameters account for the non-ideality of the system and they contain an enthalpic as well as an entropic contribution. In the original Flory-Huggins theory they are assumed to be concentration independent, but several experiments have shown that these parameters generally depend on the composition [38 - 41]. To account for such dependence the symbol χ is often replaced by another symbol, i.e. g, indicating concentration dependency.

From eq. III - 38 it is possible to derive the expressions for the chemical potentials of the components since

$$\left(\frac{\partial \Delta G_m}{\partial n_i}\right)_{P,T,n_i} = \Delta\mu_i = \mu_i - \mu_i^o$$

(III - 39)

The eventual concentration dependency of the χ parameter must be taken into account in the differentiation procedure. The influence of the different interaction parameters χ (present in the driving forces) on the solvent flux and nonsolvent flux, and thus on the membrane structures obtained, will be described later.

The other terms present in the flux equations (eqs. III - 36 and III - 37) are phenomenological coefficients, and these must also be considered with respect to membrane formation. Also these coefficients are mostly concentration dependent. There are two ways of expressing the phenomenological coefficients when the relationships for the chemical potentials are known: i) in diffusion coefficients; and ii) in friction coefficients.

From a purely theoretical point of view, both approaches can be followed. However from a more practical point of view it is preferable to transform ternary parameters into binary parameters. The latter are much more readily measured. For this reason, it is preferable to relate the phenomenological coefficients to binary friction coefficients.

Friction coefficients may be defined by the Stefan-Maxwell flux equations:

$$\frac{\partial \mu_i}{\partial x} = \nabla\mu_i = -\sum_{j=1}^{3} R_{ij} c_j (v_i - v_j) \quad (i = 1, 2, 3)$$

(III - 40)

For three components, i.e. polymer, solvent and nonsolvent, three expressions may be obtained [35]:

$$\nabla\mu_1 = -R_{12} c_2 (v_1 - v_2) - R_{13} c_3 (v_1 - v_3)$$

(III - 41)

$$\nabla\mu_2 = -R_{21} c_1 (v_2 - v_1) - R_{23} c_3 (v_2 - v_3)$$

(III - 42)

$$\nabla \mu_3 = - R_{31} c_1 (v_3 - v_1) - R_{32} c_2 (v_3 - v_2)$$

(III - 43)

R_{ij} are the friction coefficients (in this case binary parameters) and v_i and v_j are the average velocities. c_i is the concentration of component i.

The following assumptions may be made:

i) R_{13} and R_{23} are constant at constant polymer concentration. This implies that the resistance forces acting between the solvent and the polymer or between the nonsolvent and the polymer are assumed to be constant at constant polymer concentration.

ii) R_{12} is constant at constant solvent/nonsolvent ratios. Here it is assumed that the resistance forces acting between the solvent and the nonsolvent are independent of the polymer concentration. R_{12} can be measured by determining of the mutual diffusion coefficients between the solvent and the nonsolvent. R_{23}, the frictional force between the polymer and the solvent can be obtained from sedimentation coefficients. R_{13}, the frictional force between the nonsolvent and the polymer, cannot be measured and this parameter must be estimated. Both R_{13} and R_{23} depend on the polymer concentration and it is reasonable to assume that the relationship between R_{23} and the polymer concentration is equal to that between R_{13} and the polymer concentration.

Returning to the diffusion processes during membrane formation, various parameters have now been described. However, there is another problem which has not yet been discussed. In most cases there is a (large) difference between the casting thickness and the ultimate membrane thickness. This implies that during the formation process the boundary between the nonsolvent bath and the casting solution moves, as is shown in figure III - 38. For this reason, it is necessary to introduce a position coordinate to correct for this moving boundary.

The immersion process starts at time t = 0. At all times t > 0, solvent will diffuse out of the film and nonsolvent will diffuse in. If there is a net volume outflow (solvent flux larger than nonsolvent flux) then the film/bath interface is shifted from z = 0. i.e. the actual thickness is reduced. This process will continue until equilibrium is reached (at time t = t) and the membrane has been formed. In order to describe diffusion processes involving a moving boundary adequately, a position coordinate m must be introduced (eq. III - 44)
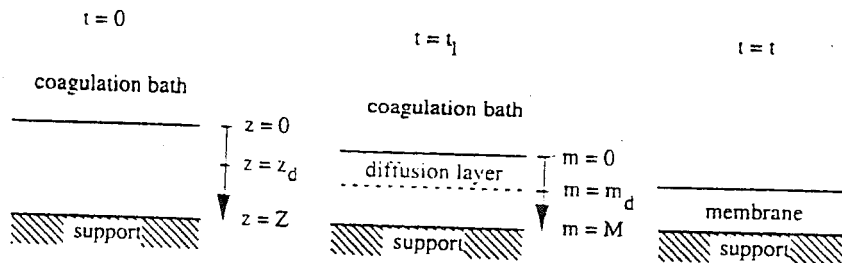
Figure III - 38.   Schematic drawing of the immersion process at different times.

[35]. The film/bath interface is now always at position m = 0, independent of the time. The position of the film/support interface is also independent of the time (see figure III - 38).

$$m(x, t) = \int_0^x \phi_3(x, t)\, dx$$

$$(III - 44)$$

$$(dm)_t = \phi_3\ (dx)_t$$

$$(III - 45)$$

In the m-coordinate

$$\frac{\partial(\phi_i/\phi_3)}{\partial t} = \frac{\partial J_i}{\partial m} \qquad i = 1, 2$$

$$(III - 46)$$

Combination of eqs. III - 36, III - 37 and III - 46 yields:

$$\frac{\partial(\phi_1/\phi_3)}{\partial t} = \frac{\partial}{\partial m}\left[v_1\,\phi_3\,L_{11}\frac{\partial\mu_1}{\partial m}\right] + \frac{\partial}{\partial m}\left[v_1\,\phi_3\,L_{12}\frac{\partial\mu_2}{\partial m}\right]$$

$$(III- 47)$$

$$\frac{\partial(\phi_2/\phi_3)}{\partial t} = \frac{\partial}{\partial m}\left[v_2\,\phi_3\,L_{21}\frac{\partial\mu_1}{\partial m}\right] + \frac{\partial}{\partial m}\left[v_2\,\phi_3\,L_{22}\frac{\partial\mu_2}{\partial m}\right]$$

$$(III- 48)$$

The main factor determining the type of demixing process is the local concentration in the film. Using eqs. III - 47 and III - 48 it is possible to calculate these concentrations (ϕ_1, ϕ_2, ϕ_3) as a function of time. Thus at any time and any place in a cast film the demixing process occurring can be calculated: in fact the concentrations are calculated as a function of place and time and the type of demixing process is deduced from these values. However, one should note that a number of assumptions and simplifications are involved in this model. Thus heat effects, occurrence of crystallisation, molecular weight distributions are not taken into account. Nevertheless, it will be shown in the next section that the model allows the type of demixing to be established on a qualitative basis and is therefore useful as a first estimate. Furthermore, it allows an understanding of the fundamentals of membrane formation by phase inversion.

III.6.9 Mechanism of membrane formation
It is shown in this section that two types of demixing process resulting in two different types of membrane morphology can be distinguished:
- *instantaneous liquid-liquid demixing*
- *delayed onset of liquid-liquid demixing*

Instantaneous demixing means that the membrane is formed immediately after

immersion in the nonsolvent bath whereas in the case of delayed demixing it takes some time before the membrane is formed.

The occurrence of these two distinctly different mechanisms of membrane formation can be demonstrated in a number of ways: by calculating the concentration profiles; by light transmission measurements; and visually.

The best physical explanation is given by a calculation of the concentration profiles. To calculate the concentration profiles in the polymer film during the (delayed demixed type of) phase inversion process, some assumptions and considerations must be made[35]:

- diffusion in the polymer solution is described by eqs. III - 34 and III - 35.
- diffusion in the coagulation bath is described by Fick's law
- no convection occurs in the coagulation bath
- thermodynamic equilibrium is established at the film/bath interface.

    μ_i (film) = μ_i (bath)   i = 1, 2, 3
- volume fluxes at the film/bath interface are equal, i.e.

    J_i (film) = J_i (bath)   i = 1, 2

In addition, a number of parameters must be determined experimentally:

- the thermodynamic binary interaction parameters (the χ parameters or the concentration dependent g parameters) appearing in the expressions for the chemical potentials.

    * g_{12}: from calorimetric measurements yielding values of the excess free energy of mixing, from literature compilations of G^E and activity coefficients, from vapour-liquid equilibria and from Van Laar, Wilson, or Margules equations or from UNIFAC.

    * g_{13}: from equilibrium swelling experiments or from inverse gas chromatography (see section).

    * g_{23}: from membrane osmometry or vapour pressure osmometry (see section)

- the binary friction coefficients which are related to the ternary phenomenological coefficients L_{ij}.

    * R_{12}: from binary diffusion measurements

    * R_{23}: from sedimentation coefficients

    * R_{13}: which cannot be determined experimentally. This parameter has to be related to R_{23}.

Two types of demixing process will now be distinguished leading to different types of membrane structure. These two different types of demixing process may be characterised by the instant when liquid-liquid demixing sets in. Figure III - 39 shows the composition path of a polymer film schematically at the very moment of immersion in a nonsolvent bath (at t <1 second). The composition path gives the concentration at any point in the film at a particular moment. For any other time another compositional path will exist.
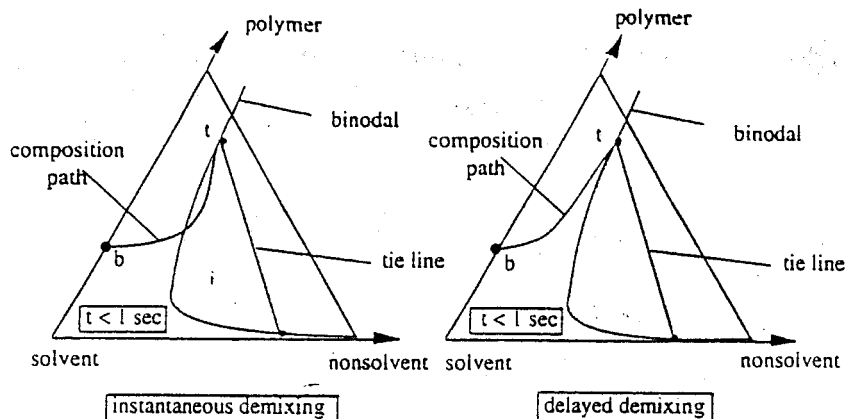
Figure III - 39.   Schematic composition path of the cast film immediately after immersion; t
                    is the top of the film and b is the bottom. The left-hand figure shows
                    instantaneous liquid-liquid demixing whereas the right-hand figure shows the
                    mechanism for the delayed onset of liquid-liquid demixing.

Because diffusion processes start at the film/bath interface, the change in composition is first noticed in the upper part of the film. This change can also be observed from the composition paths given in figure III - 39. Point t gives the composition at the top of the film while point b gives the bottom composition. Point t is determined by the equilibrium relationship at the film/bath interface μ_i (film) = μ_i (bath). The composition at the bottom is still the initial concentration in both examples. In figure III - 39 (left) places in the film beneath the top layer t have crossed the binodal, indicating that liquid-liquid demixing starts immediately after immersion. In contrast, figure III - 39 (right) indicates that all compositions directly beneath the top layer still lie in the one-phase region and are still miscible. This means that no demixing occurs immediately after immersion. After a longer time interval compositions beneath the top layer will cross the binodal and liquid-liquid demixing will start in this case also. Thus two distinctly different demixing processes can be distinguished and the resulting membrane morphologies are also completely different.

When liquid-liquid demixing occurs instantaneously, membranes with a relatively porous top layer are obtained. This demixing mechanism results in the formation of a porous membrane (microfiltration/ultrafiltration type). However, when liquid-liquid demixing sets in after a finite period of time, membranes with a relatively dense top layer are obtained.This demixing process results in the formation of dense membranes (gas separation/pervaporation). In both cases the thickness of the top layer is dependent on all kind of membrane formation parameters (i.e. polymer concentration, coagulation procedure, additives, see section III - 7).

These two types of formation mechanism can also be distinguished by the

application of numerical procedures, as well as by simple light transmission measurements or just by visual observation. In these latter cases only qualitative information can be obtained, however. Light transmission measurements enable observations of the length of time necessary before turbidity occurs. A suitable experimental set-up is shown in figure III - 40.
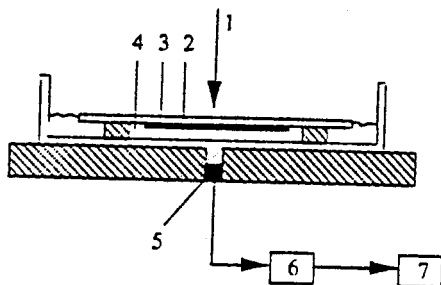
Figure III - 40.   Light transmission set-up: 1, light source: 2, glass plate; 3, cast polymer film: 4, coagulation bath: 5, detector; 6, amplifier; 7, recorder.

A cast film is immersed in a coagulation bath and the light transmittance through the film measured as a function of time. When inhomogenities appear in the film as a result of liquid-liquid demixing, the light transmittance decreases. Differences between instantaneous demixing and delayed liquid-liquid demixing can thus be observed quite readily. Some schematically drawn light transmission curves are shown in figure III - 41. From this figure it can be seen that systems a and b demix instantaneously, since the light transmission decreases very rapidly. In system c a delayed onset of demixing can be observed. with the decrease in light transmittance commencing only after a definite period of time. Delayed demixing also occurs for system d, with a relatively long period of time being necessary before the demixing process commences.

The simplest technique for discriminating between instantaneous demixing and the delayed onset of liquid-liquid demixing is via visual observation. A polymer solution is cast upon a glass plate and immersed in a nonsolvent bath. When instantaneous demixing occurs, in most cases the membrane immediately lifts off the glass plate and is no longer transparent. On the other hand, when a finite period of time is necessary to effect lift off from the glass plate or for the film to become non-transparent (opaque) a delayed onset of liquid-liquid demixing has occurred. The following two examples may be quoted: a solution of polysulfone (PSf) in dimethylformamide (DMF) when cast as a film and immersed in water shows instantaneous demixing, whereas a solution of cellulose acetate (CA) in acetone similar prepared exhibits delayed onset of demixing on water immersion.
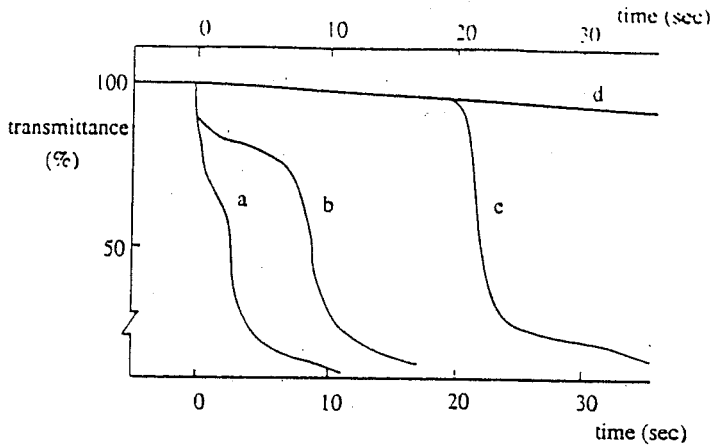
Figure III - 41. Light transmission curves: a and b, instantaneous demixing; c and d, delayed onset of liquid-liquid demixing.

The question arises as to what parameters are important for membrane morphology and how can the latter be controlled? In section III - 7 the influence of the most important membrane formation parameters will be described in relation to the membrane structure obtained. Other topics which have to be described is the determination of the various interaction parameters. The interaction parameter between solvent and nonsolvent (χ_{12} or g_{12} (concentration dependent) will be described in section III.7. Here, the determination of the other two parameters, polymer-nonsolvent (χ_{13}) and polymer-solvent (χ_{23}) will be described briefly.

Polymer-nonsolvent interaction parameter (χ_{13})
The interaction between polymer and nonsolvent is not only of interest for membrane formation but also in transport phenomena were sorption may effect drastically the performance. Sorption measurements are the most simple method to determine this interaction parameter. If a polymer is in contact with a liquid which is not a solvent, the liquid will diffuse into the poymer until equilibrium has been reaches, i.e the chemical potential of the liquid in the liquid phase is equal to the chemical potential of the liquid inside the polymer. Due to this diffusion osmotic swelling will occur, i.e. the free enthalpy change in this process contains not only a mixing term but an elastic free enthalpy term as well. The membrane or polymer can be considered as a swollen network with crosslinks caused by crystalline regions, chain entanglements or van der Waals interactions. The swelling behaviour may be described by the Flory-Rehner theory [42]. If a nonsolvent or penetrant is brought in contact with a polymer then the free energy change consists of two terms, thr free enthalpy of mixing and the elastic free enthalpy which is induced by the osmotic swelling. At equilibrium the chemical potential of the penetrant in both phases are equal, i.e [42]

$$\left(\ln \phi_1 - (1 - \frac{V_1}{V_2}) \phi_2 + \chi \phi_2^2 \right) + \frac{V_1}{M_c V_2} (\phi_2^{1/3} - 0.5 \phi_2) = 0$$

(III - 49)

The first term represents the mixing term (see also eq. III - 28) and the second one is the elastic contribution. M_c can be interpreted as the average molecular weight between two crosslinks and ϕ_1 and ϕ_2 are the volume fraction of penetrant and polymer, respectively. In cases where the interaction between polymer and penetrant is relatively low, i.e the weight increase is less than $\approx 30\%$, the elastic term may be neglected and eq. becomes.

$$\chi = - \frac{\ln (1 - \phi_2) + \phi_2}{\phi_2^2}$$

(III - 50)

By determining the weight increase the volume fraction of polymer can be estimated and then the polymer-nonsolvent interaction parameter can be determined.

polymer-solvent interaction parameter (χ_{23})

Vapour pressure depression and membrane osmometry are the most common methods to determine the polyer-solvent interaction parameter. The latter method will be described briefly. In a membrane osmometer a dilute polymer solution has been separated from pure solvent by means of a membrane. The membrane is permeable for solvent molecules but not for polymer molecules. Due to a chemical potential difference solvent molecules will diffuse from the diluted phase to the concentrated phase and this results in a pressure increase which is called the osmotic pressure π (see also section VI - 2 for a more detailed description of osmosis). The osmotic pressure is given by

$$\Delta \mu_1 = \mu_1 - \mu^{\circ}_1 = RT \ln a_1 = - \pi V_1$$

(III - 51)

from the Flory-Huggins theory the activity of the solvent has been derived as has been given. Using a serie expression for $\ln \phi_1$

$$\ln \phi_1 = \ln (1 - \phi_2) = - \phi_2 - \frac{1}{2} \phi_2^2 - \frac{1}{3} \phi_2^3 - \ldots\ldots\ldots\ldots$$

(III - 52)

Frequently only the first two terms in a series are employed and substitution of eq. III - 51 in III - 52 gives

$$RT \ln a_1 = RT \left(- \frac{V_1}{V_2} \phi_2 - (0.5 - \chi) \phi_2^2 \right) = - \pi V_1$$

(III - 53)

or

$$\pi = \frac{RT}{V_2} \phi_2 + \frac{RT}{V_1} (0.5 - \chi) \phi_2^2$$

(III - 54)

Determination of the osmotic pressure then gives the interaction parameter polymer-solvent. Frequently this parameter is concentration dependent and then more experiments are required to estimate the concentration dependency.

III.7.   Influence of various parameters on membrane morphology

In the previous section the thermodynamic and kinetic relationships have been given to describe membrane formation by phase inversion processes. These relationships contain various parameters which have a large impact on the diffusion and demixing processes and hence on the ultimate membrane morphology. It has been shown that two different types of membranes may be obtained, the porous membrane (microfiltration and ultrafiltration) and the nonporous membrane (pervaporation and gas separation), depending on the type of formation mechanism, i.e. instantaneous demixing or delayed onset of demixing, involved.

In this respect the choice of the polymer is not so important, although it directly influences the range solvents and nonsolvents that can be used. In this section the effect of various parameters on membrane morphology will be described. Two widely used polymers, polysulfone (PSf) and cellulose acetate (CA) will be taken as examples. The following factors will be described:
- the choice of solvent/nonsolvent system;
- the polymer concentration;
- the composition of the coagulation bath; and
- the composition of the polymer solution.

There are a number of other parameters, in addition to those listed, such as the use of additives (low molecular weight as well as high molecular weight components), the molecular weight distribution, the ability to crystallise or aggregate, the temperature of the polymer solution and of the coagulation bath, etc., that also influence the ultimate structure obtained after phase inversion. These latter factors will not be considered here.

III.7.1   Choice of solvent/nonsolvent system

One of the main variables in the immersion precipitation process is the choice of the solvent/nonsolvent system. In order to prepare a membrane from a polymer by phase inversion the polymer must be soluble. Although one or more solvents may be suitable for the chosen polymer, the solvent and nonsolvent must be completely miscible. Water is frequently used as a nonsolvent but other nonsolvents can also be used. Some solvents for cellulose acetate and polysulfone which are miscible with water are listed in table III.6. The solubility of these organic solvents with water must be considered further. As described in the previous section, the miscibility of components of all kind is determined by the free enthalpy of mixing

$$\Delta G_m = \Delta H_m - T \Delta S_m \qquad\qquad (III - 2)$$

For ideal solutions $\Delta H_m = 0$ and $\Delta S_m = \Delta S_{m,ideal}$. However, mixtures of organic solvents

Table III.6 Solvents for cellulose acetate and polysulfone

cellulose acetate	polysulfone
dimethylformamide (DMF)	dimethylformamide (DMF)
dimethylacetamide (DMAc)	dimethylacetamide (DMAc)
acetone	dimethylsulfoxide (DMSO)
dioxan	formylpiperidine (FP)
tetrahydrofuran (THF)	morpholine (MP)
acetic acid (HAc)	N-methylpyrrolidone (NMP)
dimethylsulfoxide(DMSO)	

and water deviate strongly from ideal behaviour, and most organic mixtures do not behave ideally because of the existence of polar interactions or hydrogen bonding. Only very weakly interacting solvents, such as alkanes, can be considered ideal. For non-ideal systems the free enthalpy of mixing for 1 mol of mixture becomes

$$\Delta G_m/RT = x_1 \ln\phi_1 + x_2 \ln\phi_2 + g_{12}(\phi) \, x_1 \, \phi_2$$ (III - 55)

where ϕ and x are the volume fraction and mole fraction respectively in the binary system. The parameter g_{12} can be considered a free energy term containing both enthalpic and entropic contributions. As can be seen from eq. III - 55 the interaction parameter is considered to be concentration-dependent and hence the symbol χ has been replaced by g; when this parameter increases the mutual affinity and miscibility decrease and when $g_{12} \Rightarrow$ > 0 the mixture will tend towards ideality.

The excess free enthalpy of mixing (G^E) is the difference between the actual free enthalpy of mixing (ΔG_m) and the ideal free enthalpy of mixing ($\Delta G_{m,ideal}$):
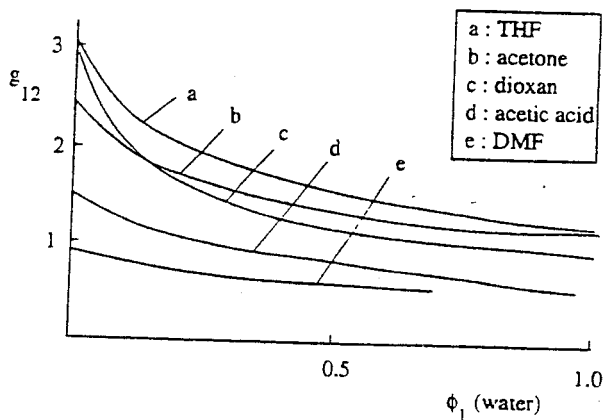
Figure III - 42. The interaction parameters g_{12} for various solvent/water systems calculated from eq. III - 58 and literature data on G^E [43]

$$G^E = \Delta G_m - \Delta G_{m,ideal} \qquad (III - 56)$$

Since

$$\Delta G_{m\ ideal} = RT (x_1 \ln x_1 + x_2 \ln x_2) \qquad (III - 57)$$

substitution of eqs. III - 55 and III - 57 into III - 56 gives

$$g_{12} = \frac{1}{x_1 \phi_2} \left[x_1 \ln \frac{x_1}{\phi_1} + x_2 \ln \frac{x_2}{\phi_2} + \frac{G^E}{RT} \right] \qquad (III - 58)$$

If G^E is known, g_{12} can be calculated as a function of composition for any binary mixture (ϕ refers to the volume fraction in the binary solution and x to the mol fraction, respectively). In fact, G^E represents the non-ideal part of the free enthalpy of mixing and can be expressed as

$$G^E = RT [x_1 \ln \gamma_1 + x_2 \ln \gamma_2] \qquad (III - 59)$$

The activity coefficients can be obtained from semi-empirical expressions such as van Laar, Margules or Wilson. These equations have been summarized in table III.7.

Table III.7   Van Laar, Margules, and Wilson equation

$$\ln \gamma_1 = \frac{A_{12}}{\left(1 + \frac{A_{12} x_1}{A_{21} x_2}\right)^2}$$

$$\ln \gamma_2 = \frac{A_{21}}{\left(1 + \frac{A_{21} x_2}{A_{12} x_1}\right)^2} \qquad \text{v Laar}$$

$$\ln \gamma_1 = A_{12}^I x_2^2 \left[1 + 2x_1 \left(\frac{A_{21}^I}{A_{12}^I} - 1 \right) \right]$$

$$\text{Margules}$$

$$\ln \gamma_2 = A_{21}^I x_1^2 \left[1 + 2x_2 \left(\frac{A_{12}^I}{A_{21}^I} - 1 \right) \right]$$

$$\ln \gamma_1 = - \ln (x_1 + \Lambda_{12} x_2) + x_2 \left[\frac{\Lambda_{12}}{x_1 + \Lambda_{12} x_2} - \frac{\Lambda_{21}}{x_2 + \Lambda_{21} x_1} \right] \quad \text{Wilson}$$

$$\ln \gamma_2 = - \ln (x_2 + \Lambda_{21} x_1) - x_1 \left[\frac{\Lambda_{12}}{x_1 + \Lambda_{12} x_2} - \frac{\Lambda_{21}}{x_2 + \Lambda_{21} x_1} \right]$$

Large compilations exist to estimate the activity coefficients in binary or ternary mixtures based on one of these expressions [44]. It can not be anticipated which of the equations fit the experimental value the best but there is a slight preference to apply the Wilson equation.

G^E can also be determined experimentally and a large number of data are available in the literature [36]. It is also possible to use vapour-liquid equilibria in determining g_{12}. For a number of mixtures of organic solvents with water, the g_{12} parameters are plotted as a function of the volume fraction of water (figure III - 42).

It can be seen from this figure that g_{12} is strongly concentration-dependent. Furthermore, acetone/water and THF/water mixtures show very high g_{12} values (low mutual affinity) whereas DMF shows very low values of g_{12} (high mutual affinity).

How does the choice of the solvent now influence the membrane structure when water is used as the nonsolvent and cellulose acetate as the polymer? The first interesting point is that the slope of the tie lines, which connect the two phases in equilibrium in the two-phase region, is less steep when the mutual affinity (or miscibility) between the solvent and the nonsolvent decreases [35,43]. The binodal and tie lines are depicted in figure III - 43 for the system water/solvent/CA, where the tie lines become steeper as the miscibility with water increases in the order DMF > dioxan > acetone >THF. Light transmission measurements conducted on the same water/solvent/CA systems are shown in figure III - 44. When DMSO (e), DMF (d) and dioxan (c) are used as the solvent, instantaneous demixing occurs. Only when the solvent is added to the coagulation bath is
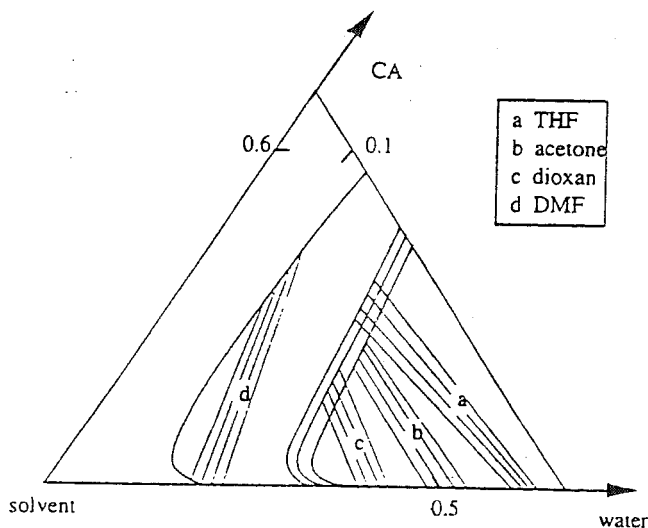
Figure III - 43. Calculated binodals and tie lines for ternary CA/solvent/water systems [35].

delayed demixing observed. In the case of dioxan about 15% solvent is required in the water bath, in the case of DMF about 45% and in the case of DMSO about 65%. This means that if the mutual affinity of the solvent and nonsolvent increases, more solvent is

required in the nonsolvent coagulation bath to effect delayed demixing. On the other hand, a delayed onset of demixing always occurs with acetone and THF even if there is no solvent in the water bath.
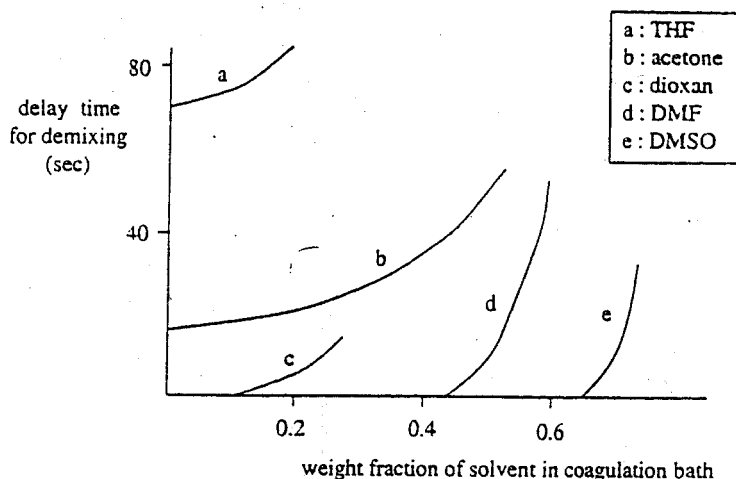
Figure III - 44.   Delay time of demixing for 15% cellulose acetate/solvent solutions in water [35].

Again a striking point is that the tendency towards a delayed onset of demixing decreases in the sequence THF > acetone > dioxan > DMF > DMSO, the same as for the decrease in mutual miscibility with water.

What is the influence of the choice of solvent/nonsolvent system on membrane morphology? As described in the previous section the two different mechanisms for membrane formation lead to two different structures, the difference between the two mechanisms being characterised by the instant at which the onset of liquid-liquid demixing occurs. From the observations depicted in figure III - 44 it is to be expected that polymers with THF or acetone as the solvent and water as the nonsolvent result in a dense membrane (delayed demixing). When DMSO and DMF are used as solvents and water as the nonsolvent, a porous type of membrane will be obtained (instantaneous demixing). Indeed, polysulfone/DMF/water, cellulose acetate/DMSO/water and cellulose acetate/DMF/water systems give ultrafiltration membranes [39]. On the other hand, cellulose acetate/acetone/water and polysulfone/THF/water systems give very dense pervaporation types of membrane without any macroporosity [41].

A number of other nonsolvents can be used besides water. However, thermodynamic mixing data are not available for all kinds of liquid mixtures and should therefore be measured or derived from group contribution theories. In contrast, light transmission measurements may readily be performed. If water is replaced by another nonsolvent, e.g. an alcohol, completely different membrane structures and consequently different membrane properties are obtained.
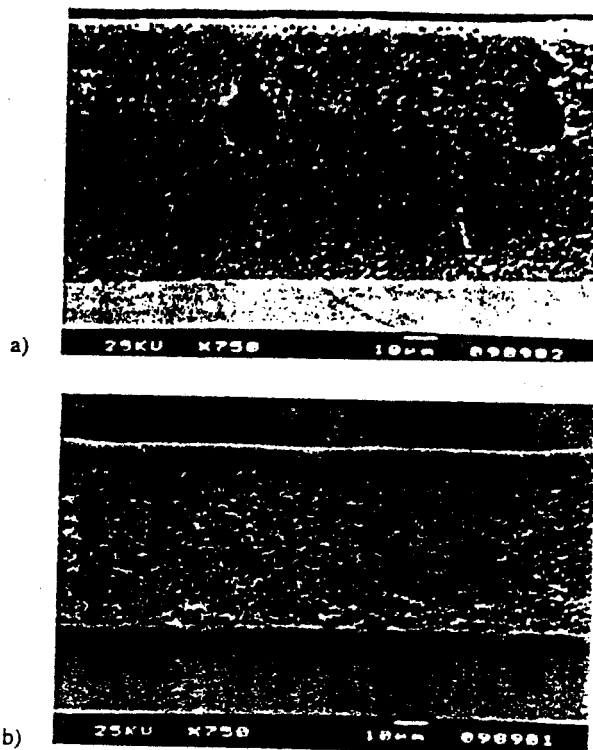
Figure III - 45. SEM cross-sections of membranes prepared from a polysulfone/DMAc solution after
a) immersion in water (porous membrane); and b) immersion in i-propanol
(nonporous membrane).

To quote an example. A polysulfone/DMAc system can be immersed in either water or i-
propanol. Since the miscibility of DMAc with water is much better than with i-propanol,
instantaneous demixing consequently occurs in water resulting in a porous membrane
with ultrafiltration properties. With i-propanol as the nonsolvent delayed demixing occurs,
which results in an asymmetric membrane with a dense nonporous top layer with
pervaporation or gas separation properties. The cross-sections of these membranes are
shown in figure III - 45.

A very large number of combinations of solvent and nonsolvent are possible all with
their own specific thermodynamic behaviour. Table III.8 shows a very general
classification of various solvent/nonsolvent pairs. Where a high mutual affinity exists a
porous membrane is obtained, whereas in the case of low mutual affinity a nonporous
membrane (or better an asymmetric membrane with a dense nonporous top layer) is
obtained. It should be noticed that this holds for ternary systems. In case of multi-
component systems with additives the thermodynaics and kinetics change, as do the
membrane properties.

Although other parameters exist which have an influence on the type of membrane
structure, the choice of solvent/nonsolvent is crucial. Fixing this parameters still leaves a

number of degrees of freedom in the system such as polymer concentration, addition of solvent to the nonsolvent bath, addition of nonsolvent to the polymer solution, the temperature of the coagulation bath and of the polymer solution and the addition of additives (low molecular weight, high molecular weight) to the casting solution or to the coagulation bath. Some of these parameters will be discussed in the sections below.

Table III.8   Classification of solvent/nonsolvent pairs

solvent	nonsolvent	type of membrane
DMSO	water	porous
DMF	water	porous
DMAc	water	porous
NMP	water	porous
DMAc	n-propanol	nonporous
DMAc	i-propanol	nonporous
DMAc	n-butanol	nonporous
trichloroethylene	methanol/ethanol/propanol	nonporous
chloroform	methanol/ethanol/propanol	nonporous
dichloromethane	methanol/ethanol/propanol	nonporous

III.7.2   Choice of polymer

The choice of polymer is an important factor because it limits the solvents and nonsolvents that can be used in the phase inversion process.

Table III.9.   Polymers from which ultrafiltration membranes have been prepared using DMF or DMAc as the solvent and water as the nonsolvent to yield porous membranes polymer concentration: 10 to 20%

polymer[1]

polysulfone
poly(ether sulfone)
poly(vinylidene fluoride)
polyacrylonitrile
cellulose acetate
polyimide
poly(ether imide)
polyamide (aromatic)

[1] for chemical structure, see chapter II

With porous (ultrafiltration/microfiltration) membranes, membrane performance is mainly determined by the pore size of the membrane. The choice of membrane material then becomes important with respect to fouling (adsorption effects; hydrophilic/hydrophobic character) and to the thermal and chemical stability. In contrast, for nonporous membranes the choice of polymer directly affects the membrane performance, because the intrinsic membrane separation properties (solubility and diffusivity) depend on the chemical structure and hence on the choice of polymer (see chapters II and V).

For porous membranes obtained by instantaneous demixing, the separation properties are mainly determined by the choice of solvent/nonsolvent. Indeed this type of structure can almost be considered to be independent of the choice of polymer. Table III - 9 gives a list of polymers from which ultrafiltration membranes have been made using DMAc or DMF as the solvent and water as the nonsolvent. The polymer concentration varied from 10-20% and immersion precipitation occurred at room temperature.

III.7.3   Polymer concentration

Another parameter influencing the ultimate membrane properties is the concentration of the polymer. Increasing the initial polymer concentration in the casting solution leads to a much higher polymer concentration at the interface. This implies that the volume fraction of polymer increases and consequently a lower porosity is obtained. Figure III - 46 [35] shows the calculated composition paths for the system cellulose acetate/dioxan/water system obtained by varying the initial polymer concentration in the casting solution (10% and 20% CA).
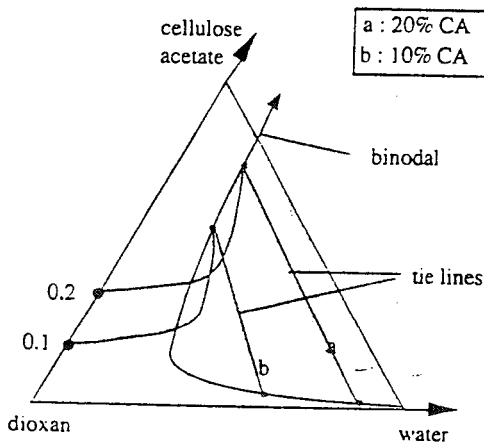
Figure III - 46.   Calculated composition paths for the system CA/dioxan/water for varying CA concentrations in the casting solution [32].

Instantaneous demixing occurs in both cases (confirmed experimentally by light transmission measurements, see figure III - 44), but with a higher initial polymer

concentration in the casting solution a higher polymer concentration at the film interface is obtained that results in a less porous top layer and a lower flux. In table III.10 the pure water fluxes exhibited by polysulfone ultrafiltration membranes are given as a function of the polymer concentration in the casting solution. At low polymer concentrations (12 - 15%) typical ultrafiltration membranes are obtained, but upon increasing the polymer concentration the resulting pure water flux can be reduced to zero although demixing occurs still instantaneously.

Table III.10   Pure water flux through polysulfone membranes

polymer conc. (%)	flux ($l.m^{-2}.h^{-1}$)
12	200
15	80
17	20
35	0[†]

System: water/DMAc/polysulfone; $\Delta P = 3$ bar; T = 20°C.

† : very low in terms of ultrafiltration fluxes
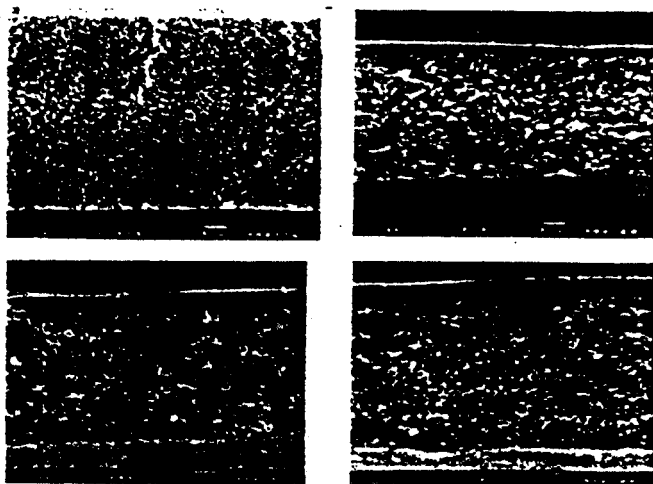
Figure III - 47.   Cross-sections of membranes obtained from the polysulfone/DMAc/i-propanol system with the following varying polymer concentrations in the casting solution (a) 15%; (b) 20%; (c) 25%; (d) 30%.

For nonporous membranes (obtained by using poorly miscible solvent/nonsolvent pairs), the influence of the polymer concentration is also very clear. As the delay time for liquid-liquid demixing is increased the distance from the film/bath interface in the film also increases, so that the first formed nuclei of the dilute phase are formed at a greater distance in the film from the film/bath interface. Thus the thickness of the dense top layer increases with increasing polymer concentration, as is clearly shown in figure III - 47 for the polysulfone/DMAc/i-propanol system.

III.7.4 Composition of the coagulation bath

The addition of solvent to the coagulation bath is another parameter which strongly influences the type of membrane structure formed. The maximum amount of solvent that can be added is determined roughly by the position of the binodal. When the binodal shifts towards the polymer/solvent axis, more solvent can be added. In the polysulfone/DMAc/water system the binodal is located close to the polysulfone/DMAc axis so that membranes can still be obtained when even up to 90% DMAc has been added to the coagulation bath. In the CA/acetone/water system the binodal is located more towards the CA/water axis and so that up to a maximum of 65% dioxan can be added to the coagulation bath to obtain a composition within in the binodal area. The addition of solvent to the coagulation bath results in a delayed onset of liquid-liquid demixing.

Indeed, it is even possible to change from porous to nonporous membranes by adding solvent to the coagulation bath. Figure III - 48 shows the composition paths for the CA/dioxan/water system with varying amounts of dioxan in the coagulation bath.
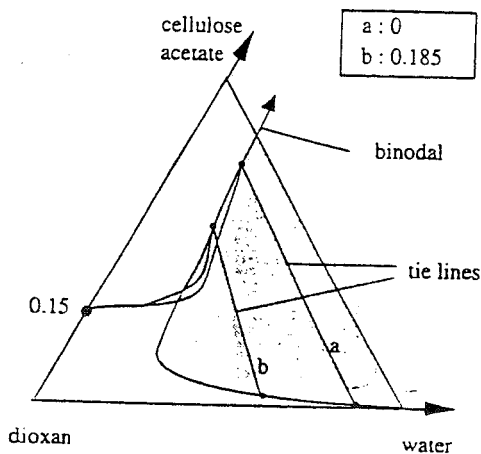
Figure III - 48. Calculated initial composition paths for the CA/dioxan/water system with varying volume fractions of dioxan (0 and 0.185, respectively) in the coagulation bath. Initial polymer concentration: 15 vol.% [35].

If the coagulation bath just contains pure water (figure III - 48, tieline a), instantaneous demixing will occur as shown in figure III - 44, because the initial composition path will cross the binodal. This has been confirmed by light transmission measurements. Also with 18.5 vol % dioxan in the coagulation bath, the composition path crosses the binodal and instantaneous demixing occurs (figure III - 48, tieline b). The composition path does not cross the binodal with dioxan concentrations higher than 19 vol % (see also curve c in figure III - 37), which means a delayed onset of liquid-liquid demixing. This has also been confirmed by light transmission measurements. Another remarkable point arising from figure III - 48 is that an increasing solvent (dioxan) content in the coagulation bath leads to a decrease in the polymer concentration in the film at the interface. In fact two opposing effects appear to operate: delayed demixing tends to produce nonporous membranes with thick and dense top layers, whereas low interfacial polymer concentration tends to produce more open top layers.

III.7.5   Composition of the casting solution

In most of the examples discussed so far the casting solution has consisted solely of polymer and solvent. However, the addition of nonsolvent has a considerable effect on the membrane structure. The maximum amount of nonsolvent that can be added to a polymer solution can be deduced from the ternary diagram, in the same way as the case of the maximum amount of solvent which can be allowed in the coagulation bath. The only requirement is that no demixing may occur, which means that the composition must be in the one-phase region where all the components are completely miscible with each other.
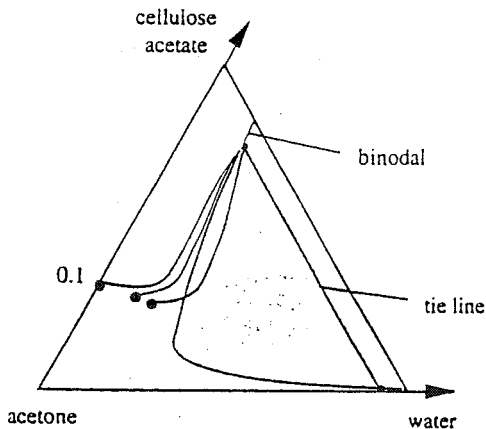
Figure III - 49.   Calculated composition paths for the CA/acetone/water system with varying water content (0, 12.5 and 20%) in the casting solution [35].

On adding nonsolvent to a polymer solution, the composition shifts in the direction of the liquid-liquid demixing gap. In this case, figure III - 49 illustrates the calculated

composition paths for the CA/acetone/water system, as varying amounts of water are added to the polymer solution. When no water is present in the casting solution, membrane formation occurs via the delayed demixing mechanism. This implies that nonporous membranes can be obtained. From calculations it can be shown that as the water content in the polymer solution is increased the composition path shifts to the binodal and eventually crosses it. Instantaneous demixing now occurs, so this is an example where transition from delayed demixing to instantaneous demixing occurs by the addition of nonsolvent to the casting solution. Again these calculations have been confirmed by light transmission measurements as shown in figure III - 50. With no water in the casting solution, delayed demixing is clearly observed with the transmittance remaining almost 100% for up to 25 seconds. In contrast when sufficient water is added, instantaneous demixing occurs after the addition of 11% or more. Under these circumstances there is an immediate decrease in the transmittance to lower values. The addition of nonsolvent to the coagulation bath is a method to obtain a more open structure and this method is widely used in practice. Generally, another nosolvent is added than the one which is used as coagulation medium.
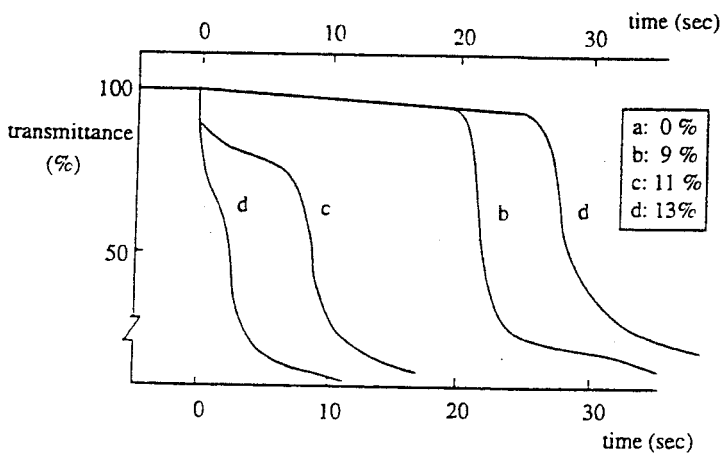
Figure III - 50.   Light transmission measurements in the CA/acetone/water system on the addition of varying amounts of water to the casting solution [35].

VI.7.6   Preparation of porous membranes - summary

From the previous sections it can now be summarized which factors promotes the formation of a porous membrane;
*   low polymer concentration
*   high mutual affinity between solvent and nonsolvent
*   addition of nonsolvent to the polymer solution
*   lowering of activity of nonsolvent (vapour phase instead of coagulation bath)
*   addition of a second polymer to the polymer solution, such as polyvinylpyrrolidone

III.7.7   *Formation of integrally skinned membranes*

Integrally skinned membranes can be characterised by a defect-free thin toplayer, suitable for gas separation, vapour permeation or pervaporation supported by an open structure. The toplayer has about the same properties as a homogeneous film. The basic requirements of these membranes are similar to composite membranes;

*   toplayer should be thin and absolutely defect-free
*   sublayer should be very open with a negligible resistance

These different structures can be correlated to the two mechanism of membrane formation, toplayer by a delayed onset of demixing, sublayer by instantaneous demixing. Moreover, a polymer concentration profile should be generated as shown schematically in figure III - 49, with a high polymer concentration at the top side and a low polymer concentration at the bottom side. Such a profile can be obtained in two ways;

*   introduction of an evaporation step before immersion in a nonsolvent bath (dry-wet phase inversion). As a result of this evaporation step the volatile solvent will evaporate from the surface and a driving force has been generated for diffusion of solvent from the bottom side to the top side. This process may be considered to be convection driven.
*   immersion in a nonsolvent with a low mutual affinity to the solvent (wet phase inversion)

It is possible to achieve a high polymer concentration at the top side by direct immersion in the coagulation bath without any evaporation step. This can be achieved by immersion in a nonsolvent with a low mutual affinity. This results in a high ratio of solvent outflow versus nonsolvent inflow (in fact only the solvent should diffuse out of the polymer film) and a non-linear profile is established as well. This may be called a diffusion driven process. Both concepts will be discussed briefly.
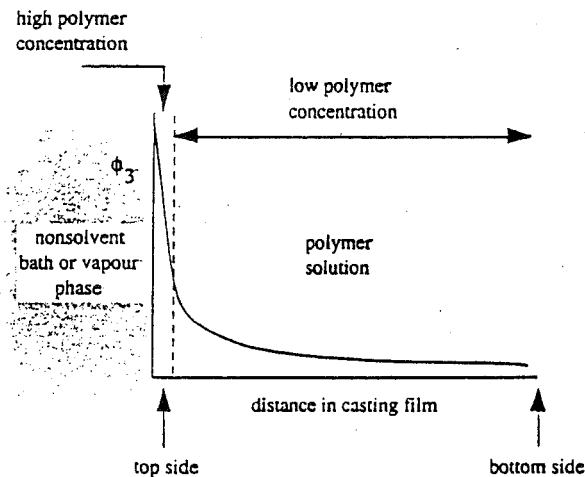
Figure III - 51.   Schematic drawing of the volume fraction of polymer (ϕ_3) in the casting solution after a short period of time

7.1 Dry-wet phase separation process

itroduction of an evaporation step before immersion in a nonsolvent bath (dry-wet
inversion) seems to be a logical way to prepare defect-free asymmetric membranes.
ain problem here is not to obtain a defect-free toplayer (the evaporation of a solvent
ı polymer solution results in a homogeneous membrane !) but to obtain a sublayer
negligible resistance. Two directions have been followed to achieve this
ion of nonsolvent to the polymer solution [45,46].

addition of a less volatile nonsolvent to a polymer solution with a volatile solvent a
sition is created which lies close to the binodal demixing gap and upon evaporation
ent the composition is shifted into the two phase demixing gap and result in a
aneous demixing and an open structure. During evaporation the nascent film
es turbid indicating the onset of phase separation. Integrally skinned asymmetric
anes with intrinsic gas separation properties have been obtained from a number of
ls polysulfone, polycarbonate, polyimide, polyestercarbonate and polyetherimide.
n thickness of these membranes is less than 0.1 μm and completely defect-free.
use of a nonvolatile 'good' solvent and a volatile 'bad' solvent (' evaporation
: delayed demixing') [47].

ithout the addition of nonsolvent in the polymer solution a rather open structure
obtained. The feature of this process is to combine a volatile 'bad' solvent with a
atile 'good' solvent as solvent system. Both are solvents for the polymer but have
lifferent affinity to the nonsolvent, water. The 'bad' solvent has a low affinity for
 can be expressed by a high excess free enthalpy of mixing whereas the 'good'
has a high affinity for water and a low or sometimes even a negative excess free
 of mixing.
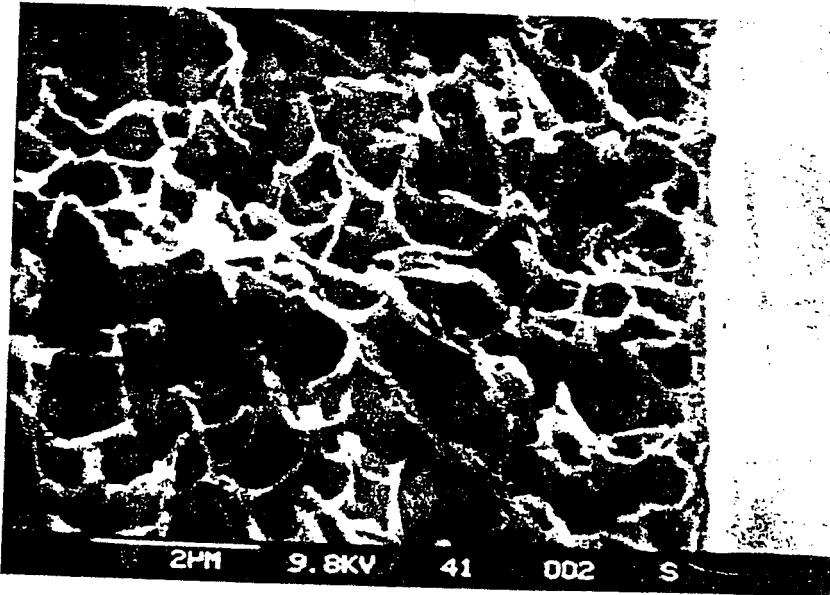
52.   Cross-section of a PPO-OH membrane from the system PPO-OH/THF/DMF and
        immersed in water after a certain evaporation time. Toplayer = 100 nm [47].

An example of such a solvent mixture is THF/DMF or THF/NMP with water as nonsolvent. As shown in the previous section, the affinity between THF and water is quite low whereas DMF and NMP show a high affinity for water. A polymer solution containing a polymer, e.g. modified PPO and THF and NMP as solvent is allowed to evaporate for a certain period of time anf then immersed into water. An integrally skinned membrane is obtained with a defect-free toplayer (see figure III - 52). The affinity between solvent and nonsolvent can be obtained from thermodynamic data such as excess free enthalpy of mixing which can be obtained from VLE data, or calculated from the van Laar equation, the Wilson equation or UNIVAC or UNIQUAC data.

III.7.7.2   Wet-phase separation process

It is also possible to prepare completely defect-free asymmetric membranes without any evaporation step by direct immersion in a nonsolvent bath using the dual bath procedure [45 - 48]. In this process the polymer solution is immersed in different nonsolvent baths consecutively. The first nonsolvent (bath) has a very low affinity to the solvent resulting in a delayed onset of demixing and an increase of polymer concentration. After a short period of time (in the order of seconds) the solution is immersed in a second nonsolvent with a high affinity resulting in instantaneous demixing and a rather open structure. A triple spinneret, as shown in figure III - 8, is very convenient to achieve this. Here, the first nonsolvent is already introduced through the outer orifice. Figure III - 53 shows a cross-section of a hollow fiber membrane from the system PES/NMP/glycerol/water.
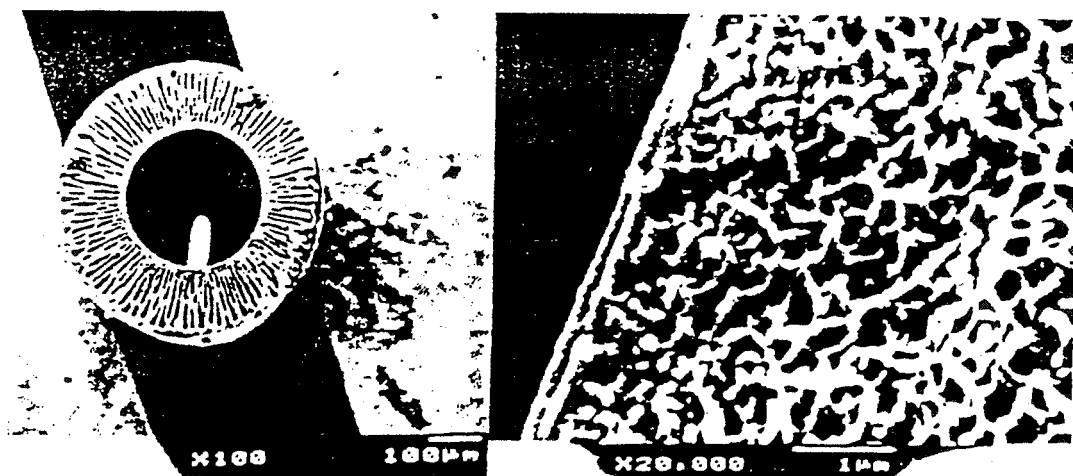
Figure III - 53   Cross-section of a PES hollow fiber obtained from a dual-bath process (left) and a magnification (20,000 x) of the toplayer side of the cross-section (right) [50].

The polymer solution is brought into contact with the glycerol. During this time no phase separation occurs but due to the outdiffusion of NMP the polymer concentration at the topside of the solution increases. The second coagulation bath contains water and the demixing occurs immediately. In this way a thin dense toplayer is obtained supported by a porous sublayer. Table III.11 summarizes some results of integrally skinned membranes prepared from different polymers with both the wet-dry and wet phase separation techniques. All membranes intrinsic selectivities indicating that no defects are present.

Table III.11   Selectivity, permeability, and $P/\ell^{\#}$ values for various concepts

material	system	selectivity	P/ℓ	method*	ref.
PES	CO_2/CH_4	41	16.1	W	50
PSf	CO_2/CH_4	41	10.3	W	51
PSf	O_2/N_2	6.0	14.5	D/W	46
PPO-OH	O_2/N_2	3.4	4.0	D/W	47
PI	O_2/N_2	5.9	95	D/W	46

$\#$ P/ℓ : 10^{-6} cm^3 (STP)/cm^2.s.cmHg (CO_2 or O_2)

* W = wet phase inversion and D/W = dry-wet phase inversion

III.7.8   Formation of macrovoids

Asymmetric membranes consist of a thin top layer supported by a porous sublayer and quite often macrovoids can be observed in the porous sublayer. Figure III - 54 illustrates two ultrafiltration membranes from polysulfone and polyacrylonitrile, where the existence of these macrovoids can be clearly observed.

The presence of macrovoids is not generally favourable, because they may lead to a weak spot in the membrane which is to be avoided especially when high pressures are applied, such as in gas separation. For this reason it is necessary to avoid macrovoid formation as much as possible, which can be achieved when the mechanism of macrovoid formation is understood.

In what membrane-forming systems do macrovoids actually appear? The examination of many systems indicates that systems those exhibiting instantaneous demixing often show macrovoids, whereas when a delayed onset of demixing occurs macrovoids are absent. Hence, it would seem that the mechanism which determines the type of membrane formed, i.e. the onset of liquid-liquid demixing, also determines whether or not macrovoids are present. This means that the parameters that favour the formation of porous membranes may also favour the formation of macrovoids.

The main parameter involved is the choice of solvent/nonsolvent pair. A high affinity between the solvent and the nonsolvent is a very strong factor in the formation of an ultrafiltration/microfiltration type of membrane. Solvent/water pairs with DMSO, DMF, NMP, DMAc, triethylphosphate and dioxan as the solvent exhibit very high mutual affinities (see also figure III - 42) and macrovoids can be found in membranes prepared from these systems irrespective of the polymer chosen for their preparation.

(a)   b;
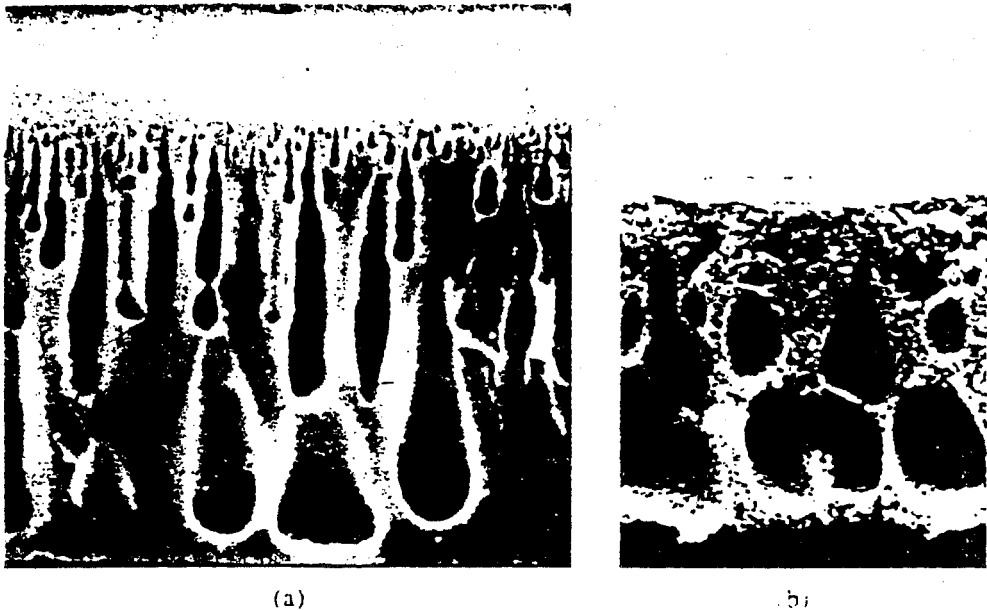
Figure III - 54.   SEM cross-sections of polyacrylonitrile (a) and polysulfone (b) ultrafiltration
                          membranes.

Besides the miscibility of the solvent and the nonsolvent, other parameters which affect the
instant of onset of liquid-liquid demixing also have an influence on the presence of
macrovoids. However, before discussing these parameters, it is first necessary to describe
the mechanism of macrovoid formation. In this respect, two phases in the formation
process have to be considered: i) initiation; and ii) propagation or growth.

     Many approaches have been described in the literature, for both the initiation and
growth process [52 - 55]. Here, the macrovoid formation is believed to be a result of the
liquid-liquid demixing process, where the nuclei of the polymer-poor phase are also those
responsible for macrovoid formation. Growth takes place because of the diffusional flow
of solvent from the surrounding polymer solution. Most of the macrovoids start to develop
just beneath the top layer, initiated by some of the nuclei which are formed directly beneath
this layer. A nucleus can only grow if a stable composition is induced in front of it by
diffusion. Growth will cease if a new stable nucleus is formed in front of the first formed
nucleus. A schematic drawing is shown in figure III - 55. It is assumed in this figure that
liquid-liquid demixing occurs instantaneously, with the first droplets of the polymer-poor
phase being formed at t = 1. The polymer solution in front of the droplets is still
homogeneous and remains stable, i.e. no new nuclei are formed. In the meanwhile
diffusion of solvent (and nonsolvent) occurs into the first nuclei. In this way growth of
macrovoids occurs and this growth continues until the polymer concentration at the
macrovoid/solution interface becomes so high that solidification occurs.

In the case of a delayed onset of liquid-liquid demixing, nucleation is not possible until a certain period of time has elapsed. In the meantime the polymer concentration has increased in the top layer. After a finite time has elapsed nucleation starts in the layer beneath the top layer. However, the composition now in front of these first-formed nuclei is such that the formation of new nuclei has been initiated.
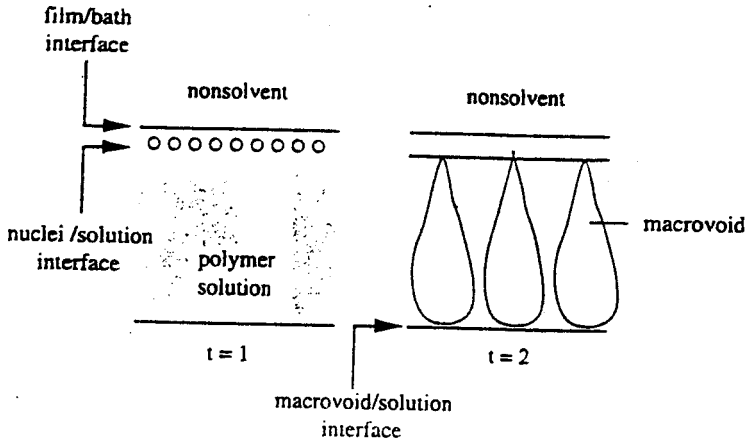
Figure III - 55. Schematic representation of the growth of macrovoids at two different times during instantaneous demixing.

The parameters that influence the onset of liquid-liquid demixing also determine the occurrence of macrovoids in systems that show instantaneous demixing. The main parameter is the choice of the solvent/nonsolvent pair, but other parameters such as the addition of a nonsolvent to the casting solution, the addition of solvent to the coagulation bath and the polymer concentration can be varied to prevent macrovoid formation.

As discussed in the previous section, systems in which the solvent-nonsolvent pairs exhibit high mutual affinity show instantaneous demixing and a tendency to macrovoid formation. Examples are DMSO/water, DMAc/water, DMF/water and NMP/water with various polymers such as polyamide, polysulfone, cellulose acetate, etc. Indeed, the CA/dioxan system with pure water as a coagulant shows macrovoids. However, by adding the solvent to the coagulation bath and promoting delayed demixing, the tendency for macrovoid formation also decreases (see figure III - 44). With 10% dioxan present in the coagulation bath macrovoids are still present, whereas the addition of 20% and 30% dioxan to the coagulation leads to the complete absence of macrovoids. One more important point must not be forgotten. Prevention of macrovoid formation in microfiltration/ultrafiltration membranes by encouraging delayed onset of liquid-liquid demixing also results in the densification of the top layer, which is unwanted. Another method of preventing macrovoid formation is the addition of additives (low molecular weight or high molecular weight components) to the casting solution.

III.8.   Inorganic membranes

Inorganic membranes have become an important type of membranes due to its specific properties compared to polymeric membranes. The upper temperature limit of polymeric membranes will never exceed 500°C but inorganic materials such as ceramics (siliciumcarbide, zirconiumoxide, titaniumoxide) can withstand very high temperatures and are very suitable to be applied harsh environments, e.g. high temperature applications such as in membrane reactors. For this purpose inorganic composite membranes have been developed consisting of various layers. The total membrane may be various millimetres in thickness but the actual toplayer is only a few micrometers or smaller and the pores size can be below 1 nm. Figure III - 56 gives a schematic drawing of such a multi-layered structure.

reverse osmosis/gas separation
ultrafiltration layer
microfiltration layer
substrate
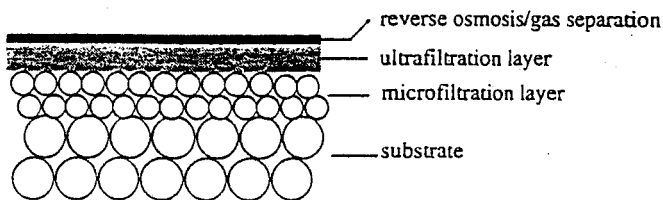
Figure III - 56.   Schematic drawing of a multi-layer inorganic membrane.

The preparation of the inorganic membranes will be discussed only briefly and the reader is referred to a number of review articles and books for more details [56 - 60]. The course macrostructure of the substrate is obtained by various methods such as isostatic pressing of dry powder, extrusion or slip-casting of ceramic powders with the addition of binders and plasticizers. These supports are then sintered to give a support with a pore sizes in the range of 5 - 15 μm and a porosity of 30 to 50% (see figure III - 56, substrate). Upon this layer a thin layer is applied by e.g. suspension coating (for instance γ-Al$_2$O$_3$) with a narrow pore size distribution. This layer has typical pore size of 0.2 to 1 μm (macropores) and can be use as microfiltration membrane. To make the pore sizes smaller nanoparticles are required. In order to stabilise these particles and to obtain a thin defect-free layer the so-called sol-gel process is widely employed. In this way pore diameters in the nanometer range (mesopores) are obtained with typical ultrafiltration properties. To make the membranes suitable for reverse osmosis or gas separation a further densification is required which can be done by various techniques, such as vapour deposition. Furthermore, to enhance specific transport, i.e. surface diffusion, the chemical nature of the internal surface is often modified as well.

III.8.1   The sol-gel process
The development of the sol-gel process in the beginning of the eighties can be considered as the breakthrough in inorganic membranes comparable to the Loeb-Sourirajan process

for the preparation of asymmetric polymeric membranes. Different types of microfiltration membranes were known for a long time, based on metals or carbon but the number of applications of these were limited due to the relatively large pore size. Through the sol-gel process a mesoporous layer is formed with ultrafiltration properties while gas separation is possible through Knudsen flow (see chapter V). In addition these layers can be considered as the basis for further densification. Two different routes are widely used, the colloidal suspension route and the polymeric gel route. The basic scheme is shown in figure III - 58. Both preparation routes make use of a precursor which may be hydrolyzed and polymerized. These processes must be controlled to obtain the required structure. An alkoxide is frequently employed as precursor and the hydrolysis and polymerization (condensation) reaction is shown below in figure III - 57. The colloidal suspension starts from a sol which has been obtained after hydrolysis. A sol can be defined as a colloidal dispersion of particles in a liquid. The process starts with a precursor which is often an alkoxide such as aluminium tri-sec butoxide (ATSB). This precurser is then hydrolyzed by the addition of water which yields an hydroxide, e.g. in the case of an aluminium based precursor aluminumhydroxide (γ-AlOOH) or boehmite is obtained. This partially hydrolyzed alkoxide is now through the OH groups able to react with other reactants and a polyoxometalate is formed. The viscosity of the solution will increase which is an indication that the polymerization proceeds. The sol is peptized by the addition of an acid (e.g. HCl or HNO_3) to form a stable suspension. Often an organic polymer such as polyvinylalcohol (PVA) (20-30 wt%) is added. In this way the viscosity of the solution increases which results in a lower tendency of pore penetration and it reduces the formation of cracks due to stress relaxation. By changing the surface charge of the particles (zeta potential) or by increasing the concentration the particles tend to agglomerate
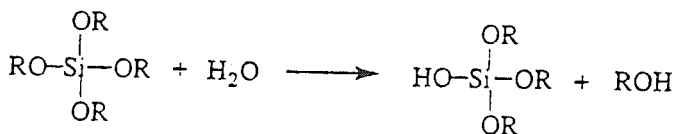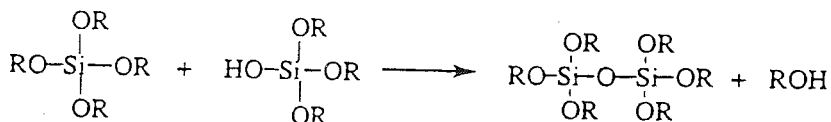
Figure III - 57.   Hydrolysis and condensation reaction of an alkoxide precursor

and a gel is obtained. This gel can be defined as a three-dimensional network structure and the compactness of the structure is dependent on the pH, concentration and nature of the ions to stabilize the colloidal suspension. Drying of these gel structures is regarded as the most critical step in the formation of these membranes. Since the particles are quite small high capillary forces are generated which may exceed 200 MPa for very small pores and resulting in cracks. There are various methods to circumvent this problem. One way is by super-critical drying in which capillary forces are drastically reduced. Another and widely applied method is the addition of organic binders which are able to relax generated stresses. This binder can be effectively removed by a heat treatment. After drying the membrane is sintered at a certain temperature and the final morphology is stabilised. In the polymer gel route a precursor has been selected with a low hydrolysis rate. By addition of small amounts of water an inorganic polymer has been formed which finally result in a polymer network (a gel !). The water required for this process can be added directly but very slowly or can be generated by a chemical reaction, e.g. an esterification reaction. Not all ceramic materials are equally suited for either reaction route and dependent on the system and the structures required a suitable system can be chosen. Furthermore, there are a number of parameters with a large influence on the final structure. Especially the calcination temperature to yield the oxide form and the final structure can be used to adjust the required pore sizes (see also figure IV - 17).
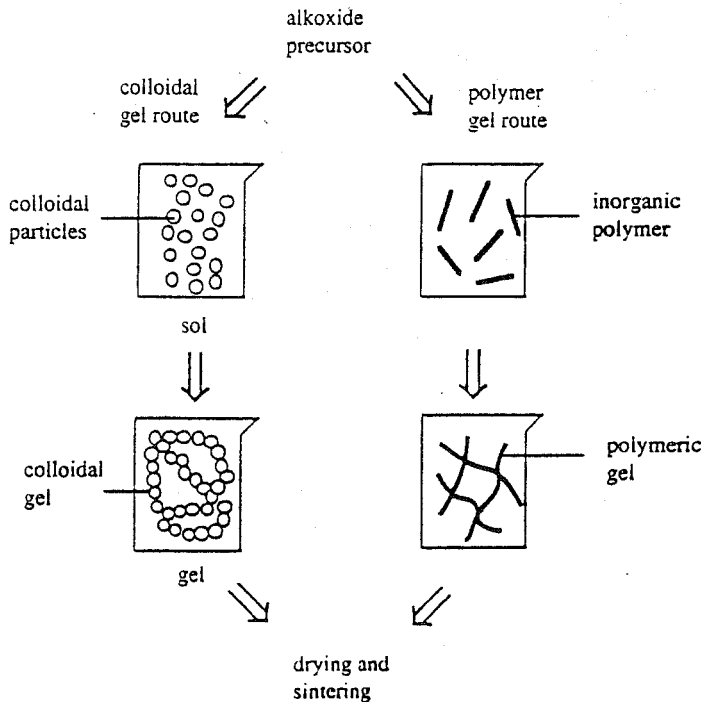
Figure III - 58.   Schematic drawing of the preparation of ceramic membranes by the sol-gel process [56.57]

III .8.2   Membrane modification

The sol-gel process results in structures with pore sizes in the nanometer range. In order to prepare ceramic membranes suitable for gas separation or reverse osmosis a further densification of the structure is required. Various techniques can be used to achieve this and the structures are given in figure III - 59. Ceramic membranes are very suited for high temperature applications, e.g. in membrane reactors in which they contain the catalytically active sites and function as separation barrier as well. One way to obtain a catalically active membrane is by covering the surface by a catalyst (fig III - 59a). Different catalyst can be used in combination with a suitable inorganic membrane, e.g. γ-Al$_2$O$_3$, palladium, platinum, silver, molybdenesulfide [59,60]. The structure shown schematically in figure III - 59b is a typical structure for a catalytically active membrane only the catalyst is not deposited as a continuous layer but rather as nanoparticles. Structure c is typical obtained by a coating process of an inorganic polymeric gel on top of a support. For this purpose silicate or alkoxides are used and by the addition of water polymerization occurs. The chain length and density of the layer can be controlled by the amount of water, temperature and time. Finally structure III - 59d is a structure obtained by chemical vapour deposition (CVD). In this way constraints are formed in the porous system which may be catalytically active as well.

(a)   (b)

(c)   (d)
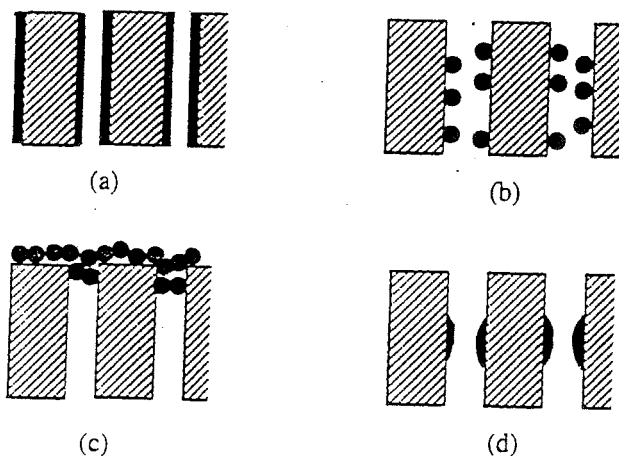
Figure   III - 59.   Schematic drawing of surface modification of ceramic membranes.
(a) Internal deposition of pores by monolayer or multi-layer; (b) pore-plugging of nanoparticles; (c) coating layer on top of the membrane and (d) constrictions at sites in the toplayer [59].

III.8.3   Zeolite membranes

Zeolite membranes have gained much interest recently. Zeolites are crystalline microporous aluminasilicates. It is built up by a three dimensional network of SiO$_4$ and AlO$_4$ tetrathedra [61 - 63]. Zeolites have a very defined pore structure and figure III - 60 gives a schematic drawing of the structures of zeolite LTA (type A) and silicalite-1. Due to

the high amount of aluminium, zeolite LTA is a very hydrophilic zeolite. The pore size depend on the type of cation and Ca^{2+}, Na^+ and K^+ gives 5A, 4A, and 3A, respectively. On the other hand silicalite-1 is a very hydrophobic zeolite since it does not contain any aluminium and has no excess of charge which must be compensated by a counter-ion.

Table III.12   Some properties of zeolites [63,64]

Name	pore size (Å)	Si/Al	structure
Type A	3.2 - 4.3	1	3D
ZSM-5	5.1 - 5.6	10 - 500	2D
silicalite-1	5.1 - 5.6	∞	2D
Theta-1	4.4 - 5.5	> 11	1D
Offretite	3.6 - 6.7	3 - 4	3D
Mordenite	2.6 - 7.0	5 - 6	2D
Faujasite	7.4	1.5 - 3	3D

Zeolite A contains a high amount of aluminium which implies the presence of a large number of cations. The size of the pores is dependent on the size of the cation. Another zeolite, Faujasite, has a similar structure.

Silicalite, a pure silica zeolite has a completely different structure. The structure which is built up in this case by ten oxygen atoms, is characterized by a two-dimensional pore
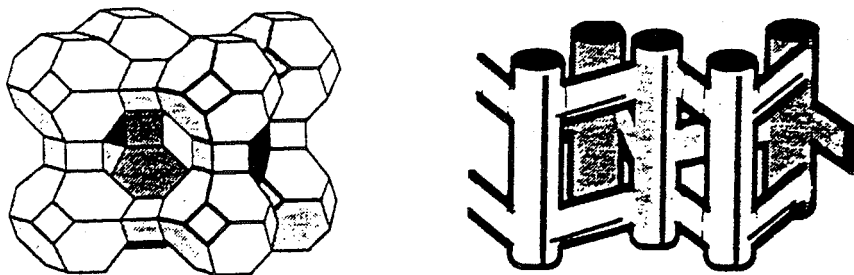
Figure III - 60.   Schematic drawing of the structures of zeolite A (left) and silicate-1 (right).

structure, one with straight channels and the other with a more sinusoidal type of structure. If these structures are applied in membranes very defined pores are obtained for specific separations. Recently, various investigators [65 - 67], have been tried to develop a zeolite toplayer in a multi-layered membrane. For instance in the case of silicalite-1, the support is immersed in a sol of SiO_2 in water with some additives. Now the zeolite is grown under specific conditions e.g in an autoclave and the final structure is obtained after calcination.

III.8.4.   Glass membranes

Besides ceramics, metals, and carbon, glass is another material from which membranes can be prepared. Two well known glasses are Pyrex and Vycor, both containing SiO_2, B_2O_3 and Na_2O. The ternary phase diagram of the system SiO_2, B_2O_3 and Na_2O is shown schematically in figure III - 61 [68,69]. Various miscibility gaps can be observed and when a homogeneous melt at 1300 - 1500 °C is cooled down to 500 to 800°C at certain compositions phase separation occurs. One of these compositions consists of 70 wt.% SiO_2, 23 wt.% B_2O_3 and 7 wt.% Na_2O which is located in the 'Vycor glass region'. Demixing occurs into two phases, one phase consists mainly of SiO_2 which is not soluble in mineral acids. The other phase is richer in B_2O_3 and this compound can be leached out of the structure resulting in a porous matrix with pores in the μm to nm range. A careful temperature control may give a rather narrow pore size distribution. A disadvantage of these membranes is the poor mechanical stability and the susceptibility of the material (surface) for all kinds of reaction at elevated temperature with components which are present in the feed solution. On the other hand, the surface can easily be modified with all kinds of compounds which can be applied to change the separation properties.
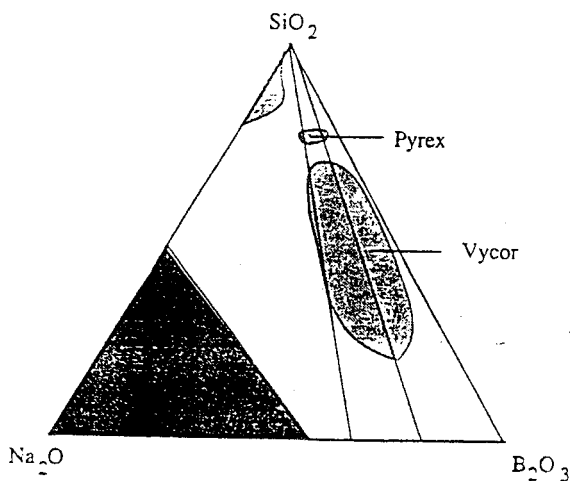
Figure III - 61.   Phase diagram of the system SiO_2, B_2O_3 and Na_2O

III.8.5   Dense membranes

Besides porous membranes dense (nonporous) inorganic membranes may be applied as well. Examples of these membranes are thin metal plates such as palladium and silver and alloys of these metals. In most cases alloys are employed to reduced the brittleness of pure palladium. These metal/alloys are impermeable to all substances except for atomic oxygen and hydrogen which implies for instance that palladium has an infinitely high separation factor for hydrogen over all kinds of gases. Hydrogen is not transported as 'molecular hydrogen' but as 'hydrogen atom'. Molecular hydrogen is dissociated at the palladium surface into hydrogen atoms which diffuse through palladium (or the palladium/silver alloy) and recombines and desorbs at the other surface. However, the low permeability is a drawback and this can be partly solved by making a composite membrane with a very thin palladium layer applied by a deposition technique upon a porous support. Also in the field of immobilized liquid membranes (see chapter VI) nonporous inorganic materials may be applied for specific separation properties such as molten salts incorporated into porous inorganic membranes have very high separation factors towards e.g. oxygen, ammonia, carbon dioxide [70].

III.9.   Solved problems

1. In a binary system solvent (1) - polymer (2) shifts the location of the critical point of the binodal to the solvent axis with increasing molecular weight of the polymer (see figure III - 23). Derive that the polymer volume fraction at the critical point is equal to
$$\phi_{2,c} = (1 + n^{1/2})^{-1}$$

III.10.   Unsolved problems

1. Membranes are frequently prepared by an immersion precipitation process in which three components are used: polymer (P), solvent (S), en nonsolvent (NS). Consider a system that demixes at 30% by weight of nonsolvent independently on the polymer concentration. The critical point is located at 5% by weight polymer.

a) Draw the ternary system with the demixing region. Define the various points and the various regions of the triangle. (An 'empty' ternary phase diagram can be found after the solved problems).

The polymer solution A has the following composition: 20% by weight polymer, 70% by weight solvent and 10% by weight nonsolvent.

b) Draw the location of polymer solution A in the ternary phase diagram

The coagulation bath B has the following composition: 90% by weight nonsolvent and 10% solvent.

c) Indicate in the ternary phase diagram where (on which line !) the final compositions of the membrane is located. If the polymer solution A changes from composition how does the final composition change after demixing?

Consider two systems:

system 1 : consisting of polymer and solvent and the coagulation bath consisting of pure nonsolvent.

system 2 : consisting of polymer and solvent and coagulation bath of system B (see 1c).

d) Compare the magnitude of the solvent and nonsolvent flow for the two systemsand and the implications to the rate of demixing

2. Immersion precipitation is one of the most important techniques to prepare phase inversion membranes. During this process demixing can occur *instantaneously* or *delayed*.

a) Explain briefly both types of demixing processes

With light transmission experiments the occurrence of instantaneous or delayed demixing can easily be shown
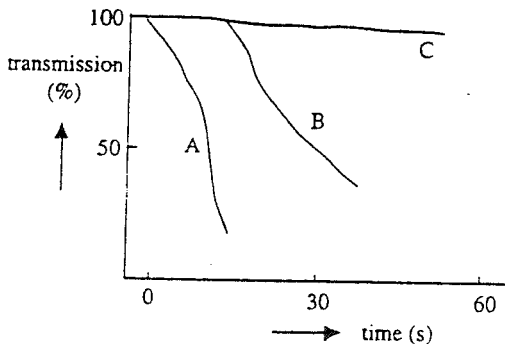
b) Indicate which of the curves represents a membrane forming system with instantaneous demixing ?

By the addition of solvent to the nonsolvent bath demixing can be controlled. For the ternary system cellulose acetate/solvent (D and E)/water the following result is obtained from light transmission.

delayed
demixing
(s)

50

D

E

10   30   50

conc. of solvent in
nonsolvent bath (weight%)
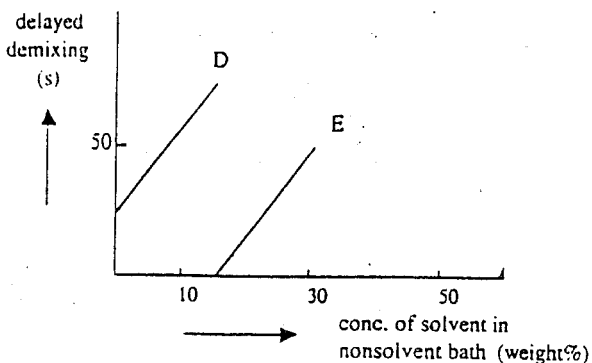
c) Indicate which of the systems show instantaneous demixing in the case that no solvent has been added to the nonsolvent bath

The occurrence of delayed demixing is often determined by the low affinity between solvent and nonsolvent. g_{12} is the interaction parameter between solvent and nonsolvent.

$$g_{12} = 1/x_1 \, v_2 \, [\, x_1 \ln (x_1/v_1) + x_2 \ln (\, x_2/v_2) + G^E/RT]$$

d) Is the g_{12} interaction parameter relatively high or low in the case of a low affinity between solvent and nonsolvent.

e) Draw qualitatively ΔG_m (free enthalpy of mixing), ΔG_{ideal} (ideal free enthalpy of mixing) and G^E (excess free enthalpy of mixing) as a function of the composition of a solvent/nonsolvent   pair with a low mutual affinity.

3. The T-x diagram for a binary polymer-solvent system may be as follows

T_1

T

T_2

.A

solvent   polymer
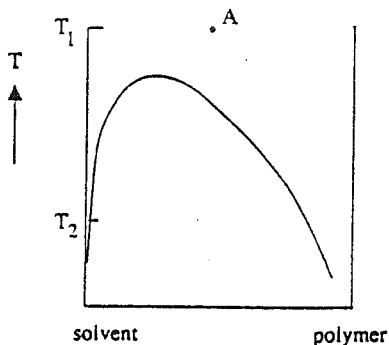
a) Draw schematically the ΔG_m curves at T_1 and T_2
b) Why has the T - x diagram an asymmetric character ?

c) What membrane porosity do you obtain by cooling a solution A from T_1 to T_2 (assuming that a homogeneous porous membrane is obtained).
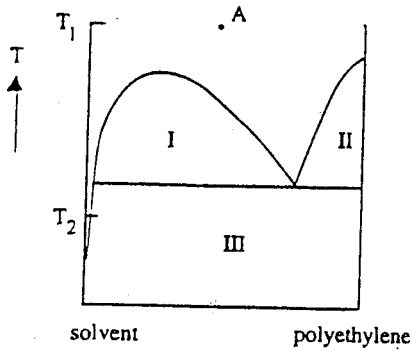
The figure above shows schematically the $T - x$ diagram for the system polyethylene/nujol.

d) Identify the regions I, II, and III.

e) Describe the phenomena occurring when cooling down a solution A slowly from T_1 to T_2

f) Draw the spinodal and indicate how spinodal demixing may occur in these kinds of systems ?

4. Membrane formation frequently takes place by immersion precipitation in which three components are involved; solvent (S), nonsolvent (NS) and polymer (P). A given ternary phase diagram shows as follows
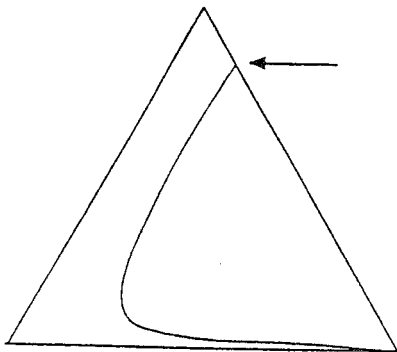
a. Indicate the areas and the points

b. Explain how this phase diagram has been constructed (What is the relation with ΔG_m)

c. What is the physical significance of the point indicated by the arrow ?

Membrane formation is not only determined by thermodynamics but also by kinetics. The flux of nonsolvent (subscript 1) and solvent (subscript 2) can be represented as follows

$$J_i = - L_i \, \Delta \mu_i$$

d. What does the ratio $\Delta \mu_1 / \Delta \mu_2$ mean ?

solvent in coagulation bath
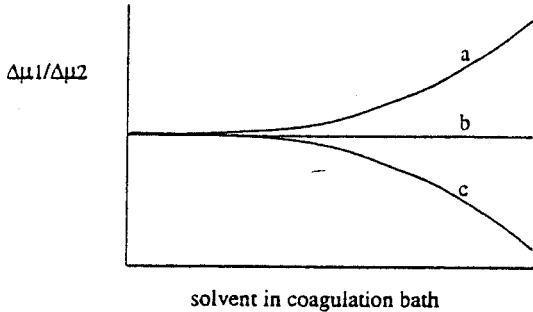
e. Which of the curves is correct and why ? What does this imply for the type of demixing

5. For nonpolar components the solubility parameter theory is very useful and activity coefficients may be estimated from this theory.

a. Derive for component 1 of a binary mixture that the activity coefficient is given as
$RT \ln\gamma_1 = V_1 \, \phi_2^2 \, (\delta_1 - \delta_2)^2$
with $\Delta H_m = V \, \phi_1 \, \phi_2 \, (\delta_1 - \delta_2)^2$
and $\Delta H_m = RT \, n_1 \phi_2 \, \chi$
$\delta_{benzene} = 18.8 \ (J/cm^3)^{0.5}$ $V_{benzene} = 89 \ cm^3/mol$
$\delta_{cyclohexane} = 16.8 \ (J/cm^3)^{0.5}$ $V_{cyclohexane} = 109 \ cm^3/mol$

b. Why is the solubility parameter of benzene greater than of cyclohexane ?
c. Calculate the activity coefficients of benzene and cyclohexane in an equimolar mixture $(x_1 = x_2 = 0.5)$ at 25°C.
d. Calculate the Flory-Huggins interaction parameter χ_{12} at $x_1 = x_2 = 0.5$.

6. A membrane is prepared by an immersion precipitation process from a ternary system consisting of polymer (P), solvent (S) and nonsolvent (NS). A certain demixes at a nonsolvent concentration of 20% by weight, independent on polymer concentration. The critical point is located at 1% of polymer. A student want to make membranes from the following initial polymer solutions.

solution	wt.% P	wt.% S	wt.% NS
A	10	90	0
B	20	80	0
C	20	70	10
D	10	60	30

a. Draw the ternary phase diagram with the regions and points and give the 4 compositions in this diagram.

Membranes were prepared from this solution by immersion in 100% nonsolvent. One solution did not yield membranes, one solution gave a dense structure whereas the other two solution gave porous structures

b. Indicate which structures are obtained from which solutions and explain briefly.

In an other case solution B is used for some experiments in different coagulation baths

coagulation bath	wt.% NS	wt.% S
I	100	0
II	90	10
III	80	20

c. Give in the phase diagram the final compositions of the obtained membranes and indicate whether porous or nonporous membranes are obtained.

7. The activity of toluene in a toluene/polyphenyleneoxide (PPO) solution has been determined from vapour pressure measurements. At a volume fraction of toluene of ϕ_1 = 0.75 the activity a_1 = 0.99. Determine the interaction parameter $\chi_{tol/PPO}$. The molecular weight of PPO is 10^5 g/mol.

8. The weight fraction of water in cellulose diacetate (density = 1.3 g/ml) at 20°C is 0.15. Determine the interaction parameter $\chi_{CA/H2O}$.

9. The vapour pressures and vapour compositions of mixtures of water (1) and N-methylpyrrolidone (2) at 20°C are given below.

x_1	0	0.3	0.5	0.8	1.0
y_1		0.9753	0.9918	0.999	
p (mmHg)	0.13	3.6	7.0	13.9	18.8

Calculate the interaction parameters at the given compositions (N.B. Calculate first the activity coefficients)
water: M_w = 18 g/mol and density = 1.0 g/l
NMP: M_w = 99 g/mol and density = 1.03 g/l

10. Membranes can be prepared from a binary system polymer/solvent. A schematic drawing of the free enthalpy of mixing ΔG_m, is shown below
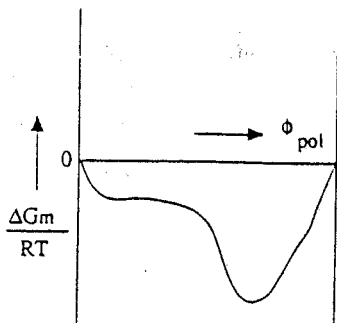
a. Transfer this curve in a T - ϕ diagram
b. How does the binodal change as χ increases.

11. The following cloud points were found for the system polysulfone/DMAc/water

% PSf	% H_2O	% DMAc
5.0	4.0	91.0
10.0	3.75	86.25
15.0	3.5	81.5
20.0	3.25	76.75
25.0	3.0	72.0

a. Draw the binodal.
b. Give in the ternary diagram the compositions with a constant polymer/nonsolvent ratio of 4/1.
c. Can you estimate the polymer/nonsolvent interaction

12. The excess free enthalpy of mixing for the binary system ethanol (1)-chloroform (2) at 50°C for three different compositions is given below;

x_1	0.25	0.50	0.75
G^E (J/mol)	620	680	350

Determine the binary interaction parameters for these compositions (ρ_{EtOH} = 0.78 g/ml and ρ_{CHCl_3} = 1.2 g/ml).

13. The solubility parameters and molar volumes of some alcohols and of silicone rubber (PDMS) are tabulated below. Calculate the χ interaction parameter of the various alcohols towards silicone rubber and compare these with the Δ values. What is your conclusion ?

	δ_d[†]	δ_p	δ_h	v_m[‡]
methanol	7.4	6.0	10.9	40.7
ethanol	7.7	4.3	9.5	58.7
propanol	7.8	3.3	8.5	75.2
butanol	7.8	2.8	7.7	92.0
silicone rubber	7.8	0.05	2.3	

[†] δ in $(cal/cm^3)^{0.5}$ and [‡] v_m in cm^3/mol

III.12. Literature

1. Zsigmondy, R., and Bachman, W., *Z. Anorg. Allgem. Chem.*, **103** (1918), 119
2. Strathmann, H., Koch, K., Amar, P., and Baker, R.W., *Desalination*, **16** (1975) 179
3. Ferry, J.D., *Chem. Rev.*, **18** (1936) 373
4. Maier, K., and Scheuermann, E., *Kolloid Z.*, **171** (1960) 122
5. Kesting, R.E., *J. Appl. Polym. Sci.*, **17** (1973) 177
6. Lloyd, D.R., Barlow, J.W., *AIChE. Symp. Ser.*, **84** (1988), 28
7. Kesting, R.E., *Synthetic Polymeric Membranes*, McGraw Hill, New York, 1985
8. Manjikian, S., Loeb, S., and Mc. Cutchan, J.W., *Proc. First. Symp. Water Des.* (1965) 165
9. Frommer, M.A. and Lancet, D., in Lonsdale, H.K., and Podall, H.E., (eds.), *Reverse Osmosis Membrane Research* , Plenum Press, NY, 1972, p. 85
10. Koenhen, D.M., Mulder, M.H.V., and Smolders, C.A., *J. Appl. Polym. Sci.*, **21** (1977), 199
11. Guillotin, M., Lemoyne, C., Noel, C., and Monnerie, L., *Desalination*, **21** (1977) 165
12. Blume, I., Internal Report, University of Twente
13. Deryagin, B.M., and Levi, S.M., *Film coating theory*, The Focal press, London, 1959
14. Ellinghorst, G., Niemoller, H., Scholz, H., and Steinhauser, H., *Proceedings of the Second International Conference on Pervaporation Processes in the Chemical Industry*, Bakish, R., (ed.), San Antonio, 1987, p. 79
15. Hildebrand, J., and Scott, R., *Solubility of Nonelectrolytes*, Reinhold, New York, 1949.
16. Hansen. C.M., *J. Paint. Technol..*, **39** (1967) 104
17. Froehling, P.E., Koenhen, D.M., Bantjes, A., and Smolders, C.A., *Polymer*, **17** (1976) 835
18. Barton. A.F.M., *Handbook of Solubility Parameters and Cohesion Parameters*, Boca Raton, Florida, 1983
19. Koenhen, D.M., Smolders, C.A., *J. Appl. Polym. Sci.*, **19** (1975) 1163
20. Wijmans. J.G., Smolders, C.A., *Eur. Polym. J.*, **13** (1983), 1143
21. Mulder, M.H.V., Kruitz, F., and Smolders, C.A., *J. Membr. Sci.*, **11** (1982) 349
22. Flory, P.J., *Principles of Polymer Chemistry*, Cornell University Press, Ithaca, 1953
23. Smolders, C.A., and Van Aartsen, J.J., and Steenbergen, A., *Kolloid. Z. Z. Polym.*, **243** (1971) 14
24. Altena. F.W., and Smolders, C.A., *Macromolecules*, **15** (1982) 1491
25. Tan, H.M., Moet, A., Hiltner, A., and Baer, E., *Macromolecules*, **16** (1983) 28
26. Reuvers. A.J., Altena, F.W., and Smolders, C.A., *J. Polym. Sci. Pol. Phys. Ed.*, **24** (1986) 793
27. Wijmans, J.G., Rutten, H.J.J., Smolders, C.A., *J. Polym. Sci., Polym. Phys.* **23** (1985) 1941
28. Kelley, F.N., and Bueche, F., *J. Pol. Sci.*, **50** (1961) 549
29. Gaides. G.E., and McHugh, A.J., *Polymer*, **30**, (1989) 2085

30. Castro, A.J., US Patent, 4, 247, 498 (1980)

31. Tsai, F-J., Torkelson, J.M., *Macromolecules*, 23 (1990) 775

32. Nohmi, T., US Patent, 4, 229, 297 (1980)

33. Mahoney, R.M., et al., US Patent, 4, 115, 492 (1978)

34. Tseng, H-S., Proceedings ICOM 90, Chicago, USA (1990), p.16

35. Reuvers, A.J., *Ph.D. Thesis*, University of Twente, 1987

36. Wisniak, J., and Tamir, A., *Mixing and Excess Thermodynamic Properties*, Elsevier, Amsterdam, 1978.

37. Rabek, J.F., *Experimental Methods in Polymer Chemistry*, Wiley, Chichester, 1980

38. Koningsveld, R., and Kleintjes, L.A., I^2-*Procestechnologie*, no.6 (1986) 9

39. Wijmans, J.G., *Ph.D. Thesis*, University of Twente, 1984

40. Altena, F.W, *Ph.D. Thesis*, University of Twente, 1982

41. Mulder, M.H.V., *Ph.D. Thesis*, University of Twente, 1984

42. Flory, P.J., and Rehner, J., J. Chem. Phys., 11 (1943) 521

43. Altena, F.W. and Smolders, C.A., *Macromolecules*, 15, (1982), 1491

44. Gmehling, J. and Onken, U., *Vapour-liquid Equilibrium Data Collection*, Dechema, Frankfurt, Germany, 1977

45. Pinnau, I., Wind, J., Peineman, K.V., *Ind. Eng. Chem. Res.*, 29 (1990) 2028

46. Pinnau, I., PhD Thesis, University of Texas at Austin, 1991

47. Mulder, M.H.V., Nardello, G., Sisto, R, submitted to *Gas Separation & Purification*

48. Mulder, M.H.V., Internal Publication University of Twente, 1982

49. Hof, J van 't, PhD Thesis, University of Twente, 1988

50. Li, S.G., Koops, G.H., Mulder, M.H.V., Boomgaard, T. v.d., and Smolders, C.A., *J. Membr. Sci.*, 94 (1994) 329

51. Koops, G.H., Nolten, J.A.M., Mulder, M.H.V., Smolders, C.A., *J. Appl. Pol. Sci.*, 54 (1994) 385

52. Graig, J.P., Knudsen, J.P, and Holland, V.F., *Text. Res. J.*, 32 (1962) 435

53. Gröbe, V., and Meyer, K., *Faserf. Textiltechn.*, 10 (1959) 214

54. Strathmann, H., and Kock, K., *Desalination*, 21 (1977) 241

55. Cabasso, I., : 'Membrane technology', in A.R. Cooper (ed.), *Ultrafiltration Membranes and Applications, Polymer Science and Technology*, Vol.13, Plenum Press, NY, 1980, p. 47

56. Burggraaf, A.J., and Keizer, K., Synthesis of Inorganic Membranes, in '*Inorganic Membranes, Synthesis, Characteristics, and Applications* ', Ed. Bhave, R.R., Van Nostrand Reinhold, New York, 1991

57. Cot, L., Guizard, C., Julbe, A., and Larbot, A., Preparation and Application of Inorganic Membranes, in ' *Membrane Processes in Separation and Purification*', Eds. Crespo, J.G. and Böddeker, K.W., Kluwer Academic Publishers, Dordrecht, The Netherlands, 1994.

58. Keizer, K., Uhlhorn, R.J.R. and Burggraaf, A.J., Gas Separation using inorganic Membranes, in '*Membrane Separation Technology, Principles and Applications*, (Eds. Noble, R.D. and Stern, S.A.), Elsevier, Amsterdam, 1995

59. Keizer, K., Zaspalis, V.T., de Lange, R.S.A., Harold, M.P., and Burggraaf, A.J., Membrane reactors for partial oxidation and dehydrogenation reactions, in ' *Membrane*

Processes in Separation and Purification', Eds (Crespo, J.G. and Böddeker, K.W.), Kluwer Academic Publishers, Dordrecht, The Netherlands, 1994., p. 395.

60. Falconer, J.L., Noble, R.D., and Sperry, D.P., Catalytic membrane reactors, in *'Membrane Separation Technology, Principles and Applications*, (Eds.Noble, R.D. and Stern, S.A.), Elsevier, Amsterdam, 1995

61. Breck, D.W., *Zeolite Molecular Sieves: Structure, Chemistry and use*, John Wiley & Sons, 1974,

62. Vaughan, D.E.W., *Chem. Eng. Progr.*, **84** (1988) 25,

63. Meier, W.M., Olson, D.H., *Atlas of Zeolite structure types*, 3rd edition, Butterworth-Heineman 1992.

64. Ruthven, D.M., *Chem. Eng. Progr.*, **84** (1988) 42.

65. Geus, E.R., Mulder, A., Vischjager, D.J., Schoonman, J., and van Bekkum, H., Key Engineering Materials, **61 & 62** (1991) 57,

66. Geus, E.R., den Exter, M.J., and van Bekkum, H., *J. Chem. Soc. Faraday Trans.*, **88** (1992) 3102

67. Jia, M.-D., Peinemann, K.-V., and Behling, R.-D., *J. Membr. Sci.*, **82** (1993) 15

68. Schnabel, R., German Patent, Nr. 2,454,111, (1976)

69. Schnabel, R., and Vaulant, W., *Desalination*, 24 (1978) 249

70. Pez, G.P., *US Patent* 4.612,209 (1986)

IV CHARACTERISATION OF MEMBRANES

IV. 1.   Introduction

Membrane processes can cover a wide range of separation problems with a specific membrane (membrane structure) being required for every problem. Thus, membranes may differ significantly in their structure and consequently in their functionality. Many attempts have been made to relate membrane structure to transport phenomena, in an effort to provide a greater understanding of separation problems and possibly predict the kind of structure needed for a given separation.

Membranes need to be characterised to ascertain which may used for a certain separation or class of separations. A small change in one of the membrane formation parameters can change the (top layer) structure and consequently have a drastic effect on membrane performance. Reproducibility is also often a problem. Membrane characterisation is necessary to relate structural membrane properties such as pore size, pore size distribution, free volume and crystallinity to membrane separation properties. Although membrane manufacturers give very definite and straightforward information for example about membrane cut-off, pore size and pore size distribution no attempt is made to place this information in a more comparative framework. The question arises as to what information can be obtained from characterisation measurements which will help us in the prediction of membrane performance for a given application. One useful piece of information is a distinction between intrinsic membrane properties and actual membrane applications. For example, the membrane flux for ultrafiltration in food- and dairy applications is usually less than 10% of the pure water flux, with the application of microfiltration giving an even larger difference between the pure water flux and process fluxes. The large discrepancy is mainly caused by concentration polarisation and fouling. These phenomena will be described in chapter VII, but they are implicit factors which must form part of membrane characterisation.

Membrane characterisation leads to the determination of structural and morphological properties of a given membrane. Irrespective of the structure developed, the first requirement after membrane preparation is to characterise the latter using simple techniques. Since membranes range from porous to nonporous depending on the type of separation problem involved, completely different characterisation techniques will be required in each case. To obtain an impression about size of particles and molecules to encountered, it is useful to consider fermentation processes since a wide range of particles and molecules with various dimensions are found in these cases. Other than suspended particles (micro-organisms such as yeasts, fungi and bacteria), a wide variety of products may be produced with different molecular weights; these include low molecular weight products such as alcohols (especially ethanol in wines, beers and distilled spirits),

carboxylic acids (citric acid, lactic acid and gluconic acid) and L-amino acids (alanine, leucine, histidine, phenylalanine and glutamic acid) together with high molecular weight components such as enzymes.

Some typical dimensions of small particles, molecules and ions are given in table IV.1, from which it can be seen that the particles to be separated cover a range of five orders of magnitude in size.

Table IV.1   Apparent dimensions of small particles, molecules and ions
(from ref. 1).

species	range of dimensions (nm)		
yeasts and fungi	1000	-	10000
bacteria	300	-	10000
oil emulsions	100	-	10000
colloidal solids	100	-	1000
viruses	30	-	300
proteins/polysaccharides (Mw. 10^4-10^6)	2	-	10
enzymes (Mw. 10^4-10^5)	2	-	5
common antibiotics (Mw. 300-1000)	0.6	-	1.2
organic molecules (Mw. 30-500)	0.3	-	0.8
inorganic ions (Mw. 10-100)	0.2	-	0.4
water (Mw. 18)	0.2		

Such components can only be separated from each other through the use of different membranes, ranging from microfiltration to reverse osmosis.

IV.2.   Membrane characterisation

Before describing the membrane characterisation methods available and the purpose for which they can be employed, it is important to realise the wide range of pore sizes which must be covered (see table IV.1). In general, it may be stated that membrane characterisation becomes progressively more difficult as the pore size decreases. Various pore sizes have their own methods of characterisation methods. Again, the membranes will be classified in two main groups, which have been depicted schematically in figure IV-1.
i) porous and ii) nonporous membranes

In microfiltration/ultrafiltration membranes, fixed pores are present which can be

characterised by several techniques. In order to avoid confusion in defining porous membranes, we will use the term 'porous' for both the microfiltration and ultrafiltration membranes instead of the frequently used definition of microporous. The definition of porous is more in agreement with the definitions adopted by the IUPAC [2 - 4]:

-    macropores > 50 nm
-    mesopores   2 nm < pore size < 50 nm
-    micropores < 2 nm.

The pore size classification given here is referred to pore diameter or more arbitrarily pore width.

This implies that microfiltration membranes are porous media containing macropores and ultrafiltration membranes are also porous with mesopores in the top layer. Hence, the definition porous covers both the macropores and mesopores. With membranes of these type it is not the membrane (material) which is characterised but the pores in the membrane. Here the pore size (and pore size distribution) mainly determines which particles or molecules are retained and which will pass through the membrane. Hence, the material is of little importance in determining the separation performance. On the other hand, with dense pervaporation/gas separation membranes, no fixed pores are present and now the material itself mainly determines the performance.
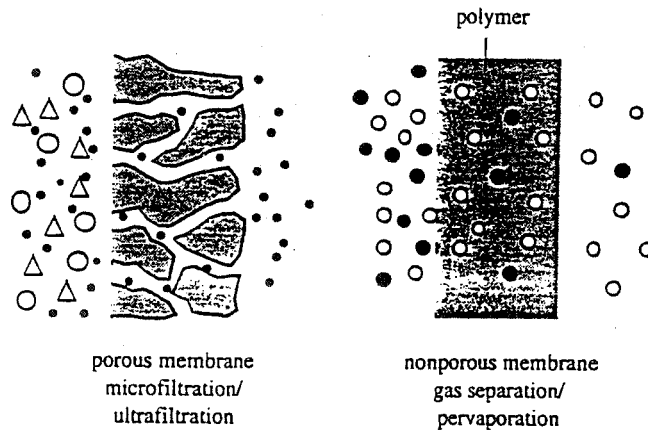
Figure IV - 1.   Schematic drawing of a porous and a nonporous membrane.

The morphology of the polymer material (crystalline, amorphous, glassy, rubbery) used for membrane preparation directly affects its permeability. Factors such as temperature and the interaction of the solvent and solute with the polymeric material, have a large influence on the segmental motions. Consequently, the material properties may change if the temperature, feed composition, etc. are changed.

In this chapter the characterisation methods described and discussed apply both to

porous as well as nonporous membranes.

IV.3.   The characterisation of porous membranes

Characterisation data for porous membranes often give rise to misunderstandings and misinterpretations. It should be realised that even when the pore sizes and pore size distributions have been determined properly the morphological parameters have been determined. However, in actual separation processes the membrane performance is mainly controlled by other factors, e.g. concentration polarisation and fouling.

One important, but often not clearly defined variable in the characterisation of porous membranes, is the shape of the pore or its geometry. In order to relate pore radii to physical equations, several assumptions have to be made about the geometry of the pore. For example, in the Poiseuille equation (see eq. IV - 4) the pores are considered to be parallel cylinders, whereas in the Kozeny-Carman equation (eq. IV - 5) the pores are the voids between the close-packed spheres of equal diameter. These models and their corresponding pore geometries are extreme examples in most cases, because such pores do not exist in practice. However, in order to interpret the characterisation results it is often essential to make assumptions about the pore geometry. In addition, it is not the pore size which is the rate-determining factor, but the smallest constriction. Indeed some characterisation techniques determine the dimensions of the pore entrance rather than the pore size. Such techniques often provide better information about 'permeation related' characteristics.

Another factor of interest is the pore size distribution in a porous ultrafiltration and microfiltration membrane. In general, the pores in these membranes do not have the same size but exist as a distribution of sizes. Figure IV-2 provides a schematic drawing of the pore size distribution in a given membrane. The membrane can be characterised by a nominal or an absolute pore size. With an absolute rating, every particle or molecule of that size or larger is retained. On the other hand, a nominal rating indicates that a percentage (95 or 98%) of the particles or molecules of that size or larger is retained.
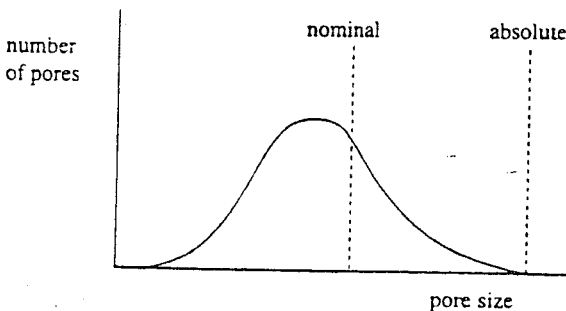
Figure IV - 2.   Schematic drawing of the pore size distribution in a certain membrane.

It should be noted that this definition does not characterise the membrane nor the pores of the membrane, but rather the size of the particles or molecules retained by it. The separation characteristics are determined by the large pores in the membrane. Another factor of interest is the surface porosity. This is also a very important variable in determining the flux through the membrane, in combination with the thickness of the top layer or the length of the pore. Different microfiltration membranes exhibit a wide range of surface porosity as discussed in chapter III, from about 5 to 70%. In contrast, the ultrafiltration membranes normally show very low surface porosities, ranging from 0.1 - 1 %.

Two different types of characterisation method for porous membranes can be distinguished from the above considerations:

- *Structure-related parameters:*
  determination of pore size, pore size distribution, top layer thickness and surface porosity.
- *Permeation-related parameters:*
  determination of the actual separation parameters using solutes that are more or less retained by the membrane ('cut-off' measurements).

It is often very difficult to relate the structure-related parameters directly to the permeation-related parameters because the pore size and shape is not very well defined. The configuration of the pores (cylindrical, packed-spheres) used in simple model descriptions deviate sometimes dramatically from the actual morphology, as depicted schematically in figure IV - 3. Nevertheless, a combination of well defined characterisation techniques can give information about membrane morphology which can be used as a first estimate in determining possible fields of application. In addition, it can serve as a feed-back for membrane preparation.
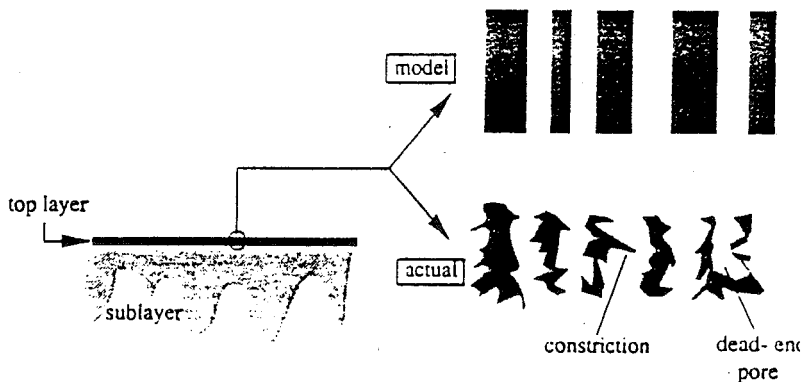
Figure IV - 3. Comparison of an ideal and the actual structure in the top layer of an ultrafiltration membrane [2].

There are a number of characterisation techniques available for porous media and although both microfiltration and ultrafiltration membranes are porous, they will be discussed separately, because different techniques must be used.

IV .3.1   Microfiltration

Microfiltration membranes possess pores in the 0.1 - 10 μm range and are readily characterised with various techniques. The following methods will be discussed here:
- scanning electron microscopy
- bubble-point method
- mercury intrusion porometry
- permeation measurements

The first three methods listed involve the measurement of morphological or structural-related parameters whereas the last method is a typical permeation-related technique.

IV.3.1.1 Electron microscopy (EM)

Electron microscopy (EM) is one of the techniques that can be used for membrane characterisation. Two basic techniques can be distinguished: scanning electron microscopy (SEM) and transmission electron microscopy (TEM).
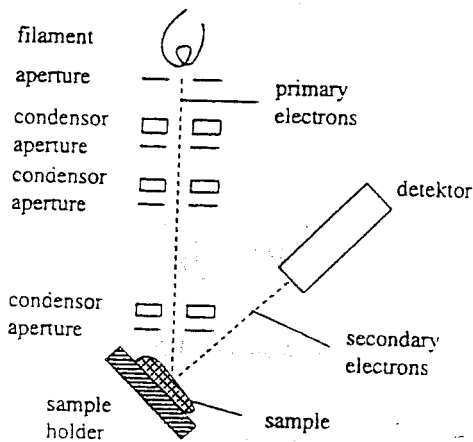
Figure IV - 4.   The principle of scanning electron microscopy.

Of these two techniques, scanning electron microscopy provides a very convenient and simple method for characterising and investigating the porous structure of microfiltration

membranes. (In addition, the substructure of other asymmetrical membranes can also be studied.) The resolution limit of a simple electron microscope lies in the 0.01 μm (10 nm) range, whereas the pore diameters of microfiltration membranes are in the 0.1 to 10 μm range. Resolutions of about 5 nm (0.005 μm) can be reached with more sophisticated microscopes.

The principle of the scanning electron microscope is illustrated in figure IV - 4. A narrow beam of electrons with kinetic energies in the order of 1-25 kV hits the membrane sample. The incident electrons are called primary (high-energy) electrons, and those reflected are called secondary electrons. Secondary electrons (low-energy) are not reflected but liberated from atoms in the surface; they mainly determine the imaging (what is seen on the screen or on the micrograph). When a membrane (or polymer) is placed in the electron beam, the sample can be burned or-damaged, depending on the type of polymer and accelerating voltage employed. This can be avoided by coating the sample with a conducting layer, often a thin gold layer, to prevent charging up of the surface. The preparation technique is very important (but often overlooked) since bad preparation techniques give rise to artefacts. Other important problems are associated with drying of a wet sample because the capillary forces involved damage the structure. Various methods can be employed to prevent this, e.g., the use of a cryo-unit, or replacing the water in the membrane for a liquid with a lower surface tension prior to drying.

The latter method is probably the more simple one. Water has a high surface tension (γ = 72.3 10^{-3} N/m), and on replacing it by another liquid with a much lower surface tension this also reduces the capillary forces acting during drying. The choice of the liquid used depends on the membrane structure, since all the liquids must be non-solvents for the membrane. An example of a typical sequence of liquids is: water, ethanol, butanol, pentane or hexane. The last solvent in this sequence, an alkane, has a very low surface tension (hexane: γ = 18.4 10^{-3} N/m) and can be easily removed.

In polymers with a high to very high water sorption, problems can arise because the structure may be damaged or altered upon drying. For these types of sample low-temperature scanning electron microscopy (LTSEM) may be used where a so-called cryo-unit is connected to the microscope. The wet samples are quenched in liquid nitrogen and brought into the cryo-unit where the frozen water is partly sublimed. The frozen water takes care of electron conduction but it also possible to coat the sample with a gold layer by a deposition technique. Without this deposition technique the magnifications attained is not very high and also that freezing can damage the structure. However, this is a very useful technique for highly swollen samples.

Scanning electron microscopy allows a clear view of the overall structure of a microfiltration membrane; the top surface, the cross-section and the bottom surface can all be observed very nicely. In addition, any asymmetry in the structure can be readily observed. Figure IV - 5 shows the top surface of a porous poly(ether imide) membrane [5] as observed by scanning electron microscopy (SEM) methods. Micrographs of this kind allow the pore size, the pore size distribution and the surface porosity to be obtained. Also the geometry of the pores can be clearly visualised.
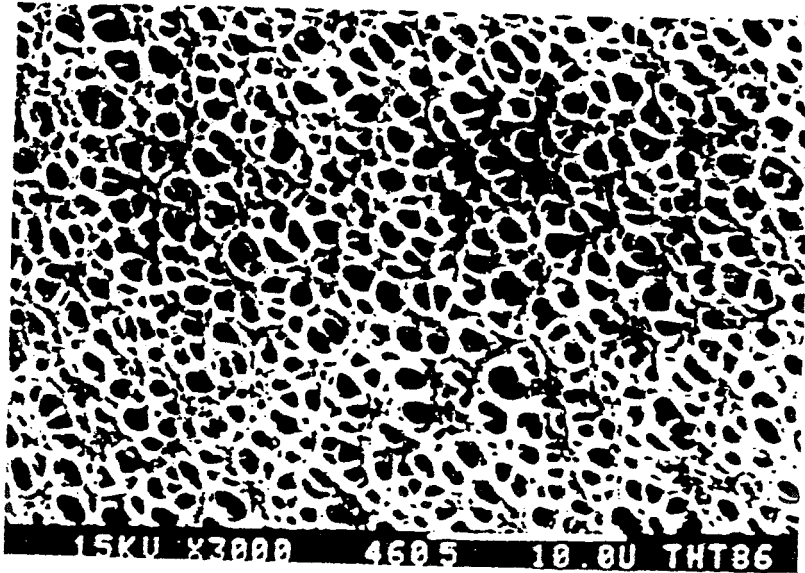
Figure IV - 5. Top surface of a porous poly(ether imide) membrane taken by SEM
methods (magnification: 3,000 x).

In summary, it can be stated that scanning electron microscopy is a very simple and useful technique for characterising microfiltration membranes. A clear and concise picture of the membrane can be obtained in terms of the top layer, cross-section and bottom layer. In addition, the porosity and the pore size distribution can be estimated from the photographs. Care must be taken that the preparation technique does not influence the actual porous structure.

IV.3.1.2   Atomic force microscopy

Atomic force microscopy is a rather new new method to characterise the surface of a membrane [6,7]. A sharp tip with a diameter smaller than 100 Å is scanning across a surface with a constant force. London - vanderWaals interactions will occur between the atoms in the tip and the surface of the sample and these forces are detected. This will result

in a line scan or profile of the surface. The use of a micro fabricated cantilever allows to operate at very low forces, less than 1 nN (= 10^{-9} N). This makes it possible to apply this technique for soft surfaces as in polymeric membranes.

In general the technique is applied at constant force between tip and surface and this give then an image of the surface in a certain direction. Figure IV - 6 gives a schematic drawing of such an image for a microfiltration membrane.
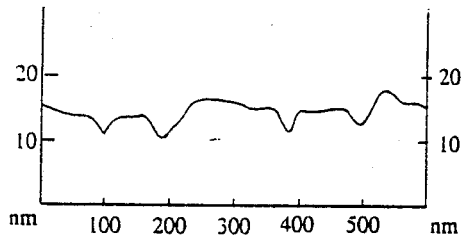
Figure IV - 6   Schematical drawing of a surface scan of an UF membrane

The surface of the membrane can be scanned in air without any pretreatment. The obtained line scans do not only reveal the possible position and size of a pore, also an indication of surface roughness or surface corrugations are obtained. Due to this surface roughness it is often difficult to obtain a pore size distribution since the surface corrugations are in the same order or larger than the pore sizes. However, in combination with electron microscopy and other technique it might be a useful technique. Also information on surface roughness might be useful when support layers are characterized for composite membranes.

In summary, the atomic force microscopy (AFM) is a method to determine the structure of a surface. The pore size and porosity can be obtained from the cross-sections of the AFM images. The advantage of this technique is that no pretreatment is required and the measurement can be carried out under atmospheric conditions. A disadvantage is that high surface roughness may result in images which are difficult to interpreted. Moreover, high forces may damage the polymeric structure.

IV.3.1.3   Bubble-point method

The bubble-point point method provides a simple means of characterising the maximum pore size in a given membrane. The method was used by Bechold even in the early years of this century. A schematic drawing of the test apparatus is given in figure IV - 7. The method essentially measures the pressure needed to blow air through a liquid-filled membrane. The top of the filter is placed in contact with a liquid (e.g. water) which fills all the pores when the membrane is wetted. The bottom of the filter is in contact with air and

as the air pressure is gradually increased bubbles of air penetrate through the membrane at a certain pressure.
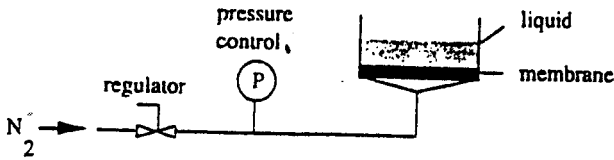
Figure IV - 7. Schematic drawing of a bubble-point test apparatus

The relationship between pressure and pore radius is given by the Laplace equation (eq. IV - 1).

$$r_p = \frac{2\gamma}{\Delta P} \cos\theta$$

(IV - 1)

where r_p is the radius of a capillary shaped pore (m) and γ the surface tension at the liquid/air interface (N/m). The principle of the bubble-point measurement is depicted schematically in figure IV - 8, from which it can be seen that the liquid on the top of the membrane wets the latter. An air bubble will penetrate through the pore when its radius is equal to that of the pore. This means that the contact angle is 0° (and $\cos\theta = 1$). Penetration will first occur through the largest pores and since the pressure is known, the pore radius can be calculated from eq. IV - 1.

This method can only be used to measure the largest active pores in a given membrane and has therefore become the standard technique used by suppliers to characterise their (dead-end) microfiltration membranes. It will be shown later on that both
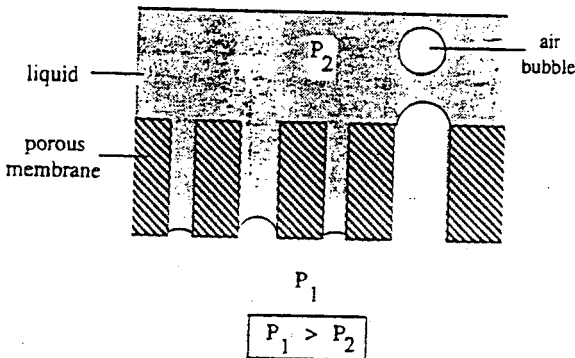
Figure IV - 8. The principle of the bubble-point method.

the permeation method and the mercury intrusion method are extensions of the bubble-point method. Since the surface tension at the water/air interface is relatively high (72.3 10^{-3} N/m), if small pores are present, it is necessary to apply high pressures. However, water can be replaced by another liquid e.g. by an alcohol (the surface tension at the t-butanol/air interface is 20.7 10^{-3} N/m). Some data calculated from eq. IV - 1 using water as the liquid are given in table IV.2. This table also gives an indication of the pressure required for a given pore radius.

Table IV.2   Relation between pressure and pore radius (eq. IV - 1)
              using water as the wetting medium

pore radius (μm)	pressure (bar)
10	0.14
1.0	1.4
0.1	14.5
0.01	145

Equation IV - 1 suggests that the method is independent of the type of liquid used. However, if different liquids, e.g. water, methanol, ethanol, n-propanol, i-propanol, are used, different values radius will be obtained for the pore radius. This is probably due to wetting effects and for this reason i-propanol is often used as a standard liquid. Other factors that influence the measurement are the rate at which the pressure is increased, the length of the pore, and the affiniyty between wetting liquid and membrane material.

In summary, the bubble-point method is a very simple technique for characterising the largest pores in microfiltration membranes. Active pores are determined with this technique. A disadvantage is that different results are obtained when different liquids are used for characterisation. In addition, the rate of pressure increase and the pore length may influence the result. Pore size distributions can be obtained by performing this technique by a stepwise increase of the pressure.

IV.3.1.4   Bubble-point with gas permeation (wet and dry flow method)
The bubble-point method gives only limited information and a another method was developed that combines the bubble-point concept with the measurement of the gas flow through the emptied pores. Here at first the gas flow is measured through a dry membrane as a function of the pressure and generally a straight line obtained (see figure IV - 8). Then

the membrane is wetted and again the gas flow is determined as a function of the applied pressure. At very low pressures the pores are still filled with the liquid and the gas flow, which is determined by diffusion through the liquid, is very low. At a certain minimal pressure (the 'bubble-point') the largest pores will be empty and the gas flow will increase by convective flow through these pores. A further increment in pressure will open smaller pores according to the Laplace equation. At the highest pressure the gas flow of the dry membrane must be equal to the wet membrane. If this is not the case there are still some smaller pores present in the membrane. The dry and wet flow are both depicted in figure IV - 9 and the pore size distribution can be determined. This method is suitable for characterisation of macropores and can be applied for microfiltration membranes with pore sizes up to 50 nm.
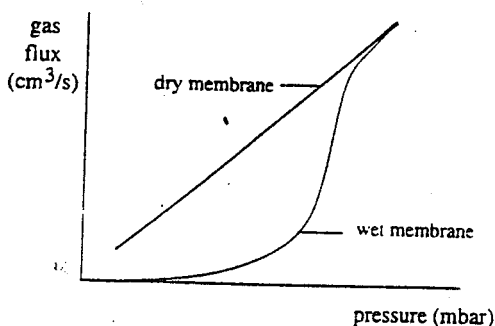
Figure IV. - 9.   Gas flux in the permeation related bubble-point measurement

IV.3.1.5   Mercury intrusion method

The mercury intrusion technique is a variation of the bubble-point method. In this technique, mercury is forced into a dry membrane with the volume of mercury being determined at each pressure. Again, the relationship pressure and pore size is given by the Laplace equation. Because mercury does not wet the membrane (since its contact angle is greater than 90° and consequently cos θ has a negative value), eq. IV . 1 is modified to:

$$r_p = - \frac{2\gamma \cos\theta}{\Delta P}$$

(IV - 2)

The contact angle of mercury with polymeric materials is often 141.3° and the surface tension at the mercury/air interface is 0.48 N/m. Hence eq. IV . 2 reduces to

$$r_p = \frac{7492}{\Delta P}$$

(IV - 3)

where r_p is expressed in nm and P in bar.

Since the volume of mercury can be determined very accurately, pore size distributions can be determined quite precisely. However, eq. IV - 2 assumes that capillary pores are present. This is not generally the case and for this reason a morphology constant must be introduced. Furthermore, very high pressures should be avoided since these may damage the porous structure and lead to an erroneous pore size distribution. Figure IV - 10 gives a schematic drawing of the result of a mercury intrusion experiment.
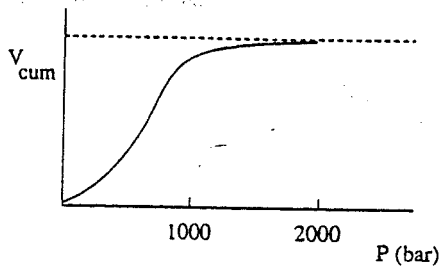
Figure IV - 10. Cumulative volume (V_{cum}) as a function of the applied pressure.

At the lowest pressures the largest pores will be filled with mercury. On increasing the pressure, progressively smaller pores will be filled according to eq. IV - 3. This will continue until all the pores have been filled and a maximum intrusion value is reached. It is possible to deduce the pore size distribution from the curve given in figure IV - 10, because every pressure is related to one specific pore size (or entrance to the pore !). The pore sizes covered by this technique range from about 5 nm to 10 μm. This means that all microfiltration membranes can be characterised as well as a substantial proportion of the ultrafiltration membranes.

In summary, both pore size and pore size distribution can be determined by the mercury intrusion technique. One disadvantage is that the apparatus is rather expensive and not widely used as a consequence. Another point is that small pore sizes require high pressures and damage of the membrane structure may occur. Furthermore, the method measures all the pores present in the structure, including dead-end pores.

IV.3.1.6 Permeability method
If capillary pores are assumed to be present, the pore size can be obtained by measuring the flux through a membrane at a constant pressure using the Hagen-Poiseuille equation.

$$J = \frac{\varepsilon \ r^2}{8 \ \eta \ \tau} \frac{\Delta P}{\Delta x}$$

$$(IV - 4)$$

Here J is the (water)flux through the membrane at a driving force of $\Delta P/\Delta x$, with ΔP being the pressure difference (N/m^2) and Δx the membrane thickness (m). The proportionality factor contains the pore radius r (m), the liquid viscosity η (Pa.s), the surace porosity of the membrane ε (= $n\pi r^2$/surface area) and the tortuosity factor τ.

The pore size distribution can be obtained by varying the pressure, i.e. by a combination of the bubble-point method and permeability methods. It is not essential that the liquid should wet the membrane.
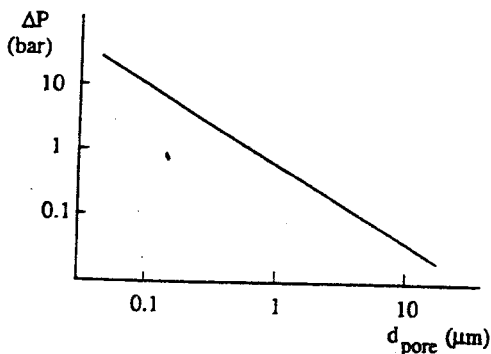
Figure IV - 11.   Wetting pressure for water as a function of the pore diameter for   porous polypropylene (Accurel).

A number of porous membranes are hydrophobic (such as polytetrafluoroethylene, poly(vinylidene fluoride), polyethylene and polypropylene) and water does not wet them. Nevertheless, water can be used as permeating liquid also for these membranes. The method itself is very simple, the (water) flux through the membrane is measured as function of the applied pressure. At a certain minimum pressure the largest pores become permeable, while the smaller pores still remain impermeable. This minimum pressure depends mainly on the type of membrane material present (contact angle), type of permeant (surface tension) and pore size. According to eq. IV - 4, the increase in (water) flux is proportional to the increase in applied pressure.

Suppose that we have an isoporous hydrophobic membrane with a number of capillaries of a given radius and that we use a liquid that does not spontaneously wet the membrane. Figure IV - 11 shows the pressure needed to wet a porous polypropylene membrane with water as a function of pore size. Very small pore diameters require a high pressure to wet the membrane. At a certain pressure, however, the membrane becomes wetted and permeable, and thereafter the flux increases linearly with increasing pressure. The idealised flux versus pressure curve is shown in figure IV - 12. However, synthetic

microfiltration and ultrafiltration membranes do generally not posses a uniform pore size, and hence breakthrough curves of the type shown in figure IV - 12 will not be observed. At a pressure below P_{min} ($= 2 \gamma / r_{max}$) the membrane is impermeable. At P_{min} the largest pores become permeable, and as the pressure increases smaller and smaller pores become permeable. Finally, when a pressure P_{max} is reached, the smallest pores become permeable. The flux at a certain pressure is due to the contribution of all pores that are available, i.e. assuming cylindrical pores the Hagen-Poisseuile equation can be applied in
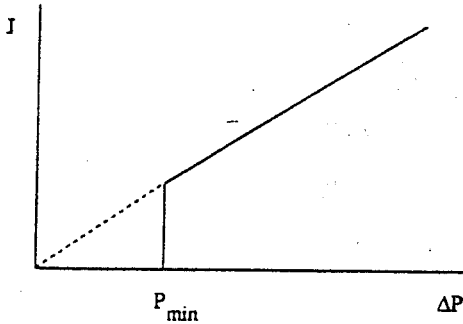
Figure IV - 12. Flux versus pressure curve for a membrane possessing a uniform pore size.

which n_i is the number of pores of radius r_i (eq. IV - 5). From the flux-pressure characteristic a pore size distribution can be estimated.

$$J = \frac{\pi \sum_i (n_i \, r_i^4)}{8 \, \eta \, \tau \, l} \, \Delta P$$

$$(IV - 5)$$
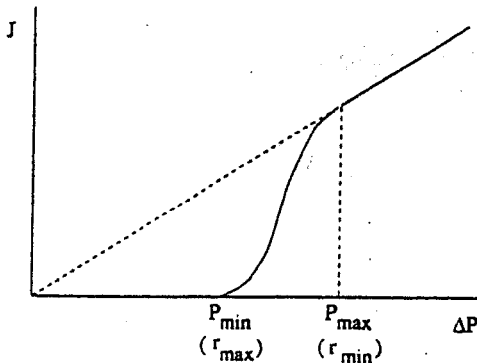
Figure IV - 13. Flux versus pressure curve for a membrane exhibiting a pore size distribution.

When the pressure is increased further the flux increases linearly with pressure. (see figure IV - 13). The Hagen-Poiseuille relationship assumes that the pores in the membrane are cylindrical but generally this is not the case. Therefore, these limitations should be considered carefully in applying this equation. The Kozeny-Carman equation can be used instead of the Hagen-Poiseuille equation. It is assumed in this equation that the pores are interstices between close-packed spheres as can be found in sintered structures. The flux is given by eq. IV - 6.

$$ J = \frac{\varepsilon^3}{K \eta \ S^2 \ (1 - \varepsilon)^2} \frac{\Delta P}{\Delta x} $$

(IV - 6)

where K is a membrane constant, called the Kozeny-Carman constant, which is dependent on the pore shape and tortuosity. Here, ε is the porosity and S is the specific surface area.

The permeability method can be used both for microfiltration and ultrafiltration membranes. As with most methods of characterisation, one of the main problems encountered is the pore geometry. As mentioned above, the Hagen-Poisseuille equation assumes that the pores are cylindrical whereas the Kozeny-Carman equation assumes that the pores are interstices between close-packed spheres. Such pores are not commonly found in synthetic membranes.

In summary, it can be concluded that the permeability method has the distinct advantage of experimental simplicity, especially when liquids are used. However, the pore geometry is very important in this method and since this is not generally known the experimental results are often difficult to interpret.

IV.3.2   Ultrafiltration

Ultrafiltration membranes can also be considered as porous. However, this structure is typical more asymmetric compared to microfiltration membranes. Such asymmetric membranes consist of a thin top layer supported by a porous sublayer, with the resistance to mass transfer being almost completely determined by the top layer. For this reason, the characterisation of ultrafiltration membranes involves the characterisation of the toplayer; i.e. its thickness, pore size distribution and surface porosity. Typical pore diameters in the toplayer of an ultrafiltration membrane are generally in the range of 20 - 1000 Å. Because of the small pore sizes, microfiltration characterisation techniques cannot be used for ultrafiltration membranes. The resolution of an ordinary scanning electron microscope is generally too low to determine the pore sizes in the toplayer accurately. Furthermore, mercury intrusion and bubble-point methods cannot be used because the pore sizes are too small, so that very high pressures would be needed, which would destroy the polymeric structure. However, permeation experiments can still be used and this method can be extended by the use of various types of solute. The following characterisation methods will be discussed here:

- gas adsorption-desorption
- thermoporometry
- permporometry
- liquid displacement
- (fractional) rejection measurements
- transmission electron microscopy

IV.3.2.1   Gas adsorption-desorption

Gas adsorption-desorption is a well-known technique for determining pore size and pore size distribution in porous materials. The adsorption and desorption isotherm of an inert gas is determined as a function of the relative pressure ($p_{rel} = p/p_0$, i.e. the ratio between the applied pressure and the saturation pressure). Nitrogen is often used as adsorption gas and the experiments are carried out at boiling liquid nitrogen temperature (at 1 bar). The adsorption isotherm starts at a low relative pressure. At a certain minimum pressure the smallest pores will be filled with liquid nitrogen (with a minimum radius size of about 2 nm). As the pressure is increased still further, larger pores will be filled and near the saturation pressure all the pores are filled. The total pore volume is determined by the quantity of gas adsorbed near the saturation pressure. Desorption occurs when the pressure is decreased, starting at the saturation pressure. The desorption curve is generally not identical to the adsorption curve, e.g. a hysteresis effect can be observed (see figure IV - 14). The reason for this is that capillary condensation occurs differently in adsorption and desorption. Due to the concave meniscus of the liquid in the pore, nitrogen evaporates at a lower relative pressure because the vapour pressure of the liquid is reduced. The lowering of the vapour pressure for a capillary of radius r is given by the Kelvin relationship:

$$\ln \frac{p}{p_0} = - \frac{2 \gamma \, V}{r_k \, R \, T} \cos \theta$$

(IV - 7)

the contact angle θ being assumed to be zero ($\cos\theta = 1$).

This relation can be simplified for nitrogen adsorption-desorption to with r_k expressed in nm:

$$r_k = - \frac{4.1}{\log \dfrac{p}{p_0}}$$

(IV - 8)

and the pore radius may be calculated from:

$$r_p = r_k + t$$

(IV - 9)

where t is the thickness of the adsorbed layer of vapour in the pores, r_k is the Kelvin radius and r_p the pore radius ($r_k < r_p$). The thickness of the t-layer can be estimated from calibration curves.
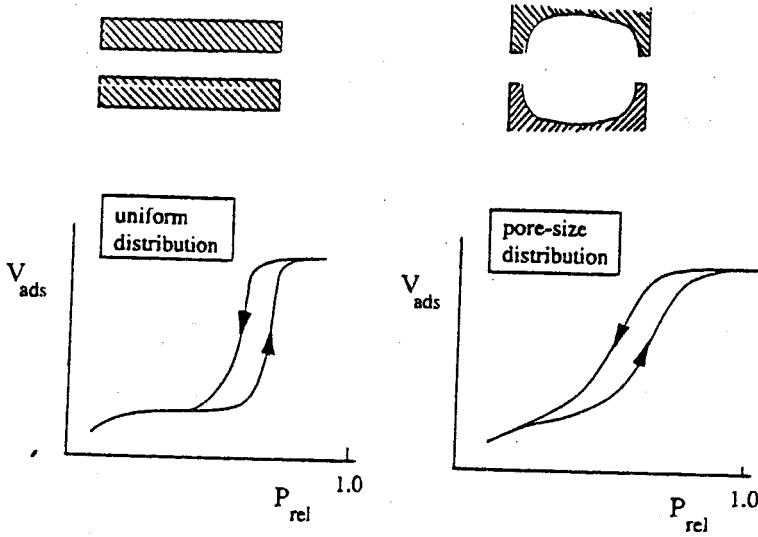
Figure IV - 14. Nitrogen adsorption-desorption isotherm for porous material containing cylindrical type of pores. Uniform pore distribution (left) and pore size distribution (right).
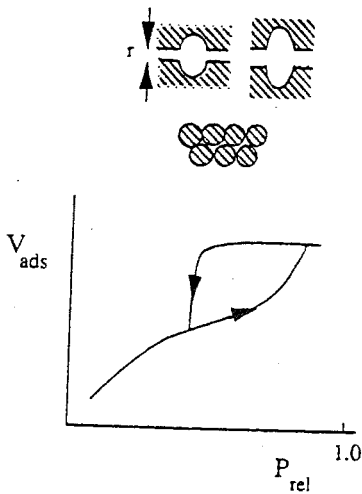
Figure IV - 15. Nitrogen adsorption-desorption isotherm for a porous material where the pores are assumed to be voids between close-packed spheres (and also for a system of parallel plates, see also figure IV - 15).

Gas adsorption-desorption isotherms for systems containing pores corresponding to various geometries are given in figures IV - 14 and IV - 15. The adsorption- desorption isotherms for systems containing typical cylindrical type pores are given in figure IV - 14. Where a pore size distribution exists, both adsorption and desorption curves show a slow increase/decrease as a function of the relative pressure. However, where a uniform pore distribution exists, a sudden increase/decrease occurs corresponding to that specific pore size. For pores with an ink bottle shape, as with voids in a system of close-packed spheres, the adsorption curve increases slowly but desorption takes place at the same relative pressure because all of the pore entrances have the same size (see figure IV - 14).

This method is generally not very accurate in membranes with a large pore size distribution and without a definite pore geometry. However, the morphology is better defined in ceramic membranes and the pore size distribution is often very sharp. Some examples are given in figures IV - 16 and IV - 17. The gas adsorption-desorption isotherm of an alumina (Al_2O_3) membrane calcined at 400°C is given in figure IV - 15 [8].
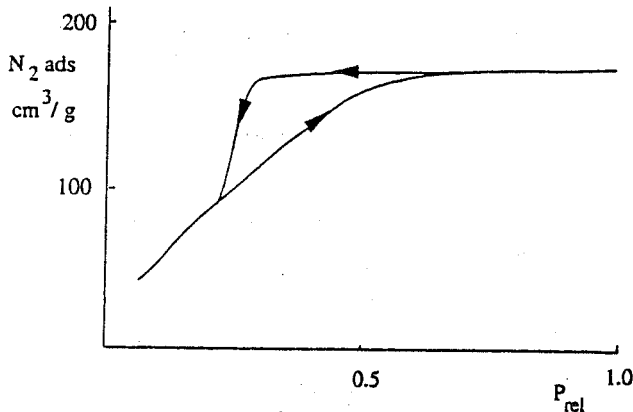
Figure IV - 16. Adsorption-desorption isotherm of an alumina membrane calcined at 400°C [8].

The pores in membranes of this type are formed by packing plate-shaped crystals in a parallel fashion. Slit-shaped pores where the slit width and plate thickness are about the same [8] are obtained in this way .

The pore size distribution of some ceramic alumina membranes (Al_2O_3) treated at various temperatures are given in figure IV - 17. These distribution curves were calculated from the corresponding adsorption-desorption isotherms and demonstrate that the alumina membranes all possess a narrow pore size distribution with individual pores being slit-shaped.
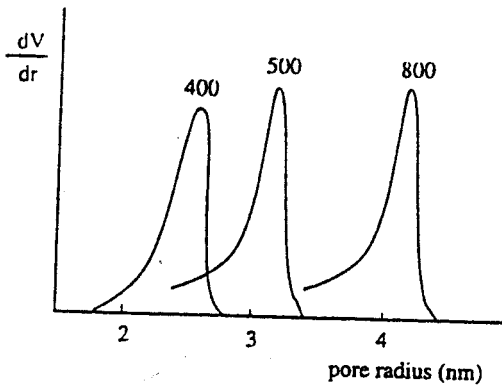
Figure IV - 17. Pore size distributions of alumina membranes calcined at various temperatures [8].

In summary, it may be concluded that the gas adsorption-desorption method is simple if a suitable apparatus is available. The main problem is to relate the pore geometry to a model which allows the pore size and pore size distribution to be determined from the isotherms. Dead-end pores which do not contribute towards transport are measured by this technique. Ceramic membranes often give better results because their structure is generally more uniform and the membranes less susceptible to capillary forces.
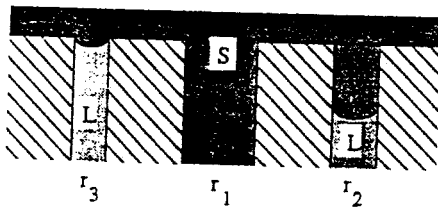
Figure IV - 18. Schematic drawing of the extent of undercooling in relation to the pore diameter. L=liquid (water); S=solid (ice); r=pore radius ($r_1 > r_2 > r_3$).

IV.3.2.2   Thermoporometry

Thermoporometry is based on the calorimetric measurement of a solid-liquid transition (e.g. of pure water) in a porous material and can be applied to determine the pore size in porous membranes [9 - 11]. This may be the pores in the skin of an asymmetric membrane, the temperature at which the water in the pores freezes (the extent of undercooling) depending on the pore size. As the pore size decreases the freezing point of water decreases. Each pore (pore size) has its own specific freezing point. For cylindrical

pores containing water, the following equation for melting can be derived [9]:

$$r_p \;=\; 0.68 \;-\; \frac{32.33}{\Delta T}$$

$$(IV - 10)$$

where r_p is the pore radius (nm) and ΔT the extent of undercooling (°C). Brun derived as well a relation between the heat effect w (J/g) and the melting point depression.

$$w = - 0.155 \, \Delta T^2 \;-\; 11.39 \, \Delta T \;-\; 332$$

$$(IV - 11)$$
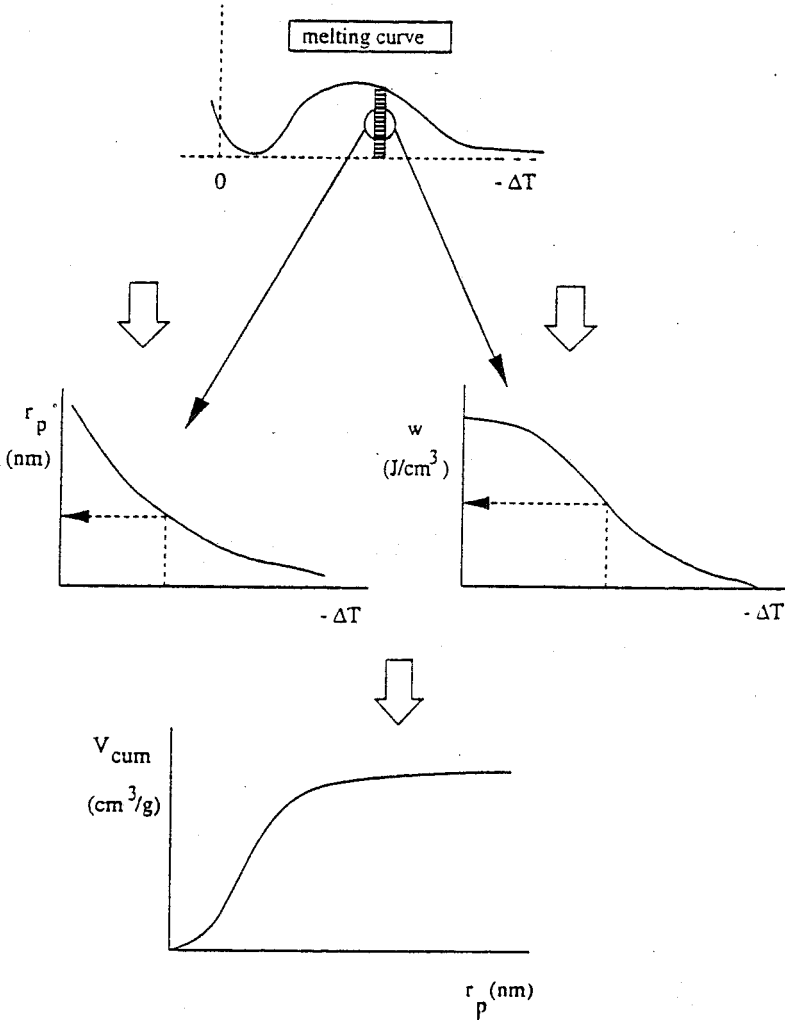
Figure IV - 19.   Schematic drawing showing how to obtain a pore size distribution from a DSC melting curve.

It can be seen from eq. IV - 10 that as the pore radius becomes smaller the extent of undercooling increases. Figure IV - 18 provides a schematic drawing for the freezing of a liquid (water) in a porous medium as a function of the pore size. It is assumed that the temperature has been decreased to such an extent that all the water in the pore r_1 has become ice. Water has started just to freeze in pore r_2 while all the water is still liquid in pore r_3. If the temperature is lowered still further, the water in pore r_3 will also freeze. The heat effect of the liquid-solid transition ('freezing or melting') is measured by means of a Differential Scanning Calorimeter (DSC).

Figure IV - 19 shows how a pore size distribution may be obtained from a melting curve (It is better to follow the melting curve rather than the crystallisation curve because melting is less susceptible to kinetic effects). The melting curve is measured as a function of the degree of undercooling $(-\Delta T)$ using DSC. Because the relationship between the extent of undercooling and the pore radius is known (eq. IV - 10), and also between the heat effect (in J/cm^3) and extent of undercooling, the cumulative pore volume can be obtained as a function of the pore radius.
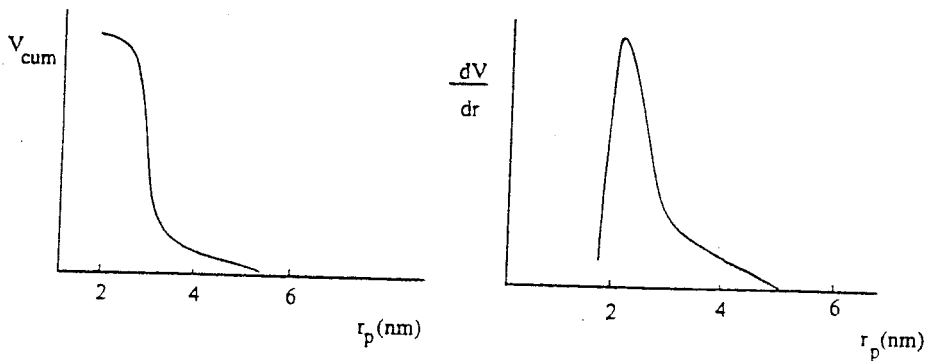
Figure IV - 20.   Cumulative pore volume and pore size distribution for a PPO membrane [12].

Figure IV - 20 gives the cumulative pore volume and the pore size distribution for a PPO poly(phenylene oxide) ultrafiltration membrane determined by thermoporometry [12]. Figure IV - 21 gives the pore size distribution of a ceramic membrane determined by two methods: gas adsorption-desorption and thermoporometry [13]. Both curves (and hence both methods) are in good agreement with each other. Similar results were found by Cuperus for γ-alumina membranes [14].

In summary, it may be concluded that thermoporometry is a simple method if a DSC apparatus is available. As with all the other methods, an assumption has to be made about the pore geometry, in order to calculate the pore size and the pore size distribution. All pores are measured with this technique, including dead-end pores. Furthermore, the pore size distribution can also be determined.
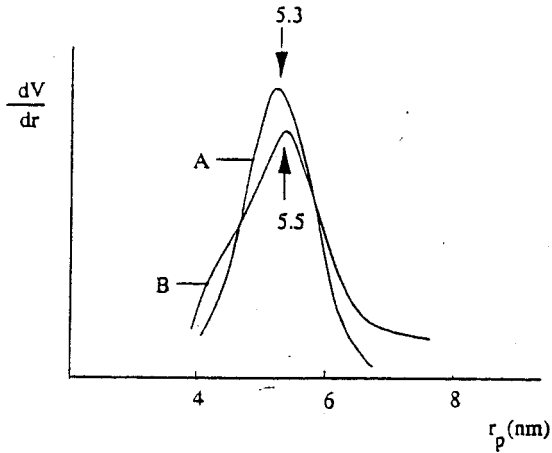
Figure IV - 21. Pore size distribution for a ceramic membrane determined by thermoporometry (A) and gas adsorption-desorption (B) [13].

IV.3.2.3   Permporometry

Thermoporometry has the disadvantage that all pores present in the membrane, in the sublayer as well as in the toplayer, are characterised including 'dead-end' pores that make no contribution towards transport. However, another rather new technique, permporometry, only characterises the active pores [14,15]. This means that in asymmetric membranes where transport is determined by the thin toplayer, information can be obtained about pore size and pore size distribution of the active pores in this toplayer. Permporometry is based on the blockage of pores by means of a condensable gas, linked with the simultaneous measurement of gas flux through the membrane. Such blockage is based on the same principle of capillary condensation as adsorption - desorption hysteresis (see section IV - 3.2.1). A schematic drawing of the experimental set-up employed is given in figure IV - 22.
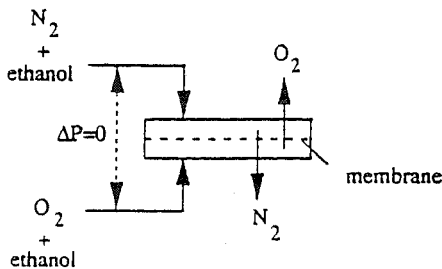
Figure IV - 22. Experimental set-up employed in permporometry

In the example illustrated ethanol is taken to be the condensable gas. It is important that the vapour should not swell the membrane, because if this occurs the pore sizes will change and erroneous results will be obtained. Hence, the affinity of the vapour and the polymer must be very low ('inert vapours') and also the vapour pressure should be readily adjusted over the whole range. The choice of the organic vapour also influences the method in another way, because the thickness of the t-layer (adsorbed monolayer) is dependent on the type of vapour employed. In order to interpret the results correctly, the thickness of this t-layer has to be determined (or calculated). During the experiment there is no difference in hydrostatic pressure across the membrane and gas transport proceeds only by diffusion, the flow of one of the two non-condensable gases being measured (for example that of oxygen can be measured with an oxygen selective electrode).

The principle of the method is shown schematically in figure IV - 23. At a relative pressure p_r ($p_r = p/p°$) equal to unity, all the pores are filled with liquid and no gas permeation occurs. On reducing the relative pressure, the condensed vapour is removed from the largest pores in accordance with the Kelvin equation (eq. IV - 7), and the diffusive gas flow through these open pores is measured. On reducing the relative pressure still further, smaller pores become available for gas diffusion. When the relative pressure is reduced to zero, all the pores are open and gas flow proceeds through them all.

Because a certain pore radius (Kelvin radius r_k !) is related to a specific vapour pressure (eq. IV - 7), a measurement of the gas flow provides information about the number of these specific pores. Reducing the vapour pressure allows the pore size distribution to be obtained.
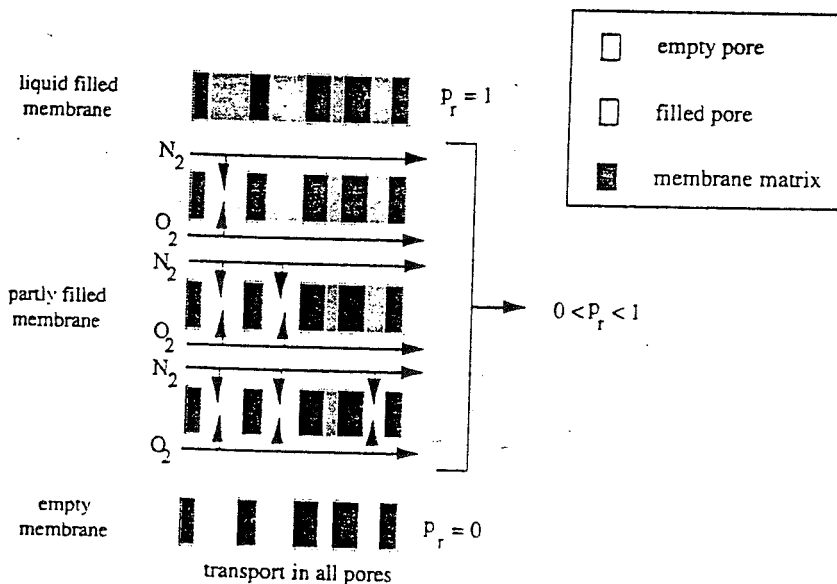
Figure IV - 23.   The principle of permporometry [15].

Figure IV - 24 gives an example of the pore size distribution obtained for an asymmetric poly(phenylene oxide) (PPO) membrane as determined by gas adsorption/desorption, thermoporometry and permporometry methods.

This particular membrane has a narrow pore size distribution, which is somewhat unusual for polymeric membranes obtained by phase inversion. Furthermore, the agreement between the methods is quite reasonable, with permporometry giving the highest value and adsorption-desorption the lowest. It should be noted that permporometry only measures active pores whereas adsorption-desorption and thermoporometry measure active, dead-end and even small pores in the sublayer.
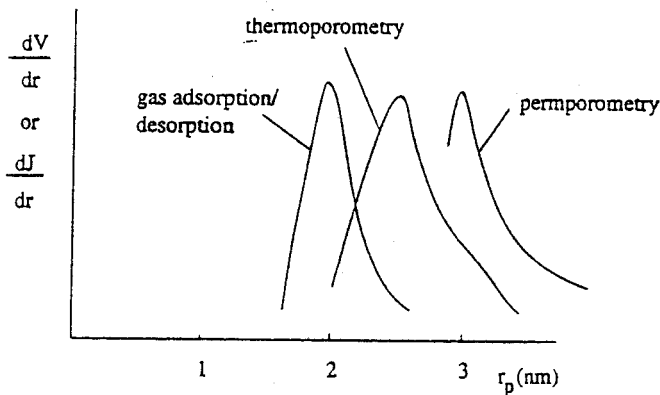
Figure IV - 24.   Pore size distribution of a PPO membrane measured by gas adsorption/desorption, permporometry and thermoporometry methods [16].

In summary, permporometry is more complicated than any of the other methods discussed so far because of experimental difficulties. The principal problem is the difficulty of maintaining the same vapour pressure on both sides of the membrane so that some time is necessary before thermodynamic equilibrium is attained and to control the gas flow accurately. Furthermore, the method is difficult to employ with hollow fibers. The advantage of this method is that only active pores are characterised.

IV.3.2.4   Liquid displacement

The liquid displacement method for determination of the pore size distribution was already introduced in the early century by Bechold [17] and Erbe [18] and further developed by Munari [19,20]. This method is similar to the gas flow bubble-point method (see IV . 3.1.2) method. The difference is that instead of a gas a liquid is used to displace a second liquid which has already been present in the pores of the membranes. A schematic drawing is given in figure IV - 25. For this method two immiscible liquids are employed. One of

these liquids is used to fill the pores of the membrane and a second liquid is used to
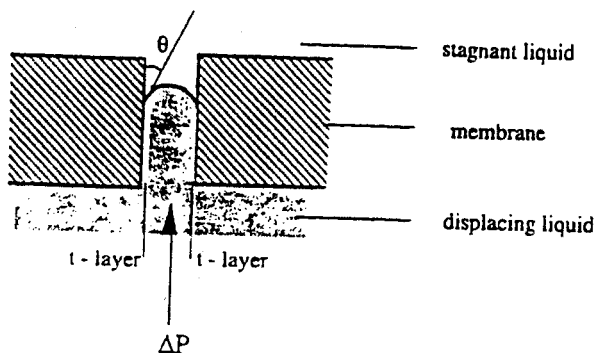
Figure IV - 25. The principle of the liquid displacement method

displace the pore-filling liquid. This can be achieved when a certain pressure is employed as given by the Laplace equation (eq. IV - 1). γ is the surface tension between the two liquids and by a proper choice a low value of γ can be obtained, two orders of magnitude lower than the surface tension at a water/air interface. Table IV.3 summarizes the interfacial tension of various liquid/air and liquid/liquid interfaces.

Table IV.3 Surface tension of various liquid/air and liquid/liquid interfaces at 25°C.

phase 1	phase 2	γ (mN/m)
water	air	72.0
methanol	air	22.6
ethanol	air	21.8
hexane	air	18.4
iso-pentane	air	13.7
water	iso-butanol	1.85

Displacement will start at the largest pores resulting in a flux which can be described by the Hagen-Poisseuille equation (eq. IV - 4). The flow can be measured with a mass flow meter. By increasing the pressure the liquid in smaller pores will be displaced and this will cause an enhancement of the flux through the membrane. In this way the flux is obtained as a function of the pore radius and from this curve the pore size distribution can be calculated. Figure IV - 26 gives the pore size distribution of a celgard (X10 400) membrane [21]. The membrane is wet with iso-butanol which is then displaced by water. It can be observed that the mean pore radius is about 13 nm, which is smaller than the

value given by the supplier. However, the pore sizes in a celgard membrane are not clearly defined (see figure VI - 4b) and the liquid displacement method will characterise the smallest constraints. The method can be carried out in two ways. i) the pressure is varied stepwise and the liquid flow is measured or ii) a fixed flow is varied stepwise (by an
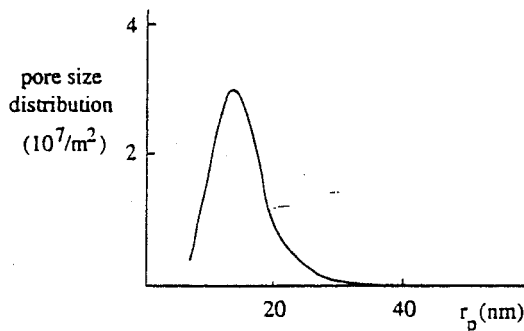
Figure IV - 26. Pore size distribution of a celgard membrane as determined by liquid displacement [21].

HPLC pump) and the pressure is measured. The former method is more easily to perform with flat membranes but with a hollow fiber system pressure build-up may result in irreproducible values and the second method is preferred.

In summary, liquid displacement is another method to determine the pore size distribution in microporous and mesoporous materials. The advantage of this method is that only active pores are characterised. A drawback may the occurrence of swelling due to the stagnant liquid that changes the pore sizes. Moreover, the set-up is rather complex and a pressure build-up may occur which interferes with the measurements.

IV.3.2.5   Solute rejection measurements

Many manufacturers use the concept of 'cut-off' to characterise their ultrafiltration membranes. Cut-off is defined as that molecular weight which is 90% rejected by the membrane. Cut-off values of a membrane are often used in an absolute fashion ('this membrane has a cut-off value of 40,000', implying that all solutes with a molecular weight greater than 40,000 are more than 90% rejected). Figure IV - 27 gives a schematic comparison between a membrane with a so-called 'sharp cut-off' and a membrane with a 'diffuse cut-off'. However, it is not possible to define the separation characteristics of a membrane by a single parameter, i.e. the molecular weight of the solute. Other parameters

are even more important, such as the shape and flexibility of the macromolecular solute, its interaction with the membrane material and, last but not least, the occurrence of concentration polarisation phenomena. Concentration polarisation and membrane fouling can have a drastic effect on the separation characteristics. Furthermore, cut-off values are often defined in different ways under different test conditions (pressure, cross-flow velocity, geometry of the test cell, concentration and type of solute, molecular weight distribution of solute) which makes it difficult to compare the results. When three different types of solute with the same molecular weight are considered, for example a globular protein (albumin), a branched polysaccharide (dextran) or a linear flexible molecule [poly(ethylene glycol)], three completely different rejection characteristics can be observed, as a function of the molecular weight. In other words, if solutes are used with the same molecular weight then three different cut-off values are obtained. Moreover, if a solution containing two solutes with a large difference in molecular weight (for example, γ-globulin, M_w = 150,000) and the other with a lower molecular weight (for example, albumin, M_w = 69,000), then the separation of the lower molecular weight solute is influenced by the presence of that with the higher molecular weight as a result of boundary layer effects. The high molecular weight solute is retained completely and the polarisation/fouling layer so formed has a considerable influence on the permeation of the low molecular weight solute. It is also possible that the solute with the higher molecular weight blocks the pores. Thus the influence of one upon the other is large in this.
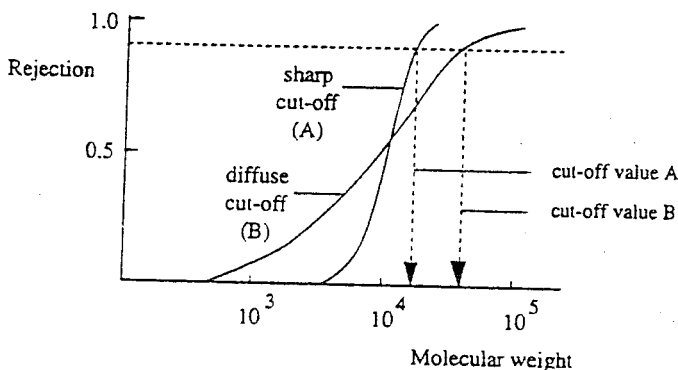
Figure IV - 27. Rejection characteristics for a membrane with a 'sharp cut-off' compared with those of a membrane with a 'diffuse cut-off'.

In order to characterise the real (intrinsic) properties of the membrane, these boundary layer phenomena must be taken into account. Modified cut-off values are obtained in this way and in some cases this seems to be a good approach. The method can be improved further by taking a test molecule as dextran which has both a broad molecular weight distribution and a relatively low adsorption tendency. Using gel permeation

chromatography (GPC) or high performance liquid chromatography (HPLC), the molecular weight distribution of both the feed and permeate in a given test run can be determined. A typical result is shown in figure IV - 28.

The fractional rejection R_{Mi} may be defined according to eq. IV - 12.

$$R_{Mi} = 1 - \frac{c_{Mi \text{ (permeate)}}}{c_{Mi \text{ (feed)}}} \qquad (IV - 12)$$

which indicates that each polymeric chain with a corresponding molecular weight has its own rejection value. This value can be obtained from the molecular weight distribution curves associated with the feed and permeate (figure IV - 28). Instead of the concentration terms (c_{Mi}) which appear in eq. IV - 12, it is sometimes more convenient to use weight fractions (w_{Mi}).
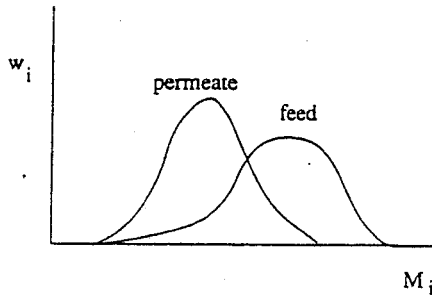
Figure IV - 28. Typical molecular weight distribution of dextran in the feed and permeate of a given test run.

$$R_{Mi} = \frac{w_{Mi \text{ (feed)}} - w_{Mi \text{ (permeate)}} (1 - R_{overall})}{w_{Mi \text{ (feed)}}} \qquad (IV - 13)$$

with $R_{overall}$ being given by

$$R_{overall} = 1 - \frac{c_p}{c_f} \qquad (IV - 14)$$

Although the weight fraction of every species in the feed and permeate can be obtained directly from the HPLC curves (see figure IV - 28), concentration polarisation and fouling can often change these characteristics quite drastically. This means that the retention given by eq. IV - 12 is an observed value. Because of concentration polarisation (and in some cases fouling), the concentration at the membrane surface can be much higher and it is this concentration that must be taken into account if real or intrinsic retention values are to be determined. Thus eq. IV - 12 becomes:

$$R_{M,} = 1 - \frac{c_{M, (permeate)}}{c_{M, (membrane)}}$$

(IV - 15)

The concentration at the membrane surface [c_{Mi}(membrane)] cannot be measured directly and must be calculated from equations incorporating boundary layer phenomena (see chapter VII). Another approach is to employ experimental conditions such that c_{Mi} (membrane) $\approx c_{Mi}$ (feed). This implies that the experiments should be carried out at low driving forces (low pressures) and very low feed concentrations.

An even more simple approach on solute rejection based on hydrodynamics was already developed by Ferry in 1936 [22] assuming a simple sieving mechanism. The rejection of a non-adsorbing spherical molecule can be related to the ratio of the solute radius and the pore radius, $\lambda = r_s/r_p$.

$$R = [\lambda(2 - \lambda)]^2$$

(IV - 16)

Although the Ferry equation is based on a rather simple concept since it does not take into account surface effects (adsorption), flow induced deformation, hindered diffusion and other interactive and hydrodynamic effects, it may be helpful as a first estimate of the rejection of a solute in relation to the pore size of the membrane. Several investigators have shown that this simple concept can be well applied when the pore size is larger than the solute size, i.e., when $\lambda < 1$. A number of similar equations have been derived [23,24] showing about the same type of retention curves as obtained from eq. IV - 16.
A polymer chain in solution can be considered as a random coil. The size of the macromolecular solute can be expressed as the radius of gyration r_g or as the hydrodynamic radius or Stokes-Einstein radius r_h. If there is a possibility of rotation about covalent bonds in the polymer backbone there is a continuous motion and in fact there is no well defined shape. In solution the chain is rather coiled than stretched and therefore it is better to define coil dimensions.
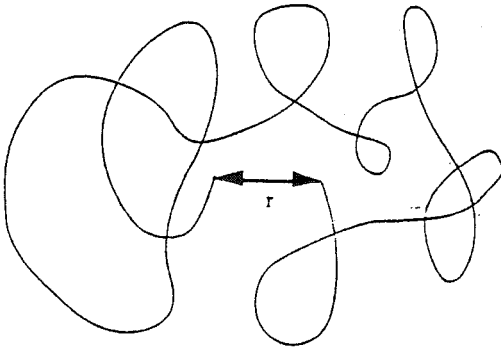
Figure IV - 29.   Schematic drawing of a random coil.

The size of the coil can be described by the root-mean-square of the end-to-end distance r of the chain $<r^2>^{0.5}$, the radius of gyration r_g or the Stokes-Einstein or hydrodynamic radius r_h. Figure IV - 29 shows a schematic drawing of such a random coil with the end-to-end distance r. The conformation of the coil is determined by the length of the chain, the intramolecular forces, the type of solvent and the temperature. As the molecular weight of the chain increases the dimensions of the coil increases with the square root of the molecular weight. The end-to-end distance is related to the radius of gyration and often expressed by

$$<r^2> = 6 . <r_g^2> \qquad\qquad (IV - 17)$$

The radius of gyration can be determined experimentally by viscosity measurements, gel permeation chromatography (GPC), and light scattering.

The dimensions of a coil are also often expressed by the Stokes-Einstein radius or the hydrodynamic radius r_h. For many polymer solutions there is an empirical relation between the (bulk) diffusion coefficient D_b and the molecular weight M_w.

$$D_b = a \; M_w^{-b} \qquad\qquad (IV - 18)$$

where a and b are constants characteristic for a polymer and a solvent or class of solvents. From the diffusion coefficient the Stokes-Einstein radius can be determined

$$r_h = \frac{k\,T}{6\,\pi\,\eta\,D_b} \qquad\qquad (IV - 19)$$

If the empirical relations between the diffusion coefficient and the molecular weight have been determined the Stokes-Einstein can be determined easily. The radius of gyration and the hydrodynamic radius are within a certain ratio, $0.55 < r_h/r_g < 0.80$ [25,26], which means that either one of the radii can be used to express the coil dimensions. The dimensions are strongly dependent on type of solvent and temperature. When the interaction of solvent and polymer increases and with increasing temperature the radius of gyration increases and the coil becomes more extended. In addition by decreasing the solvent power or decreasing the temperature the coil becomes more compact and finally this can result in phase separation. In the case of flexible polymers the intramolecular interactions are minimal and these polymers are able to deform under stress. In contrast to these flexible chains, proteins are characterized by strong intramolecular interactions (hydrogen bonding) and in many proteins there are covalent crosslinks between cysteine units of the various chains. The rotation of the bonds in the backbone is severely hindered and this results in a stable globular structure with a rather well-defined radius. When the solute dimensions have been estimated and the pore dimatere is known then the retention can be predicted from eq. IV - 16.

In summary, solute rejection measurements provide a very simple technique for indicating the performance of a given membrane. For this reason they are very frequently used for

the industrial assessment of membranes. However, quantitative predictions of membrane performance are difficult to be obtained by such methods since other factors such as adsorption and concentration polarisation also influence the permeation rate and membrane selectivity.

IV.4.   Characterisation of ionic membranes

Ionic membranes are characterised by the presence of charged groups. Charge is, in addition to solubility, diffusivity, pore size and pore size distribution, another principle to achieve a separation. Charged membranes or ion-exchange membranes are not only employed in electrically driven processes such as electrodialysis and membrane electrolysis. There are a number of other processes that make use of the electrical aspects at the interface membrane-solution without the employment of an external electrical potential difference. Examples of these include reverse osmosis and nanofiltration (retention of ions), microfiltration and ultrafiltration (reduction of fouling phenomena), diffusion dialysis and Donnan dialysis (combination of Donnan exclusion and diffusion) and even in gas separation and pervaporation charged membranes can be applied
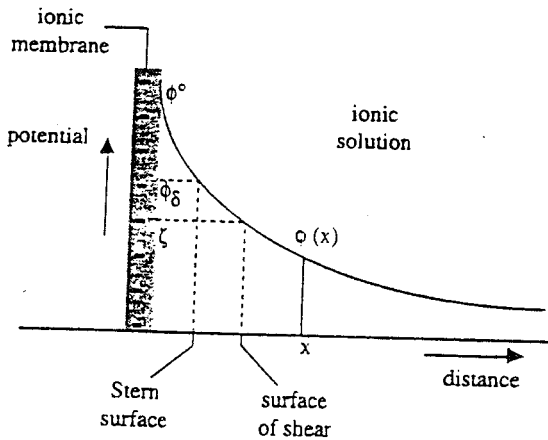
Figure IV - 30.   Simplified representation of the electrical potential as a function of distance.

although in these latter membranes the ionic groups will not be dissociated and can rather be considered as a highly polar group. In this chapter mainly the characterisation of the ionic membranes will be emphasized and transport phenomena and processes which make use of this principle are described in chapters V and VI, respectively.

If an ionic membrane is in contact with an ionic solution a distribution of ions in

the solution will be established as well as a distribution inside the membrane (Donnan equilibrium). These Donnan effects will be discussed in chapter V and here only the effects in the solution and interface will be considered. If the membrane has a negative fixed charge, ions of opposite charge (positively charged ions or counter-ions) will be attracted towards the membrane surface while ions of the same charge (negatively charged ions or co-ions) are repelled from the membrane surface. In this way an electric double layer has been formed.

Figure IV - 30 represents a simplified representation of the electrical potential as a function of the distance from the surface. Two regions can be observed in the electric double layer, a layer of 'fixed ions' at the surface which are rather immobile since the ions are bound to the surface by electric forces. Further away from the surface the ions become more mobile and this layer is called the diffusive region. Between these two regions is the so-called Stern-layer and the potential at this distance from the wall is called the Stern potential ϕ_s. The exact location of this Stern layer can not be determined. If the ionic solution is forced to flow along the surface, the mobile ions will flow along a layer of more immobile ions and this shear plane can be determined experimentally. The potential at this shear plane is called the ζ (zeta) potential (see figure IV - 30) and it is assumed that this is only a little smaller than the Stern potential. Often it is assumed that the ions in the solution are uniformly distributed and the electrical potential decreases exponentially with distance. This can be described by

$$\phi = \phi^\circ \exp(-\kappa x) \qquad\qquad\qquad\qquad (IV - 20)$$

At a distance of κ^{-1} (which is referred as the Debye length) the potential has been decreased to a value of $\exp(-1) = 1/e = 0.37$, and this value is frequently taken as the potential which gives the thickness of the double layer. The specific properties of the ionic membranes can be expressed by parameters as surface charge, zeta (ζ) potential, electrical resistance and ionic permeability.

IV.4.1   Electrokinetic phenomena

Interestic phenomena occur when a charged surface is in contact with an electrolyte solution and when an electrical potential or an hydrodynamic pressure difference is applied. Observation of these so-called electrokinetic phenomena can provide information about the charge density and the zeta (ζ) potential of the surface. The zeta (ζ) potential gives in fact the effective surface charge and this parameter may be obtained from streaming potential measurements. A streaming potential is generated when an ionic solution is forced to flow through a charged pore, capillary or slit by an applied hydrodynamic pressure due to a simultaneously transfer of mass and charge. In the case of a charged porous microfiltration or ultrafiltration membrane the solution flows through the pores (see figure IV - 31a) while in the case of a nonporous membrane a slit may be formed between two surface and the solution flows in between two parallel membranes (see figure IV - 31b). The electrical potential difference ($\Delta\phi$) which has been generated by

the flow of ions due to an applied driving force ΔP is determined by a high resistance voltmeter. By varying the applied pressure (ΔP) the electrical potential difference is measured. The streaming potential $(\Delta\phi/\Delta P)_{I=0}$ is related to the ζ potential by the Helmholtz-Smoluchowski equation [27]

$$\frac{\Delta\phi}{\Delta P} = \frac{\varepsilon \zeta}{\eta \kappa}$$

(IV - 21)
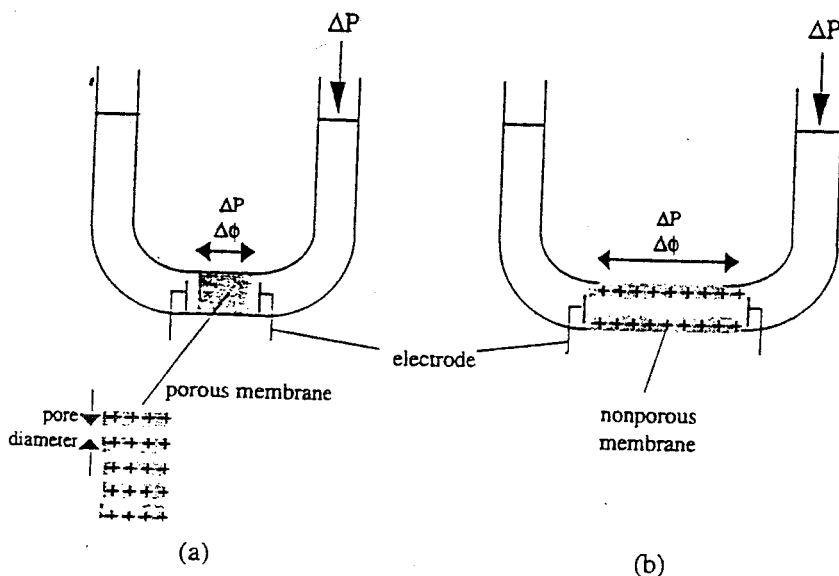
Figure IV - 31.   Apparatus for measuring the streaming potential. A pressure is applied across a membrane and the electrical potential is measured. (a) porous membrane and (b) nonporous membrane

where κ is the electrical conductivity of the solution ($\Omega^{-1}.m^{-1}$), ε the permittivity of the solution or the dielectric constant ($\varepsilon = \varepsilon_o \varepsilon_r$ with ε_o being the permittivity of vacuum, $\varepsilon_o = 8.85 \ 10^{-12} \ C^2/Nm^2$, and ε_r is the relative dielectric constant, $\varepsilon_r = 80$ for water), and η the viscosity (Pa.s). At a given ionic strength these parameters are constant and ζ can be obtained from the slope of a $\Delta\phi$ - ΔP plot. Note that the $\Delta\phi$ - ΔP plot gives a straight line if the various parameters are constant. At very low electrolyte concentrations surface conductivity will occur as well and the conductivity term of eq. IV - 21 must be corrected see e.g. ref 27).   The streaming potential is independent on flow geometry, i.e., a capillary or a slit give the same results providing that the charge densities are the same. The determination of the potential provides information of the effective surface charge.

However, it must be realised that the ζ potential is not a constant but dependent on the ionic environment. It is dependent on two parameters, the surface charge of the membrane and of the ionic strength. The surface charge may be strongly dependent on pH. The ionic strength both depends on the concentration and on the valence of the ions involved.

$$I = 0.5 \, \Sigma \, c_i \, z_i^2 \hspace{5cm} (IV - 22)$$

An increase of the ionic strength results in a decrease of the double thickness (κ^{-1}) and of the ζ potential (see figure IV - 32).
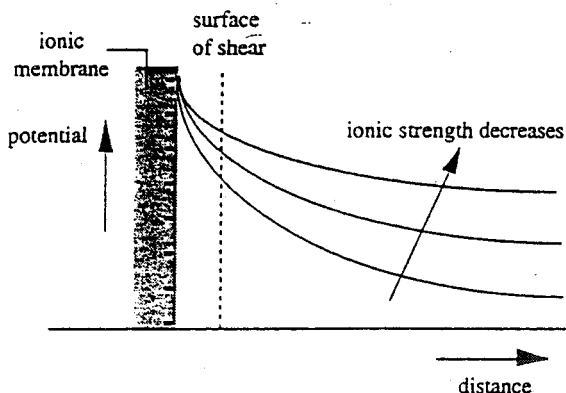
Figure IV - 32.   Potential as a function of the distance for various ionic strengths.

Figure IV - 33 gives the ζ potentials of porous alumina (Al_2O_3) and zirconia (ZrO_2) as a function of the pH. It can be clearly seen at which pH the membranes are positively charged or negatively charged.
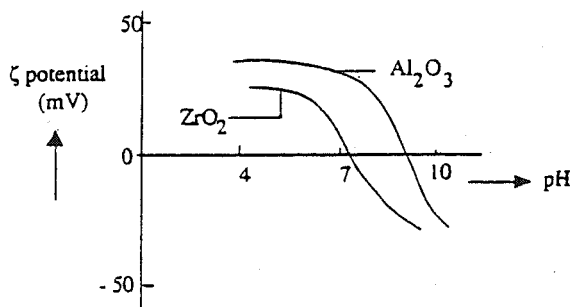
Figure   IV - 33. ζ potentials of alumina (Al_2O_3) and zirconia (ZrO_2) as a function of pH [28]

From these experiment the iso-electric point (IEP) of both membranes, i.e the point without effective charge. can clearly be observed. The rejection behaviour towards ionic species may well be predicted as a function of the pH if the surface charge is known (see chapter V).

IV.4.2.   Electro-osmosis

Electro-osmosis is another electrokinetic phenomenon in which an electric field is applied across a charged porous membrane or a slit of two charged nonporous membranes (see figure IV - 31). Due to the applied potential difference an electric current will flow and water molecules will flow with the ions (electro-osmotic flow) generating a pressure difference. As can be derived from nonequilibrium thermodynamics (see chapter V) the following equation can be obtained indicating that both phenomena, electro-osmose and streaming potential, are similar.

$$\frac{dV}{dt} = \frac{\varepsilon \, I \zeta}{\eta \, \kappa}$$

(IV - 23)

with dV/dt being the generated flow rate and I the current. A unique relationship between electro-osmosis and streaming potential can be obtained by combining eqs. IV - 21 and IV - 23.

$$\frac{\Delta \phi}{\Delta P} = \frac{dV/dt}{I}$$

(IV - 24)

IV.5.   Characterisation of nonporous membranes

Nonporous membranes are used to perform separations on a molecular level. However, rather than molecular weight or molecular size, the chemical nature and morphology of the polymeric membrane and the extent of interaction between the polymer and the permeants are the important factors to consider. Transport through nonporous membranes occurs by a solution-diffusion mechanism and separation is achieved either by differences in solubility and/or diffusivity.   Hence such membranes cannot be characterised by the methods described in the previous section, where the techniques involved mainly characterised the pore size and pore size distribution in the membranes. The determination of the physical properties related to the chemical structure is now more important and in this respect the following methods will be described:

i)   permeability
ii)   other physical properties
iii) plasma etching
iv)   surface analysis

One of the principal and simplest method of characterising a nonporous membrane is to determine its permeability towards gases and liquids. The permeabilities of oxygen and nitrogen through various polymers were given in chapter II (table II - 5) and it can be seen from this table that they vary by up to six orders of magnitude or more depending on the type of polymer used. Generally elastomers are more permeable than glassy polymers, but the highest permeability found to date is for the glassy polymer polytrimethylsilylpropyne (PTMSP). Despite this observation, the physical state, be it rubbery or glassy, remains an important factor. Whether a polymer is in the glassy or rubbery state is determined by its glass transition temperature; the various structural parameters determining the location of T_g having been described in chapter II. Although, the glass transition temperature is not directly related to the permeability, it is still an important parameter. Methods for determining T_g will be described later in this chapter. In turn, although the permeability coefficient is an intrinsic material property, it is not just simply a constant. Its value is very dependent on factors such as sample history and the test conditions employed together with the type of gas used. In this latter respect helium, hydrogen, nitrogen, argon and oxygen may be considered as inert or non-interacting gases, i.e. the polymer morphology is not changed by the presence of these gases. Other gases such as carbon dioxide, sulfur dioxide, hydrogen sulfide and ethylene are interacting gases. In addition, with glassy polymers the permeability or permeability coefficient decreases with increasing pressure due to non-ideal sorption (see chapter V).

Various physical methods can be used to characterise the parameters that affect the permeability. Such methods mainly determine the membrane morphology. Two structural parameters that affect membrane permeability very strongly are the glass transition temperature (T_g) and the crystallinity. As discussed in chapter II, only polymers exhibiting a regular chain configuration are capable to crystallise. Two factors are important in any investigation of polymer crystallisation: the degree of crystallinity, and the size and shape of crystalline regions. The degree of crystallinity gives the fraction of crystalline material in the semi-crystalline polymer. The crystalline regions are dispersed throughout an amorphous (continuous) phase (see figure IV - 34).

Since transport proceeds mainly via the amorphous regions, it is very important to know
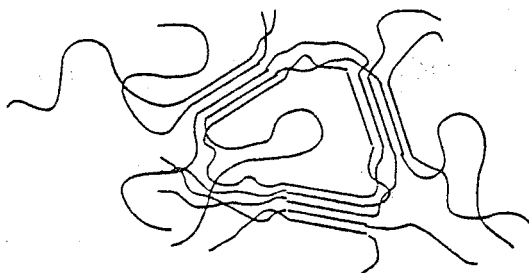
Figure IV - 34.   Morphology of a semi-crystalline polymer (fringed-micelle model)

the degree of crystallinity in the polymer. Hence, the characterisation of crystallinity data gives information which may be related directly to the permeability behaviour. Glass transition temperatures and the degree of crystallinity are known for most of the commercial available polymers. If not, they can be determined with simple techniques: by differential scanning calorimetry (DSC) or differential thermal analysis (DTA) (a number of other techniques such as chromatography and dilatometry can be used as well). The degree of crystallinity can be determined by DSC and DTA, and by X-ray diffraction or X-ray scattering methods, and by density measurements and by spectroscopy (IR and NMR). These techniques will be described very briefly below. Other methods used to characterise the chemical structure of composite membranes will be described later in this chapter.

IV.5.1 Permeability methods

Permeability measurements can be made using a simple experimental set-up, a schematic drawing of such a gas permeability test apparatus being given in figure IV - 35.
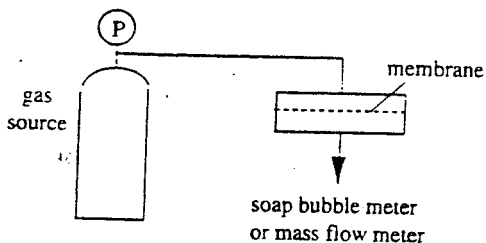
Figure IV - 35.   Gas permeability set-up.

The cell containing a homogeneous membrane of known thickness is pressurised with a chosen gas. The extent of gas permeation through the membrane is measured by means of a mass flow meter or by a soap bubble meter. More sophisticated set-ups employ a calibrated volume connected to the permeate side with the small pressure increase in the calibrated volume being measured with a pressure transducer. The gas permeability or permeability coefficient P can be determined from the steady-state gas flow if the membrane thickness ℓ is known, since

$$J = P / \ell$$

(IV - 25)

where J is the gas flow per unit pressure ($cm^3.cm^{-2}.s^{-1}.cmHg^{-1}$) and ℓ the membrane thickness (cm). P is expressed per unit membrane area, per unit time per unit driving force ($cm^3.cm.cm^{-2}.s^{-1}.cmHg^{-1}$ or $m^3.m.m^{-2}.h^{-1}.bar^{-1}$). Often the permeability is also expressed in Barrer (1 Barrer = 10^{-10} $cm^3.cm.cm^{-2}.s^{-1}.cmHg^{-1}$). The diffusion coefficient can also be determined from the initial part of the permeation experiment by

using the so-called time-lag method (see chapter V). This P/ℓ value, which is the normalised flux, is very often used to determine in composite gas separation membranes the contribution of the sublayer resistance in relation to the overall resistance. This means that also in characterising support layers the P/ℓ-value is used frequently.

Through the use of various gases and various polymers, complete compilations of permeability coefficients have been obtained. The permeability of liquids has also been determined by this means. The experimental set-up in this case is quite similar to that employed for gas permeability experiments. A schematic drawing of a simple pervaporation test apparatus is given in figure IV - 36. The pure liquid is contained in the reservoir on the upstream side of the membrane, its temperature being controlled by means of heating coils. Vacuum is applied on the downstream side and the pressure is measured via any suitable vacuum gauge (Pirani or Macleod) . The downstream pressure must be less than about one-tenth of the saturation pressure of the pure liquid at that temperature in order to obtain a maximum driving force (see also chapter VI, under pervaporation).
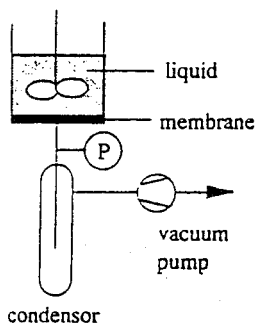
Figure IV - 36. Liquid permeability (pervaporation) set-up.

The liquid permeating through the membrane is evaporated on the downstream side and collected in the condenser which is cooled with liquid nitrogen or another cooling agent. The amount of liquid can be determined simply by weighing.

IV.5.2   Physical methods
Important physical properties associated with polymers (or membranes) such as the glass transition temperature, their crystallinity and density can be determined by a large number of techniques. Some of these will be described briefly to enable a better understanding to be obtained concerning permeability through nonporous polymeric films.

IV.5.2.1   DSC/DTA methods
Differential Scanning Calorimetry (DSC) and Differential Thermal Analysis (DTA) are in

fact identical techniques used to measure transitions or chemical reactions in a polymer sample. DSC determines the energy (dQ/dt) necessary to counteract any temperature difference between the sample and the reference, whereas DTA determines the temperature difference (ΔT) between the sample and the reference upon heating or cooling. A schematic DSC-curve for a semi-crystalline polymer is shown in figure IV - 37, illustrating possible heat effects. Such DSC-curves allow the glass transition temperature and the degree of crystallinity to be obtained. Indeed both first-order and second-order transitions can be observed in figure IV - 37. First-order transitions such as crystallisation and melting give narrow peaks, the peak area being proportional to the enthalpy change in the polymer and the enthalpy change being related to the amount of crystalline material present, i.e.
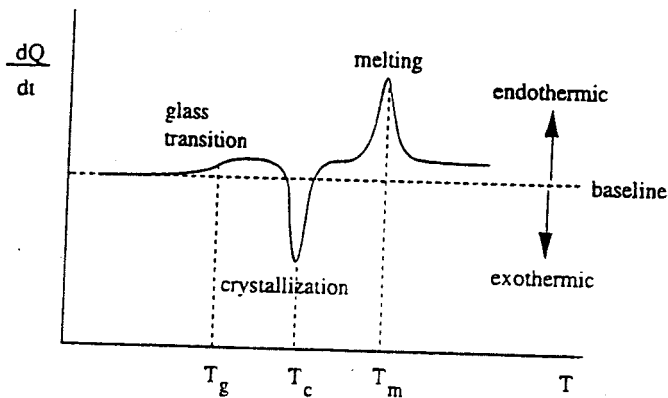
Figure IV - 37.   Schematic DSC-curve for a semi-crystalline polymer.

allowing an estimation of the degree of crystallinity. The glass transition corresponds to a second-order transition. These second-order transitions are characterised by a shift in the base line resulting from a change in the heat capacity. The glass transition temperature can be determined from figure IV - 37 and by employing the method outlined in figure IV - 38. In the latter case, the glass transition temperature is the point of intersection of the tangents (or the inflection point). The degree of crystallinity can be obtained from the area under the peak corresponding to melting per unit weight of polymer. This gives the enthalpy of fusion (J/g). To calculate the crystallinity, the enthalpy of fusion for the 100% crystalline material must be known. Data of these kinds are not generally available. In those cases the melting curve must be compared with the calibration curves of samples of known density and crystallinity to enable the degree of crystallinity to be obtained. Crystallinity and density are directly related to each other. As the degree of crystallinity increases the density also increases because the density of the crystalline regions is greater than that of amorphous regions. This implies that information on the degree of crystallinity can be obtained by density measurements.
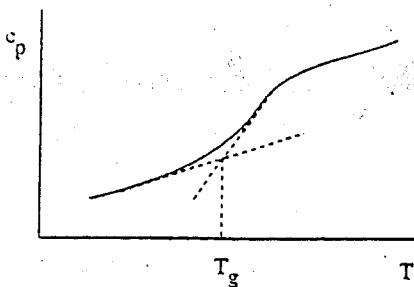
Figure IV - 38. Determination of the glass transition temperature.

IV.5.2.2 Density measurements

IV.5.2.2.1   Density gradient columns

The density of the polymer or its reciprocal the specific volume is also a very important parameter in many respects. It may be related to free volume, diffusivity and permeability. Moreover, it may give information on the crystalline content. Membranes prepared from high-density polymers tend to have lower permeabilities. The density decreases and vice versa the specific volume increases, as the temperature raises, but when the glass transition temperature has been passed, the density decreases even more rapidly (see also figure II - 9).

The overall density of a polymer can be determined via a number of techniques such as picnometry and dilatometry, and through the use of a density gradient column. A schematic drawing of such a column is given in figure IV - 39.
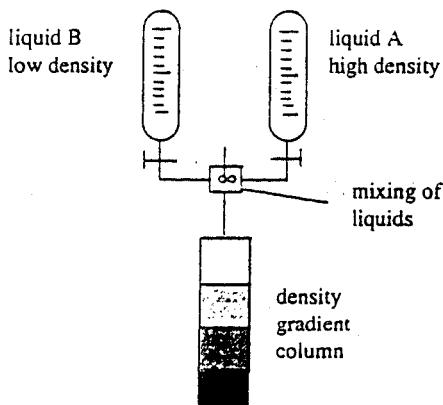
Figure IV - 39.   Schematic drawing of a density gradient column.

The density gradient in the column is obtained by mixing two liquids, one with a high density and one with a low density, with each other in defined quantities. Often aqueous inorganic solutions such as that of sodium bromide are used for polymers with densities $\rho > 1$ cm^3/g. The overall density (ρ) of a polymer sample can be obtained by measuring its flotation level.

IV.5.2.2.2   Density determination by the Archimedes principle

The density determination of a polymer may be performed by a simple experiment based on the Archimedes principle. A polymer sample has been immersed in a liquid with known density. The upward pressure which is generated by immersion of the polymer sample into the liquid is equal to the weight of the displaced volume and this can be measured by a balance. A schematic drawing is given in figure IV - 40.
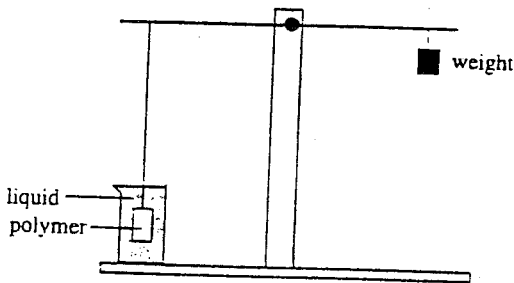
Figure IV - 40.   Schematic drawing of the density measurement by the Archimedes principle.

IV.5.2.3   Wide-angle X-ray diffraction (WAXS)

X-ray diffraction is another technique which can provide information about polymer morphology. Wide-angle X-ray diffraction is an especially good technique for obtaining information about the size and shape of crystallites, and about the degree of crystallinity in solid polymers. A schematic drawing of the technique is given in figure IV - 41, while figure IV - 42 gives a plot of the scattering intensity as a function of the diffraction angle.
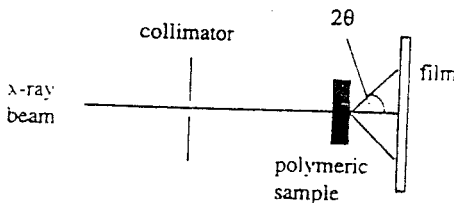
Figure IV - 41.   Schematic drawing of the WAXS technique.

As shown in figure IV - 41, an X-ray beam is allowed to impinge on the polymer sample and the intensity of the scattered X-rays is determined as a function of the diffraction angle (2θ). Crystalline regions show coherent scattering patterns and a sharp peak can be observed in the diffraction versus intensity curve whereas an amorphous phase gives a broad peak. The degree of crystallinity can be obtained by measuring the area under each peak. However, it is often difficult to discriminate between crystalline and amorphous scattering, which implies that the degree of crystallinity cannot be determined very accurately. Also the presence of small crystallites is difficult to characterise, because they exhibit similar scattering effects as the amorphous material. However, small crystallites tend to broaden the peaks and sometimes information about crystal size can be obtained from such broadening.
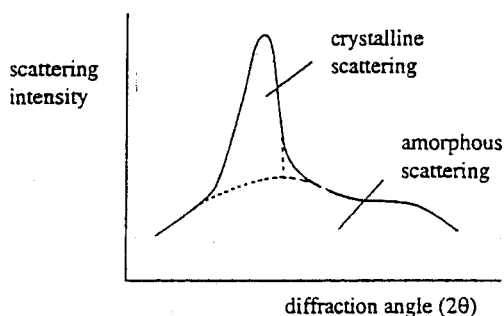
Figure IV - 42. A typical plot of scattering intensity versus diffraction angle obtained from wide-angle X-ray diffraction (WAXS).

The spacing between two adjacent planes may be obtained from the Bragg relationship.

$$n \lambda = 2 d \sin\theta \qquad\qquad (IV - 26)$$

The method has recently also been used to determine the interchain distance in amorphous polyimides from measurements of the maximum in the amorphous scattering [29,30]. It is clear from figure IV - 42 that amorphous scattering will give rise to a broad band, which implies a d-spacing distribution. However, this approach may be considered critically since it uncertain whether eq. IV - 26 may be used for amorphous scattering to obtain quantitative information about interchain distances.

IV.5.3   Plasma etching
Plasma etching is a new technique which allows the measurement of the thickness of the top layer in asymmetric and composite membranes. The uniformity of the structure in the

top layer as well as the properties of the layer just beneath the top layer and of the the sublayer can also be determined. This process involves a reaction between the surface of a polymeric membrane and a plasma produced in a glow discharge. This leads to the slow removal of the top layer. Volatile products such as CO_2, CO, NO_x, SO_x, and H_2O are removed by means of a vacuum system [31]. A schematic drawing of the principle is given in figure IV - 43.
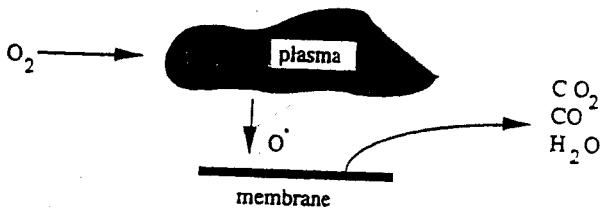
Figure IV - 43. Principle of plasma etching.

By measuring the gas transport properties as a function of the etching time, information can be obtained about the morphology and thickness of the thin nonporous top layer. Because top layer thicknesses are generally within the range of 0.1 to 5 μm, the etching rate must be low (of the order of 0.1 μm/min). An example of the results obtained in an etching experiment involving PES [poly(ether sulfone)] hollow fibers is
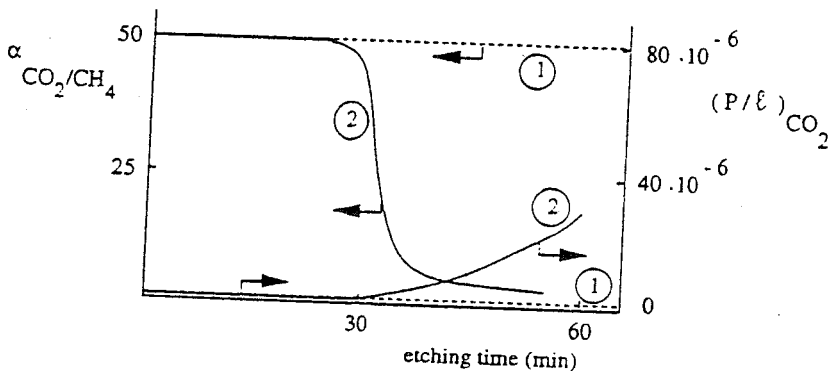
Figure IV - 44. Selectivity and permeation rate as a function of the etching time with PES hollow fibers. Dashed line 1 : untreated fibers ; Curve 2 : etched fibers [31].

given in figure IV - 44. Asymmetric PES hollow fibers have a selectivity for CO_2/CH_4 of about 50 and a CO_2 flux (P/ℓ) of $1.4 \ 10^{-6}$ $cm^3.cm^{-2}.s^{-1}.cmHg^{-1}$. For short etching times when only a portion of the top layer is removed, it is expected that the selectivity should

remain unchanged. In fact, the flux should increase in proportion to the decrease in the top layer thickness, but this was not found in this experiment. It is probable that not only is material removed but polymer modification also takes place and as a result there is a change in permeability. As etching progresses the total top layer is ultimately removed and the porous substructure is reached. The selectivity now drops drastically and the flux also increases (curve 2 in figure IV - 44 obtained after 30 minutes). The value of the flux when the complete top layer has been removed gives a measure of the resistance of the sublayer.

IV.5.4   Surface analysis methods
It is often desirable to alter the surface properties of a membrane, for example to reduce adsorption or to introduce specific groups that can be used for affinity membranes. Surface modification can also be used as a method of changing the separation properties of a material.

In composite membranes, the membrane properties are determined by an extremely thin layer. When this layer is applied via a polymerisation reaction, e.g. plasma polymerisation, interfacial polymerisation, or in-situ polymerisation, the chemical nature of this layer is often not known exactly. Hence, it becomes necessary to determine the surface properties by surface analysis.

Surface analysis methods are based on the concepts outlined schematically in figure IV - 45.

electron
ion
photon
neutral particle
electric field
heat
                          surface

electron
ion
photon
neutral particle
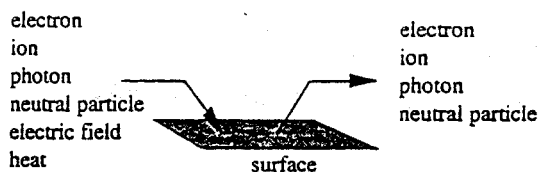
Figure IV - 45.   Basic concepts involved in surface analysis.

A solid surface is excited by means of radiation or particles bombardment and the emission products, which provide information about the presence of specific groups, atoms, or bonds, are detected. The following techniques are frequently used [32 - 36] :
ESCA: Electron Spectroscopy for Chemical Analysis
XPS: X-ray Photoelectron Spectroscopy
SIMS: Secondary Ion Mass Spectrometry
AES: Auger Electron Spectroscopy
A schematical drawing of the transitions involved in ESCA/XPS and AES is given in figure IV - 46. XPS or ESCA are two names for one and the same technique, with excitation occurring by means of photons (hv) and with photoelectrons constituting the

emission products. With AES, excitation takes place via electrons and leads to the removal of core electrons from the K shell. The resulting vacancy is filled by an electron from another shell (e.g. an L shell). The energy liberated in this way ($E_K - E_L$) can be transferred to an electron from another shell which is then emitted. In the case of XPS, the binding energies of the electrons in the molecules are measured. The absolute binding energies of electrons in a given element have fixed values and are characteristic of that element. Differences in the chemical environment lead to small changes in the binding energies, i.e.
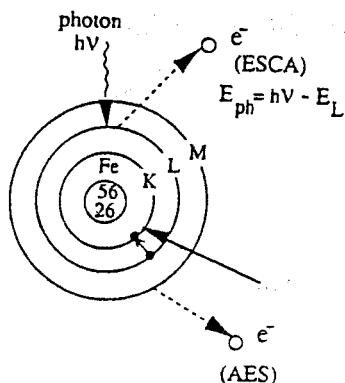
Figure IV - 46.   Schematic drawing of the electron transitions involved in ESCA/XPS and AES measurements.

to chemical shifts. The chemical shift depends on the nature of the binding and on the electronegativity of the attached groups. For example, the binding energy of C_{1s} electrons is 285.0 eV. The binding energies of C_{1s} electrons in Nylon-6 are shown in figure IV - 47 [37], which indicates that the binding energy of a C_{1s} electron of a carbon attached to hydrogen or to another carbon atom has a value close to 285 eV. However, carbon atoms attached to nitrogen exhibit a chemical shift of 1.3 eV while carbon in a carbonyl group has a chemical shift of about 2.8 eV. Another example is given in figure IV - 48. Here the C_{1s} spectra of polyethyleneterephthalate (PET) and of PET where the surface has been etched with oxygen and argon [34] are illustrated.
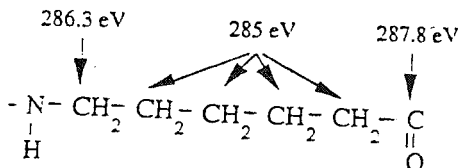
igure IV - 47.   Binding energies of C_{1s} in Nylon-6 [37].

The spectrum of PET clearly shows a chemical shift associated with the C_{1s} peak of the carboxyl group and of the ether group. The spectrum of the argon-etched surface reveals that the proportion of the carboxyl groups (- COO^-) has been reduced whereas oxygen etching leads to no change in the chemical structure. From the core level spectra of the various elements distinguished (e.g. C_{1s}, N_{1s}, O_{1s}, F_{1s}) the ratio of these elements in the top layer can be determined.
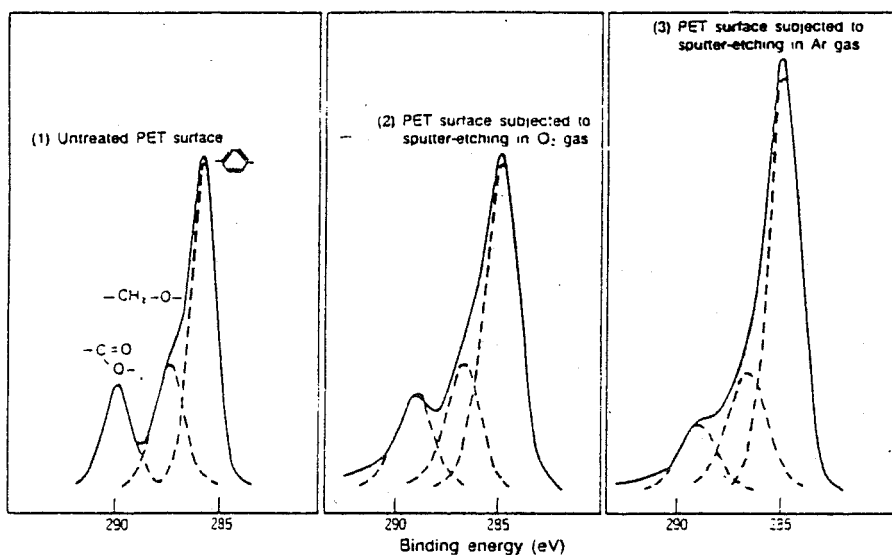
Figure IV - 48. C_{1s} spectra of PET and of PET etched with oxygen and with argon as determined by XPS methods [32].

ESCA/XPS methods can detect atoms to a depth of 0.5 - 10 nm which makes this technique most useful for the determination of surface structures.

SIMS is another technique frequently used for surface analysis. SIMS makes use of (primary) ions as the exciting source with (secondary) ions being the emission products. The primary ions used are usually noble gas ions (Ar^+ or Xe^+) with energies in the keV range which enable them to penetrate the solid a few atomic layers. The energy involved in this process leads to the emission of neutral or charged surface particles, which are analysed by a mass spectrometer. All elements and compounds can be determined with this technique. Problems may occur because of charge build-up (see also at scanning electron microscopy) and ion-induced reaction at the surface.

Another technique for surface analysis is Fourier Transform Infrared Spectroscopy

(FT-IR). As in conventional infrared spectroscopy, FT-IR detects absorptions in the infrared region (4000 - 400 cm^{-1}) but detection involves the use of an interferometer rather than a monochromator. The penetration depth is of the order of a few micrometers. A combination of surface analysis techniques (e.g. XPS, SIMS and FT-IR) is often required to elucidate the chemical structure in the top layer.

IV.6.   Solved problems

1. A Nuclepore membrane is characterised with permporometry using cyclohexane as condensable vapour. At a relative pressure of 0.78 a high oxygen flux can be observed which does not increase further upon decreasing the relative vapour pressure. The t-layer of cyclohexane in the pore is 0.5 nm. The experiment is performed at 34°C.

a. Calculate the vapour pressure of cyclohexane at 34°C at a relative pressure of 0.78.
b. What can you say about the pore size distribution in this membrane ?
c. What is/are the pore radius/radii in this membrane ?

2. The following numbers have been extracted from a brochure on track-etch membranes.

pore diameter (μm)	number of pores (number/cm^2)
5.0	5.0×10^5
1.0	1.3×10^7
0.2	3.2×10^8
0.05	4.0×10^9

Calculate the porosity and the water flux at 1 bar

IV.7.   Unsolved problems

1. The 'bubble-point' method is a simple method to characterize microfiltration membranes.

a. Do two wettable membranes from different materials with the same pore size distribution show the same bubble-point ?
b. What is the bubble-point for a membrane with the following pore size distribution and water as liquid ($\gamma_{water/air} = 72.8$ mN/m) ?
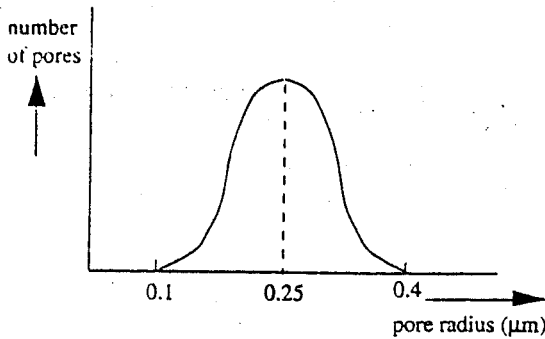
c. What is the error if the contact angle between liquid and polymer is not $0°$ but $20°$?

d. Wetting occurs if there is a high interaction between liquid and polymer. What process interferes if the interaction becomes high and what happens with the measurement ?

e. Is it possible to characterize ultrafiltration membranes ($r_p \approx 1$ nm) with this technique using water ? And using ethanol ? (The surface tension water/air and ethanol/air are given in table IV - 3).

2. Calculate the porosity of a membrane with a pore diameter of 0.2 µm and a number of pores of 10^9 pores/cm²

3. Permporometry is a recent characterisation technique for ultrafiltration membranes.

a. Which membrane characteristic is characterized with this technique ?

For a given membrane the following bimodal pore distribution has been determined experimentally.
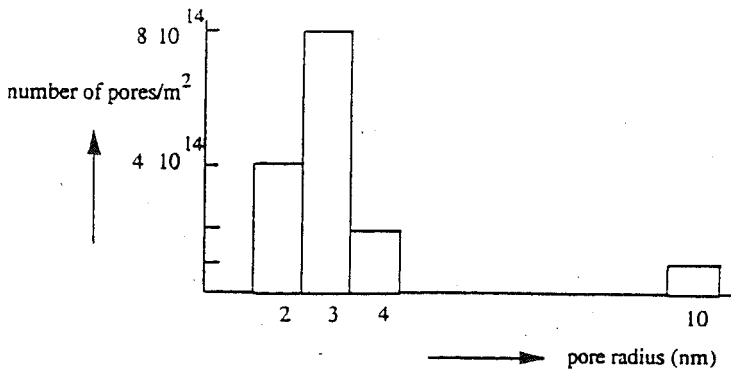
b. Do you think that the pores of 10 nm contribute to the flux ? Explain.

The water flux through these membranes can be described by the Poissueille equation.

c. Calculate the theoretical flux of water at $\Delta P = 1$ bar based on this figure for an asymmetric membrane with a toplayer thickness of 1 μm. Furthermore, a tortuosity of $\tau = 1.5$ is given and the viscosity of water is $\eta = 10^{-3}$ Pa.s.

d. What is the contribution of the 10 nm pores to the total flux ?

4. Cuprophan (regenerated cellulose) is frequently used as membrane in hemodialysis. The properties are obtained because of swelling in water by which 'pores' are formed. The membrane has a cut-off value of about 6000 g/mol.

a. The cut-off value is determined by spherical particles with a density of 1 g/cm^3 and a molecular weight of 6000. Estimate the pore size of this membrane (assume that the pore size is equal to the particle size).

b. Describe briefly two characterization techniques which are suitable and two techniques which are not suitable to characterize the membrane.

5. The density of a homogeneous film of Nylon 6.6 is 1.14 g/cm^3. The density of the crystalline fraction $\rho_{cryst} = 1.22$ g/cm^3 and of the amorphous phase $\rho_{amorph} = 1.07$ g/cm^3, respectively. Calculate the amount of crystallinity in weight fraction and in volume fraction
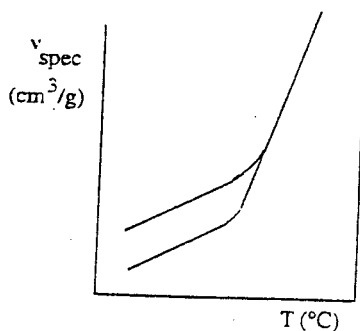
6. The figure above shows the specific volume for polyvinylacetate after cooling the polymer quickly from a temperature well above T_g. The specific volume was measured at 0.02 hours and at 100 hours after cooling. Explain which curve belongs to which time.

7. The pore size distribution of an ultrafiltration membrane van be determined by liquid displacement. If the set-up has a pressure-range of 0.1 to 5 bar and if a water/iso-butanol ($\gamma = 1.85$ mN/m) is used as a liquid mixture what will be the pore range which can be determined.

8. A polymer solved in water has a hydrodynamic radius of 15 nm. Calculate the rejection of a membrane with a uniform pore radius 0.05 μm and 0.1 μm for the case of no adsorption at the pore wall and for the case with monolayer adsorption at the pore wall.

9a. Estimate the surface porosity of the nucleore membrane from figure VI - 4.
 b. The average pore diameter of this nuclepore membrane is 0.4 μm and the thickness is 10 μm.
    At a pressure of 1 bar a water flux of 3000 l/m².h is found. Calculate the porosity.

10. Verify the dimensions of eq. IV - 21.

11. Draw schematically the DSC curve of the block copolymer of polybutylene terephtalate and polyethylene oxide (see also problem II - 9)

12. The following result has been obtained from a characterization experiment, showing the cumulative volume versus the pore radius.
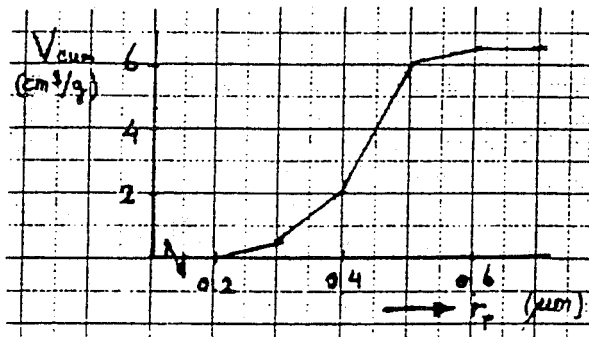
a. Which method could have been used here.
b. Calculate (draw) the pore size distribution

13. The zeta potential can be obtained from a streaming potential measurement. The following results are obtained for a nanofiltration membrane using a 10^{-3} M NaCl solution (molar conductivity $\Lambda = 126$ cm².eq^{-1}.Ω^{-1} and $\eta = 10^{-3}$ Pa.s).

P (mbar)	ϕ (mV)
50	- 26
100	- 53
150	- 79
200	- 105

Calculate ζ.

IV.8. Literature

1. Beaton, N.C., in A.R. Cooper (Ed.), *Ultrafiltration Membranes and Applications*, *Polym. Sci. Techn.*, 13 (1980) 373.

2. Cuperus, F.P., *PhD Thesis*, University of Twente, 1990

3. IUPAC Reporting Physisorption Data, *Pure Appl. Chem.*, 57 (1985) 603

4. Cuperus, F.P., Membrane News, ESMST, No. 22-23, Sept. 1990, p. 3

5. Roesink, H.D.W., *PhD Thesis*, University of Twente, 1989

6. Binnig, G., Quate, C.F., and Gerber, C., *Phys. Rev. Lett.*, 12 (1986) 930

7. Dietz, P., Hansma, P.K., Herrmann, K.H., Inacker, O., Lehmann, H.D., *Ultramicroscopy*, 35 (1991) 155

8. Leenaars, A.F.M., *PhD Thesis*, University of Twente, 1984

9. Brun, M., Lallemand, A., Quinson, J.F., and Eyraud, Ch., *Therm. Acta*, 21 (1977) 59

10. Quinson, J.F., Mameri, N., Guihard, L., and Bariou, B., *J. Membr. Sci.*, 58 (1991) 191

11. Cuperus, F.P., Bargeman, D., and Smolders, C.A., J. Membr. Sci., 66 (1992) 45

12. Smolders, C.A., and Vugteveen, E., *ACS Symp. Ser.*, 269 (1985) 327.

13. Eyraud, C., *ESMST Summerschool on Membrane Science and Technology*, Cadarache, France, 1984

14. Mey-Marom, A., and Katz, M.G., *J. Membr. Sci.*, 27 (1986) 119

15. Cuperus, F.P., Bargeman, D., and Smolders, C.A., *J. Membr. Sci.*, 71 (1992) 57

16. Cuperus, F.P. Internal publication, University of Twente

17. Bechold, H., Schlesinger, M., and Silbereisen, K., *Kolloid Z.*, 55 (1931) 172

18. Erbe, F., *Kolloid Z.*, 59 (1932) 195

19. Munari, S., Bottino, A., Capanelli, G., and Moretti, P., *Desalination*, 53 (1985) 11

20. Capanelli, G., Becchi, I., Bottino, A., Moretti, P., and Munari, S., in 'Characterization of Porous Solids', Unger, K.K. (Ed.), Elsevier, Amsterdam, 1988, p.283

21. Wienk, I., *PhD Thesis*, University of Twente, 1993.

22. Ferry, J.D., *Chem. Rev.*, 18 (1936) 373

23. Mason, E.A., Wendt, R.P., Bresler, E.H., *J. Membr. Sci.*, 6 (1980) 283

24. Munch, W.D., Zestar, L.P., and Anderson, J.L., *J. Membr. Sci.*, 5 (1979) 77

25. Schmidt, M., and Burchard, W., *Macromolecules*, 15 (1982) 1604

26. Tanford, C., *Physical Chemistry of Macromolecules*, Wiley, New York, 1961

27. Shaw, D.J., *Introduction to Colloid and Surface Chemistry*, Butterworth, London, 1970

28. Julbe, A., private communication

29. Kim, T-H, Koros, W.J., Husk, G.R., *Sep. Sci.*, 23 (1988) 1611

30. Stern, S.A., Mi, Y., Yamamoto, H., St. Clair, A.K., *J. Polym. Sci. Polym. Phys.*, 27 (1989), 1887

31. B. Chapman, *Glow discharge processes; sputtering and plasma etching*, John Wiley, New York, 1980.

32. Hof, J. v.'t, *PhD Thesis*, University of Twente, 1988

33. Nitto Denko, Technical Report, The 70th Anniversary Special Issue, 1989

34. Langsam, M., Anand, M, and Karwacki, E.J., *Gas Separation and Purification*, 2 (1988) 162

35. Oldani, M., and Schock, G., *J. Membr. Sci.*, **43** (1989) 243

36. Bartels, C.R., *J. Membr. Sci.*, **45** (1989) 225

37. Fontijn, M., Bijsterbosch, B.H. and v.'t Riet, K., *J. Membr. Sci.*, **36** (1987) 141

38. Dilks, A., in J.V. Dawk (ed.), *Development in polymer characterisation*', Appl. Science Publ.vol. 2, p. 14

V   TRANSPORT IN MEMBRANES

V.1.   Introduction

A membrane may be defined as a permselective barrier between two homogeneous phases. A molecule or a particle is transported across a membrane from one phase to another because a force acts on that molecule or particle. The extent of this force is determined by the gradient in potential, or approximately by the difference in potential, across the membrane (ΔX) divided by the membrane thickness (ℓ), i.e.

$$\text{driving force} = \frac{\Delta X}{\ell} \quad [\text{N/mol}]$$

(V - 1)

Two main potential differences are important in membrane processes, the chemical potential difference ($\Delta\mu$) and the electrical potential difference (ΔF) (the electrochemical potential is the sum of the chemical potential and the electrical potential). Other possible forces such as magnetical fields, centrifugal fields and gravity will not be considered here.
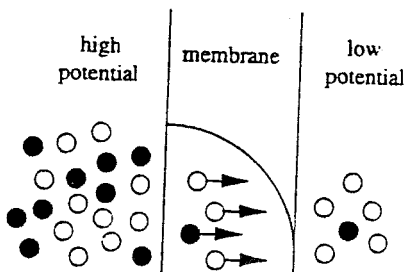
Figure V - 1.   Passive membrane transport of components from a phase with a high potential to one with a low potential.

In passive transport, components or particles are transferred from a high potential to a low potential (see figure V - 1). The driving force is the gradient in potential ($= \partial X/\partial x$). Instead of differentials it is often more useful to use differences ($\partial X/\partial x \approx \Delta X/\Delta x$). The average driving force (F_{ave}) is equal to the difference in potential across the membrane divided by the membrane thickness:

$$F_{ave} = - \Delta X/\ell$$

(V - 2)

If no external forces are applied to this system, it will reach equilibrium when the potential difference has become zero. Equilibrium processes are not relevant and will therefore not be considered. When the driving force is kept constant, a constant flow will occur through the membrane after establishment of a steady state. There is a proportionality relationship between the flux (J) and the driving force (X), i.e.

flux (J) = proportionality factor (A) * driving force (X)   (V - 3)

An example of such a linear relationship is Fick's law, which relates the mass flux to a concentration difference.

Phenomenological equations are generally black box equations that tell us nothing about the chemical and physical nature of the membrane or how transport is related to the membrane structure. The proportionality factor A determines how fast the component is transported through the membrane or, in other words, A is a measure of the resistance exerted by the membrane as a diffusion medium, when a given force is acting on this component.
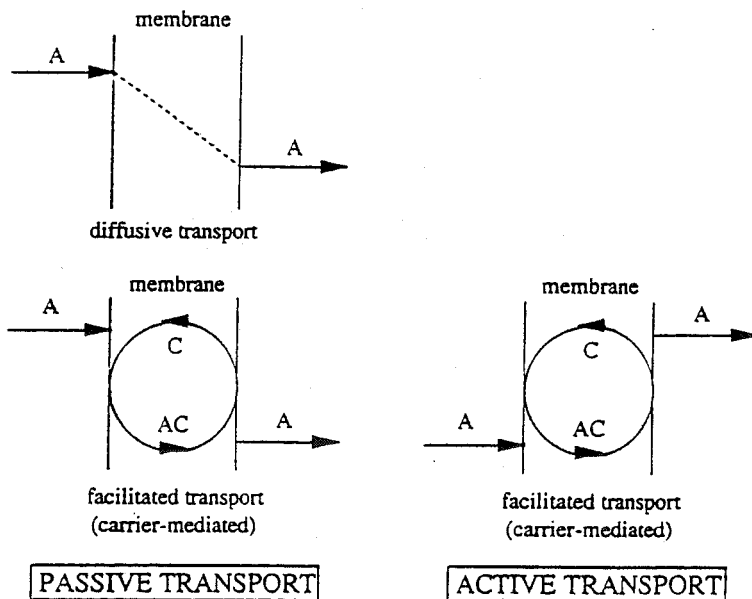
Figure V - 2.   Schematic drawing of two basic forms of transport, i.e. passive transport and active transport (C is carrier and AC is carrier-solute complex).

Another form of passive transport is 'facilitated' transport or 'carrier-mediated' transport.

Here transport of a component across a membrane is enhanced by the presence of a (mobile) carrier. The carrier interacts specifically with one or more specific components in the feed and an additional mechanism (besides free diffusion) results in an increase in transport. Sometimes components are transported against their chemical potential gradient in carrier-mediated transport. In these cases transport proceeds in a co-current or counter-current fashion, which means that another component is also transported simultaneously with with the 'real' driving force being the chemical potential gradient of the second component. Components can also be transported against their chemical potential gradient. This is only possible when energy is added to the system, for example by means of a chemical reaction. Active transport is mainly found in living cell membranes where the energy isprovided by ATP. Very specific and often very complex carriers are also found in biological

systems. Only passive transport will be considered in this book and the reader interested in more information on active transport is referred to books on biological membranes [e.g. ref. 1]

The basic forms of transport are summarised in figure V - 2. In the case of multi-component mixtures, fluxes often cannot be described by simple phenomenological equations because the driving forces and fluxes are coupled. In practice, this means that the individual components do not permeate independently from each other. For example a pressure difference across the membrane not only results in a solvent flux but also leads to a mass flux and the development of a solute concentration gradient. On the other hand, a concentration gradient not only results in diffusive mass transfer but also leads to a build-up of hydrostatic pressure.

Osmosis is one of the phenomena that result of coupling between a concentration difference and a hydrostatic pressure. Coupling also occurs with other driving forces. Thus electro-osmosis arises as a result from coupling between an electrical potential difference and a hydrostatic pressure difference. Such coupling phenomena cannot be described by simple linear phenomenological equations, but are better discussed in terms of non-equilibrium thermodynamics. Membrane transport will be described using non-equilibrium thermodynamics in the first part of this chapter. Then various permeation models will be given that relate membrane structure to transport.

V.2. Driving forces

As indicated in the previous section transport across a membrane takes place when a driving force. i.e. a chemical potential difference or an electrical potential difference, acts on the individual components in the system. The potential difference arises as a result of differences in either pressure, concentration, temperature or electrical potential. Membrane processes involving an electrical potential difference occur in electrodialysis and other related processes. The nature of these processes differs from that of other processes involving a pressure or concentration difference as the driving force, since only charged molecules or ions are affected by the electrical field.

Most transport processes take place because of a difference in chemical potential $\Delta\mu$. Under isothermal conditions (constant T), pressure and concentration contribute to the chemical potential of component i according to

$$\mu_i = \mu_i{}^o + RT \ln a_i + V_i\, P \tag{V - 4}$$

The first term on the right hand side ($\mu_i{}^o$) is a constant. The concentration or composition is given in terms of activities a_i in order to express non-ideality.

$$a_i = \gamma_i\ x_i \tag{V - 5}$$

where γ_i is the activity coefficient and x_i the mole fraction. For ideal solutions the activity coefficient $\gamma_i \Rightarrow 1$, and the activity a_i becomes equal to the mole fraction x_i.

The chemical potential difference $\Delta\mu_i$ can be subdivided into a difference in composition and a difference in pressure according to

$$\Delta\mu_i = RT\, \Delta\ln a_i + V_i\, \Delta P \tag{V - 6}$$

The composition contribution (activity or mole fraction) is equal to the product of RT and the logarithm of the composition. At room temperature RT is equal to ≈ 2500 J/mole. The pressure contribution is equal to the product of the (partial) molar volume and the difference in pressure. The molar volume of liquids is small; thus water, for example, has a molar volume of $1.8\ 10^{-5}$ m^3/mol (18 cm^3/mol) and an 'ordinary' organic solvent (molecular weight 100 g/mol, density 1 g/ml) a molar volume of 10^{-4} m^3/mol. If we take, for example, a pressure difference over the membrane of 50 bar ($= 5\ 10^6$ N/m^2), then the product of $v_i\ \Delta P$ is ≈ 100 J/mol for water and ≈ 500 J/mol for the solvent.

A simple method of comparing driving forces is to make them dimensionless. As shown in figure V - 1, the driving force is the potential gradient, and the average driving force is the potential difference across the membrane divided by the membrane thickness (eq. V - 1). If the chemical potential and the electrical potential are considered to be the driving force and assuming ideal conditions, i.e. $a_i = x_i$ and $\Delta \ln x_i \approx (1/x_i)\, \Delta x_i$, eq. V - 2 becomes

$$F_{ave} = \frac{RT}{\ell}\frac{\Delta x_i}{x_i} + \frac{z_i\,\mathcal{F}}{\ell}\,\Delta E + \frac{V_i}{\ell}\,\Delta P \tag{V - 7}$$

On multiplying eq. V - 7 by a factor ℓ/RT ($=$ mol/N) the driving forces become dimensionless:

$$F_{dim} = \frac{\Delta x_i}{x_i} + \frac{z_i\,\mathcal{F}}{RT}\,\Delta E + \frac{V_i}{RT}\,\Delta P \tag{V - 8}$$

or

$$F_{dim} = \frac{\Delta x_i}{x_i} + \frac{\Delta E}{E^{\bullet}} + \frac{\Delta P}{P^{\bullet}}$$

(V - 9)

where $P^{\bullet} = \frac{RT}{V_i}$ and $E^{\bullet} = \frac{RT}{z_i \mathscr{F}}$

The magnitude of the various driving forces being the pressure, electrical potential or concentration, can easily be compared with each other using eq. V - 9. The concentration term $\Delta x_i / x_i$ is often equal to unity, while the pressure term is strongly

Table V. 1 Estimated values of P*

component	P*
gas	P
macromolecule	0.003 ......0.3 MPa
liquid	15 .... 40 MPa
water	140 MPa

dependent on the kind of component involved (i.e. on the molar volume). Some approximate values are given in table V.1. For gases, P* is equal to P (assuming that the gas behaves ideally).The electrical potential depends on the valence z_i

$$E^{\bullet} = \frac{RT}{\mathscr{F} \, z_i} = \frac{8.3 \quad 300}{10^5 \, z_i} \approx \frac{1}{40 \, z_i}$$

(V - 10)

Electrical potential is a very strong driving force in comparison to pressure, which is very weak. A concentration term of unity equates to an electrical potential difference of 1/40 V (for $z_i = 1$) whereas a pressure of 1200 bar is needed to produce the same driving force for water transport. This means that in the pervaporation of water through a dense membrane, a downstream pressure of zero ($P_2 \Rightarrow 0$) leads to the same flux as an infinite upstream pressure ($P_1 \Rightarrow \infty$).

V.3. Nonequilibrium thermodynamics

Flux equations derived from irreversible thermodynamics give a 'real' description of transport through membranes. In this description the membrane is considered as a black box and no information is obtained or is required about the structure of the membrane. Thus, no physico-chemical view is obtained how the molecules or particles permeate through the membrane. Because of the limitations of this approach with respect to the

nature of the membrane and the separation mechanism, only a short introduction will be given. Detailed information can be found in a number of excellent handbooks [1 - 3]. One of the strong points of this concept is that the existence of coupling of driving forces and/or fluxes can be shown and described very clearly. Therefore some examples will be given to demonstrate the existence of these coupling phenomena.

Transport processes through membranes cannot be considered as thermodynamic equilibrium processes and therefore only the thermodynamics of the irreversible processes can be used to describe membrane transport. In irreversible processes (and thus in membrane transport) free energy is dissipated continuously (if a constant driving force is maintained) and entropy is produced. Entropy is continuously produced if transport occurs across a membrane, i.e. due to a driving force a flow is produced. This entropy production is in most cases irreversible energy loss or exergy loss. The rate of entropy increase due to the irreversible process is given by the dissipation function ϕ. This dissipation function can be expressed as the summation of all irreversible processes, each can be described as the product of conjugated flows (J) and forces (X).

$$\phi = T \frac{dS}{dt} = \Sigma J_i X_i \tag{V - 11}$$

The flows do not only refer to the transport of mass but also to the transfer of heat and of electric current. The fluxes are expressed relative to the fixed membrane as reference frame with constant boundaries.

Close to equilibrium it can be assumed that each force is linearly related to the fluxes (eq. V - 12) or each flux is linearly related to the forces (eq. V - 13). This latter approach is often used in membrane transport.

$$X_i = \Sigma R_{ij} \cdot J_j \tag{V - 12}$$

and

$$J_i = \Sigma L_{ij} \cdot X_j \tag{V - 13}$$

Considering eq. V - 13 then for single component transport a very simple relation is obtained with only one proportionality coefficient. If the driving force is the gradient in the chemical potential then

$$J_1 = L_1 X_1 = - L_1 \frac{d\mu_1}{dx} \tag{V - 14}$$

In the case of the transport of two components 1 and 2 there are two flux equations with four coefficients (L_{11}, L_{22}, L_{12} and L_{21}). (In the case of transport of three components there are three flux equations and nine coefficients). In the absence of an electrical potential the driving force is the chemical potential gradient

$$J_1 = -L_{11} \frac{d\mu_1}{dx} - L_{12} \frac{d\mu_2}{dx}$$

(V - 15)

$$J_2 = -L_{21} \frac{d\mu_1}{dx} - L_{22} \frac{d\mu_2}{dx}$$

(V - 16)

The first term on the right hand side of eq. V - 15 corresponds to the flux of component 1 under its own gradient, while the second term gives the contribution of the gradient of component 2 to the flux of component 1. L_{12} is a coupling coefficient and represents the coupling effect. L_{11} is called the main coefficient.

According to Onsager the coupling coefficients are equal, hence

$$L_{12} = L_{21}$$

(V - 17)

This means that three phenomenological coefficients have to be considered. Two other restrictions also apply, i.e.

$$L_{11} \text{ (and } L_{22}) \geq 0$$

(V - 18)

$$L_{11} \cdot L_{22} \geq L_{12}^2$$

(V - 19)

The coupling coefficients may be either positive or negative. Usually the flux of one component increases the flux of a second component, i.e. there is a positive coupling. Positive coupling often results in a decrease in the selectivity.

Non-equilibrium thermodynamics have been applied to all kinds of membrane processes, as well as to dilute solutions consisting of a solvent (usually water) and a solute [5,6]. The characteristics of a membrane in such systems may be described in terms of three coefficients or transport parameters: the solvent permeability L , the solute permeability ω and the reflection coefficient σ. Using water as the solvent (index w) and with a given solute (index s), the dissipation function (entropy production) in a dilute solution is the sum of the solvent flow and solute flow multiplied by their conjugated driving forces:

$$\phi = J_w \cdot \Delta\mu_w + J_s \cdot \Delta\mu_s$$

(V - 20)

The chemical potential difference for water ($\Delta\mu_w$) is given by

$$\Delta\mu_w = \mu_{w,2} - \mu_{w,1} = V_w (P_2 - P_1) + RT (\ln a_2 - \ln a_1)$$

(V - 21)

where the subscript 2 refers to phase 2 (permeate side) and the subscript 1 refers to phase 1 (feed side). Expressing the osmotic pressure as (see chapter VI)

$$\pi = \frac{RT}{V_w} \ln a$$

(V - 22)

eq. V - 21 becomes

$$\Delta\mu_w = V_w \ (\Delta P - \Delta\pi) \tag{V - 23}$$

Writing the chemical potential difference for the solute as:

$$\Delta\mu_s \ = \ V_s \, \Delta P \ + \ \frac{\Delta\pi}{\overline{c_s}} \tag{V - 24}$$

and substituting eq. V - 23 and eq. V - 24 into eq. V - 20, the dissipation function may be expressed as:

$$\phi \ = \left(J_w \ V_w + J_s \ V_s\right) \Delta P \ + \left(\frac{J_s}{\overline{c_s}} - J_w \ V_w\right) \Delta\pi \tag{V - 25}$$

where the first term on the right-hand side represents the total volume flux (J_v), i.e.

$$J_v \ = \ J_w \cdot \ V_w \ + \ J_s \cdot V_s \tag{V - 26}$$

while the second term on the right-hand side represents the diffusive flux (J_d), i.e.

$$J_d \ = \ \frac{J_s}{\overline{c_s}} - J_w \ V_w \tag{V - 27}$$

Hence, the dissipation function can be written as:

$$\phi \ = \ J_v \cdot \Delta P \ + \ J_d \cdot \Delta\pi \tag{V - 28}$$

and the corresponding phenomenological equations as

$$J_v \ = \ L_{11} \cdot \ \Delta P \ + \ L_{12} \cdot \ \Delta\pi \tag{V - 29}$$

$$J_d \ = \ L_{21} \cdot \ \Delta P \ + \ L_{22} \cdot \ \Delta\pi \tag{V - 30}$$

The same restrictions concerning the magnitude of the various coefficients as mentioned previously apply, i.e.

$$L_{12} = L_{21} \tag{V - 17}$$

$$L_{11} \geq 0 \text{ and } L_{22} \geq 0 \tag{V - 18}$$

$$L_{11} \cdot L_{22} \geq L_{12}^2 \tag{V - 19}$$

The first assumption reduces the number of coefficients to three. The flux equations indicate that even if there is no difference in hydrodynamic pressure across the membrane ($\Delta P = 0$) there is still a volume flux (see eq. V - 29), and if the solute concentration on both sides of the membrane is the same ($c_1 = c_2 \Rightarrow \Delta\pi = 0$) there is still a solute flux when $\Delta P \neq 0$ (eq.V - 30). This is a very illustrative example of the occurrence of coupling, i.e. solvent flow because of solute transport and solute flow because of solvent transport.

The flux equations also allow some characteristic coefficients to be derived. When there is no osmotic pressure difference across the membrane ($\Delta\pi = 0 \Rightarrow c_1 = c_2$ or $\Delta c = 0$), eq. V - 29 indicates that a volume flow occurs because of a pressure difference (ΔP). This flow can be described as:

$$(J_v)_{\Delta\pi=0} = L_{11} \cdot \Delta P \qquad\qquad\qquad\qquad (V - 31)$$

or

$$L_{11} = \left(\frac{J_v}{\Delta P}\right)_{\Delta\pi = 0} \qquad\qquad\qquad\qquad (V - 32)$$

L_{11} is called the hydrodynamic permeability or water permeability of the membrane and is often referred to as L_p. Some average values of L_p using water as the solvent are given in table V.2.

Table V. 2   Some estimated values of L_p for various pressure driven membrane processes as obtained from experimental data

process	L_p ($l/m^2.hr.atm$)
reverse osmosis	< 50
ultrafiltration	50 - 500
microfiltration	> 500

When there is no hydrodynamic pressure difference across the membrane ($\Delta P = 0$) eq. V - 30 indicates that diffusive solute flow occurs because of an osmotic pressure difference

$$(J_d)_{\Delta P=0} = L_{22} \cdot \Delta\pi \qquad\qquad\qquad\qquad (V - 33)$$

or

$$L_{22} = \left(\frac{J_d}{\Delta\pi}\right)_{\Delta P = 0} \qquad\qquad\qquad\qquad (V - 34)$$

L_{22} is called the osmotic permeability or solute permeability and is often referred to as ω.

The third parameter, the reflection coefficient σ, can be derived from steady-state permeation measurements. When no volume flux occurs ($J_v = 0$) under steady state conditions then according to eq. V - 29:

$$L_{11}. \Delta P + L_{12}. \Delta \pi = 0 \qquad\qquad\qquad (V - 35)$$

or

$$(\Delta P)_{J_v = 0} = - \frac{L_{12}}{L_{11}} \Delta \pi \qquad\qquad\qquad (V - 36)$$

From eq. V - 35 it can be seen that, when the hydrodynamic pressure difference is equal to the osmotic pressure difference, L_{11} is equal to L_{12}, i.e. there is no solute transport across the membrane and the membrane is completely semipermeable. Membranes are not usually completely semipermeable and the ratio L_{12}/L_{11}, which is called the reflection coefficient σ [44], i.e.

$$\sigma = - \frac{L_{12}}{L_{11}} \qquad\qquad\qquad (V - 37)$$

is less than unity. The reflection coefficient is a measure of the selectivity of a membrane and usually has a value between 0 and 1.

$$\sigma = 1 \implies \text{ideal membrane, no solute transport} \qquad\qquad\qquad (V - 38)$$

$$\sigma < 1 \implies \text{not a completely semipermeable membrane: solute transport} \qquad\qquad\qquad (V - 39)$$

$$\sigma = 0 \implies \text{no selectivity.} \qquad\qquad\qquad (V - 40)$$

Substitution of eq. VI - 37 into eqs. VI - 29 and VI - 30 gives the following transport equations for the volume flux J_v and the solute flux J_s:

$$J_v = L_p (\Delta P - \sigma \Delta \pi) \qquad\qquad\qquad (V - 41)$$

$$J_s = \overline{c_s} (1 - \sigma) J_v + \omega \Delta \pi \qquad\qquad\qquad (V - 42)$$

Eqs. V - 41 and V - 42 indicate that transport across a membrane is characterised by three transport parameters, i.e. the water (solvent) permeability L_p, the solute permeability ω and the reflection coefficient σ. All these parameters can be determined experimentally. If the solute is not completely retained by the membrane then the osmotic pressure difference is not $\Delta \pi$ but $\sigma . \Delta \pi$ (see eq. V - 41). When the membrane is freely permeable to the solute ($\sigma = 0$), the osmotic pressure difference approaches zero ($\sigma . \Delta \pi \implies 0$) and the volume

flux is described as:

$$J_v = L_p \cdot \Delta P \qquad (V - 43)$$

This is a typical equation for porous membranes where the volume flux is proportional to the pressure difference (see, for example, the Kozeny-Carman and Hagen-Poiseuille equations for porous membranes).

The water permeability coefficient can be obtained via eq. V - 43 using experiments with pure water. Because the osmotic pressure difference is zero, there is a linear relationship between the hydrodynamic pressure ΔP and the volume (water) flux J_v (eq. V - 43), and from the slope of the corresponding flux-pressure curve the water permeability coefficient L_p can be obtained. Figure V - 3 is a schematic representation of the volume flux plotted as a function of the applied pressure for a more open membrane (high L_p) and a more dense membrane (low L_p).
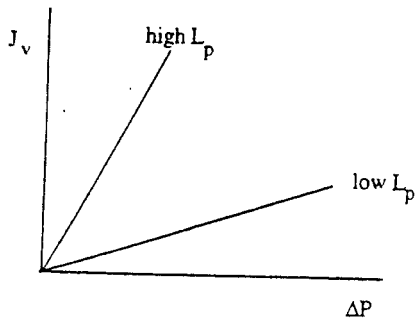
Figure V - 3.   Schematic representation of pure water flux as a function of the applied pressure.

The solute permeability ω can be obtained from eq. V - 42 and is given by

$$\left(\frac{J_s}{\Delta\pi}\right)_{J_v = 0} = \omega = \frac{\overline{c_s}\left(L_{11} L_{22} - L_{12}^2\right)}{L_{11}} = \overline{c_s}\left(L_{22}/L_{11} - \sigma^2\right) L_{11} \qquad (V - 44)$$

Both coefficients, the solute permeability ω and the reflection coefficient σ can be obtained by performing an osmotic and diffusion experiment. Also reverse osmosis can be applied. By rearranging eq. V - 42, the following equation is obtained:

$$\frac{J_s}{\Delta c} = \omega + (1 - \sigma) J_v \frac{\overline{c}}{\Delta c} \qquad (V - 45)$$

where Δc is the concentration difference between the feed and the permeate and $\overline{c}$ is the

mean logarithmic concentration [$\bar{c} = (c_f - c_p)/\ln(c_f/c_p)$]. By plotting $J_s/\Delta c$ versus $(J_v \bar{c})/\Delta c$, the solute permeability ω may be obtained from the intercept and the reflection coefficient σ from the slope of the resulting straight line (see figure V - 4). In cases where the pores become larger (from reverse osmosis to nanofiltration to ultrafiltration) or when the polymer has been highly swollen such as in dialysis, the major contribution towards the retention of a given solute is its molecular size in relation to that of the pore. This implies that an approximate relationship exists between the reflection coefficient and the solute size. The solute size may be expressed by the Stokes-Einstein equation (eq. V - 46).

$$r = \frac{kT}{6 \pi \eta D}$$

(V - 46)
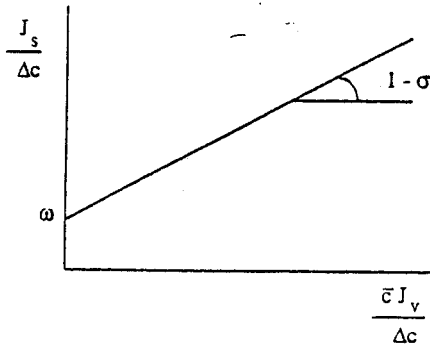
Figure V - 4.   Schematic drawing to obtain solute permeability coefficient ω and reflection coefficient σ according to eq. V - 45.

Although this equation is only strictly valid for spherical and quite large particles, it can be used as a first approximation for smaller molecules.

In order to compare the relationship between particle size (as expressed by the Stokes-Einstein radius) and the reflection coefficient σ, Nakao et al. [7] have performed

Table V - 3. Some characteristic data for low molecular weight solutes [7]

Solute	molecular weight	Stokes radius (Å)	σ
polyethylene glycol	3000	163	0.93
vitamin B12	1355	74	0.81
raffinose	504	58	0.66
sucrose	342	47	0.63
glucose	180	36	0.30
glycerine	92	26	0.18

ultrafiltration experiments with a number of low molecular weight organic solutes using rather dense ultrafiltration membranes. The results obtained are given in table V - 3 and clearly show, that at least qualitatively, the reflection coefficient increases with increasing solute size, i.e. the membrane becomes more and more selective. However, thisthermodynamic approach provides no information about the transport mechanism inside the membrane. Furthermore the various coefficients are not very easy to determine, especially in multi-component transport.

The above example (eqs. V - 20 till V - 42) clearly shows how coupling between water transport and salt transport could be described. Other phenomena can also be described; thus coupling between heat transfer and mass transfer arises in thermo-osmosis. Here, a temperature difference across the membrane not only results in heat transfer, but can also lead to mass transfer. Moreover, coupling between electrical potential difference and hydrostatic pressure arises in electro-osmosis, where solvent transport can occur via an electrical potential difference across the membrane in the absence of a difference in hydrostatic pressure. As an example of the coupled transport occurring during electro-osmosis, let us consider the case of a porous membrane separating two (aqueous) salt solutions. Transport can occur because of an electrical potential difference (ions) or because of a pressure difference (solvent). Again, entropy production can be described as the sum of conjugated fluxes and forces, i.e.

$$\phi = T \frac{dS}{dt} = \Sigma J_i \ X_i = J . \Delta P + I . \Delta E \qquad \text{(V - 47)}$$

or

$$I = L_{11} \Delta E + L_{12} \Delta P \qquad \text{(V - 48)}$$

$$J = L_{21} \Delta E + L_{22} \Delta P \qquad \text{(V - 49)}$$

From these equations it is clear that an electric current can be induced both because of an electrical potential difference and a pressure difference. Furthermore, a volume flux results from both an electrical potential difference and a pressure difference.

Assuming that Onsager's relationship applies $(L_{12} = L_{21})$, four different conditions can be distinguished:

i) In the absence of an electric current $(I = 0)$, an electrical potential develops because of the pressure difference. This phenomenon is called a streaming potential.

$$(\Delta E)_{I=0} = - \frac{L_{12}}{L_{11}} \Delta P \qquad \text{(V - 50)}$$

ii) When the pressure difference is zero $(\Delta P = 0)$, transport of solvent occurs because of an electric current. This phenomenon is called electro-osmosis.

$$(J)_{\Delta P = 0} \quad = \quad \frac{L_{21}}{L_{11}} \; I \tag{V - 51}$$

iii) When the solvent flux across the membrane is zero ($J = 0$), a pressure ('electro-osmotic pressure') is built up because of an electrical potential difference.

$$(\Delta P)_{J = 0} \quad = \quad - \; \frac{L_{21}}{L_{22}} \; \Delta E \tag{V - 52}$$

iv) In the absence of an electrical potential difference ($\Delta E = 0$), an electrical current is generated because of solvent flow across the membrane.

$$(I)_{\Delta E = 0} \quad = \quad \frac{L_{12}}{L_{22}} \; J \tag{V - 53}$$

In the previous chapter it has been described how these electrokinetic phenomena can be used to obtain information about the properties at the membrane-solution surface, e.g. surface charge of the membrane, zeta potential, and electrical double layer.

The thermodynamics of irreversible processes are very useful for understanding and quantifying coupling phenomena. However, structure-related membrane models are more useful than the irreversible thermodynamic approach for developing specific membranes. A number of such transport models have been developed, partly based on the principles of the thermodynamics of irreversible processes, both for porous and nonporous membranes. Again, two types of structure will be considered here: porous membranes, as found in microfiltration/ultrafiltration, and nonporous membranes of the type used in pervaporation/gas separation.

Transport occurs through the pores in porous membranes rather than the dense matrix, and structure parameters such as pore size, pore size distribution, porosity and pore dimensions are important and have to been taken into account in any model developed. The selectivity of such membranes is based mainly on differences between particle and pore size. The description of the transport models will involve a discussion of all these various parameters. In dense membranes, on the other hand, a molecule can only permeate if it dissolves in the membrane. The extent of such solubility is determined by the affinity between the polymer (membrane) and the low molecular weight component. Because of the existence of a driving force, the component within the membrane is then transported from one side to the other via diffusion. Selectivity in these membranes is mainly determined by differences in solubility and/or differences in diffusivity. Hence the important transport parameters are those that provide information about the thermodynamic interaction or affinity between the membrane (polymer) and the permeant. In this respect, large differences exist between gaseous and liquid permeants. Interaction between polymers and gases is low in general low, whereas strong interactions often exist between polymers and liquids. As the affinity increases in the system the polymer network will tend to swell and this swelling has a considerable effect on transport. Such effects must be considered in any description of transport through dense membranes.

V.4. Transport through porous membranes

Porous membranes are used in microfiltration and ultrafiltration processes. These membranes consist of a polymeric matrix in which pores within the range of 2 nm to 10 μm are present. A large variety of pore geometries is possible and figure V - 5 gives a schematic representation of some of the characteristic structures found. Such structures exist over the whole membrane thickness in microfiltration membranes and here the resistance is determined by the total membrane thickness. On the other hand, ultrafiltration membranes generally have an asymmetric structure, where the porous top-layer mainly determines the resistance to transport. Here, the transport length is only of the order of 1 μm or less.

(a)   (b)   (c)
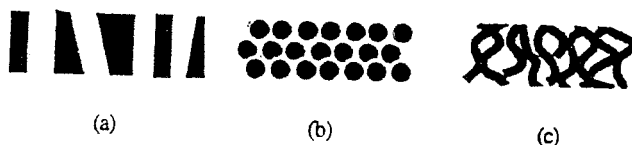
Figure V - 5. Some characteristic pore geometries found in porous membranes.

The existence of these different pore geometries also implies that different models have been developed to describe transport adequately. These transport models may be helpful in determining which structural parameters are important and how membrane performance can be improved by varying some specific parameters.

The simplest representation is one in which the membrane is considered as a number of parallel cylindrical pores perpendicular or oblique to the membrane surface (see figure V - 5a). The length of each of the cylindrical pores is equal or almost equal to the membrane thickness. The volume flux through these pores may be described by the Hagen-Poiseuille equation. Assuming that all the pores have the same radius, then we may write:

$$J = \frac{\varepsilon \, r^2}{8 \, \eta \, \tau} \frac{\Delta P}{\Delta x}$$

$$(V - 54)$$

which indicates that the solvent flux is proportional to the driving force, i.e. the pressure difference (ΔP) across a membrane of thickness Δx and inversely proportional to the viscosity η. The quantity ε is the surface porosity, which is the fractional pore area (ε is equal to the ratio of the pore area to membrane area A_m multiplied by the number of pores n_p, $\varepsilon = n_p \cdot \pi \, r^2 / A_m$), while τ is the pore tortuosity (For cylindrical perpendicular pores, the tortuosity is equal to unity).

The Hagen-Poiseuille equation clearly shows the effect of membrane structure on transport. By comparing eq. V - 54 with the phenomenological eq. V - 43 (and writing in the latter case $\Delta P/\Delta x$ as driving force instead of ΔP), a physical meaning can be given to the

hydraulic permeability L_p in terms of the porosity (ε), pore radius (r), pore tortuosity (τ) and viscosity (η) so that the phenomenological 'black-box' equation may be related to a physical model:

$$L_p = \frac{\varepsilon \, r^2}{8 \, \eta \, \tau} \tag{V - 55}$$

The Hagen-Poiseuille eq. V - 54 gives a good description of transport through membranes consisting of a number of parallel pores. However, very few membranes posses such a structure in practice .

Membranes consisting of the structure depicted schematically in figure V - 5b, i.e. a system of closed packed spheres, can be found in organic and inorganic sintered membranes or in phase inversion membranes with a nodular top layer structure. Such membranes can best be described by the Kozeny-Carman relationship (eq. V - 56), i.e.

$$J = \frac{\varepsilon^3}{K \, \eta \, S^2 \, (1 - \varepsilon)^2} \frac{\Delta P}{\Delta x} \tag{V - 56}$$

where ε is the volume fraction of the pores, S the internal surface area and K the Kozeny-Carman constant, which depends on the shape of the pores and the tortuosity.

Phase inversion membranes frequently show a sponge-like structure, as schematically depicted in figure V - 5c. The volume flux through these membranes are described either by the Hagen-Poiseulle or the Kozeny-Carman relation, although the morphology is completely different (see also chapter IV).

V.4.1 Transport of gases through porous membranes

When an asymmetric membrane or composite membrane is used in gas separation, the gas molecules will tend to diffuse from the high-pressure to the low-pressure side. Various transport mechanisms can be distinguished depending on the structure of the asymmetric membrane or composite membrane, see figure V - 6, i.e.

— top layer (bulk diffusion)
narrow pores (Knudsen diffusion)

wide pores (viscous flow)
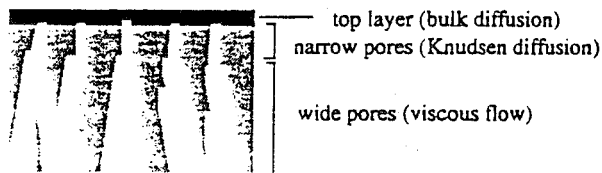
Figure V - 6. Transport in an asymmetric membrane as a result of various mechanisms.

- transport through a dense (nonporous) layer
- Knudsen flow in narrow pores
- viscous flow in wide pores
- surface diffusion along the pore wall

The rate determining step is mostly transport through the dense nonporous top layer. This type of transport will be discussed in the following section. However, it is also possible that the other mechanisms contribute to transport, i.e. the resistance of the sublayer may contribute to transport. In addition, generally ultrafiltration types of membranes are employed as sublayer. In chapter IV it has been shown already that the surface porosity may be quite low, ranging from a few procents to lower than 1%. This implies that the effective thickness is much larger than the actual toplayer thickness, as depicted in figure V - 7. The actual toplayer thickness is ℓ_o but when a molecule penetrates the film at point A the thickness is much larger as shown in figure V - 7. It is obvious that the effective thickness ℓ_{eff} is strongly dependent on the surface porosity ε of the sublayer.
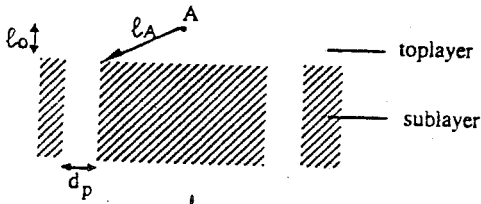
Figure V - 7.   Schematic drawing of various diffusion paths in a composite membrane.

The average diffusion length can be given by

$$\ell_{eff} = \varepsilon \ell_o + (1 - \varepsilon) \frac{\ell_A + \ell_o}{2}$$

$$(V - 57)$$

This equation shows clearly that the determination of the P/ℓ value (see IV.4.1), which is often used to characterize the resistance of the sublayer, is not sufficient and that data are required to determine the pore size distribution.

V.4.1.1   Knudsen flow

The occurrence of Knudsen flow or viscous flow is mainly determined by the pore size. For large pore sizes ($r > 10 \ \mu m$) viscous flow occurs in which gas molecules collide exclusively with each other (in fact they seem to ignore the existence of the membrane) and no separation is obtained between the various gaseous components. The flow is proportional to r^4 (see eq. V - 54). However, if the pores are smaller and/or when the pressure of the gas is reduced, the mean free path of the diffusing molecules becomes

comparable or larger than the pore size of the membrane. Collisions between the gas molecules are now less frequent than collisions with the pore wall. This kind of gas transport is called Knudsen diffusion. (see figure V - 8).

Poisseuille
flow
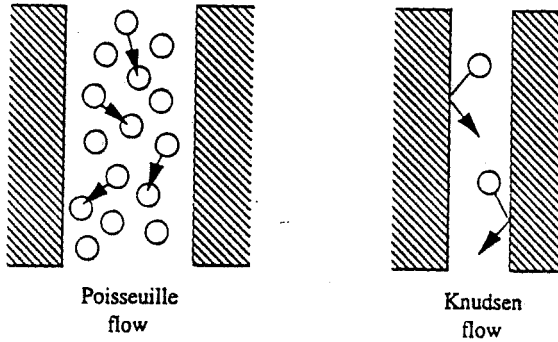
Knudsen
flow

Figure V - 8. Schematic drawings depicting Poisseuille (or viscous flow) and Knudsen flow.

The mean free path (λ) may be defined as the average distance traversed by a molecule between collisions. The molecules are very close to each other in a liquid and the mean free path is of the order of a few Ångströms. Therefore, Knudsen diffusion can be neglected in liquids. However, the mean free path of gas molecules will depend on the pressure and temperature. In this case, the mean free path can be written as:

$$\lambda = kT / (\pi \, d^2_{gas} \, P \, \sqrt{2})$$ (V - 58)

where d_{gas} is the diameter of the molecule. As the pressure decreases the mean free path increases, and at constant pressure the mean free path is proportional to the temperature. (At 25°C the mean free path of oxygen is 70 Å at 10 bar and 70 μm at 10 mbar).

In ultrafiltration membranes (those used, for example, as a support in gas permeation experiments), the pore diameter is within the range 20 nm to 0.2 μm, and hence Knudsen diffusion can have a significant effect. At low pressures, transport is determined completely by Knudsen flow [4]. In this regime the flux is given by:

$$J = \frac{\pi \, n \, r^2 \, D_k \, \Delta p}{R \, T \, \tau \, \ell}$$ (V - 59)

where D_k, the Knudsen diffusion coefficient, is given by $D_k = 0.66 \, r \, \sqrt{\dfrac{8 \, R \, T}{\pi \, M_w}}$

T and M_w are the temperature and molecular weight, respectively and r is the pore radius. Eq. V - 59 shows that the flux depends on the square root of the molecular weight, i.e. the separation between the molecules is inversely proportional to the ratio of the square root of

the molecular weights of the gases.

V.4.2. *Friction model*

Another approach used to describe transport through a porous membrane is the friction model. This considers that passage through the porous membrane occurs both by viscous flow and diffusion, i.e. that an extra term is necessary in. This implies that the pore sizes are so small that the solute molecules cannot pass freely through the pore, and that friction occurs between the solute and the pore wall (and also between the solvent and the pore wall and between the solvent and the solute). The frictional force F per mole is related linearly to the velocity difference or relative velocity. The proportionality factor is called the friction coefficient f. On considering permeation of the solvent and solute through a membrane and taking the membrane as a frame of reference ($v_m = 0$), the following frictional forces can be distinguished (subscripts s, w and m refer to solute, water (solvent) and membrane respectively):

$$F_{sm} = -f_{sm}(v_s - v_m) = -f_{sm} \cdot v_s \qquad (V-60)$$

$$F_{wm} = -f_{wm}(v_w - v_m) = -f_{wm} \cdot v_w \qquad (V-61)$$

$$F_{sw} = -f_{sw}(v_s - v_w) \qquad (V-62)$$

$$F_{ws} = -f_{ws}(v_w - v_s) \qquad (V-63)$$

The proportionality factor f_{sm} (the friction coefficient) denotes interaction between the solute and the polymer (pore wall).

Using linear relationships between the fluxes and forces in accordance with the concept of irreversible thermodynamics and assuming isothermal conditions the forces can be described as the gradient of the chemical potential, i.e.

$$X_i = -\frac{\partial \mu_i}{\partial x} \qquad (V-64)$$

However, other (external) forces acting on component i, such as the frictional force, must also be included. Thus equation V - 64 becomes

$$X_i = -\frac{\partial \mu_i}{\partial x} + F_i \qquad (V-65)$$

The diffusive solute flux can be written as the product of the mobility, concentration and driving force. The mobility m may be defined as

$$m = D/RT \qquad (V-66)$$

so that the flux then becomes

$$J_s = m_{ws} \, c_{sm} \left(-\frac{\partial \mu_s}{\partial x} + F_{sm} \right)$$

(V - 67)

where c_{sm} is the concentration of the solute in the membrane (pore). Eq. V - 67 describes the solute flux as a combination of diffusion (first term on the right-hand side) and viscous flow (second term on the right-hand side). Assuming an ideal solution, then

$$\left(\frac{\partial \mu_s}{\partial x} \right)_{P,T} = \frac{\partial \mu_s}{\partial c_{sm}} \left(\frac{\partial c_{sm}}{\partial x} \right)$$

(V - 68)

Furthermore, for dilute (ideal) solutions

$$\left(\frac{\partial \mu_s}{\partial x} \right)_{P,T} = \frac{R\,T}{c_{sm}}$$

(V - 69)

The frictional force per mole of solute is given by

$$F_{sm} = -f_{sm} \, v_s = -f_{sm} \frac{J_s}{c_{sm}}$$

(V - 70)

and relating the mobility of the solute in water to the frictional coefficient between the solute and water, then

$$m_{sw} = 1/f_{sw}$$

(V - 71)

If we define a parameter b that relating the frictional coefficient f_{sm} (between the solute and the membrane) to f_{sw} (between the solute and water), then

$$b = \frac{f_{sw} + f_{sm}}{f_{sw}} = 1 + \frac{f_{sm}}{f_{sw}}$$

(V - 72)

On combining eqs. V - 67, V - 68, V - 69, V - 71 and V - 72, the solute flux can then be written as [8]:

$$J_s = -\frac{R\,T}{f_{sw} \, b} \frac{dc_{sm}}{dx} + \frac{c_{sm} \, v_s}{b}$$

(V - 73)

The coefficient for distribution of solute between the bulk and the pore (membrane) is given by

$$K = c_{sm} / c$$

(V - 74)

while the frictional coefficient f_{sw} between the solute and water may be written as:

$$D_{sw} = RT/f_{sw} \qquad (V-75)$$

where D_{sw} is the diffusion coefficient for the solute in dilute solutions. With $J_v = \varepsilon \cdot v$, $J_i = J_s \cdot \varepsilon$ and $\xi = \tau \cdot x$, eq. V - 73 becomes

$$J_i = -\frac{K D_{sw}}{b \tau} \frac{dc}{dx} + \frac{K c J_v}{b} \qquad (V-76)$$

Because

$$c_p = J_s / v_s \qquad (V-77)$$

integration of eq. V - 76 with the boundary conditions

$$x = 0 \implies c1.sm = K \cdot cf$$

$$x = \ell \implies c2.sm = K \cdot cp$$

where c_f and c_p are the solute concentrations in the feed and permeate respectively, yields [8]

$$\frac{c_f}{c_p} = \frac{b}{K} + \left(1 - \frac{b}{K}\right) \exp\left(-\frac{\tau \ell J_v}{\varepsilon D_{sw}}\right) \qquad (V-78)$$

Plotting cf /cp (which relates to the selectivity) versus the permeate flux as expressed by the exponential factor $(\tau . \ell/\varepsilon) . (J_v /D_{sw})$, leads to the results depicted in figure V - 9.
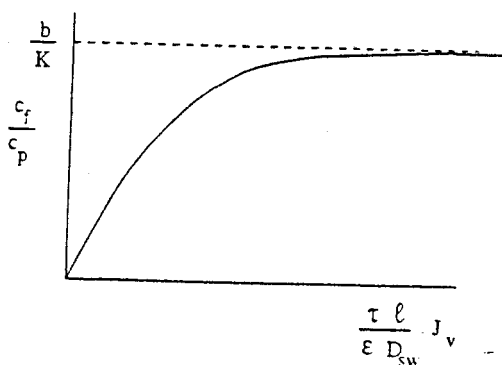

Figure V - 9. Schematic drawing of concentration reduction (c_f /c_p) versus flux as given by eq. V - 76 [8].

This figure demonstrates that the ratio c_f/c_p increases to attain an asymptotic value at b/K, a factor which has a maximum value when b is large and K is small. The friction factor b is large when the friction between the solute and the membrane (f_{sm}) is greater than the friction between the solute and the solvent (f_{sw}). The parameter K is small when the uptake of solute by the membrane from the feed is small compared to the solvent (water) uptake, i.e. when the solute distribution coefficient is small. An important point is that both the distribution coefficient (an equilibrium thermodynamic parameter) and the frictional forces (kinetic parameter) determine the selectivity.

Solute rejection is given by

$$R = \frac{c_p - c_f}{c_p} = 1 - \frac{c_f}{c_p} \tag{V - 79}$$

and from eqs. V - 77 and V - 78 it can be seen that the maximum rejection R_{max} ($J_v \Rightarrow \infty$) is given by

$$R_{max} = \sigma = 1 - \frac{K}{b} = 1 - \frac{K}{\left[1 + \frac{f_{sm}}{f_{sw}}\right]^{-1}} \tag{V - 80}$$

This equation shows how rejection is related to a kinetic term (the friction factor b) and to a thermodynamic equilibrium term (the parameter K). Spiegler and Kedem derived the following equation [6]:

$$\sigma = 1 - \frac{K_s}{K_w} \frac{\left[f_{sw} + f_{wm}\left(\frac{V_s}{V_w}\right)\right]}{f_{sw} + f_{sm}} \tag{V - 81}$$

$$\underset{\substack{\text{exclusion} \\ \text{term}}}{\hphantom{xxx}} \underset{\substack{\text{kinetic} \\ \text{term}}}{\hphantom{xxx}}$$

Again two terms can be distinguished, a thermodynamic equilibrium term (also described as the exclusion term) being the ratio of solute to water uptake (= K_s/K_w). For a highly selective membrane this term must be as small as possible, i.e. the solubility of the solute in the membrane must be as low as possible. This can be achieved by a proper choice of the polymer. In addition the kinetics, as expressed by the friction coefficients, affect the selectivity as well, as indicated by the the second term on the right-hand side of eq. V - 80.

Thus, even in this concept, selectivity is considered in terms of a solution-diffusion mechanism, with the exclusion term being equivalent to the solution part and the kinetic term to the diffusion part.

Another relation between rejection and flux has been derived by Pusch [9,10]. If the permeate concentration is given by $c_p = J_s/J_v$, then the rejection R can be written as

$$R = 1 - \frac{c_p}{c_f} = 1 - \frac{J_s}{c_f J_v}$$

(V - 82)

Substitution of eq. V - 42 into V - 82 gives

$$R = 1 - \frac{[\omega \Delta\pi + (1 - \sigma) J_v \bar{c}]}{c_f J_v}$$

(V - 83)

or

$$R = 1 - \frac{(1 - \sigma) \bar{c}}{c_f} - \frac{\omega \Delta\pi}{c_f J_v}$$

(V - 84)

Substitution of eq. V - 43 into V - 83 gives

$$R = 1 - \frac{(1 - \sigma) \bar{c}}{c_f} - (L_{22}/L_{11} - \sigma^2) \frac{\bar{c}}{c_f} \frac{L_{11} \Delta\pi}{J_v}$$

(V - 85)

From eq. V - 85 limiting conditions can be derived. The maximum rejection R^∞ is obtained as $J_v \Rightarrow \infty$. Under these conditions the rejection is given by

$$R^\infty = 1 - \frac{(1 - \sigma) \bar{c}^\infty}{c_f}$$

(V - 86)

in which c^∞ is the average solute concentration at $J_v \Rightarrow \infty$. Assuming that $c^\infty \approx c_f$ then $R^\infty = \sigma$. Furthermore if $R = \Delta\pi / \pi_f$ and substitution of eq. V - 86 into V - 85 then eq. V - 87 is obtained.

$$\frac{1}{R} = \frac{1}{R^\infty} + \left[\frac{L_{11}}{L_{22}} - (R^\infty)^2 \right] \frac{L_{11} \pi_f}{R^\infty J_v}$$

(V - 87)

From eq. V - 87 it can be seen that if the reciprocal rejection coefficient R is plotted versus the reciprocal solvent flux Jv a straight line is obtained with the reciprocal of the maximum rejection R^∞ as absissa and as slope $[L_{11}/L_{22} - (R^\infty)^2]$.

V.5.   Transport through nonporous membranes

When the sizes of molecules are in the same order of magnitude, as with oxygen and nitrogen or hexane and heptane, porous membranes cannot effect a separation. In this case nonporous membranes must be used. However, the term nonporous is rather ambiguous because pores are present on a molecular level in order to allow transport even in such membranes. The existence of these dynamic 'molecular pores' can be adequately described in terms of free volume.

Initially transport through these dense membranes will be considered via a somewhat simple approach. Thus, although there are some similarities between gaseous and liquid transport, there are also a number of differences. In general, the affinity of liquids and polymers is much greater than that between gases and polymers, i.e. the solubility of a liquid in a polymer is much higher that of a gas. Sometimes the solubility can be that high that crosslinking is necessary to prevent polymer dissolution. In addition, a high solubility also has a tremendous influence on the diffusivity, making the polymer chains more flexible and resulting in an increased permeability.

Another difference between liquids and gases is that the gases in a mixture flow through a dense membrane in a quite independent manner, whereas with liquid mixtures the transport of the components is influenced by flow coupling and thermodynamic interaction. This synergistic effect can have a very large influence on the ultimate separation, as will be shown later.

Basically, the transport of a gas, vapour or liquid through a dense, nonporous membrane can be described in terms of a solution-diffusion mechanism, i.e.

Permeability (P) = Solubility (S) x Diffusivity (D) (V - 88)

Solubility is a thermodynamic parameter and gives a measure of the amount of penetrant sorbed by the membrane under equilibrium conditions. The solubility of gases in elastomer polymers is very low and can be described by Henry's law. However, with organic vapours or liquids, which cannot be considered as ideal, Henry's law does not apply. In contrast, the diffusivity is a kinetic parameter which indicates how fast a penetrant is transported through the membrane. Diffusivity is dependent on the geometry of the penetrant, for as the molecular size increases the diffusion coefficient decreases. However, the diffusion coefficient is concentration-dependent with interacting systems and even large (organic) molecules having the ability to swell the polymer can have large diffusion coefficients.
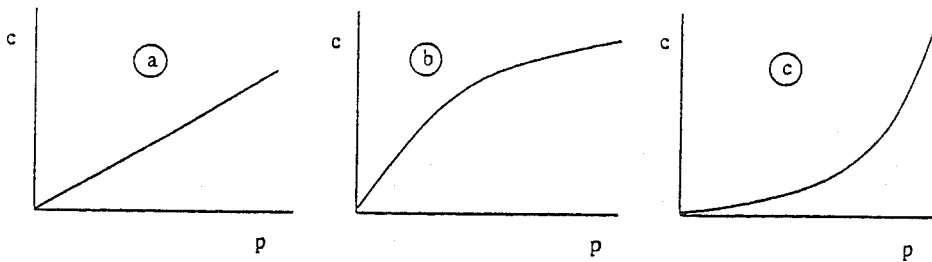

Figure V - 10. Schematic drawing of sorption isotherms for ideal and non-ideal systems.

The solubility of gases in polymers is generally quite low (< 0.2% by volume) and it is assumed that the gas diffusion coefficient is constant. Such cases can be considered as

ideal systems where Fick's law is obeyed. On the other hand, the solubility of organic liquids (and vapours) can be relatively high (depending on the specific interaction) and the diffusion coefficient is now assumed to be concentration-dependent, i.e. the diffusivities increase with increasing concentration.

Two separate cases must therefore be considered, ideal systems where both the diffusivity and the solubility are constant, and concentration-dependent systems where the solubility and the diffusivity are functions of the concentration.(Other cases can be distinguished where the solubility and the diffusivity are functions of other parameters, such as time and place. These phenomena, often termed "anomalous", can be observed in glassy polymers where relaxation phenomena occur or in heterogeneous types of membranes. These cases will not be considered further here.)

For ideal systems, where the solubility is independent of the concentration, the sorption isotherm is linear (Henry's law), i.e. the concentration inside the polymer is proportional to the applied pressure (figure V - 10a). This behaviour is normally observed with gases in elastomers. With glassy polymers the sorption isotherm is generally curved rather than linear (see figure V - 10b), whereas such strong interactions occur between organic vapours or liquids and polymer, the sorption isotherms are highly non-linear, especially at high vapour pressures (figure V - 10c). Such non-ideal sorption behaviour can be described by free volume models [11] and Flory-Huggins thermodynamics [12].

The solubility can be obtained from equilibrium measurements in which the volume of gas taken up is determined when the polymer sample is brought into contact with a gas at a known applied pressure. For glassy polymers where the solubility of a gas often deviates in the manner shown in figure V - 10b, such deviation can be described by the dual sorption theory [13 - 15], in which it is assumed that two sorption mechanisms occur simultaneously, i.e. sorption according to Henry's law and via a Langmuir type sorption. This is shown in figure V - 11.
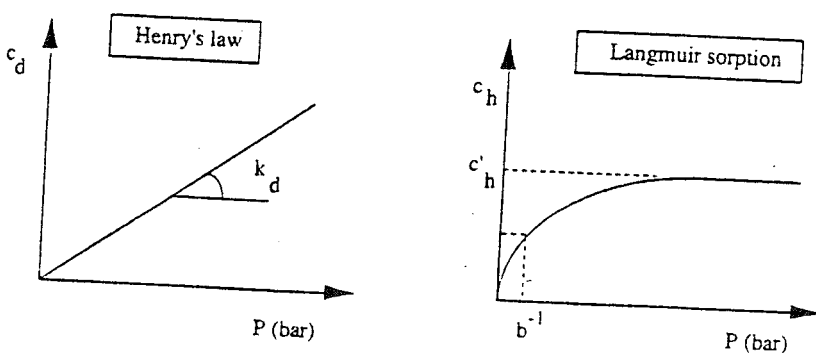
Figure V - 11 . The two contributions in the dual sorption theory: Henry's law and Langmuir type sorption.

In this case, the concentration of gas in the polymer can be given as the sum produced by the two sorption modes

$$c = c_d + c_h \tag{V - 89}$$

or

$$c = k_d P + \frac{c_h^{'} \, b \, P}{1 + b \, P} \tag{V - 90}$$

where k_d is the Henry's law constant ($[kd]$: cm3(STP).cm^{-3}.bar^{-1}) which is equal to the solubility coefficient S, b is the hole affinity constant ($[b]$: bar^{-1}) and c'h is the saturation constant ($[c'h]$: cm^3(STP).cm^{-3}). The dual sorption model often gives a good description of observed phenomena and it is very frequently used to describe sorption in glassy polymers. From a physical point of view, however, it is difficult to understand the existence of two different sorption modes for a given membrane which implies the existence of two different types of sorbed gas molecules (the dual sorption theory can also be considered as a three parameter fit).
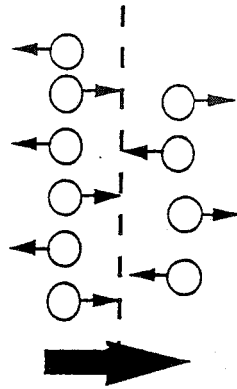
Figure V - 12.   Schematic drawing of diffusion as a result of random molecular motions.

Permeability is both a function of solubility and diffusivity (see eq. V - 88). The simplest way to describe the transport of gases through membranes is via Fick's first law (eq. V - 91).

$$J = -D \frac{dc}{dx} \tag{V - 91}$$

the flux J of a component through a plane perpendicular to the direction of diffusion being proportional to the concentration gradient dc/dx. The proportionality constant is called the

diffusion coefficient.

Diffusion may be considered as statistical molecular transport as a result of the random motion of the molecules. A (macroscopic) mass flux occurs because of a concentration difference. Imagine a plane with more molecules on one side than on the other, then a net mass flux will occur because more molecules move to the right than to the left. (as shown schematically in figure V - 12). Now, consider two planes (e.g. a thin part of a membrane) at the points x and x + δx (figure V - 13). The quantity of penetrant which enters the plane at x at time δt is equal to J . δt. The quantity of penetrant leaving the plane at x + δx is [J + (∂J/∂x)δx]δt.
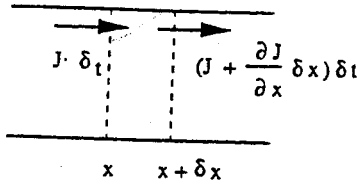
Figure V - 13. Diffusion across two planes situated at the points x and x + δx in the cross-section of a membrane (or any other medium).

The change in concentration (dc) in the volume between x and x + δx is

$$dc = \frac{[J \; \delta t - (J + \left(\frac{\partial J}{\partial x}\right) \delta x) \; \delta t \;]}{\delta x}$$

(V - 92)

which yields

$$dc = - \left(\frac{\partial J}{\partial x}\right) \delta t$$

(V - 93)

For an infinite small section and an infinite small period of time (δx ⟹ 0, δt ⟹ 0), eq. V - 93 becomes

$$\frac{\partial c}{\partial t} = - \frac{\partial J}{\partial x}$$

(V - 94)

This equation has already been used in chapter III for describing the change in composition during membrane formation.

Substitution of eq. V - 91 into eq. V - 94 yields

$$\frac{\partial c}{\partial t} = - \frac{\partial}{\partial x} \left(D \frac{\partial c}{\partial x}\right)$$

(V - 95)

If it is assumed that the diffusion coefficient is constant, then

$$\frac{\partial c}{\partial t} = -D \frac{\partial^2 c}{\partial x^2}$$

<div align="right">(V - 96)</div>

This expression, also known as Fick's second law, gives the change in concentration as a function of distance and time. At room temperature the diffusion coefficients of gases in gases are of the order of 0.05 - 1 cm²/sec, whereas for low molecular weight liquids and gases in liquids the values are of the order of 10^{-4} - 10^{-5} cm²/sec.

Table V. 4   Diffusion coefficients of noble gases in polyethylmethacrylate [16]

noble gas	diffusion coefficient (cm²/sec)
helium	$\approx 0.5 \ 10^{-4}$
neon	$\approx 10^{-6}$
argon	$\approx 10^{-8}$
krypton	$\approx 0.5 \ 10^{-8}$

The order of magnitude of the diffusion coefficients of molecules permeating through nonporous membranes depends on the size of the diffusing particles and on the nature of the material through which diffusion occurs. In general, diffusion coefficients decrease as the particle size increases (compare the Stokes-Einstein eq. V - 46). The diffusion coefficients of the noble gases in polyethylmethacrylate at 25°C are listed in table V - 4 [16].

Another example of diffusion being very dependent on the medium through which it proceeds is shown in figure V - 14. This figure is a schematic representation of the values of the diffusion coefficients in water (or in another low molecular liquid) and in a rubbery polymer as a function of the molecular weight of the diffusing component. In water, the diffusion coefficient decreases only slightly with increasing molecular weight compared to the situation with rubber. This is the normal behaviour when diffusion occurs in non-interacting systems. When concentration-dependent systems are involved, however, the membrane may swell considerably and the diffusing medium may also change significantly. Such strong interactions can have a large impact on diffusion phenomena. Because of swelling the penetrant concentration inside the polymer will increase. The diffusion coefficient also increases and under such circumstances the effect of the particle size will become less important. In general, it can be said that the effect of concentration will increase as the diffusion coefficients decrease at lower swelling values. This is shown schematically in figure V - 14 (right-hand figure), where the diffusion coefficients of a given low molecular component are plotted versus the degree of swelling. This figure
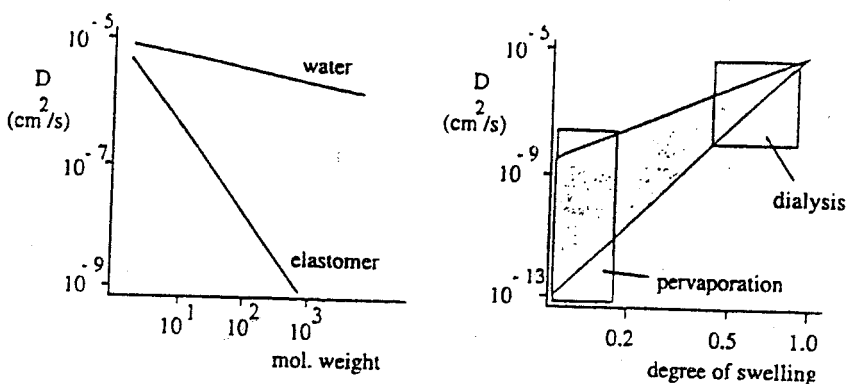
Figure V - 14.   Diffusion coefficients of components in water and in an elastomer membrane as a function of the molecular weight (left figure) and in a polymer as a function of the degree of swelling for a given low molecular weight penetrant.

shows clearly that the diffusion coefficients vary by some orders of magnitude with different degrees of swelling, resulting in the occurrence of different types of separation.

Another way of describing diffusion processes is in terms of friction. The penetrant molecules move through the membrane with a velocity v because of a force $\partial\mu/\partial x$ acting on them. This force (the chemical potential gradient) is necessary to maintain the velocity v against the resistance of the membrane. If the frictional resistance is denoted as f, the velocity is then given by

$$v = -\frac{1}{f}\left(\frac{\partial\mu}{\partial x}\right)$$

(V - 97)

Since the reciprocal of the friction coefficient is the mobility coefficient m (see also eq. V - 70), and eq. V - 97 becomes

$$v = -m\left(\frac{\partial\mu}{\partial x}\right)$$

(V - 98)

and the quantity of molecules passing through the cross-sectional area per unit time is given by

$$J = v\,c = -m\,c\left(\frac{\partial\mu}{\partial x}\right)$$

(V - 99)

The thermodynamic diffusion coefficient D_T is related to the mobility by the relation

$$D_T = m \cdot RT \tag{V - 100}$$

and since the chemical potential μ is given by

$$\mu = \mu^\circ + RT \ln a \tag{V - 101}$$

eq. V - 99 can be rewritten as

$$J = - \frac{D_T}{RT} c \left(\frac{\partial \ln a}{\partial x} \right) = - D_T \left(\frac{\partial \ln a}{\partial \ln c} \right) \left(\frac{\partial c}{\partial x} \right) \tag{V - 102}$$

and by comparison with Fick's law we obtain

$$D = D_T \left(\frac{d \ln a}{d \ln c} \right) \tag{V - 103}$$

Since for ideal systems the activity a is equal to the concentration c and $D = D_T$, eq. V - 102 will reduce to Fick's law. However, for non-ideal systems (organic vapours and liquids) activities must be used rather than concentrations. The fact that D_T changes with the concentration (or activity) indicates that the presence of the penetrant modifies the properties of the membrane.Both ideal and concentration dependent systems will be considered in more detail in the following section.

V.5.1   Transport in ideal systems
Graham studied the transport of gases through rubber membranes in 1861 and postulated the existence of a solution-diffusion mechanism. The same approach is followed here where it is assumed that ideal sorption and diffusion behaviour occur.
     The solubility of a gas in a membrane can be described by Henry's law which indicates that a linear relationship exists between the external pressure p and the concentration c inside the membrane, i.e.

$$c = S \ p \tag{V - 104}$$

The pressure is p_1 on the feed side ($x = 0$) and the penetrant concentration in the polymer is c_1, whereas on the permeate side ($x = \ell$) the pressure is p_2 and the penetrant concentration is c_2. Substitution of eq. V - 104 into Fick's law (eq.V - 84) and integrating across the membrane leads to:

$$J = \frac{S \ D}{\ell} (p_1 - p_2) \tag{V - 105}$$

and since the permeability coefficient P may be defined as

$$P = D \ S \tag{V - 106}$$

this leads to:

$$J = \frac{P}{\ell} (p_1 - p_2)$$

(V - 107)

This equation shows that the flux of a component through a membrane is proportional to the pressure difference across the membrane and inversely proportional to the membrane thickness. It is worth studying solubility, diffusivity and permeability more closely in respect to the solution-diffusion mechanism. Figure V - 15 shows the solubility and diffusivity of various gases in natural rubber as a function of the molecular dimensions [18], and clearly indicates that the diffusion coefficient decreases as the size of the gas molecules increases. The small molecule hydrogen has a relatively high diffusion coefficient whereas carbon dioxide having a relatively low diffusion coefficient. Such a relationship can be deduced from the Stokes-Einstein equation (eq. V - 46), when it may be shown that the frictional resistance of a (spherical) molecule increases with increasing radius with the diffusion coefficient being inversely proportional to this friction resistance, i.e.

$$f = 6\pi\eta \, r$$

(V - 108)
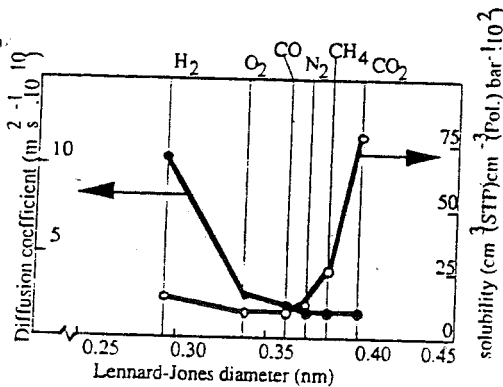
Figure V - 15. Solubility and diffusivity of various gases in natural rubber [18].

and

$$D = \frac{kT}{f}$$

(V - 109)

In contrast, the solubility of gases in natural rubber as well as in other polymers increases with increasing molecular dimensions. Since the interaction of a gas with a polymer is in general very small, helium (He), hydrogen (H_2), nitrogen (N_2), oxygen (O_2) and argon (Ar) may be considered to be non-interacting gases. However, other gases may show some interaction, and carbon dioxide (CO_2), ethylene (C_2H_4), propylene, etc.

are considered to be interacting gases.

Table V.5   Critical temperature T_c and the solubility coefficient S of various gases in natural rubber [17]

gas	T_c (K)	S ($cm^3\ cm^{-3}\ cmHg^{-1}$)
H_2	33.3	0.0005
N_2	126.1	0.0010
O_2	154.4	0.0015
CH_4	190.7	0.0035
CO_2	304.2	0.0120

The main parameter that determines the solubility is the ease of condensation, with molecules becoming more condensable with increasing diameter. The critical temperature T_c is a measure of the ease of condensation. Figure V - 16 illustrates a series of P-V isotherms for a given gas. Below a certain temperature (the critical temperature T_c) the gas can be liquefied, simply by increasing the pressure. Under these circumstances the volume is reduced and the molecules are compressed so close together that condensation occurs.
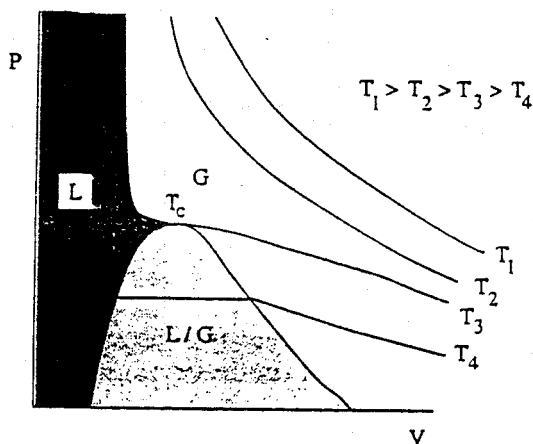
Figure V - 16. The P-V isotherms for a gas at various temperatures. The two-phase region is indicated as L/G with the shaded area corresponding to the liquid state. The critical temperature is denoted as T_c.

Table V.5 lists the critical temperature T_c of various gases together with the solubility of these gases in natural rubber. Both the critical temperature and the solubility of the gas in the polymer increase as the molecular dimensions increase. This is shown as well in figure
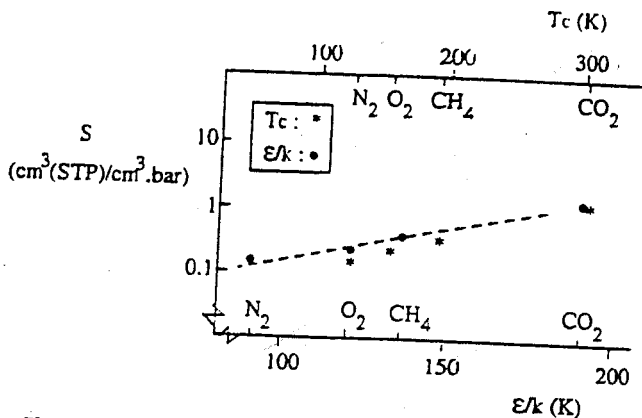
Figure V - 17. Solubility of various inert gases in silicone rubber (PDMS) as a function of critical temperarature (T_c) and Lennard-Jones potential (ε/k)

V - 17 where the solubility of oxygen, nitrogen. methane and carbon dioxide in silicon rubber are given as a function of the critical temperature and the Lennard-Jones (12,6) potential. Both parameters, the Lennard-Jones 12-6 potential, ε/k, and the critical temperature, Tc, describe adequately solubilities of non-interactive gases in polymers. The permeability of various gases in natural rubber is listed in figure V - 18, which indicates that smaller molecules do not automatically permeate faster than larger molecules. The high permeability of smaller molecules such as hydrogen and helium arises from their high diffusivity whereas a larger molecule such as carbon dioxide is highly permeable because
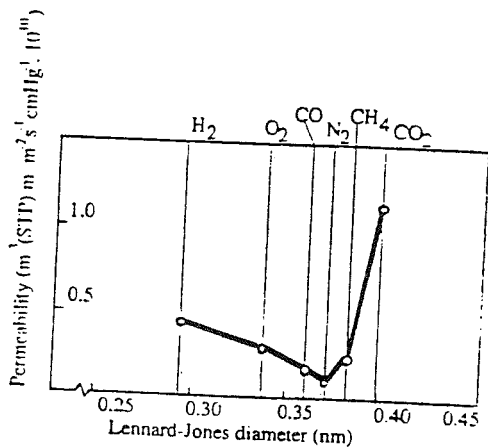
Figure V - 18. Permeability of various gases in natural rubber [18].
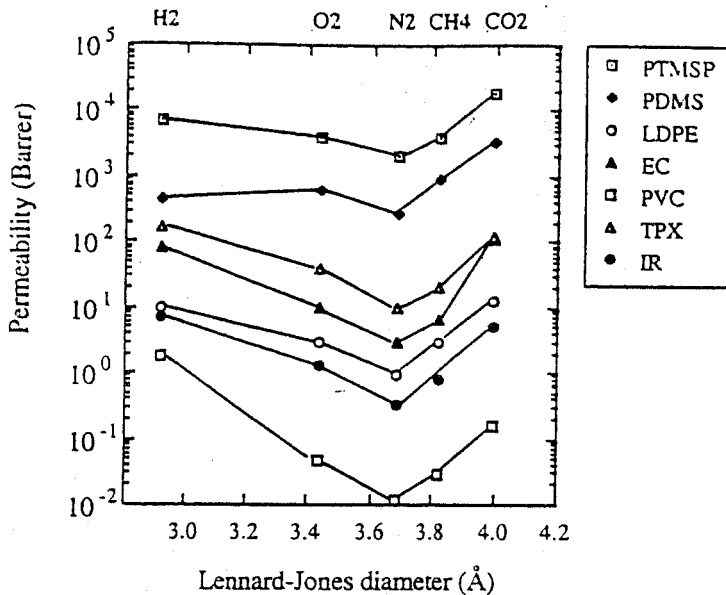
Figure V - 19. The permeability of various gases different polymers [18]. PTMSP: polytrimethylsilylpropyne; PDMS: polydimethylsiloxane; LDPE: low density polyethylene; EC: ethyl cellulose; PVC: poly(vinyl chloride); TPX: polymethylpentene; IR: polyisoprene.

of its (relatively) high solubility. The low permeability of nitrogen may be attributed to both a low diffusivity and a low solubility. Although one might expect the permeability to be strongly dependent on the nature of the polymer, the behaviour demonstrated in figures V - 16 and V - 18 is characteristic for most polymers, for highly permeable rubbery polymers as well as for low permeability glassy polymers.

V.5.1.1   Determination of the diffusion coefficient

The diffusion coefficient is constant for ideal systems as discussed here and can be determined by a permeation method, i.e. the time-lag method. If the membrane is free of penetrant at the start of the experiment the amount of penetrant (Q_t) passing through the membrane in the time t is given by [19]

$$\frac{Q_t}{\ell\, c_i} = \frac{D\, t}{\ell^2} - \frac{1}{6} - \frac{2}{\pi} \sum \frac{(-1)^n}{n^2} \exp\left[\frac{-D\, n^2\, \pi^2\, t}{\ell^2}\right]$$

$$(V - 110)$$

where c_i is the concentration on the feed side and n is an integer. A curved plot can be observed initially in the transient state but this becomes linear with time as steady-state conditions are attained (see figure V - 20). When $t \Rightarrow \infty$, the exponential term in eq. V - 110 can be neglected and it simplifies to:

$$Q_t = \frac{D \, c_i}{\ell} \left(t - \frac{\ell^2}{6 \, D} \right)$$

(V - 111)

If the linear plot of $Q_t / (\ell.c_i)$ versus t is extrapolated to the time axis, the resulting intercept, θ, is called the time lag, i.e.

$$\theta = \frac{\ell^2}{6 \, D}$$

(V - 112)

Instead of measuring a flow, the increment of the permeate pressure (p_2) can be monitored as well. In this way the time-lag can be obtained from a p_2 versus time plot.

The time-lag method is very suitable for studying ideal systems with a constant diffusion coefficient. The permeability coefficient P can be obtained from the steady-state part of this permeation experiment (eq. V - 106), which means that both the diffusion coefficient and the permeability coefficient can be determined from one experiment. More
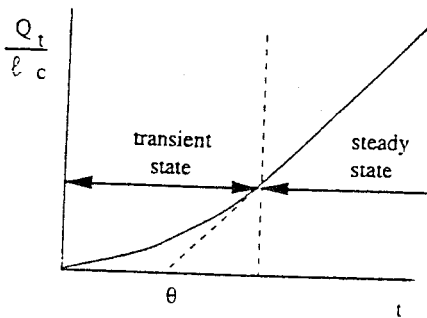
Figure V - 20. Time-lag measurement of gas permeation.

complex relationships for the time-lag must be used in concentration dependent systems [20].

V.5.1.2 Determination of the solubility coefficient

Once the diffusion coefficient D and the permeability coefficient P have been determined the solubility coefficient is known as well from the ratio P over D (see eq. V - 80).

However, various techniques can be employed to determine the solubility coefficient directly. i.e gravimetrically using a microbalance or quartz spring or by a pressure decay method. The pressure decay method has some preference due to a high accuracy [21] and can be employed in a single and dual volume concept (see figure V - 21). The concept is the same for both.
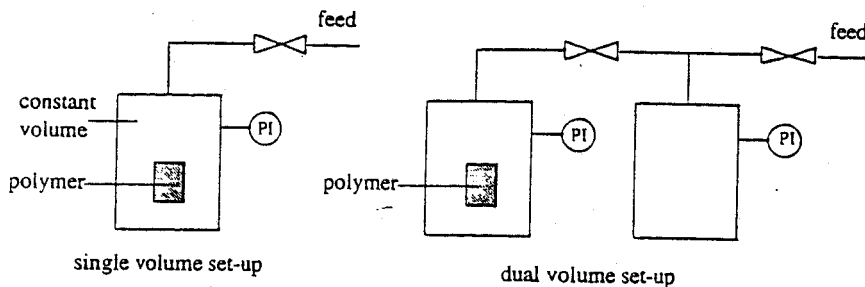
Figure V - 21.   Schematic drawing of a single volume and a dual volume pressure decay set-up

A polymer sample has been applied in a closed, constant volume. The volume has been evacuated for a certain period to remove present interfering molecules and then a gas is applied at a certain pressure. Due to sorption of the gas in the polymer the pressure decreases in time until equilibrium has been reached and the amount of penetrant inside polymer can now be calculated. From the sorption experiments an effective diffusion coefficient can be determined as well. By plotting the ratio of mass uptake at time t (M_t) over the mass uptake at infinite time (M_∞) versus the square root of time, the diffusion
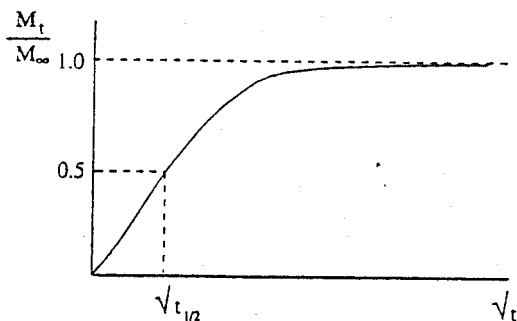
Figure V - 22.   Sorption isotherm or relative mass uptake versus time

coefficient can be obtained from the slope according to equation V - 113 [22].

$$\frac{M_t}{M_\infty} = \frac{4}{\gamma\pi} \sqrt{\frac{Dt}{\ell^2}}$$

(V - 113)

or

$$D = \frac{0.049}{t_{1/2}/\ell^2}$$

(V - 114)

V . 5.1.3   Effect of temperature on the permeability coefficient

Transport through dense films may be considered as an activated process which can usually be represented by an Arrhenius type of equation. This implies that the temperature may have a large effect on the transport rate. The following equation expresses the temperature dependence of the permeability coefficient.

$$P = P_0 \exp(-E_P/RT)$$

(V - 115)

It can be seen that the energy of activation is more or less the same for the various gases in polyethylene and is about between 35 and 45 kJ/mol. Since the permeability coefficient depends both solubility and diffusivity both parameters must be involved to understand the temperature effect. For the solubility of non interactive gases in polymers a similar Arrhenius equation expresses the temperature effect.

$$S = S_0 \exp(-\Delta H_s/RT)$$

(V - 116)
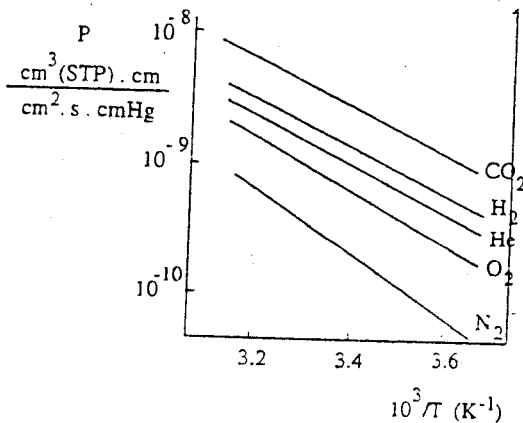
Figure   V - 23. Temperature dependence of the permeability coefficient of non interactive gases in polyethylene [23]

ΔH_s is the heat of solution and S_o is a temperature independent constant. The heat of solution which contains both a heat of mixing term and a heat of condensation can be either positive (endothermic) or negative (exothermic). For small non interactive gases such as nitrogen, helium, methane or hydrogen this heat of solution term has a small positive value which indicates that the solubility increases slightly with increasing temperature. For large molecules such as organic vapours the situation is much more complex. Here, the heat of sorption is negative and the solubility decreases with increasing temperature.

A similar temperature effect can be observed for the diffusion of gases in a polymer. The process can be considered as a thermally activated process and also the diffusion coefficient follows an Arrhenius behaviour

$$D = D_o \exp(-E_d/RT) \qquad\qquad (V - 117)$$

with E_d being the activation energy for diffusion and D_o a temperature independent constant or a preexponential factor (D_o as given here incaution should not be confused with D_o in equation which represents the diffusion coefficient at zero concentration). This equation holds for the simple non-interactive gases, for the large interactive organic vapours the diffusion coefficient is not a constant but concentration dependent and also the temperature dependency is quite complex.

Combination of eq V - 88 with V - 116 and V - 117 gives equation V - 115.

$$P = D_o S_o \exp\left(-\frac{\Delta H_r + E_d}{RT}\right) = P_o \exp\left(-\frac{E_p}{RT}\right) \qquad\qquad (V - 115)$$

For small noninteractive gases the temperature effect of the permeability coefficient is more determined by diffusion since the solubility does change so much with temperature. In this case permeability and diffusivity dependence are about the same. For the larger molecules the situation is more complex since two effects diffusion and solubility are opposing. Furthermore, both parameters are concentration dependent and should be considered from component to component.

A very interesting phenomenon can be observed by comparing the values of the activation energy of permeation in elastomeric and glassy polymers. A famous example is polyvinyl acetate with a glass transition temperature of 29°C [24]. This T_g value allows permeability measurements above and below the glass transition temperature, i.e. in the rubbery state and the elastomeric state. A schematic drawing is given in figure V - 24 and from the slopes it can be seen that the activation energy for permeation is higher in the elastomeric region than in the glassy region, despite much more segmental mobility and rotational freedom in the rubbery phase. This example indicates that values for activation energy can not be related explicitly to the ease of permeation.
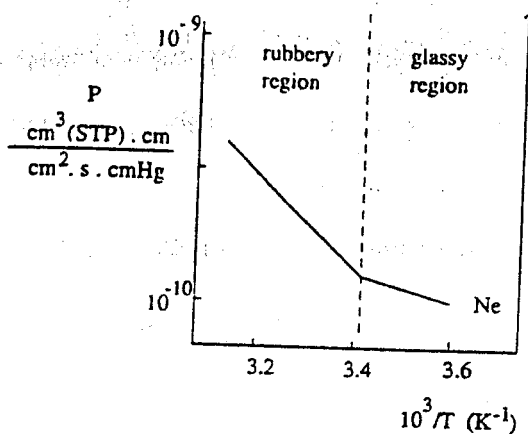
Figure V - 24. Temperature dependence of the permeability of neon in polyvinylacetate [24]

V.5.2 Interactive systems

If only the size of the molecules is considered, it might be expected that large organic molecules in the vapour state would have low permeability coefficients compared to simple gases.
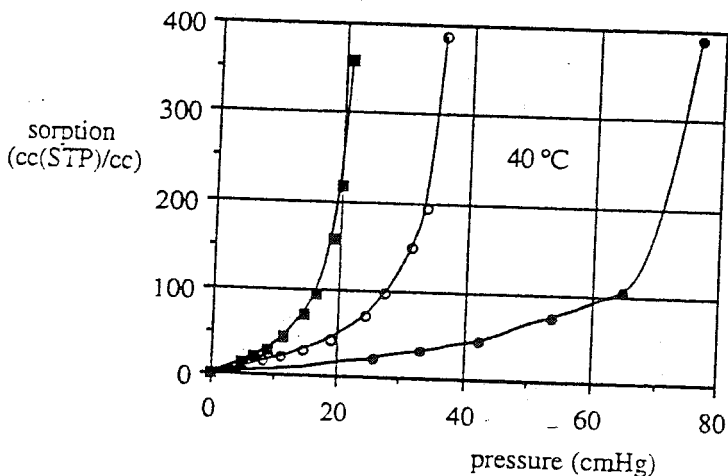
Figure V - 25. Solubility of dichloromethane (●), trichloromethane (o) and tetrachloromethane (■) in polydimethylsiloxane as a function of the vapour pressure [25].

The permeability coefficients of various components in polydimethylsiloxane (PDMS) [25] listed in Table V.6 clearly indicate that the permeabilities of large organic molecules such as toluene or trichloroethylene can be 4 to 5 orders of magnitude higher than those of small molecules such as nitrogen. These large differences in permeability arise from differences in interaction and consequently in solubility. Higher solubility increases segmental motion and hence the free volume is increased. Furthermore since the solubility is non-ideal, this means that the solubility coefficient is a function of concentration (or activity). Since high solubilities occur in glassy as well as in rubbery polymers, the diffusion coefficients are also concentration-dependent in such a way that the diffusivities increase with increasing penetrant concentration. For such non-ideal systems, the main difference with ideal systems is that solubility can no longer be described by Henry's law and the diffusion coefficient is not a constant.

Table V.6. Permeabilities of various components in
polydimethylsiloxane at 40°C [25]

Component	Permeability (Barrer)
nitrogen	280
oxygen	600
methane	940
carbon dioxide	3200
ethanol	53,000
methylene chloride	193,000
1,2-dichloroethane	269,000
carbon tetrachloride	290,000
chloroform	329,000
1,1,2-trichloroethane	530,000
trichloroethylene	740,000
toluene	1,106,000

Information on non-ideal or concentration-dependent solubility coefficients can be obtained from sorption isotherms. Figure V - 25 depicts the solubility of dichloromethane (CH_2Cl_2), trichloromethane $(CHCl_3)$ and tetrachloromethane (CCl_4) in polydimethylsiloxane (PDMS) as a function of the vapour pressure [25]. The curves obtained indicate that no linear relationships exists between concentration and pressure, so that Henry's law no longer applies to systems exhibiting strong interactions. The solubility coefficient deviates quite strongly from ideal behaviour especially at high activities.

A convenient method of describing the solubility of organic vapours and liquids in polymers is via Flory-Huggins thermodynamics [11], a detailed description having already

been given in chapter III. The activity of the penetrant inside the polymer is given by

$$\ln a_i = \ln\left(\frac{p_i}{p^o}\right) = \ln \phi_i + \left(1 - \frac{V_i}{V_p}\right)\phi_p + \chi \ \phi_p^2$$

(V - 118)

where χ is the interaction parameter. When this parameter is large ($\chi > 2$) the interaction are small, but strong interactions exist for small values ($0.5 < \chi < 2.0$) and high permeabilities may be expected (Under some circumstances $\chi < 0.5$, but the polymer must be crosslinked in these cases). The diffusion coefficient is concentration dependent. However, no unique relationship exists for the concentration dependence of the diffusion coefficient, because it varies from polymer to polymer and from penetrant to penetrant and an empirical exponential relationship is often used, i.e.

$$D = D_o \ \exp(\gamma \cdot \phi)$$

(V - 119)

Here, D_o is the diffusion coefficient at zero concentration, ϕ the volume fraction of the penetrant and γ is an exponential constant. D_o can be related to the molecular size , i.e., D_o is relatively large for small molecules (water) and small for large molecules (benzene), see table V.7.

Table V. 7   Effect of penetrant size on D_o in poly(vinyl acetate) [26]

	V_m (cm^3/mole)	D_o (cm^2/s)
water	18	1.2 10^{-7}
ethanol	41	1.5 10^{-9}
propanol	76	2.1 10^{-12}
benzene	91	4.8 10^{-13}

However, the diffusivity is influenced to a much greater extent by the factor γ and the volume fraction of penetrant within the membrane, because both these terms appear in the exponent. The quantity γ can be considered as a plasticising constant indicating the plasticising action of the penetrant on segmental motion (It may even occur that the penetrant acts as an anti-plasticiser that decreases the permeability but this is very exceptional and will not be considered further). For simple gases which hardly show any interaction with the polymer, $\gamma \Rightarrow 0$, and eq. V - 119 reduces to a constant diffusion coefficient.

The concentration dependence of the diffusion coefficient can be described adequately by the free volume theory [10], which assumes that the introduction of a penetrant increases the free volume of the polymer. It is shown in the following section that this theory may also lead to a relationship between log D and the volume fraction of the

penetrant in the polymer which is similar to eq. V - 119.

V.5.2.1   *Free volume theory*

A simple way of expressing the concentration dependence of the diffusion coefficient has been given above in eq. V - 119. A more quantitative approach is based on the free volume theory.

It was shown in chapter II that a large difference in permeability often depends on whether a polymer is in the glassy or rubbery state. In the glassy state, the mobility of the chain segments is extremely limited and the thermal energy too small to allow rotation around the main chain. Only a few segments have sufficient energy for mobility although some mobility can occur in the side groups.
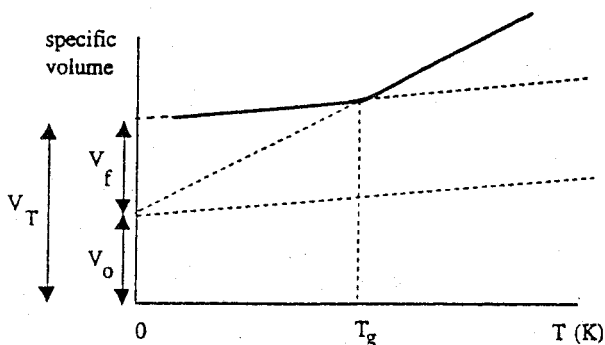
Figure V - 26. Specific volume of an amorphous polymer as a function of the temperature.

Above the glass transition temperature, i.e. in the rubbery state, the mobility of the chain segments is increased and 'frozen' microvoids no longer exist. A number of physical parameters change at the glass transition temperature and one of these is the density or specific volume. This is shown in figure V - 26 where the specific volume of an amorphous polymer has been plotted as a function of the temperature.

The free volume V_f may be defined as the volume generated by thermal expansion of the initially closed-packed molecules at 0 K.

$$V_f = V_T - V_o \qquad\qquad\qquad (V - 120)$$

where V_T is the observed volume at a temperature T and V_o is the volume occupied by the molecules at 0 K. The fractional free volume v_f is defined as the ratio of the free volume (V_f) to the observed volume (V_T), i.e.

$$v_f = \frac{V_f}{V_T}$$

$$\text{(V - 121)}$$

The observed or specific volume at a particular temperature can be obtained from the polymer density whereas the volume occupied at 0 K can be estimated from group contribution [27,28].

Using the free volume concept based on viscosity, a fractional free volume $v_f \approx 0.025$ has been found for a number of glassy polymers and this value is now considered to be a constant ($v_f \approx v_{f,Tg}$). Above T_g, the free volume increases linearly with temperature according to

$$v_f = v_{f,Tg} + \Delta\alpha \, (T - T_g)$$

$$\text{(V - 122)}$$

where $\Delta\alpha$ is the difference between the value of the thermal expansion coefficient above T_g and below T_g.

Simha and Boyer [29] have used the free volume concept to describe glass transition temperatures and they have derived a value of $v_f = 0.11$, which is far higher than that quoted above. However, these two values should be considered to be quite genuine, not only because they differ by so much but because in the case of diffusion not all the free volume is available for transport.

The free volume approach is very useful for describing and understanding transport of small molecules through polymers. The basic concept is that a molecule can only diffuse from one place to another place if there is sufficient empty space or free volume. If the size of the penetrant increases, the amount of free volume must also increase. The probability of finding a 'hole' whose size exceeds a critical value is proportional to $\exp(-B/v_f)$, where B expresses the local free volume needed for a given penetrant and v_f is the fractional free volume. The mobility of a given penetrant depends on the probability of it finding a hole of sufficient size that allows its displacement. This mobility can be related to the thermodynamic diffusion coefficient (see eq. V - 100), which in turn is related to the exponential factor according to [11]:

$$D_T = R T A_f \exp\left(- \frac{B}{v_f}\right)$$

$$\text{(V - 123)}$$

A_f is dependent on the size and the shape of the penetrant molecules while B is related to the minimum local free volume necessary to allow a displacement. Eq. V - 123 shows that the diffusion coefficient increases with increasing temperature, and also that the diffusion coefficient decreases as the size of the penetrant molecule increases, since B increases.

In the case of non-interacting systems (polymer with 'inert' gases such as helium, hydrogen, oxygen, nitrogen or argon), the polymer morphology is not influenced by the presence of these gases which means that there is no extra contribution towards the free volume. For such systems eq. V - 123 predicts a straight line when lnD is plotted versus

the reciprocal of the fractional free volume (v_f)$^{-1}$, assuming that A_f and B are independent of the polymer type. Such behaviour has been observed for a number of systems [30 - 32] which suggests that the diffusivity of a given (non-interacting) gas molecule can be determined from density measurements alone when a lnD versus (v_f)$^{-1}$ plot is available. Because of its simplicity this approach is very useful. However, recent data obtained for polyimides deviate from this linear behaviour [33,34], which suggests that the assumptions behind eq. V - 123 are not completely correct and that A_f and B may be a function of the polymer type or that polymer-dependent parameters need to be incorporated in the equation. A more sophisticated approach to free volume theory has been given by Vrentas and Duda [36,37], but their theory contains a number of other parameters that have to be determined from experiments.

So far only non-interacting systems with $v_f = f(T)$ have been considered. However, in interacting systems (e.g organic vapours) the free volume is a function of the temperature and the penetrant concentration [$v_f = f(\phi,T)$]. Under these circumstances the free volume will increase if the penetrant concentration increases and if additivity is assumed then

$$v_f(\phi,T) = v_f(0,T) + \beta(T) \; \phi \qquad\qquad (V - 124)$$

where $v_f(0,T)$ is the free volume of the polymer at temperature T in the absence of penetrant and ϕ is the volume fraction of penetrant. The quantity $\beta(T)$ is a constant characterising the extent to which the penetrant contributes to the free volume.

According to eq. V - 123, the diffusion coefficient at zero penetrant concentration $D_{c \to 0}$ or D_0 is given by

$$D_0 = R\,T\,A_f \exp\left(- \frac{B}{v_f(0,T)}\right) \qquad\qquad (V - 125)$$

Combination of eqs. V - 123 and V - 125 gives

$$\ln \frac{D_T}{D_0} = \frac{B}{v_f(0,T)} - \frac{B}{v_f(\phi,T)} \qquad\qquad (V - 126)$$

or

$$\left[\ln \left(\frac{D_T}{D_0}\right)\right]^{-1} = \frac{v_f(0,T)}{B} + \frac{v_f(0,T)^2}{\beta(T)\,B\,\phi} \qquad\qquad (V - 127)$$

This relationship shows that $[\ln (D_T/D_0)]^{-1}$ is related linearly to ϕ^{-1}. This has been confirmed for several systems [10].

The empirical exponential relationship (eq.V - 104) and the relationship derived from free volume theory (eq.V - 127) are similar when $v_f(0,T) \gg \beta(T) \; \phi$, implying that

plots of lnD versus φ should be linear. This behaviour has been observed for a number of systems [10]. Deviations from linearity mean that the empirical relationship (eq.V - 123) may not be suitable and that a more sophisticated approach towards free volume may give better results [35,36].

For gas molecules it has been assumed that solubility may be described via Henry's law, i.e. the solubility of a gas in a polymer is related linearly to the external pressure. Henry's law does not apply to organic vapours and liquids and the concentration inside the polymer under these circumstances can best be described by Flory-Huggins thermodynamics (see eq. V - 118).

The relationship between the measured diffusion coefficient D and the thermodynamic diffusion coefficient D_T is

$$D_i = D_T \frac{d\ln a_i}{d\ln \phi_i}$$

(V - 128)

the differences between the two diffusion coefficients increasing at larger penetrant concentrations. The factor ($d\ln a_i / d\ln \phi_i$) can be obtained by differentiation of eq. V - 118 with respect to $\ln \phi_i$

$$\frac{d\ln a_i}{d\ln \phi_i} = 1 - \left(2\chi + 1 - \frac{V_i}{V_p}\right)\phi + 2\chi \phi^2$$

(V - 129)

The thermodynamic diffusion coefficient is equal to the observed diffusion coefficient only for ideal systems and at low volume fractions; $\phi_i \longrightarrow 0$ giving $d\ln a_i / d\ln \phi_i \longrightarrow 1$ and $D = D_T$.

V . 5.2.2   *Clustering*

The free volume approach also gives very satisfactory results for interacting systems. Deviations may be caused by clustering of the penetrant molecules, i.e. the component diffuses not as a single molecule but in its dimeric or trimeric form. This implies that the size of the diffusing components increases and that the diffusion coefficient consequently decreases. For example, water molecules experience strong hydrogen bonding which means that 'free' water molecules may diffuse accompanied by clustered (dimeric, trimeric) molecules. The extent of clustering will also depend on the type of polymer and other penetrant molecules present.

The clustering ability may be described by the Zimm-Lundberg theory [37]. The the following equation (the cluster function) has been derived, which gives an indication of the ability or probability of molecules to cluster inside a membrane. In cases where this occurs this will have a large effect on the transport properties since a clustering of molecules will show a much lower mobility than the corresponding free molecules. The presence of clustered components can be determined with help of the cluster integral G_{11}:

$$\frac{G_{11}}{V_1} = \left(\frac{1}{\phi_1} - 1\right)\left(\frac{\partial \ln\phi_1}{\partial \ln a_1}\right) - \frac{1}{\phi_1}$$

(V - 130)

where V_1 and ϕ_1 are the molar volume and volume fraction of penetrant, respectively. For ideal systems $\partial \ln\phi/\partial \ln a = 1$, which implicates that $G_{11}/V_1 = -1$, and no clustering occurs. When $G_{11}/V_1 > -1$, clustering will occur.

V.5.2.3   Solubility of liquid mixtures

The thermodynamics of polymeric systems have already been described in detail in chapter III, where it was shown that a basic difference exists between a ternary system (a binary liquid mixture and a polymer) and a binary system (polymer and liquid). In the former case not only the amount of liquid inside the polymer (overall sorption) is an important parameter but the composition of the liquid mixture inside the polymer is especially so. This latter value, the preferential sorption, represents the sorption selectivity.

Figure V - 27 provides a schematic drawing of a binary liquid feed mixture (volume fractions v_1 and v_2) in equilibrium with a polymeric membrane (volume fractions ϕ_1, ϕ_2 and ϕ_3). The concentration of a given component i in the binary liquid mixture in the ternary polymeric phase is given by:
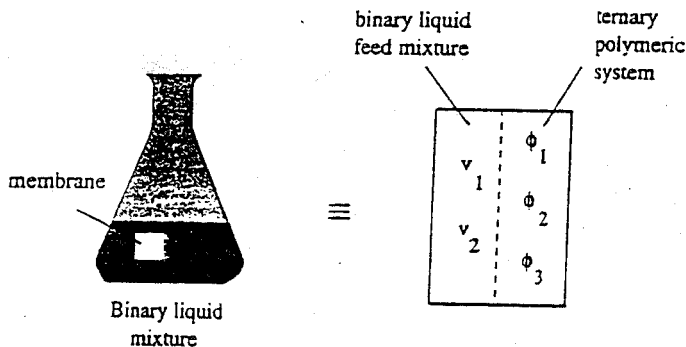

Figure   V - 27.   Schematic drawing of a binary liquid feed mixture in equilibrium with the polymeric membrane.

$$u_i = \frac{\phi_i}{\phi_1 + \phi_2} = \frac{\phi_i}{1 - \phi_3} \qquad i = 1,2$$

(V - 131)

The preferential sorption is then given by

$$\varepsilon = u_i - v_i \qquad\qquad i = 1,2 \tag{V - 132}$$

and the condition for equilibrium between the binary liquid phase and ternary polymeric phase is given by equality of the chemical potentials in the two phases. If the polymer free phase is denoted with the subscript f (feed) and the ternary phase with the subscript m (membrane), then

$$\Delta\mu_{f,i} = \Delta\mu_{m,i} + \pi \; V_i \qquad\qquad i = 1,2 \tag{V - 133}$$

Expressions for the chemical potentials are given by Flory-Huggins thermodynamics [11] (see chapter III). When $V_1/V_3 \approx V_2/V_3 \approx 0$ and $V_1/V_2 = m$, using concentration-independent Flory-Huggins interaction parameters and eliminating π gives [38];

$$\ln\left(\frac{\phi_1}{\phi_2}\right) - \ln\left(\frac{v_1}{v_2}\right) = (m - 1)\,\ln\frac{\phi_2}{v_2} - \chi_{12}\left(\phi_2 - \phi_1\right) - \chi_{12}\left(v_1 - v_2\right) - \phi_3\left(\chi_{13} - m\,\chi_{23}\right) \tag{V - 134}$$

This equation, which gives the composition of the liquid mixture inside the membrane, can be solved numerically when the interaction parameters and volume fraction of the polymer are known.

However, Flory-Huggins interaction parameters for these systems are generally concentration-dependent and this leads to a much more complex expression which also contains the partial derivatives of the interaction parameters relative to concentration. For the sake of simplicity we will follow the approach given in eq. V - 134. When the sorption selectivity α_{sorp} is defined as

$$\alpha_{sorp} = \frac{\left(\phi_1 / \phi_2\right)}{\left(v_1 / v_2\right)} \tag{V - 135}$$

then the left-hand side of eq. V - 121 becomes equal to the logarithm of the sorption selectivity. The following factors, which are important with respect to preferential sorption, can be deduced from eq. V - 134, i.e.
- the difference in molar volume
If only entropy effects are considered the component with the smaller molar volume will be sorbed preferentially. Indeed, this factor makes a considerable contribution towards the preferential sorption of water in many systems. The effect increases with increasing polymer concentration and reaches maximum value when $\phi_3 \Rightarrow 1$. Table V.8 lists some

values of molar volumes (With liquid mixtures it is better to speak of partial molar volumes but here volume changes upon mixing are neglected.)

Table V. 8. Ratio of molar volumes at 25°C of
various organic solvents with water
($V_1 = 18$ cm^3/mol)

solvent	V_1/V_2
methanol	0.44
ethanol	0.31
propanol	0.24
butanol	0.20
dioxane	0.21
acetone	0.24
acetic acid	0.31
DMF	0.23

- the affinity towards the polymer

In terms of the enthalpy of mixing, the component with the highest affinity to the polymer will make a positive contribution towards preferential sorption. When ideal sorption is assumed, this factor only influences the solubility, i.e. the highest affinity leads to the highest solubility.

- mutual interaction

The influence of mutual interaction with the binary liquid mixture on preferential sorption depends on the concentration in the binary liquid feed and on the value of χ_{12}. For organic liquids this parameter varies quite considerably with composition and in these cases the constant interaction parameter χ_{12} should be replaced by a concentration-dependent interaction parameter g_{12} (ϕ). Some examples of the concentration dependence of this parameter have been given already in chapter III (fig. III - 28). Because of large variations in composition, preferential sorption will vary accordingly.

The preferential sorption of many systems has been studied and it has been shown that for many different polymeric materials with a wide variety of different liquid mixtures that the component which is preferentially sorbed also permeates preferentially [39].

V.5.2.4 *Transport of single liquids*

Concentration-dependent systems can also be described by Fick's law using concentration-dependent diffusion coefficients. The following empirical relationship is often used.

$$D_i = D_{0,i} \exp(\gamma_i \cdot c_i) \qquad\qquad (V - 136)$$

where $D_{0,i}$ is the diffusion coefficient at $c_i \Rightarrow 0$ and γ is a plasticising constant expressing the influence of the plasticising action of the liquid on the segmental motions. Substitution of eq. VI - 136 into Fick's law and integration across the membrane using the boundary conditions

$$c_i = c_{i,1}{}^m \qquad \text{at} \quad x = 0$$
$$c_i = 0 \qquad\quad \text{at} \quad x = \ell$$

yields the following equation:

$$J_i = \frac{D_{0,i}}{\gamma\,\ell} \exp(\gamma\, c_{i,1}{}^m - 1) \qquad\qquad (V - 137)$$

This represents the flux of a pure liquid through a membrane, and indicates which parameters determine the flux: $D_{0,i}$, γ and ℓ are constants and the main parameter is the concentration inside the membrane $(c_{i,1}{}^m)$. As this concentration increases so the permeation rate increases. This implies that the permeation rate for single liquid transport is determined mainly by the interaction between the polymeric membrane and the penetrant. For a given penetrant, the flux through a particular polymeric membrane will increase if the affinity between the penetrant and the polymer increases.

V.5.2.5 Transport of liquid mixtures

The transport of liquid mixtures through a polymeric membrane is generally much more complex than that of a single liquid. For a binary liquid mixture, the flux can also be described in terms of the solubility and the diffusivity, such that they may influence each other strongly.

Two phenomena must be distinguished in multi-component transport: i) flow coupling and ii) thermodynamic interaction. Flow coupling may be described via non-equilibrium thermodynamics (see earlier in this chapter), the following equations being obtained for a binary liquid mixture:

$$- J_i = L_{ii}\, d\mu_i/dx + L_{ij}\, d\mu_j/dx \qquad\qquad (V - 15)$$

$$- J_j = L_{ji}\, d\mu_i/dx + L_{jj}\, d\mu_j/dx \qquad\qquad (V - 16)$$

The first term on the right-hand side of eq. VI - 15 describes the flux of component i due to its own gradient while the second term describes the flux of component i due to the gradient of component j. This second term also represents the coupling effect. If no coupling occurs ($L_{ij} = L_{ji} = 0$), the flux equations reduce to simple linear relationships.

These linear relationships assume that the components permeate through the membrane independently of each other. This is not generally the case as can be simply demonstrated by comparing the pure component data with those of the mixture. It is even possible for a component with a very low permeability, e.g. water in polysulfone shows a much higher permeability in the presence of a second component, e.g. ethanol. This second component has a much higher affinity towards the polymer and consequently a higher (overall) solubility is obtained which allows water permeation.

Coupling phenomena are difficult to describe, predict or even to measure quantitatively. However, when thermodynamic interactions (or preferential sorption) are considered in relation to selective transport, it is possible to obtain indirect information about flow coupling.

V.5.3   The effect of crystallinity

A large number of polymers are semi-crystalline, i.e. they contain an amorphous and a crystalline fraction. The presence of crystallites may strongly influence membrane performance with regard to both the transport of gases and liquids. If the diffusion takes place primarily in the amorphous regions and if the crystallites are considered to be impermeable, the amount of crystallinity directly influences the diffusion rate and hence the flux.

The diffusion coefficient can be described as a function of the crystallinity in the following manner [40]:

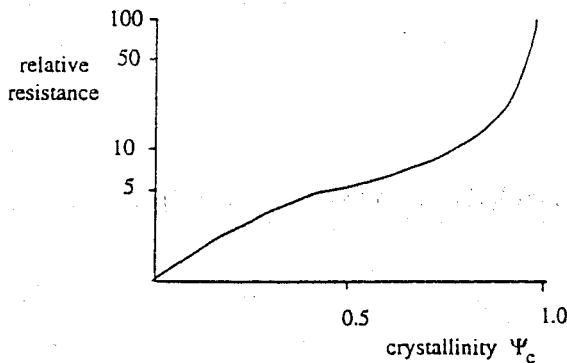$$D_i = D_{i,o} \left(\frac{\psi_c^{\,n}}{B} \right) \qquad\qquad (V - 138)$$

Figure V - 28.   The effect of crystallinity on diffusion resistance [40].

where Ψ_c is the fraction of crystalline material present, B is a constant and n an exponential factor (n < 1). Diffusion resistance as a function of the crystallinity is depicted in figure V - 28. This figure shows that low amounts of crystallinity ($\Psi_c < 0.1$) have little influence on diffusion resistance, but as crystallinity increases the resistance may become very high. However, in most membranes the crystallinity is quite low and consequently, the effect of crystallinity on the permeation rate is often fairly small.

V.6. Transport through membranes. A unified approach.

A number of 'macroscopic' models have been given in the preceding paragraphs in an attempt describe the large differences in the separation principles involved in various membrane processes and membranes, with the extremes being observed for porous membranes (microfiltration/ultrafiltration) and nonporous membranes (gas separation/pervaporation). The model descriptions can be classified as those based on a phenomenological approach and on non-equilibrium thermodynamics, and those mechanistic models such as the pore model and the solution-diffusion model. The phenomenological models are so-called 'black-box' models and provide no information as to how the separation actually occurs. Mechanistic models try to relate separation with structural-related membrane parameters in an attempt to describe mixtures. These latter models also provide information on how separation actually occurs and which factors are important.

We shall try to cover all the membrane processes within one model at the end of this chapter, in order to relate the various membrane processes with each other in terms of driving forces, fluxes and basic separation principles. To do so, the starting point must be a simple model, such as a generalised Fick equation [41] or a generalised Stefan-Maxwell equation [42]. In order to describe transport through a porous membrane or through a nonporous membrane, two contributions must be taken into account, the diffusional flow (v) and the convective flow (u). The flux of component i through a membrane can be described as the product of velocity and concentration, i.e.

$$J_i = c_i (v_i + u) \qquad\qquad (V - 139)$$

The contribution of convective flow is the main term in any description of transport through porous membranes. In nonporous membranes, however, the convective flow term can be neglected and only diffusional flow contributes to transport. It can be shown by simple calculations that only convective flow contributes to transport in the case of porous membranes (microfiltration). Thus, for a membrane with a thickness of 100 μm, an average pore diameter of 0.1 μm, a tortuosity τ of 1 (capillary membrane) and a porosity ε of 0.6, water flow at 1 bar pressure difference can be calculated from the Poisseuille equation (convective flow), i.e.

$$J_w = \frac{\varepsilon \, r^2}{8 \, \eta \, \tau} \frac{\Delta P}{\Delta x} \approx \frac{0.6 \; 0.25 \; (10^{-7})^2 \; 10^5}{8 \; 10^{-3} \; 10^{-4}} \approx 2 \; 10^{-3} \; m/s$$

The driving force for diffusion is the difference in chemical potential, and both the concentration (activity) and the pressure contribute to this driving force. However, it can be assumed that the 'concentration' (or activity) on either side of the membrane is equal in microfiltration and hence the pressure difference must be the only driving force. Indeed, diffusive water flow as a result of this driving force is very small, as can be demonstrated as follows. The chemical potential difference can be written as:

$$J_i = u = k \cdot \Delta P$$

porous
membrane

$$J_i = c_i \, (v_i + u)$$

membrane

$$J_i = c_i \, v_i$$

nonporous
membrane
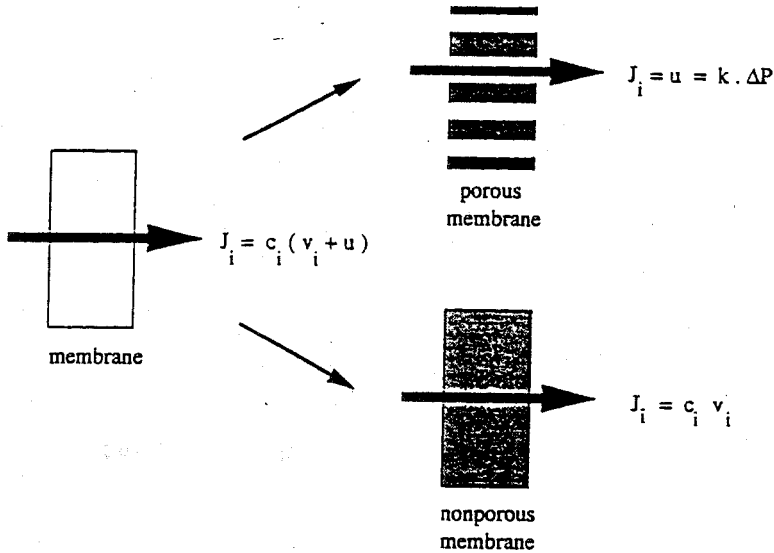
Figure V - 29.   Convective and diffusive flow in a porous and a nonporous membrane.

$$\Delta \mu_w = v_w \cdot \Delta p = 1.8. \; 10^{-5}. \; 10^5 = 1.8 \; J/mol$$

$$J_w = L_p \frac{d\mu}{dx} \approx \frac{D_w}{R\,T} \frac{\Delta \mu_w}{\Delta x} = \frac{10^{-9} \; 2}{2500 \; 10^{-4}} \approx 10^{-8} \; m/s$$

and a comparison of the value for the convective and diffusive contributions indicates quite clearly that diffusion can be neglected in this case.

Considering only the extreme cases, it can be stated that transport in porous membranes occurs by convection and in nonporous membranes by diffusion. However, in going from porous to nonporous membranes, an intermediate region exists where both

contributions have to be taken into account.

The last part of this chapter will be devoted to a comparison of membrane processes where transport occurs through nonporous membranes. A solution-diffusion model will be used where each component dissolves into the membrane and diffuses through the membrane independently [41]. A similar approach was recently followed by Wijmans [43]. As a result, simple equations will be obtained for the component fluxes involved in the various processes which allows to compare the processes in terms of transport parameters.

The flux of a component through a membrane may be described in terms of the product of the concentration and the velocity, i.e. convective flow makes no contribution (see eq. V - 139). Hence,

$$J_i = c_i. \; v_i$$

$$\text{(V - 140)}$$

The mean velocity of a component in the membrane is determined by the driving force acting on the component and the frictional resistance exerted by the membrane, i.e.

$$v_i \; = \; \frac{X_i}{f_i}$$

$$\text{(V - 141)}$$

The driving force is given by the gradient $d\mu/dx$. The frictional coefficient can be related to the thermodynamic diffusion coefficient D_T. If ideal conditions are assumed, i.e. if the thermodynamic diffusion coefficient is equal to the observed diffusion coefficient, eq. V - 140 then becomes

$$J_i \; = \; \frac{D_i \; c_i}{R \, T} \; \frac{d\mu_i}{dx}$$

$$\text{(V - 142)}$$

The chemical potential can be written as

$$\mu_i = \mu^\circ_i + \; RT \ln a_i + V_i . \; (p - p^\circ)$$

$$\text{(V - 6)}$$

and substitution of eq. V - 6 into eq. V - 142 gives

$$J_i \; = \; \frac{D_i \; c_i}{R \, T} \left[R \, T \frac{d\ln a_i}{dx} \; + \; V_i \; \frac{dP}{dx} \right]$$

$$\text{(V - 143)}$$

Figure V - 30 gives a representation of the process conditions necessary for describing transport through nonporous membranes, where the superscripts m and s refer to membrane and feed/permeate side, respectively. If it is assumed that thermodynamic equilibrium exists at the membrane interfaces, i.e. that the chemical potential of a given component (liquid or gas) at the feed/membrane interface is equal in both the feed and the membrane, and furthermore, that the pressure inside the membrane is equal to the pressure

on the feed side, the following equations may be obtained[41]:

Figure V - 30.   Process conditions for transport through nonporous membranes.

at the feed interface (phase 1/membrane):

$$\mu_{i,1}{}^m = \mu_{i,1}{}^s \;\;\Rightarrow\;\; a_{i,1}{}^m = a_{i,1}{}^s \qquad\qquad\qquad (V - 144)$$

and at the permeate interface (membrane/phase 2):

$$\mu_{i,2}{}^m \; = \; \mu_{i,2}{}^s \;\;\Rightarrow\;\; a_{i,2}{}^m \; = \; a_{i,2}{}^s \exp\left[\frac{-V_i(P_1 - P_2)}{R\,T}\right] \qquad (V - 145)$$

The activities at the feed interface can be written as

$$c_{i,1}{}^m \cdot \gamma_{i,1}{}^m = c_{i,1}{}^s \cdot \gamma_{i,1}{}^s \qquad\qquad\qquad (V - 146)$$

while the activities at the permeate interface are

$$c_{i,2}{}^m \; \gamma_{i,2}{}^m \; = \; c_{i,2}{}^s \; \gamma_{i,2}{}^s \exp\left[\frac{-V_i(P_1 - P_2)}{R\,T}\right] \qquad (V - 147)$$

If the solubility constant K_i is defined as the ratio of the activity coefficients, we can write:

$$K_{i,1} \; = \; \frac{\gamma_{i,1}{}^s}{\gamma_{i,1}{}^m} \quad \text{and} \quad K_{i,2} \; = \; \frac{\gamma_{i,2}{}^s}{\gamma_{i,2}{}^m} \qquad\qquad (V - 148)$$

or

$$c_{i,1}{}^m \; = \; K_{i,1} \cdot c_{i,1}{}^s \quad \text{and} \quad c_{i,2}{}^m \; = \; K_{i,2} \cdot c_{i,2}{}^s \qquad (V - 149)$$

Furthermore, if it is assumed that the diffusion coefficient is concentration-independent, Fick's law (eq. V - 83) can be integrated across the membrane to give

$$J_i = - \frac{D_i}{\ell} (c_{i,2}{}^m - c_{i,1}{}^m)$$

$$(V - 150)$$

After substitution of eqs. V - 146, V - 147 and V - 148 into eq. V - 150 one arrives at

$$J_i = \frac{D_i}{\ell} \left(K_{i,1} \ c_{i,1}{}^s - K_{i,2} \ c_{i,2}{}^s \exp\left[\frac{-V_i (P_1 - P_2)}{R T}\right]\right)$$

$$(V - 151)$$

and if $\alpha_i = K_{i,2} / K_{i,1}$ (i.e. the solubility coefficients are similar at both interphases) and $P_i = K_i \cdot D_i$, then eq. V - 151 converts into

$$J_i = \frac{P_i}{\ell} \left(c_{i,1}{}^s - \alpha_i \ c_{i,2}{}^s \exp\left[\frac{-V_i (P_1 - P_2)}{R T}\right]\right)$$

$$(V - 152)$$

Eq. V - 152 is the basic equation used to compare various membrane processes when transport occurs by diffusion [41]. The phases involved in such processes are summarised in table V.9.

Table V. 9. Phases involved in diffusion controlled membrane processes

Process	Phase 1	Phase 2
reverse osmosis	L	L
dialysis	L	L
gas separation	G	G
pervaporation	L	G

V.6.1   Reverse osmosis

Reverse osmosis is normally used with aqueous solutions containing a low molecular weight solute, which is often a salt. It can also be used for aqueous solutions containing very small amounts of organic solutes. This process involves the application of pressure to the liquid feed mixture as driving force, the total flux being given by the sum of the water flux J_w and the solute flux J_s. With highly selective membranes the solute flux can be neglected (in fact even with less selective membranes the solvent flux is large compared to the solute flux).

$$J_{total} = J_w + J_s \approx J_w$$

$$(V - 153)$$

since $\Delta\pi = RT/V_i \cdot (\ln c_{w,2}{}^s / c_{w,1}{}^s)$ and $\alpha_i = 1$, the water flux J_w may be written as

$$J_w = \frac{D_w \, K_w \, c_{w,1}{}^s}{\ell}\left(1 - \exp\left[\frac{-V_i\,(\,P_1 - P_2 - \Delta\pi)}{R\,T}\right]\right)$$

(V - 154)

or

$$J_w = \frac{P_w \, c_{w,1}{}^s}{\ell}\left(1 - \exp\left[\frac{-V_i\,(\,P_1 - P_2 - \Delta\pi)}{R\,T}\right]\right)$$

(V - 155)

For small values of x, the term

$$1 - \exp(-x) \approx -x$$

(V - 156)

and since

$$K_w \cdot c_{w,1}{}^s = c_{w,1}{}^m$$

(V - 157)

eq. V - 154 becomes

$$J_w = \frac{D_w \, c_{w,1}{}^m}{\ell}\left(\left[\frac{V_w\,(\,\Delta P - \Delta\pi)}{R\,T}\right]\right)$$

(V - 158)

This equation gives the water flux through a membrane as a function of the pressure difference. This equation can also be written in a simple form as:

$$J_w = A_w\,(\Delta P - \Delta\pi)$$

(V - 159)

with $A_w = D_w \cdot c_{w,1}{}^m \cdot V_w \,/\, R\,T \cdot \ell$. A_w is called the water permeability coefficient and frequently the symbol L_p is used as well. Eq. V - 159 is generally applied both for reverse osmosis and nanofiltration.

Reverse osmosis membranes are generally not completely semipermeable and a simple equation can also be derived for the solute flux. Thus from eq. V - 151, with $\alpha_j = 1$, the solute flux J_s can be written as

$$J_s = \frac{D_s \, K_s}{\ell}\left(c_{s,1}{}^s - c_{s,2}{}^s \exp\left[\frac{-V_s\,(\,P_1 - P_2 - \Delta\pi)}{R\,T}\right]\right)$$

(V - 160)

and since the exponential term is approximately unity (see section V - 6.4), eq. V - 160 becomes

$$J_s = \frac{D_s \, K_s \, \Delta c}{\ell}$$

(V - 161)

or

$$J_s = B. \Delta c$$

$$(V - 162)$$

where $B = D_s . K_s / \ell$ and is called the solute permeability coefficient. Eq. V - 162 expresses in a simple way how the solute flux in reverse osmosis is proportional to the concentration difference, whereas the water (or solvent) flux is proportional to the applied pressure or effective pressure difference (eq. V - 159).

V.6.2   Dialysis

In dialysis, liquid phases containing the same solvent are present on both sides of the membrane in the absence of a pressure difference. The pressure terms can therefore be neglected and the following equation may be obtained from eq. V - 152 if $\alpha_i = 1$.

$$J_i = \frac{P_i}{\ell} (c_{i,1}{}^s - c_{i,2}{}^s)$$

$$(V - 163)$$

or

$$J_i = \frac{P_i \Delta c}{\ell}$$

$$(V - 164)$$

This simple equation describes the solute flux in dialysis indicating that it is proportional to the concentration difference. Separation arises from differences in permeability coefficients: thus macromolecules have much lower diffusion coefficients and distribution coeffients than low molecular weight components.

V.6.3   Gas permeation

In gas permeation or vapour permeation, both the upstream and downstream sides of a membrane consist of a gas or a vapour. However, eq. V - 152 cannot be used directly for gases. The concentration of a gas in a membrane can be written as

$$c_{i,1}{}^m = p_{i,1}{}^s . K_i$$

$$(V - 165)$$

and combination of eq. V - 165 with eq. V - 150

$$J_i = \frac{P_i}{\ell} (p_{i,1}{}^s - p_{i,2}{}^s)$$

$$(V - 166)$$

where $P_i = K_i . D_i$

It can be seen from this equation that the rate of gas permeation is proportional to the partial pressure difference across the membrane. Eq. V - 166 is widely used to describe the gas or vapour flux across a membrane.

V.6.4   *Pervaporation*

Pervaporation is a membrane process in which the feed side is a liquid while the permeate side is a vapour as a result of applying a very low pressure downstream. Hence, on the downstream side $P_2 \Rightarrow 0$ (or $a_2{}^s \Rightarrow 0$) and the exponential term in eq. V - 164 is equal to unity and can be neglected ($\Delta P \approx 10^5$ N/m^2, $V_i = 10^{-4}$ m^3/mol, RT ≈ 2500 J/mol $\Rightarrow$ $\exp(-V_i.\Delta P/RT) \approx 1$). If the partial pressure is put equal to the activity, then:

$$\gamma_i{}^s . c_i{}^s = p_i \qquad\qquad (V - 167)$$

and eq. V - 165 becomes

$$J_i = \frac{P_i \; c_{i,1}{}^s}{\ell}\left(1 - \frac{p_{i,2}{}^s}{p_{i,1}{}^s}\right) \qquad\qquad (V - 168)$$

From eq. V - 168 it can be seen that when the permeate pressure ($p_{i,2}{}^s$) increases the flux of component i decreases. As the permeate pressure ($p_{i,2}{}^s$) is equal to the feed pressure($p_{i,1}{}^s$) then the flux of component i becomes zero.

V.7.   Transport in ion-exchange membranes

Reverse osmosis can be used for the separation of ions from an aqueous solution. Neutral membranes are mainly used for such processes and the transport of ions is determined by their solubility and diffusivity in the membrane (as expressed by the solute permeability coefficient, see eq. V - 162). The driving force for ion transport is the concentration difference, but if charged membranes or ion-exchange membranes are used instead of neutral membranes ion transport is also affected by the presence of the fixed charge. Teorell [45] and Meyer and Sievers [46] have used a fixed charge theory to describe ionic transport through these type of systems. This theory is based on two principles: the Nernst-Planck equation and Donnan equilibrium.

If an ion-exchange membrane in contact with an ionic solution is considered, then ions with the same charge as the fixed ions in the membrane are excluded and cannot pass through the membrane. This effect is known as Donnan exclusion and can be described by equilibrium thermodynamics which allow the chemical potential of the ionic component in the two phases present to be calculated when an ionic solution is in equilibrium with an ionic membrane. Thus, in the ionic solution itself:

$$\mu_i = \mu_i{}^\circ + RT \ln m_i + RT \ln \gamma_i + z_i \mathcal{F} \psi \qquad\qquad (V - 169)$$

where activities are better employed than concentrations because electrolyte solutions generally behave non-ideal (Ideal behaviour may be assumed at very low concentrations.) The activity of a cation or anion is expressed here as the product of the molal concentration

In the membrane:

$$\mu_i{}^m = \mu^o{}_i{}^m + RT \ln m_i{}^m + RT \ln \gamma_i{}^m + z_i \mathcal{F} \psi^m$$

(V - 170)

Quantities with the subscript m refer to the membrane phase. At equilibrium the electrochemical potentials in both phases are equal, thus

$$\mu_i = \mu_i{}^m$$

(V - 171)

If the reference states for both phases are also assumed to be equal ($\mu^o{}_i = \mu^o{}_i{}^m$), the following equation may be obtained, with $E_{don} = \psi^m - \psi$.

$$\frac{m_i}{m_i{}^m} = \frac{\gamma_i{}^m}{\gamma_i} \exp\left(\frac{z_i \, \mathcal{F} \, E_{don}}{R \, T}\right)$$

(V - 172)

$$E_{don} = \frac{R \, T}{z_i \, \mathcal{F}} \ln\left(\frac{\gamma_{i,m} \, m_{i,m}}{\gamma_i \, m_i}\right)$$

(V - 173)

or

$$E_{don} = \frac{R \, T}{z_i \, \mathcal{F}} \ln\left(\frac{a_{i,m}}{a_i}\right)$$
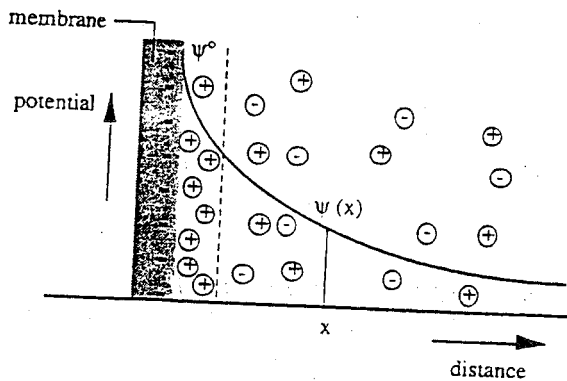
(V - 174)

Figure V - 31. Schematic drawing of the ionic distribution at the membrane-solution interface (membrane contains fixed negatively charged groups) and the corresponding potential as a function of the distance.

or , for the case of dilute solutions where $a_i \approx c_i$

$$E_{don} = \frac{RT}{z_i \mathcal{F}} \ln\left(\frac{c_{i,m}}{c_i}\right)$$

(V - 175)

This equation enables some simple calculations to be undertaken. For a given monovalent ionic solute at a concentration difference of 10, the equilibrium potential difference established at the interface is $E_{don} = [(8.314 * 298)/ (96500)] \ln (1/10) = -59$ mV.

In fact an additional term $\pi .V_i$, i.e. the swelling pressure originating from the swelling of the crosslinked polymeric network, has to be added to the right-hand side of eq V - 175. This term, however, has little influence on the ionic distribution. The swelling pressure is mainly determined by the concentration of the fixed charge (ion-exchange capacity).

The Donnan potential gives the potential build-up at the membrane-solution interface, which is determined by the ionic distribution as shown schematically in figure V - 31 [2,47]. Indeed, this ionic distribution largely determines the transport of charged molecules. In this example depicted in figure V - 31, the anions are repelled from the interface, since they have the same charge as the fixed charge on the ion-exchange membrane.

Let us now consider an ion-exchange membrane with a fixed negative charge (R^-) with Na^+ as the counterion placed in contact with a dilute sodium chloride (NaCl) solution, as shown in figure V - 32. If it is assumed that the solution behaves ideal, the activities can be put equal to the concentrations ($a_i = c_i$). The Na^+ and Cl^- ions and the water molecules can freely diffuse from the solution to the membrane phase, although the Na^+ ions can only diffuse in combination with a Cl^- ion. At equilibrium, the electrochemical potentials are equal in both phases.

$$Na^+ \longleftrightarrow Na^+$$
$$Cl^- \longleftrightarrow Cl^-$$
$$H_2O \longleftrightarrow H_2O$$
$$R^-$$
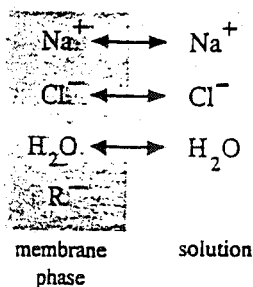
membrane   solution
phase

Figure V - 32. Donnan equilibrium established when an ionic membrane with a fixed negative charge is placed in contact with aqueous NaCl solution.

This means that under ideal conditions (activity coefficients $\longrightarrow 0$)

$$[c_{Na^+}]^m .[c_{Cl^-}]^m = [c_{Na^+}] . [c_{Cl^-}]$$

(V - 176)

where the superscript m refers to the membrane phase. Because of electrical neutrality

$$\Sigma\, z_i\, c_i = 0 \qquad\qquad\qquad (V\text{ - }177)$$

which means

$$[c_{Na^+}]^m = [c_{Cl^-}]^m + [c_{R^-}]^m \qquad\qquad (V\text{ - }178)$$

$$[c_{Na+}] = [c_{Cl^-}] \qquad\qquad\qquad (V\text{ - }179)$$

Combination of eqs. V - 176 and V - 178 gives

$$[c_{Cl^-}]^m \cdot ([c_{Cl^-}]^m + [c_{R^-}]^m) = [c_{Na^+}] \cdot [c_{Cl^-}] \qquad (V\text{ - }180)$$

Substitution of eq. V - 179 into V - 180 gives

$$[c_{Cl^-}]^m \cdot [c_{R^-}]^m + ([c_{Cl^-}]^m)^2 = ([c_{Cl^-}])^2 \qquad (V\text{ - }181)$$

or

$$\frac{[c_{Cl^-}]}{[c_{Cl^-}]^m} = \sqrt{\frac{[c_{R^-}]^m}{[c_{Cl^-}]^m} + 1} \qquad\qquad (V\text{ - }182)$$

For a dilute solution eq. V - 182 reduces to

$$[c_{Cl^-}]^m = \frac{([c_{Cl^-}])^2}{[c_{R^-}]^m} \qquad\qquad (V\text{ - }183)$$

This equation gives the ionic or 'Donnan equilibrium' of charged solutes in the presence of a charged membrane (or charged macromolecules) possessing a fixed charge density R^-.

If the concentration in the feed is low and the concentration of the fixed charge (R^- in the above example) is high, the Donnan exclusion is very effective. However, with increasing feed concentration, this exclusion becomes less effective. For instance, in the case of brackish water with a concentration of 590 ppm NaCl (≈ 0.01 eq/l $\approx 10^{-5}$ eq/ml) and a membrane with a wet-charge density of $\approx 2 \cdot 10^{-3}$ eq/ml, the co-ion (chloride) concentration in the membrane as estimated from eq. V - 183 will be approximately $5 \cdot 10^{-8}$ eq/ml. This example indicates that the concentration of the co-ion in the membrane is very low and is strongly dependent both on the feed concentration and on the fixed charge density in the membrane.

Ionic solutions do not generally behave in an ideal manner and eq. V - 183 must therefore include activity coefficients in order to correct for the non-ideality. Introducing the mean ionic activity coefficients $\gamma_\pm$ (for a univalent cation and anion $\gamma_\pm = (\gamma^+ \cdot \gamma^-)^{0.5}$, where γ^+ and γ^- are the activity coefficients of the cation and anion, respectively), eq. V -

181 becomes

$$\frac{[c_{Cl}] \; [\gamma_{\pm}]}{[c_{Cl}]^m \; [\gamma_{\pm}]^m} = \sqrt{\frac{[c_R]^m}{[c_{Cl}]^m} + 1} \qquad\qquad\qquad \text{(V - 184)}$$

Ion-exchange membranes are frequently used in combination with an electrical potential difference (as in electrodialysis, for example see chapter VI, where electrical driven membrane processes are involved). Two forces now act on the ionic solutes; a concentration difference and an electrical potential difference. Under these circumstances transport of an ion can be described by a combination of these two processes, i.e. a Fickian diffusion and an ionic conductance. The resulting equation is known as the Nernst-Planck equation:

$$J_i = -D_i \frac{dc}{dx} + \frac{z_i \mathcal{F} c_i D_i}{R T} \frac{dE}{dx} \qquad\qquad\qquad \text{(V - 185)}$$

Processes driven by electric potentials will be described further in chapters VI and VII. In cases where ions are transported across a charged membrane without an electropotential difference such as in nanofiltration, reverse osmosis or ('dense') ultrafiltration membranes a convective term has to be included and the ionic transport is now determined by three contributions, an electrical, a diffusive and a convective term, respectively.

$$J_i = J_{i,dif} + J_{i,elec} + J_{i,conv} \qquad\qquad\qquad \text{(V - 186)}$$

This equation is called the extended Nernst-Planck equation where in addition to eq. V - 185 a convective term has been introduced [2,48]. In absence of coupling phenomena and assuming ideal conditions the extended Nernst-Panck equation can be given as

$$J_i = -D_i \frac{dc}{dx} + \frac{z_i \mathcal{F} c_i D_i}{R T} \frac{dE}{dx} + c_i J_v \qquad\qquad\qquad \text{(V - 187)}$$

V.8.   Solved problems

1. A time-lag technique is used to determine the diffusion coefficient of CO_2 in PVC (membrane thickness is 30 μm). This experiment is carried out at various feed pressures (p_1). The permeate side (p_2) is evacuated and then the pressure increase is measured as a function of time. The following results are obtained for the steady-state region;

p_1 (CO_2) (mmHg)	dp_2/dt (mmHg/s)
1000	34.5
2000	81.6
3000	130.4
4000	190.5
5000	256.4

The abscissa at $t = 0$ is equal to the negative value of p_1, the feed pressure.

a. Calculate the diffusion coefficient of CO_2 at the various feed pressures and explain the result

b. If helium is used as gas instead of CO_2, give then a schematic drawing of a p_2 - t curve for $p_1 = 1000$ mmHg and $p_1 = 3000$ mmHg

2. Calculate the water flux through a typical microfiltration (MF) and ultrafiltration (UF) membrane at 1 bar and 298 K. Assume that the tortuosity factor is 1.2.

	MF	UF
ε (porosity)	0.6	0.02
r_p (pore radius)	0.2 μm	2 nm
ℓ (thickness)	100 μm	1 μm

3. The oxygen permeability and some other physical parameters of various polyvinylidene polymers are summarized below (J.Mohr and D.R. Paul, JAPS, 42(1991) 1711).

	ρ (g/cm^3)[a]	V_w (cm^3/mol)[b]	P_{O_2} (Barrer)[c]
polyethylene	0.854	20.46	15.7
polyisobutene	0.910	40.90	2.1
polyvinylidenefluoride	1.670	25.56	0.39
polyvinylidenechloride	1.780	38.03	

[a] density of amorphous fraction
[b] Van der Waals volume
[c] permeability of amorphous fraction

a. Calculate the fractional free volumes of the various polymers
b. Estimate the permeability of PVDC

V.9.   Unsolved Problems

1a. Natural gas often contains small amounts of nitrogen which can be removed by membrane technology. The critical temperature of nitrogen is 126 K and of methane is 191 K. The kinetic diameter of nitrogen is 3.64 Å and of methane the diameter is 3.8

Å. Explain whether polymers will be generally nitrogen or methane selective ?

b. Many polyimides show a selectivity for nitrogen. Is this due to diffusivity, solubility or a combination ?

2. For a three layer composite membrane frequently a highly permeable selective layer is used as intermediate layer and is sometimes named as 'gutter layer'. Upon this 'gutter layer' the active layer is deposited. Derive an equation for the selectivity of this membrane for a gas mixture consisting of A and B in which thickness of each layer and the gas permeabilities are included (Assume that the resistance of the support layer is negligible).

3. Calculate the diffusion coefficient of nitrogen (radius 1.9 Å) in water, in silicon rubber (SR) and in polyimide (PI), respectively, at 25°C. The permeabilities of nitrogen in SR and PI are 280 and 0.1 Barrer, and the solubilities are 0.15 $(cm^3(STP)/cm^3)$ in SR and 0.1 $(cm^3(STP)/cm^3)$ in PI at 2 bars, respectively.

4. Already in 1830 Mitchell performed gas separation experiments. One of the experiments was as follows; a wide mouthed bottle was filled with hydrogen and the aperture was covered by a kind of elastomeric film (see drawing). Hydrogen may be considered to behave ideal.
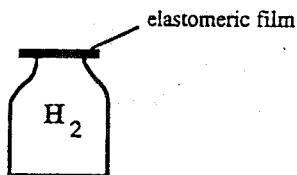
elastomeric film

a) Describe what happens (Give also a drawing)
b) If the bottle was covered by a glassy polymer instead of the elastomeric film with a permeability coefficient for hydrogen being 10^4 less what happens then ?
c) Give a qualitative drawing of the permeability coefficient, solubility coefficient and diffusion coefficient of hydrogen in both materials as a function of pressure.

Rubbery materials are frequently used for the separation of organic vapours from air.

d) Is the high permeability for the organic vapour compared to air due to a high solubility or a high diffusivity. Explain.
e) How does the solubility coefficient of the organic vapour change as a function of the partial vapour pressure outside the membrane.

5. The solubility of gases can be described by Henry's law ('ideal behaviour') and by the

'dual sorption'.

a. What is the difference between the two models ? Explain briefly

b. Explain the physical weakness and the perfect experimental fitting of the dual sorption model

c. Give the permeability as a function of the pressure for both models assuming that the diffusion coefficient remains constant.

The permeability of CO_2 in polyvinylchloride (PVC) is described as follows
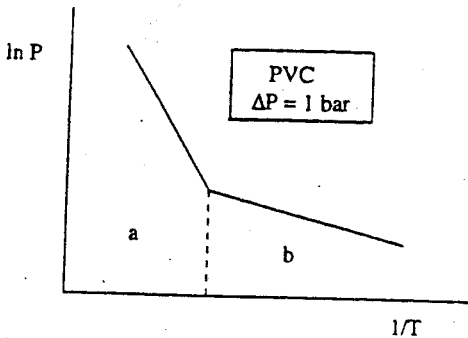
d. Indicate the regions a en b and explain the temperature of the inflection point

CO_2 is well known for its plasticising effects in glassy polymers and in polyvinylchloride (PVC) this effect starts above 10 bar.

e. When the above figure is measured at 15 bar instead of 1 bar, does the point of inflection shift ? If so, in what direction. Explain briefly.

g. Draw schematically the permeability of CO_2 in polyimide as a function of pressure (note the plasticising effect !).

h. CO_2 is present in the air (0.03 vol.%). When a gas separation experiment is carried out with air at a pressure of 100 bar to what extent does P_{CO2} differ from the P_{CO2} measured at 1 bar using pure CO_2 ?

6. The molecular mass of the noble gases increases in the order Helium (He), Neon (Ne), Krypton (Kr) and Xenon (Xe).

a. Show qualitatively (in a drawing) the variation of the diffusion coefficients of these gases in a given polymer ? Does it make a difference whether a glassy or a rubbery polymer is used ?

b. Give in a drawing of the solubility (not the solubility coefficient !) of the various gases in a rubber as a function of the pressure ?

c. Give a qualitative drawing of the permeability of argon in silicone rubber.

For a given polymer A the solubility of helium is 10 times at low and the diffusivity is 1000 times at high compared to argon.

d. What is the selectivity of the polymer A for the helium / argon mixture ?

Three balloons are filled with helium, argon, and air respectively. The pressure in the balloons is 1.0004 bar, while the pressure outside is 1 bar.

e. Show in a drawing what happened with the balloons after 1 day ? (The balloons did not escape to heaven since they were captured in your membrane laboratory).

7. The diffusivity of organic vapours and of organic liquids in polymers is mostly far from ideal and frequently concentration dependent. Show how the thermodynamic diffusion coeffient, or rather the ratio of the thermodynamic diffusion coefficient versus mutual diffusion coefficient changes as the volume fraction ϕ of the penetrant changes from $\phi = 0.02$ to $\phi = 0.5$ while the binary interaction parameter of polymer/penetrant is $\chi = 0.6$.

8. Park (ref. 15) found for the diffusion coefficient (D) of benzene in polyvinylacetate (PVAc) the following concentration dependency.
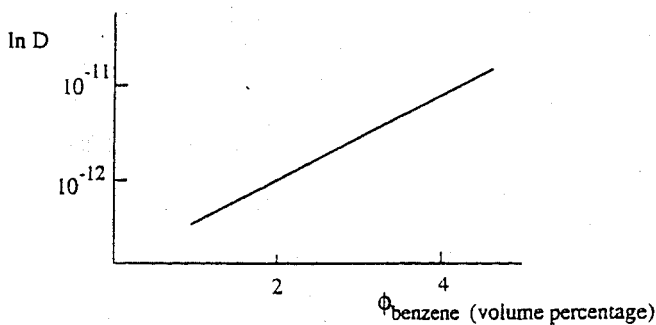
a. By which mathematical relation is D related to the concentration of benzene in the membrane
b. Estimate the plasticing constant from this graph
c. The interaction of water, methanol, propanol, and benzene with PVAc decreases in this sequence. Show how D varies in this sequence (Give a qualitative drawing) ?
d. Indicate how D_0 varies in this sequence ?

9. Show the relative magnitude of the various quantities appearing in the electrochemical potential for an electrodialysis system with the following characteristics.
$\Delta\phi = 0.01$ V; $\Delta x = 0.05$ cm; $V_m = 18$ cm³/mol; $\Delta P = 0.1$ bar; T = 300 K; $c'/c'' = 2$

10. The tortuosity factor of a microfiltration membrane (thickness 100 μm) is often difficult to determine. One way to achieve this is filling the pores with water and measuring the CO_2 flux across the membrane in a system with at one side CO_2' and on the other side no CO_2. The measured flux at 25°C was $J_{CO2} = 1.56 \ 10^{-4}$ mol/m².s and the diffusion coefficient of CO_2 in water is $D = 1.92 \ 10^{-9}$ m²/s. Calculate the tortuosity factor when the surface porosity is 30% ?

11. In a composite membrane the thin dense toplayer (thickness 0.2 μm) is supported by a porous sublayer with an uniform pore size ($r_p = 50$ nm) and neglible resistance. Calculate the effective thickness of the toplayer with a surface porosity of the sublayer of 0.1 (10%), 0.01 (1%) and 0.001 (0.1%) ?

12. The flux in pervaporation can be described by Fick's law. Derive for a component the concentration in the membrane as a function of the distance (i.e. the concentration profile) in a steady-state process for a system with a constant diffusion coefficient and with an exponential diffusion coefficient and draw these concentration profiles. Derive an equation for the concentration dependent diffusion coefficient as a function of the distance in the membrane and draw this diffusion profile.

13. Calculate the partial vapour pressure and the chemical potential of oxygen in air at: 1 bar and 298 K and at 10 bar and 298 K (Assume that air consist of 21 mol% of oxygen).
$S°_{O_2} = 205.1$ J/mol.K.

14. Calculate the chemical potential of water at 25°C and 1 bar, at 25°C and 100 bar and at 1 bar and 90°C, respectively. $H°_{f,H2O} = -285.8$ kJ/mol, $S°_{H2O} = 69.9$ J/mol.K and $c_p = 75.3$ J/mol.K).

15. The sorption isotherms of methane, argon, helium, ethane, nitrogen and carbon dioxide in poly(norbornene) at 25°C have been studied by Yampolskii et al. and are given below.
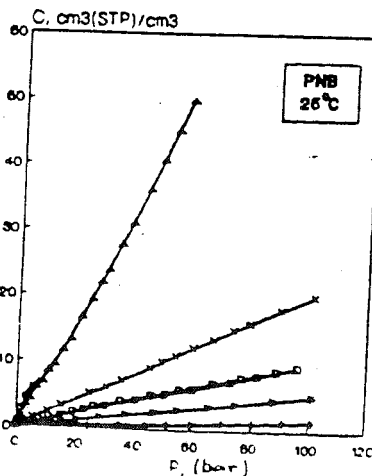
a. Is polynorbornene a glass or a rubber at 25°C.
b. Indicate which isotherm belongs to each gas?
c. Estimate the solubility coefficient of each gas in poly(norbornene).

16. The permeability coefficients of nitrogen and ethylene (in Barrer) in Butyl rubber at various temperatures are given below.

	40°C	60°C	80°C
nitrogen	9.5	29	74
ethylene	28	86	230

Calculate the activation energies of both components in butyl rubber.

17. The reflection coefficient of a nanofiltration membrane for glucose (Mw = 180 g/mol), sucrose (Mw = 342 g/mol) and mannose (Mw = 504 g/mol) has been determined in a diffusion cell. One compartment is filled with a sugar solution of 18 g/l, the other with pure water. A volume increase of 1.0 % for glucose, 0.7% for sucrose and 0.56% for mannose have been observed in 45 minutes. The water permeability coefficient of the membrane is, $L_p = 10^{-5}$ g/cm^2.s.bar.The volume in the sugar compartment is 56 ml and the membrane area is 13.2 cm^2.Calculate the reflection coefficients of the various sugars.

18. The three characteristic parameters σ, L_p and ω can be determined from two experiments; in the first experiment 4.6 ml of water has been permeated in 1 hour in a cell with a diameter of 7.5 cm whereas 10 bars of pressure has been applied. In the second experiment 1 g of sucrose (Mw: 342 g/mol) is dissolved in 100 ml of water. One compartment of a dialysis cell with a volume of 44 ml is filled with this solution whereas the other contains pure water. After two hour the liquid volume in the sucrose compartment has been increased 0.57 ml while the sucrose concentration has been decreased with 1.16%.

19. The sorption of carbon dioxide in polyimide has been measured with the pressure decay method in a single pressure volume set-up at 25°C. The volume of the cell is 250 cm^3 and the volume of the polymer sample is 0.3 cm^3. At 1 bar and at 8 bar of carbon dioxide pressure a pressure decay of 1.46 kPa and 5.58 kPa, respectively have been measured.
a. Calculate the sorption values at 1 and 8 bar assuming ideal gas behaviour.
b. Shows carbon dioxide in polyimide Henry behaviour? Explain

20. Determine the solubility coefficient of trichloromethane in PDMS at 40°C at activity 0.3 and 0.9 respectively (Use figure V-18).

21. A cuprophane dialysis membrane separates two compartments with a volume of 100 ml. The left compartment contains a solution of 5.10^{-3} M sodiumpolyacrylate and the right compartment a solution of 10^{-3} M sodiumchloride. The membrane is permeable

for the Na^+ and Cl^- ions but not for the negatively charged polyacrylate ions. Calculate the sodium and chloride concentrations at both side of the membrane at equilibrium.

22. A negatively charged membrane is able to retain ions by a Donnan exclusion mechanism. Calculate the membrane selectivity ($\equiv$ ratio anion concentration in membrane over anion concentration in solution, c_s^m/c_s) for an 1 mmol/liter solution of sodium chloride solution, sodium sulfate and calcium chloride. The amount of fixed charges in the polymer is 0.02 eq/liter (swollen polymer).

V.10. Literature

1. Prigogine, I., *Thermodynamics of irreversible processes*, Thomas Springfield, Illinois, 1955

2. Lakshminarayanaiah, N., *Transport phenomena in membranes*, Academic Press, Orlando, USA,. 1969

3. Katchalsky, A., and Curran P.F., *Non-equilibrium processes in biophysics*, Harvard University Press, 1965

4. Mason. E.A., and Malinauskas. A.P., *Gas transport in porous media: The dusty gas model*, Elsevier, Amsterdam, 1983

5. Kedem, O., and Katchalsky, A., *Biochim. Biophys. Acta.*, **27** (1958) 229

6. Spiegler, K.S., and Kedem, O., *Desalination*, **1** (1966) 311

7. Nakao, S.I., and Kimura, S.J., *J. Chem. Eng. Japan*, **14** (1981) 32

8. Jonsson, G., and Boessen, C.E., *Proc. 6th. Symp. Fresh Water from the Sea*, 1978, Vol. 3, p. 157

9. Pusch, W., *Ber. Bunsen-Ges. Phys.Chem.*, **81** (1977) 269

10. Pusch. W., *Chem.-Ing.-Tech.*, **45** (1973) 1216.

11. Fujita, H., *Fortschr. Hochpolym. Forsch.*, **3** (1961) 1

12. Flory, P.J., *Principles of Polymer Chemistry*, Cornell Univ. Press, Ithaca, 1953

13. Vieth, W.R., Howell, J.M., and Hsieh, H.J., *J. Membr., Sci.*, **1** (1976) 177

14. Paul, D.R., and Koros, J.W., *J. Polym. Sci. Polym. Phys*, **14** (1976) 675

15. Petropolous, J.H., *J. Polym. Sci. A-2*, **8** (1970) 1797

16. Park, G.S.,: 'Transport in polymers', in: Bungay, P.M., Lonsdale, H.K., and de Pinho (eds.), *Synthetic Membranes: Science, Engineering, and Applications*, Reidel Publishing Company, Dordrecht, 1986, p. 57

17. Brown. W.R., and Park, G.S., *J. Paint. Technol.*, **42** (1970) 16

18. Baker. R.W., and Blume, I., Chemtech., **16** (1986) 232

19. Crank, J., *The mathematics of diffusion*, Clarendon Press, Oxford, 1975

20. Frisch. H.L., *J. Phys. Chem.*, **62** (1957) 93

21. Koros, W.J., and Paul, D.R., *J. Polym. Sci., Polym. Phys.*, **14** (1976) 1903

22. Mc Call. D.W., *J. Polym. Sci.*, **16** (1975) 151

23. Stern, S.A., Gareis, P.J., Sinclair, T.F., Mohr, P.H., *J. Appl. Pol. Sci.*, **7** (1963)

2035

24. Meares, P., *J. Am. Chem.Soc.*, **76** (1954) 3415

25. Blume, I., Internal publications, University of Twente

26. Kokes, R.J., and Long, F.A., *J. Am. Chem. Soc.*, **75** (1953) 6142

27. Bondi, A., *J. Phys. Chem.*, **68** (1964) 411

28. Sugden, S., *J. Chem. Soc.*, (1927), 1786

29. Simha, R., and Boyer, R.F., *J. Chem., Phys.*, **37** (1962) 1003

30. Muruganandam, N., Koros, W.J., Paul, D.R., *J. Polym. Sci. Polym. Phys.*, **25** (1987) 1999

31. Barbari, T., Koros, W.J., and Paul, D.R., *J. Polym. Sci. Polym. Phys.*, **26** (1988) 709

32. Min, K.E., and Paul, D.R., *J. Polym. Sci. Polym. Phys.*, **26** (1988) 1021

33. Tanaka, K., Kita, H., Okamoto, K, Nakamura, A., Kusuki, Y., *J. Membr. Sci.*, **47** (1989) 203

34. Hensema, E., Mulder, M.H.V., and Smolders, C.A., to be published

35. Vrentas, J.S., and Duda, J.L., *J. Polym. Sci., Polym. Phys.*, **15** (1977) 403

36. Vrentas, J.S., and Duda, J.L., *J. Polym. Sci., Polym. Phys.*, **15** (1977) 417

37. Zimm, B.H., and Lundberg, J.L., *J. Phys. Chem.*, **60** (1956) 425

38. Mulder, M.H.V., Franken, A.C.M., and Smolders, C.A., *J. Membr. Sci.*, **22**, (1985), 155

39. Mulder, M.H.V.; 'Thermodynamics principles of Pervaporation' in R.Y.M. Huang (ed.), *Pervaporation Membrane Separation Processes*, Elsevier, Amsterdam, 1991, Chapter 4.

40. Bitter, J.G.A., *Desalination*, 51 (1984) 19

41. Lee, C.H., *J. Appl. Polym. Sci.*, **19** (1975) 83

42. Wesselingh, J.A., and Krishna, R., *Mass Transfer*, Ellis Horwood, New York, 1990

43. Wijmans J.G., *J. Membr. Sci.*, (1995)

44. Staverman, A.J., *Rec. Trav. Chim.*, **70** (1951) 344

45. Teorell, T., *Proc. Soc. Exp. Biol. Med.*, **33** (1935) 282

46. Meyer, K.H., and Sievers, J-F., *Helv. Chim. Acta*, **19** (1936) 649

47. Helfferich, F., *Ion-Exchange*, McGraw-Hill, New York, 1962

48. Dresner, L., *Desalination*, **10** (1972) 27

VI   MEMBRANE PROCESSES

VI.1.   Introduction

All membrane processes have the common feature that separation is achieved via a membrane. The membrane can be considered to be a permselective barrier existing between two homogeneous phases. Transport through the membrane takes place when a driving force is applied to the components in the feed. In most the membrane processes the driving force is a pressure difference or a concentration (or activity) difference across the membrane. Parameters such as pressure, concentration (or activity) and even temperature may be included in one parameter, the chemical potential μ.

$$\mu = f(T, P, a \text{ or } c)$$

$$(VI - 1)$$

At constant temperature T, the chemical potential of component i in a mixture is given by

$$\mu_i = \mu^°_i + RT \ln a_i + V_i P$$

$$(VI - 2)$$

where $\mu^°_i$ is the chemical potential of 1 mol of pure substance at a pressure P and temperature T. For pure components the activity is unity, i.e. $a = 1$, but for liquid mixtures the activity is given by the product of mole fraction x_i and activity coefficient γ_i

$$a_i = x_i \cdot \gamma_i$$

$$(VI - 3)$$

For ideal mixtures the activity coefficient is unity, i.e. $\gamma_i = 1$, so that the activity is equal to the mole fraction, i.e. $a_i = x_i$. However, since many non-aqueous mixtures are non-ideal, activities rather than concentrations should be used.

For perfect gases, the chemical potential is given by

$$\mu_i = \mu^°_i + RT \ln x_i + RT \ln P$$

$$(VI - 4)$$

where p_i is the partial pressure. Because

$$p_i = x_i P$$

$$(VI - 5)$$

eq. VI - 4 can be written as

$$\mu_i = \mu^°_i + RT \ln p_i$$

$$(VI - 6)$$

Gases deviate from ideality as well and in fact fugacities should be used instead of partial pressures. Eq. VI - 6 then becomes

$$\mu_i = \mu^\circ_i + RT \ln f_i \qquad\qquad (VI - 7)$$

where f_i is the fugacity. The fugacity is given by the product of fugacity coefficient ϕ_i and the partial pressure p_i

$$f_i = \phi_i \, p_i \qquad\qquad (VI - 8)$$

Table VI.1 gives an example of the difference between pressure and fugacity for carbon dioxide at various pressures at 300 K. It can be seen that for high pressures the discrepancy between pressure and fugacity can be quite large. Other gases show the same behaviour which indicates that in the case of high pressure applications the use fugacities is preferred.

Table   VI.1. The fugacity of carbon dioxide at 300 K [1]

pressure (P) (bar)	fugacity (f) (bar)	f/P
1	0.995	0.995
5	4.9	0.976
25	22.0	0.880
50	38.1	0.761
60	42.8	0.713

The fugacity of a gas may normally be calculated if the equation of state is known. The fugacity coefficient ϕ is related to the compressibility factor z, which is given by

$$z = \frac{P \overline{V}}{R T} \qquad\qquad (VI - 9)$$

For an ideal gas z is of course unity. For many real gases virial equations are known in which the compressibility factor has been expanded in powers of V or P (see eq. VI - 10).

$$z = \frac{P \overline{V}}{R T} = 1 + B' P + C' P^2 + \ldots\ldots \qquad\qquad (VI - 10)$$

B' and C' are called the pressure-series virial coefficients. B' is the second virial coefficient and C' the third virial coefficient. The fugacity coefficient can be obtained from the compressibility factor according to

$$\ln \phi = \int_0^p \frac{z-1}{P} \, dP \qquad\qquad (VI - 11)$$

From eqs. VI - 11 and VI - 8 the fugacity can now be calculated and the actual driving

force can then be determined accurately.

Another driving force in membrane separations is the electrical potential difference. This driving force only influences the transport of charged particles or molecules. The membrane processes discussed in this chapter may be classified according to their driving forces. Such a classification is given in table VI. 2.

Table VI.2 Classification of membrane processes according to their driving forces

pressure difference	concentration (activity) difference	temperature difference	electrical potential difference
microfiltration ultrafiltration nanofiltration reverse osmosis piezodialysis	pervaporation gas separation vapour permeation dialysis diffusion dialysis carrier-mediated transport	thermo-osmosis membrane distillation	electrodialysis electro-osmosis membrane electrolysis

Before describing these various processes an introduction is given on osmotic phenomena, because such phenomena are very important in membrane processes especially in pressure-driven processes.

VI.2.   Osmosis

An osmotic pressure arises when two solutions of different concentration (or a pure solvent and a solution) are separated by a semipermeable membrane, i.e. one which is permeable to the solvent but impermeable to the solute. This situation is illustrated schematically in figure VI - 1a. Here the membrane separates two liquid phases: a concentrated phase 1 and a dilute phase 2.
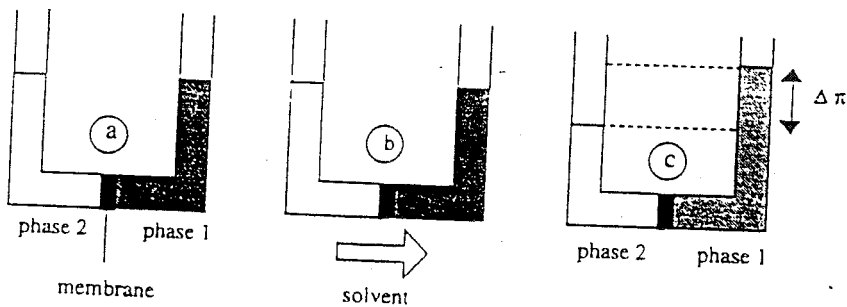

Figure VI - 1   Schematic illustration of osmotic processes

Under isothermal conditions the chemical potential of the solvent in the concentrated phase (phase 1) is given by

$$\mu_{i,1} = \mu_{i,1}{}^\circ + RT \ln a_{i,1} + V_i \, P_1 \tag{VI - 12}$$

while the chemical potential of the solvent in the dilute phase (phase 2) is given by

$$\mu_{i,2} = \mu_{i,2}{}^\circ + RT \ln a_{i,2} + V_i \, P_2 \tag{VI - 13}$$

The solvent molecules in the dilute phase have a higher (more negative !) chemical potential than those in the concentrated phase. This chemical potential difference causes a flow of solvent molecules from the dilute phase to the concentrated phase (the flow is proportional to $-\partial\mu/\partial x$). This is shown in figure VI - 1b. This process continues until osmotic equilibrium has been reached, i.e. when the chemical potentials of the solvent molecules in both phases are equal (see figure VI - 1c):

$$\mu_{i,1} = \mu_{i,2} \tag{VI - 14}$$

Combination of eqs. VI - 12, VI - 13 and VI - 14 gives,

$$RT \, (\ln a_{i,2} - \ln a_{i,1}) = (P_1 - P_2) \, V_i = \Delta\pi \, . \, V_i \tag{VI - 15}$$

This hydrodynamic pressure difference $(P_1 - P_2)$ is called the osmotic pressure difference $\Delta\pi$ $(\Delta\pi = \pi_1 - \pi_2)$. When only pure solvent is situated on one side of the membrane (phase 2), i.e. $a_{i,2} = 1$, then eq. VI - 15 becomes

$$\pi = -\frac{RT}{V_i} \ln a_{i,1} \tag{VI - 16}$$

with π the osmotic pressure of phase 1. For very low solute concentrations $(\gamma_i \Rightarrow 1)$ eq. VI - 16 can be simplified further by applying Raoult's law:

$$\ln a_i = \ln \gamma_i \, x_i \approx \ln x_i \approx \ln (1 - x_j) = -x_j \tag{VI - 17}$$

$$\pi = \frac{RT \, x_j}{V_i} \tag{VI - 18}$$

with $x_j = n_j/(n_i + n_j)$. For a dilute solution, $x_j \approx n_j/n_i$ and

$$\pi \, n_i \, V_i = n_j \, RT \tag{VI - 19}$$

Because $n_i \, V_i \approx V$ (for dilute solutions)

$$\pi \, V = n_j \, RT \tag{VI - 20}$$

and since $n_j / V = c_j / M$, then

$$\pi = c_j \, RT \,/\, M$$

$$(VI - 21)$$

This simple relationship between the osmotic pressure π and the solute concentration c_j, is called the van 't Hoff equation. It can be seen that the osmotic pressure is proportional to the concentration and inversely proportional to the molecular weight. If the solute dissociates (as for instance in salts) or associates, eq. VI - 21 must be modified. When dissociation occurs the number of moles increases and hence the osmotic pressure increases proportionally, whereas in the case of association the number of moles decreases as does the osmotic pressure. The osmotic pressure difference in microfiltration and ultrafiltration applications are quite low, whereas it has to be taken into account in reverse osmosis.

Substantial deviations from van 't Hoff's law occur at high concentrations and with macromolecular solutions as will be described in chapter VII. In this case the osmotic pressure can be expressed by a virial expansion in which the van 't Hoff equation is the first term (eq. VI - 22).

$$\pi = \frac{RT}{M} c + B c^2 + \dots\dots$$

$$(VI - 22)$$

Often a more simple exponential relationship has been applied for macromolecular solutions.

$$\pi = a \cdot c^n$$

$$(VI - 23)$$

Here, a is a constant and n an exponential factor with a value greater than 1. Hence, if the concentration is high the osmotic pressure can be high as well and this concept may be used to describe concentration polarization, i.e. although the osmotic pressure of the bulk solution is still low, the concentration at the wall may have increased drastically as does the osmotic pressure (see chapter VII.5, osmotic pressure model)

VI.3.   Pressure driven membrane processes

VI.3.1.   Introduction

Various pressure-driven membrane processes can be used to concentrate or purify a dilute (aqueous or non-aqueous) solution. The characteristic of these processes is that the solvent is the continueous phase and that the concentration of the solute is relatively low. The particle or molecular size and chemical properties of the solute determine the structure, i.e. pore size and pore size distribution. necessary for the membrane employed. Various processes can be distinguished related to the particle size of the solute and consequently to membrane structure. These processes are microfiltration, ultrafiltration, nanofiltration and reverse osmosis. The principle of the four processes is illustrated in figure VI - 2.
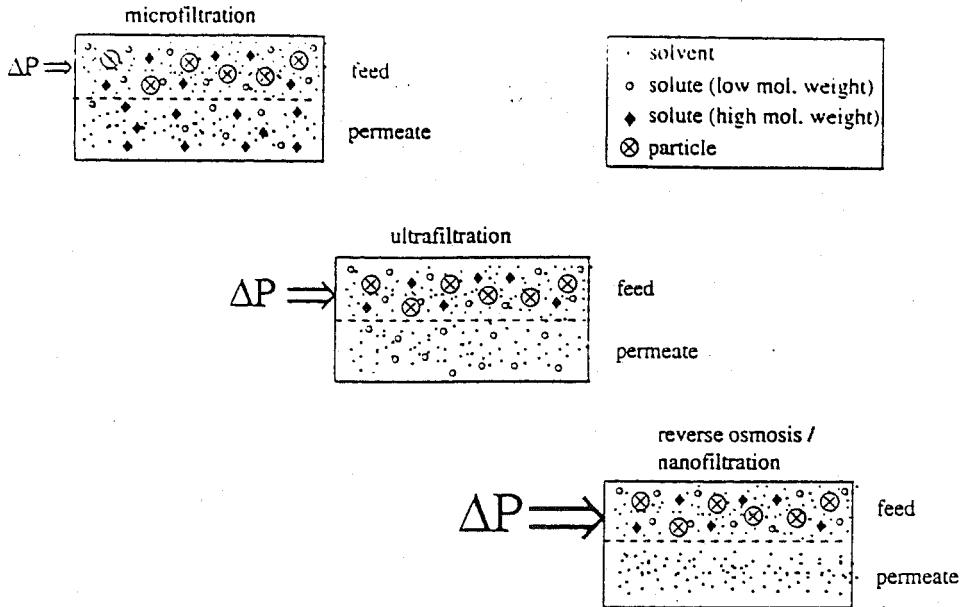
microfiltration

reverse osmosis /
nanofiltration

Figure VI - 2.   Schematic representation of microfiltration, ultrafiltration, nanofiltration and reverse osmosis.

Because of a driving force, i.e. the applied pressure, the solvent and various solute molecules permeate through the membrane, whereas other molecules or particles are rejected to various extents dependent on the structure of the membrane. As we go from microfiltration through ultrafiltration and nanofiltration to reverse osmosis, the size (or molecular weight) of the particles or molecules separated diminishes and consequently the pore sizes in the membrane must become smaller. This implies that the resistance of the membranes to mass transfer increases and hence the applied pressure (driving force) has to be increased to obtain the same flux. However, no sharp distinction can be drawn between the various processes. A schematic drawing of the separation range involved in these various processes is given in figure VI - 3. It is possible to distinguish between the various processes in terms of membrane structure. In the case of microfiltration, the complete membrane thickness may contribute towards transport resistance, when a symmetrical porous structure is involved. The membrane thickness can extend from 10 μm to more than 150 μm. However, most microfiltration membranes possess an asymmetric structure build-up with a toplayer thickness in the order of 1 μm. Ultrafiltration, nanofiltration and reverse osmosis membranes have an asymmetric structure as well with a thin, relatively dense toplayer (thickness 0.1-1.0 μm) supported by a porous substructure (thickness ≈ 50-150 μm). The hydraulic resistance is almost completely located in the toplayer, the sublayer having only a supporting function.
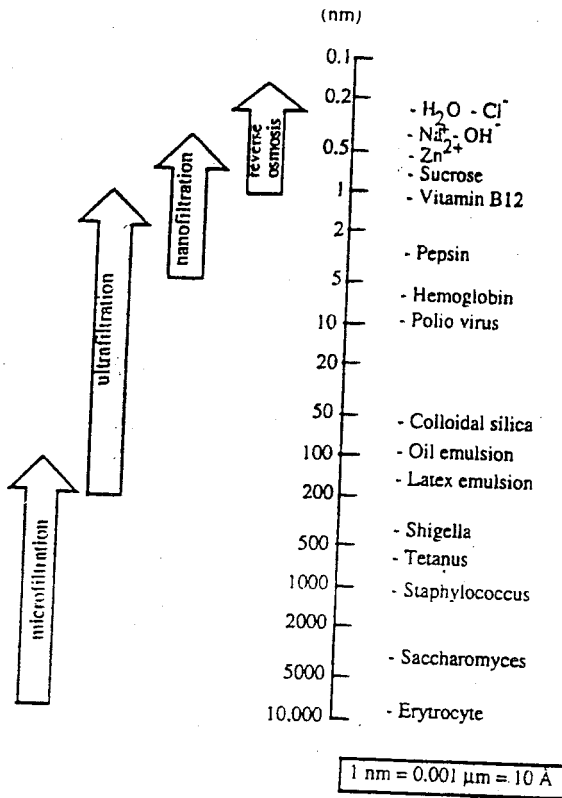
(nm)

- 0.1
- 0.2 — H$_2$O - Cl$^-$
- — Na$^+$- OH$^-$
- 0.5 — Zn^{2+}
- — Sucrose
- 1 — Vitamin B12
- 2 — Pepsin
- 5 — Hemoglobin
- 10 — Polio virus
- 20
- 50 — Colloidal silica
- 100 — Oil emulsion
- 200 — Latex emulsion
- 500 — Shigella
- — Tetanus
- 1000 — Staphylococcus
- 2000
- 5000 — Saccharomyces
- 10,000 — Erytrocyte

reverse osmosis / nanofiltration / ultrafiltration / microfiltration

| 1 nm = 0.001 μm = 10 Å |

Figure VI - 3. Application range of microfiltration. ultrafiltration, nanofiltration and reverse osmosis.

The flux through these (and other) membranes is inversely proportional to the (effective) thickness. and because they possess an asymmetrical structure with toplayer thicknesses less than 1 μm membranes of this type became of commercial interest. A comparison of the various pressure driven processes is given in table VI.4.

VI.3.2 Microfiltration

Microfiltration is the membrane process which most closely resembles conventional coarse filtration. The pore sizes of microfiltration membranes range from 10 to 0.05 μm, making the process suitable for retaining suspensions and emulsions.

The volume flow through these microfiltration membranes can be described by Darcy's law. the flux J through the membrane being directly proportional to the applied pressure:

$$J = A \cdot \Delta P$$

(VI - 24)

where the permeability constant A contains structural factors such as the porosity and pore

Table VI.4. Comparison of various pressure driven membrane processes

microfiltration	ultrafiltration	nanofiltration/ reverse osmsosis
separation of particles	separation of macromolecules (bacteria, yeasts)	separation of low MW solutes (salts, glucose, lactose, micropollutents)
osmotic pressure[#] negligible	osmotic pressure[#] negligible	osmotic pressure high ($\approx 1 - 25$ bar)
applied pressure low (< 2 bar)	applied pressure low ($\approx 1 - 10$ bar)	applied pressure high ($\approx 10 - 60$ bar)
symmetric structure asymmetric structure	asymmetric structure	asymmetric structure
thickness of separating layer symmetric $\approx 10 - 150$ μm asymmetric ≈ 1 μm	thickness of actual separating layer $\approx 0.1 - 1.0$ μm	thickness of actual separating layer $\approx 0.1-1.0$ μm
separation based on particle size	separation based on particle size	separation based on differences in solubility and diffusivity

In absence of concentration polarization (see chapter VII).

size (pore size distribution). Furthermore, the viscosity of the permeating liquid is also included in this constant. For laminar convective flow through a porous system both the Hagen-Poiseuille and the Kozeny-Carman equations can be applied. If the membrane consists of straight capillaries, the Hagen-Poiseuille relationship can be used with $A \approx \varepsilon$ r^2:

$$J = \frac{\varepsilon \, r^2}{8 \, \eta \, \tau} \frac{\Delta P}{\Delta x} \qquad\qquad (VI - 25)$$

where r is the pore radius, Δx is the membrane thickness, η is the dynamic viscosity and τ is the tortuosity factor which is unity in the case of cylindrical pores. It can be seen that the flux $J \approx r^4$!.

When a nodular structure exists, i.e. an assembly of spherical particles, the Kozeny-Carman equation can be employed:

$$J = \frac{\epsilon^3}{K \eta S^2} \frac{\Delta P}{\Delta x}$$

(VI - 26)

where K is a dimensionless constant which depends on the pore geometry, S is the surface area of the spherical particles per unit volume, and ϵ is the porosity. For spherical particles and assuming $K = 5$ then eq. VI - 26 can be written as

$$J = \frac{\epsilon^3 d^2}{\eta \; 180 \; (1 - \epsilon)^2} \frac{\Delta P}{\Delta x}$$

(VI - 27)

In both eqs. VI - 25 and VI - 26 (or VI - 27), the viscosity appears as an inversely proportional parameter. Also both equations relate the volume flow to simple structural parameters such as porosity ϵ and pore radius r.

In order to optimise microfiltration membranes, it is essential to ensure that the structural parameters are such that the (surface) porosity is as high as possible with the pore size distribution as narrow as possible. It should be realised that the convective flow as described by these equations only involves membrane-related parameters and none which apply to the solutes.

VI.3.2.1   Membranes for microfiltration

Microfiltration membranes may be prepared from a large number of different materials based on either organic materials (polymers) or inorganic materials (ceramics, metals, glasses).

Various techniques can be employed to prepare microfiltration membranes from polymeric materials:
-   sintering
-   stretching
-   track-etching
-   phase inversion.

Such preparation techniques have already been discussed in detail in chapter III. Figure VI - 4 shows SEM micrographs of some characteristic polymeric microfiltration membranes obtained by phase inversion (IV - 4a), stretching (IV - 4b) or track-etching (IV - 4c).

Frequently, inorganic membranes are used instead of polymeric membranes because of their outstanding chemical and thermal resistances. In addition, the pore size in these membranes can be better controlled and as a consequence the pore size distribution is generally very narrow (see also chapter IV). Various techniques can be used to prepare ceramic membranes with some important ones being:
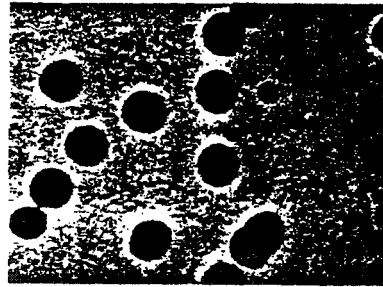-   sintering
-   sol/gel process
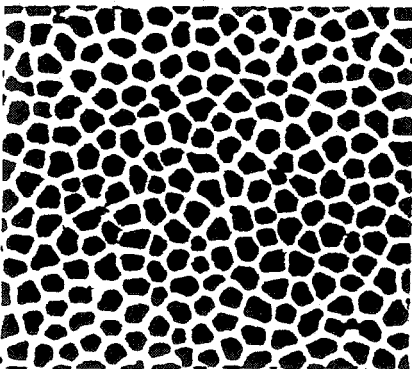-   anodic oxidation
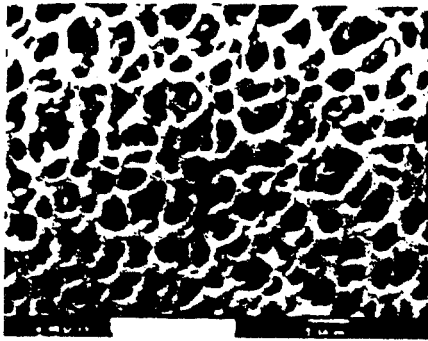
(a)
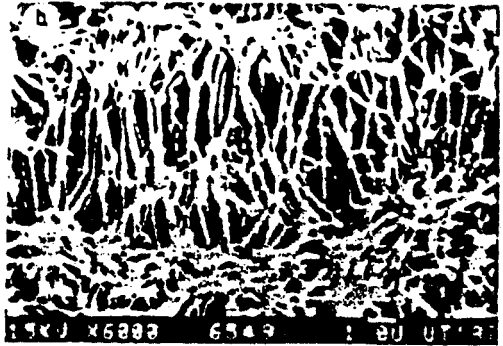
(b)

(c)

Figure VI - 4. Polymeric microfiltration membranes: (a) phase inversion; (b) stretching; and (c) track etching

Two typical structures are depicted in figure VI - 5.

(a)

(b)

Figure VI - 5. Ceramic microfiltration membranes: (a) Anotec®, anodic oxidation (surface); and (b) US Filter®, sintering (cross-section, upper part).

These SEM photographs clearly show that the porosity and pore size distribution differ substantially for the various membranes depicted. Table VI.5 summarises the effect of the preparation method on the porosity and the pore size distribution.

Table VI.5 Porosities and pore size distributions achieved by various preparation methods

process	porosity	pore size distribution
sintering	low/medium	narrow/wide
stretching	medium/high	narrow/wide
track-etching	low	narrow
phase inversion	high	narrow/wide

These various techniques allow to prepare microfiltration membranes from virtually all kinds of materials of which polymers and ceramics are the most important. Synthetic polymeric membranes can be divided in two classes, i.e. hydrophobic and hydrophilic. Various polymers which yield hydrophobic and hydrophilic membranes are listed below. Ceramic membranes are based mainly on two materials, alumina (Al_2O_3) and zirconia (ZrO_2). However, other materials such as titania (TiO_2) can also be used in principle. A number of organic and inorganic materials are listed below:

- hydrophobic polymeric membranes polytetrafluoroethylene (PTFE, teflon)
  poly(vinylidene fluoride) (PVDF)
  polypropylene (PP)
  polyethylene (PE)

- hydrophilic polymeric membranes cellulose esters
  polycarbonate (PC)
  polysulfone/poly(ether sulfone) (PSf/PES)
  polyimide/poly(ether imide) (PI/PEI)
  (aliphatic) polyamide (PA)
  polyetheretherketone (PEEK)

- ceramic membranes alumina (Al_2O_3)
  zirconia (ZrO_2)
  titania (TiO_2)
  silicium carbide (SiC)

Other materials such as glass (SiO_2), carbon and various metals (stainless steel, palladium, tungsten, silver) have also been used for preparing microfiltration membranes.
  Microfiltration membranes, possessing pores in the range 0.1 - 2 μm, are relatively easy to characterise (see chapter IV). The main techniques employed are Scanning Electron Microscopy (SEM), bubble-point measurements, mercury porometry and

permeation measurements. The main problem encountered when microfiltration is applied (in the laboratory or in an industrial scale) is flux decline. This is caused by concentration polarisation and fouling (the latter being the deposition of solutes inside the pores of the membrane or at the membrane surface). Quite often considerable flux declines can be observed with values for process fluxes approximately 1% of the pure water flux being not unrealistic. This implies that for industrial applications the Hagen-Poiseuille and the Kozeny-Carman relations are of no relevance and other relations must be used. These phenomena will be discussed in detail in chapter VII. To reduce fouling as much as possible it is important that careful control is exercised over the mode of process operation. Basically, two process modes exist, i.e. dead-end and cross-flow filtration (see also chapter VIII). In dead-end filtration the feed flow is perpendicular to the membrane surface, so that the retained particles accumulate and form a type of a cake layer at the membrane surface. The thickness of the cake increases with filtration time and consequently the permeation rate decreases with increasing cake layer thickness. In cross-flow filtration the feed flow is along the membrane surface, so that part of the retained solutes accumulate. A schematic drawing of these processes is shown in figure VI - 6.

Adsorption phenomena may also play an important role in fouling and hence it is important to the select an appropriate membrane material. Hydrophobic materials of the type mentioned above have a larger tendency to foul in general, especially in the case of proteins. Furthermore, such hydrophobic materials (e.g. polytetrafluoroethylene) are not wetted by water and no water will flow through the membrane at normal applied pressures. This non-wettability is another disadvantage and such membranes have to be pretreat, for example with alcohol, prior to use with aqueous solutions.
Flux decline still occurs despite a proper choice of the process mode since it is an implicit part of the process and the membranes must be cleaned periodically. This implies that the choice of the membrane material is also important with respect to its stability relative to the
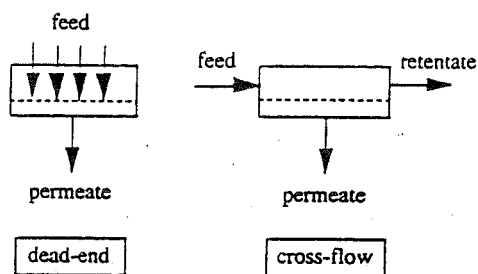

Figure VI - 6.   Schematic representation of dead-end filtration and cross-flow filtration.

cleaning procedure. An example of a chemical which is frequently used as a cleaning agent is active chlorine, towards which many polymers are not stable. Furthermore, resistance over a wide pH range is another requirement in chemical stability. Other applications, especially in biotechnology, require stability against steam sterilisation and this must extend over the whole module including the housing and potting materials.

Moreover, there many applications fro non-aqueous solutions in which an organic solvent is the continuous phase. Also here chemical stability is a first requirement.

All these examples clearly indicate that not only is the membrane performance important in microfiltration but particularly the chemical and thermal resistance of the materials used. Furthermore, the control of fouling is extremely important as well and this is discussed further in chapter VII.

VI.3.2.2 *Industrial applications*

Microfiltration is used in a wide variety of industrial applications where particles of a size > 0.1 μm, have to be retained from a liquid. The most important applications today are stil based on dead-end filtration using cartridges [2] and single membranes applied in all kinds of (analytical) laboratories. For the larger scale applications dead-end filtration will slowly be replaced by across-flow filtration. One of the main industrial applications is the sterilisation and clarification of all kinds of beverages and pharmaceuticals in the food and pharmaceutical industries. This can be done at any temperature, even at low temperatures. Microfiltration is also used to remove particles during the processing of ultrapure water in the semiconductor industry. New fields of application are biotechnology and biomedical technology. In biotechnology, microfiltration is especially suitable in cell harvesting and as a part of a membrane bioreactor (involving a combination of biological conversion and separation). In the biomedical field, plasmapheresis which involves the separation of plasma with its value products from blood cells appears to have an enormous potential. A number of applications are summarised below [2-4]:
- cold sterilisation of beverages and pharmaceuticals
- cell harvesting
- clarification of fruit juice, wine and beer
- ultrapure water in the semiconductor industry
- metal recovery as colloidal oxides or hydroxides
- waste-water treatment
- continuous fermentation
- separation of oil-water emulsions
- dehydration of latices

VI.3.2.3 *Summary of microfiltration*

membranes:	(a)symmetric porous
thickness:	≈ 10 -150 μm
pore sizes:	≈ 0.05 - 10 μm
driving force:	pressure (< 2 bar)
separation principle:	sieving mechanism
membrane material:	polymeric, ceramic
main applications:	- analytical applications
	- sterilisation (food, pharmaceuticals)
	- ultrapure water (semiconductors)

- clarification (beverages)
- cell harvesting and membrane bioreactor (biotechnology)
- plasmapheresis (medical)
- water treatment

VI.3.3   Ultrafiltration

Ultrafiltration is a membrane process whose nature lies between nanofiltration and microfiltration. The pore sizes of the membranes used range from 0.05 µm (on the microfiltration side) to 1 nm (on the nanofiltration side). Ultrafiltration is typically used to retain macromolecules and colloids from a solution, the lower limit being solutes with molecular weights of a few thousand Daltons. Ultrafiltration and microfiltration membranes can both be considered as porous membranes where rejection is determined mainly by the size and shape of the solutes relative to the pore size in the membrane and where the transport of solvent is directly proportional to the applied pressure. Such convective solvent flow through a porous membrane can be described by the Kozeny-Carman equation (see eq. VI - 27) for example. In fact both microfiltration and ultrafiltration involve similar membrane processes based on the same separation principle. However, an important difference is that ultrafiltration membranes have an asymmetric structure with a much denser toplayer (smaller pore size and lower surface porosity) and consequently a much higher hydrodynamic resistance.
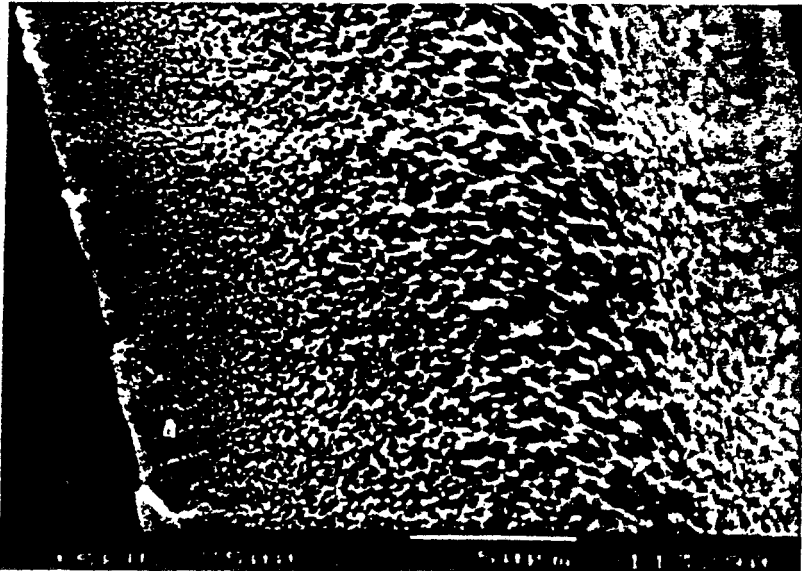
Figure VI - 7.   A scanning electron micrograph showing the cross-section of an ultrafiltration polysulfone membrane (magnification: 10,000 x).

The toplayer thickness in an ultrafiltration membrane is generally less than 1 μm with figure VI - 7 illustrating an example of an asymmetric polysulfone membrane.

The flux through an ultrafiltration membrane can be described in the same way as for microfiltration membranes, being directly proportional to the applied pressure:

$$J = K \ \Delta P$$

<div align="right">(V - 28)</div>

The permeability constant K includes all kinds of structural factors similar to microfiltration. The value of this constant K for ultrafiltration membranes is much smaller than for microfiltration membranes, being of the order of 0.5 m^3/m^2.day.bar for dense membranes up to about 5 m^3/m^2.day.bar for the more open membranes.

VI.3.3.1   Membranes for ultrafiltration

Most of ultrafiltration membranes used commercially these days are prepared from polymeric materials by a phase inversion process. Some of these materials are listed below:

- polysulfone/poly(ether sulfone)/sulfonated polysulfone
- poly(vinylidene fluoride)
- polyacrylonitrile (and related block-copolymers)
- cellulosics (e.g. cellulose acetate)
- polyimide/poly(ether imide)
- aliphatic polyamides
- polyetheretherketone

In addition to such polymeric materials, inorganic (ceramic) materials have also been used for ultrafiltration membranes, especially alumina (Al_2O_3) and zirconia (ZrO_2). Figure VI - 8 shows a multi-layer Al_2O_3 membrane in which the toplayer is prepared via a sol-gel technique [6].

Since the lower limit for preparing porous membranes by sintering is about 0.1 μm in pore diameter, this technique cannot be used to prepare ultrafiltration membranes. Such sintered porous structures can be used as the sublayer for composite ultrafiltration membranes, a technique frequently employed in the preparation of the ceramic ultrafiltration membranes. On the other hand, ultrafiltration membranes themselves are often used as sublayers in composite membranes for reverse osmosis, nanofiltration, gas separation and pervaporation.

Ultrafiltration is often applied for the concentration of macromolecular solutions where the large molecules have to be retained by the membrane while small molecules (and the solvent) should permeate freely. In order to choose a suitable membrane, manufacturers often used the concept of 'cut-off' but this concept should be considered critically (see chapter IV).

Figure VI - 8.   SEM photograph of a multi-layer inorganic Al_2O_3 membrane [6].

There are a number of other techniques besides cut-off measurements for characterising ultrafiltration membranes. However, typical methods for microfiltration membranes, such as mercury intrusion or scanning electron microscopy cannot be used for the characterisation of ultrafiltration membranes. For this reason, other techniques have been developed such as thermoporometry, liquid displacement and permporometry as have been discussed in chapter IV. Other more general techniques which are applicable are gas adsorption-desorption, permeability measurements and 'modified cut-off' measurements.

An important point which must be considered is that as in microfiltration the process performance is not equal to the intrinsic membrane properties in actual separations. The reason for this is again the occurrence of concentration polarisation and fouling. The macromolecular solute retained by the membrane accumulates at the surface of the membrane resulting in a concentration build-up. At steady state, the convective flow of the solute to the membrane is equal to the diffusional back-flow from the membrane to the bulk. Further pressure increase will not result in an increase in flux because the resistance of the boundary layer has increased (see chapter VII) so that a limiting flux value (J_∞) is attained (see figure VI - 9). As in microfiltration, these boundary layer phenomena mainly determine the process performance. Thus, intrinsic properties are not all that important in membrane development, but rather its chemical and thermal resistance and ability to reduce fouling tendency. The number of membrane applications increase as they become more resistant to higher temperatures (> 100°C), to a wide range of pH (1 to 14) and to organic solvents. Furthermore, as in microfiltration, module and system design are very important for reducing fouling as much as possible at a minimal cost.

VI.3.3.2   Applications
Ultrafiltration is used over a wide field of applications involving situations where high molecular components have to be separated from low molecular components. Applications
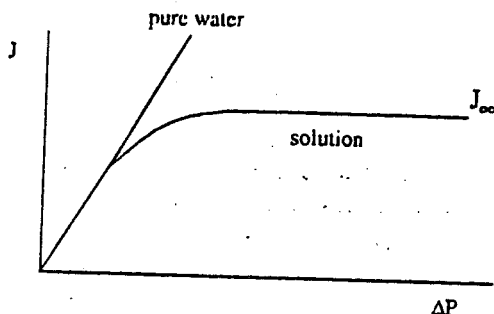
Figure VI - 9. Schematic drawing of the relationship between flux and applied pressure in ultrafiltration.

can be found in fields such as the food and dairy industry, pharmaceutical industry, textile industry, chemical industry, metallurgy, paper industry, and leather industry [4,7-9]. Various applications in the food and dairy industry are the concentration of milk and cheese making, the recovery of whey proteins, the recovery of potato starch and proteins, the concentration of egg products, and the clarification of fruit juices and alcoholic beverages.

Ultrafiltration membranes have been used up until now for aqueous solutions, but a new and developing field is in non-aqueous applications. For these latter applications, (new) chemical resistant membranes must be developed from more resistant polymers but inorganic membranes can be used as well.

VI.3.3.3 Summary of ultrafiltration

membranes:	asymmetric porous
thickness:	$\approx$ 150 μm (or monolithic for some ceramics)
pore sizes:	$\approx$ 1 - 100 nm
driving force:	pressure (1 - 10 bar)
separation principle:	sieving mechanism
membrane material:	polymer (e.g. polysulfone, polyacrylonitrile)
	ceramic (e.g. zirconium oxide, aluminium oxide)
main applications:	- dairy (milk, whey, cheese making)
	- food (potato starch and proteins)
	- metallurgy (oil-water emulsions, electropaint recovery)
	- textile (indigo)
	- pharmaceutical (enzymes, antibiotics, pyrogens)
	- automotive (electro paint)
	- water treatment

VI.3.4   Reverse osmosis and nanofiltration

Nanofiltration and reverse osmosis are used when low molecular weight solutes such as inorganic salts or small organic molecules such as glucose, and sucrose have to be separated from a solvent. Both processes are considered as one process since the basic principles are the same. At the end of this section the differences will be emphasized. The difference between ultrafiltration and nanofiltration/reverse osmosis lies in the size of the solute. Consequently, denser membranes are required with a much higher hydrodynamic resistance. Such low molecular solutes would pass freely through ultrafiltration membranes. In fact, the nanofiltration and reverse osmosis membranes can be considered as being intermediate between open porous types of membrane (microfiltration/ultrafiltration) and dense nonporous membranes (pervaporation/gas separation). Because of their higher membrane resistance, a much higher pressure must be applied to force the same amount of solvent through the membrane. Moreover, the osmotic pressure has to be overcome (The osmotic pressure of seawater, for example, is about 25 bar).
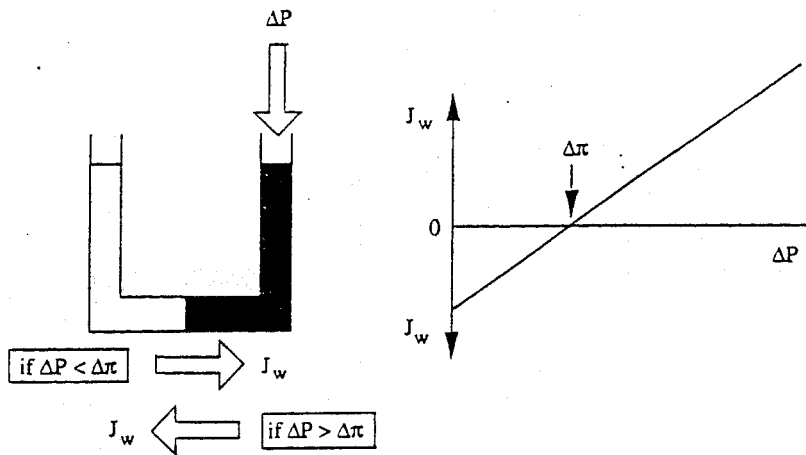
Figure VI - 10. Schematic drawing of water flow (J_w) as a function of applied pressure (ΔP).

Figure VI - 10 presents a schematic drawing of a membrane separating pure water from a salt solution. The membrane is permeable to the solvent (water) but not to the solute (salt). In order to allow water to pass through the membrane, the applied pressure must be higher than the osmotic pressure. As can be seen from figure VI - 10, water flows from the dilute solution (pure water) to the concentrated solution if the applied pressure is smaller than the osmotic pressure. When the applied pressure is higher than the osmotic pressure water flows from the concentrated solution to the dilute solution (see also figure VI - 1). The effective water flow can be represented by eq. VI - 29 if it is assumed that no solute

permeates through the membrane:

$$J_w = A \ (\Delta P - \Delta \pi)$$

<div align="right">(VI - 29)</div>

In practice, the membrane may be a little permeable to low molecular solutes and hence the real osmotic pressure difference across the membrane is not $\Delta \pi$ but $\sigma \ \Delta \pi$, where σ is the reflection coefficient of the membrane towards that particular solute (see also chapter V). When R < 100%, then σ < 1 and eq. VI - 21 now becomes

$$J_w = A \ (\Delta P - \sigma \ \Delta \pi)$$

<div align="right">(VI - 30)</div>

In the description considered here, we assume that the solute is completely retained by the membrane.

The water permeability coefficient A (also defined as the hydrodynamic permeability coefficient) is a constant for a given membrane and contains the following parameters (see also chapter V - 6.1).

$$A = \frac{D_w \ c_w \ V_w}{R \ T \ \Delta x}$$

<div align="right">(VI - 31)</div>

The value of A, which is a function of the distribution coefficient (solubility) and the diffusivity, lies roughly in the range $3.10^{-3} - 6.10^{-5} \ m^3.m^{-2}.h^{-1}.bar^{-1}$ for reverse osmosis while for nanofiltration the permeabilities range from 3.10^{-3} to $2.10^{-2} \ m^3.m^{-2}.h^{-1}.bar^{-1}$.

The solute flux can be described by

$$J_s = B \ \Delta c_s$$

<div align="right">(VI - 32)</div>

where B is the solute permeability coefficient and Δc_s the solute concentration difference across the membrane ($\Delta c_s = c_f - c_p$). The value of B lies in the range $5.10^{-3} - 10^{-4} \ m.h^{-1}$ for reverse osmosis with NaCl as solute with the lowest value for high rejection membranes. For nanofiltration membranes the retention for the various salts may vary considerably, e.g. the retention for NaCl may range from about 5 to 95 %, i.e. it is not very useful to give a range for the solute permeability coefficient for this process. The solute permeability coefficient B is a function of the diffusivity and the distribution coefficient as given by eq. VI - 33.

$$B = \frac{D_s \ K_s}{\Delta x}$$

<div align="right">(VI - 33)</div>

From eq. VI - 29 it can be seen that when the applied pressure is increased the water flux increases linearly. The solute flux (eq. VI - 32) is hardly affected by the pressure difference and is only determined by the concentration difference across the membrane.

The selectivity of a membrane for a given solute is expressed by the retention

coefficient or rejection coefficient R:

$$R = \frac{c_f - c_p}{c_f} = 1 - \frac{c_p}{c_f}$$

$$(VI - 34)$$

Consequently, as the pressure increases the selectivity also increases because the solute concentration in the permeate decreases. The limiting case R_{max} is reached as $\Delta p \Rightarrow \infty$. With $c_p = J_s/J_w$ and combining eqs. VI - 29, VI - 32 and VI - 34, the rejection coefficient can be written as:

$$R = \frac{A(\Delta P - \Delta \pi)}{A(\Delta P - \Delta \pi) + B}$$

$$(VI - 35)$$

Eq. VI - 35 is very illustrative since the only variable which appears in this equation is ΔP, assuming that the constants A and B are independent of the pressure (see also chapter VIII).

The pressures used in reverse osmosis range from 20 to 100 bar and in nanofiltration from about 10 to 20 bar, which are much higher than those used in ultrafiltration. In contrast to ultrafiltration and microfiltration, the choice of material directly influences the separation efficiency through the constants A and B (see eq. VI - 34). In simple terms, this means that the constant A must be as high as possible whereas the constant B must be as low as possible to obtain an efficient separation. In other words, the membrane (material) must have a high affinity for the solvent (mostly water) and a low affinity for the solute. This implies that the choice of material is very important because it determines the intrinsic membrane properties. The difference to ultrafiltration/ microfiltration, where the dimensions of the pores in the material determine the separation properties and the choice is mainly based upon chemical resistance, is obvious.

VI.3.4.1   Membranes for reverse osmosis and nanofiltration
The flux through the membrane is as important as its selectivity towards various kinds of solute. When a given material has been selected on the basis of its intrinsic separation properties, the flux through the membrane prepared from this material can be improved by reducing its thickness. The flux is approximately inversely proportional to the membrane thickness and for this reason most reverse osmosis membranes have an asymmetric structure with a thin dense toplayer (thickness $\leq$ 1 μm) supported by a porous sublayer (thickness $\approx$ 50 - 150 μm), the resistance towards transport being determined mainly by the dense toplayer. Two different types of membrane with an asymmetric structure can be distinguished: i) (integral) asymmetric membranes; and ii) composite membranes.

In integral asymmetric membranes, both toplayer and the sublayer consist of the same material. These membranes are prepared by phase inversion techniques. For this reason it is essential that the polymeric material from which the membrane it to be prepared is soluble in a solvent or a solvent mixture. Because most polymers are soluble in one or more solvents, asymmetric membranes can be prepared from almost any material.

However, this certainly does not imply that all such membranes are suitable for every reverse osmosis application because the material constants A and B must have optimal values for a given application. Thus for aqueous applications, e.g. the desalination of seawater and brackish water, hydrophilic materials should be used (high A value) with a low solute permeability.

An important class of asymmetric reverse osmosis membrane prepared by phase inversion are the cellulose esters, especially cellulose diacetate and cellulose triacetate. These materials are very suitable for desalination because of their high permeability towards water in combination with a (very) low solubility towards the salt. However, although the properties of membranes prepared from these materials are very good, their stability against chemicals, temperature and bacteria is very poor. Typical operation conditions of such membranes are over the pH range 5 to 7 and at a temperature below 30°C, thus avoiding hydrolysis of the polymer. The extent of this hydrolysis decreases as the degree of acetylation increases, and for this reason cellulose diacetate is less resistant than cellulose triacetate. Biological degradation is also a severe problem whilst another limitation of cellulose acetate membranes is their rather poor selectivity towards small organic molecules other than carbohydrates such as glucose or sucrose.

Other materials that have been used frequently for reverse osmosis membranes are aromatic polyamides. These materials also show high selectivities towards salts but their water flux is somewhat lower. Polyamides can be used over a wider pH range, approximately from 5 - 9. The main drawback of polyamides (or of polymers with an amide group -NH-CO in general) is their susceptibility against free chlorine Cl_2 which causes degradation of the amide group. Asymmetric membrane as well as symmetric membranes have been prepared from these polymers by melt or dry spinning to obtain hollow fibers with very small dimensions (outside diameters of such hollow fibers < 100 μm). The membrane thickness of these fibers is about $\approx$ 20 μm with the result that the permeation rate has decreased dramatically. However, this effect is counteracted by the extremely high membrane surface area in a given volume element, with values up to 30,000 m^2/m^3 (see also chapter VIII).

A third class of material that have been used are the polybenzimidazoles, polybenzimidazolones, polyamidehydrazide and polyimides. The chemical structures of these materials have been given in chapter II.

Composite membranes constitute the second type of structure frequently used in reverse osmosis while most of the nanofiltration membranes are in fact composite membranes. In such membranes the toplayer and sublayer are composed of different polymeric materials so that each layer can be optimised separately. The first stage in manufacturing a composite membrane is the preparation of the porous sublayer. Important criteria for this sublayer are surface porosity and pore size distribution and asymmetric ultrafiltration membranes are often used. Different methods have been employed for placing a thin dense layer on top of this sublayer;
- dip coating
- in-situ polymerisation
- interfacial polymerisation

- plasma polymerisation

Table VI.6. Example of monomers used for interfacial polymerisation

HN—NH + COCl—⟨⟩—COCl ⟶ —N—N—C(=O)—⟨⟩—C(=O)—

piperazine   m-terephthaloylchloride   polyamide

H₂—CH₂—NH + COCl—⟨⟩—COCl ⟶ —CH₂—CH₂—N—C(=O)—⟨⟩—C(=O)—N—CH₂—CH₂—
                    COCl   O=C
                                                      O⁻Na⁺

polyethyleneimine   trimesoylchloride   polyamide

water-soluble   organic solvent-   product
monomer   soluble monomer
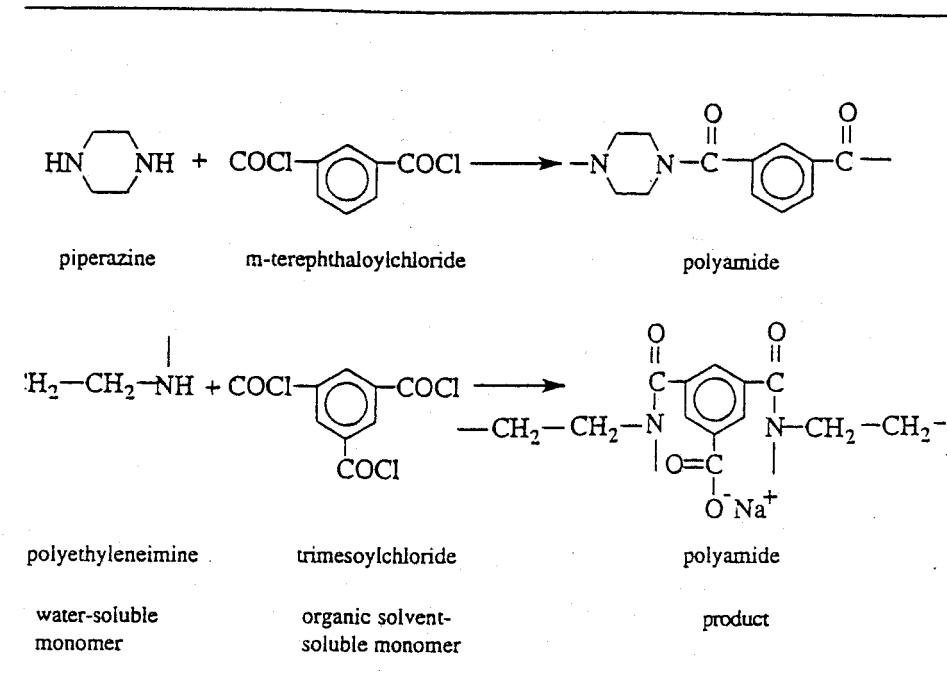
These various methods have been discussed in chapter III. Since reverse osmosis membranes may be considered as intermediate between porous ultrafiltration membranes and very dense nonporous pervaporation/gas separation membranes, it is not necessary that their structure to be as dense as for pervaporation/gas separation. Most composite reverse osmosis and nanofiltration membranes are prepared by interfacial polymerisation (see chapter III . 6) in which two very reactive bifunctional monomers (e.g. a di-acid chloride and a di-amine) or trifunctional monomers (e.g. trimesoylchloride) are allowed to react with each other at a water/organic solvent interface and a typical network structure is obtained. Another example of monomers used for interfacial polymerisation are given in table VI.6 (see also table III.1).

VI.3.4.2   Applications
Reverse osmosis can be used in principle for a wide range of applications, which may be roughly classified as solvent purification (where the permeate is the product) and solute concentration (where the feed is the product).

Most of applications are in the purification of water, mainly the desalination of brackish and especially seawater to produce potable water [10-13]. The amount of salt present in brackish water is between 1000-5000 ppm, whereas in seawater the salt concentration is about 35,000 ppm. Another important application is in the production of ultrapure water for the semiconductor industry.

Reverse osmosis is used as a concentration step particularly in the food industry (concentration of fruit juice, sugar, coffee), the galvanic industry (concentration of waste streams) and the dairy industry (concentration of milk prior to cheese manufacture).

Tabel VI.7. Comparison of retention characteristics between nanofiltration (NF) and reverse osmosis (RO)

solute	RO	NF
monovalent ions (Na, K, Cl,NO_3)	> 98%	< 50%
bivalent ions (Ca, Mg, SO_4,CO_3)	> 99%	> 90%
bacteria and virusses	> 99%	< 99%
microsolutes (Mw > 100)	> 90%	> 50%
microsolutes (Mw < 100)	0 - 99%	0 - 50%

Nanofiltration membranes are the same as reverse osmosis membranes only the network structure is more open. This implies that the retention for monovalent salts as Na^+ and Cl^- become much lower but the retention for bivalent ions such as Ca^{2+} and CO_2^{2-} remains very high. In addition the retention is high as well for micropollutants or microsolutes such as herbicides, insecticides, and pesticides and for other low molecular components such as dyes and sugars. It is clear that the application of both processes is different; when a high retention is required for NaCl with high feed concentrations reverse osmosis is the preferred process. In other cases with much lower concentrations, divalent ions and microsolutes with molecular weights ranging from 500 to a few thousand Dalton nanofiltration is the preferred process. Since the water permeability is (much) higher in nanofiltration the capital cost for a certain application will be lower. Table VI.7 compares qualitatively the rejection characteristics of nanofiltration and reverse osmosis towards some solutes.

VI.3.4.3   Summary of nanofiltration

membranes:	composite
thickness:	sublayer ≈ 150 μm; toplayer ≈ 1 μm
pore size:	< 2 nm
driving force:	pressure (10 - 25 bar)

separation principle: solution-diffusion
membrane material: polyamide (interfacial polymerisation)
main applications: - desalination of brackish water
                         - removal of micropollutents
                         - water softening
                         - waste water treatment
                         - retention of dyes (textile industry)

VI.3.4.4   *Summary of reverse osmosis*

---

membranes: asymmetric or composite
thickness: sublayer ≈ 150 μm; toplayer ≈ 1 μm
pore size: < 2 nm
driving force: pressure: brackish water 15 - 25 bar
                                 seawater 40 - 80 bar
separation principle: solution-diffusion
membrane material: cellulose triacetate, aromatic polyamide,
                       polyamide and poly(ether urea) (interfacial polymerisation)
main applications: - desalination of brackish and seawater
                       - production of ultrapure water (electronic industry)
                       - concentration of food juice and sugars (food industry), and
                         the concentration of milk (dairy industry).

VI.3.5   *Pressure retarded osmosis*

Pressure retarded osmosis (PRO) is a process derived from reverse osmosis. This process enables to generate energy from a concentration difference [14]. The principle is shown in figure VI - 11. If a semipermeable membrane separates a concentrated salt solution from water or a dilute solution then osmosis occurs and water flows from the dilute solution (or pure water) to the concentrated solution. Only when a pressure is applied higher than the osmotic pressure water flows from the concentrated solution to the diluted solution. The osmotic water flow can be used to generate electricity by means of a turbine.

The water flow at a pressure $\Delta P < \Delta \pi$ can be described by VI - 36 assuming complete rejection.

$$J_v = A \ (\Delta \pi - \Delta P) \hspace{4cm} (VI - 36)$$

The power E (Watt or J/s) per unit membrane area is given by the product of flux and pressure difference, i.e.

$$E = J_v \cdot \Delta P = A \ (\Delta \pi - \Delta P) \cdot \Delta P$$

(VI - 37)

The power is at maximum ($E = E_{max}$) at $dE/d(\Delta P) = 0 \implies \Delta P = 0.5 \ \Delta \pi$, which implies that

$$E_{max} = \frac{A}{4} \ \Delta \pi^2$$

(VI - 38)

This equation clearly shows the effect of the osmotic pressure on the maximum power. This process was evaluated on the basis of experiments with existing membranes and seawater as saline solution. In this case about 1.5 W/m^2 was produced but as a more concentrated solution is used the energy production will increase drastically. However, there are a number of practical problems.
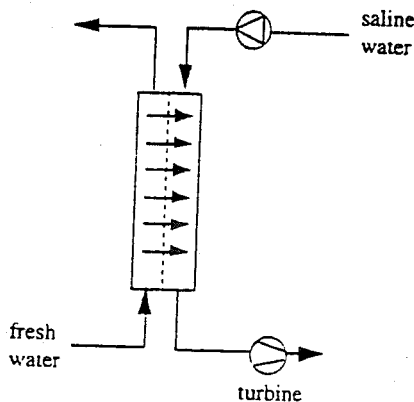
Figure   VI - 11   Principle of pressure retarded osmosis.

- osmosis; because of osmosis the concentration of the concentrated solution will decrease and consequently the osmotic pressure decreases.
- salt flux: when the membrane is not perfectly semipermeable (R < 100%) a salt flux occurs from the concentrated to the dilute side and as a result the osmotic pressure will decrease.
- concentration polarisation. The severest problem is the occurrence of concentration polarisation (see chapter VII) which implies that the concentration at both membrane surfaces is different from that in the bulk (see figure VI - 12). The salt flux will cause an increased concentration in the sublayer, which can be considered as a stagnant layer, causing a decrease in effective osmotic pressure difference. This effect will decrease as J_s $\implies$ 0, which means that perfect semipermeable membranes (R = 100%) must be developed.
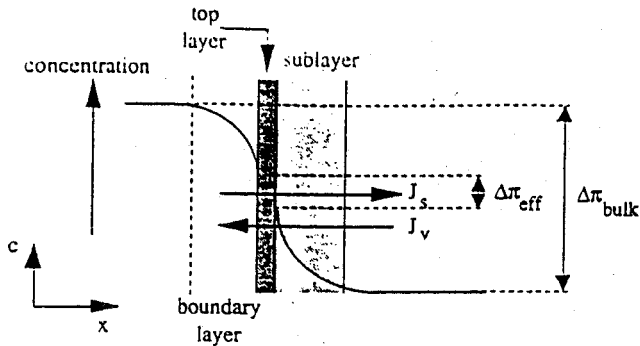
Figure VI - 12. Concentration polarisation in pressure retarded osmosis.

VI.3.5.1   Summary of pressure retarded osmosis

membranes:	asymmetric or composite
thickness:	sublayer $\approx$ 150 μm; toplayer $\approx$ 1 μm
pore size:	< 2 nm
driving force:	concentration difference (osmotic pressure)
separation principle:	solution-diffusion
membrane material:	cellulose triacetate, aromatic polyamide,
	poly(ether urea) (interfacial polymerisation)
main applications:	- production of energy

VI.3.6   Piezodialysis

Another membrane process which uses pressure as the driving force is piezodialysis [15-17]. This process is applied with ionic solutes where in contrast to reverse osmosis, the ionic solutes permeate through the membrane rather than the solvent, which is usually water. A schematic drawing of the process is given in figure VI - 13.

If a pressure is applied at one side of the membrane an electromotive force (ΔE) will be generated   which is proportional to the applied pressure difference (ΔP).   The proportionality constant is called the electric osmotic coefficient β. This coefficient is negative for anion-exchange membranes and positive for cation-exchange membranes

$$\Delta E = -\beta \Delta P \qquad\qquad\qquad\qquad (VI - 39)$$
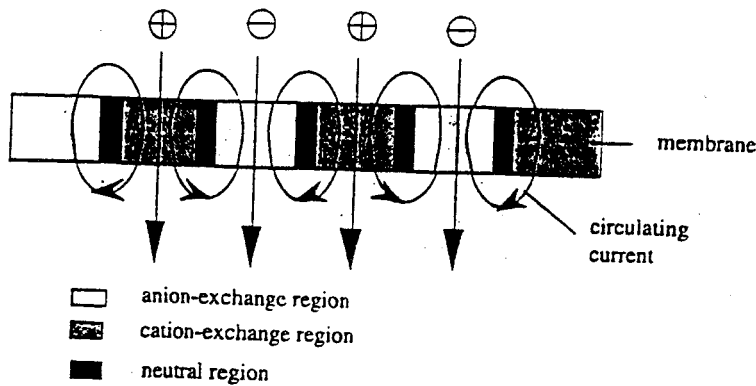
Figure VI - 13. The transport of ions through a mosaic membrane during piezodialysis

So-called mosaic membranes must be used for this process. These are ion-exchange membranes possessing both cation-exchange and anion-exchange groups separated by a neutral region. Due to the generation of a current loop, anions will be transported through the anion-exchange region and cations are trasnported through the cation-exchange region. Electroneutrality is maintained by the simultaneous passage of cations and anions through the membrane. Since ion transport is favoured relative to solvent transport, the salt concentration in the permeate is higher than that in the feed. This allows a dilute salt solution to be concentrated and a salt enrichment by a factor of two can be achieved. An increase in salt flux can be obtained by increasing the ion-exchange capacity of the membrane. Although the basic principle of the piezodialysis process has been demonstrated in the laboratory, it has not been employed on a commercial scale.

VI.3.6.1   Summary of piezodialysis

membranes:	mosaic membranes (with cation-exchange regions adjacent to anion-exchange regions)
thickness:	$\approx$ few hundred μm
pore size:	nonporous
driving force:	pressure, up to 100 bar
separation principle:	ion transport (Coulomb attraction and electroneutrality)
membrane material:	cation/anion-exchange membrane
application:	salt enrichment

VI.4.   Concentration difference as the driving force

VI.4.1   Introduction

In many processes, including those in nature, transport proceeds via diffusion rather than convection. Substances diffuse spontaneously from a high to a low chemical potential. Processes which make use of a concentration difference as the driving force are gas separation, vapour permeation, pervaporation, dialysis, diffusion dialysis, carrier mediated processes and membrane contactors (In pervaporation, gas separation and vapour permeation it is preferred to express the driving force as a partial pressure difference or an activity difference rather than concentration difference). On the basis of differences in structure and functionality it is possible to distinguish between processes that use a synthetic solid (polymeric or sometimes ceramic or zeolitic) membrane (gas separation, dialysis and pervaporation) and those that use a liquid (with or without a carrier) as the membrane.

Whereas the pressure driven processes microfiltration, ultrafiltration, nanofiltration and reverse osmosis are more or less similar processes, dialysis, gas separation and pervaporation differ quite considerably from each other. The basic feature that they have in common is the use of a nonporous membrane. It should be noticed that the term nonporous gives no information about the permeability of a certain species. It was shown in chapter II that the permeability of a gas through an elastomeric and a glassy material may differ by more than five orders of magnitude, despite both materials being nonporous. This difference arises from large differences in segmental motion which is very restricted in the glassy state or by the presence of a large free volume.
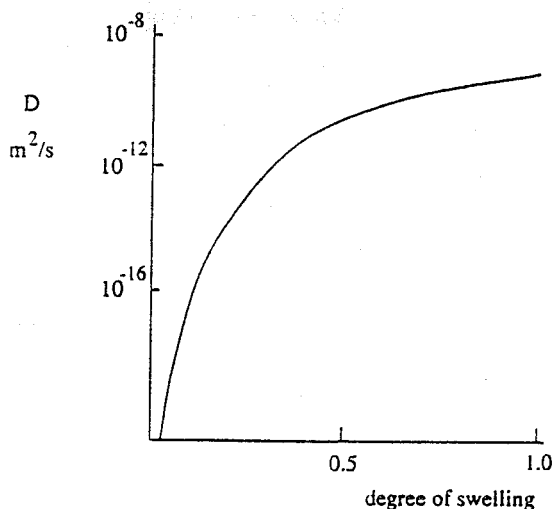
Figure VI - 14. Diffusivity as a function of the degree of swelling in nonporous polymers.

The presence of crystallites can further reduce the mobility. A factor that enhances segmental mobility, or chain mobility in general, is the presence of low molecular penetrants. Increasing concentrations of penetrants (either gas or liquid) inside the polymeric membrane leads to an increase in the chain mobility and consequently to an increase in permeability (or diffusivity). The concentration of penetrant inside the polymeric membrane is determined mainly by the affinity between the penetrant and the polymer and the concentration (or activity) of the penetrant in the feed. In gas separation with inert gases such as helium, hydrogen, nitrogen and oxygen, there is hardly any interaction between the gas molecules and the membrane material and the gas concentration in the membrane is very low at low feed pressures. The gas molecules must diffuse through a rigid membrane structure in the case of glassy materials with the state of the polymer being hardly effected by their presence. However, even for 'low affinity' penetrants of this type, there is a difference between the inert nitrogen and carbon dioxide, for example. In contrast, with liquid penetrants the solubility in the membrane may be appreciably higher which results in an enhanced chain mobility. An even greater interaction between liquid and membrane may occur in dialysis resulting in a much greater swelling of the polymer which allows relatively large molecules diffuse through this kind of open membrane. Figure VI - 14 shows schematically how the diffusion coefficient of a low molecular weight component changes as the degree of swelling of the membrane increases (the swelling of the membrane being defined as the weight fraction of penetrant inside the membrane relative to the weight fraction of dry polymer). It will be seen that the diffusion coefficient can vary over the range 10^{-19} to 10^{-9} m^2/s. This demonstrates quite clearly, that the mobility of the polymer chains increases with increasing swelling so that a situation is attained where the diffusivity is comparable to diffusion in a liquid (the diffusion coefficient in liquids is $\approx 10^{-9}$ m^2/s). Thus swelling, as a result of interaction between the penetrant and the polymer, is a very important factor in transport through nonporous membranes.

Figure VI - 14 demonstrates that the diffusion coefficient can change by up to 10 orders of magnitude. Thus the diffusion coefficient of benzene in poly(vinyl alcohol) at zero penetrant concentration is less than 10^{-19} m^2/s [18], whereas the diffusion coefficient of water in hydrogels is greater than 10^{-9} m^2/s, which is virtually equal to value of the self-diffusion coefficient of water.

VI.4.2   Gas separation

Gas separation is possible even with the two extreme types of membrane considered, i.e. porous and nonporous. The transport mechanisms through these two types of membrane, however, are completely different as discussed already in chapter V.

VI.4.2.1   Gas separation in porous membranes

When gas transport takes place by viscous flow (as in the case of a microfiltration membrane, for example), no separation is achieved because the mean free path of the gas molecules is very small relative to the pore diameter. By decreasing the pore diameter of

the pores in the membrane the mean free path of the gas molecules may become greater than the pore diameter. This kind of gas flow is called Knudsen flow which may be expressed by the equation:

$$J \;=\; \frac{\pi\, n\, r^2\, D_k\, \Delta p}{R\,T\,\tau\,\ell}$$

(VI - 40)

where D_k, the Knudsen diffusion coefficient, is given by $D_k = 0.66 \; r \; \sqrt{\dfrac{8\,R\,T}{\pi\,M_w}}$

T and M_w are the temperature and molecular weight, respectively and r is the pore radius. Eq. VI - 40 shows that the flow is inversely proportional to the square root of the molecular weight and the latter is the only parameter which determines the flow for a given membrane and a given pressure difference. Hence, the separation of two gases by a Knudsen flow mechanism depends on the ratio of the square root of their corresponding molecular weights. This means that low separation factors are generally obtained. High separation can only be achieved via a cascade operation involving a number of modules connected together (see chapter VIII). For economical reasons this is very unattractive and thus the only commercial application of this method to date has been the enrichment of uranium hexafluoride ($^{235}UF_6$), a very expensive material. The separation factor obtained in the separation of $^{235}UF_6$ from $^{238}UF_6$ is extremely low (the ideal separation factor is 1.0064, but this factor will not be attained in the practical situation). A plant employing this application method using porous ceramic membranes operates in France (at Tricastin). However, there is another aspect to Knudsen flow. Where the transport of gases occurs through nonporous membranes, as will be discussed in the following section, Knudsen flow is not involved. However, when these nonporous membranes are used in a composite membrane where a dense toplayer is supported by a porous substructure, Knudsen flow may contribute to the total flow depending on the pore sizes in the sublayer.

VI.4.2.2   Gas separation through nonporous membranes
Gas separation through nonporous membranes depends on differences in the permeabilities of various gases through a given membrane. Figure VI - 15 gives a schematic drawing of a nonporous membrane separating two gas phases.
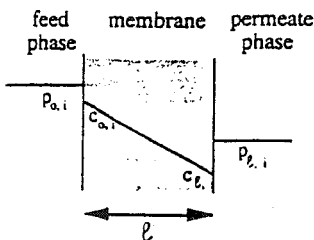
Figure VI - 15.   Nonporous membrane separating two gas phases

Fick's law is the simplest description of gas diffusion through a nonporous structure, i.e.

$$J = - D \frac{dc}{dx}$$

(VI - 41)

where J is the flow rate through the membrane, D is the diffusion coefficient and the driving force dc/dx is the concentration gradient across the membrane. Under steady-state conditions this equation can be integrated to give:

$$J_i = \frac{D_i \left(c_{o,i} - c_{\ell,i} \right)}{\ell}$$

(VI - 42)

where $c_{o,i}$ and $c_{\ell,i}$ are the concentrations in the membrane on the upstream side and downstream side, respectively, whereas ℓ is the thickness of the membrane.

The concentrations are related to the partial pressures by Henry's law which states that a linear relationship exists between the concentration inside the membrane (c_i) and the (partial) pressure of gas outside the membrane (p_i), i.e.

$$c_i = S_i \cdot p_i$$

(VI - 43)

where S_i (cm³(STP)/cm³.bar) is the solubility coefficient of component i in the membrane. Henry's law is mainly applicable to amorphous elastomeric polymers for the solubility behaviour is very often much more complex below the glass transition temperature, as has been described in chapter V.

Combining eq. VI - 42 with eq. VI - 43 gives

$$J_i = \frac{D_i S_i \left(p_{o,i} - p_{\ell,i} \right)}{\ell}$$

(VI - 44)

an equation which is generally used for the description of gas permeation through membranes. The product of the diffusion coefficient D and the solubility coefficient S is called the permeability coefficient P, i.e.

$$P = D \cdot S$$

(VI - 45)

so that eq.VI - 44 can be written as:

$$J_i = \frac{P_i \left(p_{o,i} - p_{\ell,i} \right)}{\ell} = \frac{P_i}{\ell} \Delta p_i$$

(VI - 46)

Eq. VI - 46 shows that the flow rate across a membrane is proportional to the difference in (partial) pressure and inversely proportional to the membrane thickness. The ideal selectivity is given by the ratio of the permeability coefficients:

$$\alpha_{i/j \; ideal} \;\; = \;\; \frac{P_i}{P_j}$$

<div style="text-align: right">(VI - 47)</div>

With a number of gaseous mixtures, the real separation factor is not equal to the ideal separation factor because of plasticisation which may occur at high (partial) pressures when a permeating gas exhibits a high chemical affinity for the polymer. Because of such plasticisation, the permeability increases but the selectivity decreases generally.
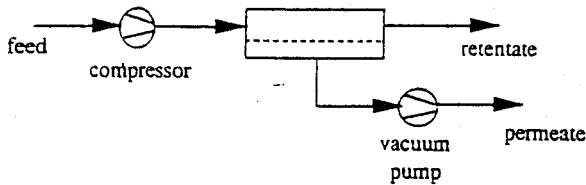
Figure VI - 16.   Schematic drawing of a gas separation process.

The real separation factor also depends on the pressure ratio across the membrane. In the case of a high pressure ratio ($p_\ell /p_o \Rightarrow 0$) the separation efficiency is a maximum and the selectivity decreases as the pressure ratio decreases (see also chapter VIII). The driving force can be established either by applying a high pressure on the feed side and/or maintaining a low pressure on the permeate side. A schematic drawing of such a gas separation process is shown in figure VI - 16.

VI.4.2.3.   Aspects of separation

The permeability coefficient P is a very characteristic parameter which is often described as a constant intrinsic parameter easily available from simple permeation experiments with membranes of known thickness (using eq. VI - 46). The permeability coefficient is often given in Barrer units. (1Barrer = 10^{-10} cm^3(STP).cm.cm^{-2}.s^{-1}.cmHg^{-1} = 0.76 10^{-17} m^3(STP).m.m^{-2}.s^{-1}.Pa^{-1}).

The dimension of the permeability coefficient indicates the invariancy with respect to the membrane thickness, the membrane area and the driving force, i.e. it is a normalized parameter. However, in the case of interactive systems where Henry's law does not apply anymore, the permeability coefficient P is no longer a constant but is related to the driving force, i.e. varying the pressure leads to different values for P and this dependency must be taken into account. To describe the fundamentals of gas separation, however, other factors relating to the nature of the polymer (i.e. chemical structure) need to be considered. Two parameters are important in this context: *i)* the glass transition temperature and *ii)* the crystallinity. The glass transition temperature determines whether a polymer is in the

glassy or in the rubbery state. Segmental motion is limited for an amorphous polymer in the glassy state, whereas in the rubbery state enough thermal energy is available to allow rotation in the main chain. The glass transition temperature is mainly determined by chain flexibility and chain interaction. These parameters have been discussed in detail in chapter II.

In general, permeability through a rubbery material (elastomer) is much higher relative to glassy polymers because of the higher mobility of the chain segments. In

Table VI.8.   The permeability of carbon dioxide and methane in various polymers [19-21,27]

polymer	P_{CO_2} (Barrer)	P_{CO_2}/P_{CH_4}
polytrimethylsilylpropyne	33100	2.0
silicone rubber	3200	3.4
natural rubber	130	4.6
polystyrene	11	8.5
polyamide (Nylon 6)	0.16	11.2
poly(vinyl chloride)	0.16	15.1
polycarbonate (Lexan)	10.0	26.7
polysulfone	4.4	30.0
polyethyleneterephthalate (Mylar)	0.14	31.6
cellulose acetate	6.0	31.0
poly(ether imide) (Ultem)	1.5	45.0
poly(ether sulfone) (Victrex)	3.4	50.0
polyimide (Kapton)	0.2	64.0

1 Barrer = 10^{-10} cm^3(STP).cm.cm^{-2}.s^{-1}.cmHg^{-1}

contrast, the selectivity of glassy polymers is higher. Table VI.8 lists the permeability of carbon dioxide (in Barrer) and the ratio of the permeabilities (the ideal selectivity) of carbon dioxide and methane in various polymers. These results indicate that elastomers exhibit high permeabilities and low selectivities whereas glassy polymers show much lower permeabilities but generally higher selectivities. There is however no unique relationship between the glass transition temperature and permeability, or in other words the permeability of a rubber is not 'a priori' greater than that of a glassy polymer. Table VI - 9 summarises some examples where the permeability of glassy polymers are higher than those of elastomers. These examples have only been given in order to demonstrate that exceptions exist to the rule that the permeability of elastomers is higher than that of glassy polymers. The rule applies in general of course, with the vast majority of elastomers having a higher permeability than most of the glassy polymers. Only in those cases where the fractional free volume of the polymer is high (e.g. polytrimethylsilylpropyne and to a

lesser extent polyphenyleneoxide) high permeabilities are obtained.

Table VI.9.   The permeability of oxygen and nitrogen for some elastomers and glassy polymers [19-21]

Polymer	Tg (°C)	P_{O2} (Barrer)	P_{N2} (Barrer)	α_{ideal} (P_{O2}/P_{N2})
PPO	210	16.8	3.8	4.4
PTMSP	≈ 200	10040.0	6745.0	1.5
ethylcellulose	43	11.2	3.3	3.4
polymethylpentene	29	37.2	8.9	4.2
polypropylene	-10	1.6	0.3	5.4
polychloroprene	-73	4.0	1.2	3.3
polyethylene LD	-73	2.9	1.0	2.9
polyethylene HD	-23	0.4	0.14	2.9

The basic concept of gas separation is governed by the permeability coefficient (P) which is equal to the product of the solubility (S) and the diffusivity (D). In comparison to liquids the affinity of gas molecules towards a polymer is generally much lower and hence the solubility of gases in polymers is quite low (generally < 0.2%). The solubility is mainly determined by the ease of condensation. Because larger molecules condense more readily, their solubility increases. This can be illustrated by the example of the noble gases. Such gases show no polymer interaction and their solubility is determined only by their ease of condensation. Hence the solubility increases with increasing size of the gas molecules (and with increasing critical temperature or boiling temperature) in the sequence: neon, argon, krypton, and xenon [22]. Thus the solubility of neon in silicone rubber is 0.04 cm^3(STP).cm^{-3}.atm^{-1} whereas for krypton a value of 1.0 cm^3(STP).cm^{-3}.atm^{-1} is found [22]. Solubility of a given gas molecule increases as its polymer affinity increases. For example the solubility of carbon dioxide in hydrophilic polymers is generally higher than in more hydrophobic polymers. The other factor affecting permeability is the diffusivity. It depends mainly on two factors: the molecular size of the gaseous penetrant and the choice of the polymer. The size of the gas molecule is reflected in the diffusion coefficient, i.e. the smaller its size the higher the diffusion coefficient. Indeed, a close examination of the dimensions of gas molecules provides some interesting results. Table VI.10 summarises the kinetic diameters of some relevant gas molecules [23].

Thus, although the molecular weight of oxygen is greater than that of nitrogen, the molecular dimensions of oxygen are smaller. Hence when the permeability is considered in terms of diffusivities oxygen will generally have a higher permeability than nitrogen. The tables of permeability coefficients (tables VI.8 and VI.9) demonstrate that this is

indeed the case, not only for glassy polymers but also for elastomers. Only in glassy polymers is the separation factor generally higher.

Table VI.10   The kinetic diameter of
some gas molecules [23]

gas molecule	diameter (Å)
He	2.6
Ne	2.75
H_2	2.89
NO	3.17
CO_2	3.3
C_2H_2	3.3
Ar	3.4
O_2	3.46
N_2	3.64
CO	3.76
CH_4	3.80
C_2H_4	3.9
C_3H_8	4.3

It has already been shown in chapter V that the thermodynamic diffusion coefficient can be expressed as:

$$D_T = \frac{kT}{f}$$

(VI - 48)

where f is the frictional coefficient. Stokes' law demonstrates that the frictional coefficient is related to the size of the diffusing molecule by:

$$f = 6\pi\eta r$$

(VI - 49)

Combination of eq. VI - 48 with eq. VI - 49 for ideal systems ($D_T = D$) gives

$$D = \frac{kT}{6\pi\eta r}$$

(VI - 50)

This relationship shows that the diffusion coefficient is inversely proportional to the molecular size. Although not very accurate for the diffusion of gases in polymers, this relationship does illustrate the link between the diffusion coefficient and the size. Relative small differences in size may have a very large effect on the diffusion coefficient. For

example, the diffusion coefficient of neon (M_w : 20 g/mol) in polymethylmethacrylate (PMMA) is approximately 10^{-10} m^2s^{-1} and for krypton (M_w : 83.8 g/mol) approximately 10^{-12} m^2s^{-1} [22] (see also chapter V). The diffusion coefficient also depends strongly on the nature of the polymer. For example the diffusion coefficient of krypton in polydimethylsiloxane is about 10^{-9} m^2s^{-1} while for the same gas in PVA values of 10^{-13} m^2s^{-1} have been reported, i.e. four orders of magnitude lower [22].

A comparison of the separation properties requires an evaluation not of the solubilities and diffusivities but rather their respective ratio. Table VI.11 lists the ratios of the solubilities (S), diffusivities (D) and permeabilities (P) for CO_2 and CH_4 in some glassy polymers [24].

Table   VI.11   Ratios of the diffusivities, solubilities and permeabilities of CO_2 and CH_4 in various polymers [24]

polymer	D_{CO_2}/D_{CH_4}	S_{CO_2}/S_{CH_4}	P_{CO_2}/P_{CH_4}
cellulose acetate	4.2	7.3	30.8
polyimide	15.4	4.1	63.6
polycarbonate	6.8	3.6	24.4
polysulfone	8.9	3.2	28.3

The affinity of carbon dioxide for a given polymer is (much) higher than that of methane. This can be clearly seen from table VI.11, where in cellulose acetate or other ester-containing polymers the solubility of CO_2 is especially high and a high solubility ratio can be found. However, it appears that high selectivities are not necessarily based on large differences in solubility, but that diffusivity or changes in diffusivity in particular have a much stronger effect on the selectivity. Thus, the polyimide shown in the table (Kapton) is a glassy polymer with a very rigid structure. Table VI.11 shows that for such polymers it is mainly the diffusivity ratio which determines the selective transport, suggesting the existence of a microstructures which is able to discriminate on a molecular level. Because molecules of almost the same size can be separated this implies that openings (in terms of free volume) with very definite dimensions exist within the polymeric matrix which allow smaller molecules to pass (much) more readily than larger ones. These kinds of very rigid structure are quite similar to those in zeolites (or molecular sieves) which also contain very definite structures. Such behaviour may be observed not only for the CO_2/CH_4 separation but also for the separation of oxygen and nitrogen. Almost all polymers have selectivity factors (or P_{O_2}/P_{N_2}) between 2 and 6 [25], but some rigid glassy polymers, similar to the polyimide mentioned above, have higher selectivities.

It is assumed that it is the very definite pore structure which exclude the larger nitrogen molecule to a greater extent than the smaller oxygen molecule. Hence, separation is determined by the selective diffusion of oxygen to nitrogen rather than specific interaction. This means that highly selective polymers capable of separating permanent

gases should be glassy polymers rather than elastomers. Furthermore, the microstructure seems to be much more important than the existence of specific interactions. However, the permeability is often very low and differences in permeability can be as much as six orders of magnitude (compare the permeabilities of various gases through poly(vinyl alcohol) or polyacrylonitrile with that through polydimethylsiloxane).

Up to this point it has been demonstrated that the permeability of a gas depends very much on the choice of the polymer. However, when different gases are used with the same polymer (membrane) large differences in permeability can be observed. This is especially true for organic vapours where differences can extend over six orders of magnitude. The difference between a gas and a vapour lies in the fact that vapours are condensable under standard conditions (0°C and 1 bar). Table VI.12 gives the permeabilities of various gases and vapours in polydimethylsiloxane [26] , the vapour values having been measured at an activity of $a = 1$ ($p = p°$).

Table VI.12.   Permeabilities of various gases and
vapours in polydimethylsiloxane [26].

Component	Permeability (Barrer)
nitrogen	280
oxygen	600
methane	940
carbon dioxide	3200
ethanol	53,000
methylene chloride	193,000
carbon tetrachloride	290,000
1,2-dichloroethane	248,000
1,1,1-trichloroethane	247,000
chloroform	329,000
trichloroethylene	740,000
toluene	1,106,000

Although the kinetic dimensions of the various organic vapour molecules are much larger than those of oxygen and nitrogen, the permeabilities are much higher. Because the permeability is determined by the solubility and the diffusivity, this suggests that the high permeability originates from a much higher solubility. Organic vapour molecules exert a plasticising action on the polymer, i.e. the polymer chains become much more flexible, alternatively the free volume increases considerably. This effect increases with increasing solubility and an exponential relation is often found.

It is also possible to derive an exponential relationship from the free volume theory   as was described in chapter V. The following empirical relationship is often used:

$$D = D_0 \exp (\phi \cdot \gamma) \qquad\qquad (VI - 51)$$

where D_0 is the diffusion coefficient at zero penetrant concentration. γ is a constant related to the plasticising effect of the penetrant on the polymer and ϕ is the volume fraction of the penetrant in the membrane. The concentration dependence of the diffusion coefficient is not the same for all polymers. D_0 is mainly determined by the penetrant size and shape, and by the choice of the polymer. For a given polymer, D_0 decreases with increasing penetrant size: for example, the value of D_0 for methanol in poly(vinyl alcohol) is about three orders of magnitude larger than the D_0 value for n-propanol [9].For a given penetrant, D_0 increases with increasing chain flexibility. Hence D_0 increases drastically in going from a glassy polymer to an elastomer; for example, the D_0 value of benzene in poly(vinyl alcohol) is about ten orders of magnitude lower than that of benzene in polydimethylsiloxane (silicone rubber). A correlation between D_0 and T_g has been proposed but glassy polymers as poly(dimethylphenylene oxide) and polytrimethylsilylpropyne also show very high permeabilities which stem from very high diffusivities.

The solubility of organic vapours in (glassy) polymers is generally much higher than that of permanent gases in the same polymer. Whereas Henry's law can be used in the latter case, with organic vapours the solubility can be described by Flory-Huggins thermodynamics, as for liquids.

VI.4.2.4   Joule-Thomson effect

A very peculiar phenomenon in gas separation is the occurrence of the Joule-Thomson effect. This occurs if a gas is expanded across a membrane, as in the case of a gas permeation process. In the case of such an (adiabatic) expansion of a real gas, the temperature may change to a large extent dependent on the type of gas and the pressure applied (for ideal gases the temperature does not change). In turn, this temperature change may have a large influence on the permeation properties, i.e., if the temperature decreases generally the flux decreases and the selectivity increases. The principle will be demonstrated by a simple experiment as shown schematically in figure VI - 17.
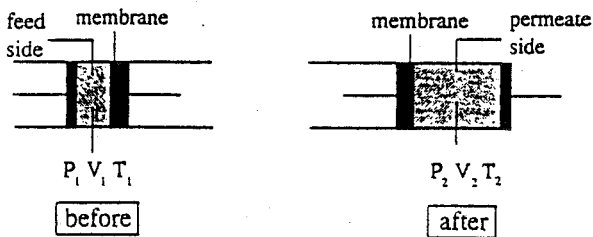
Figure VI - 17   Schematic representation of the principle of the Joule-Thompson effect

A gas passes a membrane from the high pressure side (subscript 1) to the low pressure side (subscript 2). This process is assumed to occur adiabatically, i.e. the whole system has been isolated and no heat transfer occurs ($q = 0$). The internal energy change of this process ΔU is equal to

$$\Delta U = U_2 - U_1 = -P_2 V_2 + P_1 V_1 \qquad (VI - 52)$$

or

$$U_1 + P_1 V_1 = U_2 + P_2 V_2 \qquad (VI - 53)$$

or

$$H_1 = H_2 \qquad (VI - 54)$$

This implies that this process occurs isenthalpic. The temperature change in this process is expressed by the differential equation $(\partial T/\partial P)_H$, which is called the Joule-Thompson coefficient μ_{JT}. If the enthalpy of a gas H is considered to be dependent on T and P then the total differential of H is given by

$$dH = \left(\frac{\partial H}{\partial P}\right)_T dP + \left(\frac{\partial H}{\partial T}\right)_P dT \qquad (VI - 55)$$

Furthermore,

$$\left(\frac{\partial H}{\partial T}\right)_P = c_P \qquad (VI - 56)$$

and

$$\left(\frac{\partial T}{\partial P}\right)_H = -\left(\frac{\partial T}{\partial H}\right)_P \left(\frac{\partial H}{\partial P}\right)_T \qquad (VI - 57)$$

For the enthalpy change of a reversible process we can write

$$dH = V\, dP + T\, dS \qquad (VI - 58)$$

differentiation with respect to P at constant temperature gives

$$\left(\frac{\partial H}{\partial P}\right)_T = V + T\left(\frac{\partial S}{\partial P}\right)_T \qquad (VI - 59)$$

From the Maxwell's relations we have

$$-\left(\frac{\partial S}{\partial P}\right)_T = \left(\frac{\partial V}{\partial T}\right)_P \tag{VI - 60}$$

Substitution of eqs. VI - 56, VI - 59 and VI - 60 into VI - 57 gives

$$\left(\frac{\partial T}{\partial P}\right)_H = \mu_{JT} = -\frac{1}{c_p}\left[V - T\left(\frac{\partial V}{\partial T}\right)_P\right] \tag{VI - 61}$$

Depending on the relative magnitude of the two terms between brackets the gas is either cooled or warmed upon pressurizing. Some values of μ_{JT} of various gases is given in table VI.13.

<div align="center">

Table   VI.13.   Joule-Thomson coefficient
of various gases at 1 bar and 298 K

gas	μ_{JT} (K/bar)
He	- 0.06
CO	0.01
H_2	0.03
O_2	0.30
N_2	0.25
CH_4	0.70
CO_2	1.11

</div>

It can be seen clearly that temperature decrease in gas separation depends on the type of gas. Hydrogen will give a small temperature difference only but carbon dioxide may give a tremendous temperature decrease at high applied pressure. It is clear that in in the latter case the separation performance is affected as well and that the Joule-Thomson effect should be taken into account when carbon dioxide is removed at a high pressure.

VI.4.2.5   Membranes for gas separation

Table VI.8 showed that the permeability of a given gas molecule in various polymers can change by more than six orders of magnitude. Equally, table VI.11 also shows that for a given polymer the permeability of various gas and vapour molecules can change over six orders of magnitude. This large variation in permeability shows that in principle many materials can be used as a membrane depending on the application. Gas separation is not only based on permeability but also on the selectivity, which is equal to the ratio of the permeabilities for gas mixtures.

For separation problems involving large differences in interaction, e.g. gases from

vapours, the permeability ratio is usually large (see table VI.11) and for this reason a highly permeable material may be chosen. In general, these are elastomers such as silicone rubber or natural rubber. Elastomers show rather low selectivities for some separations and glassy polymers with a much lower permeability are often used. It can be seen from eq. VI - 47 that the permeation rate (= P / ℓ) varies inversely with membrane thickness. For this reason the permeation properties can be optimised by minimising the effective membrane thickness. Therefore two types of membranes are very suitable for gas separation:
- asymmetric membranes
- composite membranes

Asymmetric membranes are mainly prepared by immersion precipitation whereas this technique is also used for the sublayer in composite membrane upon which a very thin selective layer is deposited by one of the following techniques:
- dip-coating
- interfacial polymerisation
- plasma polymerisation

All these techniques have been described in chapter III. In both asymmetric and composite membranes the hydrodynamic resistance is determined largely by the thin dense toplayer. This toplayer must be absolutely defect-free, since a few defects can significantly reduce the selectivity without having much influence on the flux. In addition, the following requirements are necessary for the porous support layer:
- it must provide mechanical support for the toplayer
- it must have an open porous network to minimise resistance to mass transfer (no closed pores !)
- it must not contain macrovoids (weak spots for high-pressure applications)
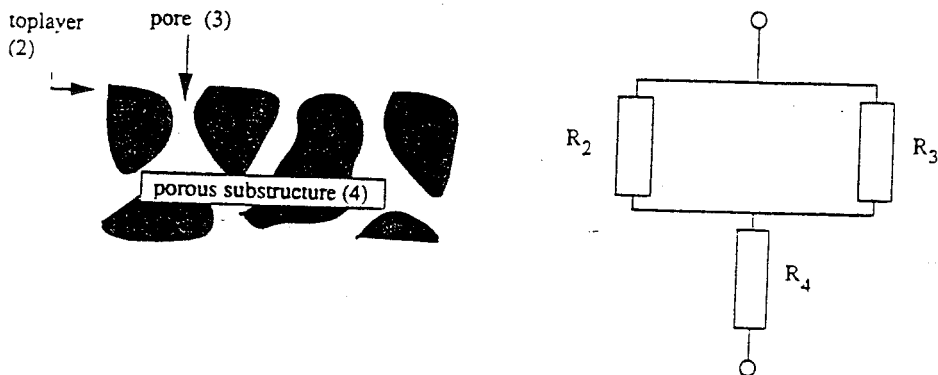
Figure VI - 18. Schematic representation of an asymmetric membrane and the corresponding electrical circuit analogue.

It is very difficult to make a defect-free thin toplayer from a glassy polymer. However, two phase inversion methods can be used to prepare a defect-free asymmetric membrane, i.e. the dual bath method [27] and the evaporation method [28.29] (see also chapter III). Another elegant method of preparing a defect-free 'asymmetric' membrane is to deposit a coating of a highly permeable polymer upon an asymmetric membrane containing some defects. This coating layer plugs the surface pores resulting in a membrane without defects [30]. It is also possible to reduce the toplayer thickness further to increase the permeation rate. At the same time it is interesting to know how many imperfections can be allowed without losing too much in selectivity. The effectiveness of this procedure can be easily be demonstrated by considering a resistance model [30]. Figure VI - 18 shows a schematic representation of an asymmetric membrane and the corresponding electrical circuit analogue. It is obvious that the surface porosity must be negligible otherwise the selectivity will decrease dramatically. By applying a thin coating layer upon these asymmetric membrane these defects will be plugged. Although an extra resistance has now been introduced, the resistance of the plugged pores is much higher than of the open pores so that a much better performance results. This can also be demonstrated by means of a resistance model which can explain the effectiveness of a highly permeable low-selective defect-free coating layer.

The gas flow through a membrane per unit area per unit time is given by

$$J = \frac{P}{\ell} \Delta p \quad \text{or} \quad \frac{J}{\Delta p} = \frac{P}{\ell} \tag{VI - 62}$$

The overall permeability P can be expressed in terms of resistances as:

$$\frac{P}{\ell} = R_{tot}^{-1} \tag{VI - 63}$$

where R_{tot} is the total membrane resistance. For the uncoated membrane the total resistance $R_{tot,un}$ is given by (see figure VI - 18)

$$R_{tot,un} = (R_2^{-1} + R_3^{-1})^{-1} + R_4 \tag{VI - 64}$$

while for the coated layer the total resistance $R_{tot,c}$ is given by (see figure VI - 19)

$$R_{tot,c} = R_1 + (R_2^{-1} + R_3^{-1})^{-1} + R_4 \tag{VI - 65}$$

If it is assumed that the resistance in the sublayer (R_4) is negligible, the flux of the uncoated (J_{un}) and coated membranes (J_c) may be written as:

$$\frac{J_{un}}{\Delta p} = \frac{P_2 + P_1 (A_2 / A_3)}{\ell_2} \tag{VI - 66}$$

and
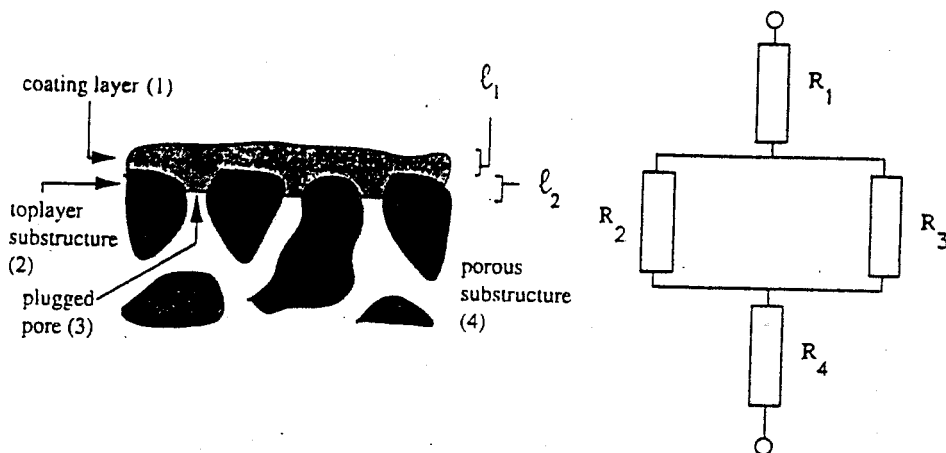
Figure VI - 19. Schematic representation of a coated asymmetric membrane and the corresponding electrical circuit analogue.

$$\frac{J_c}{\Delta p} = \left[\frac{\ell_1}{P_1} + \left(\frac{\ell_2}{P_2 + P_1 (A_2 / A_3)} \right) \right]^{-1}$$

(VI - 67)

Here, ℓ_1 is the thickness of the coating layer, ℓ_2 is the thickness of the toplayer in the substructure, A_2 is the total pore area and A_3 is the surface area of the (solid) polymer (the ratio A_2/A_3 gives the surface porosity).

Figure VI - 20 gives the flux and selectivity as a function of the surface porosity for the uncoated and coated membranes using polysulfone as support membrane and silicone rubber as coating layer as an example using the data given in table VI.8 and with a toplayer thickness of 1 μm ($\ell_1 = \ell_2 = 1$ μm). From this figure it can be seen that a coating procedure with a very permeable low-selective polymer is very effective in obtaining a defect-free layer. For the uncoated membrane any defect leads to a decrease in selectivity, whereas in coated membranes surface porosities (defects) up to 10^{-4} may be allowed without any decrease in selectivity. The permeability is hardly affected by the presence of the coating layer. Hence this method enables the uncoated membrane to be optimised with respect to flux. Although some defects might be present because of the reduction in the toplayer thickness, these will have no effect because of the coating layer.

It should be emphasised again that the performance of these composite membranes is determined by the asymmetric membrane (or the intrinsic properties of the polymer used to prepare this membrane) and the only function of the coating layer is to plug the pores (defects). The plugging of defects in a sublayer with a high permeable polymer is a special type of composite membrane since the support layer determines in fact the separation performance. In general a composite membrane has a sublayer and toplayer, and transport through the thin toplayer is the rate-determining step.
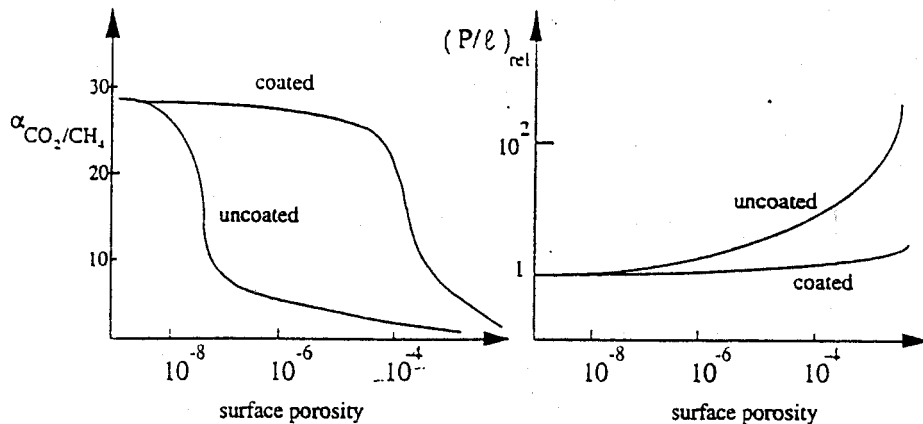
Figure VI - 20.   Selectivity and flux as a function of the surface porosity for coated and uncoated
membranes on the basis of the resistance model.

It may occur that the toplayer material has been penetrated into the sublayer and then the
overall resistance, expressed as an effective thickness, may become quite large. This is
very much the case with glassy toplayers supported by glassy supports and pore
penetration should be avoided.

Sometimes, a highly permeable third layer, e.g., polydimethylsiloxane, is used
between the sublayer and toplayer and serves as an intermediate layer or 'gutter'. When
the surface of the sublayer is highly porous, it is often difficult to deposit a thin selective
coating directly. Also when the toplayer is composed of a glassy polymer it is often
difficult to obtain this layer defect-free. Under these circumstances the three-layer
membrane or 'double composite' membrane may be a good approach [31].

Several methods capable of depositing the thin selective layer upon the support have
been described already in chapter III. Solution coating (dipcoating) is the most applied
method to prepare composite membranes fro gas separation.

VI .4.2.6   Applications
Ideal gas separation membranes possess a high flux and a high selectivity. However,
generally a trade-off can be observed, i.e., high fluxes or high permeabilities are related to
low selectivities and vice versa. To discuss gas separation applications a classification will
be made into high permeable and low permeable materials:
-   High permeable materials are used if high selectivities are not required, as for example
the production of oxygen enriched air for medical applications, combustion processes, and
sterile air for aerobic fermentation processes. Another application is the separation of
organic vapours from non-condensable gases such as nitrogen (air!) or methane (removal
of higher hydrocarbons), where high selectivities may be obtained with highly permeable
materials. The permeability of hydrophobic elastomeric materials for nitrogen and methane

is much lower than that for any organic vapour and hence it is of advantage to select a high permeable material for this application.

- If a moderate selectivity is required then then low permeable materials based on glassy polymers will be employed. In practice a balance must be found between permeability and selectivity. A large number of applications can be mentioned.

* CO_2/CH_4

This kind of separation problem arises in many applications: the purification of CH_4 from landfill drainage gas, the purification of CH_4 from natural gas and the recovery of CO_2 in enhanced oil recovery.

* H_2 or He from other gases

Hydrogen and helium have relatively small molecular sizes compared to other gases and exhibit high selectivity ratios in glassy polymers. Applications can be found in the recovery of H_2 from purge gas streams in ammonia synthesis, petroleum refineries and methanol synthesis.

* H_2S/CH_4

Besides CO_2, H_2S is often present in natural gas in appreciable concentrations. The concentration of this very toxic, highly corrosive gas has to be reduced to less than 0.2%.

* O_2/N_2

Separation can be effected to obtain both oxygen-enriched air and nitrogen-enriched air. Nitrogen-enriched air (95 - 99.9%) can be used as an inert gas in the blanketing of fuel tanks, and in the storage of food and agricultural products.

* H_2O from gases

Dehydration of natural gas, air conditioning, and drying of compressed air

* SO_2, CO_2 and NO_x from smoke or flue gas

Due to the relatively low concentrations at atmospheric pressures this application is not very suitable fro pressure driven operations (low driving force) but rather for membrane contactors, carrier mediated processes and membrane reactors.

An overview of various applications and materials can be found in literature [32-36].

VI.4.2.7   Summary of gas separation

membranes:	asymmetric or composite membranes with an elastomeric or glassy polymeric toplayer
thickness:	≈ 0.1 to few μm (for toplayer)
pore size:	nonporous (or porous < $1\mu m$)
driving force:	pressure, upstream to 100 bar or vacuum downstream
separation principle:	solution/diffusion (nonporous membranes) Knudsen flow (porous membranes)
membrane material:	elastomer: polydimethylsiloxane, polymethylpentene glassy polymer: polyimide, polysulfone
application:	- H_2 or He recovery - CH_4/CO_2 - O_2/N_2

- removal of H_2O (drying)
- organic vapours from air
- dehydration (compressed air, natural gas, air conditioning
- acid gases from flue gas

VI .4.3   Pervaporation

Pervaporation is a membrane process in which a pure liquid or liquid mixture is in contact with the membrane on the feed or upstream side at atmospheric pressure and where the permeate is removed as a vapour because of a low vapour pressure existing on the permeate or downstream side. This low (partial) vapour pressure can be achieved by employing a carrier gas or using a vacuum pump. The (partial) downstream pressure must be lower than the saturation pressure at least. A schematic drawing of this process is shown in figure VI - 21.
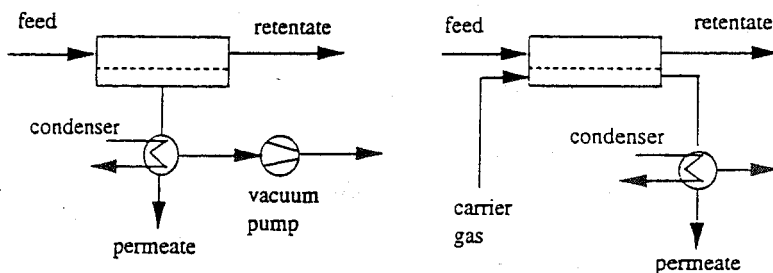
Figure VI - 21.   Schematic drawing of the pervaporation process with a downstream vacuum or an inert carrier-gas.

Essentially, the pervaporation process involves a sequence of three steps:
- selective sorption into the membrane on the feed side
- selective diffusion through the membrane
- desorption into a vapour phase on the permeate side

Pervaporation is a complex process in which both mass and heat transfer occurs. The membrane acts as a barrier layer between a liquid and a vapour phase implying that a phase transition occurs in going from the feed to the permeate. This means that the heat of vaporisation of the permeating components must be supplied. Because of the existence of a liquid and a vapour pervaporation is often considered as a kind of extractive distillation process with the membrane acting as a third component. The separation principle in distillation is based on the vapour-liquid equilibrium whereas separation in pervaporation is based on differences in solubility and diffusivity. The vapour-liquid equilibrium influences

the separation characteristics because it directly affects the driving force. Figure VI - 22 compares distillation (vapour-liquid equilibrium) with pervaporation for an ethanol-water mixture at 20°C. The pervaporation experiments were carried using a polyacrylonitrile membrane. It shows clearly the difference in concept, the pervaporation characteristic is determined by the choice of the material while the distillation characteristic is fixed by the vapour-liquid equilibrium (VLE).

Transport can be described by means of a solution-diffusion mechanism where the selectivity is determined by selective sorption and/or selective diffusion. In fact, the same type of membrane or membrane material can be used for both gas separation or pervaporation. However, the affinity of a liquid towards a polymer is generally much higher than that of a gas in a polymer so that the solubility is much higher. This effect could already be noticed in the case of organic vapours which exhibit much higher permeabilities than permanent gases such as nitrogen. In gas separation, the selectivity towards a mixture can be estimated from the ratio of the permeability coefficients of the pure gases. However, with liquid mixtures the separation characteristics are far different from those of a pure liquid because of thermodynamic interactions.
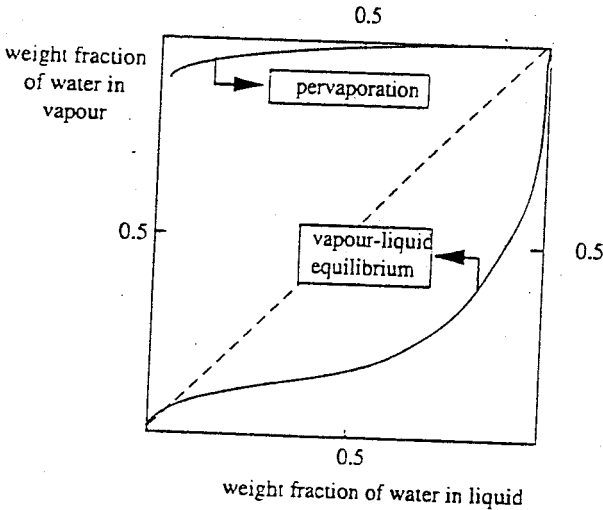
Figure VI - 22. Distillation (vapour-liquid equilibrium) and pervaporation characteristics for an ethanol-water mixture at 20°C. Pervaporation was carried out using a polyacrylonitrile membrane [38].

The low solubility of gases in polymeric materials (at $T < T_g$) can be described by Henry's law. The much higher solubility of liquids implies that Henry's law is no longer obeyed, and the Flory-Huggins theory is commonly used to provide an adequate description of the solubility of liquid mixtures and pure liquids into a polymeric material (see also chapter V).

The permeability of a given component i from a mixture of components i and j can be expressed as a function of the diffusivity (D) and the solubility (S). With liquids the main difference from gases is that the diffusivity and the solubility are not constants but are strongly dependent on the feed composition:

$$P_i = D_i (c_i, c_j) \cdot S_i (c_i, c_j) \qquad \qquad (VI - 68)$$

If another component k is taken instead of component j, both the diffusivity D_i and the solubility S_i are changed.

If poly(vinyl alcohol) is used for the separation of ethanol-water mixtures, two compositions can be distinguished: a low water concentration and a low alcohol concentration. With this low alcohol concentration (say less than 10%) the membrane is highly swollen and hardly any selectivity is obtained. With the low water concentration (say less than 10%), this same polymer membrane shows a high selectivity towards water and exhibits a reasonable flux.

Another example is that of a mixture which consists of two components which are not miscible with each other over the whole composition range, e.g. trichloroethylene-water. Pervaporation can be used to remove a small amount of water from trichloroethylene or to remove small amounts of trichloroethylene from water. If silicone rubber (polydimethylsiloxane) is used as a membrane material, good results are obtained if small amounts of trichloroethylene from water should be removed. When the same membrane material is used to remove water from almost pure trichloroethylene, the membrane becomes too highly swollen and the separation and mechanical properties are lost. Thus in order to remove traces of water another material has to be chosen, e.g. poly(vinyl alcohol). These extreme examples indicate the influence of composition on the membrane performance.

VI.4.3.1.   Aspects of separation
For single component transport, simple transport equations can be derived from linear flux-force relationships:

$$J_i = - L_i \frac{d\mu_i}{dx} \qquad \qquad (VI - 69)$$

where L_i is a proportionality or phenomenological coefficient. The chemical potential is given by

$$\mu_i = \mu^\circ_i + RT \ln a_i \qquad \qquad (VI - 70)$$

with

$$a_i = \frac{p_i}{p_i^o}$$

$$(VI - 71)$$

p^o_i being the saturation pressure of component i and p_i is its vapour pressure. Because

$$\frac{d\mu_i}{dx} = \frac{R\,T}{p_i}\,\frac{dp_i}{dx}$$

$$(VI - 72)$$

eq. VI - 69 now becomes

$$J_i = \frac{L_i\,R\,T}{p_i}\,\frac{dp_i}{dx}$$

$$(VI - 73)$$

Taking differences instead of differentials ($dp_i/dx \approx \Delta p_i /\Delta x$) where Δx is the membrane thickness ℓ and $P_i = (L_i \cdot RT)/p_i$, eq. VI - 73 becomes

$$J_i = \frac{P_i}{\ell}\,\Delta p_i$$

$$(VI - 74)$$

Eq. VI - 74 is the basic equation for liquid transport and it is the same as that for gas transport (see eq. VI - 46) and vapour transport. However, due to the (high) interaction between organic liquids and polymer the permeability coefficient P_i is dependent on composition and temperature. Both solubility and diffusivity are concentration and temperature dependent as have been discussed in chapter V. Eq. VI - 74 illustrates the important parameters involved, the permeability coefficient is a membrane- or material-based parameter. Other parameters of interest are the effective membrane thickness ℓ and the partial pressure difference Δp_i. The permeation rate is inversely proportional to the membrane thickness and proportional to the partial pressure difference across the membrane. In general eq. VI - 74 can be written as

$$J_i = \frac{P_i}{\ell}\,(\,x_i\,\gamma_i\,p_i^\circ - y_i\,p_p\,)$$

$$(VI - 75)$$

Here, x_i is the mol fraction of component i in the liquid feed, $p_i{}^\circ$ the saturation pressure of the pure component at a given temperature and γ_i is the activity coefficient of component i. The Antoine equation is normally used to determine $p_i{}^\circ$, the saturation pressure of a pure a component at a given temperature, and the values of the constants A, B, and C can be found in literature.

$$\log P = A - \frac{B}{T + C}$$

$$(VI - 76)$$

in which P is given in mmHg and T in °C. Appendix 2 at the end of the book summarizes the values of the constants A, B, and C for a number of organic solvents.

The values for the activity coefficients can be obtained from semi-empirical equations such van Laar, Margules, Wilson, UNIVAC and UNIQUAC (see chapter III). The constants, which appear in these equations can be found in literature as well [39]. At the permeate side normally ideal behaviour is assumed and the partial pressure is given by the product of pressure and mol fraction. The vapour pressure at the permeate side is minimum when a vacuum is applied in combination with liquid nitrogen temperatures (- 196°C or 77 K) which may occur in laboratory testing. In this case the driving force is determined completely by the vapour pressure of the feed liquid, which in turn can be strongly influenced by the temperature of the feed.

In the case of ideal behaviour eq. VI - 73 or VI - 74 can be transformed into Fick's law. Combining eqs. VI - 69 and VI - 70, the following equation is obtained

$$J_i \ = \ - \ L_i \, R \, T \, \frac{d \ln a_i}{dx} \tag{VI - 77}$$

or

$$J_i \ = \ - \ L_i \, R \, T \, \frac{d \ln a_i}{dc_i} \, \frac{dc_i}{dx} \tag{VI - 78}$$

The activity a_i of a component in a polymeric membrane can be described by Flory-Huggins thermodynamics [40]. Thus, the activity of a component (index i) in a polymer (index j) is given by

$$\ln a_i = \ln \phi_i \ + (1 - \ V_i/V_j) . \ \phi_j \ + \ \chi_{ij} \ \phi_j^2 \tag{VI - 79}$$

where ϕ_i is the volume fraction of the liquid inside the polymer, ϕ_j is the volume fraction of polymer and χ_{ij} is the Flory-Huggins interaction parameter. For an ideal system ($V_i = V_j$ and $\chi_{ij} = 0$), differentiation of eq. VI - 79 with respect to ϕ_i gives

$$\frac{d \ln a_i}{d \phi_i} \ = \ \frac{1}{\phi_i} \tag{VI - 80}$$

If we define the concentration dependent diffusion coefficient D_i (c) as

$$D_i(c) \ = \ L_i \, R \, T \, \frac{d \ln a_i}{dx} \tag{VI - 81}$$

then writing concentrations c instead of volume fractions ϕ and combining eqs. VI - 77, VI - 80 and VI - 81 gives Fick's law

$$J_i \ = \ - \ D_i \, (c) \ \frac{dc_i}{dx} \tag{VI - 82}$$

In eq. VI - 81. D_i (c) is the diffusion coefficient of component i in the polymer fixed frame of reference and is a function of the concentration. The liquid generally swells the polymer to a certain extent during pervaporation. Such swelling is anisotropic, since the liquid concentration on the feed side of the membrane is a maximum whereas on the permeate side the swelling is almost zero. Figure VI - 23 gives a schematic drawing of the concentration profile, or in this case an activity profile. It is assumed that thermodynamic equilibrium exists at the interfaces, i.e. the activity of the liquid in the feed and in the membrane are the same (for pure liquids this means that the activity is unity). When the vapour pressure on the permeate side is very low (or $p_2/p° \Rightarrow 0$), the activity or
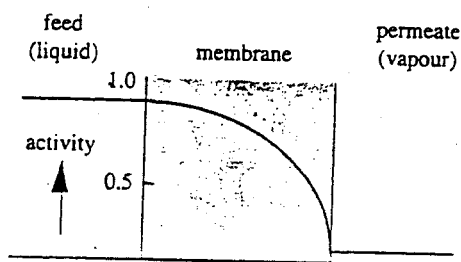
Figure VI - 23. Activity profile of a pure liquid across a membrane.

concentration varies quite considerably over the membrane and the driving force is a maximum. Consequently, the concentration-dependent diffusion coefficient will also change quite considerably across the membrane. Indeed, an exponential relationship is often used to express the concentration dependence of the diffusion coefficient, i.e.

$$D_i = D_{o,i} \exp(\gamma \cdot c_i) \qquad (VI - 83)$$

where $D_{o,i}$ is the diffusion coefficient at $c \Rightarrow 0$ and γ is a plasticising constant expressing the plasticising action of the liquid on segmental motion. Combining eqs. VI - 82 and VI - 83 and integrating across the membrane using the boundary conditions

$$c_i = c_{i,1}{}^m \quad at \quad x = 0$$
$$c_i = 0 \qquad at \quad x = \ell$$

gives the following equation:

$$J_i = \frac{D_{o,i}}{\ell} [\exp(\gamma \ c_{i,1}{}^m) - 1] \qquad (VI - 84)$$

This equation represents the flux of a pure liquid through a membrane, and indicates

which parameters determine this flux. The quantities $D_{o,i}$, γ and ℓ are constants so that the main parameter is the concentration inside the membrane ($c_{1,1}{}^m$). As the concentration just inside the membrane increases, the permeation rate also increases. This implies that the permeation rate for single liquid transport is mainly determined by the interaction between the polymeric membrane and the penetrant. For a given penetrant the flux through a particular polymeric membrane will increase if the affinity between the penetrant and the polymer increases.

The transport of liquid mixtures through a polymeric membrane is generally much more complex. In the case of a binary liquid mixture, the flux can also be described in terms of the solubility and the diffusivity but in such a way that they can have a strong influence on each other. Two phenomena must be distinguished in multi-component transport:

- flow coupling
- thermodynamic interaction

Flow coupling is described in terms of non-equilibrium thermodynamics (see chapter V) and accounts for the fact that the transport of a component is affected due to the gradient of the other component. Thermodynamic interaction is a much more important phenomenon. Due to the interaction of one component the membrane becomes more accessible for the other component since the membrane becomes more swollen, i.e. the diffusion resistances decrease. It is even possible for a component with a very low permeability, e.g. water in polysulfone, to exhibit a much higher permeability in the presence of a second component, e.g. ethanol. This second component has a much higher affinity towards the polymer and consequently a higher (overall) solubility is obtained that allows water to permeate.
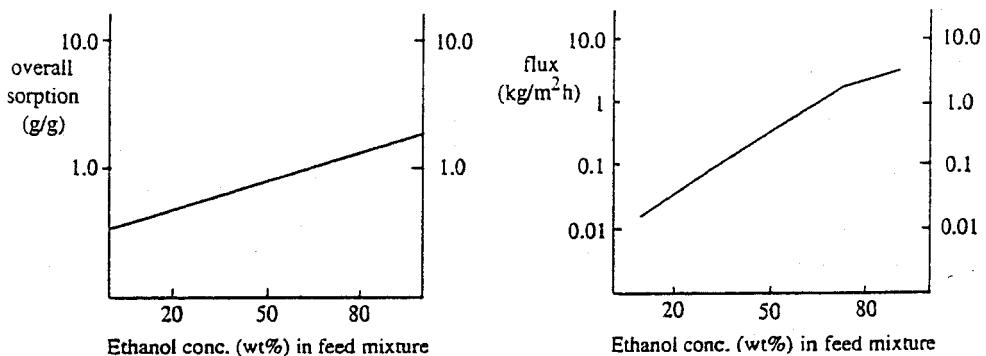
Figure VI - 24. Overall sorption (left) and pervaporation flux (right) as a function of the ethanol/toluene feed composition for a PAA-PVA polymer blend with 20% PVA [41].

The transport properties, flux and selectivity, can be correlated with two thermodynamic parameters, *i)* sorption and *ii)* preferential sorption (see also chapter V). The sorption value reflects the overall interaction of the liquid mixture towards the membrane material. Figure VI - 24 shows the sorption value (left) and the flux (right) of a mixture of toluene-ethanol in a membrane consisting of a blend of polyvinyl alcohol (PVA)-poly acrylic acid (PAA) [41]. It can be seen that with increasing alcohol concentration in the liquid mixture the overall sorption value increases. The transport resistance in this swollen network will decrease and consequently the flux (or better the permeability coefficient) will increase. In fact both the diffusivity (due to increased swelling) and the solubility (due to increased interaction) increase.
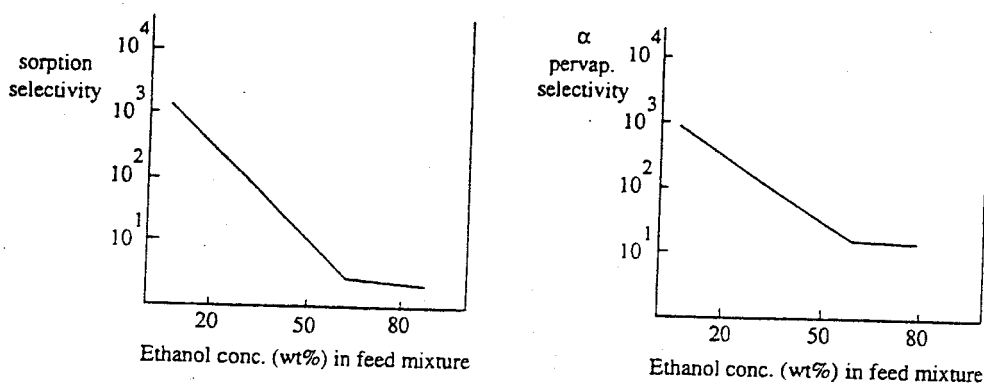
Figure VI - 25. Sorption selectivity (left) and pervaporation selectivity (right) as a function of the ethanol/toluene feed composition for a PAA-PVA polymer blend membrane with 20% PVA [41].

The second parameter of interest, sorption selectivity or preferential sorption can be correlated to the membrane selectivity in a pervaporation experiment. Figure VI - 25 shows sorption selectivity (left) and the pervaporation selectivity (right) as a function of the ethanol/toluene feed composition in a PAA-PVA blend membrane with 20% of PVA. With increasing ethanol concentration in the feed, the preferential sorption or selective uptake of ethanol from the liquid feed mixture into the membrane decreases and so does the selectivity. Also the trade-off between flux and selectivity can be seen. With increasing ethanol concentration in the feed the polymer membrane becomes more swollen, the flux increases (figure VI - 24) but the selectivity decreases (figure VI - 25). Also in cases with a low mutual affinity between the components present in the feed the same trend can be observed. Here the removal of trichloroethylene from water is given as an example. Figure VI - 26 depicts the preferential sorption and pervaporation results as a function of the concentration of trichloroethylene in water using nitrile-butadiene rubber (with a 18% nitrile content) as the membrane [42]. This figure shows that the selectivity for trichloroethylene increases exponentially with feed concentration and the same behaviour is

found for preferential sorption.The preferential sorption has been studied for many systems and it has been shown that in many different polymeric materials and with many different liquid mixtures the component that is sorbed preferentially also permeates preferentially.

Table VI.14 summarises some of these systems as an example. It can be concluded from these results that the determining factor in selective transport in pervaporation is thermodynamic interaction or preferential sorption. On the other hand the flux can be correlated to the overall sorption.
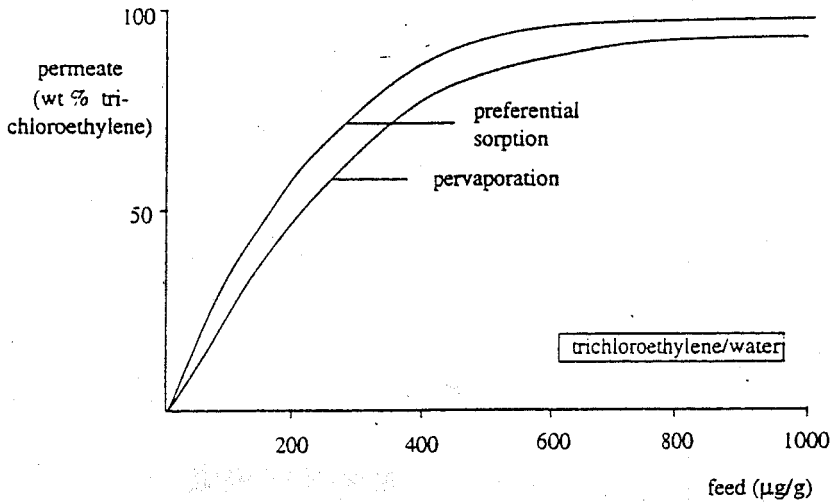
Figure VI - 26.   Experimental values for the preferential sorption and pervaporation of the system trichloroethylene/water/NBR-18 [42].

VI.4.3.2   Membranes for pervaporation

For pervaporation and gas separation, nonporous membranes are required preferably with an anisotropic morphology, an asymmetric structure with a dense top layer and an open porous sublayer, as found in asymmetric and composite membranes. The requirements for the substructure are in fact the same as for gas separation membranes:

- an open substructure to minimise resistance to vapour transport and to avoid capillary condensation.
- a high surface porosity with a narrow pore size distribution

Pressure loss on the permeate side results in an increase in partial pressure and hence in a decrease in driving force and flux. When the pores are too small, the pressure loss may be so high that even capillary condensation may occur. On the other hand, if the pores in the support layer are too large it is difficult to apply a thin selective layer directly

Table VI.14. Literature data relating to preferential sorption

binary mixture	polymer#	ref.
water/methanol	PMG, PDMS	43,44
water/ethanol	PVA, CA, PAN, PMM	45 - 49
	Selemion, PDMS	
water/propanol	PDMS	45
water/butanol	PDMS	45
ethanol/1,2-dichloroethylene	PTFE/PVP	50
ethanol/chloroform	PTFE/PVP	50
acetic acid/1,2-dichloroethylene	PTFE/PVP	50
chloroform/water	SBR, NBR	42,51
trichloroethylene/water	NBR, BR	42
benzene/water	NBR	51
toluene/water	NBR, BR	42,51
benzene/cyclohexane	PMG	48
benzene/heptane	NBR	52
o-xylene/p-xylene	CTP	53
toluene/methanol	PAA-PVA	41
toluene/ethanol	PAA/PVA	41

PMG: polymethylglutamate; PDMS: polydimethylsiloxane; PVA: polyvinylalcohol;
CA: cellulose acetate; PAN: polyacrylonitrile; PTFE: Polytetrafluoroethylene; PVP: poly
vinylpyrrolidone; SBR: styrene-butadiene rubber; NBR: nitrile-butadiene rubber; CTP:
cellulose tripropionate; PAA: polyacrylic acid;

upon the support. In addition, it is very important that the surface porosity should be high. Hence, it may be useful to consider a three-layer membrane consisting of a very porous substructure which shows no resistance, with a non-selective intermediate layer placed on this followed by a dense top layer.

The methods used to deposit the thin layer upon a support layer have been discussed in chapter III and are the same as those used in the preparation of gas separation and vapour permeation membranes. Three important techniques are:
- dip-coating
- plasma polymerisation
- interfacial polymerisation

The choice of the polymeric material depends strongly on the type of application. In contrast to gas separation, elastomers are generally no more permeable than glassy polymers. Because of the much higher affinity of liquids, their solubility is much higher with the high penetrant concentration exerting a plasticising effect on segmental motion in

the polymer chains resulting in an enhanced permeation rate. In fact, because of the high swelling the T_g value is reduced with the result that a glassy polymer may behave as an elastomer if the application temperature is above the glass transition temperature (see also chapter II).

Some further general remarks can be made with respect to polymer choice. It is important that the membrane should not swell too much otherwise the selectivity will decrease drastically. On the other hand, low sorption or swelling will result in a very low flux. Hence, the optimum is somewhere in between, and as a rough estimate an overall sorption value of about 5 - 25 % by weight is useful. It is not necessary that the polymers are crosslinked or crystalline. It is even better to use amorphous (glassy or rubbery) polymers, because crystallinity has a negative influence on the permeation rate. Crosslinked polymers should be used in those cases where the polymeric membrane swells excessively and where a crosslinked membrane shows a good performance. An example is the separation of low concentrations of chlorinated hydrocarbons from water. For extremely low concentrations of organics in water ($\approx$ 10 ppm) uncrosslinked elastomers may be used, but at higher concentrations (> 100 ppm) crosslinking is necessary to reduce the swelling which causes a drastic decrease in selectivity and to improve long term mechanical properties. Table VI.15 shows, as an example, the pervaporation results for a number of polymers used in the dehydration of ethanol through homogeneous membranes with a thickness of about 50 μm [54].

Table   VI.15   Flux and selectivity of ethanol/water through homogeneous
                      membranes [54]
                      feed: 90% by weight ethanol
                      temperature: 70°C
                      membrane thickness: 50 μm.

Polymer	flux (kg/m^2.hr)	α
polyacrylonitrile	0.007	12500
polyacrylamide	0.011	4080
polyacrylamide (high carboxyl)	0.100	2200
poly(vinyl alcohol) (98%)	0.080	350
poly(vinyl alcohol) (100%)	0.060	140
poly(ether sulfone)	0.072	52
polyhydrazide	0.132	19

The high selectivities of PVA, PAN and polyacrylamide originate mainly from two effects: the greater interaction between water and the polymer relative to ethanol and the polymer (water is a solvent for PVA and polyacrylamide !) and the small size of the water molecule (the smaller molar volume) which makes a positive contribution to the entropy of mixing and to the diffusivity. A material such as PVA can be used only at low water

concentrations otherwise it swells too much and the selectivity decreases drastically.

The separation of water from organic solvents is a relatively simple process because of large differences between the components with respect to size (molar volume) and chemical properties, such as polarity and hydrogen-bonding ability. As the components become more similar, separation becomes more and more difficult. For example, separation factors of only about two have been published for xylene isomers with respect to 'ordinary' polymers [55,56].

VI.4.3.3   Applications

Pervaporation is a complex separation process and the separation characteristics may be strongly influenced by composition. The process is used mainly to separate (or better remove) a small amount of liquid from a liquid mixture. When highly selective membranes are used, only the heat of vaporisation of the almost pure permeate has to be supplied. This separation becomes very attractive when the liquid mixture exhibits an azeotropic composition (where the liquid and vapour have the same composition). 'Ordinary' distillation cannot be used to separate such mixtures. Mixtures of an organic solvent with water exhibit an azeotrope in the composition region of the pure organic solvent. Hence it is very advantageous to use pervaporation to dehydrate these types of mixture. Other organic mixtures also show an azeotrope and table VI.16 summarises some of these mixtures with their corresponding azeotropic compositions.

Table   VI.16   Azeotropic compositions associated with some liquid mixtures.

Mixture	azeotrope (weight%)
water/ethanol	4.4/95.6
water/i-propanol	12.2/87.8
water/t-butanol	11.8/88.2
water/tetrahydrofuran	5.9/94.1
water/dioxan	18.4/81.6
methanol/acetone	12.0/88.0
ethanol/hexane	21.0/79.0
n-propanol/cyclohexane	20.0/80.0

There are many binary mixtures where the azeotrope is not located at one of the pure components but somewhere in the middle. In these cases it is not very advantageous to use pervaporation for the complete separation. However, a combination of distillation and pervaporation can be applied where pervaporation is used to break the azeotrope. This is shown schematically in figure VI - 27. It is good to realize that the actual separation is performed by distillation and pervaporation is only applied to shift the composition from

the azeotrope [57,58]. The employment of hybrid processing, the combination of two or more separation processes is in many cases much more advantageous in terms of investment (capital cost) and energy consumption (operating cost).

The last example given involves a case where the difference in relative volatilities of the components to be separated is relatively small. If membranes are available with higher selectivities than the vapour-liquid equilibrium, pervaporation can be combined with distillation as shown in figure VI - 28. This approach is very attractive in case of 'debottlenecking' of an existing distillation plant. Most pervaporation applications can be found in the chemical process industry but they are also other areas such as the food and
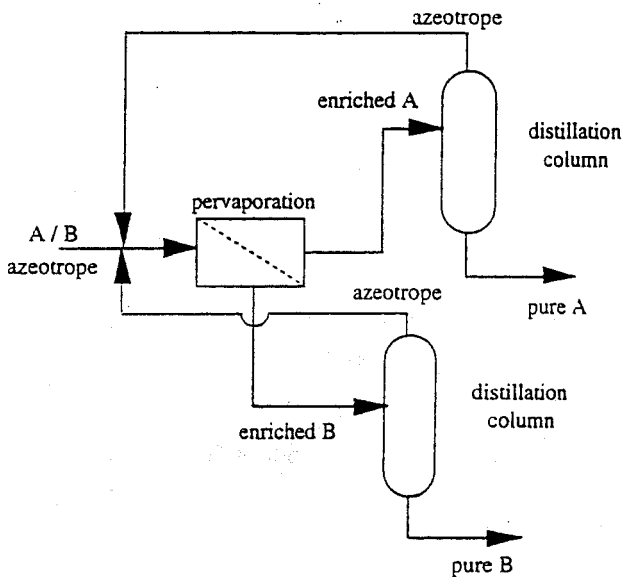
Figure VI - 27.   Schematic drawing of a hybrid distillation/pervaporation for the separation of a 50/50 azeotropic mixture.

pharmaceutical industries to concentrate heat-sensitive products or remove (concentrate) aroma compounds, for environmental problems to remove volatile organic contaminants from waste water [59-61] or in analytical applications to enrich a given component for quantitative detection [62]. Since the number of possible applications is very large it is useful to classify them into aqueous and non-aqueous mixtures. A further subclassification can then be made:

* aqueous mixtures

Two main classes can be distinguished here; either a small amount of water has to be removed from an organic solvent (dehydration) or a small amount of organic

solvent has to be removed from water:
- dehydration
    - removal of water from organic solvents. Even traces of water can be removed (e.g., from chlorinated hydrocarbons)
- removal of volatile organic compounds from water
    - alcohols from fermentation broths (ethanol, butanol and acetone-butanol-ethanol (ABE))
    - volatile organic contaminants from waste water (aromatics, chlorinated hydrocarbons)
    - removal of flavour and aroma compounds
    - removal of phenolics
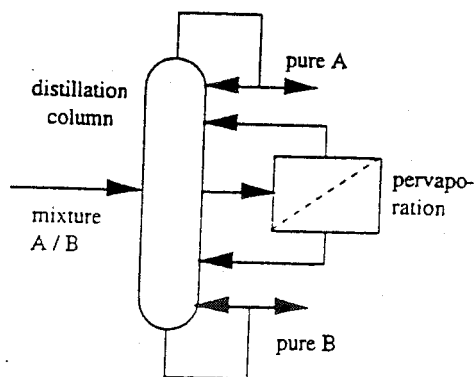
Figure VI - 28. Schematic drawing of a hybrid distillation/pervaporation process for the separation of close boiling mixtures.

* non-aqueous mixtures

A further subclassification can again be made:
- polar/ non-polar
    - alcohols/aromatics (methanol/toluene)
    - alcohols/aliphatics (ethanol/hexane)
    - alcohols/ethers (methanol/methyl-t-butylether (MTBE))
- aromatics/aliphatics
    - cyclohexane/benzene
    - hexane/toluene
- saturated/unsaturated
    - butane/butene
- isomers
    - C-8 isomers (o-xylene, m-xylene, p-xylene, styrene, ethylbenzene)

VI.4 3.4   Summary of pervaporation

---

membranes:	composite membranes with an elastomeric or glassy polymeric top layer
thickness:	≈ 0.1 to few μm (for top layer)
pore size:	nonporous
driving force:	partial vapour pressure or activity difference
separation principle:	solution/diffusion
membrane material:	elastomeric and glassy polymers
application:	- dehydration of organic solvents
	- removal of organic components from water (alcohols, aromatics, chlorinated hydrocarbons)
	- polar/non-polar (e.g. alcohols/aliphatics or alcohols/aromatics)
	- saturated/unsaturated (e.g. cyclohexane/benzene)
	- separation of isomers (e.g. C-8 isomers; o-xylene, m-xylene, p-xylene, ethylbenzene, styrene)

VI.4.4   Carrier mediated transport

A membrane has been defined as an interphase between tweo phases (see chapter 1) and only solids have been described as membrane materials so far. It is also possible to use a liquid as a membrane and the same general definition of a membrane also applies in this case: the liquid membrane or liquid film separates two phases from each other. Also here separation occurs because of differences in solubility and diffusivity in the liquid film similar to a solid film. However, when a carrier is present inside the membrane with the ability to complex with a specific solute the flux of that solute may be enhanced. The carrier may be dissolved in the liquid and in this case the carrier is mobile. On the other hand, the carrier can be bound chemically (covalently) or physically to a solid polymer. In this case the carrier is fixed and has a very restricted mobility. These two systems have been drawn in figure VI - 29. In the mobile carrier system, the carrier-solute complex diffuses across the membrane whereas in the fixed carrier system the solute jumps or 'hops' from one site to the other. It is obvious that the diffusivity in the mobile system is much higher. Between these two limits there is a large area where the continuous phase can be considered as a gel or a solvent swollen polymer and as a consequence the diffusivity will increase. In these systems the carrier can either be fixed or mobile, however, when the carrier is fixed it still has a certain mobility compared to a carrier in an unswollen system. Table VI.17 gives a rough estimate of the diffusion coefficients which can be expected in the various systems. The mobile carrier systems, which are referred to as 'liquid membranes' have been studied widely and this concept will be discussed in the next section.

Table VI.17. Diffusivities in carrier mediated systems

system	D (cm²/s)
mobile carrier system	$10^{-5} - 10^{-7}$
solvent swollen or gel system	$10^{-6} - 10^{-8}$
fixed carrier	$> 10^{-7}$
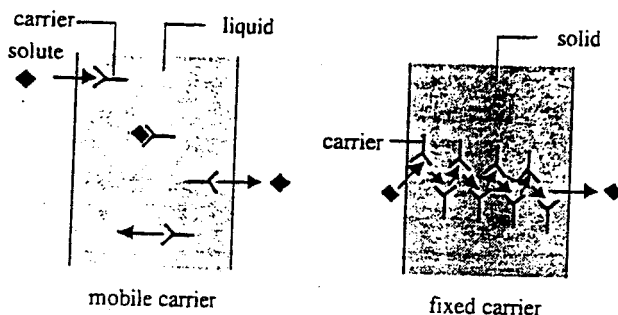
Figure VI - 29. Schematic drawing of a mobile carrier system (left) and a fixed carrier system (right).

The characteristic of a facilitated or carrier mediated transport is the occurrence of a reversible chemical reaction or complexation process in combination with a diffusion process. This implies that two cases can be distinguished:
* diffusion is rate-limiting (fast reaction)
* reaction is rate-limiting (slow reaction and relatively fast diffusion)
The latter case does not occur frequently and only the former case will be considered.

VI.4.4.1   Liquid membranes

Two basically different types of liquid membrane can be distinguished (see figure VI - 30):

i) The liquid film is immobilised within the pores of a porous membrane (figure VI - 30 left). The porous membrane serves only as a framework or supporting layer for the liquid film. This type of membrane is called an immobilised liquid membrane (ILM) or supported liquid membrane (SLM). Such membranes can easily be prepared by impregnating a (hydrophobic) porous membrane with a suitable organic solvent.

ii) The second type of liquid membrane is the emulsion liquid membrane (ELM) (figure VI - 30, right) which is also readily prepared as shown schematically in figure VI - 31. Here two immiscible phases, water and oil for example, are mixed vigorously and emulsion droplets are formed (droplet size about 0.5 - 10 μm), which are stabilised by the addition of a surfactant. A water/oil emulsion is obtained in this way. This emulsion is added to a
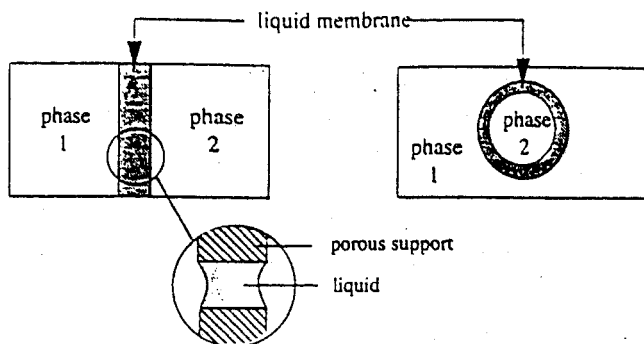
Figure VI - 30. Schematic drawing of two types of liquid membrane, left: supported liquid membrane (SLM) and right : emulson liquid membrane (ELM)

large vessel containing an aqueous phase where a water/oil/water emulsion is now formed, the oil phase being the liquid membrane in this concept.

The two phases (phase 1 and phase 2) are generally aqueous solutions, while the liquid membrane phase is an organic phase which is immiscible with water. The solubility is a very important factor with respect to the stability of these system. This stability effect will be discussed below.
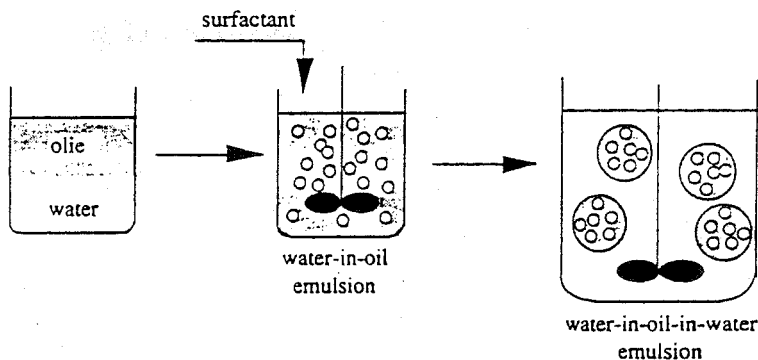
Figure VI - 31.   Preparation of an emulsion type of liquid membrane (ELM).

The liquid membranes illustrated here are only used in some specific applications because of the rather low selectivities obtained. Selectivities are mainly based on differences in the distribution coefficients of the components of phase 1 with the liquid. If the components are similar these differences are generally not very high. The diffusivities of components of comparable size are similar so that the selectivity, which is determined

by differences in solubility and diffusivity, will not be very high in general. However, in some cases this concept may be very useful as will be discussed later (see membrane contactors).

Far higher selectivities can be obtained by adding a carrier molecule to the liquid (membrane) which has a high affinity for one of the solutes in phase 1. The carrier accelerates the transport of this specific component. This type of transport is called 'carrier-mediated' transport or facilitated transport. The mechanism of facilitated transport can be demonstrated by the simple experiment depicted schematically in figure VI - 32.
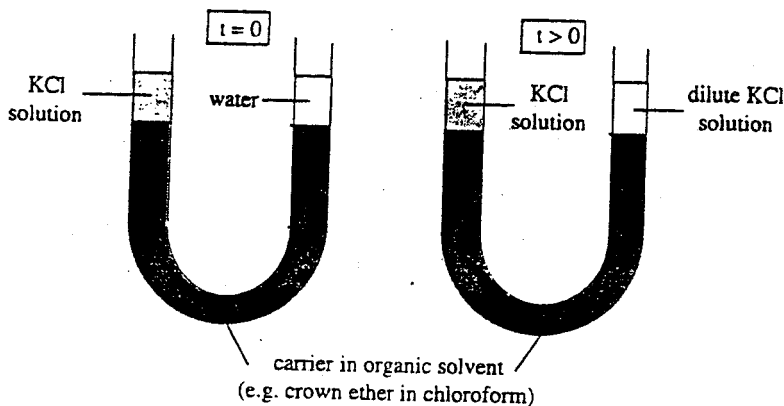
Figure VI - 32. U-tube experiment to demonstrate facilitated transport.

The bottom of an U-tube is filled with an organic liquid e.g. chloroform (with a higher density than water) containing a carrier with a high affinity to salt. Typical carriers are crown ethers which exhibit specific interactions towards a number of substances including salts. Figure VI - 33 gives the structure of a simple example of this class, 18-crown-6.
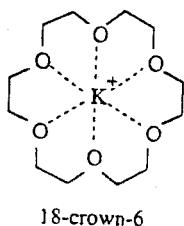
18-crown-6

Figure VI - 33. Crown ether (18-crown-6) complexed with a potassium ion.

One arm of the U-tube is filled with an aqueous potassium chloride solution whereas the

other arm is filled with water. Because of the concentration difference, the salt will diffuse from the concentrated solution to the pure water phase. However, in the absence of carrier, the transport of salt is extremely low because its solubility in the organic phase (e.g. chloroform) is very low. Adding a carrier to the organic phase that is capable to form a reversible complex with the salt (e.g. diphenyl-18-crown-6) causes transport of potassium from one side of the U-tube to the other. After a finite time the pure water phase will now contain a certain amount of KCl (note that to maintain electroneutrality the anion chloride has to diffuse along with the carrier complex). This U-tube experiment is very suitable to demonstrate the existence of facilitated or carrier-mediated transport.

The difference between 'ordinary' diffusive transport and facilitated transport is shown schematically in figure VI - 34. With carrier-mediated transport, the transport of component A is enhanced by the presence of a carrier molecule C. Component A and carrier C form the complex AC, which also diffuses through the membrane. In this case two processes occur simultaneously; part of component A is transported by diffusion ('free diffusion') whilst another part is transported by solute-carrier complex diffusion ('carrier-diffusion'). Hence an increased transport of component A can be observed.
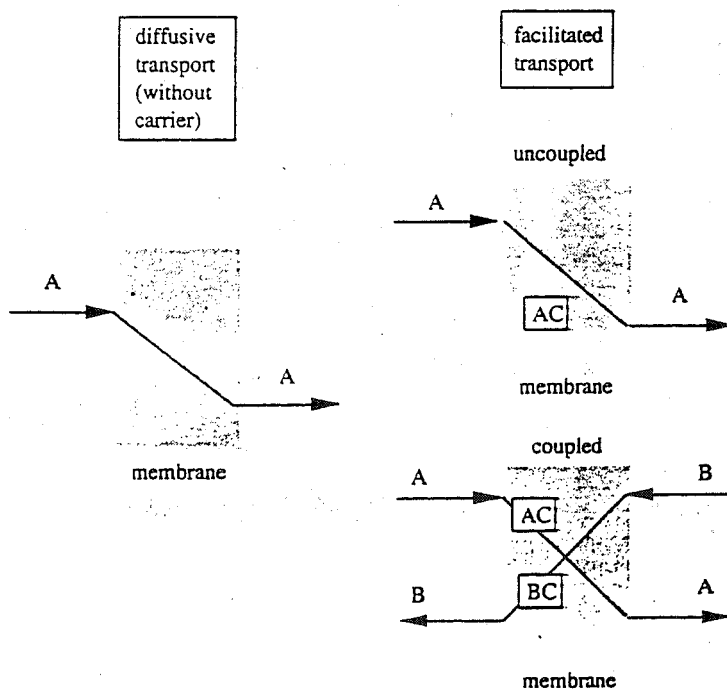
Figure VI - 34. Transport mechanism in a liquid membrane. Diffusive transport (without carrier): left-hand figure; facilitated transport (with carrier C); right-hand figures.

Two components are often involved in carrier mediated-transport, this type of transport being called coupled transport. Two types of coupled transport can be considered:

- co-coupled transport, where the two components are moving in the same direction
- counter-coupled transport, where the two components are moving in opposite directions (as illustrated in figure VI - 34).

Co-coupled transport takes place, for example, in the transport of ions (see fig. VI - 28, i.e. the example with the U-tube). If cations are transported then anions must be transported at the same time to preserve electroneutrality. Mainly counter-coupled transport will be considered here with the term coupled transport being reserved for counter-coupled transport. The coupled transport mechanism is interesting because it offers the possibility of transporting a component against its own concentration gradient, i.e. from a low concentration to a high concentration, since the real driving force is the concentration gradient of the other component. Another aspect of this process is that decomplexation is established by a high concentration of the components in the opposing phases.

The mechanism of facilitated or carrier-mediated transport is given in figure VI - 35. The following separated steps can be distinguished:

- the solute dissolves in the membrane (liquid)
- complexation takes place between the carrier and the solute A at the phase 1 (feed phase or source phase)/membrane interface
- the carrier-solute complex diffuses across the membrane
- decomplexation takes place at the membrane/phase 2 (stripping phase or receiving phase) interface
- the solute is released from the membrane phase
- The free carrier diffuses back
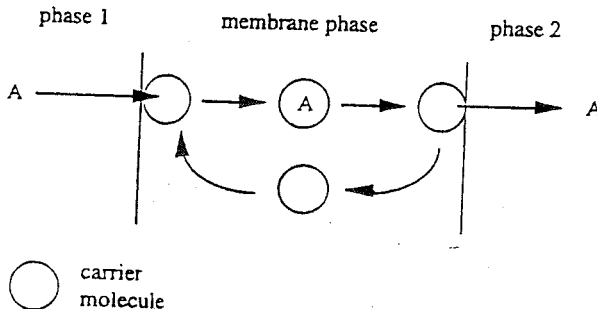
Figure VI - 35. The mechanism of carrier-mediated transport in liquid membranes with mobile carriers.

A basic feature of carrier-mediated transport is that the complexation reaction must be reversible otherwise transport will stop once all the carrier molecules have formed a complex with the solute. The affinity between the carrier and the solute may vary appreciably. Thus a strong complex, i.e. one exhibiting a high affinity between the complex and the solute, may result in a slow release while a weak complex, i.e. one exhibiting a low affinity between the solute and the carrier, could mean that only limited facilitation occurs so that the selectivity is also small. For this reason, it is essential to find an optimum. The bond energies of these reversible complexes will be in the range of 10 to 50 kJ/mol. Typical complexation reactions involving this amount of energy are, hydrogen bonding, acid-base interactions, chelation, clathration, π bond interactions [63].

As can be seen from figure VI - 35, two effects contribute to the transport of component A:
- the rate of complex formation (complexation/decomplexation) at the two interfaces.
- diffusion of the complex (and the free solutes) across the membrane

The occurrence of two different processes at the same time, i.e. chemical reaction (complexation/ decomplexation) and mass transfer (diffusion), is another characteristic of facilitated transport as has been discussed earlier. A result of these combined processes is that the flux in not proportional anymore to the driving force and furthermore at (very) low concentrations in the feed phase still appreciable fluxes can be obtained.
The mechanism of both uncoupled and coupled-facilitated or carrier-mediated transport will be described by some examples.
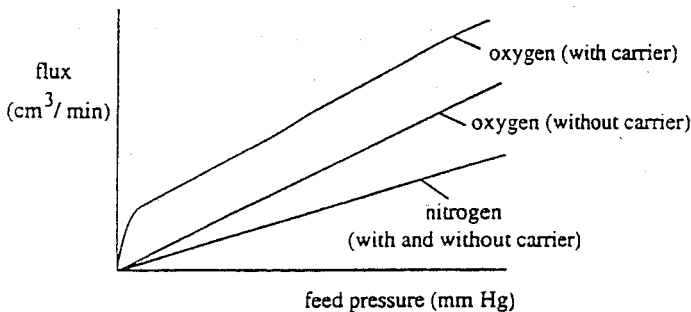
Figure VI - 36. Oxygen and nitrogen flux through water with and without carrier (cobalthistidine) [64].

An example of uncoupled transport is given in figure VI - 36 where the oxygen and nitrogen fluxes through a water film with and without the presence of a carrier are depicted. The carrier in this case was a cobalt compound. This carrier molecule forms a complex with oxygen but not with nitrogen. This figure shows that the nitrogen flux

increases with increasing pressure and that the permeation rate is not affected by the presence of carrier. The solubility of oxygen in water is greater than of nitrogen and consequently a higher flux is obtained which is enhanced in the presence of the carrier molecule. Some oxygen molecules are transported by the carrier and others are transported by 'ordinary' molecular diffusion or 'free diffusion'. This facilitated effect is greater at lower oxygen partial pressures because the carrier will be saturated at higher oxygen partial pressures (concentrations).

Ions are of interest in facilitated transport because a large number of complexing agents are available as carrier molecules, especially for ion-exchange components. An example of coupled transport is the transport of the nitrate ion (NO_3^-). Tertiary amines or quaternary ammonium salts are suitable complexing agents for anions. The affinity between an anion and an anion-exchange component is mainly determined by the charge density on the anion, which in turn is determined by the size and valence of the anion. The following affinity sequence between various anions and a quaternary ammonium salt has been observed:

$$I^- > NO_3^- > NO_2^- > Cl^- > H_2PO_4^{2-} > HSO_4^- > SO_4^{2-} > HCO_3^- > PO_4^{3-} > CO_3^{2-}$$
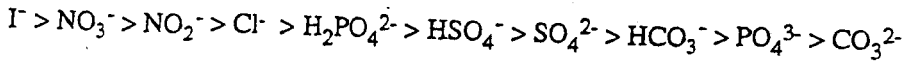
To remove the NO_3^- anion from a dilute solution via a coupled transport mechanism the other component must have a lower affinity for the carrier in comparison to nitrate, but this must not be too low, otherwise decomplexation becomes very difficult. The chloride (Cl^-) appears to be a good component for exchange with nitrate. The coupled transport of the nitrate anion is depicted in figure VI - 37.

Nitrate in phase 1 (feed) is exchanged by Cl^- whereas the chloride in phase 2 is exchanged by the nitrate. The nitrate anion is transported against its own driving force with the actual driving force in this process being the large concentration difference in chloride
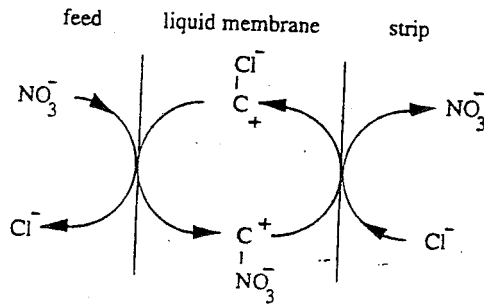
Figure VI - 37.   Counter-current transport. The chloride ion concentration in phase 2 (strip phase) is very high in comparison to the low nitrate concentration in the feed (phase 1).

ions across the membrane. Although the affinity between the nitrate ion and the carrier is

much higher relative to that of the chloride ion, decomplexation in phase 2 (strip phase) can occur when a very high chloride ion concentration has been established. The equilibrium reaction for this process is

$$RCl + NO_3^- \iff RNO_3 + Cl^-$$

Very high concentration factors can be obtained with coupled facilitated transport processes of this kind.

VI.4.4.2   Aspects of separation [65]
As has been shown in figure VI - 36, the transport of oxygen through water can be enhanced by the addition of a specific carrier. Two mechanisms contribute to the total oxygen flux through the membrane, i.e. the oxygen molecules form a complex with the carrier and this carrier molecule diffuses through the membrane. The second part is the 'normal' Fickean diffusion of dissolved oxygen across the membrane.

Figure VI - 38 shows the concentration profiles when diffusion occurs via Fickean diffusion (molecular oxygen) and by diffusion of a carrier-oxygen complex (complexed oxygen). Both transport mechanisms occur simultaneously. Let us first consider the simple case, i.e. one-component transport. The permeant A can react with the carrier C to form a carrier-solute complex AC

$$A + C \iff AC$$
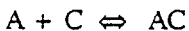
This complex can then be transported across the membrane either in the uncomplexed or complexed form. The total flux of component A will then be the sum of the two contributions, i.e.

$$J_A = \frac{D_A}{\ell} \left(c_{A,o} - c_{A,\ell} \right) + \frac{D_{AC}}{\ell} \left(c_{AC,o} - c_{AC,\ell} \right) \qquad (VI - 85)$$

The first term on the right-hand side of eq. VI - 85 represents permeant diffusion according to Fick's law, where D_A is the diffusion coefficient of (the uncomplexed) component inside the liquid film while $c_{A,o}$ is the concentration of component A just inside the liquid film. The second term represents carrier-mediated diffusion with the flux being proportional to the driving force, which in this case is the concentration difference of complex across the liquid film. D_{AC} is the diffusion coefficient of the complex and $c_{AC,o}$ is the concentration of the carrier-solute complex at the interface. The equilibrium constant of the complexation reaction is given by

$$K = \frac{c_{AC,o}}{c_{A,o} \, c_C} \qquad (VI - 86)$$

The average carrier concentration at any place in the membrane is given by

$$\bar{c} = c_C + c_{AC_o}$$

(VI - 87)

with c_c is the concentration of free carrier and c_{ACo} is the concentration of complexed carrier at a certain point in the membrane. Substitution of eq. VI - 86 and VI - 87 into VI - 85 and assuming that the membrane concentrations at the permeate or strip side are neglectible ($c_{A\ell} \approx c_{AC\ell} \approx 0$), then the total flux of component A is obtained

$$J_A = \frac{D_A}{\ell} c_{A_o} + \frac{D_{AC}}{\ell} \left(\frac{K \bar{c} c_{A_o}}{1 + K c_{A_o}} \right)$$

(VI - 88)

since the partition or distribution coefficient $k = c_{Ao}/c_{Af}$ in which c_{Af} is the concentration of component A in the feed eq. VI - 88 becomes

$$J_A = \frac{D_A k}{\ell} c_{A_f} + \frac{D_{AC}}{\ell} \left(\frac{K k \bar{c} c_{A_f}}{1 + K k c_{A_f}} \right)$$

(VI - 89)
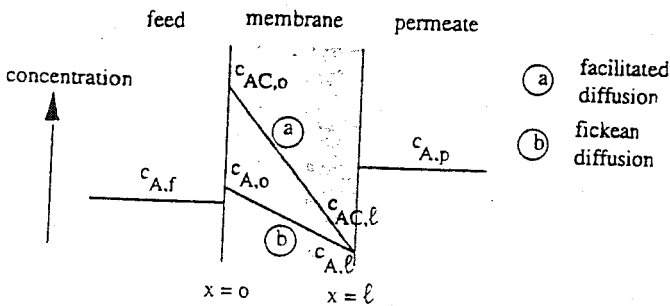
Figure VI - 38.   Schematic drawing of the concentration profiles arising from free oxygen diffusion via Fick's law (curve b) and by facilitated diffusion (curve a).

Two limiting cases can be observed from figure VI - 38 and eq. VI - 85 :
i) the first term, i.e. Fickean diffusion, is rate-determining.
This will be the case when the reaction rate is low compared to the diffusion rate, in other words when the concentration of the carrier-solute complex AC is much lower than the concentration of free A ($c_{A,o} \gg c_{AC,o}$) .
ii) diffusion of the complex, i.e. the second term, is rate-determining.
This will be the case when the reaction rate is fast and the permeation rate of the complex is much higher than that of the uncomplexed permeant ($c_{AC,o} \gg c_{A,o}$).
The ratio between the reaction rate and the diffusion rate is given by the Damköhler number. The second Damköhler number is defined as $\ell^2/(D \cdot t_{0.5})$, where $t_{0.5}$ is the half-

life of the complexation reaction (reaction time constant), D the diffusion coefficient of the free component and ℓ the membrane thickness. The diffusion coefficient divided by the square of the membrane thickness can be considered as the diffusion time constant. If $\ell^2/(D \cdot t_{0.5}) \gg 1$ then the reaction rate is very fast and diffusion of the free permeant can be neglected (for example, with a membrane thickness of 10 μm, a $t_{0.5}$ value of about 10^{-7} sec and a D value of 10^{-9} m^2.sec^{-1}, the Damköhler number is very large, being in the range of 10^6). On the other hand, at low Damköhler numbers the free diffusion of the uncomplexed permeant is rate-determining and no facilitation occurs in this case with the total flux being equal to the Fickean flux. Figure VI - 39 gives the ratio of the total flux or facilitated flux to the Fickean flux as a function of the Damköhler number.

A flux ratio of 10 (total flux/Fickean flux) has been chosen arbitrarily to indicate the region where facilitated transport is the rate-determining step (region II) [66].
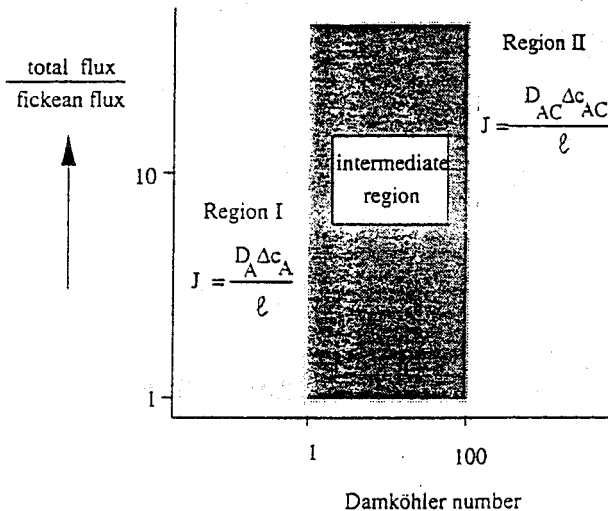
Figure VI - 39. Schematic drawing of the ratio of the total flux to the Fickean flux as a function of the Damköhler number [59].

In this region the diffusion of the complex determines the total permeation rate, which means that the first term on the right-hand side of eq. VI - 85 can be neglected relative to the second term and transport is determined by the carrier-solute complex. The Damköhler number can be high even when the reaction rate constant is small, i.e. when the solubility of the solute into the liquid membrane is extremely low.

In absence of concentration polarization the flux of a component can be described by eq. VI - 85. But in general, also in carrier mediated transport boundary layer effects should be taken into account. Figure VI - 40 shows the concentration profile of a component (for

example, the nitrate anion) which is transported against its concentration gradient in a coupled transport process (counter-transport). The other component involved in this process (the chloride ion) is not included in this drawing. If the profile is followed it can be seen that an extra resistance occurs at both interphases due to concentration polarisation. These boundary layer resistances may be comparable or even dominating over the diffusional resistance.
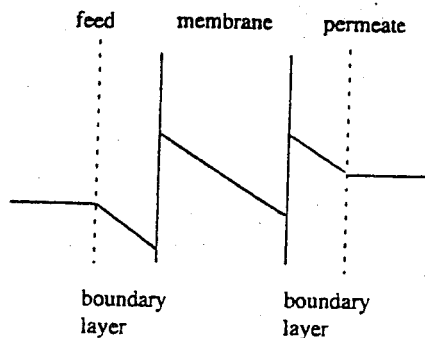
Figure VI - 40.   Schematic drawing of the concentration profile in a liquid membrane process.

The chemical reaction which occurs during this coupled process is

$$RCl + NO_3^- \iff RNO_3 + Cl^-$$
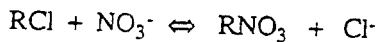
and the equilibrium constant K for this reaction is given by

$$K = \frac{[RNO_3]_o \; [Cl^-]_w}{[RCl]_o \; [NO_3^-]_w}$$

$$(VI - 90)$$

where the concentrations refer to the organic phase (subscript o) and the aqueous phase (subscript w). If the solubilities of the ions in the organic phase are very low, then the concentration of the carrier-solute complex determines the ion concentrations in this phase. This implies that the equilibrium constant is equal to the ratio of the distribution coefficients on the feed side because

$$k_{NO_3} = \frac{[NO_3^-]_o}{[NO_3^-]_w} = \frac{[RNO_3]_o}{[NO_3^-]_w}$$

$$(VI - 91)$$

and

$$k_{Cl^-} = \frac{[Cl^-]_o}{[Cl^-]_w} = \frac{[RCl]_o}{[Cl^-]_w}$$

$$(VI - 92)$$

The specific character of the carrier is determined by the ratio of the distribution coefficients $k_{NO_3^-}/k_{Cl^-}$, and if this ratio is high then the carrier is very selective.

Three processes must be considered in any description of the overall transport [67]. The nitrate flow in the boundary layer (J_{bl}) is given by

$$J_{bl} = - D_{bl} \frac{d[NO_3^-]_w}{dx} \tag{VI - 93}$$

while the flow of nitrate across through the interface J_i, which is determined by the ease of complexation, is given by

$$J_i = k_1 [NO_3^-]_w - k_{-1} [NO_3^-]_m \tag{VI - 94}$$

where k_1 and k_{-1} are rate constants and $[NO_3^-]_w$ and $[NO_3^-]_m$ are the interfacial nitrate concentrations in the aqueous (w) and organic phase (m) respectively.

The nitrate flux through the membrane phase (J_m) is given by

$$J_m = - D_m \frac{d[NO_3^-]_m}{dx} \tag{VI - 95}$$

and under steady-state conditions the fluxes are equal (otherwise accumulation would occur), i.e. $J_{bl} = J_i = J_m$, and, in addition, are equal to the overall flux J. If the differentials are considered as differences (dc/dx = $\Delta c/\Delta x$), then combination of eqs. VI - 93, VI - 94 and VI - 95 gives

$$J = \frac{k_1 [NO_3^-]_w}{k_1 \dfrac{\delta}{D_{bl}} + k_{-1} \dfrac{\ell}{D_m} + 1} \tag{VI - 96}$$

where δ is the thickness of the boundary layer and ℓ is the membrane thickness.
If the nitrate concentration in the feed, $[NO_3^-]_w$, is not remained constant then the flux can be given by

$$J = - \frac{V}{A} \frac{d[NO_3^-]_w}{dt} \tag{VI - 97}$$

where V is the total feed volume and A is membrane area. Assuming that the rate of complexation is very fast, then

$$\frac{k_1}{k_{-1}} = \frac{[NO_3^-]_o}{[NO_3^-]_w} = k_{NO_3} \tag{VI - 98}$$

By dividing both the numerator and the denominator by k_{-1} and neglecting 1 in the denominator, eq. VI - 96 becomes [67]

$$\frac{J}{[NO_3^-]_w} = \frac{k_{NO_3}}{k_{NO_3} \frac{\delta}{D_{bl}} + \frac{\ell}{D_m}} = P$$

(VI - 99)

If permeation is only determined by the diffusion process through the liquid membrane, i.e., boundary layer phenomena can be neglected, then the permeability coefficient P can be written as $P = k_{NO3} \cdot D_m/\ell$. However, when the boundary layer effects predominate, then $P = D_{bl} / \delta$ which is equal to the mass ransfer coefficient in the boundary layer.

Combination of eqs. VI - 97 and VI - 99, and integration with the boundary conditions

$c = c_o$ at $t = 0$
$c = c$ at $t = t$

leads to the following equation:

$$\ln\left(\frac{c}{c_o}\right) = -\frac{A}{V} P t$$

(VI - 100)

This equation shows that the concentration decreases exponentially with time since the permeability coefficient is concentration-independent. This behaviour, which is often observed, is shown schematically in figure VI - 41.
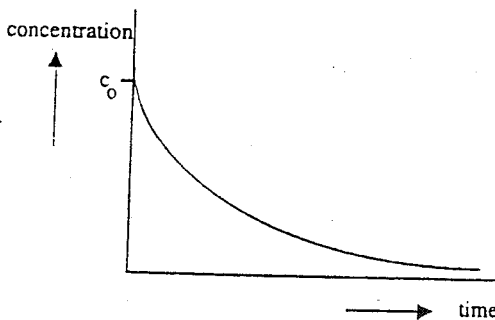
Figure VI - 41.   Removal of solute from the feed phase as a function of time as described by eq. VI - 100.

VI.4.4.3   *Liquid membrane development*

In describing membrane development, both types of liquid membranes should be distinguished, i.e. the supported liquid membrane (SLM) and the emulsion liquid membrane (ELM).

Supported liquid membranes consist of three main components:

- support membrane
- organic solvent
- carrier

Because a free liquid film is not very stable, the function of the porous support membrane is to act as a framework. However, even in the presence of such a framework the liquid membrane will not remain stable for any length of time. This is one of the main problems with this process as will be discussed towards the end of this section. In fact, all types of membrane materials can be used as the support membrane provided they are stable under the experimental conditions employed and have suitable chemical properties. Indeed,

Table VI.18.   Some porous membranes frequently used as supports
                 for supported liquid membranes (SLM)

preparation technique	material
stretching	polypropylene (Celgard)
	polytetrafluoroethylene (Gore-Tex)
phase inversion	polypropylene (Accurel)
	polyethylene

highly stable materials such as polyethylene, polypropylene and poly(vinylidene fluoride) are often used as supports. The surface porosity and overall porosity of such support materials should be high in order to obtain an optimal flux. Table VI.18 lists some hydrophobic porous membranes frequently used as porous polymeric support. In addition to the materials mentioned above, other more dense membranes can be used in principle such as polysulfone and cellulose acetate. As well as the porosity, membrane thickness also directly determines the permeation rate because the flux is inversely proportional to the membrane thickness, suggesting that the membrane should be as thin as possible. However, when the membrane thickness decreases the Damköhler number also decreases since these two effects are opposing each other. When two opposing effects operate in this fashion, an optimum situation will always exist depending on the system and the system conditions used. When high Damköhler numbers apply, the complexation rates are so fast that the overall flux is completely determined by diffusion across the membrane. Consequently, the flux will be inversely proportional to the membrane thickness under these conditions in the absence of concentration polarization.

VI.4.4.4   *Choice of organic solvent*
Some basic requirements apply regarding the choice of organic solvent in SLM systems.

Thus, if an aqueous system is involved, solubility in the aqueous phase should be extremely low and the volatility should also be low. In addition, the organic liquid must be a solvent for both the carrier and the carrier-solute complex.

Another important factor is the viscosity of the organic phase since the presence of a carrier or carrier-solute complex increases the viscosity of the liquid phase in many cases. The effect of the viscosity on the diffusion coefficient can be illustrated by the Stokes-Einstein equation which shows that the diffusion coefficient is inversely proportional to the viscosity, i.e.

$$D = \frac{kT}{6 \pi \eta r}$$

(VI - 101)

where η is the viscosity of the organic phase. Table VI.19 lists the viscosities of some organic solvents often used in liquid membranes.

On increasing the carrier concentration, two effects are once again counteracting. On the one hand, the flux will increase (see eq. VI - 89), on the other hand an increasing carrier concentration will increase the viscosity, hence reducing the diffusion coefficient and leading to a decreased flux.

Another very severe problem with SLM is the instability of the liquid film with time which causes the process to cease because of loss of the organic phase. Although it is essential for the solubility of the organic phase in the aqueous phase to be as low as possible, even if the solubility meets this requirement or even if the aqueous phase is saturated with the solvent the process becomes unstable after a finite period of time.

Table VI.19.   Viscosities at T = 298 K of
                some solvents used in LM processes [68]

solvent	viscosity $g.cm^{-1}.s^{-1}$
o-dichlorobenzene	0.013
1-octanol	0.076
dibutylphthalate	0.154
o-nitrophenyl octyl ether	0.128
o-nitro diphenylether	0.161

The reason for this instability may be the emulsification of the organic phase [69]. This is shown schematically in fig. VI - 42. The organic phase tends to form small emulsion droplets due to shear forces when the feed solution is flowing along its surface. These emulsion droplets diffuse out of the organic phase so that eventually the organic phase is completely removed. In order to develop a stable supported liquid membrane, the

experimental conditions should be chosen so that emulsion formation is prevented. Other factors that may contribute as well are solvent loss, carrier loss, and osmotic effects. Since high ion strength are involved in these system high osmotic pressure differences are generated which may instabilize the liquid film. One approach to solve these problems is by gelation of the liquid membrane phase [69]. This means that the liquid film has the properties of a highly swollen crosslinked polymer (a 'gel') rather than that of a liquid. Although the diffusion coefficient will be lower in a gel phase compared to the liquid, the stability of the layer will have been improved. A gelled 'liquid' layer can be obtained by adding a small amount of a polymer to the organic phase capable of forming a gel at low solvent concentrations. Polymers which are useful in this respect are poly(vinyl chloride) (PVC), polyacrylonitrile (PAN) and polymethylmethacrylate (PMMA).
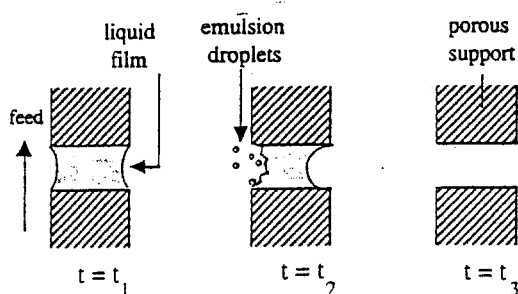
Figure VI - 42.   Schematic representation of the emulsification of the organic phase in supported liquid membranes[69].

VI.4.4.5   Choice of carrier

The choice of the carrier is a key factor in facilitated transport. High selectivities are obtained if the carrier is very specific to one solute, a measure of this selectivity being given by the ratio of the distribution coefficients. In fact, every specific solute needs its own specific carrier which makes the selection of the carrier very important but also very difficult. Much information about carrier selection can be obtained from liquid extraction. It is beyond the scope of this book to mention all the different carrier molecules that have been been described to date but some classes of carrier molecules can be mentioned:

- oximes
- (tertiary) amines
- crown ethers
- cobalt complexes
- calixarenes

The structures of some of these carrier molecules are depicted in table VI - 20.

Table VI.20 Structures of various carriers: oximes, tertiary amines, calixarenes and crown ethers
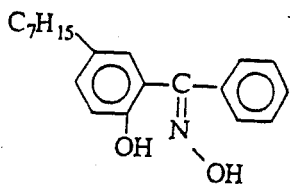
LIX 65N®
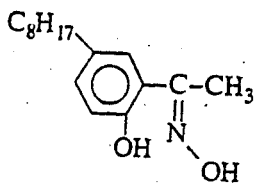
SME 529®

oxime
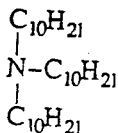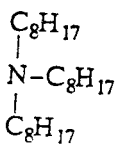
alamine 336 ®

tertiary amine
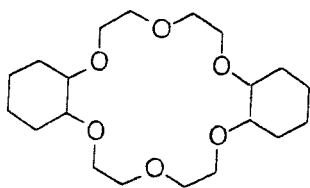
dicyclohexano-18-crown-6

crown ether
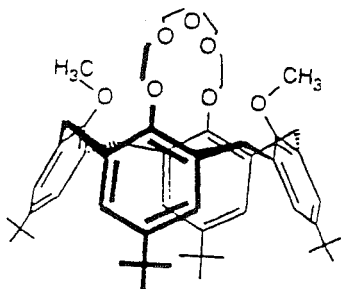
calixarene

VI.4.4.6   Applications

The number of applications is very large and various classes can again be distinguished [66,70-72], e.g. the separation of cations, anions, gases and organic molecules.

Both cations and anions can be easily removed via facilitated transport because a wide range of carriers is available. Among the numerous cations that can be recovered by liquid membranes, the following may be mentioned: copper (Cu^{2+}), mercury (Hg^{2+}), nickel (Ni^{2+}), cadmium (Cd^{2+}), zinc (Zn^{2+}) and lead (Pb^{2+}).

Anions can also be transported by liquid membranes, e.g. nitrate (NO_3^-), chromate ($Cr_2O_7^{2-}$) and uranyl ($UO_2(SO_4)_2^{2-}$).

Gases constitute a completely different type of class which can be removed by facilitated transport. Examples here are the separation of oxygen from nitrogen, the removal of H_2S from natural gas, and NH_3, NO_x and SO_2 from waste gases. Finally, the last applications class is the separation of organic mixtures. An example here is the separation of hydrocarbons (aliphatic/aromatic as benzene/hexane and the separation of isomeric xylenes) and the removal of phenol from waste water.

VI.4.4.7   Summary of carrier mediated transport

membranes:	supported liquid membranes (SLM)
	emulsion liquid membranes (ELM)
	fixed carrier membranes
	solvent swollen membranes
thickness:	20 -150 μm (SLM)
	$\approx 0.1 - 1$ μm (ELM)
pore size:	nonporous (liquid !)
driving force:	concentration difference
separation principle:	affinity to carrier (carrier mediated transport)
supporting membrane material:	hydrophobic porous membrane
applications:	- removal of specific ions
	* cations (cadmium, copper, nickel, lead)
	* anions (nitrate, chromate)
	- removal of gases
	* oxygen/nitrogen separation
	* removal of H_2S, CO_2, SO_2, CO, NH_3
	- separation of organic liquids
	- removal of phenol

VI.4.5 Dialysis

Dialysis is a process where solutes diffuse from one side of the membrane (the feed side) to the other side (the dialysate or permeate side) according to their concentration gradients. Separation between the solutes is obtained as a result of differences in diffusion rates across the membrane arising from differences in molecular size and difference in solubility. A typical concentration profile is shown in figure VI - 43a. Often boundary layer effects contribute as well and then the concentration profile as given in figure VI - 43b apply.

(a)   (b)
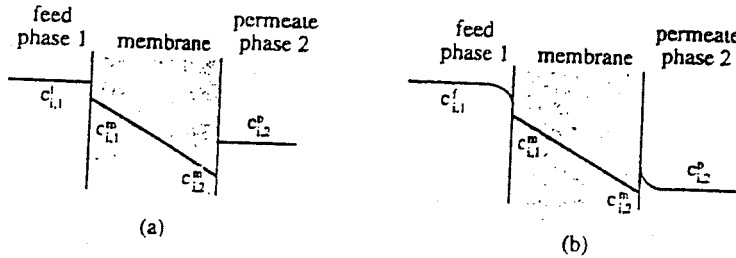
Figure VI - 43. Concentration profiles for dialysis without boundary layer resistance (a) and with bounadry layer resistances (b).

In order to obtain a high flux, the membranes should be as thin as possible. Figure VI - 44 gives a schematic drawing of the dialysis process where feed stream and dialysate or permeate stream are flowing counter-currently (see also chapter VIII).
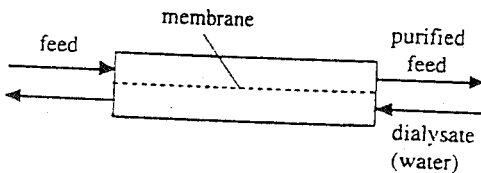
Figure VI - 44. Schematic drawing of the dialysis process.

Transport in dialysis proceeds via diffusion through nonporous membranes, and in order to reduce the diffusive resistance the membranes are highly swollen. As a result of such swelling, the diffusion coefficients are high in comparison to those in the unswollen membrane. The differences may be quite large; thus the diffusion coefficient of a low molecular solute within a polymer can vary from about 10^{-19} m²/s in a glassy (crystalline) polymer up to about 10^{-9} m²/s for a highly swollen polymer, with the permeation rate varying in a similar fashion (see figure VI - 14). This means that the

resistance increases with increasing molecular weight and decreasing swelling value. Low molecular ionic (salts) and neutral solutes (urea) readily pass through the membrane, whereas the higher molecular weight components exhibit much higher resistances.

Dialysis, or 'ordinary' dialysis as discussed in this section, is referred to as the diffusion of neutral molecules. If electrolytes are separated with neutral membranes or with charged membranes, then 'Donnan effects' arising from the unequal distribution of ions, interfere with the normal dialysis process. This type of dialysis is called Donnan dialysis or diffusion dialysis and these processes will be described in section VI.4.6.

VI.4.5.1 Transport

Dialysis is a diffusion process and at steady-state transport can be described by Fick's law which gives after integration across the membrane (see figure VI - 43a) the following equation

$$J_i = \frac{D_i}{\ell}\left(c_{i,1}^m - c_{i,2}^m\right)$$

(VI - 102)

or by introducing the equilibrium distribution coefficient K_i

$$J_i = \frac{D_i K_i}{\ell}\Delta c_i = \frac{P_i}{\ell}\Delta c_i$$

(VI - 103)

where D_i is the solute diffusion coefficient, K_i the distribution or partition coefficient ($K_i = c_{i,1}^m / c_{i,1}^f = c_{i,2}^m / c_{i,2}^f$), ℓ the membrane thickness and Δc_i the concentration difference between the feed and the permeate ($\Delta c_i = c_{i,1}^f - c_{i,2}^p$). At the same time as solute flux occurs an osmotic solvent flow takes place in the opposite direction from the low concentration side to the high concentration side. This osmotic flow is proportional to the osmotic pressure difference. The solute and solvent flows do not occur independently but are coupled (see chapter V). Because of solute diffusion the concentration difference decreases, the osmotic pressure difference decreases and hence the solvent flow decreases. On the other hand, solvent flow also causes a decrease in the solute concentration on the high concentration side, so that the concentration difference decreases and this results in a decreased solute flow.

Also in dialysis the transport resistance is not determined only by the membrane but frequently boundary layer resistances have to be taken into account. This is drawn schematically in figure VI - 43b. The overall mass transfer coefficient k_o is obtained by the sum of the three resistances according to

$$\frac{1}{k_o} = \frac{\ell}{P_i} + \frac{1}{k_1} + \frac{1}{k_2}$$

(VI - 104)

where k_1 and k_2 are the mass transfer resistances in feed and permeate boundary layers respectively and $P_i = D_i \ K_i$. The solute flux can also be given in terms of an overall mass transfer coefficient.

$$J_i = k_o \ (c^f_{i,1} - c^P_{i,2})$$

(VI - 105)

VI.4.5.2 Membranes

Dialysis is mainly used to separate low molecular weight components from those of high molecular weight. Such a separation mechanism is based on differences in molecular weight as expressed by the Stokes-Einstein equation. Although dialysis is mainly employed with aqueous solutions, the process itself is not limited solely to such solutions. To achieve sufficient permeation rates the membrane must be highly swollen, which in turn implies that the membrane selectivity will decrease. An optimum must therefore be found between the diffusion rate and swelling. In addition, the membrane should be as thin as possible.

Hydrophilic polymeric materials, e.g. cellophane and cuprophane, which are both regenerated celluloses have been used for aqueous applications. Other hydrophilic materials used include cellulose acetate (CA) or saponified cellulose acetate, poly(vinyl alcohol) (PVA), polyacrylic acid (PAA), polymethylmethacrylate (PMMA), copolymers of ethylene and vinyl acetate (EVA) or ethylene and vinyl alcohol (EVAL), of polycarbonate and polyether, and more hydrophobic materials such as polycarbonates (PC).

VI.4.5.3 Applications

By far the most important application is hemodialysis where membranes are used as artificial kidneys for people suffering from renal failure [73,74]. Dialysis membranes can completely replace the kidney and are capable of removing toxic low molecular components such as urea, creatinine, phosphates and uric acid. This is achieved by pumping the blood through a dialyser which is often a hollow fiber module, containing one of the above mentioned membranes. One of the main requirements for the membrane materials is blood compatibility. Often heparin, an anticoagulant, is added to the blood before it enters the membrane unit. In addition to the toxic components, non-toxic vital low molecular solutes will also diffuse through the membrane. For example electrolytes such as sodium and potassium will diffuse in this way, if pure water is taken as the second phase. Because the electrolyte balance is very important, physiological salt solutions are used as the dialysate so that there is no driving force for the transport of these ions under these circumstances.

Porous membranes are used as well to remove metabolic wastes from blood. This process is called hemofiltration and employs membranes of the ultrafiltration type. Both

processes, hemodialysis and hemofiltration, are different in origin: the former is based on diffusion while the latter is based on convection. Because the flow rates in hemofiltration are much higher, care must be taken to avoid dehydration of the patient.

Other applications worthy of mention are the recovery of caustic soda from colloidal hemicellulose during viscose manufacture [75] and the removal of alcohol from beer [76]. Also in biotechnology and the pharmaceutical industry to remove salts from bioproducts and for fractionation.

VI.4.5.4   *Summary of dialysis*

membranes:	homogeneous
thickness:	10 - 100 μm
driving force:	concentration differences
separation principle:	difference in diffusion rate, solution–diffusion
membrane material:	hydrophilic polymers (regenerated cellulose such as cellophane and cuprophane, cellulose acetate, copolymers of ethylene-vinyl alcohol and of ethylene-vinyl acetate)
main applications:	- hemodialysis (removal of toxic substances from blood) - alcohol reduction in beer - desalination of enzymes and coenzymes - alkali recovery in pulp and paper industry

VI.4.6.   *Diffusion dialysis*

Diffusion dialysis is a diffusion process in which ions are transported across an ionic membrane due to a concentration difference and can be described in a similar way as the dialysis process. The flux of an ion i across a membrane is in absence of concentration polarization given by

$$J_i = \frac{P_i}{\ell} \Delta c_i$$

(VI - 106)

where P_i is the permeability coefficient of a specific ion across the membrane. Eq. VI - 106 can not be applied in general. Due to the presence of ions in combination with an ionic membrane Donnan equilibria are built-up and the transport is given by the Nernst-Planck equation which includes except for a concentration difference also an electrical potential difference. Protons and hydroxyl ions are not very effectively retained by a Donnan potential and this allows to remove these ions from other ions with the same

charge. In an basic solution (pH > 7) an cation-exchange membrane is applied and this membrane is able to retain all anions except for hydroxyl ions and in this way caustic soda can be recovered from a salt solution (Figure VI - 45a left). The same accounts for an acid salt solution. Here a positively charged anion-exchange membrane is applied and this membrane retains all cations except for protons and a separation can be achieved between protons and other cations (Figure VI - 45a right). In this way the acid can be recovered.

The other concept is shown in figure VI - 45b and this process is often referred to as Donnan dialysis. Since there is in fact not a fundamental difference between diffusion dialysis and Donnan dialysis, the former name is preferred and will be used. Also here ion exchange membranes are applied and figure VI - 45b left shows a cation-exchange membrane. Since the membrane is permeable for cations, H^+ will diffuse from the left compartment (phase I) to the right compartment (phase II).

(a)

(b)
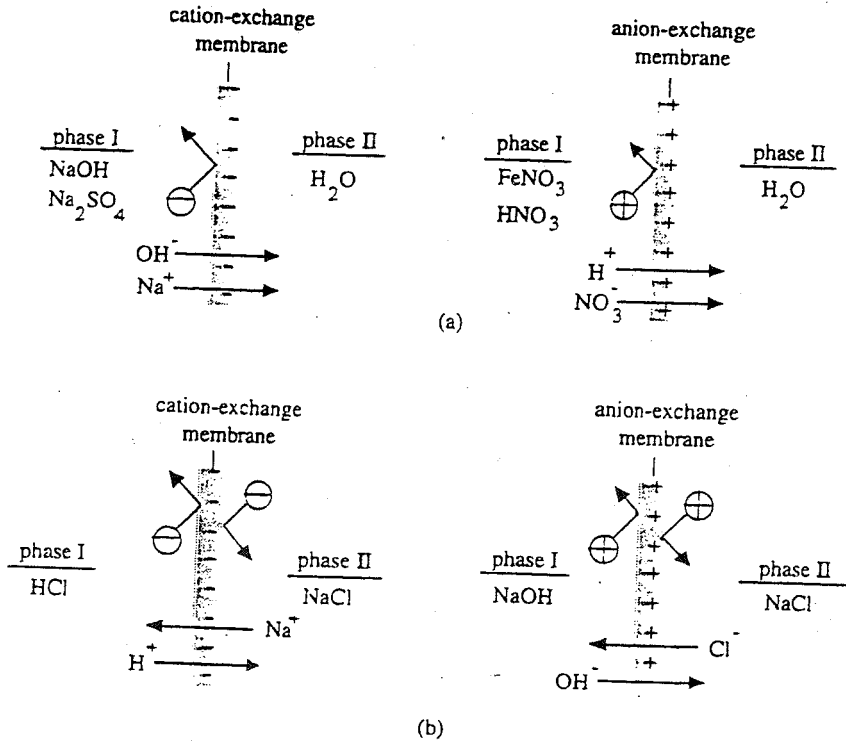
Figure VI - 45   Principle of diffusion dialysis (a) and Donnan dialysis (b) for a cation and anion exchange membrane.

At the same time Na$^+$ will diffuse in the other direction since there is a driving force (a concentration difference) but also because electroneutrality must be remained. Since the mobility of the H$^+$ ions is larger an electrical potential will be generated which accelerates the Na$^+$ flux. These processes can certainly not described anymore by the simple equation VI - 106 and here the Nernst-Planck equation should be employed. Figure VI - 45b right shows the same principle, only anion-exchange membranes have been applied and the anions are the diffusing components.

VI.4.6.1.   Applications

Diffusion dialysis type of processes are from an engineering point of view rather simple and energy efficient processes in which feed and permeate are pumped counter-currently, like most dialysis type of processes. No external driving force such as pressure difference or an electrical potential difference are required. A simplified process scheme is shown in figure VI - 46.
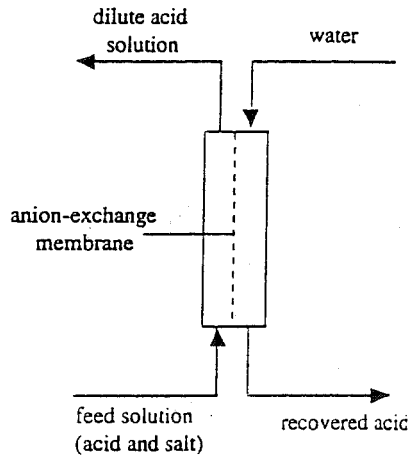
Figure VI - 46.   Schematic drawing of a diffusion dialysis process to recover acid from a salt
                      solution

HF and HNO$_3$ are often used as etching agents for stainless steel. In order to recover the acid, diffusion dialysis can be applied since the protons can pass the membrane but the Fe^{3+} ions can not. Other applications are the recovery of acids from ion exchange regeneration and in metal-refining. Also in alkaline solutions the process can be applied to recover the hydroxyl ions. Examples can be found for instance in the textile industry (mercerising process), and hydrolurgy (metal-plating).

VI.4.6.2   Summary of diffusion dialysis

membranes:	ion-exchange membranes
thickness:	≈ few hundreds of μm (100 - 500 μm)
driving force:	concentration differences (and electrical potential difference)
separation principle:	Donnan exclusion mechanism
membrane material:	cation-exchange and anion-exchange membranes (similar to electrodialysis)
main applications:	
processes	- acid recovery from etching, pickling and metal refining
	- alkali recovery from textile and metal refining processes

VI.5.   Thermally driven membrane processes

VI.5.1   Introduction

Most membrane transport processes are isothermal processes with either concentration, pressure or electrical potential difference as the driving force.

When a membrane separates two phases held at different temperatures, heat will flow from the high-temperature side to the low-temperature side. This transport of heat can be expressed by a simple phenomenological equation, i.e. Fourier's law (see chapter I . 5), where the heat flow is related to the corresponding driving force, the temperature difference. The process of heat conduction across a homogeneous membrane is shown schematically in figure VI - 47. The heat flux is given by

$$J_h = -\lambda \frac{dT}{dx}$$

(VI - 107)

in which the proportionality constant λ is the thermal conductivity or heat conductivity. Table VI.21 summarizes some values of λ in various media.

Table VI.21   Heat conductivity values in various media

medium	λ (W/m °C)
gases	0.02
organic liquids	0.2
water	0.6
polymers	2.0
metals	20 - 200

Integration of eq. VI - 107 across the membrane at steady-state flow and constant λ gives

$$J_h = \frac{\lambda}{\ell}(T_o - T_\ell) \qquad\qquad (VI - 108)$$

In addition to the heat flow a mass flow also occurs, a process called thermo-osmosis or thermo-diffusion. No phase transitions occur in these processes.

Another thermally driven membrane process is membrane distillation. Here, a porous membrane separates two liquids which do not wet it. If the liquids differ in temperature, the resulting vapour pressure difference causes vapour molecules to permeate from the high-temperature (high vapour pressure) side to the low-temperature (low vapour pressure) side. The basic concept of membrane distillation will be described below.
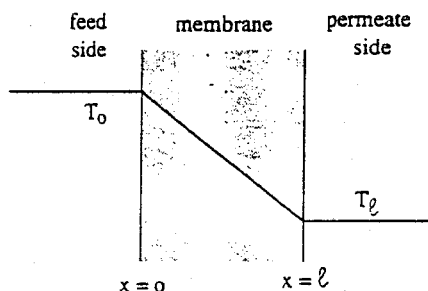
Figure VI - 47.   Temperature profile across a homogeneous membrane

VI.5.2   Membrane distillation

Membrane distillation is a process in which two liquids or solutions at different temperatures are separated by a porous membrane. The liquids or solutions must not wet the membrane otherwise the pores will be filled immediately as a result of capillary forces. This implies that non-wettable porous hydrophobic membranes must be used in the case of aqueous solutions. A schematic representation of a membrane distillation process is given in figure VI - 48.

When the phases contain pure water and there is no temperature difference, the system is in equilibrium and no transport occurs. If the temperature of one of the two phases is higher than that of the other, a temperature difference exists across the membrane, resulting in a vapour pressure difference. Thus, vapour molecules will transport through the pores of the membrane from the high vapour pressure side to the low vapour pressure side. Such transport occurs in a sequence of three steps:
- evaporation on the high-temperature side.
- transport of vapour molecules through the pores of the hydrophobic porous membrane.

- condensation on the low-temperature side

Membrane distillation is one of the membrane processes in which the membrane is not directly involved in separation. The only function of the membrane is to act as a barrier between the two phases. Selectivity is completely determined by the vapour-liquid equilibrium involved. This means that the component with the highest partial pressure will show the highest permeation rate. Thus, in the case of an ethanol/water mixture where the membrane is not wetted at low ethanol concentrations, both components will be transported through the membrane but the permeation rate of ethanol will always be relatively higher. With salt solutions, for example NaCl in water, only water has a vapour pressure, i.e. the vapour pressure of NaCl can be neglected, which means that only water will permeate through the membrane and consequently very high selectivities are obtained.
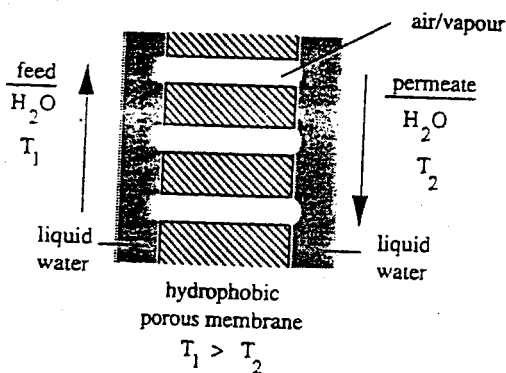
Figure VI - 48. Schematic representation of membrane distillation.

The transport of volatile components through the membrane can be described by phenomenological equations in which the flux is proportional to the driving force, i.e. the temperature difference across the membrane. The temperature difference results in a vapour pressure difference (temperature and vapour pressure are related according to the Antoine equation

The flux may be described by the phenomenological equation:

$$J_i = B \cdot \Delta p_i$$

(VI - 109)

in which the flux is related to two parameters, the membrane-based parameter B and the system-based parameter Δp. The proportionality factor B is determined by membrane parameters such as the material (hydrophobic/hydrophilic), pore structure, porosity and membrane thickness. The main structural parameters are the porosity, which must be as

high as possible and the membrane thickness. The pore size distribution must be narrow, particularly on the larger pore side because the largest pores will be wetted first. In contrast, the system-based parameter Δp is mainly determined by the temperature difference ΔT.

Other parameters of interest are the hydrodynamic conditions (flow velocity) and module design, because they determine the effect of temperature polarisation and hence influence the driving force (see chapter VII).

VI.5.2.1 Process parameters

Membrane distillation is based on the concept that distillation takes place across a porous membrane. The main requirement is that the membrane must not be wetted. If wetting occurs, the liquid will penetrate spontaneously into the pores of the membrane. The wettability is determined by the interaction between the liquid and the polymeric material, with no wetting occurring at low affinity. Information about wettability can be obtained by contact angle measurements, i.e. a drop of liquid is placed upon a nonporous flat (and smooth) surface and the contact angle is measured. For low affinity the contact angle θ will have a value greater than 90°, whereas with high affinity the value of θ will be less than 90°. In the latter case the liquid will wet the surface. This is shown schematically in figure VI - 49.
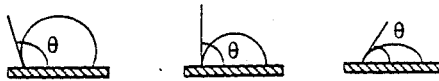
Figure VI - 49. Contact angles of liquid droplets on a solid (nonporous) material.

If the material is porous, the liquid will penetrate into the pores when wetting occurs ($\theta <$ 90°). This can be described by the Laplace equation:

$$\Delta p = -\frac{2\gamma_l}{r}\cos\theta \qquad\qquad (VI - 110)$$

If $\theta > 90°$ then $\cos\theta < 0$ and $\Delta p > 0$, and only if a finite pressure is applied (according to the Laplace equation) the liquid will penetrate into the membrane. As can be seen from eq. VI - 110, the wettability depends on three factors:
- pore size (r)
- surface tension of the liquid (γ_l)
- surface energy of the membrane material (θ or $\cos\theta$)

The wetting pressure is inversely proportional to the membrane pore size. Figure VI - 50 gives the pressure needed to wet a porous teflon membrane with water as a function of

the pore size.

The second parameter that determines the wettability is the surface tension of the liquid. This is related to intermolecular forces such as dispersion forces, polar forces and hydrogen bonding. In a hydrocarbon such as hexane, only weak dispersion forces act and consequently the surface tension is low. On the other hand, in cases where hydrogen bonding occurs such as in water, the intermolecular forces are very strong and as a result the surface tension is high. Table VI.22 summarises the surface tensions of some liquids.
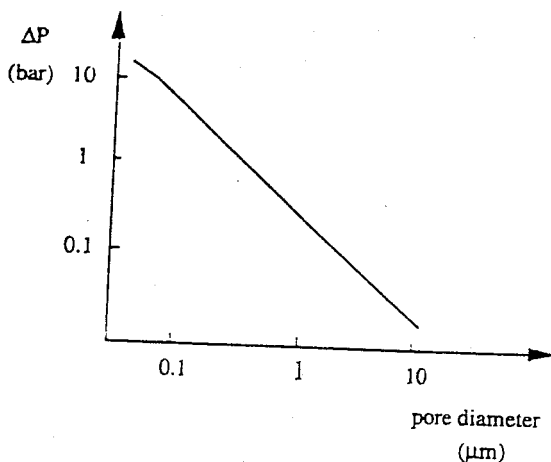
Figure VI - 50. Wetting pressure (liquid entry pressure) for a porous polytetrafluoroethylene (PTFE) membrane.

When a liquid is brought into contact with a (smooth) polymeric surface, various contact angles between the liquid and the polymer are observed depending on the affinity between the liquid and the polymer. Three different cases can be distinguished as shown in figure VI - 49. If the contact angle is greater than 90°, the liquid does not wet the

Table VI.22. Surface tension of some liquids at 20°C [77]

liquids	surface tension (γ_l) (10^3 N/m)
water	72.8
methanol	22.6
ethanol	22.8
glycerol	63.4
formamide	58.2
n-hexane	18.4

surface. This will occur when the interaction between liquid and polymer is very small, as for example with water/polypropylene. When the contact angle is smaller than 90° the liquid wets the surface, and when $\theta = 0$ the liquid spreads out over the surface.

Table VI.23. Surface energies of some polymers [77]

polymer	surface energy (γ_s) ($10^3 \cdot$ N/m)
polytetrafluoroethylene	19.1
polytrifluoroethylene	23.9
polyvinylidenefluoride	30.3
polyvinylchloride	36.7
polyethylene	33.2
polypropylene	30.0
polystyrene	42.0

The third important factor is the surface tension of the polymer. Wetting is favoured when the solid polymer has a high surface energy. Table VI.23 summarises the values of the surface energy of some polymers. To avoid wetting the maximum pore size must be small, the surface tension of the liquid high (for example, water) and the surface energy of the membrane material low such as with polypropylene (PP), polyethylene (PE), polytetrafluoroethylene (PTFE) and poly(vinylidene fluoride) (PVDF). Since teflon has the lowest surface energy this material has the lowest wetting tendency. When organic
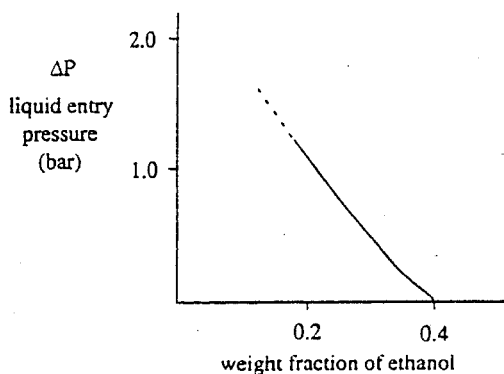
Figure VI - 51. Liquid entry pressure as a function of the weight fraction of ethanol for a porous polypropylene (Accurel) membrane with a pore diameter of 0.1 µm [78].

solvents are present in the water then the surface tension decreases. Figure VI - 51 shows the pressure needed to wet a porous polypropylene membrane (Accurel) as a function of the ethanol concentration in water [78]. With increasing ethanol concentration, the surface tension of the liquid decreases and consequently the pressure needed to wet the porous membrane decreases. At 30 - 40% ethanol in the liquid, the surface tension of the feed is so low that spontaneous wetting occurs. In order to determine the wettability of a liquid or liquid mixture, a critical surface tension must be defined and determined [78].

VI.5.2.2   Membranes

The requirements for the membranes used in membrane distillation are very clear. To avoid wetting, the surface energy of the polymer must be as low as possible. This means that very hydrophobic materials such as polytetrafluoroethylene, poly(vinylidene fluoride), polyethylene or polypropylene must be used in combination with liquids with high surface tension such as water. Because the selectivity is determined by the vapour-liquid equilibrium, the membrane cannot be optimised further. However, the flux can be optimised and here the most important parameter is the porosity (surface porosity and overall porosity). A higher porosity is often associated with increasing pore size but this factor also favours wettability. Thus a high porosity (70 to 80%) with pore sizes in the range of 0.2 to 0.3 μm is desirable. The maximum pore size is of especial interest because wettability is related to this and hence the largest pores must not be too different from the average pore size. Furthermore, it is important that the membranes should be as thin as possible. Indeed, the porous membranes used in this process can be exactly the same as those used in microfiltration.

VI.5.2.3   Applications

The applications are determined by the wettability of the membrane, which implies that mainly aqueous solutions containing inorganic solutes can be treated. The surface tension of these solutions differs little from that of water. The applications can be classified as to whether; i) permeate is the desired product or ii) retentate is the desired product.
i) the production of pure water
In most applications the permeate is the product of interest. A high quality permeate can be obtained with membrane distillation, as for example [79]
- water for the semiconductor industry
- boiler feed water for power plants
- desalination of seawater

The quality of the permeate remains high even at high feed concentrations. Figure VI - 52 gives the flux and selectivity (here expressed as conductivity) of a porous polypropylene membrane as a function of the sodium chloride concentration. With increasing salt concentration the flux shows some decline, because of a decrease in vapour pressure depression.
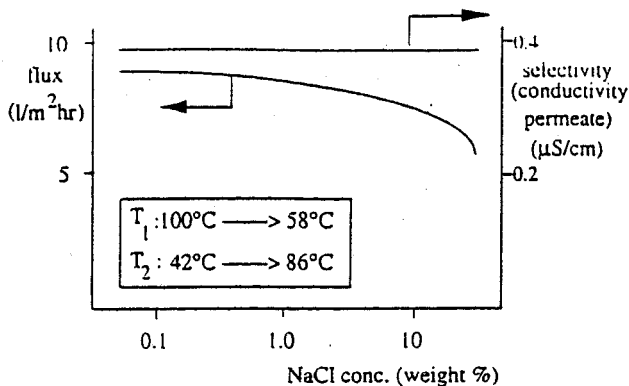
Figure VI - 52. Flux and selectivity as a function of the NaCl concentration for a porous polypropylene membrane (Accurel) [79].

On the other hand, the quality of the permeate is independent of the feed concentration. Whereas in seawater desalination reverse osmosis is strongly affected by the osmotic pressure of the (highly) concentrated feed solutions, membrane distillation can handle even higher salt concentrations without a substantial decrease in membrane performance.

The removal of volatile organic components (VOC's), such as chlorinated hydrocarbons or aromatics, from an aqueous solution is another application. These volatile contaminants are often present in very low concentrations in surface water or industrial effluent.

ii) The concentration of solutions

Membrane distillation can be used for the concentration of solutions in some cases, e.g.

- waste water treatment
- concentration of salts, acids, etc.

iii) The removal of volatile bioproducts

Volatile bioproducts, such as ethanol, butanol, acetone or aroma compounds, may be prepared by fermentation and these can be removed by membrane distillation.

Finally the process design will be considered briefly. In the simplest type of construction two compartments are separated by a membrane. Evaporation occurs on the high-temperature side and hence the temperature of this liquid will decrease. In contrast, condensation occurs on the low-temperature side and the temperature will increase. In commercial installations the process will be carried out in a counter-current flow, which allows a constant temperature difference to be set up across the membrane (the vapour pressure difference is not constant!). Figure VI - 53 gives an example of such a counter-current set-up.

90°C ──────▶ ┌─────────────────┐ ────▶ 50°C
85°C ◀────── │   feed   │ ◀──── 45°C
             │ - - - - - - - - │
             │   permeate   │
             └─────────────────┘
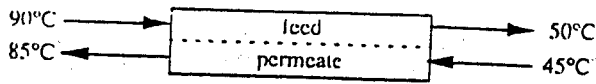
Figure VI - 53. Schematic drawing of a counter-current set-up [79].

The temperature of the feed solution decreases but the temperature of the permeate increases. A substantial portion of the heat is transferred from the feed side to the permeate side and part of this energy can be recovered. This is shown schematically in figure VI - 54 in which a membrane distillation unit is shown combined with a heat-exchanger. The high-temperature permeate stream flows along the heat exchanger thereby increasing the temperature of the inlet feed stream. However, it is also possible to carry out the same process without heat recovery.

Another class of applications are aqueous solutions containing low concentrations of a volatile component such as occur in mixtures of ethanol/water or trichloroethylene/water. Here also a vacuum can be applied instead of water on the permeate side, resulting in a high driving force ($p_2 \Rightarrow 0$). Because the separation is based on a vapour-liquid equilibrium, the permeate is enriched in the volatile component. Although this process is sometimes referred to as pervaporation it is in fact a membrane distillation process. Membrane distillation can have a distinct advantage over distillation, especially for small-scale applications, because of the large surface area per volume as can be found in hollow fiber and capillary modules.
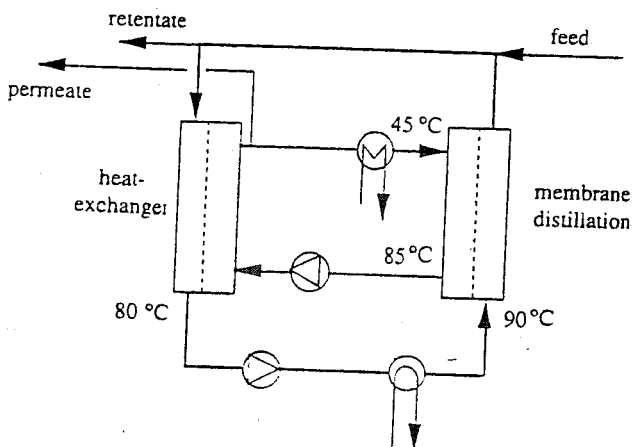
Figure VI - 54. Schematic drawing of a membrane distillation unit combined with a heat-exchanger in order to recover a part of the energy [79].

VI.5.2.4   Summary of membrane distillation

membranes:	symmetric or asymmetric porous
thickness	20 - 100 μm
pore size:	≈ 0.2 - 1.0 μm
driving force:	vapour pressure difference
separation principle:	vapour-liquid equilibrium
membrane material	hydrophobic (polytetrafluoroethylene, polypropylene)
application:	production of pure water
	- laboratories
	- semiconductor industry
	- desalination of seawater
	- production of boiler feed water
	- concentration of aqueous solutions
	removal of VOC's
	- contaminated surface water (benzene, TCE)
	- fermentation products (ethanol, butanol)
	- aroma compounds

VI.6.   Membrane contactors

In the previous section it was shown that distillation can occur across a membrane. Also for extraction, another widely industrially used separation process, ths a membrane analogue. These membrane processes are generally referred to as membrane contactors. (There are quite a number of other names which are used such as pertraction, perstraction, gas absorption, membrane based solvent extraction, liquid-liquid extraction, membrane based gas absorption and stripping, hollow-fiber contained liquid-membrane); we will use here the general name membrane contactors both for gas phase and liquid phase processes. The separation performance in these processes is determined by the distribution coefficient of a component in two phases and the membrane acts only as an interface, similar to membrane distillation. In general, it is not the enhanced mass transfer but rather the the large area per volume as can be found in hollow fiber and capillary modules, that makes this process more attractive than conventional dispersed-phase contactors. For instance for packed and trayed columns typical surface areas per volume are in the range of 30 to 300 m^2/m^3 whereas in membrane systems values can be found of 1600 to 6600 m^2/m^3 [80]. Other advantages are the elimination of flooding and entrainment of the dispersed phase. Disadvantages must be mentioned as well, and the first one is that an additional phase, the membrane phase, is added. Dependent on the type of membrane and the system applied, this membrane phase may contribute to the overall mass transfer resistance. The instability of the system may constitute another problem. If for instance a pressure is applied that exceeds the wetting pressure, liquid penetration may occur. On the other hand if a gas phase is used with a low pressure the

liquid phase may be evaporated. In the case of two liquid phases, the membrane phase may be removed due to slowly dissolution, or emulsion formation.

A distinction will be made between gas-liquid (G - L) and liquid-liquid (L - L) membrane contactors and these will be described consecutively. In the G - L contactors one phase is a gas or a vapour and the other phase is a liquid whereas in the L - L contactors both phases are liquids. A schematic drawing is given in figure VI - 55. The gas-liquid membrane contactor can be further divided in a process where a gas or a vapour is transferred from the gas phase to a liquid phase (figure VI - 55a) and a process where a gas or a vapour is transferred from the liquid phase to the gas phase (figure VI - 55b).
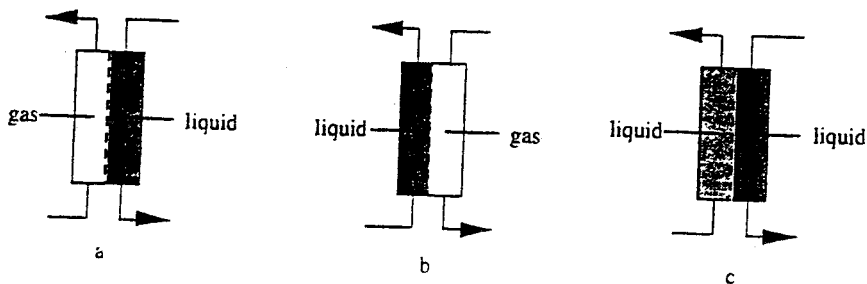
Figure VI - 55. Schematic drawing of various membrane contactors. a. gas-liquid contactor; b. liquid-gas contactor; c. liquid-liquid contactor.

If a component i is transferred from the feed phase to the permeate phase three steps can be considered in general; transport from the feed phase to the membrane, then diffusion through the membrane followed by transfer from the membrane to the permeate phase. The flux of component i is conveniently expressed in terms of an overall mass transfer coefficient

$$J_i = k_{ov,i} \, \Delta c_i$$

$$(VI - 111)$$

with

$$\frac{1}{k_{ov,i}} = \frac{1}{k_i \, (feed)} + \frac{1}{k_i \, (membrane)} + \frac{1}{k_i \, (receiving \ phase)}$$

$$(VI - 112)$$

If the mass transfer resistance is completely in the membrane phase then eq. VI - 112 reduces to

$$J_i = \frac{D_i \, K_i}{\ell} \, \Delta c_i = \frac{P_i}{\ell} \, \Delta c_i$$

$$(VI - 113)$$

in which K_i is the distribution coefficient of component i from the feed phase into the membrane phase. D_i is the diffusion coefficient of component i in the membrane and Δc_i is the bulk concentration difference. Generally, the mass transfer resistance in the boundary layers cannot be neglected and these must be calculated or estimated from mass transfer correlations as will be discussed in chapter VII. In the following two sections the gas-liquid en liquid-liquid membrane contactor will be described.

IV.6.1   Gas-liquid membrane contactor

IV. 6.1.1. Introduction

The most widely used application of G - L contactors is in blood oxygenation. In these so-called oxygenators pure oxygen or air is flow at one side of the membrane, most hollow fibers, while the blood flows at the other side. Due to a gradient in partial pressure oxygen will diffuse into the blood and carbon dioxide will diffuse from the blood to gas phase.

In general porous membranes are used in membrane contactors in which the membrane primarily acts as a barrier between the phases (It is also possible that nonporous membranes are used in this case, e.g. silicone rubber membranes. This will be considered at the end of this section, see figure VI - 59). Now two concepts are possible where the pores are either filled with the gas phase or with the liquid phase.
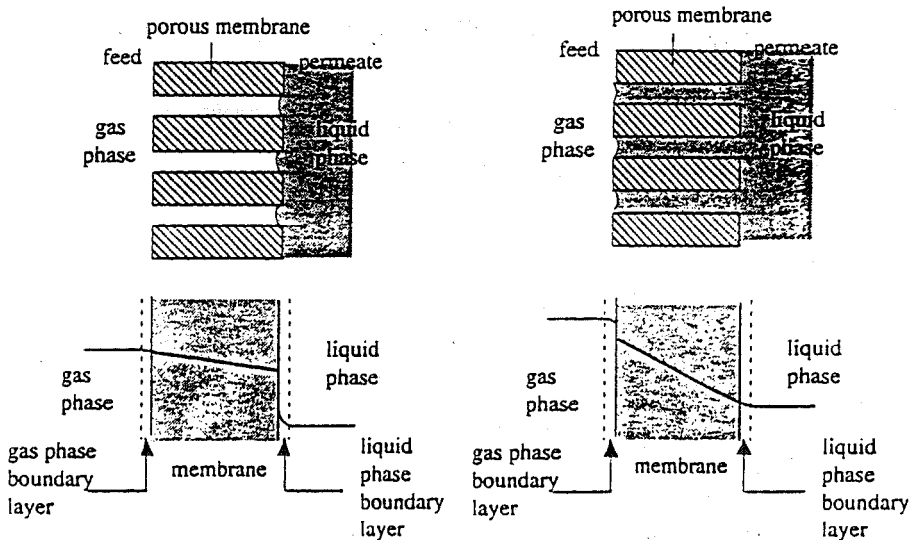
Figure V - 56.   Gas-liquid contactors with a non-wetted membrane (left side) and a wetted membrane (right side). The corresponding concentration profile are shown in the lower figures.

If a hydrophobic membrane is used such polytetrafluoroethylene, polyethylene, polypropylene, with an aqueous solution as the liquid phase that not wets the membrane then pores of the membrane are filled with the gas phase (see figure VI - 56 left). The liquid must be prevented from wetting which means that the wetting pressure may not exceeded (see for wetting pressure at section VI.3.5 membrane distillation). On the other hand, if a hydrophylic membrane is used the aqueous phase will wet the membrane (figure VI - 56 right). The corresponding solute concentration profiles are given as well in figure VI - 56 and these profiles indicate that in the case of a gas phase and a liquid phase the mass transfer resistant is normally located in the latter phase. Except for aqueous solutions non-aqueous solutions are applied as well. A few applications will mentioned to show the possibilities of this concept. Except for blood oxygenators membrane contactors may be applied in oxygen transfer systems in fermentation processes and aerobic waste water treatment without bubble formation. In these cases the feed phase and membrane phase is the gaseous phase and the permeate phase is the aqueous phase. A similar application is carbon dioxide transfer to beverages (water, lemonades or beer). When oxygen is removed from water by e.g. nitrogen stripping, the feed phase is a liquid and the permeate phase is a gas (see figure VI - 55b). A number of examples have been given so far where a specific component is removed from a gas phase and transferred into a liquid phase. If this specific component is the product of interest it must be removed two systems may be applied, an absorption stage and a desorption stage, as shown schematically in figure VI - 57. This approach has been employed in the separation of saturated/unsaturated hydrocarbons (paraffin/olefin separation) such as ethane/ethylene and propane/propylene. Since the unsaturated
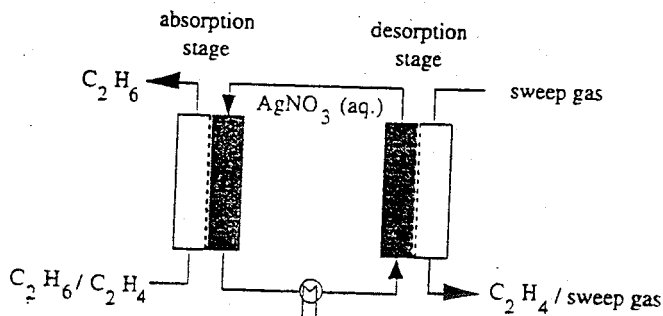
Figure VI - 57. Separation of ethane/ethylene in an absorption/desorption stage membrane contactor

ethylene and propylene gases may complex with silver ions, an aqueous silver nitrate solution can be used in an absorption stage to remove the unsaturated component. In order to desorb this gaseous component a sweep stream can be applied in a desorption step and now the fraction rich in ethane is obtained from the outlet stream of the absorption stage and the fraction rich in ethylene from the sweep stream of the desorption

stage. Only a relatively small recirculation stream of an aqueous silver nitrate solution is required. Other examples are the removal of acid gases such as CO_2, H_2S, CO, SO_2 and NOx from flue gas, biogas and natural gas and the removal of NH_3.

IV.6.2   Liquid-liquid membrane contactor

IV.6.2.1. Introduction

The liquid-liquid membrane contactor is characterised by two liquid streams separated by a porous or nonporous membrane. In case of a porous membrane the feed phase may either wet or not wet the membrane. Firstly we will consider the case where the feed is an organic solvent from which a solute has to be removed while the permeate phase is an aqueous phase. If now a hydrofobic porous membrane is used the membrane will be wet and the pores will be filled. At the permeate side an aqueous stream is pumped now which does not wet the membrane and is not miscible with the organic solvent. An interface will formed at the permeate side (figure VI - 58a) and the actual liquid-liquid extraction will occur at this interface. If the feed is an aqueous stream and the membrane is hydrofobic then the feed will not wet the membrane. The (hydrofobic) organic solvent is now used at the permeate side and this will wet the membrane which implies that now the interface is formed at the feed/membrane side (figure VI - 58b). Figure VI - 58 also
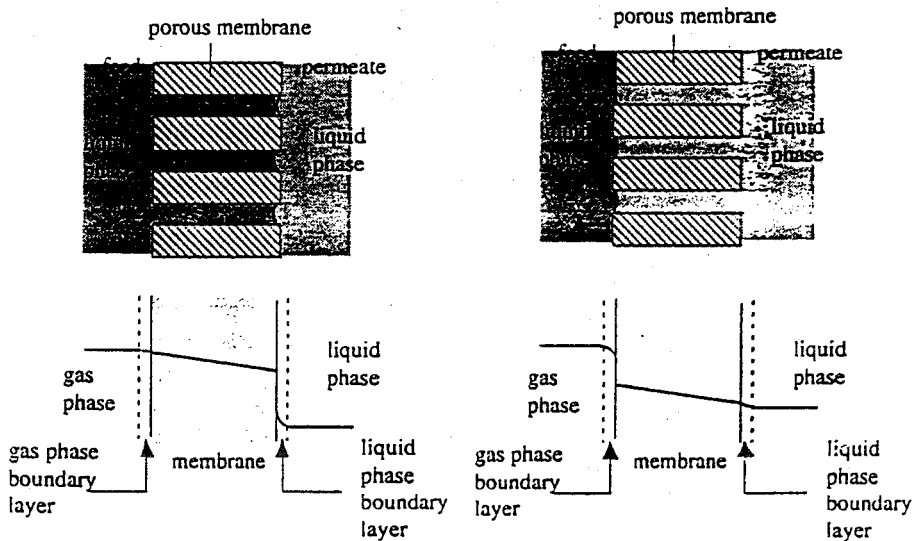
Figure VI - 58   Liquid-liquid membrane contactors with a wettable liquid feed phase (left) and a a non-wettable liquid feed phase (right). The corresponding component concentration profiles are shown in the lower figures.

shows a solute concentration profile which indicates that probably most of the mass transfer resistance will be in the boundary layer at the permeate side. However, the mass transfer resistance in each of the three phases should always be calculated or estimated for any application and module configuration in order to obtain the overall mass transfer resistance. In order to improve mass transfer in either side relatively high cross flow velocities can be applied which generate a pressure drop and this may destabilize the interface especially when surface active components are present. This problem can be partly overcome by increasing the pressure of the non-wetting liquid.

The liquid-liquid membrane contactors can be applied as an alternative for the conventional extraction process for instance to remove heavy metals, volatile organic compounds, phenol, all kind of bioproducts, and microsolutes (herbicides, insecticides and pesticides).

VI.6.3 Nonporous membrane contactors

Gas-liquid and liquid-liquid membrane contactorsdue to shear stresses, osmotic flow, and pressure gradients. This may be overcome by using either nonporous membrane contactors (G - L, L - G or L - L contactor) or by applying a coating onto the porous membrane. An example of a nonporous membrane contactor is silicone rubber which is applied in blood oxygenation. The large advantage of these nonporous systems is that there is no meniscus and the system is rather stable. On the other hand the nonporous
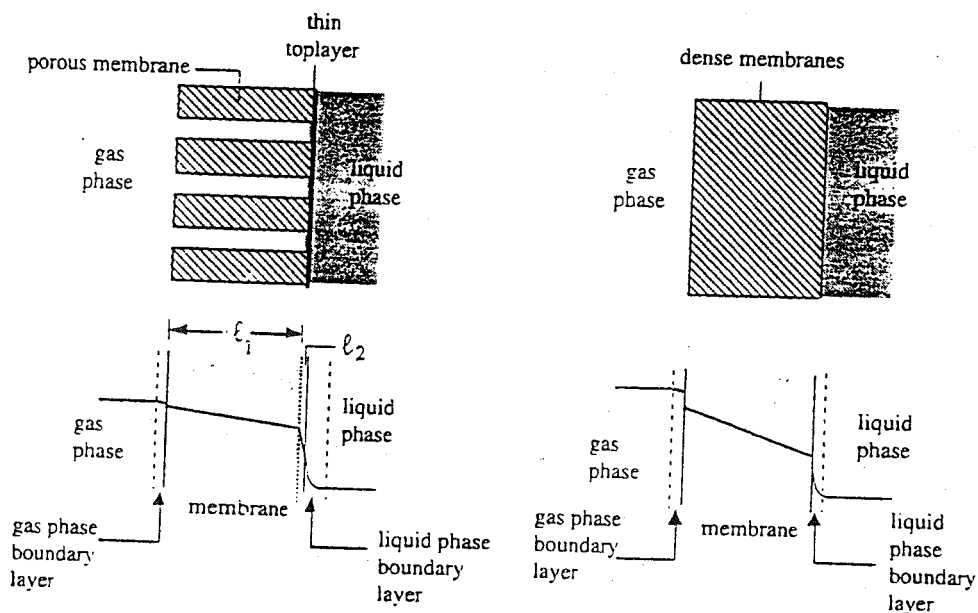
Figure VI - 59   Gas-liquid membrane contactor with a composite membrane (porous membrane, left) and a dense membrane (right)

interface constitute an additional resistance which may be overcome by swelling or by reducing the effective thickness as in coating layers. Figure VI - 59 left shows a schematic drawing of a composite membrane contactor where a coating layer has been applied upon the porous support and figure VI - 59 right shows a homogeneous membrane contactor. The mass transfer resistances in these dense layers may be reduced drastically by swelling effects and even in these cases the main resistance may be located in the liquid boundary layer at the feed side or permeate side. The overall mass transfer resistance may be determined in the same way as for porous membrane contactors, only in the case of the composite membranes, now four terms are involved, since a thin toplayer is applied. The solute concentration profiles are given as well, indicating that the toplayer may contribute substantially, but this is very much dependent on the system involved. The applications are in fact the same as in nonporous systems only the mass transfer resistances and fluxes are different.

VI.6 Summary of membrane contactors

membranes:	porous (hydrophobic or hydrophilic), nonporous, or composites
thickness	20 - 100 μm
pore size:	nonporous or 0.05 - 1.0 μm
driving force:	concentration or vapour pressure difference
separation principle:	distribution coefficient
membrane material	hydrophobic (polytetrafluoroethylene, polypropylene, silicone rubber)
application:	G - L contactors
	- SO_2, CO_2, CO, NO_x from flue gases
	- CO_2 and H_2S from natural gas
	- CO_2 from biogas
	- O_2 transfer (blood oxygenation, aerobic fermentation)
	- CO_2 transfer (beverages)
	- VOC from offgas
	- NH_3 from air (intensive farmery)
	- saturated/unsaturated (ethane/ethylene)
	L - G contactors
	- volatile bioproducts (alcohols, aroma compounds)
	- O_2 removal from water
	L - L contactors
	- heavy metals
	- fermentation products (citric acid, acetic acid, lactic acid penicillin)
	- phenolics

VI.6.5   Thermo-osmosis

Thermo-osmosis (or thermo diffusion) is a process where a porous or nonporous membrane separates two phases different in temperature. Because of the temperature difference, a volume flux exists from the warm side to the cold side until thermodynamic equilibrium is attained. This has been described as an example of coupled flow in chapter IV. There is a considerable difference between thermo-osmosis and membrane distillation, because the membrane determines the separation performance in the former process, whereas in the latter case the membrane is just a barrier between two non-wettable liquids and the selectivity is determined by the vapour-liquid equilibrium. However, the temperature difference is the driving force in both processes.

VI.7   Electrically driven membrane processes

VI.7.1   Introduction

Membrane processes in which an electrical potential difference acts as the driving force use the ability of charged ions or molecules to conduct an electrical current. If an electrical potential difference is applied to a salt solution, then the positive ions (the cations) migrate to the negative electrode (the cathode) whereas the negative ions (the anions) migrate to the positive electrode (the anode). Uncharged molecules are not affected by this driving force and hence electrically charged components can be separated from their uncharged counterparts. Electrically charged membranes are used to control the migration of the ions. Such membranes are electrically conductive. Two types of membrane can be distinguished: cation-exchange membranes allowing the passage of positively charged cations and anion-exchange membranes, that allow the passage of negatively charged anions. The transport of ions across an ionic membrane is based on the Donnan exclusion mechanism (see chapter V). The combination of an electrical potential difference and electrically charged membranes can be used in various arrangements. In this section we will describe the following concepts where ions are involved and ionic membranes are used :

* electrodialysis
* membrane electrolysis
* bipolar membranes
* fuel cells

In all cases the charged membrane constitute a selective barrier where ions are either repelled or transported dependent on the ionic charge and membrane charge. The first three processes require an electrical potential difference as driving force whereas the last process. fuel cells convert chemical energy into electrical energy in a more efficient way than conventional processes by combustion.

VI.7.2   Electrodialysis

The principle of the electrodialysis process is depicted in figure VI - 60. In this process electrically charged membranes are used to remove ions from an aqueous solution. A

number of cation- and anion-exchange membranes are placed in an alternating pattern
between a cathode and an anode. When an ionic feed solution (for example, a sodium
chloride solution) is pumped through the cell pairs, nothing will happen as long as no
direct current is applied. However, when a direct current is applied, the positively charged
sodium ions migrate to the cathode and the negatively charged chloride ions migrate to the
anode. The chloride ions cannot pass the negatively charged membrane and the cations
cannot pass the positively charged membrane. This means that the overall effect is that the
ionic concentration increase in alternating compartments accompanied by a simultaneous
decrease in ionic concentration in the other compartments. Consequently alternate dilute
and concentrate solutions are formed. Electrolysis occurs at the electrodes, with hydrogen
(H_2) and hydroxyl ions (OH^-) being produced at the negative electrode (cathode), whereas
chlorine (Cl_2), oxygen (O_2) and hydrogen ions (H^+) are produced at the positive electrode
(anode):
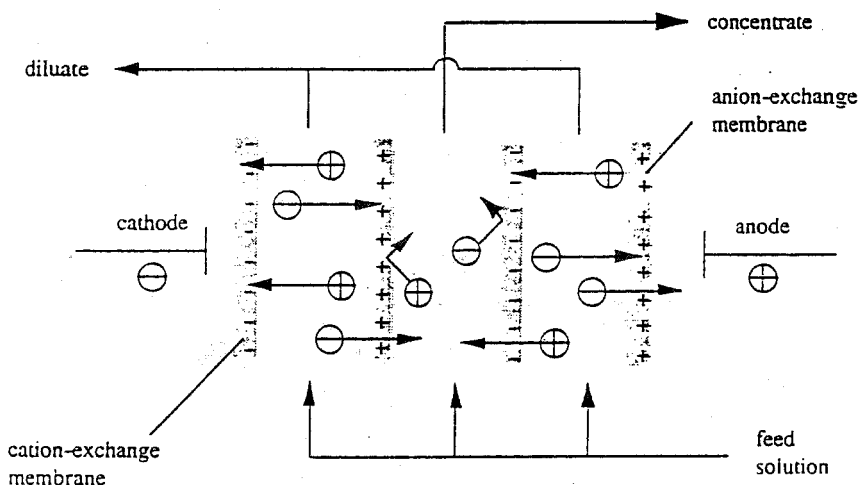
Figure   VI - 60.   The principle of electrodialysis.

The following electrode rections may occur,

cathode: $2 H_2O + 2e^- \Rightarrow H_2 + 2 OH^-$

anode: $2 Cl^- \Rightarrow Cl_2 + 2e^-$
        $H_2O \Rightarrow 1/2 O_2 + 2H^+ + 2e^-$
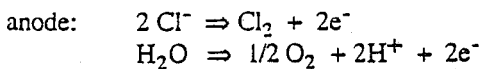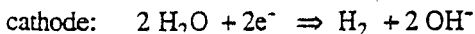
    In commercial applications several hundreds of cell pairs are assembled in a stack
and in this way the applied driving force is used very effectively. By using the concept of
an electrical potential difference in combination with electrically charged membranes, a

number of other applications are possible. Some examples will be given below to show the
flexibility of this concept.

VI.7.2.1   Process parameters

The amount of ions transported through the membrane is directly proportional to the
electrical current (ι) or current density. The electrical current required to remove a number
of ions is given by

$$\iota = z\,\mathscr{F}\,Q\,\Delta c/e \qquad\qquad\qquad (VI - 114)$$

where z is the valence, $\mathscr{F}$ is the Faraday constant (1 Faraday = 96500 coulomb/eq or
ampere-seconds/eq), Q the flow rate, Δc the concentration difference between the feed and
the permeate (diluate) (eq/l) and e the current efficiency. The current efficiency is related to
the number of cell pairs in a stack and provides information about the fraction of the total
current applied effectively used to transfer the ions. Theoretically, 1 Faraday of electricity
(which is 96,500 coulombs or 26.8 ampere of current applied for one hour) will transfer 1
gram-equivalent or equivalent of cations to the cathode (which is equal to 23 gram of
sodium) and 1 gram-equivalent or equivalent of anions to the anode (which is equal to 35.5
gram of chloride). The electric current is related to the electrical potential E by Ohm's law,

$$E = \iota\,.\,R \qquad\qquad\qquad (VI - 115)$$
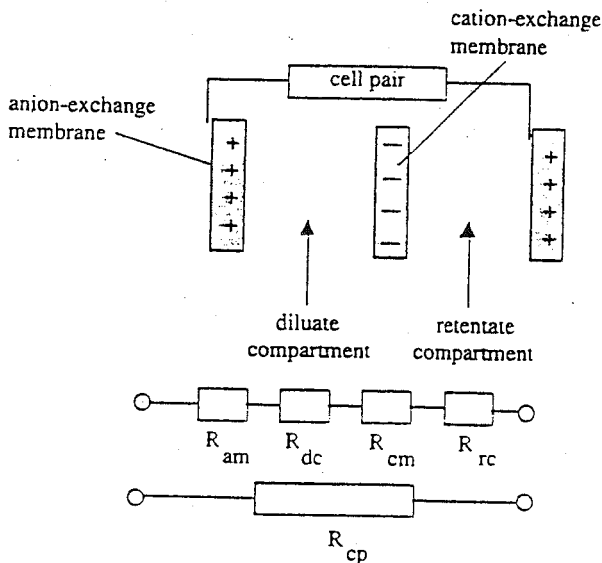
Figure VI - 61.   Resistances which apply in a cell pair.

where R is the resistance of the total membrane stack. The value of R is determined by the resistance of a cell pair R_{cp} multiplied by the number of cell pairs (N) in the stack, i.e.

$$R = R_{cp} \cdot N \hspace{6cm} (VI - 116)$$

In turn, the resistance of a cell pair is the sum of four resistances in series.

$$R_{cp} = R_{am} + R_{pc} + R_{cm} + R_{fc} \hspace{4cm} (VI - 117)$$

where

R_{cp} = resistance of one cell pair (per unit area)
R_{am} = resistance of the anion-exchange membrane
R_{pc} = resistance of the 'permeate' compartment
R_{cm} = resistance of the cation-exchange membrane
R_{fc} = resistance of the 'feed' compartment

This is shown schematically in figure VI - 61.

     The current density is determined by the applied voltage and the total resistance of the membrane stack. Increasing the current density leads to an increase in the number of ions transferred. However, the current density cannot be increased by an unlimited amount. Figure VI - 62 represents a current-voltage characteristic.
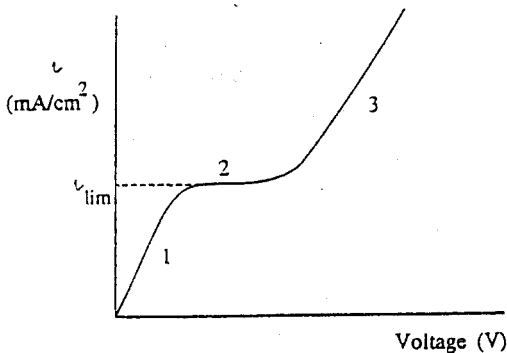
Figure VI - 62.   Current-voltage characteristic of an ion-exchange membrane

Three regions can be observed, region 1 is the Ohmic region where the electrical current or current density is related to the electrical potential difference by Ohm's law. In region 2 the current reaches a plateau value which implies that the Ohmic resistance has been increased. This is the region of the limiting current density ι_{lim}. The limiting current density (often expressed in mA/cm^2) is the current necessary to transfer all the available ions. When the

voltage is increased further no ions are available anymore to transfer the charge. This is the region of overlimiting current and water splitting will occur to generate ions. In addition all kinds of non-equilibrium processes occur in this region. The current-voltage characteristic for different ionic concentrations is shown schematically in figure VI - 63. If the ionic concentration increases then the limiting current density increases as well but the plateau value becomes less pronounced.
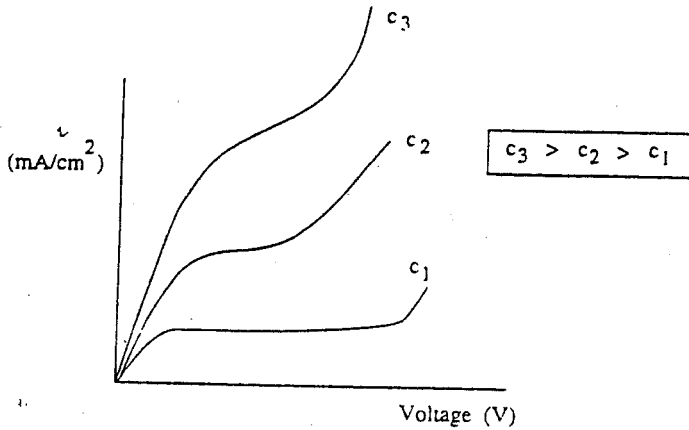
Figure VI - 63.   Current-voltage characteristic of an ion-exchange membrane for various ionic concentrations.

The current-voltage values can be plot as E/ι versus $1/\iota$ to determine the limiting current density more accurately (see figure VI - 64).
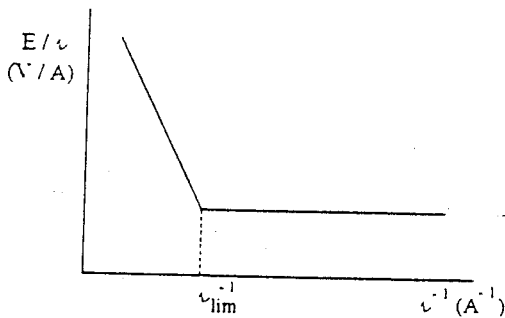
Figure VI - 64   Schematic drawing of a R (= E/ι) versus the reciprocal current.

The current density is given by

$$\iota = \frac{z \; D \; \bar{\mathcal{F}} \; (c_b - c_m)}{\delta \left(t^m - t^{bl} \right)} \qquad \qquad (VI - 118)$$

t^m and t^{bl} are the transport numbers in membrane and bounadry layer, respectively and δ is the thickness of the boundary layer. The derivation of this equation is given chapter VII. Concentration polarisation severely affects the current density and a limiting current density (ι_{lim}) is obtained as the ionic concentration at the membrane surface is reduced to zero. Thus, $\iota \Rightarrow \iota_{lim}$ as $c_m \Rightarrow 0$ and eq. VI - 118 becomes

$$\iota_{lim} = \frac{z \; D \; \mathcal{F} \; c_b}{\delta \left(t^m - t^{bl} \right)} \qquad \qquad (VI - 119)$$

Because D/δ is equal to k the mass transfer coefficient, ι_{lim} is strongly dete. There are two other effects that influences the performance of the process as well, i) osmotic flow and ii) less effective Donnan exclusion. Osmotic flow is inherently part of the process and can not be avoided. Since ions are transferred from one compartment to another an osmotic pressure difference is generated and this drives the osmotic transport of water from the diluate to the concentrated side. Secondly, in case of high ionic concentrations the Donnan exclusion becomes less effective. This effect and the less favoured energy consumption at high concentrations makes the process of electrodialysis more competitive at relatively low concentrations.

VI.7.2.2   Membranes for electrodialysis
Electrodialysis is a process in which ions are transported through membranes because of an applied electrical potential difference and as a consequence of a direct electrical current flow. In order to make the membranes selective for ions, ion-exchange membranes that either allow the transfer of anions or cations are used. Thus, the ion-exchange membranes can be sub-divided into anion-exchange and cation-exchange membranes. Anion-exchange membranes contain positively charged groups attached to a polymer, for example those derived from quarternary ammonium salts. Positively charged cations are repelled from the membrane because of this fixed charge. On the other hand, cation-exchange membranes contain negatively charged groups, primarily sulfonic or carboxylic acid groups. Negatively charged anions are now repelled by the membrane. Various structures of ion-exchange membranes have been given in chapter II. In the example given below (figure VI - 65), the polymerisation of styrene with divinylbenzene leads to a crosslinked polymer in which both cation- and anion exchange groups have been introduced. Two different types of ion-exchange membranes can be distinguished; i.e. heterogeneous and homogeneous. Heterogeneous membranes are prepared by combining ion-exchange resins
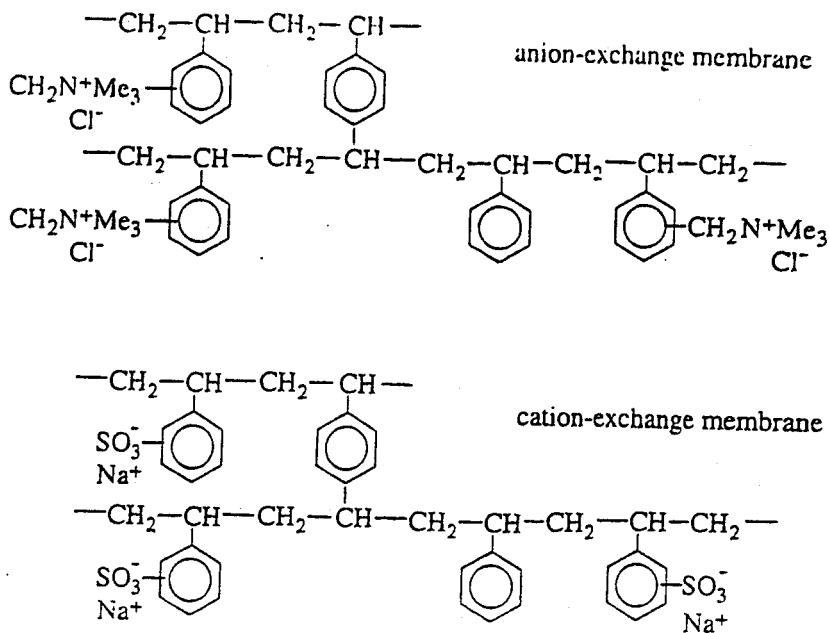
Figure VI - 65. Anion- and cation-exchange membranes based on polystyrene and divinylbenzene.

with a film-forming polymer and converting them into a film by dry-molding or calandering for example. The electrical resistance of such membranes is relatively high and their mechanical strength is relatively poor especially at high swelling values. In contrast, homogeneous membranes are obtained by the introduction of an ionic group into a polymer film. This can be achieved in different ways as shown in chapter II. The charge is distributed uniformly over the membrane and in order to reduce their extensive swelling these polymers are usually crosslinked.

The requirements for an ion-exchange membrane are a high electrical conductivity combined with a high ionic permeability. The electrical conductivity can be increased by increasing the ionic charge density, but the polyelectrolyte may then become highly swollen. These materials must therefore be crosslinked, the degree of crosslinking together with the charge density determining the sorption. As a result the diffusion coefficient of the ions inside the membrane may vary from 10^{-6} cm^2/s for a highly swollen system to 10^{-10} cm^2/s for a highly crosslinked one [81].

The basic parameters for a good membrane are:
- high selectivity
- high electrical conductivity

- moderate degree of swelling
- high mechanical strength

The electrical resistance of ion-exchange membranes lie in the range of 2 - 10 $\Omega.cm^2$ and the charge density is about 1 - 2 mequiv/g dry polymer.

VI.7.2.3   Applications

The most important application of electrodialysis is the production of potable water from brackish water [82]. A very special application is the reverse case, the production of salt. In the latter case the concentrate is the product stream whereas in the former case the diluate stream is the product. Moreover, there is an increasing number of industrial applications where ions have to be removed from a process stream such as demineralisation of whey, deacidification of fruit juices, production of boiler feed water, removal of organic acids from a fermentation broth. It is even possible to separate amino acids from each other as will be shown below.

VI.7.2.3.1   Separation of amino acids

Amino acids contain both a basic and an acidic group and because of this amphoteric character the molecule can be positively or negatively charged depending on the pH of the solution.

$$H_2NCHRCOO^- \Leftrightarrow\ ^+H_3NCHRCOO^- \Leftrightarrow\ ^+H_3NCRCOOH$$
$$\qquad (a) \qquad\qquad\qquad (b) \qquad\qquad\qquad (c)$$

At high pH, the amino acid is negatively charged (structure a) and migrates towards the anode when an electrical field is applied. At low pH, the amino acid is positively charged (structure c) and migrates towards the cathode. If structures a and c are exactly in balance, there is no net charge (structure b) and the amino acid will not migrate in an electrical field. The pH under these conditions is called the isoelectric point of the amino acid. The isoelectric point is a very characteristic parameter for a protein and different proteins have different isoelectric points. Figure VI - 66 shows how different amino acids can be separated by adjusting the pH. The cell employed is divided into three compartments in which the center compartment is adjusted to the isoelectric point (I.P.) of a specific (to be separated) protein A, one compartment is at a pH < I.P. and the one is at a pH > I.P. If a protein solution with a pH equal to that of protein A, is added to the middle compartment, the other proteins in the system will develop either a positive or a negative charge, depending on their specific isoelectric points, and will diffuse to the cathode and the anode respectively. In this way a complete separation of various proteins can be obtained by adjusting the pH value.

Figure VI - 66. Separation of amino acids.

VI.7.2.4   Summary of electrodialysis

membranes:	cation-exchange and anion-exchange membranes
thickness:	$\approx$ few hundred μm (100 - 500 μm)
pore size:	nonporous
driving force:	electrical potential difference
separation principle:	Donnan exclusion mechanism
membrane material:	crosslinked copolymers based on divinylbenzene (DVB) with polystyrene or polyvinylpyridine copolymers of polytetrafluoroethylene (PTFE) and poly(sulfonyl fluoride-vinyl ether).
application:	- desalination of water - desalination in food and pharmaceutical industry - separation of amino acids - production of salt

VI.7.3   Membrane electrolysis

In membrane electrolysis an electrolysis process is combined with a membrane separation process. The classical example is the chlor-alkali process in which sodium chloride is converted into chlorine and caustic soda. Other examples are the electrolytic recovery of (heavy) metals and the production of acid and base from the corresponding salts.

VI.7.3.1   The 'chlor-alkali' process

Whereas both cation-exchange and anion-exchange membranes are needed in some applications. only one type of ionic membrane is required in the production of chlorine and caustic soda via the 'chlor-alkali' process (Figure VI - 67). In this process only cation-exchange membranes are used, with the cell containing only two compartments separated by a negatively charged membrane.
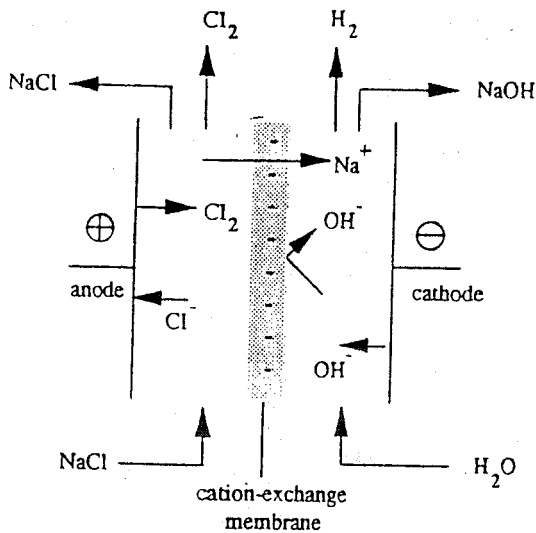
Figure VI - 67. Schematic arrangement of the 'chlor-alkali' process.

A sodium chloride solution is pumped through the left-hand compartment and electrolysis of chloride ion to chlorine gas will occur at the anode. At the same time the sodium ions migrate towards the cathode. In the right-hand compartment, electrolysis of water occurs at the cathode and hydrogen gas (H_2) and hydroxyl ions (OH⁻) are produced. The negatively charged hydroxyl ions migrate towards the anode but cannot pass the negatively charged cation-exchange membrane. In this way chlorine gas is released from the left-hand compartment whereas a sodium hydroxide solution (and hydrogen gas) is obtained from the other compartment. Unlike electrodialysis, in membrane electrolysis processes each compartment requires two electrodes as is shown schematically in figure VI - 68.
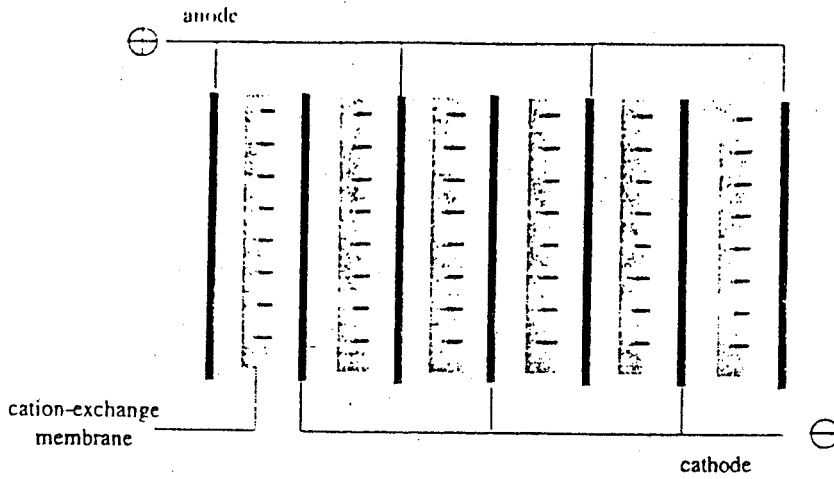
Figure VI - 68   Schematic configuration of a membrane electrolysis process

VI.7.3.2   *Bipolar membranes*

A bipolar membrane consists of a cation-exchange membrane, an anion-exchange membrane and an intermediate layer between the two membranes which are laminated together (Figure VI - 69). When an electrical potential is applied between the cathode and anode the transfer of electrical charge will be carried out by the ions present. If no ions are available, the electrical current will be transferred by the hydroxyl and hydrogen ions formed by the dissociation of water.
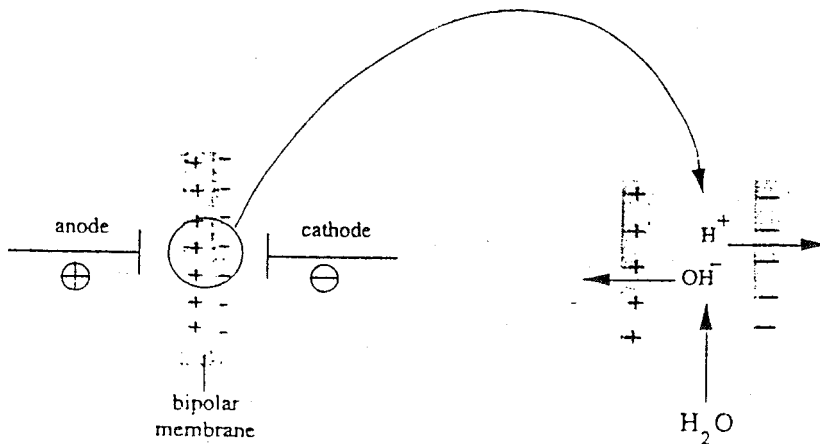
Figure VI - 69   Schematic drawing of a bipolar membrane.

An example of the application of a bipolar membrane is in the production of sulfuric acid and sodium hydroxide as shown in figure VI - 70. The bipolar membrane is placed in between a cation-exchange and an anion-exchange membrane, and a sodium sulfate solution is introduced into the membrane cell between the cation-exchange and anion-exchange membrane. The sulfate ions that pass through the anion-exchange membrane towards the anode will form sulfuric acid by association with the hydrogen ions provided by the bipolar membrane. At the same time the sodium ions that pass through the cation-exchange membrane towards the cathode will form sodium hydroxide with the hydroxyl ions from the bipolar membrane. In this way sulfuric acid and sodium hydroxide can be obtained from sodium sulfate. This process can be applied as well with mono-polar membranes in a membrane electrolysis process. In this latter process the protons and hydroxyl ions are provided by the electrolysis of water at both electrodes which implies that the energy consumption is higher than in the case of the bipolar membrane process.
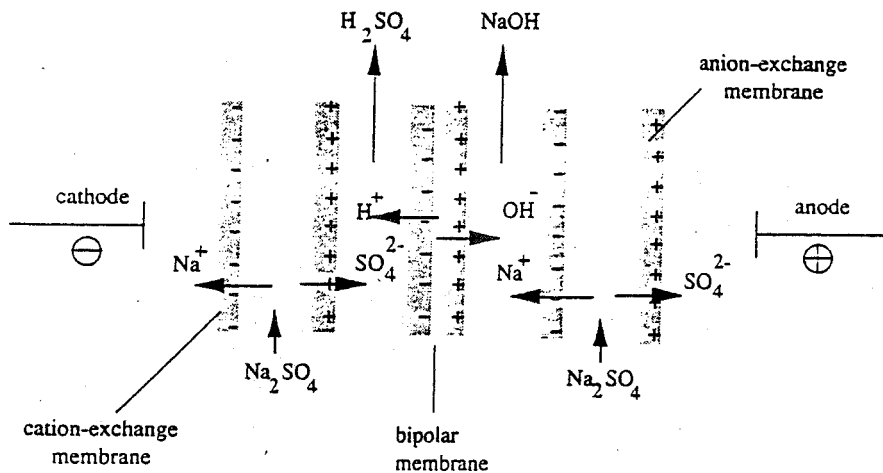
Figure VI - 70.   Production of caustic soda and sulfuric acid using bipolar membranes.

VI.7.4   *Fuel cells*

Fuel cells may be considered as a derivative of an electrical driven process. A fuel cell is a Galvanic cell in which chemical energy is directly converted into electric energy. Frequently hydrogen is used as reductor and oxygen as oxidator but other reductors can be used such as methane or methanol. A schematic drawing is given in figure VI - 71. Hydrogen is supplied at the anode compartment and is oxidised to form hydrogen ions

Anode reaction : $2H_2 \Rightarrow 4H^+ + 4e^-$
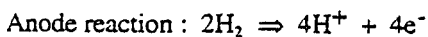
The electrons flow through the external circuit from anode to cathode. The hydrogen ions diffuse through the ion exchange membrane to the cathode compartment where a reaction occurs with oxygen and the electrons. The half reaction at the cathode is now

Cathode reaction : $4H^+ + O_2 + 4e^- \Rightarrow 2H_2O$
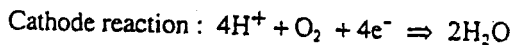
The cell reaction is $2H_2 + O_2 \Rightarrow 2H_2O$ with an electromotive force $E° = 1.2$ V. This value is obtained from the electrode potentials. Since this process is carried out isothermally and no pressure-volume work is involved, the change in free enthalpy of mixing (ΔG) is given by

$$\Delta G = - n \mathscr{F} E°$$

(VI - 120)

where n is the number of electrons transferred per molecule and $\mathscr{F}$ is the Faraday constant. ΔG can now be calculated since it is known that two electrons are transferred per mol water, $\Delta G = - (2) . (96,500) . (1.2) = - 231.6$ kJ/mol. The theoretical efficiency can be calculated if the reaction enthalpy (ΔH) is known. Under standard conditions (298 K) with water in the liquid state this is equal to the enthalpy of formation $\Delta H f° = - 285.83$ kJ/mol. This yields a theoretical efficiency of 81%. If this reaction occurs at higher temperature where water will be in the vapour phase, the efficiency is even higher since the enthalpy of formation is smaller (also the free entlapy change is smaller but not that much).

Various types of fuel cells have been developed dependent mainly on the type of electrolyte, the electrodes, and temperature. The 'solid polymer fuel cell' (SPFC) uses an cation-exchange membrane, e.g. Nafion (see figure II - 34) for ion transfer or proton transfer. This type of cell can be employed only at relatively low temperature (below 100 °C). If inorganic materials are used for ion transfer such as the 'molten carbonate fuel cell' (MCFC) and 'solid oxygen fuel cell' (SOFC) much higher temperature can be employed, between 500 and 1000 °C. Furthermore various reactants can be applied, i.e propane or methanol instead of hydrogen and hydrogen peroxide instead of oxygen.
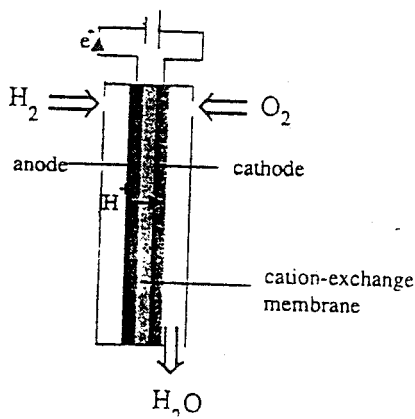
Figure VI - 71.   Schematic drawing of a fuel cell

The advantage of fuel cells as energy suppliers is the high efficiency which is generated without any waste stream (the product of the reaction between hydrogen and oxygen is water). Thermal combustion of fossil fuels such as coal, gas and oil. the traditional method of electricity production, generate large amounts of NO_x, SO_2 and CO_2

VI.7.5   Electrolytic regeneration of a mixed-bed ion-exchange resin
It has been shown in this section that combination of an electropotential difference and ionic membranes can be applied in various processes where ions are present, and there are
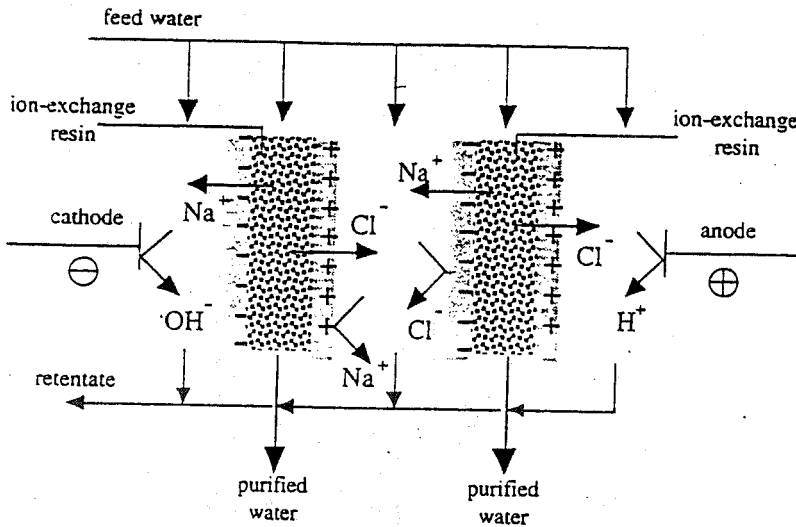
Figure VI - 72.   Principle of a continuous deionization process in which electrodialysis and ion-exchange are combined

many more possibilities than just the desalination of water. The last example given here is a hybrid process, a combination of ion-exchange and electrodialysis. Normally these processes are competitive but they can be combined in a very elegant way as shown schematically in figure VI - 72. In the production of ultrapure water with an electrical resistance of > 18 MΩ.cm, frequently ion-exchange is used. However, the regeneration of these resins is a disadvantage of this process, but the combination with electrodialysis enables a continuous regeneration without chemicals. Between anode and cathode 5 compartments can be observed which has been separated from each other by an ion exchange membrane; two electrode compartments, two compartments filled with ion-exchange resin and a compartment for the concentrated feed. The feed water enters the system and will be deionized by the ion-exchange resins. However, due to an electrical potential difference which has been applied, the free ions left in these compartments will

either diffuse to the electrode compartments or the concentrate compartment. In the concentrate compartment the presence of an ion exchange membrane with the 'proper' charge will prevent ions to diffuse into the ion exchange resin compartments. In this way two product streams and three 'retentate' streams are obtained.

VI.8.   Membrane reactors and membrane bioractors

Membranes are mainly used for concentration, purification and fractionation. However, they may be coupled to a chemical or biochemical reaction to shift the chemical equilibrium and the combination is defined as a membrane reactor or a membrane bioreactor. In the case of a membrane bioreactor the inhibitive endproduct of a bioconversion is removed to continue the reaction. In the case of membrane reactor one of the endproducts is removed to shift the reaction to the right side and consequently the conversion rate or final product concentration have been enhanced. In both cases the final result is an improvement of the productivity. Moreover, in most cases a purification step occurs as well which makes a combination of reaction and purification also from an energy point of view more favourable than conventional processes. In both membrane reactors and membrane bioreactors two basic concepts can be distinguished as illustrated by the reaction A $\Leftrightarrow$ B, i) reaction and separation are combined in one unit (figure VI - 73a) and ii) reaction and separation are not combined and the reactants are recycled along a membrane system (figure VI - 73b). The former concept is used especially in combination with inorganic membranes (ceramics, metals) and with polymeric membranes where the catalyst is coupled to the membrane. The latter concept can be applied with any membrane process and type of membranes, organic and inorganic. In fact any membrane process can be applied to remove a specific component such as microfiltration, ultrafiltration, nanofiltration, gas separation, vapour permeation, pervaporation, membrane distillation, electrodialysis, dialysis, diffusion dialysis, membrane contactors and facilitated type of processes.

(a) catalytic membrane (bio)reactor   (b) membrane recycle reactor
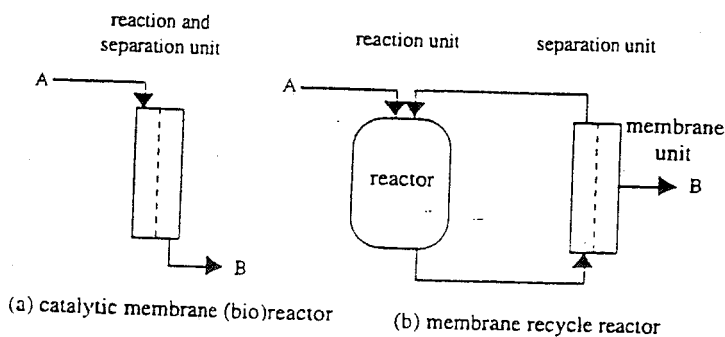
Figure VI - 73.   Two concepts of a membrane (bio)reactor: a) reaction and separation are coupled in one unit (catalytic membrane (bio)reactor and b) reaction unit and membrane unit are separated (membrane recycle reactor).

The principle of both membrane reactors and membrane bioreactors are the same but the origin is completely different. In the case of a bioreaction enzymes or microorganisms (bacteria, fungi, mammalian cells, yeasts) are applied under very specific reaction conditions. Both concepts wil be discussed briefly.

VI.8.1   Membrane reactors [83 - 87]

Most chemical reactions are equilibrium reactions and employs a catalyst to enhance the kinetics. The compounds involved in the reactions are either liquid or gaseous. In the latter case the temperature is often higher. Furthermore, the conversion is often strongly temperature dependent, which implies that each specific reaction is carried out at a specific temperature which is often higher than room temperature. The catalyst must be combined with the membrane system and various arrangements are possible. Figure VI - 74 summarizes some membrane/catalyst combinations for tubular membranes.
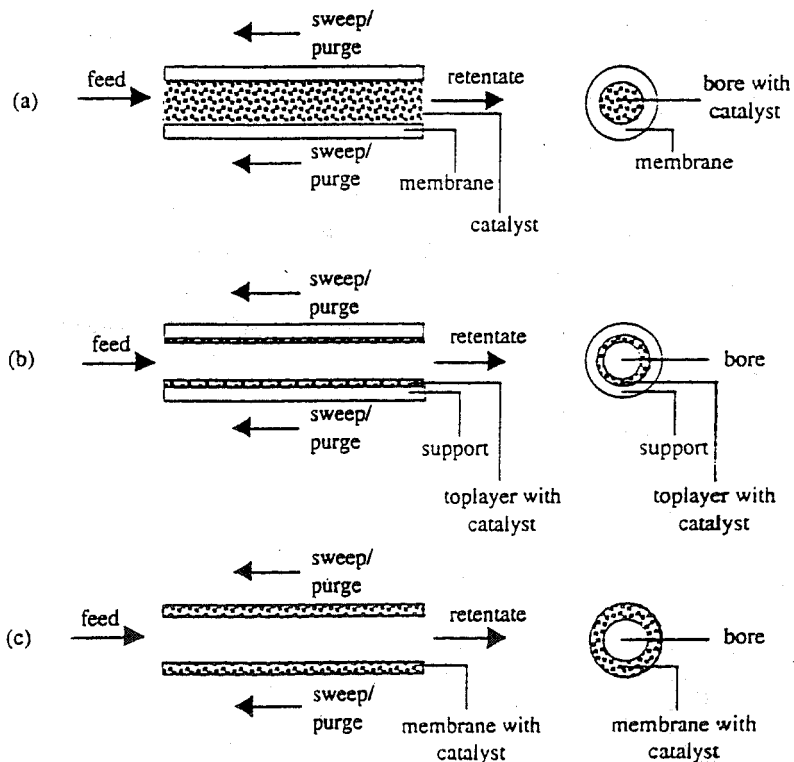
Figure VI - 74.   Schematic drawing of various membrane reactor concepts for a tubular configuration: (a) bore of the tube filled with catalyst, (b) toplayer with catalyst, and (c) membrane wall with catalyst.

The most simple and straightforward system is where the catalyst is located inside the bore of the tube (figure VI - 74a). The advantage of this system is its simplicity in preparation and operation and in case of catalyst poisoning a new catalyst can easily be introduced. In the other two arrangements the catalyst is immobilised onto the membrane, either in the toplayer (figure VI - 74b) or in the membrane wall (figure VI - 74c). In either case one of the products, not necessarily the required product, should permeate across the membrane which implies the necessity of permselective membranes under these specific conditions. At certain concentrations or partial pressures and at a certain temperature and pressure the equilibrium is completely fixed and thermodynamically determined ($\Sigma \, v_i \, \mu_i = 0$). However, by removing one of the endproducts the reaction is shifted to the right hand side and results in an enhanced conversion rate. Also the controlled addition of a reactant may enhance the productivuty. Membrane processes are well suited to remove either a gaseous or liquid compound. Furthermore they can be made catalytically active and employed at increased temperatures by employing proper materials, i.e. inorganic materials such as ceramics, zeolites or metals. Typical examples for inorganic membrane reactors are dehydrogenation where hydrogen is removed and oxidation and hydrogenation where oxygen and hydrogen are added and some of these are summarized in table VI.24.

Table VI.24. Reactions in catalytic membrane reactors [83 - 87]

dehydrogenation	ethane —> ethylene
	propane —> propene
	cyclohexane —> benzene
	cyclohexane —> cyclohexene
	ethylbenzene —> styrene
	butene —> butadiene
	isopropylalcohol —> acetone
hydrogenation	propene —> propane
	butene —> butane
	ethylene —> ethane
oxidation	carbon monoxide —> carbon dioxide
	ethylene —> ethylene oxide
	propylene —> propylene oxide

The number of possible applications are large but the commercial applications are emerging slowly due to a number of practical limititations such as low separation factor, leakage at higher temperatures, poisoning of catalyst, mass transfer limitations. Two examples will be mentioned illustrating that the possibilities of the concept are beyond the use of ceramics or zeolites as material.

VI.8.2.   *Non-selective membrane reactor [88]*

In membrane reactors, the combination of a chemical reactor with a membrane separation

process, the membrane is frequently employed to remove selectively one of the products of a mixture. It is possible as well to use non-selective membranes which are able to control the stoichiometry of the reaction. An example is the desulfurization reaction, e.g. of flue gas, by the Claus reaction

$$SO_2 + 2 H_2S \iff 3/8 S_8 + 2 H_2O$$
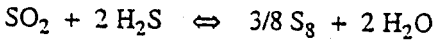
Due to fluctuations in the sulfur dioxide concentrations this reaction is very difficult to control in conventional reactor systems. The stoichiometry may be maintained by carry out the reaction within the wall of a porous ceramic membrane as shown schematically in figure VI - 75.
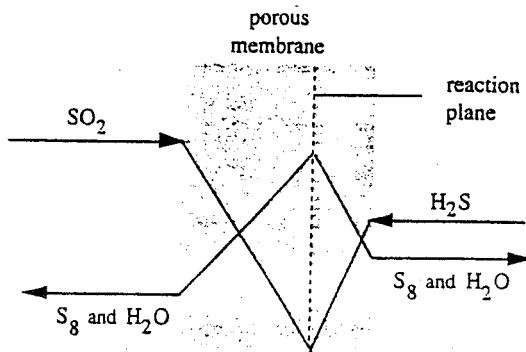
Figure VI - 75. ⁻ Schematic drawing of the concentration profiles of the various components in a non-selective membrane reactor for the Claus reaction

The membrane is macroporous with pores in the μm range without any ability to separate gases. Since this reaction is catalytically enhanced, porous α-Al_2O_3 is used as membrane (reaction interface) coated with γ-Al_2O_3 as catalyst. The reaction is carried out at elevated temperatures (T > 150 °C) and the products water and sulfur are removed as vapour. Sulfur dioxide is introduced to one side of the membrane and hydrogen sulfide at the other side and both gases will diffuse into the porous membrane and react instantaneously to sulfur and water. Somewhere inside the membrane there will be a reaction plane (see figure VI - 75). The formed products will diffuse to either side and can be obtained by condensation. Diffusion is the rate-limiting step in this reaction. If now the concentration of one of the reactants is changed then the concentration profile is changed and the reaction plane is shifted, i.e. if the sulfur dioxide concentrations is decreased the reaction plane will be shifted towards the sulfur dioxide side. In this way the stoichiometry is maintained due to the introduction of variable diffusion resistances. This concept can be applied as well for other reactions e.g. removal NOx (de-NOx).

VI.8.3   Membrane reactor in liquid phase reactions

Most of the research pertained on membrane reactors is carried out on gas phase reactions using ceramic, metal or zeolite membranes. However, the concept can be used as well for liquid phase reactions. A very specific class of reactions are the condensation or polycondensation reaction in which water is one of the products. Water is easily be removed by pervaporation (see section VI.4.3) and therefore pervaporation can be applied if the reaction temperature is not too high. As example we will use here an esterification reaction [89,90]. This reaction may be carried out in a batch reactor coupled with a pervaporation unit in which water is removed constantly (see figure VI - 76).
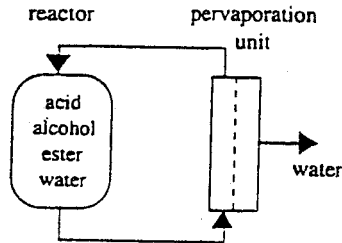
Figure VI - 76.   Combination of pervaporation and reactor in an esterification process.

The general esterification reaction is

acid + alcohol $\Leftrightarrow$ ester + water
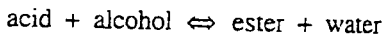
in which k_1 is the rate constant of the forward reaction and k_{-1} is the rate constant of the reverse reaction. The equilibrium constant is given by

$$K = \frac{c_{ester}\, c_{water}}{c_{acid}\, c_{alcohol}}$$

(VI - 121)

The ratio of the rate constants is equal to the equilibrium constant.

$$K = \frac{k_1}{k_{-1}}$$

(VI - 122)

The equilibrium constant is strongly temperature dependent (for reactions in the liquid phase pressure dependency is neglectible). The rate equation for the ester formation is

$$\frac{d\, c_{ester}}{dt} = k_1\, c_{alcohol}\, c_{acid} - k_{-1}\, c_{ester}\, c_{water}$$

(VI - 123)

The same rate equation holds for the formation of water

$$\frac{d\ c_{water}}{dt} = k_1\ c_{alcohol}\ c_{acid} - k_{-1}\ c_{ester}\ c_{water} \qquad (VI - 124)$$

However, water is constantly removed from the reactor through the pervaporation unit at a certain rate q_w (m^3/s)

$$q_w = J_w\ A = \frac{A\ P_w}{\ell}\ p_{w,f} \qquad (VI - 125)$$

in which A (m^2) is the membrane area, P_w (m^3.m/m^2.s.Pa) the permeability coefficient of water in the membrane, ℓ (m) the membrane thickness and $p_{w,f}$ (Pa) the partial pressure of water in the feed (The partial pressure of water at the feed side is assumed to be negligible). Using molar unit rather than volume and assuming that at low water concentrations the flow rate of water through the pervaporation unit is proportional to molar concentrations, eq. VI - 125 becomes

$$q_w = B\ c_{water} \qquad (VI - 126)$$

Combination of eq.VI - 126 with eq.VI - 124 gives

$$\frac{d\ c_{water}}{dt} = k_1\ c_{alcohol}\ c_{acid} - k_{-1}\ c_{ester}\ c_{water} - B\ c_{water} \qquad (VI - 127)$$

Eq. VI - 127 can be used to calculate the conversion rate when the water permeability coefficient of the pervaporation membrane is known. Figure VI - 77 shows a conversion curve for a value of B = 0 (traditional equilibrium batch process) and a value of B > 10.
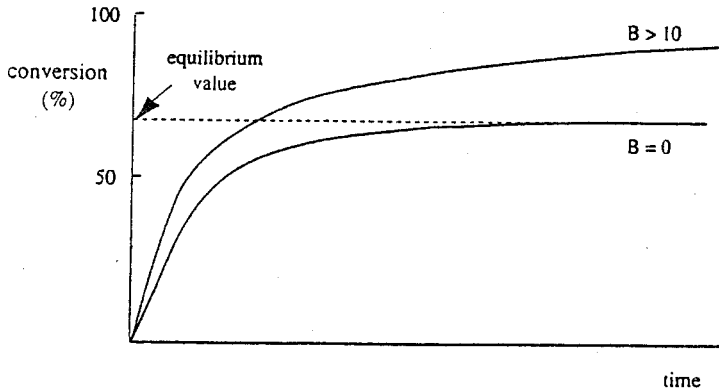
Figure VI - 77.   Conversion of an esterification without pervaporation (B = 0) and with pervaporation (B > 10)

By modifying the reactant ratio it is even possible to achieve complete conversion.

VI.8.4 Membrane bioreactors

Membrane processes can be combined with a fermentation process to improve the bioconversion in the same way as it does in chemical reactions. Since fermentation processes are inhibitory processes combination of a fermenter with a membrane separation system allows the specific removal of an inhibitory component. A typical fermentation process contains four different species; the substrate (component that is converted), the biocatalyst (microorganism such as yeast, bacteria, viruses or enzymes), nutrients (salts and co-enzymes required for the bioconversion) and product(s). Figure VI - 78 shows a schematic drawing of a batch and continuous cell recycle set-up, i.e. the fermentation broth is pumped through the membrane unit to remove the products and to retain the microorganism or enzymes. If substrate and nutrients are added and products are removed then the fermentation can be carried out continuously at much higher concentration of the biocatalyst. The choice of the membrane system depends on the product that has been prepared. Examples of low molecular weight products that can be prepared by fermentation are; alcohols (ethanol, butanol), ketones (acetone), organic acids (citric acid, acetic acid, lactic acid), amino acids (lysine), vitamins (vitamin B_{12}) and antibiotics (penicillin). For the first two groups of products (alcohols and ketones) pervaporation can be applied as membrane separation unit while for the second group electrodialysis is very attractive. Membrane bioreactors have a number of advantages; the fermentation is carried continuously, the microorganism is retained and high cell densities can be achieved, and the product can be removed selectively while nutrients and substrate are retained.

(a) batch   (b) continuous
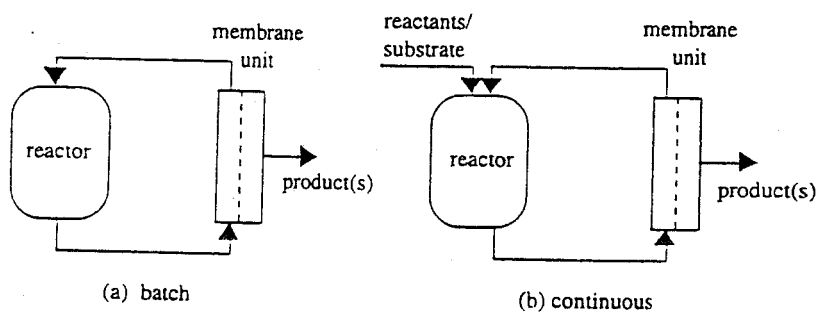
Figure VI - 78. Schematic drawing of a membrane recycle (bio)reactor in which a reactor is combined with a membrane unit.

VI.9. Solved Problems

1. Calculate the osmotic pressures of the following aqueous solution: 3% NaCl (M_{NaCl} =

58.45 g/mol) by weight. 3% albumin (M_{Alb} = 65.000 g/mol) by weight and a suspension containing 30 g/l of a solid (where the particle weight is 1 ng = 10^{-9} g) at a temperature 25°C.

2. The permeability of methane through a certain membrane has been determined at various temperatures and pressures from 5 to 70 bar. It was found that the permeability coefficient was invariant to pressure. The values of P at the various temperatures are given below.

T (°C)	P (Barrer)
10	1.8
20	3.5
30	6.3
40	10.1

a. Is the material a glass or an elastomer ?
b. Determine the activation energy

3. Ward (AIChJ, 16 (1970) 405) has derived an equation for facilitated transport for the diffusion-limited regime.

$$F = 1 + \frac{\alpha K'}{1 + K'}$$

in which F is the faciltation factor (F = total solute flux with carrier/solute flux without carrier), α the mobility ratio ($\alpha = D_{AC} \cdot c/D_A \cdot c_{A,o}$) and $K' = K \cdot c_{A,o}$.
a. derive this equation

Way and Noble (J.M.Sci., 46(1989)309 have studied the removal of hydrogen sulfide in ionexchange membranes with ethylenediamine as carrier and found the following properties.
D_A = 2.85 10^{-6} cm²/s; D_{CA} = 2.52 10^{-8} cm²/s; $c_{A,0}$ = 8.46 10^{-2} M; $\bar{c}$ = 8.32 M; ℓ = 1μm; K = 31.6
b. Calculate the facilitation factor.

4. A RO hollow fiber membrane has a water permeability of L_p = 1.6 10^{-8} m/s.bar. The external diameter is 0.1 mm. The manufacturer claims that the module flux at 60 bars and 298 K and seawater (3.0 wt% NaCl) as feed is q_p = 5 in³/day. How many fibers contains a module with a length of 1 m and calculate the flux of 1 fiber per day.

VI.10. Unsolved Problems

1. Calculate the fugacity of methane at 100 bar and at 5 bar at 50 °C. The following virial equation can be used.

$$PV/RT = 1 - 2.02 \ 10^{-3}.p + 3.72 \ 10^{-6} \ p^2 + 44 \ 10^{-12}.p^4$$

2. Plasmapheresis can be employed to separate blood plasma from blood cells. Calculate the osmotic pressure and the water flux at 200 mbar for a membrane with a water permeability coefficient of 300 l/m².h.bar. Blood contains an equivalnet of 0.9 wt%.

3. Ceramic membranes show an amphoteric character. Zirconia (ZrO_2) has an isoelectric point (IEP) at a pH = 6.5. Ultrafiltration membranes of ZrO_2 show a certain retention to sulphate ions.
   a. Explain in which case sulphate is better retained, at pH = 3 or pH = 9 ?
   b. γ-alumina (Al_2O_3) has an IEP of 9. Surface water at pH 6 frequently contains colloids with a negative charge. Is it beneficial to use γ-alumina in this case ?

4. Pressure retarded osmosis (PRO) allows to produce energy originating from an osmotic flow due to an osmotic pressure difference
   a) Is the maximum power obtained at $\Delta P = 0$?
   b) Calculate the power which can be generated from a 3% and a 15% NaCl solution respectively, and a membrane permeability of $L_p = 0.36$ kg/m².hr.bar (assume that v 't Hoff's law is still valid).
   c) What do you think are the practical limitations of this process ?

5. The hydraulic or water permeability coefficient (L_p) can be determined from a simple permeation experiment. Assume for a given membrane a L_p value of 5 10^{-4} m/hr .bar. The membrane has a rejection coefficient of 95% for NaCl and of 99.8% for Na_2SO_4 at 40 bar and 10000 ppm salt. Calculate the solute permeability coefficient for both salts.

6. Show qualitatively (in a drawing) the effect of pressure, temperature and recovery (see definition chapter VIII) on flux and permeate concentration in a reverse osmosis process.

7. A cellulose acetate membrane has a water permeability coefficient $L_p = 2.10^{-5}$ g/cm².s.bar and a solute (NaCl) permeability coefficient $B = 4.10^{-6}$ cm/s. This membrane is used for a desalination experiment. The feed concentration is 35 g/l of NaCl and the applied pressure is 60 bar. Calculate the water flux, salt flux, rejection coefficient and the concentration of NaCl in the permeate. The density of the solution is 10^3 g/l.

8. A RO membrane has a retention coefficient of 95% for a feed solution of 5000 ppm NaCl at 25°C and a pressure of 15 bar. The water permeability coefficient $L_p = 5.10^{-5}$ g/cm^2.s.bar. Calculate the retention coefficient at 30 bar.

9. The permeability coefficients of nitrogen, oxygen and toluene are 280, 600 and 1.4 10^6 Barrer, respectively. A composite membrane has been developed for the removal of toluene vapours from air. As sublayer a polyetherimide (PEI) membrane was developed which has been characterized by the nitrogen permeability and the bubble point (bp). Two membranes (A and B) have been developed with the following properties
Membrane A: $J_{N_2} = 10^{-1}$ cm^3.cm^{-2}.s^{-1}.cmHg^{-1} and a $r_{bp} = 0.5$ μm
Membrane A: $J_{N_2} = 10^{-1}$ cm^3.cm^{-2}.s^{-1}.cmHg^{-1} and a $r_{bp} = 0.1$ μm

a. Which membrane A or B, do you choose as a sublayer. Explain your choice in terms of a simple resistance model.

On top of the chosen membrane, a thin layer of silicone rubber is applied and two membranes (C and D) are prepared using the same sublayer. The oxygen and nitrogen flux are determined and the following results are obtained.
Membrane C: $J_{N_2} = 0.6 * 10^{-3}$ cm^3.cm^{-2}.s^{-1}.cmHg^{-1}
$J_{O_2} = 1.0 * 10^{-3}$ cm^3.cm^{-2}.s^{-1}.cmHg^{-1}

Membrane D: $J_{N_2} = 3.2 * 10^{-4}$ cm^3.cm^{-2}.s^{-1}.cmHg^{-1}
$J_{O_2} = 7.0 * 10^{-4}$ cm^3.cm^{-2}.s^{-1}.cmHg^{-1}

b. Which of the membranes, C or D, would you use for vapour permeation and why ?
c. With scanning electron microscopy the thickness of the silicone rubber toplayer is determined and is 0.9 μm. What can you say about the resistance of the sublayer ?
d. For a given toluene vapour mixture a selectivity factor of 120 was found at a certain permeate pressure. Compare this selectivity with the ideal selectivity and explain.

10. The following results have been obtained for the carbon dioxide permeability in PVC (polyvinyl chloride) at 1 bar and 10 bar respectively
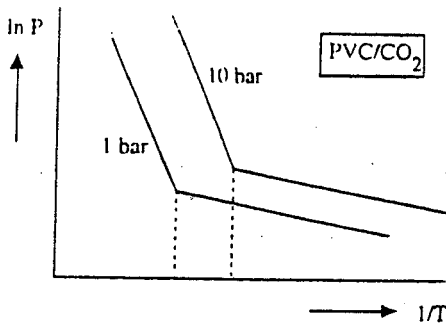
a) Explain the shift of the transition when the pressure increases from 1 bar to 10 bar.
b) What do you expect for helium as the permeating gas ?

11. The removal of volatile organic components (VOC's) from air is one of the applications of membrane technology. A feed containing 0.5 mol% of organic vapour in air is treated with a membrane with a selectivity factor of 200.

a. Give the general flux equation for the organic component.

The separation performance (i.e the permeate concentration) is dependent on the pressure ratio ($\varphi = p_{permeate}/p_{feed}$).

b. Is the organic component flux dependent of the pressure ratio φ?

Two limit cases can be considered for the separation :
a) $\varphi \ll 1$
b) $\varphi \approx 0.1 - 1$

In case a the permeate concentration of the organic vapour (x_p) is determined form the definition of the selectivity factor α.
In case b, the permeate concentration (x_p) can be approximated by
$x_p = x_f/\varphi$

c. Calculate the permeate concentration for $\varphi = 10^{-4}$ and $\varphi = 0.2$, respectively for a selectivity factor of $\alpha = 200$ and of $\alpha = 500$. Conclusion ?
A membrane with a permeability for the organic vapour of $P = 10^{-6}$ cm^3 (STP).cm/cm^2.s.cmHg) is used to remove the vapour from air (0.5 mol%).

case	1	2	3
p_{feed} (bar)	1	2	4
$p_{permeate}$ (bar)	0.2	0.4	0.8

d. Which of the following process conditions will I choose for the optimal separation performance and calculate the VOC flux in this case. (Assume that the recovery is zero. Why is that ?)

$\phi_{f,i} = 0.1$; $\phi_{p,i} = 0.4$ and $\ell = 1$ μm.

12. Outside air at 25°C and 90% relative humidity is used for air conditioning. A composite membrane with a toplayer thickness of 1 μm of polycarbonate ($P_{H2O} = 1400$ Barrer) is used to reduce the humidity to 40%. Calculate the average water flux (assume a neglible partial pressure of water at the permeate side and an average feed pressure).

13. With a Langmuir-Blodgett method very thin films can be prepared and this technique may be very useful for highly selective but low permeable polymers. A thin film with a thickness of 10 Å of a very interesting polymer XT with an oxygen permeability of 2 Barrer and a nitrogen permeability of 0.1 Barrer is applied by the Langmuir-Blodgett method on a composite membrane consisting of a polysulfone ultrafiltration membrane ($P/\ell_{O_2} = 0.1$ cm^3/cm^2 . s . cmHg) covered with a thin 1 μm thick silicon rubber layer ($P_{O_2} = 600$ Barrer and $P_{N_2} = 260$ Barrer).In this way a three-layered membrane is obtained. The silicon rubber 'gutter' layer has not been penetrated into the porous polysulfone.
   a. What is the selectivity and oxygen flux of the single XT membrane (use $\Delta p_{O_2} = 0.8$ bar).
   b. Is the silicone rubber necessary or not ?
   c. Is it justified to neglect the resistance of the polysulfone sublayer ?
   d. Calculate the oxygen flux of the 'two-layer' (polysulfone/silicone rubber) and of the 'three-layer' membrane (use $\Delta p_{O2} = 0.8$ bar). What is your conclusion ? Compare the flux of the 'three-layer' membrane also with the single XT membrane.
   e. Calculate the oxygen/nitrogen selectivity of the 'three-layer' membrane and compare with the single XT membrane. What is your conclusion ?

14. Membrane based oxygenators are frequently used as a heart-lung device. The partial pressure of oxygen in venous blood is 53 mbar.
   a. Estimate the oxygen driving force with air as supply gas at 1 bar.
      In a heart-lung device generally higher partial oxygen feed pressures are applied, i.e. $P_{O2} = 0.9$ bar. Silicone membranes with a thickness of 100 μm and a $P_{O2} = 600$ Barrer and a $P_{CO2} = 3200$ Barrer are used for the oxygen and carbon dioxide transfer.
   b. Calculate the oxygen flux
   c. Calculate the membrane area if 250 cm^3 (STP) of oxygen is required per minute
   d. Is this area sufficient to remove the CO2 from the blood. The CO2 pressure in the supply gas is negligible and the venous CO2 pressure is 60 mbar. The CO2 production rate is 200 cm^3/min.

15. Calculate the oxygen and nitrogen flux through a 10 μm thick membrane of silicone rubber with air of 20°C as feed at 1 bar and vacuum ($p_{perm} \approx 0$) at the permeate side.

The solubility coefficient (S) and diffusion coefficient (D) of the gases into silicone rubber are:

$S_{O_2} = 15 .10^{-4}$ cm^3/cm^3.cmHg $\qquad D_{O_2} = 1.6 .10^{-10}$ m^2/s

$S_{N_2} = 10 .10^{-4}$ cm^3/cm^3.cmHg $\qquad D_{N_2} = 0.9 .10^{-10}$ m^2/s

16. Good raincoats do not only retain water but they are capable to remove water vapour ('sweat'). Two different types can be distinguished; Gore-tex ® is a porous hydrofobic polymer (polytetrafluoroethylene) and Sympatex® is a nonporous hydrophilic polymer (a block-copolymer polybutylene terephtalate-polyethyleneoxide)

a. Describe the principle of these two types

b. Sympatex has a water permeability of 20,000 barrer. Calculate the water flux through a Sympatex raincoat (thickness 1 mm) assuming water saturation at 37°C at one side while the outside temperature is 20°C with a relative humidity of 80%.

17. Butyl rubber is used as material for bicycle tyres due to its low permeability for air. If a tyre contains 2400 cm^3 (STP) of air at a pressure of 2 bar, how long will it take before the tyre is completely flat. Assume that the the driving force remains constant. The thickness of the tyre is 1 mm, the surface area 2400 cm^2, and the air permeability is 0.9 Barrer.

18. In a pervaporation experiment the flux of a pure liquid (e.g. water) has been measured as a function of the permeate pressure at room temperature. The results are shown in the figure below:
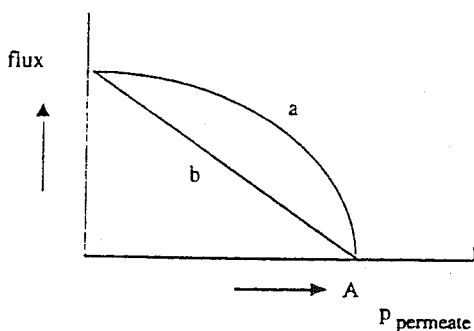
a) What does point A represent ?

b) Which curve is more realistic. a or b ? Explain.

c) How does the figure change as the feed temperature has been increased ?

d) In what direction does point A shift if ethanol (b.p. 78°C) is used as pure liquid instead of water at the same feed temperature ? Explain

Pervaporation can be applied for the removal of volatile organics such as benzene, or toluene from water. In these cases the concentration of the organics is very low (0.01 -

0.001 wt% or 10 - 100 ppm). Often composite membranes are used and the actual separating layer is an elastomer.

19. A homogeneous cellulosic ester membrane with a thickness of 20 μm is placed in a pervaporation cell with a diameter of 10 cm. The permeate side is kept at a vacuum of 1 mbar. In a steady state permeation experiment at 20°C 12.0 g of water is collected in 2 hours. Calculate the water permeability coefficient in mol.m/m².s.Pa en in cm³(STP).cm/cm².s.cmHg.

20. Isopropanol/water is separated in a pervaporation experiment at 70°C using a composite membrane with a hydrophilic toplayer with a thickness of 5 μm. It may be assumed that only water permeates through the membrane. The activity coefficient of water at infinite dilution $\gamma^{\infty} = 3.9$ and may be considered to be constant over this composition range.

The following results are obtained :

wt % H2O in feed	J_{H_2O} (kg/m².h)
1	0.04
2	0.15
3	0.5
4	0.9
5	1.4

a. Give in a graph flux versus concentration (wt %) and activity of H_2O in the feed and explain what you find

b. Calculate the water permeability coefficient (in cm³.cm/cm².s.cmHg) at each composition.

21. The water flux has been measured in a pervaporation experiment at 17°C with cellulose acetate (CA) membranes (thickness : 500 μm). A flux was found of $J = 1.1$ cm³/cm².h at 'zero' downstream pressure. The equilibrium water sorption value in CA is 0.125 g/g. From a desorption experiment of water from CA a diffusion coefficient was determined at t —>∞, D = 5,5 10-9 cm²/s.

a. Calculate the plasticisation constant γ

b. Draw the concentration profile of water in cellulose acetate in the pervaporation experiment.

22. A pervaporation experiment is carried out with a 100 μm thick elastomeric membrane and a feed solution of 10 wt% of toluene in octane. At 30°C a toluene flux of 2 g/m².h is measured with a toluene selectivity of $\alpha = 30$. Calculate the toluene flux and

selectivity at 80°C. (Assume that *i*) permeability coefficients are temperature independent, *ii*) permeate pressure is zero and *iii*) the solution behaves ideal).

23. Crown ethers are well known as carrier molecules in liquid membrane processes. A U-tube filled with chloroform in which 16-crown-8 has been dissolved. A KCl solution is placed at one tube and water at the other tube.

a. What happens with the chloride ions if potassium is transported from one side to the other side ?

b. Calculate the time to reduce the concentration of a KCl solution from 1 mmol/liter to 1 µmol/liter. Concentration polarization is assumed to be negligible. The volume is 1000 m³; the membrane area is 1 m² and the permeability coefficient of the complex is 10^{-5} m/s.

c. Does the result under b. change when concentration polarization is important ? Explain

24. From an experiment on the extraction of phenylalanine (Phe) from water by a supported liquid membrane the following results are obtained

t(h)	c_{phe} (g/l)
0	5.75
0.5	4.83
0.93	4.53
1.58	4.08
1.92	3.92
5.66	2.20

The membrane area is 25.5 cm², the feed volume is 110 ml and the mol.weight of phenylalanine is 165.2 g/mol.

a. Calculate the permeability coefficient and the flux at t = 0
b. How does the porosity of membrane affects the results ?
c. How does the choice of the carrier affect the results ?

25. A porous polypropylene membrane with a thickness of 20 µm and a porosity of 50% is filled with water. Which is the fraction of the oxygen flux that permeates through the water. Henry's law constant of oxygen in water at 298 K is 3.3 10^7 mmHg and the diffusion coefficient of oxygen in water is 2.1 10^{-5} cm²/s. The oxygen permeability in polypropylene is P = 1.6 Barrer.

26. A hydrophobic microfiltration membrane with a thickness of 100 µm, a surface porosity of 65% and a tortuosity $\tau = 2.1$ is filled with o-nitrophenyl octyl ether (o-NPOE) and separates two aqueous solutions, a feed solution with either a potassium perchlorate (KClO₄) or a sodium perchlorate (NaClO₄) solution and a permeate or strip

solution of pure water. The salt concentrations are 0.1 M (0.1 mol/liter) for both salts. The distribution coefficient of $NaClO_4 = 3.2 \cdot 10^{-5}$ and of $KClO_4 = 3.8 \cdot 10^{-5}$. The diffusion coefficients of both salts in o-NPOE are 10^{-5} cm²/s.

a. Calculate the $NaClO_4$ and $KClO_4$ flux

Calixarenes may be used as carrier molecules for facilitated ionic transport. The equilibrium constant for $KClO_4$-complexation is $9.2 \cdot 10^5$ l/mol and for $NaClO_4$-complexation is 270 l/mol. The diffusion coefficients of the carrier-salt complex is $2 \cdot 10^{-7}$ cm²/s for both salts. The carrier concentration is 10^{-2} M.

b. Calculate the carrier mediated flux for $NaClO_4$ and $KClO_4$.
c. Calculate the facilitation factor for $KClO_4$ and $NaClO_4$.

27. In diffusion dialysis often an ionic membrane is used to separate two phases as indicated in the figure below

phase 1   —   phase 2

pH = 7   —   pH = 1

CuSO4   —   H2SO4
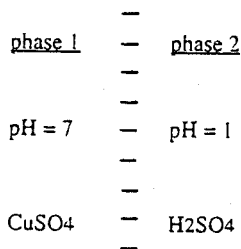
a. Explain why an ionic membrane is used.
b. Explain what happens in the process depicted in the figure and draw the directions of the various ionic flows.

28. A cellulosic membrane with a thickness of 20 µm is used in hemodialysis to remove urea from blood at 37°C. The concentration of urea (mol.weight 60 g/mol) in blood is 0.2 g/l whereas the concentration in the dialysate can be assumed to be negligible. The diffusion coefficient of urea in the cellulosic membrane is $4.5 \cdot 10^{-11}$ m²/s and the distribution coefficient is 1.5. The mass transfer coefficient at the blood side is 10^{-5} m/s and in the dialysate $4 \cdot 10^{-5}$ m/s. Calculate the urea flux and indicate the influence of the boundary layer resistance.

29. A cellophane membrane with a thickness of 50 µm shows an urea flux of 21.6 g/m².h. The feed solution contains 1 g/l urea while the permeate concentration may be assumed to be zero. The diffusion coefficient of urea in cellophane is 30.10^{-6} cm²/s. Calculate the partition coefficient.

30. Hydrophobic microfiltration membranes, such as polypropylene, are suitable for membrane distillation .

a. What kind of liquids can be used for this process if polypropylene is used as membrane and why ?
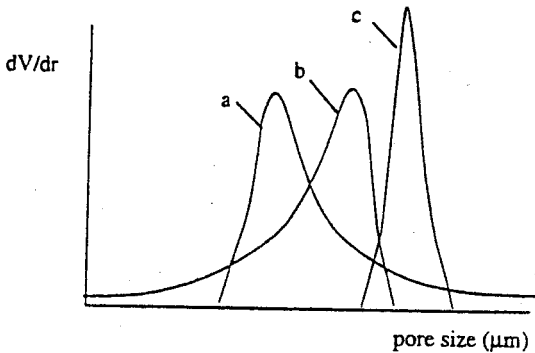
The figure shows the pore size distribution of three different porous polypropylene membranes.

b. Which one would you choose for membrane distillation and why ?

c. Membrane distillation can be employed for the preparation of potable water from seawater. What liquid will be used at the stripping side ?

d. How does the flux and the quality of the permeate change if brackish water is used as feed instead of seawater while the conditions at the permeate (stripping) remain the same ?

e. Membrane distillation will be operated in a counter-flow module. At both sides of the module the same temperature difference can be applied e.g. 10°C (90/80°C at one side and 50/40°C at the other side) ? Will the water flux be the same over the complete module ? Explain.

31. A porous polypropylene membrane with a water permeability coefficient of 4.2 10^{-7} m/s.bar is used in membrane distillation. Calculate the pure water flux for a feed temperature of 50°C and 90°C, respectively. The temperature at the permeate (distillate) side is 20°C. Neglect temperature polarization.

32. Surface water used for irrigation is desalinated with electrodialysis. The NaCl concentration of 1.2 g/l (Mw = 58.45 g/mol) must be reduced to a 200 ppm. The system contains 100 compartments, the electrical efficiency is 0.92 and the average resistance per compartment is 0.04 Ω.
Calculate the current and the electrical potential difference for this process if 10 m³/h of desalted water is required.

33. In an electrodialysis cell were the current-voltage values of a CL25T membrane determined with a 0.15 M NaCl solution at 25°C.

i (mA/cm^2)	V (V)
4	0.03
8	0.07
12	0.11
16	0.21
20	0.51
24	0.85

a. Determine the limiting current density
b. When the salt concentration increases will then ι_{lim} increase or decrease ?
c. If sodium sulphate is used instead of sodium chloride, will then ι_{lim} increase or decrease ?

34. A whey solution (20 m^3) contains 1% NaCl. How long will it take to reduce the salt content by 90% with electrodialysis. The electric efficiency is 0.9, the electric current is 100 A and there are 100 compartments.

35. Calculate the potential of a reversible methanol/oxygen fuel cell under standard conditions (1 atm. and 298 K).

	H$_f$° (kJ/mol)	S° (J/mol.K)
H$_2$O (L)	- 285.83	69.91
CH$_3$OH (L)	- 238.66	126.80
O$_2$ (G)		205.14
CO$_2$ (G)	- 393.51	213.74

VI.11 . Literature

1. Angus, S., Armstrong, B., and de Renk, K.U., *International Tables of the Fluid State*, Pergamon Press, 1976
2. Mir, L., Michaels, S.L., Goel, V., and Kaiser, R.,'Crossflow Microfiltration: Applications, Design and Cost', in Ho, W.S.W., and Sirkar, K.K., *Membrane Handbook*, Van Nostrand Reinhold, 1992, New York, p. 571
3. Porter, M.C.: 'Microfiltration', in Bungay, P.M., Lonsdale, H.K., de Pinho, M.N., (eds.), *Synthetic Membranes: Science, Engineering and Applications', Nato, ASI Series, Vol. 181.*, Reidel Publishing Company, 1986, p. 225
4. Eykamp, W.: 'Microfiltration and Ultrafiltration, in Noble, R.D., and Stern, S.A., (eds.), *Membrane Separation Technology. Principles and Applications.*, Elsevier,

Amsterdam, 1995, p.1

5. Mir, L., Michaels, S.L., Goel, V., and Kaiser, R., 'Crossflow Microfiltration: Applications, Design and Cost', in Ho, W.S.W., and Sirkar, K.K., *Membrane Handbook*, Van Nostrand Reinhold, 1992, New York, p. 571

6. Leenaars, A. and Keizer, K., University of Twente,

7. Aptel, P., and Clifton, M.: 'Ultrafiltration', in ref 3, p. 249

8 Kulkarni, S.S., Funk, E.W. and Li, N.N., 'Applications and Economics', in ref. 5, p. 446

9. Cheryan, *Ultrafiltration Handbook*, Technomic Publishing Co, Lancaster, USA, 1986

10. Lonsdale, H.K.: 'Reverse Osmosis', in ref. 3, p. 307

11. Fell, C.J.D., 'Reverse Osmosis', in ref. 4, p. 113

12. Williams, M.E., Bhattacharyya, D., Ray, R.J., McCray, S.B., 'Selected Applications', in ref. 5, p. 312

13. Amjad, Z., *Reverse Osmosis*, Van Nostrand Reinhold Inc., 1993

14. Loeb, S., J. Membr. Sci., 1 (1976) 49

15. Leitz, F.B., and Mc. Rae, W.A., *Desalination*, 10 (1972) 2933

16. Weinstein. J.N.. and Caplan. R.S., *Science*, 167 (1968) 71

17. Leitz, F.: 'Piezodialysis', in P. Meares (ed.), *Membrane Separation Processes*, Meares, Elsevier. Amsterdam, 1976, p.

18. Brown, W.R., and Park, G.S., *J. Paint Techn.*, 42 (1970) 16

19. Auvil, S.R., Srinivasan, R., and Burban, P.M., *International Symposium on Membranes for Gas and Vapour Permeation*, Suzdal, USSR, febr., 1989

20. Allen, S.M.. *J. Membr. Sci.*, 2 (1977) 153

21. Proceedings of the 4th Priestley Conference, *Membranes in Gas Separation*, Leeds, England. Sept. 1984.

22. Park, G.S.: 'Transport in Polymers'. in ref. 3, p. 57.

23. Breck, D.W., *Zeolite Molecular Sieves*. John Wiley, New York, 1974.

24. Chern, R.T., Koros, W.J., Hopfenberg, H.B., and Stannet, V.T., in: 'Material Science of Synthetic Membranes', ACS Symp. Ser., Lloyd, D.R., (ed.), 269 (1985) 25

25. Baker, R.W., and Blume, I., *Chemtechn.*, 16 (1986) 232

26. Blume, I., University of Twente, Internal report

27. van 't Hof, J.. *PhD thesis*, University of Twente, 1988

28. Peineman, K.V.. German Patent DE 3420373

29. Peineman K.V.. and Pinnau. I.. German Patent. DE 3525235

30. Henis, J.M.S.. and Tripodi, M.K., *J. Membr. Sci.*. 8 (1981) 233

31. Cabasso, I., Encyclopedia of Polymer Science and Engineering, Vol. 9, p. 509

32. Paul, D.R., and Yampolskii, Y. (Eds.). *Gas Separation*,

33. Toshima, N. (Ed.), *Polymers for Gas Separation*, VCH, Weinheim. Germany, 1991

34. Kesting, R.E.. and Fritzsche, A.K., *Polymeric Gas Separation Membranes*, John Wiley. New York. 1993

35. Zolandz. R.R.. and Fleming. G.K..' Applications'. in ref. 5, p.78

36. Cen, Y., and Lichtenthaler, Vapour Permeation', in ref. 4, p.85

37. Spillman, R., ' Economics of Gas Separation Membrane Processes', in ref. 4, p. 589

38. Mulder, M.H.V., Oude Hendrikman, J., Hegeman, H., and Smolders, C.A., *J. Membr. Sci.*, **16** (1983) 269

39. Gmehling, J. and Onken, U., *Vapour-liquid Equilibrium Collection*, Dechema, Frankfurt, Germany, 1977

40. Flory, P.J., *Principles of Polymer Chemistry*, Cornell University Press, Ithaca, 1953.

41. Park, H-C, Mulder, M.H.V., and Smolders, C.A.,

42. Nijhuis, H., *PhD Thesis*, University of Twente, 1990

43. Mulder, M.H.V., Franken, A.C.M., and Smolders, C.A., *J. Membr. Sci.*, **23** (1985) 41

44. Suzuki, F. and Onozato, K., *J. Appl. Pol. Sci.*, **28** (1983) 1949

45. Mulder, M.H.V., 'Thermodynamics of pervaporation' in R.Y.M. Huang (ed.), *Pervaporation Membrane Separation Processes*, Elsevier, 1991, Chapter 4.

46. Spitzen, J.W.F., Elsinghorst, E.J.A., Mulder, M.H.V., and Smolders, C.A., in 'Proceedings of Second International Conference on Pervaporation Processes in the Chemical Industry', R. Bakish (ed.), San Antonio, 1987, p. 96

47. Neel, J., Aptel, P., and Clement, R., *Desalination*, **53** (1985) 179

48. Itoh, T., Toya, H., Ishihara, K., and Shinihara, I., *J. Appl. Polym. Sci.*, **30** (1985) 179

49. Böddeker, K., in ' Proceedings of First International Conference on Pervaporation Processes in Chemical Industry, Ed., Bakish, R., Atlanta, 1986, p. 96

50. Aptel, P., Cuny, J., Jozefowicz, J. Neel, J., and Chaufer, B., *Eur. Polym. J.*, **14** (1978) 595

51. Brun, J.P., Larchet, C., Melet, M., and Bulvestre, G., *J. Membr. Sci.*, **23** (1985),

52. Larchet, C., Brun, J.P., and Guillou, M., *J. Membr. Sci.*, **15** (1983), 81

53. Mulder, M.H.V., and Smolders, C.A., *Sep. and Purif. Methods*, **15** (1986), 1

54. Spitzen, J.W.F., *PhD Thesis*, University of Twente, 1988

55. Mulder, M.H.V., Kruitz, F., and Smolders, C.A., *J. Membr. Sci.*, **11**, (1982) 349

56. Michaels, A.S., Baddour, F.F., Bixler, H.J., Choo, C.Y., *Ind. Eng. Chem. Process. Des. Dev.*, **1** (1962) 14

57. Wijmans, J.G., Baker, R.W., and Athayde, A.L., 'Pervaporation: Removal of organics from water and organic/organic separations', in *'Membrane Processes in Separation and Purification'*, Crespo, J.C., and Böddeker, K.W. (Eds.), Kluwer, Dordrecht, 1994, p. 283

58. Mulder, M.H.V. 'Energy requirements in membrane separation processes', in ref. 51, p. 445

59. Huang (ed.), R.Y.M., *Pervaporation Membrane Separation Processes*, Elsevier, 1991

60. Fleming, H.L., and Slater, C.S.,' Applications and Economics', in ref. 5, p. 132.

61. Néel, J., Pervaporation, in ref. 4, p. 143
62. Eustache, H., and Histi, G., *J. Membr. Sci.*, **8** (1981) 105
63. King, J.C.,' Separation processes based on reversible chemical complexation', Separation Tachnology, Rousseau (ed.), CRC, 199
64. Smith, D.R., Lander, R.J., and Quinn, J.A., in *'Recent Developments in Separation Science'*., Vol. 3, Li, N.N. (ed.), CRC Press, Cleveland Ohio, 1977,
65. Cussler, E.L., Carrier mediated transport, in ref. 32, p.
66. Schultz, J.S., in ref. 2, p. 647
67. Danesi, P.R., Horwitz, E.P., van de Grift, G.F., Chiarizia, R., *Sep. Sci. Technol.*, **16** (1981) 201
68. Handbook of Chemistry and Physics, CRC Press, Cleveland Ohio,
69. Neplenbroek, T., Ph.D Thesis, University of Twente, 1989
70. Bargeman, D., and Smolders, C.A., in ref. 2, p. 567
71. Way, J.D., and Noble, R.D., 'Facilitated Transport', in ref. 5, p. 833
72. Boyadzhiev, L., and Lazarova, Z., liquid membranes, in ref. 4, p. 283
73. Jonsson, G., 'Dialysis'. in ref. 2, p. 625
74. Kessler, S.B., and Klein, E., 'Applications', in ref. 5, p. 206
75. Nishiwaki, T., and Itoi. S., *Jap. Chem. Quarterly*, **41** (1982) 36
76. Moonen, H., and Niefind, N.J., *Desalination*, **41** (1982) 327
77. Krevelen, D.W. v., *Properties of Polymers*, Elsevier, Amsterdam, 1972
78. Franken, A.C.M., PhD Thesis, University of Twente, 1988
79. Schneider, K., and v. Gassel. T.J., *Chem . Ing-Techn.*, **56** (1984) 514
80. Reed, B.W., Semmens, M.J., and Cussler, E.L.,'Membrane Contactors', in ref. 4, p.467
81. Soldano, B.A., *Ann. N. Y. Acad. Sci.*, **24** (1953) 116
82. Strathmann, H., 'Applications', in ref. 2, p. 255
83. Zaspalis, V.T., and Burggraaf, A.J., Inorganic Membrnae Reactors to Enhance Productivity of Chemical Processes, in *'Inorganic Membranes, Synthesis, Characteristics and Applications'*, Bhave, R.R (Ed.), Van Nostrand Reinhold, New York, 1991,
84. Falconer, J.L., Noble, R.D., and Sperry. D.P., Catalytic Membrane Reactors, in *'Membrane Separations Technology, Principles and Applications'*, Noble, R.D. and Stern, S.A. Eds.), Elsevier Science B.V., Amsterdam, 1995
85. Keizer. K., Zaspalis, V.T., De Lange, R.S.A., Harold, M.P., and Burggraaf, A.J., Membrane Reactors for Partial Oxidation and Dehydrogenation Reactions', in *'Membrane Processes in Separation and Purification'*, Crespo, J.C., and Böddeker, K.W. (Eds.). Kluwer, Dordrecht, 1994.
86. Drioli. E., Aachener Membran Kolloquium, 1995, p.
87. Matson. S.L., and Quinn, J.A., Membrane Reactors, in *'Membrane Handbook '*, Ho, W.S.W., and Sirkar, K.K., Van Nostrand Reinhold, New York, 1992. p.809
88. Sloot. H.J., Versteeg, G.F, and van Swaaij, *Chem. Eng. Sci.*, **45** (1990) 2415
89. David. M.O., Gref, R., T.Q., Ngyen, Neel, J., *Trans. Chem. Eng.*, **69** part A, (1991) 335

90. H. Brüschke, Aachener Membran Kolloquium, 1995, p. 207

VII POLARISATION PHENOMENA AND

MEMBRANE FOULING

VII.1. Introduction

In order to achieve a particular separation via a membrane process, the first step is to develop a suitable membrane. However, during an actual separation, e.g. a pressure driven process, the membrane performance (or better the system performance) can change very much with time, and often a typical flux-time behaviour may be observed: the flux through the membrane decreases over time. This behaviour is shown schematically in figure VII - 1 and is mainly due to concentration polarisation and fouling.
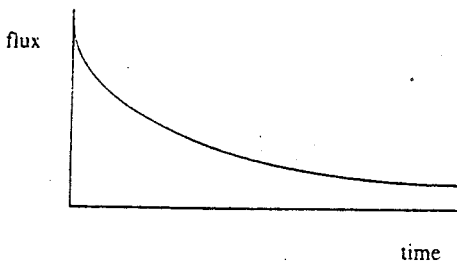
Figure VII - 1.   Flux behaviour as a function of time.

Especially in microfiltration and ultrafiltration, the flux decline is very severe with the process flux often being less than 5% that of the pure water flux. In contrast, the problem is less severe in gas separation and pervaporation.

Flux decline can be caused by several factors, such as concentration polarisation. adsorption. gel layer formation and plugging of the pores. All these factors induce additional resistances on the feed side to the transport across the membrane. The extent of these phenomena is strongly dependent on the types of membrane process and feed solution employed. Figure VII - 2 provides a schematic representation of the various resistances that can arise. The convective flux through the membrane can be written as:

$$flux = \frac{driving\ force}{viscosity\ .\ total\ resistance} \qquad\qquad (VII - 1)$$

which in the case of pressure driven processes such as microfiltration, ultrafiltration, nanofiltration and reverse osmosis, becomes

$$J = \frac{\Delta P}{\eta \ R_{tot}}$$

(VII - 2)
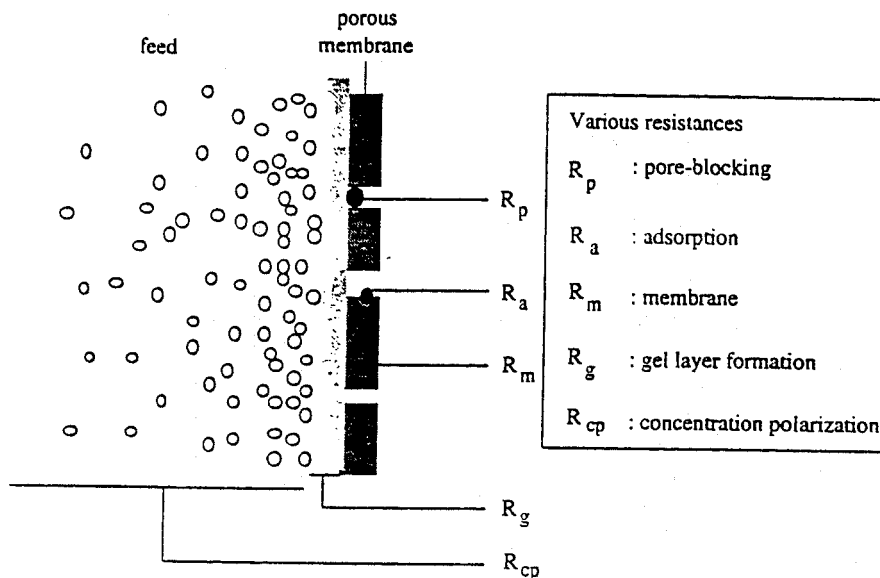
Figure VII - 2.   Overview of various types of resistance towards mass transport across a membrane in pressure driven processes.

The various resistances depicted in figure VII - 2 contribute with different extent to the total resistance, R_{tot}. In the ideal case, only the membrane resistance R_m, is involved. Because the membrane retains the solutes to a certain extent, there will be an accumulation of retained molecules near the membrane surface. This results in a highly concentrated layer near the membrane and this layer exerts a resistance towards mass transfer, i.e. a concentration polarisation resistance, R_{cp}. The concentration of the accumulated solute molecules may become so high that a gel layer can be formed which exerts the gel layer resistance, R_g. This mainly happens when the solution contains proteins. With porous membranes it is possible for some solutes to penetrate into the membrane and block the pores, leading to the pore-blocking resistance, R_p. Finally, a resistance can arise due to adsorption phenomena. i.e. the resistance R_a. Adsorption can take place upon the membrane surface as well as within the pores themselves.

Flux decline has a negative influence on the economics of a given membrane operation, and for this reason measures must be taken to reduce its incidence. Some general methods for tackling this problem will become apparent when the principles of flux decline are discussed. However, it is first necessary to distinguish between concentration

polarisation and fouling, although both are not completely independent of each other since fouling can result from polarisation phenomena.

It should be noted that another phenomenon, similar to concentration polarisation, arises from heat transfer occurring in membrane distillation and thermo-osmosis. A temperature difference across the membrane exists in these processes inducing a heat flux through the membrane with the result of temperature polarisation.

VII.2.   Concentration polarisation in pressure driven processes

Membrane processes are used to accomplish a separation since the membrane has the ability to transport one component more readily than another. For convenience, let us consider a solution consisting of a solvent and a solute as commonly found in pressure-driven membrane processes such as microfiltration, ultrafiltration and reverse osmosis. When a driving force acts on the feed solution, the solute is (partly) retained by the membrane whereas the solvent permeates through the membrane. Thus, the membrane has a certain retentivity for the solute while the solvent can permeate more or less freely. This implies that the concentration of the solute in the permeate (c_p) is lower than the concentration in the bulk (c_b), which is in fact the basic concept of membrane separations. This is shown in figure VII - 3.
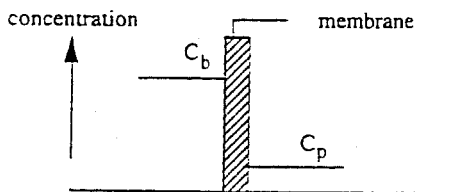
Figure VII - 3.   Membrane separation; the basic concept.

The retained solutes can accumulate at the membrane surface where their concentration will gradually increase. Such a concentration build-up will generate a diffusive flow back to the bulk of the feed, but after a given period of time steady-state conditions will be established. The convective solute flow to the membrane surface will be balanced by the solute flux through the membrane plus the diffusive flow from the membrane surface to the bulk (it should be remembered that only concentration polarisation phenomena are considered here with fouling being excluded). A concentration profile has now been established in the boundary layer (see figure VII - 4).

Suppose that the flow conditions in the feed are such that at a distance δ from the membrane surface complete mixing still occurs (concentration c_b). However, near the membrane surface a boundary layer is formed where the concentration increases and

reaches a maximum value at the membrane surface (c_m). The convective flow of solutes towards the membrane may be written as $J \cdot c$. If the solute is not completely retained by the membrane, there will be a solute flow through the membrane equal to $J \cdot c_p$. The accumulation of solute at the membrane surface leads to a diffusive back flow towards the bulk of the feed. Steady-state conditions are reached when the convective transport of solute to the membrane is equal to the sum of the permeate flow plus the diffusive back transport of the solute, i.e.

$$J c + D \frac{dc}{dx} = J c_p \qquad \text{(VII - 3)}$$
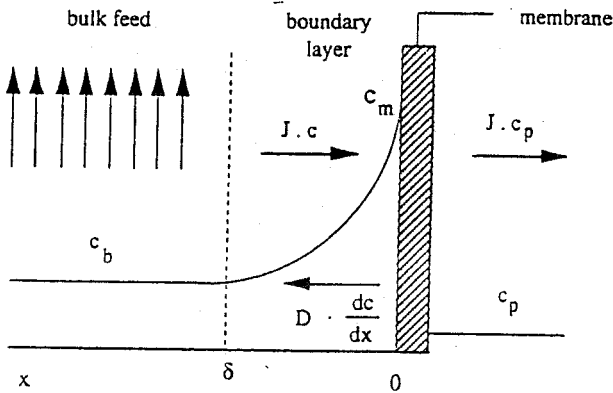
Figure VII - 4. Concentration polarisation; concentration profile under steady-state conditions.

The boundary conditions are:

$x = 0 \implies c = c_m$

$x = \delta \implies c = c_b$

so that integration of eq. VII - 3 results in

$$\ln \frac{c_m - c_p}{c_b - c_p} = \frac{J \delta}{D} \qquad \text{(VII - 4)}$$

or

$$\frac{c_m - c_p}{c_b - c_p} = \exp\left(\frac{J \delta}{D}\right) \qquad \text{(VII - 5)}$$

The ratio of the diffusion coefficient D and the thickness of the boundary layer δ is called

the mass transfer coefficient k, i.e.

$$k = \frac{D}{\delta}$$

(VII - 6)

If we introduce the equation for the intrinsic retention:

$$R_{int} = 1 - \frac{c_p}{c_m}$$

(VII - 7)

then eq. VII - 5 becomes

$$\frac{c_m}{c_b} = \frac{\exp\left(\frac{J}{k}\right)}{R_{int} + (1 - R_{int}) \exp\left(\frac{J}{k}\right)}$$

(VII - 8)

The ratio c_m/c_b is called the concentration polarisation modulus. This ratio increases (i.e. the concentration c_m at the membrane surface increases) with increasing flux J, with increasing retention R_{int} and with decreasing mass transfer coefficient k.

When the solute is completely retained by the membrane (R_{int} = 1.0 and c_p = 0), eq. VII - 5 (and eq. VII - 8) becomes

$$\frac{c_m}{c_b} = \exp\left(\frac{J}{k}\right)$$

(VII - 9)

This is the basic equation for concentration polarisation which illustrates in a simple form the two factors (the flux J and the mass transfer coefficient k) and their origin (membrane part $\Rightarrow$ J, hydrodynamics $\Rightarrow$ k) responsible for concentration polarisation.

The consequences of concentration polarisation can be summarised as follows:
- *retention can be lower*

Because of the increased solute concentration at the membrane surface, the observed retention will be lower than the real or intrinsic retention. This is generally the case with low molecular weight solutes such as salts.
- *retention can be higher*

This is especially true in the case of mixtures of macromolecular solutes where concentration polarisation can have a strong influence on the selectivity. The higher molecular weight solutes that are retained completely form a kind of second or dynamic membrane. This results in a higher retentivity for the lower molecular weight solutes.
- *flux will be lower*

The flux is proportional to the driving force where the proportionality constant can be considered as the inverse sum of all the resistances (see figure VII - 1). In those cases where concentration polarisation is very severe (microfiltration/ultrafiltration), flux decline can be quite considerably (it should be mentioned that fouling is the dominating factor in flux decline as will be discussed later) whereas in other processes, such as gas separation where concentration polarisation hardly occurs, the flux remains reasonably constant with

time.

Eq. VII - 5 or VII - 9 demonstrate the importance of the flux J and the mass transfer coefficient k in relation to concentration polarisation. The pure water flux is determined by the membrane used and this parameter is not subject to further change once the membrane has been chosen. On the other hand, the mass transfer coefficient depends strongly on the hydrodynamics of the system and can therefore be varied and optimised. The mass transfer coefficient k is related to the Sherwood number (Sh), i.e.

$$Sh = \frac{k\ d_h}{D} = a\ Re^b\ Sc^c\left(\frac{d_h}{L}\right)^d$$

$$(VII - 10)$$

where Re is the Reynolds number, Sc the Schmidt number, and a, b, c and d are constants:

$$Reynolds\ number: Re = \frac{d_h\ v}{v} = \frac{\rho\ v\ d_h}{\eta}$$

$$(VII - 11)$$

$$Schmidt\ number: Sc = \frac{v}{D} = \frac{\eta}{\rho\ D}$$

$$(VII - 12)$$

In these relationships, v is the kinematic viscosity, d_h the hydraulic diameter, η the dynamic viscosity, v the flow velocity, L the length of the tube or channel and D the diffusion coefficient. For a pipe (hollow fibers, capillary membranes or tubular membranes), the hydraulic diameter d_h = 4 A/S = 4 $(\pi/4).d^2/\pi.d$ = d. In addition, for a rectangular slit (plate-and-frame) of height h and width w, the hydraulic diameter is d_h = 4 w.h/2(w+h) = 2 w.h /(w+h).

From eq. VII - 10 it can be seen that the mass transfer coefficient k is mainly a function of the feed flow velocity (v), the diffusion coefficient of the solute (D), the viscosity, the density and the module shape and dimensions. Of these parameters, flow velocity and diffusion coefficient are the most important, viz.

k = f (v, D,module configuration)

$$(VII . 13)$$

Some semi-empirical relationships for mass transfer coefficients in pipes and channels are given in table VII.1.

Table VII.1   Mass transfer coefficients in various flow regimes

	laminar	turbulent
tube	$Sh = k.d_h/D = 1.62\ (Re.Sc.d_h/L)^{0.33}$	$Sh = 0.04\ Re^{0.75}\ Sc^{0.33}$
channel	$Sh = 1.85\ (Re.Sc.d_h/L)^{0.33}$	$Sh = 0.04\ Re^{0.75}\ Sc^{0.33}$

An overview of mass transfer correlations in membrane processes can be found in ref. 1

In microfiltration and ultrafiltration, the diffusion coefficients of the retained macromolecules, or suspended particles are small relative to those which apply to the 'retained' components in reverse osmosis, gas separation and pervaporation. In addition, the fluxes in microfiltration and ultrafiltration are large relative to those in pervaporation and gas separation. Hence, the consequences of concentration polarisation in the case of microfiltration and ultrafiltration are very severe. The consequences of fouling will be discussed later.

How can the phenomenon of concentration polarisation be reduced? This can be achieved both in terms of manipulating the flux J and the mass transfer coefficient k. This latter parameter is mainly determined by the diffusion coefficient, the flow velocity and module configuration (the module configuration will be discussed later). Because the diffusivity of the solute(s) cannot be increased (only by changing the temperature), k can only be increased by increasing the feed velocity along the membrane and by changing the module configuration (decreasing the module length, increasing the hydraulic diameter or a complete different design). When a feed is flowing through a pipe or a slit, a velocity profile will be developed after a certain entrance regime. Basically, two different flow patterns can be distinguished, i.e. laminar and turbulent flow. The velocity profiles associated with both flow patterns in a pipe are given in figure VII - 5.
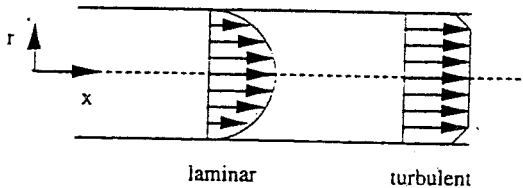
Figure VII - 5.   Fully developed laminar and turbulent velocity profiles in a pipe or slit.

A (parabolic) velocity profile can be observed over the whole cross-section for a well developed laminar flow, whereas in turbulent flow the velocity in the cross-section is constant and only in the boundary layer near the wall is the velocity lower.

Whether turbulent or laminar flow occurs is determined by the Reynolds number Re. For undisturbed flow through a straight pipe, the change from laminar to turbulent flow occurs at a Reynolds number of about 2000. The Reynolds number has a strong influence on the mass transfer, however, there are other methods available for improving mass transfer for example, using turbulence promoters, breaking the boundary layer (using corrugated membranes) or by the use of a pulsating flow. An increase in the feed temperature will also generally reduce concentration polarisation because of the increase in mass transfer coefficient (the diffusion coefficient of the retained solute will increase while the viscosity of the feed will decrease). However, an increase in feed temperature also causes an increase in the flux which opposes the effect of the improved mass transfer.

VII.2.1   Concentration profiles

So far only pressure driven processes have been considered in which a solute is typically retained and a concentration profile has been developed due to the accumulation of the solute at the membrane wall. (see figure VII - 6a and VII - 4). In other membrane processes where transport across the membrane occurs by diffusion rather than by convection it is now the fastest permeating component that is affected, i.e. if transport across the membrane is fast compared to transport across the boundary layer, a boundary layer resistance has been generated a a concentration profile has been developed as shown in figure VII - 6b.
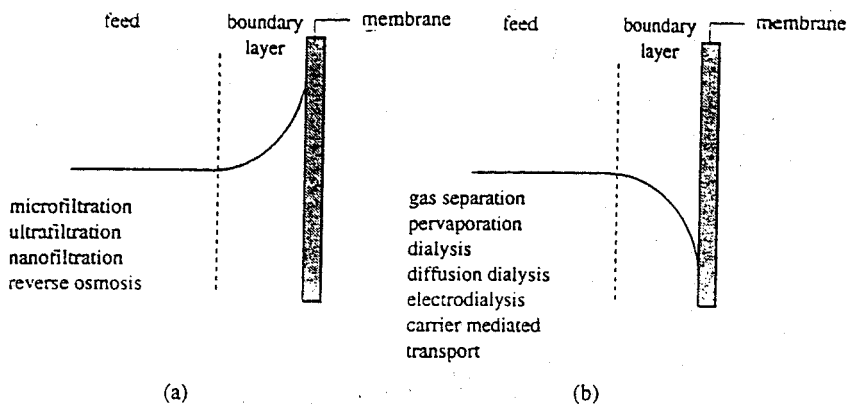
Figure VII - 6.   Concentration profiles in membrane processes; a) profile in pressure driven processes and b) profile in cases where transport occurs by diffusion

Profiles in which this latter profile can be found are electrodialysis, pervaporation, gas separation, dialysis, diffusion dialysis, facilitated transport or carrier mediated transport and membrane contactors. The extent of the boundary layer resistance varies from process to process and even for a specific process it is quite a lot dependent on application. Table VII.2 summarises the causes and consequences of concentration polarisation in various membrane processes.   The effect of concentration polarisation is very severe in microfiltration and ultrafiltration both because the fluxes (J) are high and the mass transfer coefficients k (= D/δ) are low as a result of the low diffusion coefficients of macromolecular solutes and of small particles, colloids and emulsions. Thus, the diffusion coefficients of macromolecules are of the order of 10^{-10} to 10^{-11} m²/s or less. The effect is less severe in reverse osmosis both because the flux is lower and the mass transfer coefficient is higher. The diffusion coefficients of low molecular weight solutes are roughly of the order of 10^{-9} m²/s. In gas separation and pervaporation the effect of concentration polarisation is low or can be neglected. The flux is low and the mass transfer coefficient high in gas separation (the diffusion coefficients of gas molecules are of the

Table VII.2. Consequences of concentration polarisation

membrane operation	influence	origin
reverse osmosis	moderate	k large
ultrafiltration	strong	k small/J large
microfiltration	strong	k small/J large
gas separation	(very) low	k large/J small
pervaporation	low	k large/J small
electrodialysis	strong	-
dialysis	low	J small
diffusion dialysis	low	J small/k large
carrier mediated transport	moderate	J large[#]/k large

The flux is relatively large compared to the non-facilitated process

order of 10^{-4} to 10^{-5} m^2/s). The flux is also low in pervaporation, but the mass transfer coefficient is smaller compared to gas separation and hence concentration polarisation may become somewhat more serious. When the concentration of the component in the feed which permeates selectively, is very low and the selectivity is very high as in the removal of volatile organic components such as trichloroethylene from water, the effect can become especially severe.

Concentration polarisation is not generally severe in dialysis and diffusion dialysis because of the low fluxes involved (lower than in reverse osmosis) and also because the mass transfer coefficient of the low molecular solutes encountered is of the same order of magnitude as in reverse osmosis. In carrier mediated processes and in membrane contactors the effect of concentration polarization may become moderate mainly due to the flux through the membrane. Finally, the effect of concentration polarisation may become very severe in electrodialysis. In the following sections concentration polarization will be described more in detail. In some module configurations such as plate-and-frame and spiral wound spacer materials are used in the feed compartment (see chapter VIII). These spacers effect the mass transfer coefficient and can be considered as turbulence promoters.

VII.3.   Turbulence promoters

The mass transfer coefficient is characterised by the hydrodynamic performance of the system. It was shown in the previous section that flow conditions (velocity, viscosity, density, solute diffusion coefficient) and module geometry determine the mass transfer coefficient. So far the correlations have been used for empty flow channels or tubes. However, in many systems turbulence promoters are present and these affect the mass transfer coefficient. For instance, spiral wound modules are applied in reverse osmosis, nanofiltration and ultrafiltration. These modules contain spacer materials to separate both

membranes in the feed compartment (see section VIII.3), resulting in an increased mass transfer coefficient but the pressure drop and energy consumption increase as well. The feed spacer is an essential part of the spiral wound module and figure VII - 7 shows a schematic drawing of such a spacer and a cross-section of a flow channel.
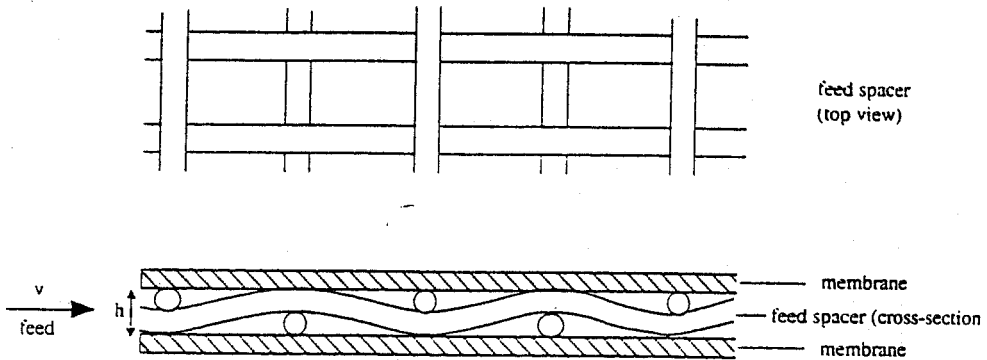
Figure VII - 7.   Schematic drawing of a spacer (upper figure) and a spacer filled channel (lower figure).

The increased mass transfer enhances the flux in two ways, the mass transfer coefficient will increase, and the wall concentration (or polarization modulus) will be lower. The mass transfer coefficient can be obtained from the Sherwood correlations with the following coefficients which assumed to be rather independent on type of spacer [2,3].

$$Sh = k.d_h/D = 0.0096 . Re^{0.5} . Sc^{0.6} \qquad (VII - 14)$$

In plate-and-frame systems, such as in electrodialysis, turbulence promoters are introduced to increase the mass transfer. Figure VII - 8 is a schematic drawing of a flow channel in which corrugations have been introduced and where Δl is the distance between successive corrugations.
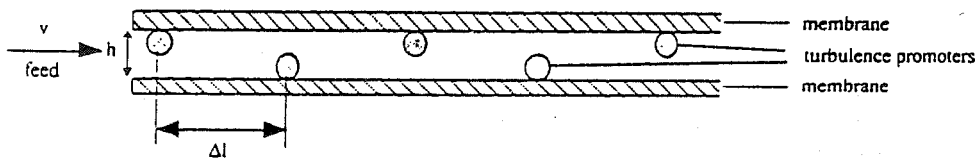
Figure VII - 8.   Schematic drawing of a flow channel with turbulence promoters

The mass transfer coefficient can be obtained from the following Sherwood relation [4],

$$Sh = \frac{k\, d_h}{D} = 1.9 \; Sc^{0.33} . Re^{0.5} \left(\frac{h}{\Delta l}\right)^{0.5}$$

(VII - 15)

These turbulence promoters are especially effective in laminar flow operations and eq. VII - 15 is typical applicable under these conditions (Re < 2000).

VII.4. Pressure drop

When a liquid flows through a pipe or a channel a pressure drop is observed across the flow geometry due to friction with the wall. The presence of a spacer or turbulence promoter in the pipe or channel will increase the friction and consequently the pressure drop increases. The pressure for a well developed flow can be given by the following correlation.

$$f = \frac{A}{Re^n}$$

(VII - 16)

Table VII.3 summarizes correlations for friction factors in various systems.

Table VII.3. Friction factors in various systems [5,6]

	channel	tube
laminar	$f = 24\, Re^{-1}$	$f = 16\, Re^{-1}$
turbulent	$f = 0.133\, Re^{-0.25}$	$f = 0.079\, Re^{-0.25}$

In can be observed that the friction factor for channel and tube are rather similar. Furthermore, in the turbulent region the friction factor is much less dependent on the Reynolds number. The pressure drop is given by the Fanning equation [6] and is related to the flow velocity by

$$\Delta p = f\, (S.L\, /A)\, 0.5 \; \rho v^2$$

(VII - 17)

in which L is the length of the tube, ρ is the density of the liquid (fluid), v the flow velocity, f the friction factor, S the circumference and A is the cross-section. This relation can be applied for a channel and a straight pipe. Substitution of the proper value of the friction factor (see table VII - 3) into eq. VII - 17 gives the value for the pressure drop in a given module geometry. From the value of the friction factor it can be observed that in the turbulent region the pressure drop is much more strongly dependent on the flow velocity. The introduction of an spacer or turbulence promoter introduce an additional resistance to

axial flow and this results in an increased friction and pressure loss. The pressure drop is very much dependent on the type of spacer. For a channel with turbulence promoters as shown in figure VII - 8, the following equation can be used [4]

$$\Delta P = 20 \left(\frac{h}{\Delta l}\right)^{0.4} Re^{-0.5} \frac{L}{h} 0.5 \, \rho \, v^2$$

(VII - 18)

in which Δl is the distance between successive turbulence promoters.

VII.5.   Characteristic flux behaviour in pressure driven membrane operations

Generally, the pure water flux through a porous membrane in pressure driven processes is directly proportional to the applied hydrostatic pressure according to

$$J = \frac{\Delta P}{\eta \, R_m}$$

(VII - 19)

where R_m is the hydrodynamic resistance of the membrane (Note that the hydrodynamic permeability L_p ($= 1 / \eta . R_m$) is often referred to as well). The hydrodynamic resistance R_m is a membrane constant and does not depend on the feed composition or on the applied pressure. The flux-force relationship for pure water is given schematically in figure VII - 9. However, when solutes are added to the water the behaviour observed is completely different especially in microfiltration and ultrafiltration. When the pressure is increased the
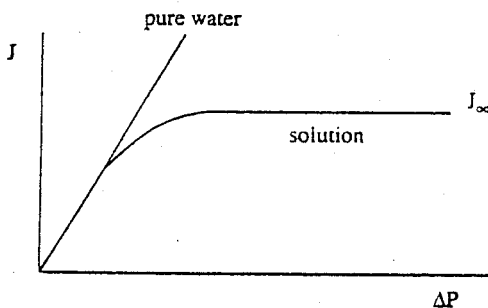
Figure VII - 9.   Flux as a function of the applied pressure both for pure water and for a solution.

flux increases, but after a finite (minimum) pressure has been attained the flux does not increase further on increasing the pressure. This maximum flux is called the limiting flux, J_{∞} (see figure VII - 9). When J in eq. VII - 10 is replaced by J_{∞}, it can be seen that the

limiting flux depends on the concentration in the bulk of the feed, c_b and on the mass transfer coefficient k. This is shown schematically in figure VII - 10.

$$J_\infty = k \ln\left(\frac{c_m}{c_b}\right) = k \ln c_m - k \ln c_b \qquad \qquad \text{(VII - 20)}$$

Figure VII - 10 demonstrates that on increasing the feed concentration, but keeping the mass transfer coefficient and the concentration at the membrane constant, the value of the limiting flux, J_∞, decreases. On the other hand, J_∞ increases when the mass transfer coefficient k is increased at constant feed concentrations.
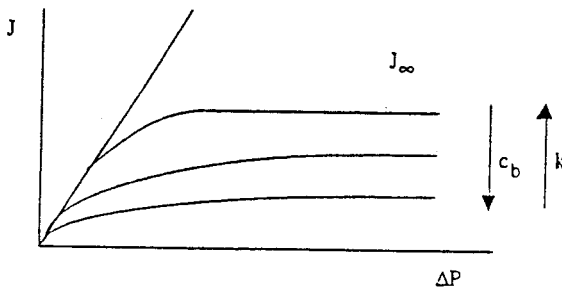
Figure VII - 10.   The flux as a function of the applied pressure for different bulk concentrations c_b and different mass transfer coefficients k.

If the results depicted in figure VII - 10 are plotted as J_∞ versus ln (c_b). a straight line is obtained. This is shown in figure VII - 11.
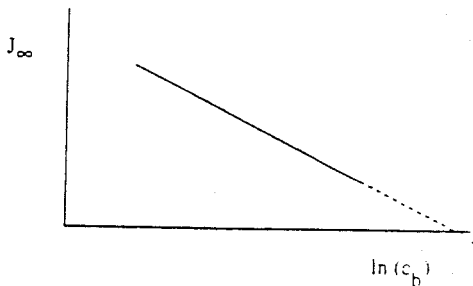
Figure VII - 11.   Limiting flux (J_∞) plotted as a function of the logarithm of the bulk concentration.

The behaviour of the limiting flux depicted is typical for ultrafiltration and to lesser extent for microfiltration. Whereas the flux increases with increasing pressure in reverse

osmosis. the flux is invariant with pressure after an initial increase in ultrafiltration. In discussing these phenomena. it must be realised that the formal description of concentration polarisation is the same for both ultrafiltration and reverse osmosis. However, the properties of concentrated macromolecular solutions, which appear in the boundary layer during ultrafiltration, are much more complex and less easy to describe than those of the concentrated solutions of simple salts encountered in reverse osmosis.

VII.6.   Gel layer model

As mentioned above, concentration polarisation can be very severe in ultrafiltration because the flux through the membrane is high, the diffusivity of the macromolecules is rather low and the retention is normally very high. This implies that the solute concentration at the membrane surface attains a very high value and a maximum concentration, the gel concentration (c_g), may be reached for a number of macromolecular solutes. The gel concentration depends on the size, shape, chemical structure and degree of solvation but is independent of the bulk concentration. The two phenomena, concentration polarisation and gel formation are shown in figure VII - 12.
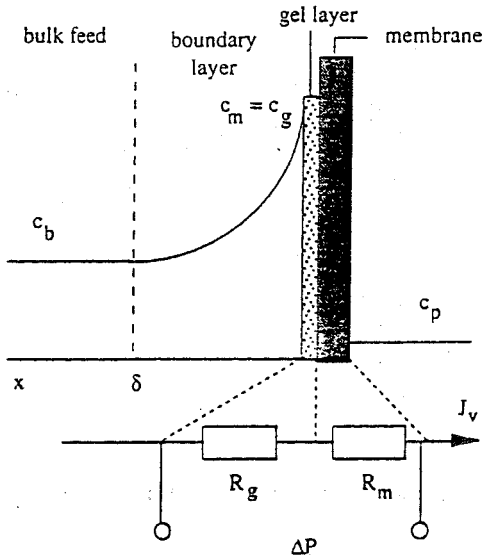
Figure VII - 12.   Concentration polarisation and gel layer formation.

Gel formation may be reversible or irreversible, a very important factor in membrane cleaning. An irreversible gel is very difficult to remove and precautions have to be taken to avoid this situation as much as possible. However, it is not important whether the gel is

reversible or irreversible for the description of the flux phenomena with the gel layer model.

The gel layer model [7-9] is capable of describing the occurrence of limiting flux as follows. Suppose the solute is completely retained by the membrane, then the solvent flux through the membrane increases with pressure until a critical concentration is reached corresponding to the gel concentration, c_g. On increasing the pressure further, the solute concentration at the membrane surface is not capable of any further increase (because the maximum concentration has been reached) and so the gel layer may become thicker and/or compacter. This implies that the resistance of the gel layer (R_g) to solvent transport increases, so that the gel layer becomes the limiting factor in determining flow. In the region of limiting flux an increase in pressure leads to an increase in the resistance of the gel layer so that the net result is a constant flux. (The osmotic pressure of the macromolecular solution is neglected in this approach). The total resistance can then be represented by two resistances in series, i.e. the gel layer resistance R_g and the membrane resistance R_m (see figure VII - 12)

For the gel layer region, this flux can be described by:

$$J_\infty = \frac{\Delta P}{\eta (R_m + R_g)} = k \ln\left(\frac{c_g}{c_b}\right) \qquad (VII - 21)$$

which suggests that if J_∞ is plotted as a function of $\ln(c_b)$ the result must be a straight line of slope -k (see figure VII - 13). It is assumed here that the gel concentration remains constant across the gel layer. The intercept of the straight line on the abscissa ($J_\infty = 0$) will give the value of $\ln(c_g)$.
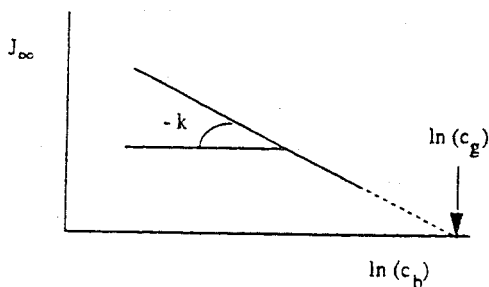
Figure VII - 13. Limiting flux (J_∞) plotted as a function of the logarithm of the concentration of the bulk feed.

Although this model may be considered to be a significant contribution to the theory of concentration polarisation and limiting flux behaviour in ultrafiltration, some drawbacks should be mentioned. In literature data have indicated that the gel concentration c_g is not a constant but depends on the bulk concentration and the cross flow velocity [16]. In

addition, different authors have reported widely varying values for c_g for a given solute [17]. Furthermore, k is assumed to be constant whereas the diffusivity of the macromolecular solute is often concentration-dependent. Finally, although proteins form a gel readily there are also many other macromolecular solutes, such as dextranes, that do not gel so easily even at very high concentrations.

VII.7. Osmotic pressure model

Macromolecules are retained by the membrane in ultrafiltration whereas low molecular weight components permeate through freely. Because the main contribution to the osmotic pressure of a solution arises from the low molecular weight solutes (the concentration of these being the same in the feed and permeate), the osmotic pressure of the retained macromolecules is often neglected.

However, for high flux values, high rejection levels and low mass transfer coefficient k values, the concentration of macromolecular solutes at the membrane surface can become quite high and hence the osmotic pressure cannot be neglected anymore. This has been commented upon by several investigators [12-16]. If the osmotic pressure at the membrane surface is taken into account, the flux equation is then given by:

$$J = \frac{\Delta P - \Delta \pi}{\eta \ R_m} \tag{VII - 22}$$

Here, ΔP is the hydraulic pressure difference and $\Delta \pi$ the osmotic pressure difference across the membrane. The value of $\Delta \pi$ is determined by the concentration at the membrane surface c_m and not by the bulk concentration c_b.

The limiting flux behaviour can also be described by this model. By increasing the pressure difference the flux increase on and hence the concentration at the membrane surface, c_m will also increases. This leads to an increase in the osmotic pressure and hence the pressure increase is (partly) counterbalanced by the osmotic pressure increase. The phenomenon of osmotic pressure has been described in a previous section of this chapter. Thus, for dilute low molecular weight solutions, a linear relationship, the so-called van 't Hoff relationship, exists between the osmotic pressure and the concentration. However, the dependence of the osmotic pressure of a macromolecular solution on the concentration is generally exponential rather than linear and can be described by

$$\pi = a. \ c^n \tag{VII - 23}$$

where a is a constant and n is an exponential factor with a value greater than 1. Indeed, for semi-dilute or concentrated polymer solutions n will have a value of 2 or greater. The constants a and n depend both on molecular weight and type of polymer. From this figure it can be seen that the deviation from van 't Hoff's relationship can become quite large for increasing macromolecular solute concentrations, especially when the exponent n is large.

Another way to account for non-ideality and to express the osmotic pressure as a function of concentration is by a virial expansion (eq. VII - 24).

$$\pi = \frac{RT}{M} c + B c^2 + \ldots\ldots$$

(VII - 24)

Applying the osmotic pressure effect to the concentration at the membrane interface (c_m), and combining eqs. VII - 23, VII - 22 and VII - 9, is also possible to calculate the flux assuming that the solutes are retained completely:
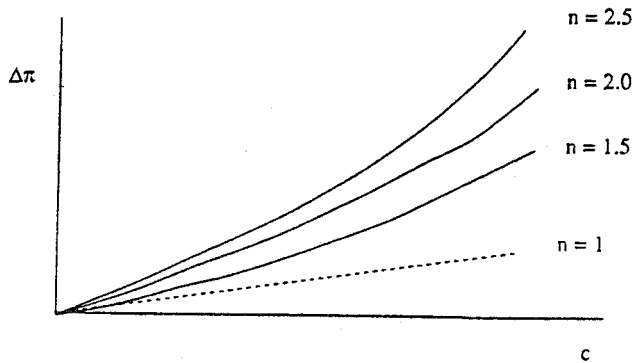
Figure VII - 14.   Schematic drawing of the osmotic pressure as a function of the concentration for various values of the exponential coefficient n.

$$J = \frac{\Delta P - a\, c_b^n \exp\left(\frac{n\, J}{k}\right)}{\eta\, R_m}$$

(VII - 25)

That the flux J does not increase linearly with an increase in the pressure P can be seen by differentiating J with respect to ΔP. The derivative $\partial J/\partial \Delta P$ shows how the flux changes with increasing pressure.

$$\frac{\partial J}{\partial \Delta P} = \left[\eta\, R_m + a\, c_b^n\, \frac{n}{k}\, \exp\left(\frac{n\, J}{k}\right)\right]^{-1}$$

(VII - 26)

Combining eqs. VII - 23 and VII - 25, and substituting the result into eq. VII - 26 leads to

$$\frac{\partial J}{\partial \Delta P} = \left(\eta \ R_m + \frac{\eta}{k} \ \Delta \pi \right)^{-1}$$

(VII - 27)

or

$$\frac{\partial J}{\partial \Delta P} = \frac{1}{\eta \ R_m} \left(1 + \frac{\Delta \pi \ \eta}{\eta \ R_m \ k} \right)^{-1}$$

(VII - 28)

The effect of a pressure increase (the derivative $\partial J/\partial \Delta P$) can be easily demonstrated from the above equations. In fact two extremes may be distinguished: $\Delta \pi$ is very high and $\Delta \pi$ approaches zero. For very high values of $\Delta \pi$ the derivative $\partial J/\partial \Delta P$ will be almost zero, i.e. the flux will not increase when the pressure increases so that the J_{∞} region has been attained. When $\Delta \pi \Rightarrow 0$, the derivative $\partial J/\partial \Delta P$ is equal to $(\eta \ R_m)^{-1}$.

Multiplying both the left-hand side and the right-hand side of eq. VII - 28 with $\eta . R_m$ leads to two dimensionless numbers:

$$\eta . R_m \left(\frac{\partial J}{\partial \Delta P} \right) \quad \text{and} \quad \left(\frac{\Delta \pi \ \eta}{\eta \ R_m \ k} \right)$$

What is the physical meaning of these numbers ?

It can be shown from eq. VII - 28 that for a pure solvent (superscript °) the following equation is obtained:

$$\left(\frac{\partial J}{\partial \Delta P} \right)^o = \frac{1}{R_m \ \eta}$$

(VII - 29)

and

$$\eta \ R_m \left(\frac{\partial J}{\partial \Delta P} \right) = \frac{\dfrac{\partial J}{\partial \Delta P}}{\left(\dfrac{\partial J}{\partial \Delta P} \right)^o}$$

(VII - 30)

Eq. VII - 30 shows that $\eta \ R_m \ (\partial J/\partial \Delta P)$ is the ratio between the slope of the plot of J versus ΔP and that of the pure solvent flux versus ΔP, i.e. it is a measure of the effectiveness of the pressure increase. The maximum slope that can be achieved in a flux versus pressure relationship is $(\partial J/\partial \Delta P)_{\text{pure solvent}}$. Hence, $R_m \ (\partial J/\partial \Delta P)$ becomes smaller when the slope of the flux versus pressure curve diminishes, i.e. the effectiveness of an increase in pressure becomes progressively less at higher pressures. This decrease in effectiveness is caused by an increase in the resistance towards transport. Because the membrane resistance R_m (or $\eta \ R_m$ in fact) is assumed to be constant, the increasing resistance must be attributed to an increase in the osmotic pressure.
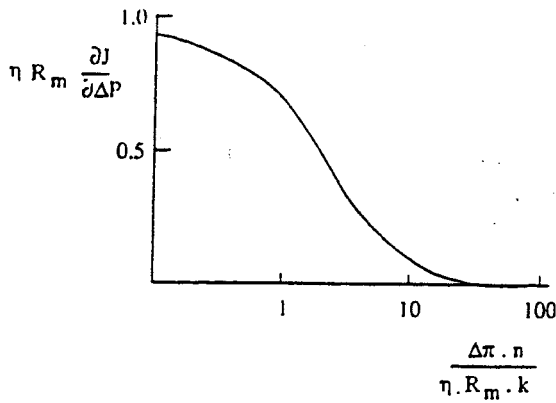
Figure VII - 15. Effectiveness of pressure increase as a function of the ratio between the osmotic resistance and the membrane resistance.

The ratio between the 'osmotic pressure resistance' and the membrane resistance is given by the second dimensionless number, i.e. $(\Delta\pi\ n)/(\eta\ R_m\ k)$. Figure VII - 15 relates these two numbers to each other.

It can be seen from this figure that $\eta\ R_m\ (\partial J/\partial\Delta P)$ becomes smaller with increasing pressure, because the osmotic pressure (or the osmotic pressure difference $\Delta\pi$ across the membrane) increases until ultimately the 'limiting flux' region is reached where the flux no longer increases (or arbitrarily increases by less than 5%) with increasing pressure.
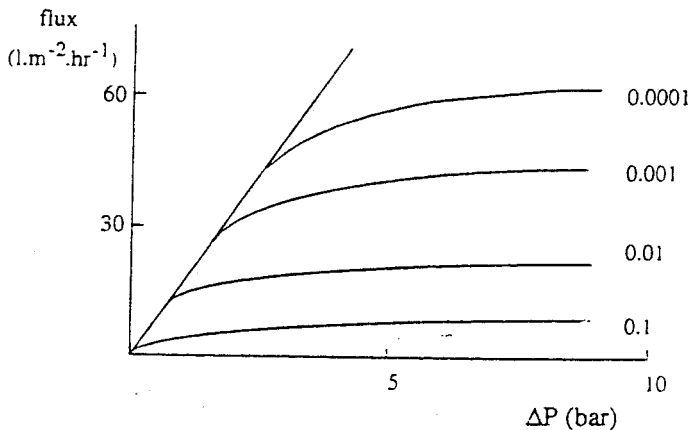
Figure VII - 16. Calculated values of the permeate flux plotted as a function of the applied pressure at varying bulk concentrations c_b and the following parameters: $a = 100$; $n = 2$; $R_m = 5\ 10^5$ bar.s / m; $k = 2\ 10^{-6}$ [16].

The influence of the osmotic pressure as a function of the applied pressure can also be demonstrated by a calculation. Using some constant parameters which are characteristic for ultrafiltration, the flux can be calculated as a function of the applied pressure by the use of eq. VII - 25. The result is given in figure VII - 16. As the pressure increases the (calculated) flux reaches the maximum, J_{∞}. However, this value of J_{∞} seems to be attained only at high applied pressures, but it should be remembered that the example is only illustrative and designed to show the effect of osmotic pressure in practice. Indeed, it is possible to reach J_{∞} at a pressure $\Delta P = 1$ bar. Furthermore, if a smaller value is used for R_m than that in figure VII - 16, then J_{∞} can be attained at even lower pressures.

How can the gel layer model and the osmotic pressure model, be related to each other? In the gel layer model, a plot of J versus $\ln(c_b)$ gives a straight line with a slope equal to -k. A similar J versus $\ln(c_b)$ relationship can be obtained from the osmotic pressure model. From eq. VII - 25 the following relationship can be derived:

$$\frac{\partial J}{\partial \ln(c_b)} = -k \left(1 + \frac{R_m \, k \, \eta}{\Delta \pi \, n} \right)^{-1} \qquad (VII - 31)$$

When $(\Delta \pi \, n)/(\eta \, R_m \, k) \gg 1$, the right-hand side of eq. VII - 31 reduces to -k. Hence the osmotic pressure model gives a linear plot in the region where R_m can be neglected with a slope equal to -k similar to that obtained from the gel layer model.
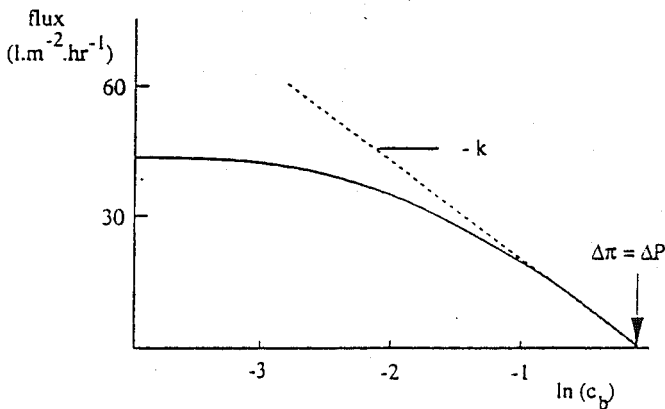
Figure VII - 17.   Flux J_{∞} as a function of the concentration in the bulk, c_b.

Figure VII - 17 depicts a plot of the flux J_{∞} as a function of the bulk concentration. When $J_{\infty} = 0$, then $\Delta P = \Delta \pi$. High values of $(\Delta \pi \, n) / (\eta \, R_m \, k)$ lead to flux decline because of osmotic pressure effects. Factors that lead to such a high value are:
- high permeate flux (because of the high driving force ΔP or the low membrane

resistance R_m)
- high bulk concentration c_b
- low mass transfer coefficient k
- high value of n (i.e. a macromolecular solute)

The considerations given above still leave the question open as to which of the two models is actually valid. A qualitative method of discriminating between the two models is provided by the J_∞ versus $\ln(c_b)$ plot, with the intercept on the absciss providing an answer. If physical-chemical reasons suggest that gelation should occur, the gel layer model may be valid and the intercept gives $c_b = c_g$. If, on the other hand, the osmotic pressure at point c is equal to the applied pressure $[\Delta P \approx \pi(c)]$, then $c_b = c_m$. However, it should be noted that often, in practice, the phenomena are much more complex than those described here. Thus, adsorption and other phenomena (see figure VII - 2) have not been taken into account. Even the way in which the pressure increments occur can lead to other results which cannot be predicted or even described by the two theories advanced above.

VII.8.   Boundary layer resistance model

Concentration polarisation phenomena lead to an increase of the solute concentration at the membrane surface. If the solute molecules are completely retained by the membrane, at steady-state conditions the convective flow of the solute molecules towards the membrane surface will be equal to the diffusive flow back to the bulk of the feed. Hence, at 100% rejection the average velocity of the solute molecules in the boundary layer will be zero. Because of the increased concentration, the boundary layer exerts a hydrodynamic resistance on the permeating solvent molecules. The solvent flux can then be represented by a resistance model in which both the boundary layer resistance (R_{bl}) and the membrane resistance (R_m) appear (assuming that no gelation occurs !). A schematic drawing of this resistance model is given in figure VII - 18.
Because both the above resistances operate in series, the solvent flux is given by eq. VII - 32:

$$J_v = \frac{\Delta P}{\eta (R_m + R_{bl})}$$

(VII - 32)

This latter equation is the basic equation of the boundary layer resistance model [17-19]. The boundary layer can be considered as a concentrated solution through which solvent molecules permeate, with the permeability of this stagnant layer depending very much on the concentration and the molecular weight of the solute. The resistance exerted by this layer is far much greater for macromolecular solutes (ultrafiltration) relative to for low molecular weight solutes (reverse osmosis). Because there is a concentration profile in the boundary layer, the permeability P of the solvent may be written as a function of the distance coordinate x with the boundaries x = 0 and x = δ.
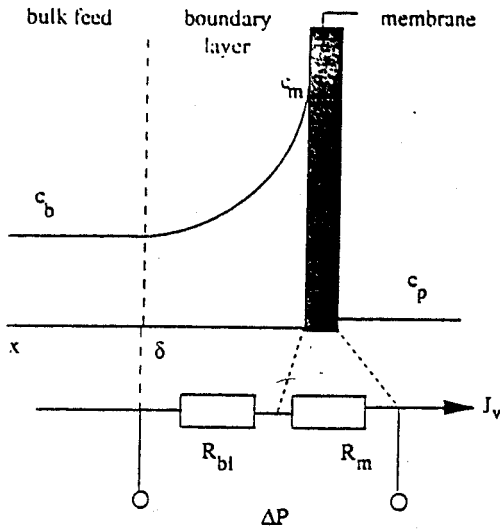
Figure VII - 18. Schematic representation of the boundary layer resistance model.

The permeability or permeability coefficient appears in the phenomenological Darcy equation [20], and because the osmotic gradient is the driving force for solvent flow in the boundary layer, the volume flux can be written as [17]:

$$J = \frac{P}{\eta} \frac{d\pi}{dx} \tag{VII - 33}$$

Integration over the boundary layer leads to

$$J = \frac{\Delta\pi_{bl}}{\eta \int_0^\delta P(x)^{-1} dx} \tag{VII - 34}$$

in which

$$R_{bl} = \int_0^\delta P(x)^{-1} dx \tag{VII - 35}$$

and hence eq. VII - 34 can be simplified to

$$J_v = - \frac{\Delta\pi_{bl}}{\eta \; R_{bl}}$$

(VII - 36)

In order to estimate the boundary layer resistance R_{bl}, it is necessary to determine the permeability P. This can be done by sedimentation measurements since a correlation exists between the permeation of a solvent through a (stagnant) polymer solution and the sedimentation of polymer molecules (or molecules as small as sucrose) through a solvent. This is shown schematically in figure VII - 19. According to Mijnlieff et al. [21] the permeability is related to the sedimentation coefficient via

$$P = \frac{\eta \; s}{(1 - v_1/v_2) \; c}$$

(VII - 37)

where v_0 and v_1 are the partial molar volume of the solvent and solute, respectively, and c is the solute concentration.

The sedimentation coefficient s can be determined by ultracentrifugation [22] in which a centrifugal field is applied to a particle or (macro)molecule. The sedimentation velocity of that particle (dr/dt) divided by the acceleration in the centrifugal field ($\omega^2 r$) is

sedimentation of the
solute

permeation of the solvent
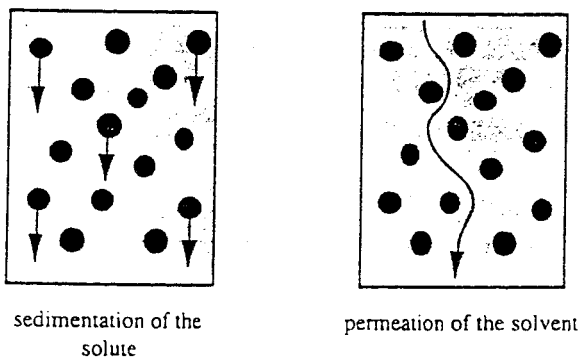
Figure VII - 19. Correlation between the sedimentation of a solute and the permeation of a solvent.

called the sedimentation coefficient s. i.e.

$$s = \frac{1}{\omega^2 \; r} \frac{dr}{dt}$$

(VII - 38)

while the concentration dependence of the sedimentation coefficient is usually expressed as

$$\frac{1}{s} = \frac{1}{s_0} \left(1 + k_1 c + k_2 c^2\right)$$

(VII - 39)

Substitution of eq. VII - 37 into eq. VII - 35 yields

$$R_{bl} = \int_0^\delta \frac{(1 - v_1/v_0) \, c}{\eta \, s} \, dx$$

(VII - 40)

and using the concentration dependence of the sedimentation coefficient s eq. VII - 40 becomes

$$R_{bl} = \int_0^\delta \frac{(1 - v_1/v_0)}{\eta \, s_0} \left[c + k_1 c^2 + k_2 c^3\right] dx$$

(VII - 41)

and hence the solute concentration in the boundary layer is a function of the distance x.

Assuming that the solute is completely retained by the membrane, the concentration of the solute in the boundary layer may then be written as:

$$c(x) = c_b \exp\left(\frac{J \, x}{D}\right)$$

(VII - 9)

since integration of $P(x)^{-1}$ over the boundary layer gives

$$c_b^n \int_0^\delta \exp\left(\frac{n \, J \, x}{D}\right) dx = \frac{D}{n \, J} \, c_b^n \left[\exp\left(\frac{n \, J}{k}\right) - 1\right] = \frac{D}{n \, J} \left(c_m^n - c_b^n\right)$$

(VII - 42)

then substitution of eq. VII - 9 into eq. VII - 41 and integration over the boundary layer gives:

$$R_{bl} = \frac{\left(1 - \frac{v_1}{v_0}\right) D}{\eta \, s_0 \, J} \left[(c_m - c_b) + \frac{k_1}{2}(c_m^2 - c_b^2) + \frac{k_2}{3}(c_m^3 - c_b^3)\right]$$

(VII - 43)

In deriving this equation it is assumed that the diffusion coefficient D is a constant and not a function of the concentration, i.e. $D \neq f(c)$.

The resistance of the boundary layer R_{bl} can be calculated if ΔP, J, R_m, c_b, k, s and D are known. It is difficult to determine the exact value of the mass transfer coefficient and an error in k has a large effect on the calculated R_{bl} since c_m is related to k via an exponential function.

It should be noted that the boundary layer resistance model is equivalent to the osmotic pressure model [16]:

$$J_v = \frac{\Delta P}{\eta (R_m + R_{bl})} = \frac{\Delta P - \Delta \pi}{\eta R_m}$$

(VII - 44)

although independent measurements are essential for both models. However, for practical purposes, the osmotic pressure model is much easier to use.

VII.9.   Concentration polarisation in diffusive membrane separations

So far concentration polarisation has been focussed on pressure driven processes in which solutes are retained to some extent by the membrane. In this way the solute concentration profile has been established by the convective flow towards the membrane and the diffusive back transport of the solute towards the bulk. However, there are many processes which are aimed to transport a specific component preferentially though a membrane, i.e., dialysis, diffusion dialysis, facilitated transport in supported and emulsion liquid membranes, pervaporation, membrane contactors. The transport in these processes are characterized by a solution-diffusion mechanism, i.e., the permeating component must dissolve into the membrane from the feed side and will then diffuse through the membrane according to a driving force. In these processes it is frequently assumed that the resistance to transport is completely determined by the membrane phase (see figure VII - 20a) and boundary layer resistances are neglected. Dependent on the hydrodynamics in the liquid feed and the resistance of the membrane for the specific permeating solute the resistance in the boundary may contribute to the overall resistance or may even be rate determining. The concentration profile for such a system is shown in figure VII - 20b in which $c^{sm}_{i,1}$ is the feed concentration of component i at the membrane surface and $c^{sm}_{i,2}$ is the permeate concentration at the membrane surface at the permeate side.

The distribution coefficient K is defined as :

(a)

(b)
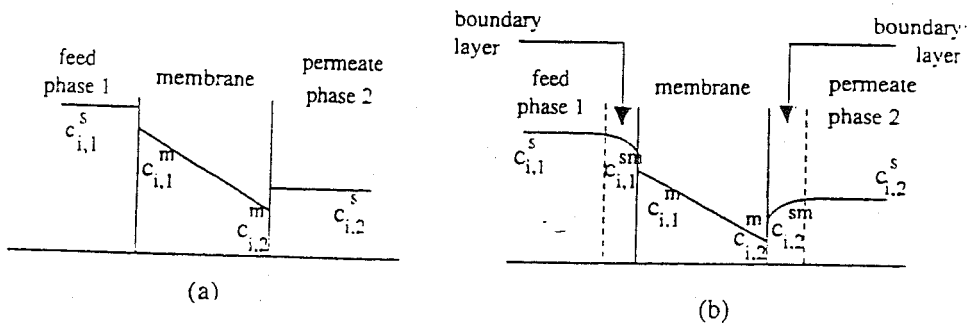
Figure VII - 20.   Concentration profiles for diffusive membrane processes: (a) without boundary layer resistances, and (b) with boundary layer resistances.

$$K = \frac{c_{i,1}^m}{c_{i,1}^{sm}} = \frac{c_{i,2}^m}{c_{i,2}^{sm}}$$

$$(VII - 45)$$

At steady state the flux equations of component i through each phase are equal. The flux of component i in the boundary layer of the feed is given by

$$J_i = k_1 (c^{sm}_{i,1} - c^s_{i,1})$$

$$(VII - 46)$$

and through the boundary layer at the permeate side by

$$J_i = k_1 (c^{sm}_{i,1} - c^s_{i,1})$$

$$(VII - 47)$$

The flux through the membrane phase is given by

$$J_i = \frac{D_i}{\ell}(c_{i,1}^m - c_{i,2}^m)$$

$$(VII - 48)$$

Substitution of eq. VII - 45 into VII - 48 gives

$$J_i = \frac{D_i . K}{\ell}(c_{i,1}^m - c_{i,2}^m) = \frac{P_i}{\ell}(c_{i,1}^m - c_{i,2}^m)$$

$$(VII - 49)$$

By addition of eqs. VII - 46, VII - 47 and VII - 49 the following equation is obtained which can be applied in general.

$$J_i = k_{ov}(c_{i,1}^s - c_{i,2}^s)$$

$$(VII - 50)$$

and the overall mass transfer coefficient k_{ov} is given by eq. VII - 51

$$\frac{1}{k_{ov}} = \frac{1}{k_1} + \frac{\ell}{P_i} + \frac{1}{k_2}$$

$$(VII - 51)$$

In many books and articles the membrane phase contribution ℓ/P_i is frequently indicated as $1/p_M$ (i.e. $\ell/P_i = 1/p_M$). $1/p_M$ has the dimension of a mass transfer coefficient while P_i (= $D_i.K$) is defined as the permeability coefficient.

This concept of resistances in series can be applied to various processes (see also chapter V.6.2 and VI.4.4.1) and the approach is to determine the mass transfer coefficients by means of the semi-empirical relationships given in table VII.1 (see also ref. [1]). When the resistances in the boundary layers are small compared to that of the membrane resistance the permeation rate is given by eq. VII - 49.

VII.10.   Concentration polarisation in electrodialysis

Although the driving forces, the separation principle and the membranes are completely different in electrodialysis from those in pressure-driven membrane processes, polarisation phenomena may severely affect the separation efficiency.

The basic principles of electrodialysis have been described in chapter VI. The mass transfer of charged molecules is the result of a driving force, an electrical potential difference and positively charged molecules (cations) are driven to the cathode and the negatively charged particles (anions) to the anode. Furthermore, diffusion will occur if a concentration difference has been generated. To illustrate the phenomenon of concentration polarisation, let us assume that a negatively charged cation-exchange membrane is placed between the cathode and anode, and that the system is immersed in a NaCl solution. The cation-exchange membrane permits only the transport of cations. When a direct current potential is applied between the cathode and the anode, the Na^+ ions move from left to right in the direction of the cathode. Because transport through the membrane proceeds faster than in the boundary layer, a concentration decrease occurs on the left-hand side of the membrane whereas a concentration increase is established at the right-hand side. A diffusive flow is generated because of the concentration gradient in the boundary layer. At steady state, a concentration profile is established (see fig. VII - 21).

The transport (flux) of cations through the membrane caused by an electrical potential difference is given by:

$$J^m = \frac{t^m \, i}{z \, \mathcal{F}}$$

(VII - 52)
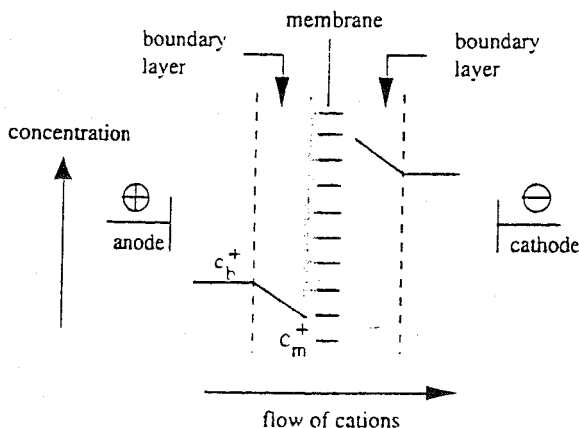
Figure VII - 21.   Concentration polarisation in electrodialysis in the presence of a cation-selective membrane.

the transport of cations in the boundary layer, which is also caused by an electrical potential difference, is given by:

$$J^{bl} = \frac{t^{bl} \, \iota}{z \, \mathcal{F}}$$ (VII - 53)

while the diffusive flow in the boundary layer is given by:

$$J_D{}^{bl} = - D \frac{dc}{dx}$$ (VII - 54)

In these various equations J^m and J^{bl} are the electrically driven fluxes in the membrane and the boundary layer, while $J_D{}^{bl}$ is the diffusive flux in the boundary layer. The transport numbers of the cation in the membrane and in the boundary layer are t^m and t^{bl}. z is the valence of the cation ($z = 1$ for Na^+); $\mathcal{F}$ is the Faraday constant; ι is the electrical current; and dc/dx is the concentration gradient in the boundary layer.

At steady state the transport of cations through the membrane is equal to the combined electrical and diffusive flux towards the membrane in the boundary layer, i.e.

$$J^m = \frac{t^m \, \iota}{z \, \mathcal{F}} = \frac{t^{bl} \, \iota}{z \, \mathcal{F}} - D \frac{dc}{dx}$$ (VII - 55)

Integration of eq. VII - 55, assuming a constant diffusion coefficient (linear concentration profile) and using the following boundary conditions,

$c = c_m$ at $x = 0$

$c = c_b$ at $x = \delta$

leads to equations for the reduced cation concentration (eq. VII - 56) and the increased cation concentration (eq. VII - 57) at the membrane surface:

$$c_m = c_b - \frac{\left(t^m - t^b\right) \, \iota \, \delta}{z \, \mathcal{F} \, D}$$ (VII - 56)

$$c_m = c_b + \frac{\left(t^m - t^b\right) \, \iota \, \delta}{z \, \mathcal{F} \, D}$$ (VII - 57)

The ohmic resistance is located mainly in the boundary layer where ion depletion has occurred. Because of such depletion the resistance in the boundary layer will increase so that part of the electrical energy may be dissipated as heat (electrolysis of water) if the concentration becomes too low. The current density ι in that layer can be obtained from eq. VII - 56.

$$\iota = \frac{z \, D \, \mathscr{F} \, (c_h - c_m)}{\delta \, (\iota^m - \iota^{bl})}$$

(VII - 58)

If the electrical potential difference is increased, the current density will increase, the cation flux will increase and consequently the cation concentration will decrease (see eq. VII - 58). When the cation concentration at the membrane surface c_m approaches zero, a limiting current density ι_{lim} is attained:

$$\iota_{lim} = \frac{z \, D \, \mathscr{F} \, c_h}{\delta \, (\iota^m - \iota^{bl})}$$

(VII - 59)

A further increase in the driving force (by increasing the difference in the electrical potential) at this point will not result in an increase in cation flux. It can be seen from eq. VII - 59 that the limiting current density depends on the concentration of cations (ions in general) in the bulk solution c_b and on the thickness of the boundary layer. In order to minimise the effect of polarisation the thickness of this boundary layer must be reduced and hence the hydrodynamics and cell design are very important. Often feed spacers and special module designs are used (see chapter VIII).

Although the phenomenon of polarisation has been illustrated by considering cation transport through cation-selective membranes, the same description applies to anions. However, the mobility of anions with the same valence in the boundary layer is a little greater than that of cations. This implies that under similar hydrodynamic conditions (equal thickness of the boundary layer, same cell construction) for the anion and cation, the limiting current density will be attained faster at a cation-exchange membrane than at an anion-exchange membrane.

VII.11.   Temperature polarisation

In comparison to isothermal membrane processes, little attention has been paid to date to polarisation phenomena in non-isothermal processes. In non-isothermal processes such as membrane distillation and thermo-osmosis, transport through the membrane occurs when a temperature difference is applied across the membrane. Temperature polarisation will occur in both membrane processes although both differ considerably in membrane structure, separation principle and practical application. In a similar manner to concentration polarisation in pressure-driven membrane processes, coupled heat and mass transfer contribute towards temperature polarisation.

The concept of temperature polarisation will be described using membrane distillation as an example. A detailed description of membrane distillation has already been given in chapter VI and a schematical representation of temperature polarisation in such a process is depicted in figure VII - 22. Two compartments filled with water are separated by a hydrophobic porous membrane (e.g. teflon). As the membrane is not wetted by

water, the pores are not filled with liquid. Because the water in one compartment is at a higher temperature (and therefore at a higher vapour pressure), transport of water vapour through the membrane pores takes place from the warm to the cold side. Thus, evaporation of water vapour occurs on the warm side of the membrane whereas condensation of the water vapour occurs on the cold side. The heat required for such evaporation has to be supplied from the bulk solution, whilst a further amount of heat is transferred through the solid polymer and through the pores by conduction. The temperature of the liquid on the warm side of the membrane will gradually decrease until a steady state is reached when the heat supplied from the bulk will be equal to the heat transferred through the membrane. For this reason, the resistance to heat transfer will be located not only in the membrane but also in the boundary layer. The difference in temperature between the liquid in the bulk and at the membrane surface is called temperature polarisation (there is a close similarity between heat transfer, figure VII - 22, and mass transfer, figures VII - 4, VII - 15 and VII - 17). The heat flux through the membrane is determined by two contributions, conduction through the membrane material and pore (air !) and by diffusion of water vapour. At steady state the heat flux ϕ through the boundary layers and membrane are equal. Thus the heat balance over the membrane from feed to permeate can be written as:

$$\phi = \alpha_1 (T_{b1} - T_{m1}) - \phi \, \Delta H_v = \frac{\lambda_m}{\ell} (T_{m1} - T_{m2}) = \alpha_2 (T_{m2} - T_{b2}) + o \, \Delta H_c \quad \text{(VII - 60)}$$
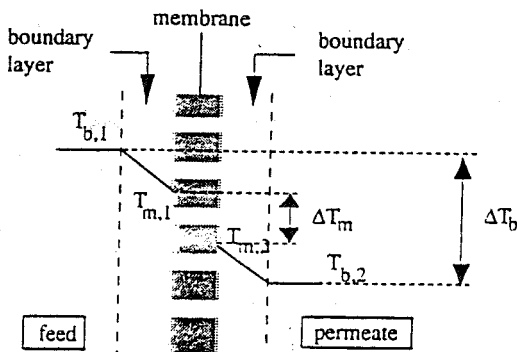
Figure VII - 22. Temperature polarisation in membrane distillation.

where α_1 and α_2 are the heat transfer coefficients on the warm side and the cold side of the membrane, respectively; $\phi \, \Delta H_v$ and $\phi \, \Delta H_c$ are the heat fluxes caused by convective transport through the pores; ℓ is the membrane thickness; and λ_m is the overall heat conductivity of the membrane.
If we assume that:
$$\phi \, \Delta H_v = - \phi \, \Delta H_c$$

$T_{b,1} - T_{m,1} = T_{m,2} - T_{b,2} = \Delta T_{bl}$ (the temperature difference in the boundary layer)

$T_{m,1} - T_{m,2} = \Delta T_m$ (the temperature difference across the membrane)

$T_{b,1} - T_{b,2} = \Delta T_b$ (the temperature difference between the bulk feed and the bulk
                                                        permeate)

$\alpha_1 = \alpha_2 = \alpha$

then the following equation can be derived [23] from eq. VII - 60:

$$\Delta T_m = \frac{\Delta T_b - \dfrac{2 \, \phi \, \Delta H_c}{\alpha}}{\left[1 + \left(\dfrac{2 \, \lambda_m}{\ell \, \alpha} \right) \right]}$$

(VII -61)

where the overall heat conductivity λ_m is the sum of two parallel resistances, the heat conductivity through the solid (polymer) λ_p and the heat conductivity through the pores filled with gas and vapour, λ_g. Assuming that the pores in the porous membrane are cylindrical and that the surface porosity is given by ε, then the overall heat conductivity λ_m is given by

$$\lambda_m = \varepsilon. \, \lambda_g + (1 - \varepsilon) . \lambda_p$$

(VII - 62)

The heat conductivity of the solid material (polymer) λ_p is, in general, 10 to 100 times greater than λ_g , the heat conductivity through the pores. Because of entrainment with water vapour molecules the convective heat flow through the membrane pores, is given by:

$$\phi \, \Delta H_c = \rho \, \Delta H_v \, J$$

(VII - 63)

Combination of eq. VII - 63 and eq. VII - 61 gives

$$\Delta T_m = \frac{\Delta T_b - \dfrac{2 \, J \, \rho \, \Delta H_v}{\alpha}}{\left[1 + \left(\dfrac{2 \, \lambda_m}{\ell \, \alpha} \right) \right]}$$

(VII - 64)

Eq. VII - 64 demonstrates that an increase in the volume flux (increase in the driving force, i.e. the temperature difference across the membrane) leads to an increase in temperature polarisation. Furthermore, a higher heat conductivity for the solid (polymer) also increases temperature polarisation, whereas an increase in the heat transfer coefficient and an increase in membrane thickness reduce this effect.

In thermo-osmosis the membrane employed does not contain any pores, viz. a dense homogeneous membrane is used. No phase transitions occur at the liquid/membrane interfaces and heat is only transferred by conduction through the solid membrane matrix.

The following equation for temperature polarisation can be derived for this process. (It should be noted that this equation is similar to eq.VII - 61, except that the enthalpies of vaporisation and condensation are not included since no phase transitions occur).

$$\Delta T_m = \frac{\Delta T_b}{\left[1 + \left(\frac{2\,\lambda_m}{\ell\,\alpha} \right) \right]}$$

(VII - 65)

The heat conductivity in the membrane, λ_m, appears in both eqs. VII - 64 and VII - 65. However, both values are not equal; the value λ_m in eq.VII -. 65 (thermo-osmosis) will be greater so that this factor will have a stronger effect on the temperature polarisation. Because a convective term which mainly depends on the volume flux appears in eq.VII - 58, the net result is that the effect of temperature polarisation is always greater in membrane distillation even when the temperature difference across the membrane is the same in both processes and when the same membrane material is used.

VII.12. Membrane fouling

The performance of membrane operations is diminished by polarisation phenomena, although the extent to which these phenomena can occur differ considerably. Thus, in microfiltration and ultrafiltration the actual flux through the membrane can be only a fraction of the pure water flux, whereas in pervaporation the effect is less severe.

With all polarisation phenomena (concentration, temperature polarisation), the flux at a finite time is always less than the original value. When steady state conditions have been attained a further decrease in flux will not be observed, i.e. the flux will become constant as a function of time. Polarisation phenomena are reversible processes, but in practice, a continuous decline in flux decline can often be observed. This is shown schematically in figure VII - 23.
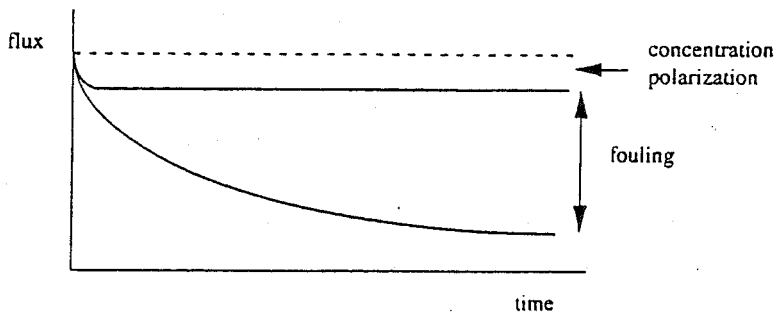
Figure VII - 23. Flux as a function of time. Both concentration polarisation and fouling can be distinguished.

Such continuous flux decline is the result of membrane fouling, which may be defined as the (ir)reversible deposition of retained particles, colloids, emulsions, suspensions, macromolecules, salts etc. on or in the membrane. This includes adsorption, pore blocking, precipitation and cake formation. Some extensive review articles have been written on fouling [18 - 21].

Fouling occurs mainly in microfiltration/ultrafiltration where porous membranes which are implicitly susceptible to fouling are used. In pervaporation and gas separation with dense membranes, fouling is virtually absent. Therefore, pressure driven processes will be emphasized but also here the type of separation problem and the type of membrane used in these processes determine the extent of fouling. Roughly three types of foulant can be distinguished:
- organic precipitates (macromolecules, biological substances, etc.)
- inorganic precipitates (metal hydroxides, calcium salts, etc.)
- particulates

The phenomenon of fouling is very complex and difficult to describe theoretically. Even for a given solution, fouling will depend on physical and chemical parameters such as concentration, temperature, pH, ionic strength and specific interactions (hydrogen bonding, dipole-dipole interactions). However, reliable values of flux decline are necessary for process design. The flux may also be described by a resistances-in-series model, in which a resistance of a cake layer is in series with the membrane resistance. The flux can be described by

$$J_v = \frac{\Delta P}{\eta (R_m + R_c)}$$

(VII - 66)
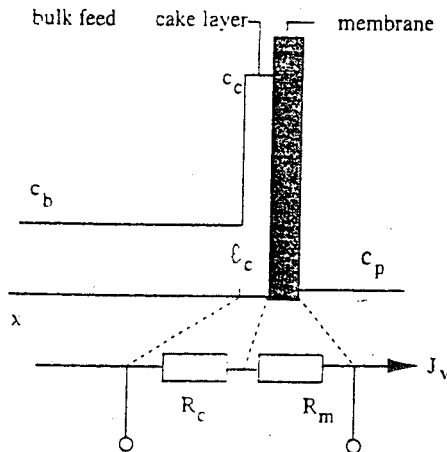
Figure VII - 24. Schematic representation of the cake-filtration model.

In this *filtration model* the solute is considered to form a "cake" or a deposition of particles at the membrane wall of constant concentration (see figure VII - 24). This cake-filtration model is frequently used to determine a fouling index. The total cake layer resistance (R_c) is equal to the specific resistance of the cake (r_c) multiplied by the cake thickness (ℓ_c). The specific cake resistance (r_c) is assumed to be constant over the cake layer.

$$R_c = \ell_c \, r_c \qquad\qquad (VII - 67)$$

The specific cake resistance is often expressed by the Kozeny-Carman relationship

$$r_c = 180 \, \frac{(1 - \varepsilon)^2}{\left[(d_s)^2 \, \varepsilon^3\right]} \qquad\qquad (VII - 68)$$

where d_s is the 'diameter' of the solute particle and ε the porosity of the cake layer. The thickness ℓ_c of the cake is equal to

$$\ell_c = \frac{m_s}{\left[\rho_s (1 - \varepsilon) A\right]} \qquad\qquad (VII - 69)$$

where m_s is the mass of the cake, ρ_s the density of the solute and A the membrane area. The mass of the cake is difficult to estimate. The effective thickness of the cake layer is in the order of several micrometers, which indicates that many monolayers ($\approx 100 - 1000$) of macromolecules are involved [22]. The thickness of the layer depends on the type of solute and especially on operating conditions and time. The growing layer of accumulates results in a continuous flux decline.
R_c the cake layer resistance can be obtained from a mass balance. In case of a complete solute rejection, $R = 100\%$ then

$$R_c = \frac{r_c \, c_b \, V}{c_c \, A} \qquad\qquad (VII - 70)$$

Now the flux may be written as

$$J = \frac{1}{A} \frac{dV}{dt} = \frac{\Delta P}{\eta \left[R_m + \frac{r_c \, c_b \, V}{c_c \, A} \right]} \qquad\qquad (VII - 71)$$

or

$$\frac{1}{J} = \frac{1}{J_w} + \left(\frac{\eta \, c_b \, r_c}{\Delta P \, c_c}\right) \frac{V}{A} \qquad\qquad (VII - 72)$$

where J_w is the pure-water flux. Figure VII - 25 shows that the reciprocal flux is indeed linearly related to the permeate volume V for various concentrations (c_b) and applied pressures (ΔP) in an unstirred dead-end filtration experiment with BSA as solute.
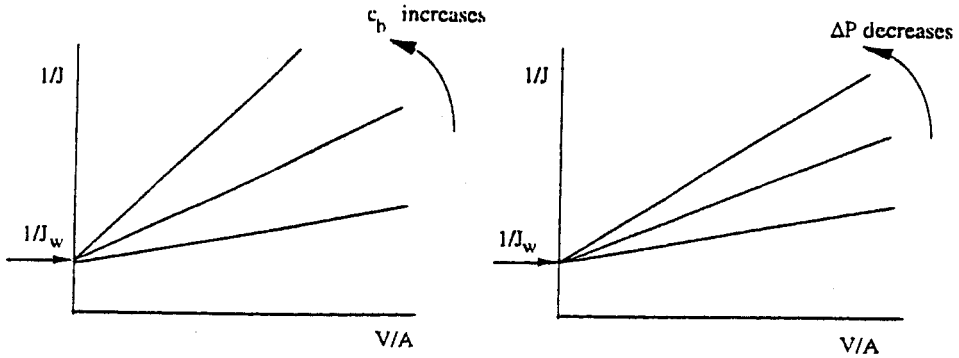
Figure VII - 25. Reciprocal flux as a function of the permeate volume for different concentrations (left figure) and applied pressures (right figure).

Frequently, the membrane resistance may be neglected and then by integration of eq. VII - 71 from t = 0 to t = t, eq. VII - 73 is obtained

$$t = \frac{\eta \; c_b \; r_c}{2 \; \Delta P \; c_c} \left(\frac{V}{A}\right)^2$$

(VII - 73)

Eq. VII - 73 is a typical relationship for unstirred dead-end filtration, showing that permeate volume $V \approx t^{0.5}$. Rewriting eq. VII - 73 in terms of the flux J shows that the flux declines with $t^{-0.5}$. This typical flux behaviour is represented in figure VII - 26.

$$J = \left(\frac{\Delta P \; c_c}{\eta \; c_b \; r_c}\right)^{0.5} t^{-0.5}$$

(VII - 74)

Eq. VII - 74 indicates that the flux decline is fully determined by the cake that has been formed onto the membrane surface and the membrane resistance can be neglected. Many sophisticated theories have been developed but since the mechanism of fouling is very complex in which many processes contribute, it is very unlikely that a single equation based on a certain theory can be applied. A simple empirical equation such as eq. VII - 75, is often very useful since it contains various contributions through the variable exponential factor
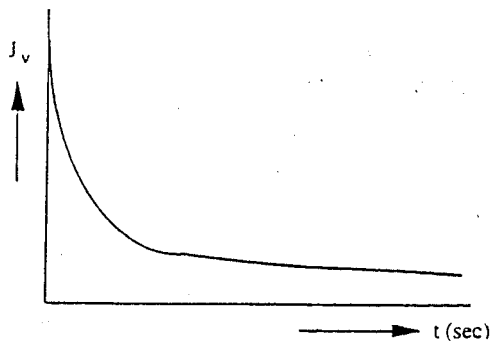
Figure VII - 26. Flux versus time according to eq. VII - 74.

$$J = J_0 t^n \qquad n < 0 \tag{VII - 75}$$

where J is the actual flux, J_0 the initial flux and the exponent n may be a function of the cross-flow velocity.

Fouling is typically associated with microfiltration and ultrafiltration due to the employment of porous membranes combined with the characteristics of the feed solution. In the case of e.g. reverse osmosis where low molecular solutes such as salts are retained the fouling tendency is low. But foulants such as organic and inorganic precipitates and suspended solids may be present as well. Since in these systems often hollow fiber and spiral wound configurations are applied fouling may occur in the feed channels since these configurations are very susceptible and measures have to be taken and this will be described in the next section.

VII.12.1   Fouling tests in reverse osmosis

A measure of the fouling tendency can be obtained by performing 'fouling tests', which can be carried out in an apparatus similar to that given in figure VII - 27. Through the use of such an apparatus the flux decline can be measured as a function of time under constant pressure, i.e. the cumulative volume will be measured as a function of time. All types of solution can be used for this test, e.g. tap water, seawater and also solutions of suspensions or emulsions. Many parameters have been advanced to describe fouling phenomena [28,29]:

- the silting index (SI)
- the plugging index (PI)
- the fouling index (FI) or the silt density index (SDI)
- the modified fouling index or the membrane filtration index (MFI).
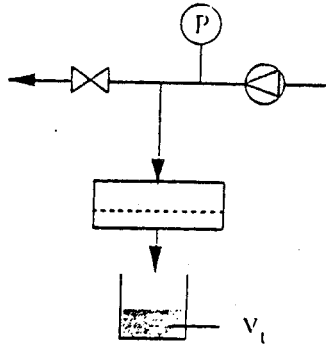
Figure VII - 27. Schematic drawing of a membrane filtration index (MFI) apparatus.

Of these parameters one, the membrane filtration index (MFI), will be described in more detail, not to give extensive information regarding the problem of fouling (such fouling phenomena are too complex to be described by a single parameter), but to illustrate the method [28]. The membrane filtration index (MFI) is based on cake filtration ('blocking filtration') as it occurs in colloidal fouling. The concept of cake filtration has been described in the previous section; the flux through the membrane can be described as the flux through two resistances in series, i.e. the cake resistance (R_c) and the membrane resistance (R_m) (see eqs. VII - 66 and VII - 71) and integration over a time t gives,

$$\frac{t}{V} = \frac{\eta \ R_m}{A \ \Delta P} + \frac{\eta \ r_c \ c_b}{2 \ A^2 \ c_c \ \Delta P} \ V$$

(VII - 76)

This equation is similar as eq. VII -73, only here the membrane resistance has been taken into account. A plot of t /V as a function of V should give a straight line after an initial linear section. The slope of this line is defined as the MFI (see figure VII - 28).
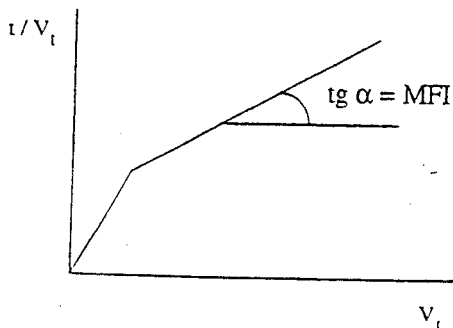
Figure VII - 28. Experimental results obtained with the apparatus depicted in figure VII - 27.

Hence

$$MFI = \frac{\eta \; r_c \; c_b}{2 \; A^2 \; c_c \; \Delta P} \qquad\qquad (VII - 72)$$

The higher the fouling potential of a given solution, the higher the MFI value will be. Figure VII - 29 gives an example of a series of MFI experiments.
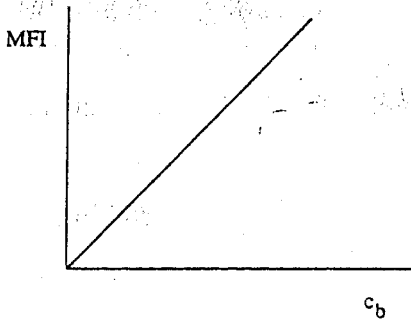
Figure VII - 29. MFI values as a function of the concentration of the fouling solute in the bulk solution [28].

The use of MFI values can have some advantages:
- by comparing various solutions, different fouling behaviour can be observed.
- a maximum allowable MFI value can be given for a specific plant.
- flux decline can be predicted to some extent.

However, there are also some drawbacks since the MFI values are only qualitative and should not be overstressed. Furthermore, MFI experiments are dead-end experiments whereas membrane filtration in practice is carried out in a cross-flow mode. Also it is assumed that the cake resistance is independent of the pressure, which is not the case in general. Finally, the MFI method is based on cake filtration whereas also other factors contribute to fouling. Nevertheless, these methods are useful as a first estimate.

VII.13.   Methods to reduce fouling

Because of the complexity of the phenomenon, the methods for reducing fouling can only be described very generally. Each separation problem requires its own specific treatment, although several approaches can be distinguished [24]:

- Pretreatment of the feed solution

Pretreatment methods employed include: heat treatment, pH adjustment, addition of complexing agents (EDTA etc.), chlorination, adsorption onto active carbon, chemical clarification, pre-microfiltration and pre-ultrafiltration. Fouling reduction starts in developing a proper pretreatment method. Often, considerable time and effort is spent on membrane cleaning whereas pretreatment is often overlooked. Sometimes very simple measures can be taken, e.g. pH adjustment is very important with proteins. In this case, fouling is minimised at the pH value corresponding to the isoelectric point of the protein, i.e. at the point at which the protein is electrically neutral. In pervaporation and gas separation, where fouling phenomena only play a minor role, pretreatment is important and often simple to accomplish. Thus, classical filtration or microfiltration methods can be used to prevent particles from entering the narrow fibers or channels on the feed side.

- Membrane properties

A change of membrane properties can reduce fouling. Thus fouling with porous membranes (microfiltration, ultrafiltration) is generally much more severe than with dense membranes (pervaporation, reverse osmosis).   Furthermore, a narrow pore size distribution can reduce fouling (although this effect should not be overestimated). The use of hydrophilic rather than hydrophobic membranes can also help reducing fouling. Generally proteins adsorb more strongly at hydrophobic surfaces and are less readily removed than at hydrophilic surfaces. (Negatively) charged membranes can also help, especially in the presence of (negatively) charged colloids in the feed. Another method is the pre-adsorption of the membrane by a component which can be easily removed.

- Module and process conditions

Fouling phenomena diminish as concentration polarisation decreases. Concentration polarisation can be reduced by increasing the mass transfer coefficient (high flow velocities) and using low(er) flux membranes. Also the use of various kinds of turbulence promoters will reduce fouling, although fluidised bed systems and rotary module systems seem not very feasible from an economical point of view for large scale applications but they may attractive for small scale applications.

- Cleaning

Although all the above methods reduce fouling to some extent cleaning methods will always be employed in practical. The frequency with which membranes need to be cleaned can be estimated from process optimisation. Three cleaning methods can be distinguished: i) hydraulic cleaning. ii) mechanical cleaning,   iii) chemical cleaning and iv) electric cleaning.

The choice of the cleaning method mainly depends on the module configuration, the type of membranes. the chemical resistance of the membrane and the type of foulant encountered.

i) hydraulic cleaning

Hydraulic cleaning methods include back-flushing (only applicable to microfiltration and

open ultrafiltration membranes), alternate pressurising and depressurising and by changing the flow direction at a given frequency . Figure VII - 30 gives a schematic representation of a filtration experiment with and without back-flushing.
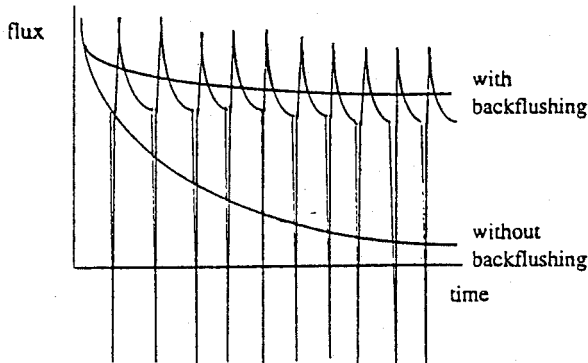
Figure VII - 30.   Schematic drawing of the flux versus time behaviour in a given microfiltration process with and without back-flushing

The principle of back-flushing is depicted in figure VII - 31. After a given period of time, the feed pressure is released and the direction of the permeate reversed from the permeate side to the feed side in order to remove the fouling layer within the membrane or at the membrane surface. Recently, a variant of this method has been developed, the 'back-shock' method [30]. Here, the time interval of back-flushing has been reduced to seconds which implies that the cake resistance remains low since it has no time to built up a layer. Consequntly, the membrane flux may remain quite high.

ii) mechanical cleaning

Mechanical cleaning can only be applied in tubular systems using oversized sponge balls.
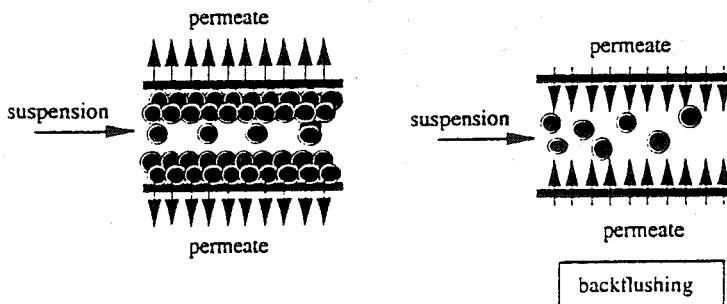
Figure VII - 31 .   The principle of back-flushing.

iii) chemical cleaning

Chemical cleaning is the most important method for reducing fouling, with a number of chemicals being used separately or in combination. The concentration of the chemical (e.g. active chlorine !) and the cleaning time are also very important relative to the chemical resistance of the membrane. Although a complete list of the chemicals used cannot be given, some important (classes of) chemicals are:

- acids (strong such as H_3PO_4 , or weak such as citric acid)
- alkali (NaOH)
- detergents (alkaline, non-ionic)
- enzymes (proteases, amylases, glucanases)
- complexing agents (EDTA, polyacrylates, sodium hexametaphosphate)
- disinfectants (H_2O_2 and NaOCl)
- steam and gas (ethylene oxide) sterilization

iv) electric cleaning

Electric cleaning is a very special method of cleaning. By applying an electric field across a membrane charged particles or molecules will migrate in the direction of the electric field. This method of removing particles or molecules from the interphase can be applied without interrupting the process and the electric field is applied at certain time intervals. A drawback of this method is the requirement to use electric conducting membranes and a special module arrangement with electrodes.

VII.14.   Compaction

Compaction is the mechanical deformation of a polymeric membrane matrix which occurs in pressure-driven membrane operations. During these processes, the porous structure densifies and as a result the flux will decline. After relaxation (effected by reducing the pressure) the flux will generally not return to its original value since the deformation process is often irreversible. Compaction will especially occur in reverse osmosis since the applied pressures are relatively high. However, in nanofiltration and ultrafiltration compaction may occur as well and the extent depends on the pressure employed and membrane morphology. In gas separation also high pressures are applied but the effect hardly occur due to the fact that pressure does not effect the structure in case of nonporous membranes. It may effect the porous sublayer and in this way increase the overall resistance.

VII.15.   Solved problems

1.   A 5% solution of sucrose (Mw = 342 g/l) is concentrated using a tubular nanofiltration membrane with an internal diameter of 6 mm. The membrane shows a complete rejection for sucrose. With a feed solution of 5 wt% , a temperature of 20°C and a pressure of 20 bar a flux is measured of 33.5 l/m^2.h at a cross-flow velocity of

0.5 m/s while at a velocity 4.5 m/s a flux is measured of 48.9 $l/m^2.h$.
Other data: $\rho = 10^3$ kg/m^3 ; $\eta = 1.1\ 10^{-3}$ Pa.s : a = 0.05 ; b = 1.1; $D_{sucr} = 4.2\ 10^{-10}$ m^2/s.

a. Calculate the concentration polarization modulus for both flow rates

b. Calculate the flux at 10 bars, assuming that the concentration polarization modulus remains the same.

c. Is this assumption of a constant concentration polarization modulus correct ?

2. An ultrafiltration membrane has a pure water flux of 210 $l/m^2.h$ at 3 bars. When an oil-water emulsion is concentrated at 4.5 bars the flux reduces to 35 due to a build-up of a cake ('emulsion') layer. The specific resistance of this cake is $r_c = 1.5\ 10^8$ m^{-2}. Calculate the thickness of the cake. The viscosity is similar to that of the water.

VII.16. Unsolved problems

1. Penicillin (mol.weight 334 Dalton) is prepared in a fermenter of 500 liter in volume. After fermentation the broth contains 3 weight % of penicillin and 5 weight% of suspended material. With diafiltration 99% of the penicillin must be removed. The ultrafiltration membranes do completely retain the suspended solids and have a rejection of 30% for the penicillin.

a. Do you in fact expect a rejection of penicillin ? Explain

The flux through the UF membrane can be described with the gel layer model

b. To what extent do flux and rejection changes when the concentration of suspended materials is 10% instead of 5% ?

In a particular experiment the mass transfer coefficient k can be represented by $k = 10^{-5}\ v^{0.75}$ (cm/s) and the gel concentration is $c_g = 200$ kg/m^3

c. How much time does it take to remove 99% of the penicillin with a membrane system with an area of 2 m^2 and a cross flow velocity of 1 m/s ? And much time with a velocity of 5 m/s ?

2. Microfiltration is frequently used in waste water treatment. The water contains suspended particles with a diameter of 1 μm. For a small scale application a capillary module is used with a length of 0.5 meter containing 400 fibers with an internal diameter of 1 mm. The waste liquid is fed through bore of the fibers with a velocity of 5 m/s.
Calculate the permeate flow rate of this module at an inlet pressure of 1.5 bar and calculate the pressure drop ? (For the flux calculation the gel layer model may be

applied with a ratio $c_m/c_b = 10$. Furthermore, the viscosity of the suspension is equal to the viscosity of water)

3. An unstirred dead-end Amicon ultrafiltration cell ($A = 38.5$ cm²) is used for the filtration of a solution of Bovine Serum Albumin (BSA) of 4 g/l at 1 bar and a 20°C. The membrane has a rejection of 100% for BSA. Assume that cake filtration occurs and that the specific cake resistance remains constant. A fixed permeate volume of 4 ml is collected each time and the results are given below

J_v (l/m².hr)	V (ml)
19.5	4
10.7	8
7.4	12
5.7	16

a. Estimate the pure water flux
b. Calculate r_{bl}/c_{bl}, the flux decline index
c. Indicate qualitatively the dependence of r_{bl}/c_{bl} on the applied pressure
    The boundary layer concentration can be determined when sedimentation data of BSA are known. The reciprocal of the sedimentation coefficient is given as a function of the BSA concentration.
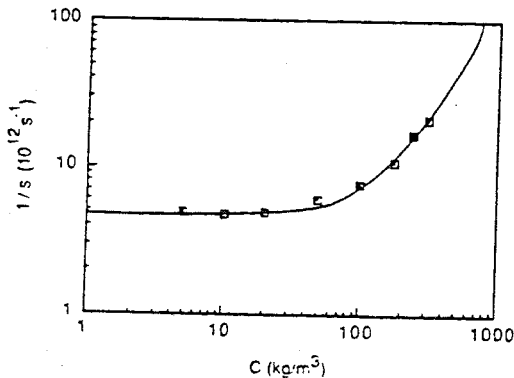
d. Calculate c_{bl}
    Other data: $\eta = 10^{-3}$ Pa.s; $v_1 = 0.75 \cdot 10^{-3}$ m³/kg; $v_o = 1.0 \cdot 10^{-3}$ m³/kg

4a. Determine the specific resistance of an adsorbed layer of Bovine Serum Albumin (BSA) and of a suspension, both with a cake porosity of 0.35 at 25°C.

The diffusion coefficient of BSA in water is $6.9 \cdot 10^{-11}$ m²/s and of the suspension in water $D = 10^{-13}$ m²/s, respectively. The viscosity is $\eta = 10^{-3}$ Pa.s

b. Determine the flux ratio through both cakes assuming that cake thickness and

pressure drop over the cake are equal.

5. Determine the gel concentration of Human Serum Albumin (HSA) from the following ultrafiltration results

conc. (wt%)	flux (l/m^2.hr)
2	196
3	165
4	146
5	125

6. The following data are obtained for an ultrafiltration experiment with an oil emulsion in a tubular module with an internal diameter of 17 mm and a length of 0.5 m at 25°C. The applied pressure is 6 bars and the cross flow velocity is 4 m/s. The viscosity of the emulsion $\eta = 1.5.10^{-3}$ Pa.s and the density is equal to the density of water (1 g/ml). The emulsion droplets have a diameter of 0.2 µm.

conc. (wt%)	flux (l/m^2.hr)
0.4	85
0.6	83
0.8	81
1.2	78

a. Calculate the mass transfer coefficient from the experimental data, assuming that the film model applies, and from the Sherwood correlations.

7. A microfiltration system contains modules with 200 capillaries with an internal diameter of 1.5 mm and a length of 0.5 m. These membranes are used to concentrate a cell suspension. The diameter of the cells is 5 µm and the flow rate is 2 m^3/h. Calculate the membrane surface area, the Reynolds number and the mass transfer coefficient.

8. Calculate the pressure drop and the Reynolds number in a tubular membrane (d = 10 mm), a capillary (d = 2 mm) and a hollow fiber (d = 100 µm) with a length of 1 m for pure water at a cross flow velocity of 0.5, 1.0 and 5.0 m/s, respectively.

9. Fouling can often be described by cake filtration

a. Give the general flux equation assuming that both resistances are in series.

With microfiltration often the following result is found, as shown schematically below.
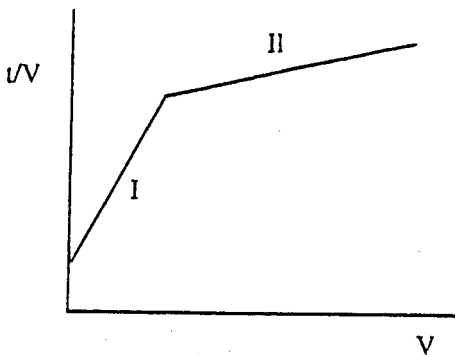
b. Describe briefly the characteristic parts I and II of the figure
c. Transform the above figure in a flux - time figure
d. What does it mean when part II lies horizontally ?

A membrane with a pure water flux of 1000 $l/m^2.h$ at 1 bar is used for yeast filtration.
e. Determine the membrane resistance (The viscosity of water is 10^{-3} Pa.s).

The membrane resistance can be obta'ned graphically. From what part of the curve you would do this, I or II and why ?
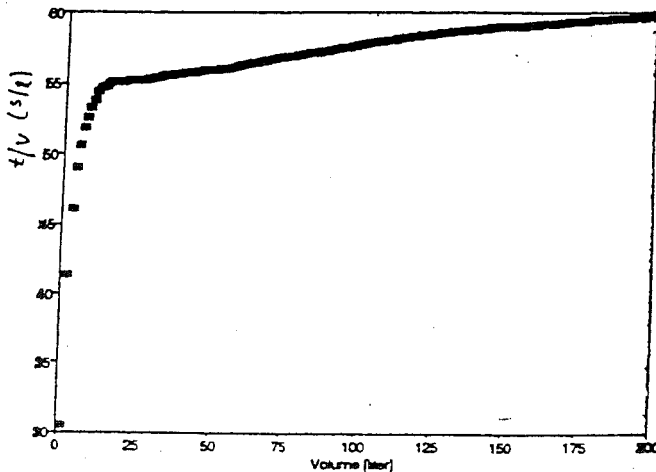
The filtration of yeast gives the following result as shown in the figure above.

f. Determine the membrane resistance and compare your answer with e.
    Take: $\eta = 2.5 \cdot 10^{-3}$ Pa.s; $\Delta P = 1$ bar; $A = 0.4$ m^2

10. A polyimide membrane is used in an ultrafiltration experiment with a solution of 5 g/l of polystyrene (mol.weight 100.000) in ethyl acetate. The experiment is performed in a dead-end cell with a diameter of 10 cm and a stirrer speed is applied of 180 rpm. A flux is observed of 16 kg/m².h. Calculate the concentration of polystyrene at the membrane wall.
Other data: $\eta_{ethyl\ acetate} = 0.455$ cp and $\rho_{ethyl\ acetate} = 0.9$ g/ml, while the hydrodynamic radius of polystyrene in ethyl acetate is 6.8 nm.

11. Calculate the pressure drop in a sheet-flow ED stack and in a tortuous path stacks with and without spacer. The stack contains 100 cell pairs. The simension of one compartment is, length of 1 m, a width of 0.5 m and a height of 1 mm. The tortuous path is divided in 5 sections. The average velocity is 10 cm/s for the sheet-flow stack and 25 cm/s for the tortuous path stack. Density and viscosity are equal to that of water. Other data are:
$D = 1.5\ 10^{-9}$ m²/s and $\Delta l/h = 10$

12. A desalination experiment with brackish water (1000 ppm NaCl) with cellulose acetate hollow fibers gives a flux of 2000 l.m².day. The intrinsic rejection is 94 % and the mass transfer coefficient is k = 5.4 10⁻⁶ m/s.
Calculate the polarization modulus and the permeate concentration.

13. Sirkar et al. (J.Membr. Sci., 43 (1989) 259) have developed a hollow fiber liquid membrane permeator in which between a bundle of hydrophobic porous hollow fibers the aqueous phase with carrier is present. This concept can be applied e.g. to remove sulfur dioxide from air. The feed flows through the lumen of one fiber (F) and the sweeping gas (S) flows counter-currently through the next fiber.
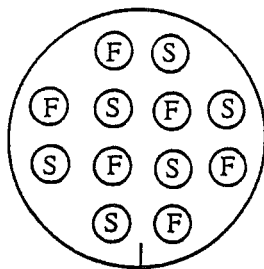
liquid phase carrier

a. Draw the concentration profile of sulfur dioxide
b. Give the general flux equation for sulfur dioxide (use the overall mass transfer coefficient)
c. Give an expression for the overall mass transfer coefficient.

14. An albumin solution with a concentration of 2.5% is concentrated in an Amicon cell with a diameter of 10 cm and a stirrer speed of 3500 rpm. The diffusion coefficient is $D = 6.10^{-11}$ m^2/s and viscosity and density are equal to that of water. Calculate the mass transfer coefficient and the flux at 5 bar under 'limiting flux conditions'. (The gel concentration $c_g = 45\%$)

15. The volume of a fermentation broth must be reduced from 1100 liters to 100 liters. This is achieved by microfiltration. A module is used with a length of 0.5 m which contains 320 fibers with a diameter of 2 mm and a membrane thickness of 0.5 mm and with the feed at the outside ('outside-in'). The flux can be described by

    $$J_t = J_o . t^{-0.5}$$

    with $J_o = 100$ l/m^2.h. How long will this process last ?

16. A 'back-shock' method is employed on the process described in problem 14. Now every 10 seconds 1/10 of the pore volume is 'backflushed' and the flux remains constant (i.e. 100 l/m^2.h). If the overall porosity of the membranes is 50%, how long does the volume reduction last. (The back-shock time may be neglected).

17. A RO membrane gives a flux of 2000 l/m^2.day and an intrinsic rejection of $R_{int} = 94$ % with a solution of 0.1 % NaCl. The mass transfer coefficient is $k = 5.4 \ 10^{-5}$ m/s. Calculate the polarization modulus and the observed rejection.

18 An ultrafiltration membrane shows a pure water flux of 100 l/m^2.h at 2 bars. This membrane is used to concentrate a polymer solution. After a certain period a constant flux is obtained of 10 l/m^2.h at 5 bars. The permeability of the formed gellayer containing particles with a size of 5 nm and a porosity of 50% can be described by Kozeny-Carmann.
a. Can I neglect the membrane resistance ?
b. Calculate the gellayer thickness.
   Now the pressure is increased to 6 bars
c. Calculate the flux and gellayer thickness.

19. A membrane distillation experiment is carried out with tap water as feed and a polypropylene membrane with a thickness of 300 μm and a porosity of 75%. The feed temperature is 70 °C and the permeate temperature is 20 °C. The waterflux is 12 l/m^2.h. The heat conductivity in polypropylene is 0.2 W/m.K and in air (pore !) is 0.02 W/m.K. The heat transfer coefficients at feed side and permeate side are assumed to be equal and independent on temperature, $\alpha = 5000$ W/m^2.K. The heat of vapourization is 40.7 kJ/mol.
    Calculate the temperature polarisation (assume heat of vapourization ≈ heat of

condensation).

20. Calculate the pressure drop in a capillary (d = 1 mm and L = 1 m) at a velocity of 1 m/s at 25 °C and at 45 °C. (η_{25} = 10^{-3} Pa.s and η_{45} = $0.65.10^{-3}$ Pa.s).

21. A solution of 0.1 % PEG is concentrated in a dead-end cell (diameter = 10 cm and ω = 300 rpm) and in a cross-flow capillary module (diameter of fiber = 5 mm, L = 1 m and v = 1 m/s) at room temperature. The viscosity and density of the PEG solution is equal to that of water while the diffusion coefficient of PEG in water at 25°C is 5.7 10^{-7} cm²/s. Calculate the mass transfer coefficient in both devices.

22. The following results are obtained in an ultrafiltration experiment with a polyethylene glycol solution in a dead-end cell.

flux, J (l/m².h)	40.1	37.2	31.8	28.7
bulk conc., c_b (weight%)	1.16	1.34	1.71	2.05
observed retention, R_{obs}	83.6	85.8	86.5	87.3
membrane conc., c_m (wt %)	13.6	13.8	14.1	14.3

a. Determine the mass transfer coefficient grafically
b. Calculate the intrinsic retention for these four samples
c. Calculate the flux from the osmotic pressure model and compare with the observed flux (ΔP = 5.2 bar; L_p = 28.7 l/m².h.bar). The osmotic pressure of the PEG solution is given by the following equation π = 0.0244.c + 0.0161.c² + 0.000193.c³, with the concentration c in weight %.

VII.17. Literature

1. Gekas, V., and Hallström, B., *J. Membr. Sci.*, **30** (1987) 153
2. Schock, G., and Miguel, A., *Desalination*, **64** (1987) 339
3. Costa da, M.J., Fane, A.G., Fell, C.J.D., and Franken, A.C.M., *J. Membr. Sci.*, **62** (1991) 275.
4. Sonin, A.A., and Isaacson, M.S., *Ind. Eng. Process Des. Develop.*, **13** (1974) 241.
5. Probstein, R.F., Sonin, A.A., Gur-Arie, E., *Desalination*, **11** (1972) 165
6. Beek, W.J., and Mutzall, K.M.K., *Mass transport phenomena*, John Wiley, New York, 1977.
7. Bixler, H.J., Nelsen, L.M., and Bluemle Jr., L.W., *Trans. Amer. Soc. Artif.Int. Organs*, **14** (1968) 99.
8. Blatt, W.F., Dravid, A., Michaels, A.S., and Nelsen, L.M., in: *'Membrane Science and Technology'*, Flinn, J.E. (ed.), Plenum Press, New York, 1970.
9. Porter, M.C., *Ind. Eng. Chem. Prod. Res. Dev.*, **11** (1972) 234
10. Nakao, S-I., Nomura, T., and Kimura, S., *AIChE J.*, **25** (1979) 615
11. Dejmek, P., PhD Thesis, Lund Institute of Technology, Sweden, 1975.

12. Kozinsky, A.A., and Lightfoot, E.N., *AIChE J.*, **17** (1971) 81

13. Goldsmith, R.L., *Ind. Eng. Chem. Fundam.*, **10** (1971) 113

14. Vilker, V.L., Colton. C.K., and Smith, K.A., *AIChE Journal*, **27** (1981) 637

15. Jonsson. G., *Desalination*, **51** (1984) 61

16. Wijmans, J.G., Nakao, S-I, and Smolders, C.A., *J. Membr. Sci.*, **20** (1984) 115

17. Wijmans, J.G., Nakao. S-I, van den Berg, J.W.A., Troelstra, F.R., and Smolders, C.A., *J. Membr. Sci.*, **22** (1985) 117

18. Nakao, S-I, Wijmans, J.G., and Smolders, C.A., *J. Membr. Sci.*, **26** (1986) 165

19. van den Berg, G.B.. and Smolders, C.A., *J. Membr. Sci.*, **40** (1989) 149

20. Darcy, H., *Les fontaines publique de la ville Dijon*, 1856.

21. Mijnlieff, P.F., and Jaspers, W.J.M., *Trans. Faraday Soc.*, **67** (1971) 1837

22. Svedberg, T., and Pedersen, K.O., *The Ultracentrifuge*, Clarendon Press, Oxford, 1940

23. Bellucci, F., *J. Membr. Sci.*, **9** (1981) 285

24. Fane, A.G., and Fell. C.J.D., *Desalination*, **62** (1987) 117

25. Matthiasson, E. and Sivik, B., *Desalination*, **35** (1980) 59

26. Belfort, G., Davis, R.H.. Zydney, A., *J. Membr. Sci.*, **96** (1994) 1

27. Marshall, A.D.. Munro. P.A., and Traghard, G., *Desalination*, **91** (1993) 65

28. Schippers, J.C. and Verdouw. J., *Desalination*, **32** (1980) 137

29. Mulder, M.H.V., Polarization phenomena and membrane fouling, in 'Membrane Separation Technology. Principles and Applications', Eds. Noble, R.D., and Stern, S.A., Elsevier. Amsterdam, 1993, Ch. 2.

30. Jonsson, NAMS 1994, Breckenridge

27. Gekas, V, and Hallström, B., J. Membr. Sci., **30** (1987) 153

VIII

MODULE AND PROCESS DESIGN

VIII.1.   Introduction

In order to apply membranes on a technical scale, large membrane areas are normally required. The smallest unit into which the membrane area is packed is called a module. The module is the central part of a membrane installation. The simplest design is one in which a single module is used. Figure VIII - 1 gives a schematic drawing of such a single module design.
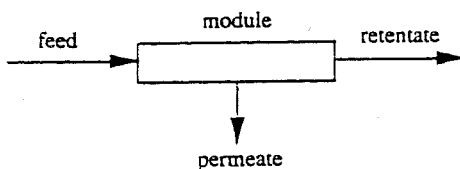
Figure   VIII - 1.   Schematic drawing of a module.

A feed inlet stream enters the module at a certain composition and a certain flow rate. Because the membrane has the ability to transport one component more readily than another, both the feed composition and the flow rate inside the module will change as a function of distance. By passage through, the feed inlet stream is separated into two streams, i.e. a permeate stream and a retentate stream. The permeate stream is the fraction of the feed stream which passes through the membrane whereas the retentate stream is the fraction retained.

A number of module designs are possible and all are based on two types of membrane configuration: i) flat; and ii) tubular. Plate-and-frame and spiral-wound modules involve flat membranes whereas tubular, capillary and hollow fiber modules are based on tubular membrane configurations. The difference between the latter types of module arises mainly from the dimensions of the tubes employed, as is shown in table VIII.1.

Table   VIII.1   Approximate dimensions
of tubular membranes

configuration	diameter (mm)
tubular	> 10.0
capillary	0.5 - 10.0
hollow fiber	< 0.5

If tubular/hollow fiber membranes are packed close together in a parallel fashion than the membrane area per volume is only a function of the dimensions of the tube. Table VIII.2 shows the membrane surface area per volume as a function of the radius of a tube, and clearly demonstrates the difference in membrane area per volume for tubular systems (r ≈ 5 mm) and hollow fiber systems (r ≈ 50 μm = 0.05 mm).

Table VIII.2   Surface area per volume for some tube radii

tube radius (mm)	surface area per volume (m^2/m^3)
5	360
0.5	3600
0.05	36,000

In general however, a system does not consist of just one single module but of a number of modules arranged together as a system. In fact. each technical application has its own system design based on the specific requirements. Two basic system designs will be described here, the single-pass system and the recirculation system.

The choice of module configuration, as well as the arrangement of the modules in a system, is based solely on economic considerations with the correct engineering parameters being employed to achieve this. Some aspects to be considered are the type of separation problem, ease of cleaning, ease of maintenance, ease of operation, compactness of the system, scale and the possibility of membrane replacement. This chapter describes the basic principles of module and process design, where only the most general types of module configuration and flow characteristics will be discussed.

VIII.2.   Plate-and-frame module

A schematic drawing of a plate-and-frame module is given in figure VIII - 2. This design provides a configuration which is closest to the flat membranes used in the laboratory. Sets of two membranes are placed in a sandwich-like fashion with their feed sides facing each other. In each feed and permeate compartment thus obtained a suitable spacer is placed. The number of sets needed for a given membrane area furnished with sealing rings and two end plates then builds up to a plate-and-framestack. The packing density (membrane surface per module volume) of such modules is about 100-400 m^2/m^3. Figure VII - 3 shows a schematic flow path in a plate-and-frame module. In order to reduce channelling, i.e. the tendency to flow along a fixed pathway and to establish an uniform flow distribution so-called 'stop discs' have been introduced.
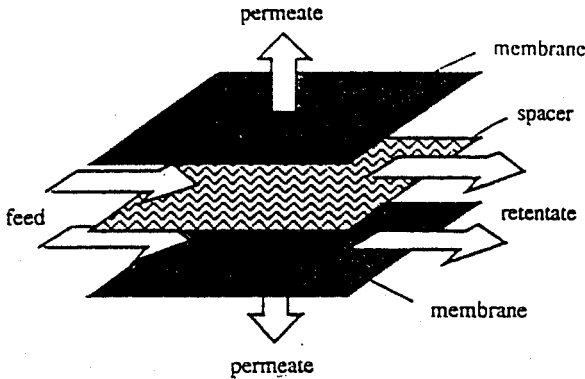
Figure VIII - 2. Schematic drawing of a plate-and-frame module.
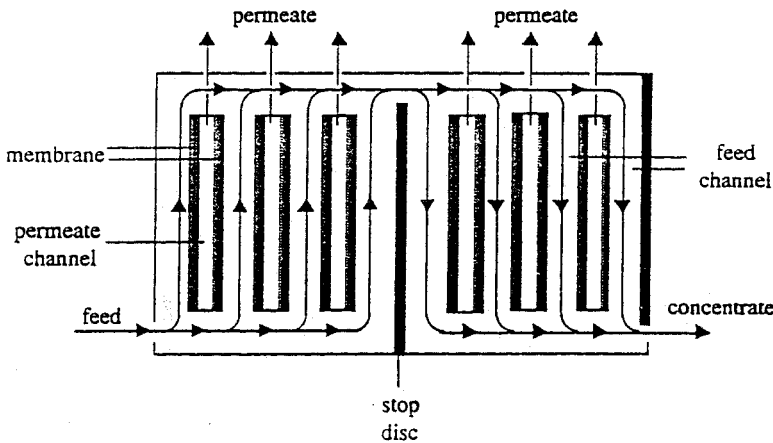
Figure VIII - 3. Schematic flow path in plate-and-frame-module

In electrodialysis special stack designs are applied mainly based on two concepts: tortuous path and sheet flow. In the latter design a spacer material is used to improve mass transfer and to reduce concentration polarization. Also the former design, the tortuous path has been developed for the same reason, reduction of concentration polarization by applying a proper spacer material [1]. By applying a high cross flow velocity the residence time of the feed in a feed channel would be quite low. A gasket is used now to transform the flat plate into a long tortuous narrow channel, as is shown schematically in figure VIII - 4.

feed
in

feed
out
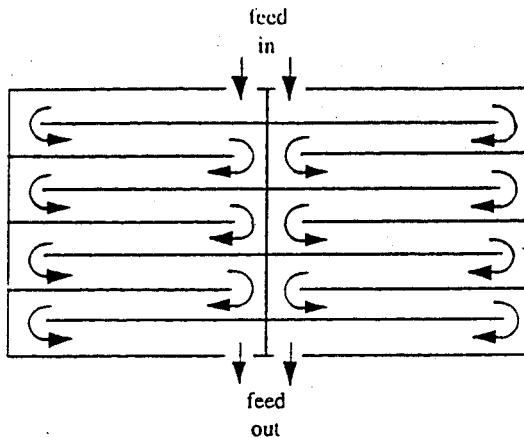
Figure VIII - 4.   Tortuous-path plate [1].

VIII.3.   Spiral-wound module

The spiral-wound module is the next logical step from a flat membrane. It is in fact a plate-and-frame system wrapped around a central collection pipe, in a similar fashion to a sandwich roll. Membrane and permeate-side spacer material are then glued along three edges to build a membrane envelope. The feed-side spacer separating the top layer of the two flat membranes also acts as a turbulence promoter. This module is shown schematically in figure VIII - 5.
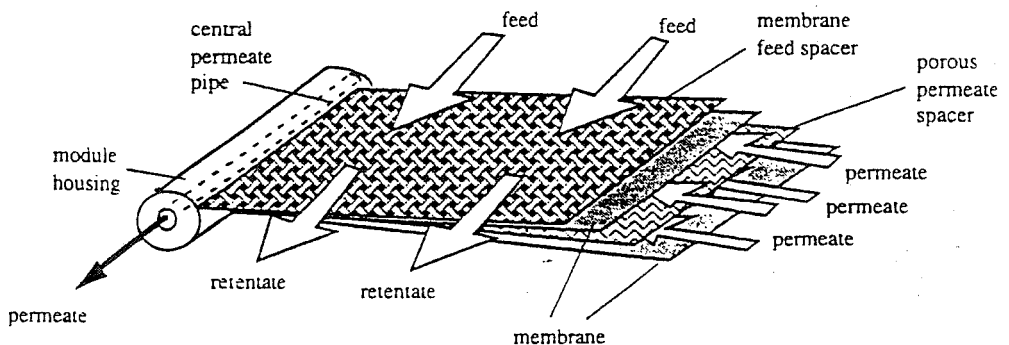
Figure VIII - 5.   Schematic drawing of a spiral-wound module.

The feed flows axial through the cylindrical module parallel along the central pipe

whereas the permeate flows radially toward the central pipe. The packing density of this module (300 - 1000 m²/m³) is greater than of the plate-and-frame module but depends very much on the channel height, which in turn is determined by the permeate and feed-side spacer material. A cross-section of the feed channel with spacer is shown in figure VIII - 6. As has been discussed in chapter VII, the presence of such a spacer has a large influence on the mass transfer and the pressure drop.

permeate channel
membrane
feed spacer
membrane
permeate channel
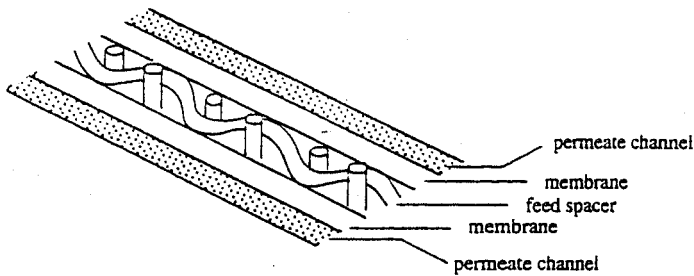
Figure VIII - 6.   Cross-section of a spiral wound 'envelope'

Usually, a number of spiral-wound modules are assembled in one pressure vessel (see figure VIII - 7) and are connected in series via the central permeate tubes.

central permeate pipe

feed

permeate

retentate
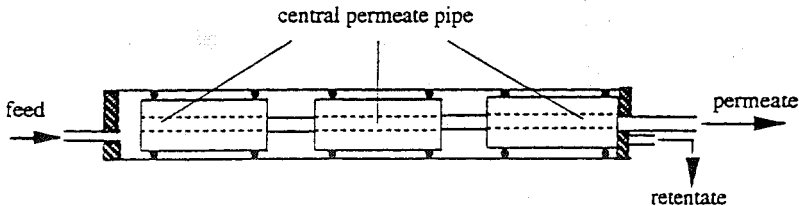
Figure VIII - 7.   Schematic drawing of a pressure vessel containing three spiral-wound modules arranged in series.

VIII.4.   Tubular module

In contrast to capillaries and hollow fibers, tubular membranes are not self-supporting. Such membranes are placed inside a porous stainless steel, ceramic or plastic tube with the diameter of the tube being, in general, more than 10 mm. The number of tubes put together in the module may vary
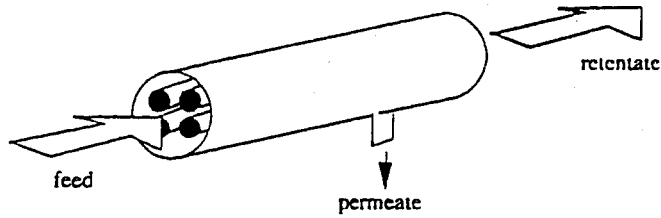
Figure VIII - 8.   Schematic drawing of tubular module.

from 4 to 18, but is not limited to this number. A schematic diagram is given in figure VIII - 8. The feed solution always flows through the centre of the tubes while the permeate flows through the porous supporting tube into the module housing. Ceramic membranes are mostly assembled in such tubular module configurations. However, the packing density of the tubular module is rather low, being less than 300 m^2/m^3. The monolithic module is a special type of ceramic module. Here a number of tubes have been introduced in a porous ceramic 'block', e.g. an α-Al$_2$O$_3$. The inner surfaces of these tubes are then covered by a thin toplayer of γ-alumina (γ-Al$_2$O$_3$), or zirconia (ZrO$_2$), for instance by a sol-gel process (see figure VI - 8). A schematic drawing of a cross-section of such a monolithic module is shown in figure VIII - 9.
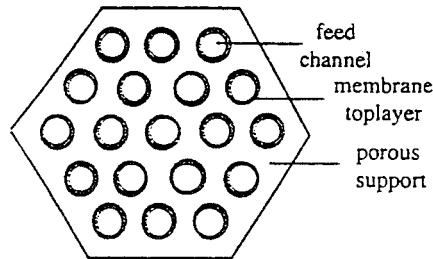
Figure VIII - 9.   Cross section of a monolithic ceramic module

VIII . 5   Capillary module

The capillary module consists of a large number of capillaries assembled together in a module, as shown schematically in figure VIII - 11. The free ends of the fibers are potted with agents such as epoxy resins, polyurethanes, or silicone rubber.

The membranes (capillaries) are self-supporting. Two types of module arrangement can be distinguished: *i)* where the feed solution passes through the bore of the capillary
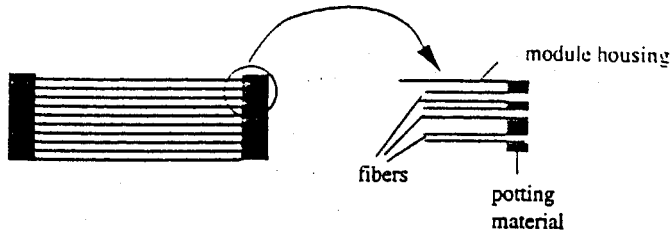
Figure   VIII - 10. Capillary module.

(lumen) whereas the permeate is collected on the outside of the capillaries (figure VIII - 11a, "inside-out"); and *ii)* where the feed solution enters the module on the shell side of the capillaries (external) and the permeate passes into the fiber bore (figure VIII - 11b, "outside-in"). The choice between the two concepts is mainly based on the application where parameters such as pressure, pressure drop, type of membrane available, etc. are important. Depending on the concept chosen, asymmetric capillaries are used with their skin on the inside or on the outside.
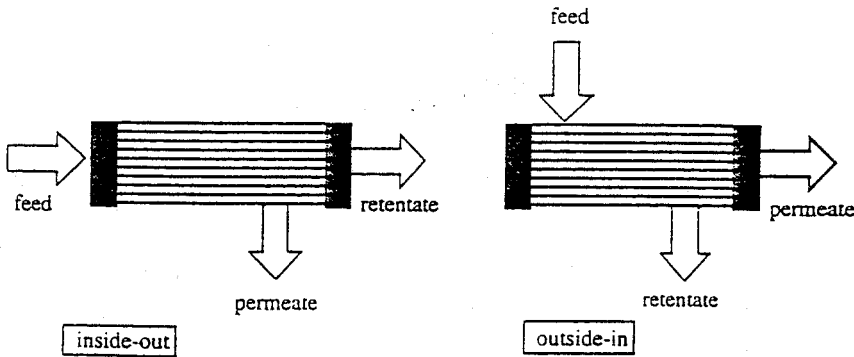
Figure VIII - 11.   Schematic drawing of a capillary module/hollow fiber module.(left) 'inside-out' or
'tube-side feed; 'outside-in' or 'shell-side feed' (right)

When porous ultra- or microfiltration membranes are employed, the capillaries mostly have a gradient in pore size across the membrane. In this case the location of the smallest pores (inside or outside) determines which of the two configurations is used. A packing density of about 600 - 1200 m^2/m^3 is obtained with modules containing capillaries, in between those existing in tubular and hollow fiber modules.

VIII.6.   Hollow fiber module

The difference between the capillary module and the hollow fiber module is simply a matter of dimensions since the module concepts are the same. Again with hollow fiber modules, the feed solution can enter inside the fiber ("inside-out") or on the outside ("outside-in") (see figure VIII - 10). In reverse osmsosis, the feed mainly flows either radially or parallel along the fiber bundle, whereas the permeate flows through the bore side of each fiber. The hollow fiber module is the configuration with the highest packing density, which can attain values of 30,000 m^2/m^3. An example of a special module of the 'outside-in' variety is shown in fig. VIII - 11. A perforated central pipe is located in the center of the module through which the feed solution enters. In this concept the fibers are arranged in a loop and are potted on one side, the permeate side. One of the disadvantages of the 'outside-in' type is that channelling may occur. This means that the feed has a tendency to flow along a fixed path thus reducing the effective membrane surface area. With a central pipe, the feed solution is more uniformly distributed throughout the module so that the whole surface area is more effectively used.

The hollow fiber module is used when the feed stream is relatively clean, as in gas separation and pervaporation. Hollow fiber modules have also been used in the case of seawater desalination, another relatively clean feed stream, but here a very effective pre-treatment is required. The module construction given in figure VIII - 12 (left figure) is that of a typical reverse osmosis module. In gas separation the module will be of the 'outside-in' type to avoid high pressure losses inside the fiber and to attain a high membrane area (see figure VIII - 12, right figure).
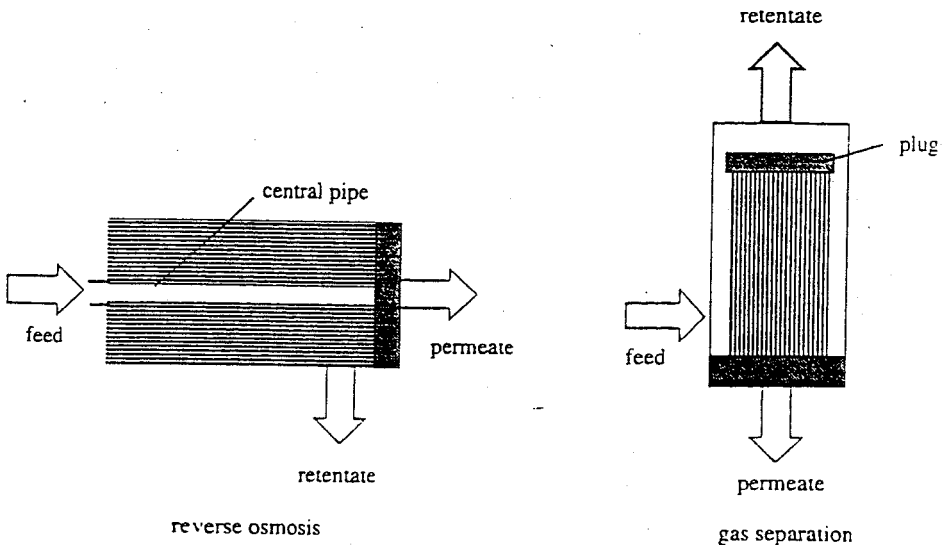
Figure VIII - 12. Special hollow fiber construction for reverse osmosis (left) and gas separation (right).

In pervaporation it is more advantageous to use the 'inside-out' type to avoid increase in permeate pressure within the fibers, but the 'outside-in' concept can be used as well with short fibers. Another advantage of the inside-out concept is that the very thin selective top layer is better protected, whereas a higher membrane area can be achieved with the outside-in concept.

New module concepts have been developed mainly to reduce fouling and concentration polarization as much as possible. One way to achieve this is by changing the flow geometry, e.g. transversal instead of tangential. This transversal flow module using hollow fibers or capillary membranes with the top layer outside [2 - 5] is such an example. In this type of module the feed is flowing perpendicular to the fibers, as indicated schematically in figure VIII - 13, and this results in an enhancement of the mass-transfer in the boundary layer. In this concept the fibers act in fact as turbulence promoters. The fibers can be arranged in different ways as shown in this figure. This type of module design is not only of interest for the pressure driven processes such as microfiltration, ultrafiltration and reverse osmosis, but also for pervaporation, liquid membranes and membrane contactors where the boundary layer resistance may become very important as well.
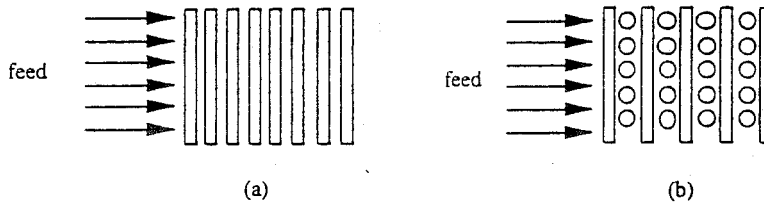
Figure VIII - 13. Schematic drawing of a transversal flow module with fibers arranged parallel-in-line (a) and crossed-in-line (b).

VIII.7.   Comparison of module configurations

The choice of the module is mainly determined by economic considerations. This does not mean that the cheapest configuration is always the best choice because the type of application is also very important. In fact, the functionality of a module is determined by the type of application. The characteristics of all the modules described above can be compared qualitatively (see table VIII.3).

Although the costs of the various modules may vary appreciably, each of them has its field of application. Despite being the most expensive configuration, the tubular module is well suited for applications with 'a high fouling tendency' because of its good process control and ease of membrane cleaning. In contrast, hollow fiber modules are very susceptible to fouling and are difficult to clean. Pretreatment of the feed stream is most important in hollow fiber systems.

Often it is possible to choose between two or more different types which are

competitive with each other, for example hollow fiber and spiral-wound modules in seawater desalination, gas separation and pervaporation. In dairy applications mainly tubular or plate-and-frame modules are used.

Table   VIII.3   Qualitative comparison of various membrane configurations

	tubular	plate-and-frame	spiral-wound	capillary	hollow fiber
packing density	low	- -> very high			
investment	high	- -> low			
fouling tendency	low	- -> very high			
cleaning	good	- > poor			
membrane replacement	yes/no	yes	no	no	no

The cost of sophisticated pretreatment procedures can contribute to the total costs (capital and operating costs) to a substantial extent.

VIII.8.   System design

The design of membrane filtration systems can differ significantly because of the large number of applications and module configurations. The module is the central part of a membrane installation and is often referred to as the separation unit. A number of modules (separation units) connected together in series or parallel is called a stage. The task of an engineer is to arrange the modules in such a way that an optimal design is obtained at the lowest product cost.
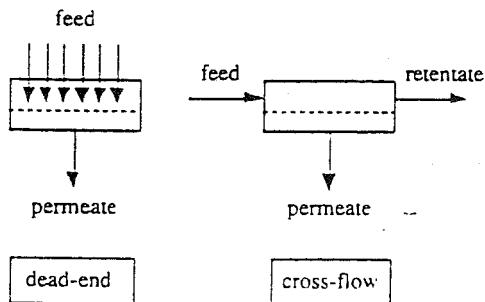
Figure VIII - 14.   Schematic drawing of two basic module operations: (a) dead-end and (b) cross-flow

The simplest design is the dead-end operation (figure VIII - 14a). Here all the feed is forced through the membrane, which implies that the concentration of rejected components in the feed increases and consequently the quality of the permeate decreases with time. This concept is still used very frequently in microfiltration.
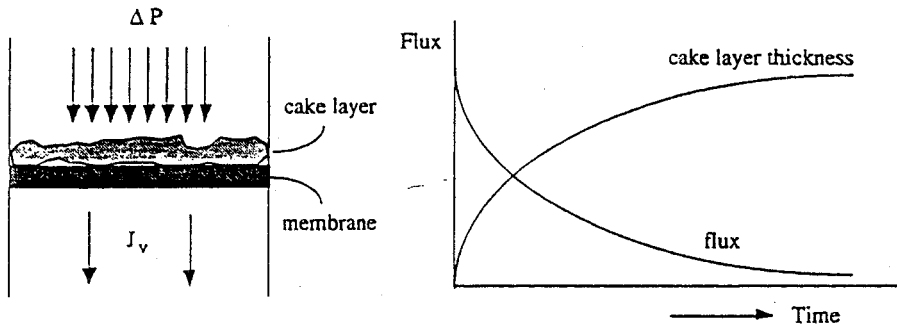
Figure VIII - 15. Flux decline in dead-end filtration.

For industrial applications, a cross-flow operation is preferred because of the lower fouling tendency relative to the dead-end mode (figure VIII - 14b). In the cross-flow operation, the feed flows parallel to the membrane surface with the inlet feed stream entering the membrane module at a certain composition. The feed composition inside the module changes as a function of distance in the module, while the feed stream is separated into two: a permeate stream and a retentate stream. The consequences of fouling in dead-end systems are shown schematically in figure VIII - 15. In dead-end filtration, the cake grows with time and consequently the flux decreases with time. Flux decline is relatively smaller with cross-flow and can be controlled and adjusted by proper module choice and cross-flow velocities.

VIII.9.   Cross-flow operations

To reduce concentration polarisation and fouling as far as possible, the membrane process is generally operated in a cross-flow mode. The proper choice of the module is the next crucial step. For a given module design and feed solution, the cross-flow velocity is the main parameter that determines mass transfer in the module. Various cross-flow operations can be distinguished and we shall consider the following cases here:
- co-current
- counter-current
- cross-flow with perfect permeate mixing
- perfect mixing
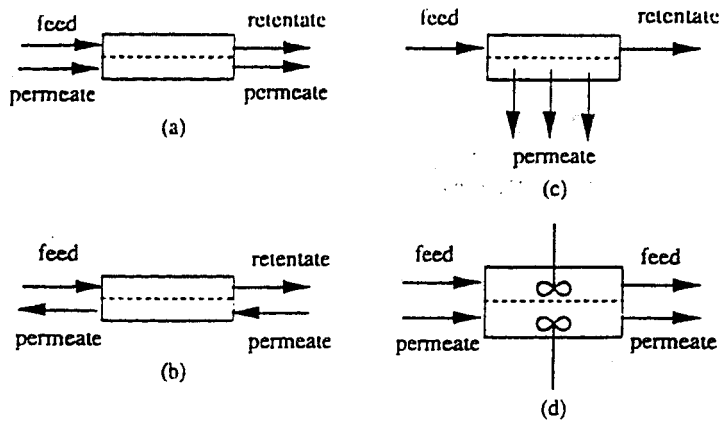
Figure VIII - 16 Schematic drawing of some cross-flow operations: (a) co-current; (b) counter-current; (c) cross-flow; (d) perfect mixing.

Schematic drawings of these various operations are given in figure VIII - 16. In co- and counter-current operations, the feed and permeate stream flow co-currently (parallel plug flow) or counter-currently along the membrane. Plug flow conditions can be defined by the so-called Péclet number (Pé), which is a measure of the ratio of mass transport by convection and by diffusion. Pé = v L/D, where v is the velocity, L is the length of the channel or pipe and D is the diffusion coefficient. If convection is dominant over diffusion then the Péclet number is much greater than unity, Pé >> 1. In the cross-flow mode with perfect permeate mixing, it is assumed that plug flow occurs on the feed side whereas mixing occurs so rapidly on the permeate side that the composition remains the same.
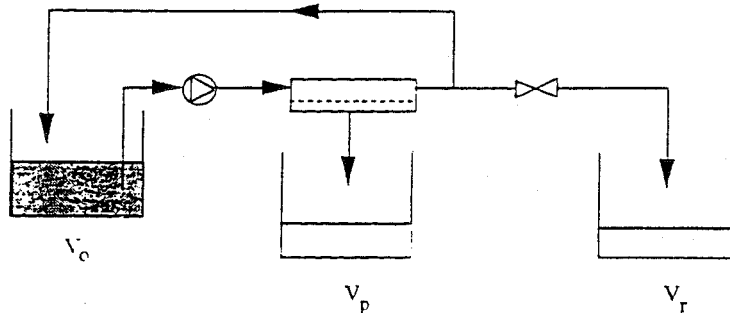
Figure VIII - 17. Schematic diagram of a batch system.

As far as the cross-flow operations are concerned, counter-current flow gives the best results followed by cross-flow and co-current flow, respectively as can be demonstrated by process

calculations. The worst results are obtained in the perfect mixing case. In practice, systems generally operate in the cross-flow mode with perfect permeate mixing. The flow scheme in the module is one of the principal variables determining the extent of separation achieved. In principle, two basic methods can be used in a single-stage or a multi-stage process: i) the 'single-pass system' and ii) the 'recirculation system'. A batch system can also be used for small-scale applications. A schematic diagram of a batch system is given in figure VIII - 17, while a schematic representation of the single-pass and recirculation systems are given in figure VIII - 18.
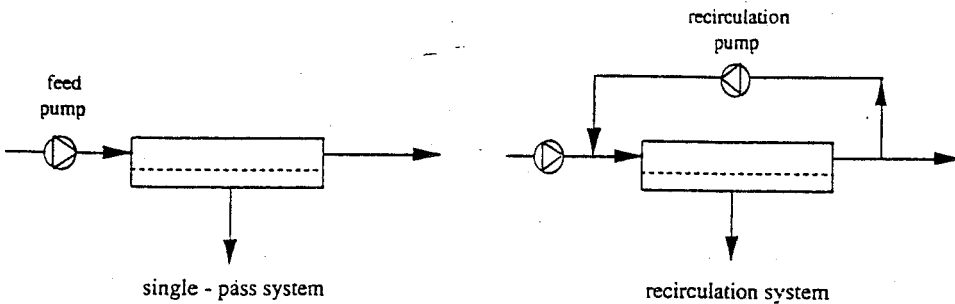
Figure VIII - 18.   Schematic representation of the single-pass and recirculation systems.

In the single-pass system the feed solution passes only once through the single or various modules, i.e. there is no recirculation. Hence the volume of the feed decreases with path length. In a multi-stage single-pass design, this loss of volume is compensated by arranging the modules in a 'tapered design' ('christmas tree design'). This is shown in figure VIII - 19. In this arrangement the cross-flow velocity through the system remains virtually constant. A characteristic of this system is that the total path length and the pressure drop are large. The volume reduction factor, i.e. the ratio between the initial feed volume and the volume of the retentate, is determined mainly by the configuration of the 'christmas tree' and not by the applied pressure.
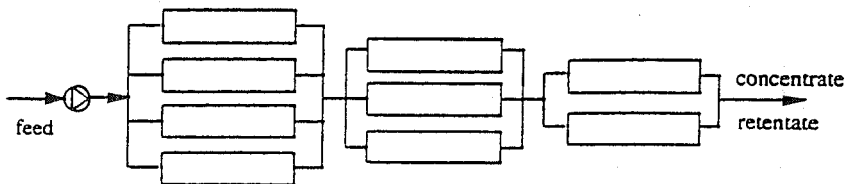
Figure VIII - 19.   Single-pass system (tapered cascade or 'christmas tree').
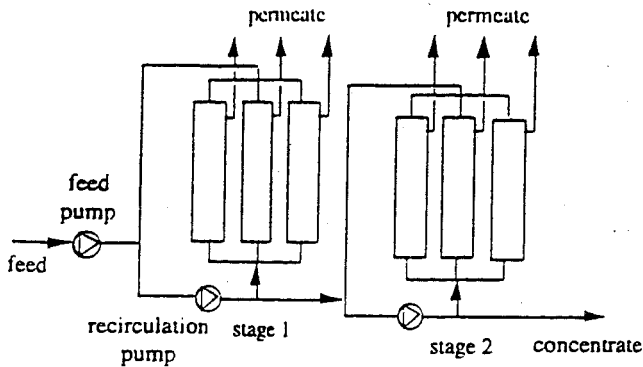
Figure VIII - 20.   Two-stage recirculation system.

The second system is the recirculation system or 'feed recycle system' (see figure VIII - 20). Here the feed is pressurised by a pump and allowed to pass several times through one stage, consisting of several modules. Each stage is fitted with a recirculation pump which maximises the hydrodynamic conditions, whereas the pressure drop over each single stage is low. The flow velocity and pressure can be adjusted in every stage. The feed recycle system is much more flexible than the single-pass system and is to be preferred in cases where severe fouling and concentration polarisation occur as in microfiltration and ultrafiltration. On the other hand, with relatively simple applications such as the desalination of seawater the single-pass system can be applied on economical grounds.

VIII.10.   Hybrid dead-end/cross flow system

The advantage of dead-end systems is the high recovery, the feed is completely passing the membrane. However. in the previous chapter it was shown that in case of microfiltration and ultrafiltration a tremendous flux decline is obtained. On the other hand, cross-flow systems allow a much better fouling control but the recovery is much lower. A hybrid dead-end/cross flow process may combine the advantages of both processes and this concept is very beneficial in microfiltration and ultrafiltration where back-flushing is possible and essential [6]. A schematic drawing of such a system is shown in figure VIII - 21. The feed is flowing to the system with valve A open and valve B closed. Due to fouling the flux will decline and after a certain period of time back-flushing occurs with valve B open to allow a bleed stream. Then valve A is closed while valve has been opened up now and the process repeats. In this way a high flux can be achieved continuously at a high recovery.
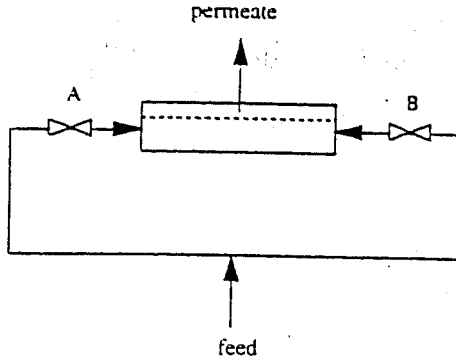
Figure VIII - 21. Schematic drawing of a hybrid dead-end/cross flow system

VIII.11. Cascade operations

Often the single-stage design does not result in the desired product quality and for this reason the retentate or permeate stream must be treated in a second stage. A combination of stages is called a cascade. A well-known example of a cascade operation occurs in the enrichment of uranium hexafluoride (^{235}U) with porous membranes. In this process transport through the membrane proceeds by a Knudsen mechanism and the selectivity is very low.
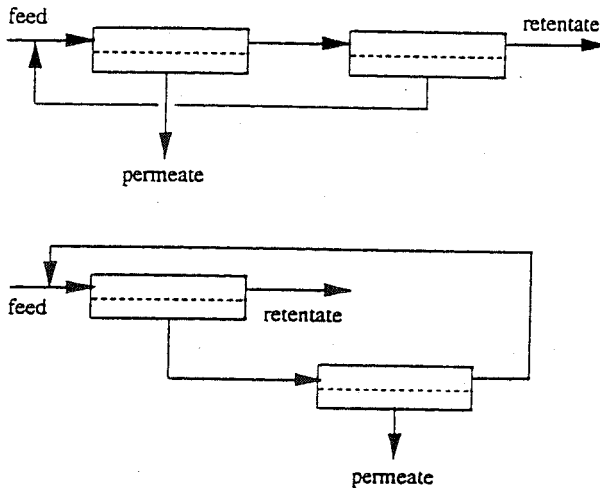
Figure VIII - 22. Two-stage membrane process.

In a cascade operation, employing a large number of units, where the permeate of the first stage is the feed of the second stage and so on, it is possible to obtain a very high product purity. An example of a two-stage operation process is given in figure VIII - 22. The type of design depends on whether the permeate or the retentate is the desired product. When more stages are required, the optimisation of the process becomes very complex and difficult. Two examples of a three-stage process are given in figures VIII - 23 and VIII - 24.
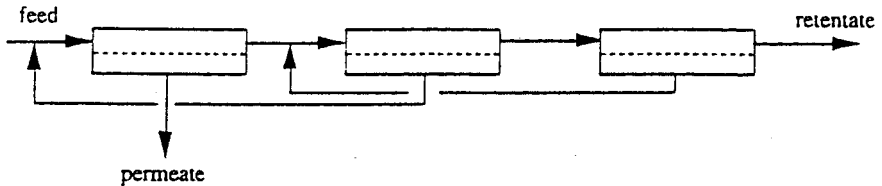
Figure VIII - 23   Three-stage membrane process with product recycle.

Figure VIII - 23 shows a three-stage process in which the permeate is recycled, similar to the design in figure VIII - 22 (top figure). Figure VIII - 24 depicts a more complex three-stage design of the type developed for the separation of natural gas (CO_2/CH_4 separation). This is said to be superior to the single-stage and two-stage design [7]. Multi-stage design becomes very complex because of the large number of variables involved in the optimisation procedure. A more detailed description of the engineering aspects of membrane separation can be found in the books of Hwang and Kammermeyer [8] and of Rautenbach and Albrecht [9].
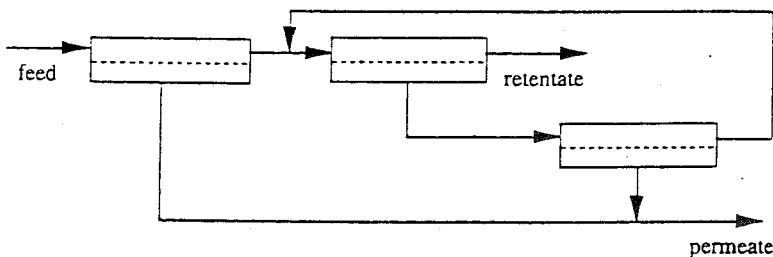
Figure VIII - 24.   Three-stage gas separation membrane process [7].

VIII.12.   Some examples of system design

The development from a membrane in the laboratory to its large scale commercial application is a long procedure. The heart of a membrane separation process is the membrane while that of a system is the module. Module design is based on various technical and economical

aspects relative to the specific separation problem. Modules can be arranged in a single-stage or multi-stage system. Indeed system design is as important as membrane development. In many cases the membrane system cannot be used directly and often pretreatment is necessary to facilitate the membrane process. However, the costs of the pretreatment can contribute appreciably to the overall costs. Pretreatment is important and necessary in micro-, ultra- and reverse osmosis. In pervaporation, vapour permeation and gas separation, where the feed streams are generally much cleaner and do not contain many impurities, only simple pretreatment are required.

Some examples of system design and plant design will be given here. A more comprehensive account of system design can be found in the book by Rautenbach and Albrecht [9].

VIII.12.1   Ultrapure water

The quality of the water must be extremely high in the semiconductor industry so that potable water is inadequate. Ions, bacteria, organics and other colloidal impurities have to be removed as much as possible and membrane processes are frequently used in this respect.
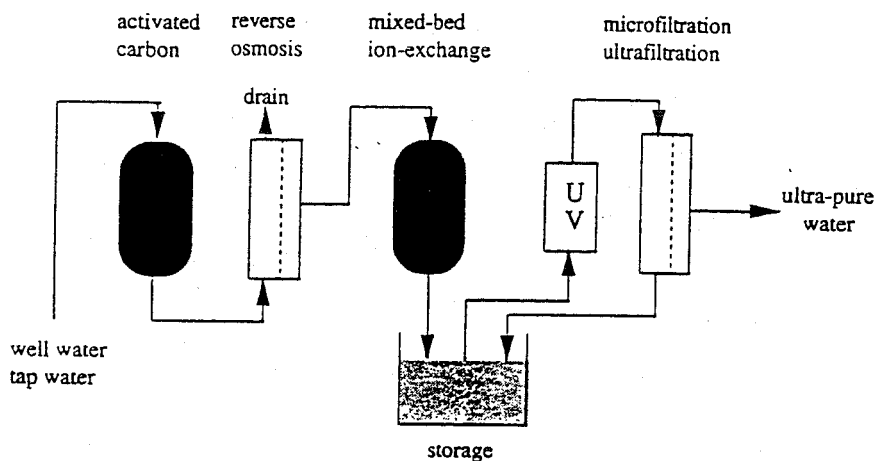
Figure VIII - 25.   Flow diagram for an ultrapure water production system.

This is a typical example in which a single membrane process does not give a high quality product and a combination of separation processes (hybrid processing) is necessary. In order to construct a separation unit, the specifications of ultrapure water have to be considered, see table VIII.4. Important parameters are conductivity, total organic carbon (TOC), and the number of particles and bacteria.

Table VIII.4   Specifications for ultrapure water [10]

Electrical resistance (MΩ.cm)	> 18
Number of particles (ml⁻¹)	< 10
Bacteria count (ml⁻¹)	< 0.01
TOC (ppb)	< 20

A hybrid separation system, i.e. a combination of reverse osmosis and ion-exchange, is used to achieve the required water quality. Pretreatment is also necessary and depends on the quality of the source water. A flow diagram of an ultrapure water production system is given in figure VIII - 19. Iron (if present) is removed in a pretreatment step and this pretreated water is then fed into an activated carbon column.This is then subjected to a high-performance reverse osmosis (RO) unit to remove salts and organic solutes. The RO permeate is then treated in a mixed-bed ion-exchanger. To obtain the desired water quality (18 MΩ cm water without organics or other particles) a post-treatment involving ultraviolet sterilisation, ion-exchange polishing and ultrafiltration to remove particles coming from the ion-exchange beds is applied.

VIII.12.2   Recovery of organic vapours

The emission of organic vapours into air is a serious environmental problem. Because of the large difference between the permeability of nitrogen (air) and those of all kinds of organic vapours (see chapter V and VI), membrane processes can be applied to recover and effect the re-use of organic vapours especially at high vapour concentrations.
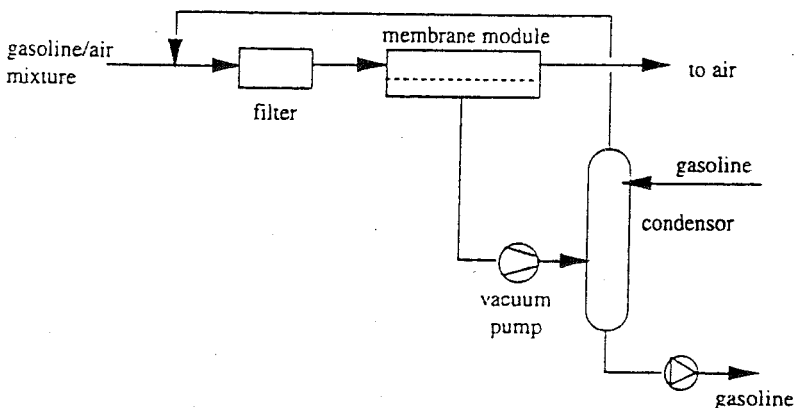
Figure VIII - 26. Flow diagram of membrane separation system for the recovery of gasoline vapours [10 - 12].

A typical example of a high vapour concentration occurs in fuel tanks (oil, gasoline). When these tanks are filled with fuel, large amounts of organic vapours are emitted into the air, although mainly because of governmental regulations this is no longer allowed. A flow diagram of a membrane separation system for the recovery of gasoline vapours is shown in figure VIII - 26. Since the feed stream is quite clean, pretreatment is simple involving only a filter to remove particles. The retentate stream contains a low concentration of organic vapour and may be emitted while the permeate is condensed and re-used. This application can be employed with all kinds of organic vapour/air mixtures.

VIII.12.3   Desalination of seawater

Desalination of seawater is one of the most important applications of membrane processes. A number of techniques are available to produce fresh water, such as distillation (multi-stage flash evaporation, MSF), electrodialysis, membrane distillation, freezing, and reverse osmosis.
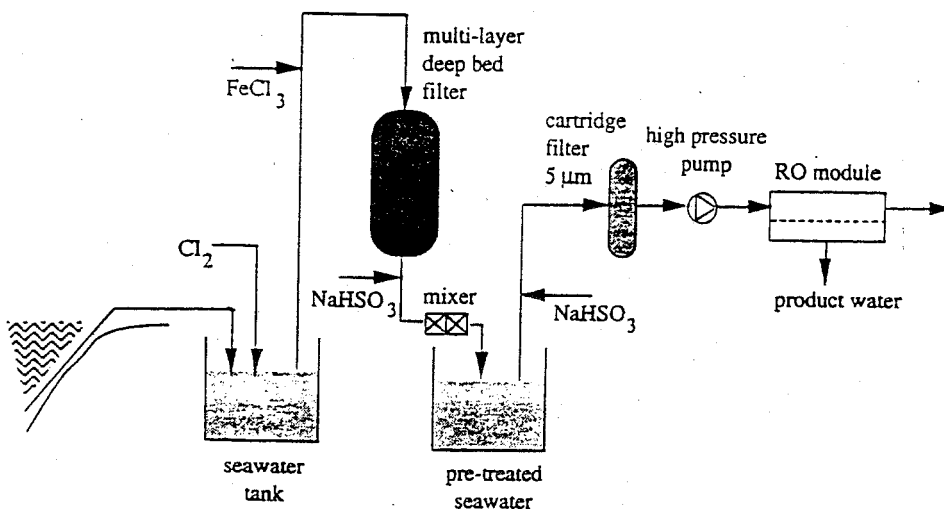
Figure VIII - 27.   Flow diagram of a reverse osmosis system for seawater desalination [13].

MSF still remains the most important technique used in this field but reverse osmosis is being applied to an increasing extent. A flow diagram of a single-stage reverse osmosis system is shown in figure VIII - 27 [13]. High-performance RO membranes exhibit a salt rejection > 99% which means that a single-stage RO system can give a product purity of about 300 ppm of salt. To improve the quality further, a two-stage (or multi-stage) system is often used. Although seawater is a relatively clean feed stream, pretreatment is necessary to

reduce fouling and to avoid membrane damage. Flocculation agents such as iron chloride or polyelectrolytes are added in order to remove suspended solids, but scaling can be a very severe problem. Scaling is the precipitation of salts which arises because their solubility products have been exceeded. The precipitation of calcium salts ($CaSO_4$, $CaCO_3$) or silica (SiO_2) in particular at the membrane surface can cause a problem in the case of seawater. To reduce scaling, the pH is adjusted by the addition of acid (calcium, barium, magnesium salts will not precipitate at low pH values and silica at high pH values). Chlorine is then added to remove bacteria and algae. With membrane materials which are not resistant to free chlorine (e.g. polyamides), a treatment with sodium hydrogen sulphite ($NaHSO_3$) is necessary to remove the chlorine.

VIII.12.4   Dehydration of ethanol

The dehydration of all kinds of organic solvents can be carried out by pervaporation. This process is very attractive, especially in those cases where water forms an azeotrope with the solvent at low water content. A typical case is ethanol/water with an azeotropic composition of 96% ethanol by weight. Purification of ethanol can also be achieved via a hybrid process; distillation up to 96% and pervaporation to > 99%, see figure VIII - 28.
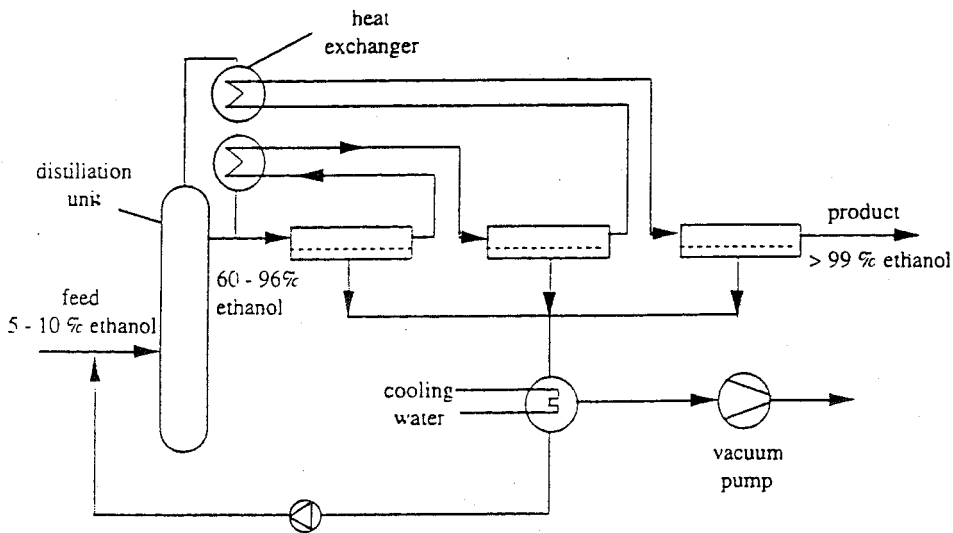
Figure VIII - 28.   Flow diagram of a hybrid process for pure alcohol production, combining distillation with pervaporation.

The pervaporation feed coming from the distillation unit contains no impurities and no pretreatment is necessary in this case. System design for pervaporation differs from that of other membrane processes. Pervaporation is the only process where a phase transition

occurs in going from the feed to the permeate. The heat of evaporation is supplied from the feed stream which implies that the temperature will decrease from the inlet feed stream to the retentate stream. As a consequence, the driving force will decrease and the flux and selectivity will decrease. For this reason, the system is divided into a number of small units with the retentate being reheated before it enters the next module. Furthermore, it is very advantageous to operate at high feed temperatures, firstly because of higher permeation rates. The permeation rate through the membranes obeys an Arrhenius type of relationship so that the flux roughly doubles with every 10°C temperature rise. In the second place condensation can occur at room temperature, which means that cooling water (10 - 20°C) can be used as the condensing liquid.

VIII.12.5   Economics

Whether or not a membrane process or another separation process is used for a given separation is based entirely on economic considerations. What factors determine the economics of a process? It will be clear that no (precise) answer can be given to this question. In fact, the costs have to be calculated for every specific separation problem and for this reason the economics will only be considered very general.

The cost of a given installation is determined by two contributions, i.e. the capital costs and the operating cost. The capital cost, the installation investment, can be divided into three parts:
- membrane modules
- costs of piping, pumps, electronics, vessels
- pretreatment and post-treatment

In order to calculate the cost per liter or cubic meter or kg of product, the capital costs are depreciated over a finite period, often 10 years. Interest has to be paid over this time on this amount of money. In contrast, the operating costs can be divided into:
- power requirement
- membrane replacement
- labour
- maintenance

Those readers who are more interested in process economics are referred to a number of articles and books (see e.g. [14]).

VIII.13.   Process parameters

Membrane performance is characterised by the retention and the permeation rate. The feed concentration is generally constant in laboratory set-ups but when a module, a stage or a system is considered the feed concentration entering differs from the outlet (retentate) concentration. This implies that the composition on the feed side changes with distance. As a result the selectivity (or retention) and flux through the membrane are a function of the distance in the system. In order to design a membrane system the process parameters have to be defined.

The description given here can be applied in general. However, a distinction must be made for pressure-driven processes such as microfiltration, ultrafiltration and reverse osmosis. Here the feed consists of a solvent (usually water) and one or more solutes. In general, the concentration of the solute(s) is low and the separation characteristics of the membrane are always related to the solute(s). On the other hand, in liquid separation (pervaporation) and gas separation the terms solvent and solute are best avoided.

Figure VIII - 29 shows a schematic drawing of a system with the inlet stream, the feed, divided into two other streams, the retentate and the permeate streams.
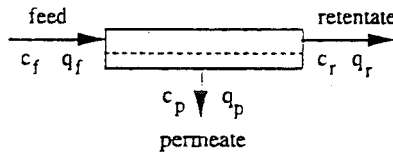
Figure VIII - 29.   Schematic drawing of a membrane system.

The feed stream enters the system with a solute concentration c_f ($kg.m^{-3}$) and a flow rate q_f ($m^3 s^{-1}$) (In the case of pervaporation and gas separation, the concentrations of the components are usually given in mole fractions). The solute is retained by the membrane to a certain extent whereas the solvent can freely pass through the membrane. Hence the solute concentration increases with distance and will have the value c_r in the retentate with the retentate flow rate being q_r. The concentration in the permeate is c_p and the permeate flow rate is q_p.

The recovery or yield (symbol S) is defined as the fraction of the feed flow which passes through the membrane:

$$\text{Recovery (S)} \equiv \frac{q_p}{q_f} \qquad\qquad\qquad\qquad \text{(VIII - 1)}$$

The recovery ranges from 0 to 1 and is a parameter of economic importance. Commercial membrane processes are often designed with a recovery value as high as possible. However, the recovery also influences the membrane or process performance. In laboratory set-ups the recovery usually approaches zero ($S \Rightarrow 0$), which implies maximum separation performance. With increasing recovery, the performance declines

because the concentration of the less permeable component increases.

Another important process parameter is the volume reduction (VR), which is defined as the ratio between the initial feed flow rate and the retentate flow rate. The volume reduction indicates the extent to which a certain solution has increased in concentration:

$$VR = \frac{q_f}{q_r} \qquad \text{(VIII - 2)}$$

In batch operations, the volume reduction VR is defined as:

$$VR_{batch} = \frac{V_f}{V_r} \qquad \text{(VIII - 3)}$$

where V_f and V_r are the initial and final volume respectively.

The retention or retention coefficient which expresses the extent to which a solute is retained by the membrane is also important. The retention R is defined as:

$$R = \frac{c_f - c_p}{c_f} = 1 - \frac{c_p}{c_f} \qquad \text{(VIII - 4)}$$

In the case of the separation of a (organic) liquid and a gas, the selectivity rather than the retention is defined in terms of a separation factor α. The separation factor always involves two components (see also chapter I). The selectivity α is defined as:

$$\alpha_{A/B} = \frac{y_A / y_B}{x_A / x_B} \qquad \text{(VIII - 5)}$$

Now that the basic process parameters necessary to design, or at least make a rough estimate regarding the design, of a complete system have been defined, some examples will be given for different membrane processes. In the following sections simple equations relating the various process parameters to each other will be derived for some processes.

VIII.14. Reverse osmosis

The principle of reverse osmosis is based on a large difference between the solvent flow and the solute flow. The solvent flow (J_w in this case, since we will consider water as solvent) is given by:

$$J_w = A (\Delta P - \Delta \pi) \qquad \text{(VIII - 6)}$$

where A is the permeability constant. If the membrane is completely semipermeable there will be no solute flux. However, this does not occur in practice although membranes are available with a very low solute flux. The solute flux J_s, which is based on the concentration difference, is given by:

$$J_s = B \ (c_f - c_p) \tag{VIII - 7}$$

where B is the solute permeability coefficient

Both equations show that the water flux depends on the effective pressure difference whereas the solute flux is hardly affected by the pressure difference and is determined solely by the concentration difference. The permeate concentration can be expressed as:

$$c_p = \frac{J_s}{J_w} = \frac{B \ (c_f - c_p)}{J_w} \tag{VIII - 8}$$

or rearranged to give

$$c_p = \frac{B \ c_f}{J_w + B} \tag{VIII - 9}$$

Combining eq. VIII - 9 with eq. VIII - 4 gives

$$R = 1 - \frac{B \ c_f}{c_f(J_w + B)} = 1 - \frac{B}{J_w + B} \tag{VIII - 10}$$

or

$$\frac{J_w \ (1 - R)}{R} = B \tag{VIII - 11}$$

For high values of the retention coefficient (R > 90%), eq. VIII - 11 reduces to

$$J_w \cdot (1 - R) = \text{constant} \tag{VIII - 12}$$

Eq. VIII - 12 shows that as the pressure increases the water flux (J_w) also increases and consequently the retention coefficient R increases. Although the equations given here show how the flux and rejection in reverse osmosis are related to each other for a given membrane, they must be considered simply illustrative. They show very clearly and in a (mathematically) simple way how important membrane parameters are related to each other, but they cannot be used to calculate the situation in a process or system under practical conditions. The feed solution becomes more concentrated in going from the inlet stream (c_f) to the outlet stream (c_r). and if it is assumed that the retention coefficient R of the membrane remains constant (independent of feed concentration) the permeate concentration will also increase and varies from (1 - R) c_f to (1 - R) c_r. Equations will now be derived for cross-flow reverse osmosis that relate the permeate concentration (c_p) and retentate concentration (c_r) to volume reduction and rejection [1]. In this derivation it is assumed that the process conditions remain constant (no pressure drop, no change in osmotic pressure and that the rejection coefficient R is independent of feed concentration).

Under steady state conditions, the mass balance equations may be written as:

- water $q_f = q_p + q_r$ (VIII - 13)

- solute $q_f \cdot c_f = q_p \cdot c_p + q_r \cdot c_r$ (VIII - 14)

Substitution of eqs.   VIII - 1 and VIII - 13 into eq. VIII - 14 gives

$$c_r = \frac{(c_f - S\ c_p)}{1 - S}$$ (VIII - 15)

where S is the recovery ($S = q_p / q_f$).
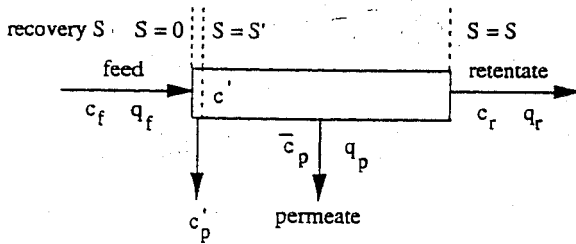
Figure   VIII - 30.   Schematical representation of the reverse osmosis process.

The module (or process) is divided into an infinite number of small segments. Figure VIII - 30 shows such a segment at the entrance of the module. The outlet feed concentration in this segment is equal to c' while the permeate concentration is equal to c_p'. If the small segment is considered (see figure VIII - 30), then eq. VIII - 15 becomes

$$c' = \frac{\left(c_f - S'\ c_p'\right)}{1 - S'}$$ (VIII - 16)

where c' is a concentration somewhere in between the initial concentration (c_f) and the retentate concentration (c_r). For the small segment c' is only a little higher than c_f. c_p' is the average permeate concentration in this segment (from $S = 0$ to $S = S'$) and can be expressed as

$$c_p' = \frac{1}{S'} \int (1 - R)\ c'\ dS$$ (VIII - 17)

Substitution of eq. VIII - 16 into eq. VIII - 17 gives:

$$c' = \frac{1}{\left(1 - S'\right)} \left[c_f - \int (1 - R)\ c'\ dS' \right]$$ (VIII - 18)

Differentiation with respect to S' gives

$$\frac{d[c'(1 - S')]}{dS'} = \frac{dc_f}{dS'} - (1 - R) c'$$

(VIII - 19)

and since $dc_f/dS' = 0$, then eq. VIII - 19 becomes

$$(1 - S') \frac{dc'}{dS'} + c' \frac{d(1 - S')}{dS'} = - (1 - R) c'$$

(VIII - 20)

or

$$\frac{dc'}{dS'} = \frac{R c'}{(1 - S')}$$

(VIII - 21)

$$\int \frac{dc'}{c'} = - \int \frac{R d(1 - S')}{(1 - S')}$$

(VIII - 22)

Integration over the whole system between the boundaries 0 to S and c_f to c_r gives

$$c_r = c_f (1 - S)^{-R}$$

(VIII - 23)

and

$$c_p = c_f (1 - R) (1 - S)^{-R}$$

(VIII - 24)

As the permeate concentration is not constant it is better to use an average permeate concentration c_p. Rewriting eq. VIII - 13 yields:

$$q_f \cdot c_f = q_p \cdot c_p + q_r \cdot c_r$$

(VIII - 25)

where c_p is the average concentration and eq. VIII - 15 becomes

$$c_r = \frac{(c_f - S \bar{c}_p)}{1 - S}$$

(VIII - 26)

and combining eq. VIII - 26 with eq. VIII - 23 yields

$$\bar{c}_p = \frac{c_f}{S} \left[1 - (1 - S)^{1 - R} \right]$$

(VIII - 27)

These equations show how the concentrations in the retentate and permeate are related to the recovery S and the retention coefficient R. In reverse osmosis and

ultrafiltration the retentate or the permeate is sometimes the product of interest, and often there are special requirements with respect to the retentate concentration and the permeate concentration. Eqs. VIII - 23 and VIII - 27 enable a fast and simple estimation to be carried out.

It can be seen that as the recovery increases the permeate concentration also increases. These simple equations allow the prediction of how large the maximal recovery may be if a certain permeate concentration cannot be exceeded. For example, with a feed concentration of 2000 ppm sodium chloride and a membrane having a retention of 95%, then eq. VIII - 4 (assuming zero recovery, $S = 0$) shows that the permeate concentration c_p $= 100$ ppm. For a recovery of 80% ($S = 0.8$), the average permeate concentration calculated via eq. VIII - 27 will be $c_p = 193$ ppm, which is almost twice as much. The equations derived here will be used later in a calculated example.

VIII.15.   Diafiltration

A complete separation between high molecular and low molecular solutes cannot be achieved with the cascade designs given above. To obtain complete separation (a problem that often occurs in biotechnology or the pharmaceutical and food industries), the retentate is diluted with solvent (water) so that the low molecular weight solutes are washed out. This type of operation is called diafiltration (dilution mode) and a schematic drawing is given in figure VIII - 31. Diafiltration is not another membrane process or membrane operation but is just simply a design to obtain a better purification or fractionation. Ultrafiltration units are often used as membrane process in this design.
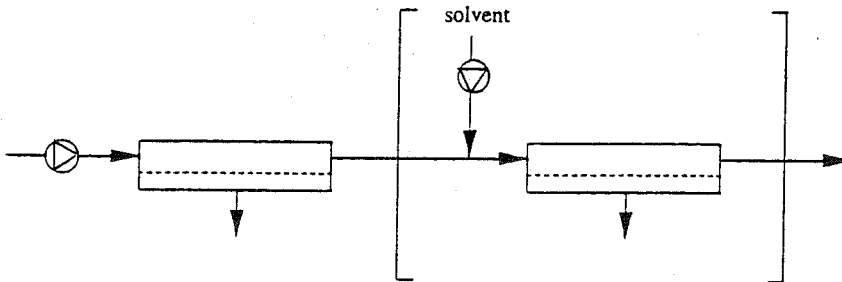
Figure   VIII - 31.   Schematic drawing of diafiltration arrangement.

As can be seen from fig. VIII - 31, after a pre-concentration step the retentate is diluted with solvent until the desired purification has been obtained.

Diafiltration can be considered as a continuous stirred tank reactor (CSTR) with a membrane placed in the outlet stream. This implies that the equations for diafiltration will be rather similar to those for a CSTR with the difference that a rejection coefficient will appear in the case of diafiltration. Figure VIII - 32 shows a schematic drawing of a continuous stirred tank reactor (CSTR) and of a diafiltration system. In a CSTR all the

solutes present (low and high molecular weight) are washed out, whereas in diafiltration the high molecular weight component is retained and the low molecular component permeates through the membrane.
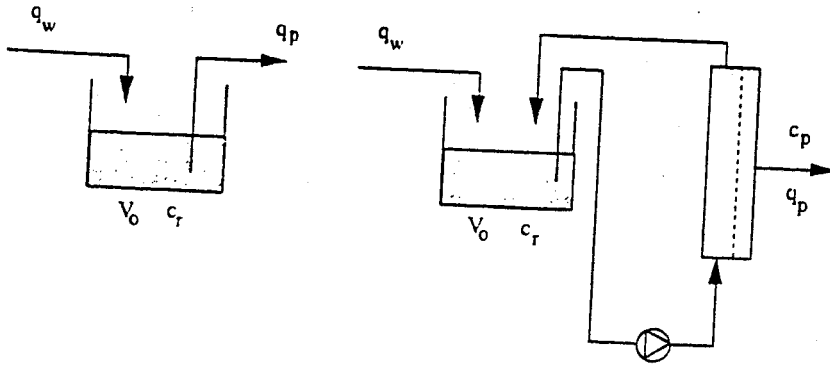
Figure VIII - 32. Schematic drawing of a continuous stirred tank reactor, CSTR (left) and a diafiltration system (right).

In diafiltration, the feed is streamed continuously along a membrane unit (e.g. an ultrafiltration unit). The ultrafiltration membrane completely retains the high molecular weight solutes, it being assumed that the low molecular weight solutes (e.g. salts) can pass through the membrane ($R = 0$). The volume in the feed tank remains constant because water is added at a rate equal to the permeation rate. If it is assumed that the macromolecules remain in the feed tank, then mass balance equations can be written, both for water and for the low molecular weight solute. The amount of solute in the feed tank per unit time must be equal to the permeation rate of the salt. The mass balance equations are:

- water: $\qquad q_w = q_p$

$$(VIII - 28)$$

- solute : $\qquad q_p c_p = - V_0 \dfrac{dc_r}{dt}$

$$(VIII - 29)$$

where

$$c_p = (1 - R) c_r$$

$$(VIII - 30)$$

and R is equal to the membrane retention for the low molecular weight solute. Integration of eq. VIII - 29 with the boundary conditions

$t = 0 \qquad c_r = c_r^{\circ}$

$t = t \qquad c_r = c_r^{1}$

yields

$$\frac{c_r^t}{c_r^o} = \exp\left[\frac{- q_w \ t \ (1 \ - \ R)}{V_o}\right]$$

(VIII - 31)

The total volume of water at time t is given by

$$V_w = q_w \cdot t$$

(VIII - 32)

and substitution of eq. VIII - 32 into eq. VIII - 31 gives

$$\frac{c_r^t}{c_r^o} = \exp\left[\frac{- V_w \ (1 \ - \ R)}{V_o}\right]$$

(VIII - 33)

As the membrane is freely permeable to low molecular weight solutes ($R = 0$), then eq. VIII - 33 indicates that 37% of the low molecular solute is still present with an amount of water equal to the initial volume V_o and that at least five times the initial volume V_o is needed to remove more than 99% of the low molecular weight solute (or to reduce the ratio c_r^t/c_r^o to less than 0.01). Since the membrane has a certain retention coefficient for the low molecular component, even more water is needed than predicted above. In practice, the membrane does not exhibit complete retention for one component whilst being freely permeable to the other.

Eq. VIII - 33 is very similar to that derived for a CSTR. Indeed, by setting $R = 0$ (no membrane !), eq. VIII - 33 reduces to the CSTR equation:

$$\frac{c_r^t}{c_r^o} = \exp\left[- \frac{V_w}{V_o}\right]$$

(VIII - 34)

However, no fractionation is obtained with a CSTR because both high and low molecular weight solutes are washed out.

VIII.16. Gas separation and vapour permeation

Simple equations can be derived to estimate the membrane area for a given gas separation separation problem. Here it is assumed that the permeability coefficients remain constant and the separation occurs under isothermal condition. The calculations are dependent on the flow pattern in the module. The most simple equations are obtained by assuming complete mixing both in feed and permeate. This concept may be found in systems which operate at low recovery. Most gas separation systems resembles cross-flow conditions, i.e. plug flow at the feed side and complete mixing at the permeate side. These two concepts will be discussed here. In case of counter-current and co-current flow conditions the equations are somewhat different and the derivations applicable for these systems can be found in literature. For vapour permeation the same approach can be used, however the

permeability coefficient is not a constant anymore but dependent on the vapour activity (see chapter V).

VIII.15.1   Gas separation under complete mixing conditions

Complete mixing implies that the concentrations at the feed side are constant at each point in the module and are equal to the retentate concentrations. Also at the permeate side the concentrations are the same at any point (see figure VIII - 33)
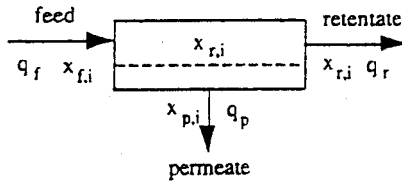
Figure   VIII - 33.   Gas separation with perfect mixing at feed side and permeate side

The overall mass balance is

$$q_f = q_p + q_r$$ (VIII - 35)

while the mass balance for component i is equal to

$$q_{f,i} = q_{p,i} + q_{r,i}$$ (VIII - 36)

or

$$q_f \cdot x_{f,i} = q_p \cdot x_{p,i} + q_r \cdot x_{r,i}$$ (VIII - 37)

The recovery has been defined as the fraction of the feed that has permeated through the membrane (In gas separations often the term 'cut' or 'stage cut' is used instead of recovery).

$$S = \frac{q_p}{q_f}$$ (VIII - 38)

Dividing eq. VIII - 38 by q_f gives for the permeate concentration the following equation

$$x_{p,i} = \frac{x_{f,i} - x_{r,i}(1 - S)}{S}$$ (VIII - 39)

and

$$x_{r,i} = \frac{x_{f,i} - S\ x_{p,i}}{(1 - S)}$$

(VIII - 40)

The equation describing the flux of a gas i through a membrane assuming perfect mixing can be written as

$$J_i = \frac{P_i}{\ell}\ \Delta p_i = \frac{P_i}{\ell}\ (x_{r,i}\ p_h - x_{p,i}\ p_\ell)$$

(VIII - 41)

where P_i is the permeability coefficient of component i, ℓ the membrane thickness, p_h the pressure on the feed side (high-pressure side), p_ℓ the pressure on the permeate side (low-pressure side), and $x_{r,i}$ and $x_{p,i}$ are the constant mole fractions of component i in the feed and the permeate, respectively. A similar equation can be written for component j. The permeate flow rate of component i, $q_{p,i}$, is given by

$$q_{p,i} = q_p\ x_{p,i} = J_i\ A = \frac{A\ P_i}{\ell}\ (x_{r,i}\ p_h - x_{p,i}\ p_\ell)$$

(VIII - 42)

and for component j

$$q_{p,j} = q_p\ (1 - x_{p,i}) = J_j\ A = \frac{A\ P_j}{\ell}\ [(1 - x_{r,i})\ p_h - (1 - x_{p,i})\ p_\ell]$$

(VIII - 43)

dividing eq VIII - 42 by eq. VIII - 43 gives

$$\frac{x_{p,i}}{1 - x_{p,i}} = \frac{P_i}{P_j}\frac{[\ x_{r,i} - \frac{p_h}{p_\ell}x_{p,i}\ ]}{[\ (1 - x_{r,i}) - \frac{p_h}{p_\ell}(1 - x_{p,i})\ ]}$$

(VIII - 44)

This is a quadratic function in $x_{p,i}$ with the form as eq. VIII - 45 and relates the permeate composition $x_{p,i}$ to the pressure ratio p_h/p_ℓ, the ideal selectivity P_i/P_j and the retentate concentration $x_{r,i}$.

$$a\ x^2_{p,i} + b\ x_{p,i} + c = 0$$

(VIII - 45)

The permeate concentration $x_{p,i}$ is obtained by solving eq. VIII - 45

$$x_{p,i} = B - \left[B^2 - \frac{\left(\frac{P_i}{P_j}\right)\ p_h}{\left(\frac{P_i}{P_j} - 1\right)\ p_\ell}\ x_{r,\ i} \right]^{0.5}$$

(VIII - 46)

or

$$x_{p,i} = B - \left[B^2 - \frac{\alpha}{(\alpha - 1) \, P_r} \, x_{r,i} \right]^{0.5}$$

$$\text{(VIII - 46a)}$$

where

$$B = 0.5 \left[1 + \frac{1}{(\alpha - 1) \, P_r} + \frac{x_{r,i}}{P_r} \right]$$

$$\text{(VIII - 47)}$$

with $P_r = p_\ell / p_h$ and $\alpha = P_i / P_j$.

In order to relate the permeate concentration $x_{p,i}$ to the feed concentration equation VIII - 40 has been substituted into equation VIII - 44 and now a quadratic equation is obtained similar to equation VIII - 43 which can be solved to obtain $x_{p,i}$.

$$[P_r (1 - S)(1 - \alpha) + S (\alpha - 1)] \, x^2_{p,i} +$$

$$(S - 1)(P_r (\alpha - 1) + 1) + x_{f,i}(1 - \alpha) - \alpha \cdot S] \, x_{p,i} + \alpha \cdot x_{f,i} = 0 \qquad \text{(VIII - 48)}$$

VIII.16.2   Gas separation under cross-flow conditions

Most of the current gas separation systems operate under cross-flow conditions, plug flow at the feed side and perfect mixing at the permeate side. In fact the permeate side is not really perfectly mixed but there is rather an average concentration. The feed concentration in the module gradually changes from the feed inlet concentration ($x_{f,i}$) to the retentate concentration ($x_{r,i}$). Figure VIII - 34 gives schematic representation of the cross-flow case. A mass balance over the differential membrane area dA gives for component i and j the following expressions

$$- d (q' \, x'_i) = \frac{P_j}{\ell} (x'_i \, p_h - x_{p,i} \, p_\ell) \, dA$$

$$\text{(VIII - 49)}$$
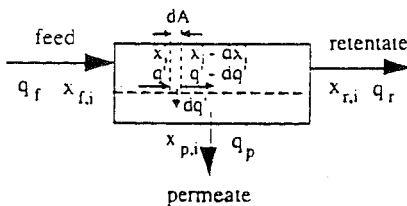
Figure VIII - 34.   Flow diagram of a cross-flow design

and for component j

$$- dq' (1 - x'_i) = \frac{P_j}{\ell} [(1 - x'_i) \, p_h - (1 - x_{p,i}) \, p_\ell] \, dA \qquad \text{(VIII - 50)}$$

The superscript ' indicates the high pressure feed side. The permeate concentration $x_{p,i}$ can be expressed as

$$x_{p,i} = \frac{d (x'_i \, q')}{d (x'_i \, q') + d ([1 - x'_i] \, q')} = \frac{d (x'_i \, q')}{dq'} \qquad \text{(VIII - 51)}$$

For component j the same equation can be derived

$$1 - x_{p,i} = \frac{d ([1 - x'_i] \, q')}{d (x'_i \, q') + d ([1 - x'_i] \, q')} = \frac{d ([1 - x'_i] \, q')}{dq'} \qquad \text{(VIII - 52)}$$

substitution of eqs VIII - 49 and VIII - 50 in VIII - 51 and VIII - 52, respectively followed by dividing the latter two gives

$$\frac{x_{p,i}}{1 - x_{p,i}} = \frac{P_i}{P_j} \frac{[\bar{x}_i - \frac{p_h}{p_\ell} x_{p,i}]}{[(1 - \bar{x}_i) - \frac{p_h}{p_\ell} (1 - x_{p,i})]} \qquad \text{(VIII - 53)}$$

This equation is similar to eq. VIII - 44 for the complete mixing case, only the feed concentration is now dependent on the place in the module. In fact, the module may be considered to be divided in an infinite number of small modules where complete mixing occurs. Eq. VIII - 50 was solved analytically by Weller and Steiner [15,16], while Hwang and Kammermeyer gave a numerical solution [8]. Here, the approach of Hogsett and Mazur will be used because of its simplicity [17]. Hogsett and Mazur assume an average concentration between feed and retentate which may be well expressed by the log mean concentration. When the feed and retentate concentrations differ quite considerably $(x_r/x_f < 0.5)$, the system may be divided into a number of steps with $x_r/x_f = 0.5$ because otherwise the error in the calculations will become too large. The log mean average feed concentration x may be defined as:

$$\bar{x}_i = \frac{x_{f,i} - x_{r,i}}{\ln\left(\frac{x_{f,i}}{x_{r,i}}\right)} \qquad \text{(VIII - 54)}$$

The composition of the permeate is obtained by solving eq. VIII - 53

$$x_{p,i} = B - \left[B^2 - \frac{\alpha}{(\alpha - 1) \, P_r} \bar{x}_i \right]^{0.5} \qquad \text{(VIII - 55)}$$

where

$$B = 0.5 \left[1 + \frac{1}{(\alpha - 1) \, P_r} + \frac{\bar{x}_i}{P_r} \right]$$

(VIII - 56)

With these two models, perfect mixing and cross-flow gas separation and vapour separation can be well described. Other configurations will not be described here but the reader is referred to a number of articles and books (see e.g.ref. 8 and 9). The derivations and solutions are rather similar to the ones given above and the results do not differ significantly in general. In addition, these flow patterns are, at least in gas separation and vapour permeation are not commonly applied.

The membrane area can now be determined from eq. VIII - 57.

$$A = \frac{q_{p,i}}{J_i} = \frac{q_p \, x_{p,i}}{J_i}$$

(VIII - 57)

VIII.17.   Pervaporation

Both driving force and permeability coefficient are temperature and concentration dependent. Compared to gas separation the same equations can be applied but the calculations become somewhat more complex. Two process configurations will be discussed here, complete mixing at feed side and permeate side, the easiest case to calculate and secondly cross-flow at feed side and complete mixing at the vapour side. Commercial pervaporation systems operate under conditions similar to the latter system. Co-current and counter-current systems can be calculated as well but will not be considered here. The reader is referred to literature (see e.g. Hwang and Kammermeyer [8] or Albrecht and Rautenbach [9]).
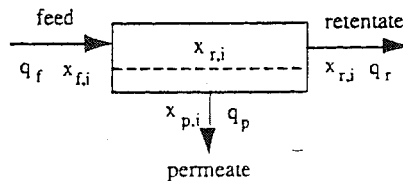
Figure VIII - 35.   Pervaporation with perfect mixing at feed side and permeate side.

VIII.16.1   Complete mixing in pervaporation
The equations for the complete mixing case are similar to the ones derived for gas separation. The retentate composition can be obtained from the mass balances (see eq. VIII - 40)

$$x_{r,i} = \frac{x_{f,i} - S\ x_{p,i}}{(1 - S)} \qquad\qquad (VIII - 40)$$

where the recovery S has been defined in the same way as in gas separation ($S = q_p/q_f$). The selectivity for a perfect mixed system with components i and j is given by

$$\alpha_{i/j} = \frac{x_{p,i} / x_{p,j}}{x_{r,i} / x_{r,j}} = \frac{x_{p,i}/(1 - x_{p,i})}{x_{r,i}/(1 - x_{r,i})} \qquad\qquad (VIII - 58)$$

or

$$x_{p,i} = \frac{\alpha_{i/j} \cdot x_{r,i}}{x_{r,i}(\alpha_{i/j} - 1) + 1} \qquad\qquad (VIII - 59)$$

Here i is assumed to be the more permeable component. Combination of eqs. VIII - 40 with VIII - 59 gives eq. VIII - 60 which is quadratic in permeate concentration $x_{p,i}$ and linear in feed concentration $x_{f,i}$ and recovery S.

$$[S\ (\alpha_{i/j} - 1)]\ x^2_{p,i} - [\ x_{f,i}(\ \alpha_{i/j} - 1) + (1 - S) + \alpha_{i/j} \cdot S]\ x_{p,i} + \alpha_{i/j} \cdot x_{f,i} = 0 \quad (VIII - 60)$$

If the permeate concentration and feed concentration are known the recovery can be determined from eq. VIII - 61.

$$S = \frac{\alpha_{i/j}\ x_{p,i} - (\alpha_{i/j} - 1)\ x_{f,i}\ x_{p,i} - x_{p,i}}{(\alpha_{i/j} - 1)(x_{p,i} - x_{p,i}^2)} \qquad\qquad (VIII - 61)$$

If the permeate concentration and recovery are known the feed concentration can be determined from eq. VIII - 62

$$x_{f,i} = \frac{(1 - \alpha_{i/j})\ x_{p,i} - (\alpha_{i/j} - 1)\ S\ x_{p,i}^2 + \alpha_{i/j}\ S\ x_{p,i}}{\alpha_{i/j} - (\alpha_{i/j} - 1)\ x_{p,i}} \qquad\qquad (VIII - 62)$$

The recovery can be obtained as well from an energy balance. For the complete mixing case the temperature at the feed side is constant and the energy balance is given

$$q_f\ c_{p,f}\ (T_f - T') = q_r\ c_{p,r}\ (T_r - T') + q_f\ c_{p,p}\ (T_p - T') + \Delta H_{vap}\ q_p \qquad (VIII - 63)$$

where ΔH_{vap} is the heat of vapourisation and c_p the heat capacity. Since there is thermal equilibrium between the feed side and permeate side $T_r = T_p$. Eq. VIII - 63 can be further simplified since the reference temperature T' can be chosen arbitrarily, hence $T_r = T_p = T'$

$$q_f \, c_{p,f} \, (\, T_f - T_r \,) \; = \; \Delta H_{vap} \, q_p \qquad\qquad\qquad\qquad\qquad \text{(VIII - 64)}$$

and

$$S \; = \; \frac{c_{p,f} (\, T_f - T_r \,)}{\Delta H_{vap}} \qquad\qquad\qquad\qquad\qquad\qquad \text{(VIII - 65)}$$

The flux of component i is given by

$$J_i \; = \; \frac{P_i}{\ell} \, \Delta p_i \qquad\qquad\qquad\qquad\qquad\qquad\qquad \text{(VIII - 66)}$$

Since the liquid feed does generally not behave ideally, whereas the gas phase is assumed to be ideally eq. VIII - 65 now becomes

$$J_i \; = \; \frac{P_i}{\ell} \left(x_{r,i} \, \gamma_i \, p_i^o - x_{p,i} \, p\ell \right) \qquad\qquad\qquad\qquad \text{(VIII - 67)}$$

where γ_i is the activity coefficient of component i in the mixture and p_i^o the saturation pressure of the pure component i at temperature T and when $x_{r,i}$ and $x_{p,i}$ are known the flux can be calculated. The membrane area can be determined from eq. VIII - 57, similar to gas separation.

VIII.17.2 *Cross-flow in pervaporation*

A more realistic flow pattern is cross-flow at the feed side and perfect mixing at the permeate side. Compared to the complete mixing case in the former section there is a distinct difference. Firstly, the concentration of component i at the feed change gradually across the system from feed inlet $x_{f,i}$ to retentate $x_{r,i}$. Moreover. the temperature is decreasing as well across the feed side and finally the permeability coefficient P_i is concentration and temperature dependent. A system may now be divided into a number of segments where the permeability coefficient is supposed to be constant but may be different in the next stage. Therefore, the concentration dependency of the permeability coefficient should be determined independently. Now the same equations can be applied as has been derived for gas separation. The number of stages is mainly dependent on the concentration dependency of the permeability coefficient and of the flux. The flux in a certain stage is now given by

$$J_i \; = \; \frac{\overline{P}_i}{\ell} \left(\overline{x}_i \, \gamma_i \, p_i^o - x_{p,i} \, p\ell \right) \qquad\qquad\qquad\qquad \text{(VIII - 68)}$$

in which x_i is the log mean concentration and P_i the average permeability coefficient.

VIII.18. Electrodialysis

Electrodialysis has been the first membrane process of commercial impact on a large scale. The process engineering of electrodialysis, or in general from electrical driven processes, is completely different since ions are transferred due to an electrical potential difference. The heart of the electrodialysis system is the membrane stack which consists of 200 to 600 cell pairs. The basic requirements of a system are membrane stack, power supply and pumps for feed, dilute and concentrate. The system may have a number of stacks parallel or in series. Figure VIII - 36 shows a flow diagram of a single-stage electrodialysis
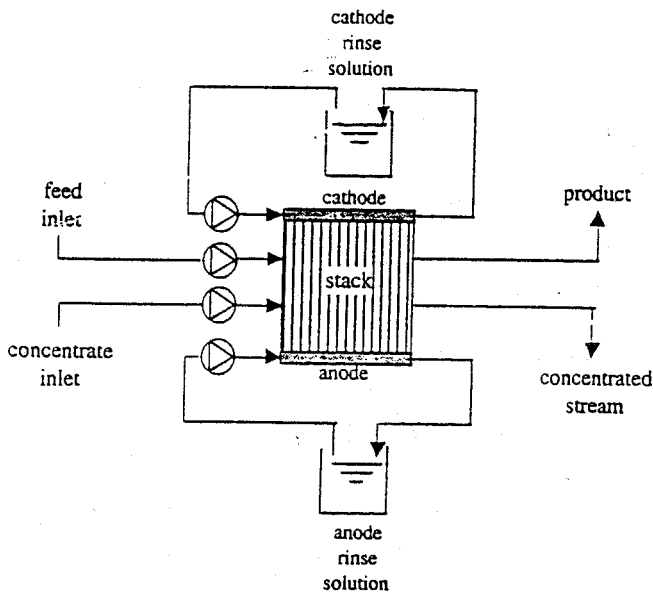
Figure   VIII -   36. Flow diagram for a single-stage electrodialysis process

process. There are a number of process parameters that influence the engineering and economics and one of the main parameters is the limiting current density i_{lim}. Any system should operate below i_{lim} and a value of the current density is taken, $i_{actual} \approx i_{lim}$. The calculations to determine the required membrane area are rather straight forward [18]. The basic equation is given by the current which is needed to remove a certain amount of ions (eq. VIII - 69).

$$I = \frac{z \, \mathcal{F} \, q \, \Delta c}{\xi}$$

(VIII - 69)

$\mathcal{F}$ is the Faraday constant (96500 Coulombs/equivalent), q is the flow rate (l/s), Δc the

concentration difference between feed and product stream (eq/l) and the ξ is the current utilisation. The current utilisation is related to the electrical efficiency and is defined as the product of number of cells n and the electrical efficiency. The electrical efficiency indicates how efficient the current is used to achieve the separation. It depends on the efficiency of the membrane (η_s) which is determined by the membrane selectivity, the efficiency due to water transport (η_w) and the efficiency due to leakage of current through the manifold in which the membranes have been clamped (η_m). The electrical efficiency is always less than 1.0 since all the efficiencies are less than 1.0, a value of 0.9 may be considered as a realistic estimate.

$$\xi = n \cdot \text{electrical efficiency} = n \, \eta_s \eta_w \eta_m \qquad \text{(VIII - 70)}$$

The current density i is given by

$$i = \frac{I}{A_m} \qquad \text{(VIII - 71)}$$

where A_m is the area of a cation or anion exchange membrane. An electrodialysis stack contains a number of cell pairs and the total area is given by

$$A = n \, A_m \qquad \text{(VIII - 72)}$$

The total membrane area required for a certain separation can now be obtained by substitution of equations VIII - 71 and 72 into VIII - 69

$$A = \frac{z \, \mathscr{F} \, q \, n \, (c_{feed} - c_{product})}{i \, \xi} \qquad \text{(VIII - 73)}$$

the electrical efficiency and the total number of cells are given by eqs. VIII - 74 and VIII - 75

$$\text{electrical efficiency} = \frac{\mathscr{F} \, q \, \Delta c}{n \, I} \qquad \text{(VIII - 74)}$$

and

$$n = \frac{\mathscr{F} \, q \, \Delta c}{\text{electrical efficiency } I} \qquad \text{(VIII - 75)}$$

The energy consumption is given by

$$E = n \, I^2 \, R_{cp} \, t \qquad \text{(VIII - 76)}$$

with R_{cp} being the resistance of a cell pair and n the number of cell pairs in a stack. The resistance of a cell is determined by the resistance of the membrane and the solution

resistance. The solution resistance is inversely proportional to the salt concentration and since the dilute compartment has a lower salt concentration the resistance is determined by this compartment. A combination of eq. VIII - 69 and VIII - 76 gives the energy consumption as a function of the applied current and the electrical resistance, the current utilization and the amount of salt removed

$$E = \frac{n \ I z \mathcal{F} R_{cp} \Delta c \, q \, t}{\xi}$$

(VIII - 77)

The total energy consumption of the process is now given by the contribution of the electrical energy to drive the ionic transfer and by the energy of the pumps to circulate the various solutions (see figure VIII - 36). Generally two or three pumps are required; for the concentrated and depleted streams and for the anode- and cathode-rinse solutions. The energy consumption can be calculated from eq. VIII - 78.

$$E_p = \frac{q_v \ \Delta P}{\eta}$$

(VIII - 78)

in which E_p is the energy requirement of the pump, q_v is the flow rate which has to be pumped, ΔP is the pressure drop and η the pump efficiency..

VIII.18.   Dialysis

Dialysis is the most frequent used membrane process. Here the feed solution flows on one side of the membrane while a solvent stream (dialysate) flows on the other side. Due to a driving force, a concentration difference, solutes may diffuse through the membrane. Generally, dialysis is used with aqueous solutions but the process can be applied as well for non-aqueous solutions. The applications can be found in a wide variety of industries but far the most important one is hemodialysis in artificial kidney. In this application the blood of persons with a kidney failure is treated in a dialysis process to remove toxic small molecular weight metabolites such as urea, creatinine, uric acid and others. In this application blood flows on one side of the membrane whereas dialysing fluid which contains vital salts such as sodium, potassium, calcium, and magnesium that may not be removed from the blood, flows on the other side. The small organic solutes diffuse through the membrane and the process is continued until the concentration of the toxic components have been reduced to a certain level.
Diffusion dialysis in another process which operates according to the same principle. In this process protons or hydroxyl ions are removed from an aqueous stream.
Dialysis is normally operated in a counter-current configuration and a schematic flow scheme is shown in figure VIII - 37.
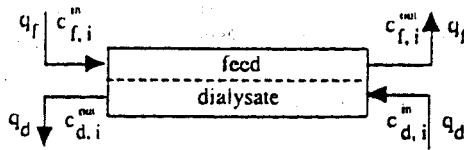
Figure VIII - 37.   Schematic drawing of a counter-current flow

The flow rates of feed and dialysate can be considered to be constant and only solutes are transported through the membrane. The flux of solute i through the membrane is given by

$$J_i = k_{i,ov} \left(\overline{c_{f,i}} - \overline{c_{d,i}} \right)$$ (VIII - 79)

with $c_{f,i}$ and $c_{d,i}$ as the average feed and dialysate concentration. $k_{i,ov}$ is the overall mass transfer coefficient which can be obtained from a resistance model.

$$\frac{1}{k_{i,ov}} = \frac{1}{k_{i,feed}} + \frac{1}{k_{i,dial}} + \frac{\ell}{P_i}$$ (VIII - 80)

$k_{i,feed}$ and $k_{i,dial}$ are the mass transfer coefficients of solute in the feed and dialysate boundary layer respectively, ℓ is the membrane thickness and P_i is the permeability coefficient of the membrane for component i. The transfer rate of component i through the membrane is given by

$$q_i = k_{i,ov} A \left(\overline{c_{f,i}} - \overline{c_{d,i}} \right)$$ (VIII - 81)

Different equations can be derived for various flow geometries which describe the removal efficiency of a solute from a solution [19,20]. The average concentration of feed and dialysate can be adequately described by the logarithmic mean concentration and for a counter-current flow the average concentration difference is given by

$$\left(\overline{c_{f,i}} - \overline{c_{d,i}} \right) = \frac{\left(c_{f,i}^{in} - c_{d,i}^{out} \right) - \left(c_{f,i}^{out} - c_{d,i}^{in} \right)}{\ln \dfrac{\left(c_{f,i}^{in} - c_{d,i}^{out} \right)}{\left(c_{f,i}^{out} - c_{d,i}^{in} \right)}}$$ (VIII - 82)

Furthermore

$$q_i = q_f \left(c_{f,i}^{in} - c_{f,i}^{out} \right) = q_d \left(c_{d,i}^{out} - c_{d,i}^{in} \right)$$ (VIII - 83)

Now the removal efficiency is given by

$$\frac{\left(c_{f,i}^{in} - c_{f,i}^{out}\right)}{\left(c_{f,i}^{in} - c_{d,i}^{in}\right)} = \frac{1 - \exp\left[\frac{k_{i,ov} A}{q_f}\left(1 - \frac{q_f}{q_d}\right)\right]}{\frac{q_f}{q_d} - \exp\left[\frac{k_{i,ov} A}{q_f}\left(1 - \frac{q_f}{q_d}\right)\right]} \quad . \tag{VIII - 84}$$

For other flow geometries the same equations can be derived, for instant for co-current flow equation VIII - 82 becomes

$$\left(\overline{c_{f,i}} - \overline{c_{d,i}}\right) = \frac{\left(c_{f,i}^{in} - c_{d,i}^{in}\right) - \left(c_{f,i}^{out} - c_{d,i}^{out}\right)}{\ln\frac{\left(c_{f,i}^{in} - c_{d,i}^{in}\right)}{\left(c_{f,i}^{out} - c_{d,i}^{out}\right)} -} \tag{VIII - 85}$$

Now the fractional solute removal is given by

$$\frac{\left(c_{f,i}^{in} - c_{f,i}^{out}\right)}{\left(c_{f,i}^{in} - c_{d,i}^{in}\right)} = \frac{1 - \exp\left[-\frac{k_{i,ov} A}{q_f}\left(1 + \frac{q_f}{q_d}\right)\right]}{\frac{q_f}{q_d} + 1} \tag{VIII - 86}$$

VIII.20. Energy requirements

A membrane separation process is an irreversible process, energy is dissipated continuously if transport occurs through a membrane. The flux is related to the driving
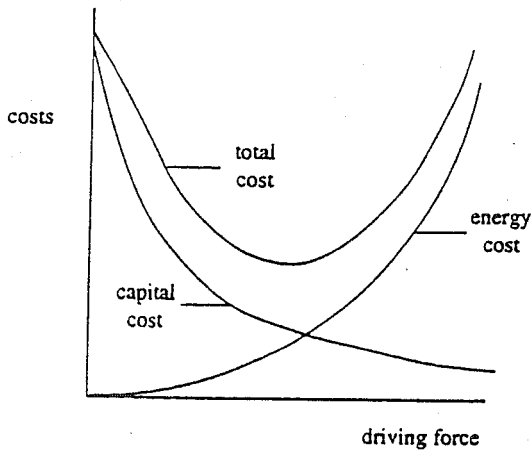
Figure VIII - 38. Schematic drawing of capital cost (investment) and energy cost as a function of driving force.

force, i.e., if the driving force increase the energy consumption increases and the flux increases. The driving force is a typical engineering parameter, by increasing the driving force, the flux increases and the required membrane area necessary for a certain application decreases and consequently the investment costs decrease. On the other hand the energy consumption for this separation process increases. Dependent on the type of process and the energy prize an optimum may be found as indicated in figure VIII - 38. Each separation process requires a minimum amount of work which is determined by the second law of thermodynamics. A reversible separation process requires as much as work as a reversible mixing process. However, the actual energy consumption is generally much higher than this minimum amount to make a membrane separation process economic feasible. The devices that can be used to establish a driving force, a hydrodynamic pressure difference (ΔP), a partial pressure difference (Δp_i) or a concentration difference (Δc_i) will be discussed briefly [21]. The electrical driven processes have been described in section VIII.17.

VIII.20.1. *Pressure driven processes*

A schematic drawing for pressure driven membrane processes is given in figure VIII - 39, in which the devices are shown (feed pump. circulation pump, turbine) which consume energy (feed pump, circulation pump) or recover energy (turbine). Depending on the flow rate, pressure difference, cross-flow velocities, membrane area, and the specific energy recovery system, the energy consumption may vary a lot from application to application.
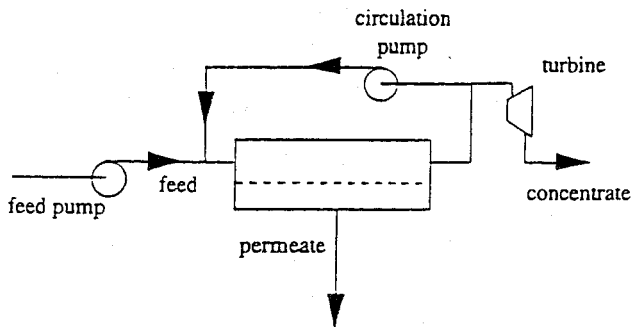
Figure VIII - 39. Schematic drawing of power devices applied in pressure driven membrane processes

The feed pump is used to pressurize the feed to a required pressure. In ultrafiltration and microfiltration flux decline is very severe due to concentration polarization and fouling. To reduce this effect as much as possible, the mass transfer in the boundary layer must be improved and this can be achieved by increasing the cross-flow velocity. In most cross-flow membrane operations, two pumps are employed, a feed pump to pressurize the feed and a circulation pump to adjust the cross-flow velocity. The aim of the circulation pump is to maintain a high cross-flow velocity. Since low hydrodynamic pressures are required in

microfiltration and ultrafiltration, combined with relatively high cross-flow velocity, the energy consumption is determined by the circulation pumps and not by the feed pumps. The energy consumption to pressurize a liquid from P_1 to P_2 is given by

$$E_p = \frac{q_v \; \Delta P}{\eta}$$

(VIII - 87)

where q is the flow rate (m³/s) and ΔP the pressure difference or pressure drop (N/m²). The efficiency η of a pump is generally between $0.5 \leq \eta \leq 0.8$.

In the case of high pressure applications such as reverse osmosis and nanofiltration, a turbine may be utilized to recover part of the energy. A liquid turbine is a device in which the liquid does work on the turbine blades at the expense of its kinetic energy. Hence, the process is expansion of a liquid from high pressure to low pressure in which work is produced. The process is in fact the opposite of compression and the same equation can be derived for the work only the efficiency η is now in the nominator.

$$E_t = - \; \eta \; q_v \; \Delta P$$

(VIII - 88)

Hence, for a turbine, the power is given as and the efficiency of a turbine normally lies between $0.5 \leq \eta \leq 0.8$. In the solved problems some examples have been worked.

VIII.20.2   Partial pressure driven processes

The partial pressure difference is typical the driving force in gas separation, pervaporation and vapour permeation. In the case of gas separation either the feed is pressurized by a compressor or the permeate side is kept at a low partial pressure by means of a vacuum pump. Sometimes a combination of both is used, as for instance in vapour permeation, a compressor to pressurize the feed to a few bar and a vacuum pump at the permeate side to adjust the partial pressure difference. Neglecting potential - and kinetic energy terms the actual work of a gas compressor is equal to that of a liquid compressor (pump). However, since a gas is compressible the final equations as the energy consumption differ completely. Gases do generally not behave ideally and the compression often occurs in several stages. Here it will be assumed that the gas behaves ideally and that compression is carried out isothermally, and then the power is given as

$$E = - \; \frac{1}{\eta} \int n \; RT \; dP = - \; \frac{n \; RT}{\eta} \ln \frac{P_2}{P_1}$$

(VIII - 89)

n is the number of moles which are compressed per second. This is a very simple equation which allows the calculation of the energy requirement in gas and vapour separations in which the feed stream is pressurized. Most compressors are better described by an adiabatic process which makes the equations somewhat different. In some applications such as air separation and vapour recovery a vacuum pump is employed at the permeate side to generate a partial pressure. A vacuum pump is in fact a compressor operating at a

pressure below atmospheric. For the vacuum pump the same equations apply as for the compressor. Figure VIII - 40 gives an overview of the mechanical devices which may be applied in gas separation and which either consume energy (compressor, vacuum pump) or recover energy (turbine).
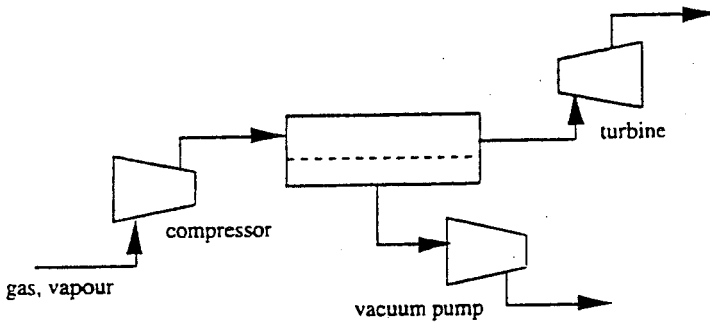
Figure VIII - 40. Schematic drawing of gas separation

VIII.20.3   Concentration driven processes

Dialysis and diffusion dialysis are membrane processes that consumes generally not much energy. The energy consumption E_p is determined by the pumps to circulate the feed and permeate (dialysate) stream along the membrane (eq. VIII - 87). If concentration polarisation becomes severe higher cross-flow velocities may be required to increase the solute mass transfer coefficient and consequently the energy consumption will increase.

VIII.21. Solved problems

1. Derive the following equation for a counter-current dialysis device in which the dialysate flow rate is high, i.e. $q_d \gg q_f$.

$$c_{f,out} = c_{f,in} \cdot \exp\left(-\frac{k_{ov} \cdot A}{q_f}\right)$$

2. An equimolar mixture of carbon dioxide and nitrogen is separated by a module containing composite membranes with an EPDM toplayer with a thickness of 1 μm. The feed pressure is $p_h = 2.5$ bar and the permeate pressure $p_p = 0.5$ bar. The feed rate is $q_f = 36$ m^3 (STP)/h. The permeability for the two gases is $P_{CO_2} = 81$ Barrer and $P_{N_2} = 5.3$ Barrer, respectively. Assume that perfect mixing occurs at feed side and permeate side.
   Calculate the permeate composition, the carbon dioxide recovery, and the carbon dioxide flux.

3. A cell suspension is concentrated in a batch MF process from 1% to 10%. Due to an effective backshock method the flux remains at 100 l/m^2.h. The fermentor has a volume of 1m^3 and the membrane area is 1.5 m^2. Calculate the batch processing time assuming that the membrane has a rejection of 100%.

4. The desalination of seawater or brackish water is usually carried out in a tapered module arrangement. Only one high-pressure feed pump is required in this design and a tapered module arrangement maintains high cross-flow velocity. Potable water (total dissolved solids (NaCl) < 250 ppm) can be obtained from seawater in a single stage design using high-performance membranes. Calculate the required membrane area and energy consumption of a 1000 m^3/day single-stage seawater desalination plant. In order to recover part of the energy consumption, a turbine is included in the process. The data necessary for the calculation are given in the table below.

Design data for a single stage seawater desalination plant

permeate flow rate	q_p : 1000 m^3/day
pressure difference	ΔP : 55 bar
flux	J : 1.3 m^3/ m^2 day (at 15 bar, T = 16°C and 1500 ppm NaCl)
rejection	R : 99.5 %
salt concentration	c_f : 35,000 ppm NaCl

recovery	S : 0.3
pump efficiency	η_{pump} : 0.65
turbine efficiency	$\eta_{turbine}$: 0.75
membrane area per module	A_{module} : 3 m^2

5. Ultrafiltration is used in a wide range of applications, mainly in the food, dairy, textile, metallurgy and pharmaceutical industries. The feed is generally an aqueous solution containing macromolecular solutes, emulsions or suspended solids. Flux decline due to concentration polarisation and fouling presents a serious problem. To reduce this phenomenon, high cross-flow velocities are required.

The concentration of aqueous feed solutions is a typical ultrafiltration application and recirculation systems are generally used. An example of concentrating a colloidal solution with a solute concentration of 50 kg/m^3 to 200 kg/m^3 will be given. Calculate the required membrane area and pump energy both for a single-stage recirculation process and a two-stage recirculation process with cross-flow velocities of 1, 2 and 3 m/s, respectively. Membrane rejection is assumed to be 100% whilst osmotic pressures are neglected. Furthermore, the flux can be described as:

$$J = k \ln (c_g / c_b).$$

where c_g is the gel concentration (see chapter VII). The mass transfer coefficient of the solutes are related to the velocities by $k = 2\ 10^{-5}\ v^{0.75}$. The design data are listed in the table below.

TABLE   Relevant data for the calculations

feed solute conc.	c_f :	50 kg/m^3
retentate solute conc.	c_r :	200 kg/m^3
rejection	R :	100%
feed flow rate	q_f :	3.6 m^3/h (10^{-3} m^3/s)
pure water permeability	A :	7.5 10^{-6} m/s bar
gel concentration	c_g :	300 kg/m^3

6. Calculate the membrane area required and the energy consumption for a product stream of 10 m^3/h of air enriched to 30% oxygen in a single-stage process at zero recovery ($x_f \approx x_r$). The feed is air containing 21% oxygen. Composite membranes are available with polydimethylsiloxane (silicone rubber) top layer of thickness 1 μm: polydimethylsiloxane has a P_{O_2} value of 600 Barrer and a selectivity factor α_{O_2/N_2} of 2.2. The

pressure ratio is 5 (p_h = 1 bar and p_ℓ = 0.2 bar).

7. Calculate the membrane area and power consumption necessary to produce 10 m³/h of 95% N_2 in a single-stage process using asymmetric poly(phenylene oxide) membranes. The characteristics of the membrane and the process data are given in the table

TABLE . Relevant data necessary for the calculations

nitrogen feed conc.	x_f : 0.79
nitrogen retentate conc.	x_r : 0.95
selectivity	α_{O_2/N_2} : 4.2
retentate flow rate	q_r : 10 m³/h
oxygen permeability	P_{O_2} : 50 Barrer
membrane thickness	ℓ : 1 μm
upstream pressure	P_h : 10 bar
downstream pressure	P_ℓ : 1 bar

VIII.22.   Unsolved problems

1. In a complete mixed module the solute feed concentration is 10 g/l at a rate of 5 m³/h, the permeate has a concentration 1 g/l at a rate of 4 m³/h and the retentate concentration is 46 g/l at a rate of 1 m³/h. Calculate the retention, the selectivity factor, the recovery and the volume reduction.

2. Calculate the packing density (in m²/m³) of a hollow fiber module with fibers of an external diameter of 100 μm.

3. A red pepper farmer in Italy wants to prepare process water from a brackish water source with a single stage RO-unit. The source contains 3000 ppm of salt (NaCl) and the required water quality must be at least 200 ppm (i.e. the water must contain less than 200 ppm of NaCl). The required capacity is 10 m³/hour and four different modules are available.

Membrane	retention[#]	flux per module[#]
A	90 %	480 l/hour
B	95 %	320 l/hour
C	97 %	200 l/hour
D	98 %	80 l/hour

[#] Retention and flux are determined with a solution of 3000 ppm salt (NaCl) and

a pressure of 28 bar.

Develop a single-pass installation with a minimum membrane area and with a recovery of 75%. The maximum applied pressure is 42 bar. (PS. Chose first the module which meets the criteria)

4. Calculate the oxygen concentration in the permeate at various selectivities and a constant pressure ratio of $p_\ell/p_\ell = 5$ at zero recovery $(x_f \approx x_r)$. The separation factors are ; $\alpha = P_{O_2}/P_{N_2} = 2.0,\ 2.2,\ 3.0,\ 5.0$ and 10.0. The feed is air containing 21% oxygen.

5. Calculate the oxygen concentration in the permeate at various pressure ratios and a constant selectivity $\alpha = 5$ at zero recovery $(x_f \approx x_r)$. The pressure ratios are ; $p_R/p_\ell = 2.0,\ 3.0,\ 5.0,\ 10,\ 20,\ 100$ and ∞. The feed is air containing 21% oxygen.

6. A landfill produces biogas containing 40% CO_2 and 60% CH_4. The methane can be recovered and reused. For this purpose a membrane is available with a selectivity of carbon dioxide over methane of 50 and a permeabilty for CO_2 of 50 Barrer. This process can be operated in the compressor mode or in the vacuum mode.
    The pressure at the feed side p_{feed} $(= p_h)$ and the permeate side $p_{permeate}$ $(= p_\ell)$ varies as follows.

case	1	2	3	4	5	6
P_{feed} (bar)	1	2	4	5	10	20
$P_{permeate}$ (bar)	0.2	0.2	0.2	1	1	1

a. Which of the 'cases' gives the highest flux
b. Which of the cases gives the highest concentration of CO_2 in the permeate.

The energy balance of this application should be positive (i.e. the energy input should be lower than the energy value of the recovered methane stream). The heat of combustion of methane is 213 kJ/mol.

c. Calculate for case 6 in a single-stage cross-flow process the methane recovery
d. Calculate for case 6 in a single-stage cross-flow process the energy consumption and the amount of energy which has been recovered from a gas stream of 200 m³ (STP)/hour. Furthermore, the methane concentration in the retentate must be at least 90%. The effective membrane thickness is 1 µm and the efficiency of the compressor $\eta = 0.6$. The logarithmic mean concentration may be used as an average concentration at the feed side for this calculation.

7.   Gas separation with hollow fibers can be applied at very high pressures, more than 100 bar. Two configurations are possible *i)* feed at tube-side ('inside-out'), or *ii)* feed at shell side ('outside-in').

a.   Which configuration has your preference. Explain.

For the preparation of oxygen enriched air membranes can be applied with a relatively low selectivity and a high flux. Often the vacuum mode is applied in which the permeate flow rate is negligible to feed flow rate ($q_f \gg q_p$). For the preparation of 30% of oxygen enriched air frequently composite membranes are applied with a silicone rubber toplayer .

b.   Calculate the membrane area for a stream of 100 m³ (STP)/hr 30% enriched air using a cross-flow system.

oxygen feed conc. (x_{O_2})	: 0.21 (mole fraction)
nitrogen feed conc. (x_{N_2})	: 0.79 (mole fraction)
P_{O_2}	: 600 Barrer
P_{N_2}	: 280 Barrer
membrane thickness ℓ	: 1 μm
feed pressure p_h	: 1 bar
permeate pressure p_ℓ	: 0.2 bar

c.   Which flux is larger J_{O_2} of J_{N_2} ? Explain.

For this application two options are possible, pressure at feed side (I) with p_h = 5 bar and p_ℓ = 1 bar or vacuum at permeate side (II), data above
d.   Does the required membrane area change when either option is chosen.
e.   For what system (I or II) do you choose based on energy considerations (assume that efficiencies of vacuum pump and compressor are the same).
f.   Calculate the energy requirement for system I. Efficiency of compressor is 0.6.

8.   A 1% by weight albumin (Mol weight: 65000 g/mol) solution with a flow rate of 360 liter/hr must be concentrated to 10% by weight in a single-stage process. The gelation concentration of albumin is 200 kg/m³. The membranes used do completely retain the albumin. Calculate the required membrane area at a cross-flow velocity of 0.5, 1.0 and 5.0 m/s, respectively. The flux can be described by the gel polarization model while the mass transfer coefficient can be described as
$k = 2.10^{-5} \, v^{0.75}$ (m/s)

9.   An aqueous solution of 100 kg (V_o) contains 1% by weight NaCl and 1% by weight of albumin. In order to purify the protein, a complete separation between the salt and the protein must be established.This can be achieved by

diafiltration.

a. Calculate the required amount of water (V_w) necessary to reduce the NaCl concentration to 0.01 % by weight, using membranes with a protein retention $R_{protein} = 100\%$ and a 5% retention for the salt.

If, instead of albumin, an antibioticum with a molecular weight of 500 must be separated from the salt, diafiltration can be used as well. The membrane has a rejection for the antibioticum $R_{protein} = 100\%$ and again a 5% retention for the salt.

b. Calculate now the required amount of water necessary to reduce the NaCl concentration to 0.01 % by weight

c. Calculate the fraction of antibioticum (δ) which is wasted out when a membrane is employed with an antibioticum rejection of R = 90% and R = 99 %, respectively.

10. Vapour permeation is a process which may be applied to recover organic vapours from air

a. How does the solubility of toluene (vapour) and nitrogen in silicone rubber change as a function of the partial pressure (Give a drawing).

From a feed stream of 100 m^3(STP)/h of 20 vol% of toluene in air the toluene content must be reduced below 2%. Three cases can be distinghuised

	case 1	case 2	case 3
feed pressure (bar)	1	2	5
permeate pressure (bar)	0.1	0.2	1

b. In which of the three cases is the highest permeate toluene concentration obtained ?

c. Calculate the toluene flux and the membrane area for case 1 and 2
    Other prameters:
    membrane thickness :   1 µm
    selectivity :   30
    toluene permeability :9000 Barrer
    The toluene permeability may be considered as a constant and the logarithmic mean value may be used for the average toluene concentration at the feed side.

d. What is the error in the membrane area by assuming using at the feed side the step-procedure instead of the log mean value ?

11. The maximum permeate concentration which can be obtained in vapour or gas separation at a certain feed and permeate pressure under zero recover (or zero stage-cut) conditions (S —> 0).

   a. Calculate under these conditions the permeate composition for a membrane with a selectivity factor of 200 for toluene vapour in air and a pressure ratio of 10, 100, and 1000 respectively. The concentration of toluene is 0.5 vol%.
   b. In practical applications no higher pressure ratio's are used than about 10. What is your conclusion ?
   c. If the membrane has a selectivity of about 500 is then the permeate composition improved at the same pressure ratio of 10 ?

12. A single pass reverse osmosis plant is used for the desalination of seawater (3.5wt% NaCl).
   The composite membranes in this system have a salt rejection of 99.3 % and a pure water flux of 1500 l/m^2 day measured at 25 bar. The applied pressure is 55 bars and the temperature is 25°C.v 't Hoffs' law may be used to calculate the osmotic pressure.
   For this process I can choose between the following recoveries; S= 0.3; 0.4; 0.5; and 0.6.

   a. Which recovery will I choose and why ?
   b. Determine the permeate concentration at the chosen recovery.
   c. Calculate the membrane area for a small installation with a capacity of 1 m^3/hr.

13. An effluent stream of 3 m^3/h containing 7.6 g/l of sodium sulfate at 20°C is treated in a hybrid process; reverse osmosis for concentration and production of clean process water and membrane electrolysis for the conversion of sodium sulfate into sulfuric acid (15%) and caustic soda which is used for neutralisation.
   The recovery in the RO process is 92.5% and the salt rejection is R = 99.5%. A pressure of 60 bar is applied and the water permeability coefficient is L_p = 10 l/m^2.h.bar. In the membrane electrolysis process a current density is applied of i = 10 A/dm^2 and the electrical efficiency is 50%.
   a. Calculate the membrane area in the RO process
   b. Calculate the membrane area in the membrane electrolysis process.

14. Show that in case of $\alpha \gg p_h/p_l$, eq. VIII - 55 reduces to $x_p = x_f/\phi$, with $\phi = p_l/p_h$

15. Sweetening of citrus fruit can be performed by electrodialysis where citrate ions are replaced by hydroxyl ions.
   a. Give a schematic drawing of the process

b.   Calculate the membrane area and the energy consumption necessary to reduce the citrate content from 15 g/l to 7.5 g/l for a flow rate of 500 l/h. The mol. weight of citrate is 300 g/l. Other data; $E = 150$ V; $i = 100$ A/m²; current efficiency = 0.8; average resistance per compartment, $R_{comp} = 0.03$ Ω

16. Surface water with 5000 ppm NaCl must be desalted to a product quality of less than 300 ppm salt at a rate of 25 m³/h. The membranes have a rejection of 97% (at 5000 ppm and $\Delta P = 15$ bar) and a water permeability coefficient of 3.0 l/m².h.bar. Calculate for a single pass system the required membrane area and the power consumption for an applied pressure of 15 bar and 30 bar, respectively.

17. Membranes can be used for drying of compressed air. Generally about 20°C temperature difference is maintained between users temperature and dew point temperature (i.e. the temperature at which water in air is saturated).
a.   In what season do you have to remove more water, in summer (T = 25°C) or in winter (T = 0°C). The mol. weight of air is 29 g/mol.
b.   Air at 25°C has a relative humidity of 30%. Calculate the dew point.
c.   Calculate the required membrane area to reduce the relative humidity of the compressed air from 60% to 30% at a flow rate of 1 m³(STP)/h and a feed pressure of 8 bar in summer (T = 25°C) and in winter (T = 0°C). Asymmetric poly phenyleneoxide (PPO) membranes are used with a toplayer thickness of 1 μm and a $P_{H_2O} = 4000$ Barrer. (The flow of air through the membranes may be neglected).

18. Tubular nanofiltration membranes are used for the concentration of low molecular proteins. The feed contains 1 % (by weight) of proteins and this must be concentrated to 20%. The feed rate is 3.6 m³/h. The membrane has a rejection of 100% for the protein and a water permeability coefficient of 4.35 l/m².h.bar. Calculate the membrane area for a single pass recirculation system. The velocity in the recirculation system remains 2 m/s and the applied pressure is 40 bar. Concentration polarization may not be neglected. The osmotic pressure of the protein solution is given by $\pi = a\,c^n$ with n = 1.2 and a = 0.7 bar (c in weight %).

19. Nitric acid is recovered from a 316 steel etching bath with diffusion dialysis. The inlet stream contains 100 g/l nitric acid and 25 g/l iron(II)nitrate. The outlet feed concentration is 19.4 g/l of nitric acid and 22.6 g/l of iron(II)nitrate. The inlet feed and dialysate flow rates are both 250 l/h, and the inlet dialysate is pure water and the dialysate contains no iron (II)nitrate. The average nitric acid concentration at the diluate side is 44 g/l (dialysate inlet is pure water and outlet is 88 g/l). The membrane has a water permeability coefficient $L_p = 240$ l/m².day.bar.

a. Calculate the osmotic flow (use logarithmic mean values as average value for concentrations at feed side)
b. Calculate the membrane area.
c. Calculate the HNO_3 recovery.

20. Nitrogen enrichment from air for blanketing can be operated with pressure at the feed side or with vacuum at the permeate side or with a combination. The following three cases are considered:

case	I	II	III
p_{feed}	1	5	2.5
p_{perm}	0.2	1	0.5

Which of these cases operates at minimum energy consumption if 10 m³ (STP)/h of 95% nitrogen is required.
For this application membranes are applied with a selectivity of $\alpha = 4.4$ and an oxygen permeability of $P_{O2} = 16.8$ Barrer. The efficiency of the compressor and of the vacuum pump is 0.7.

21. In the treatment of biogas the Joule-Kelvin effect cannot be neglected. A biogas feed contains an equimolar mixture of methane to carbon dioxide. If a pressure of 50 bar is applied at the feed side at 30°C calculate then the recovery S at which the permeate temperature has been decreased below 0°C.(Assume that only carbon dioxide permeates through the membrane and that heat transfer is much faster than mass transfer). The Joule-Kelvin coefficient of carbon dioxide is, $\mu_{JK} = 1.2$ K/bar.
$T_r - T_f = (p_f - p_p) \ln (1 - S)$

22. A dialyzer with a membrane area of 1 m² is used to remove urea from blood. How long will take to reduce the urea concentration from an initial concentration of $c_{f,urea} = 0.3$ g/l to 0.1 g/l . The blood flow rate is 240 ml/min and the 'body' volume V = 50 liter. The overall mass transfer $k_{ov} = 3.2 \ 10^{-6}$ m/s and the dialysate flow rate is high compared to the blood flow rate.

23. Nanofiltration is used to purify a surface water that has been polluted with mainly three pesticides; bentazone (10 µg/l), lindane (14 µg/l) and dieldrin (17 µg/l). The membrane rejection for these micropollutants is 92%, 95% and 90%, respectively.
a. Calculate the maximum recovery if the total concentration of pesticides in the permeate may not exceed 5 µg/l.

b. Calculate the maximum recovery if the concentration of one component may not exceed 2 µg/l and the total concentration may not exceed 5 µg/l.

24. A RO system is applied for the desalination of brackish water. The inlet feed is $q_f = 10$ m^3/h with a concentration of 3 g/l NaCl. The recovery is 80%. Calculate the permeate concentration for a complete mixing system and a cross-flow system (plug flow at the feed side and complete mixing at the permeate side). The retentate concentation is 14.5 g/l in the complete mixing case.

25. A batch microfiltration process is employed to concentrate a cell suspension from 1% to 10% from a fermentation broth. Due to an effective backshock method the flux remains at 100 l/m^2.h. The initial fermentation volume is 0.5 m^3 and the MF membrane area is 0.5 m^2. Calculate the batch processing time assuming that the membrane has a retention of 100%.

26. A 1% protein solution (V_o = 1 m^3) is concentrated in a batch process to 1/15 of the original volume. Calculate the protein permeate concentration in a perfect mixed system and a plug flow system at the feed side. The protein retention is 99%.

27. Calculate the minimum membrane area for the two-stage process in solved problem VIII-1.

28. Calculate the minimum energy requirements in microfiltration, ultrafiltration, nanofiltration and reverse osmosis. The concentration of the solutes in the various processes are : the suspended particles in microfiltration 30 g/l   (particle weight is 1 ng (nanogram), in ultrafiltration 3 gew.% albumin (Mw = 65,000 g/mol), in nanofiltration 0.3 gew.% NaCl, and in reverse osmosis 3 gew.% NaCl, respectively. Compare the values with the heat of evaporation, ΔHvap = 40.6 kJ/mol.

29. An equimolar gas mixture consisting of components A and B   is separated by a membrane (P_A = 50 Barrer and P_B = 5 Barrer) in a complete mixed system. The feed flow rate is 10^{-4} cm^3/s. The feed pressure is 80 cmHg and the permeate pressure is 20 cmHg. The membrane thickness is 2.54 mm.
Calculate the permeate composition, the recovery and membrane area.

30. A batch pervaporation process is applied to remove butanol from a fermentation broth. A volume reduction of 13% is observed when the butanol concentration has been decreased from 6% to 0.6%. Calculate

the butanol permeate concentration.

VIII.23.   Literature

1. Huffman, E.L., and Lacey, R.E., 'Engineering and Economic Considerations in Electromembrane Processing', in Lacey, R.E., and Loeb, S., *Industrial Processing with Membranes*, Wiley-Interscience, New York, 1972, p. 39
2. Baudet, J., US Patent 3,993,816 (1976).
3. Nichols, R.W., US Patent 4,959,152 (1990).
4. Yang, M.C., and Cussler, E.L., *AIChE Journal*, 32 (1986) 1910.
5. Knops, F.N.M., Futselaar, H., and Rácz, I.G., *J. Membr. Sci.*, 73 (1992), 153
6. Blume, I., Roesink, H.D.W., and Koenhen, D.M., Preprints of the Aachener Membran Kolloquium, 1995, p.53.
7. Spillman, W., *Chemical Engineering Progress*, January 1989, p.41
8. Hwang, S.T., and Kammermeyer, K., *Membranes in separations*, John Wiley, New York, 1975
9. Rautenbach, R., and Albrecht, R., *Membrane Processes*, John Wiley, New York, 1989
10. Nitto Denko Technical Report, The 70th Anniversary Special Issue, 1989
11. Ohlrogge,K, Peinemann, K.-V., Wind, J, and Behling, R.-D., *Sep. Sci.,Techn.*, 25 (1990) 1375
12. Wijmans, J.G., Baker, R.W., and Athayde, A.L., Pervaporation: Removal of organics from water and organic/organic separations, in Crespo, J.G., and Böddeker, K.W., Membrane Processes in Separation and Purification, Kluwer Academic Publishers, Dordrecht, Netherlands, 1995, p.283
13. Toray, Technical Bulletin
14. Saltonstall, C.W., and Lawrence, R.W., *Desalination*, 42 (1982) 247
15 Weller, S., and Steiner, W.A., *Chem. Eng. Progr.*, 46 (1950) 585
16. Weller, S., and Steiner, W.A., *Appl. Pol. Sci.*, 21 (1950) 279
17. Hogsett, J.E., and Mazur, W.H., *Hydrocarbon Processing*, 62, aug. 1983, p. 52
18. Korngold, E., *Electrodialysis: membranes and mass transport*, in 'Synthetic Membrane Processes, Belfort.G. (Ed.), Academic Press, New York, 1984, p. 192
19. Michaels, A.S., *Trans. Amer. Soc. Artif. Intern. Organs*, 12 (1966) 387
20. Klein, E., Ward, R.A., and Lacey, R.E., *Membrane Processes - dialysis and electrodialysis*, in 'Handbook of Separation Process Technology', Rousseau, R.W., John Wiley, New York, 1987
21. Mulder, M.H.V., *Energy requirements in membrane separation*

processes, in Crespo, J.G., and Böddeker, K.W., Membrane Processes in Separation and Purification, Kluwer Academic Publishers, Dordrecht, Netherlands, 1995, p.445

Ternary phase diagram (for problems of chapter III)

Polymer

Solvent

Nonsolvent
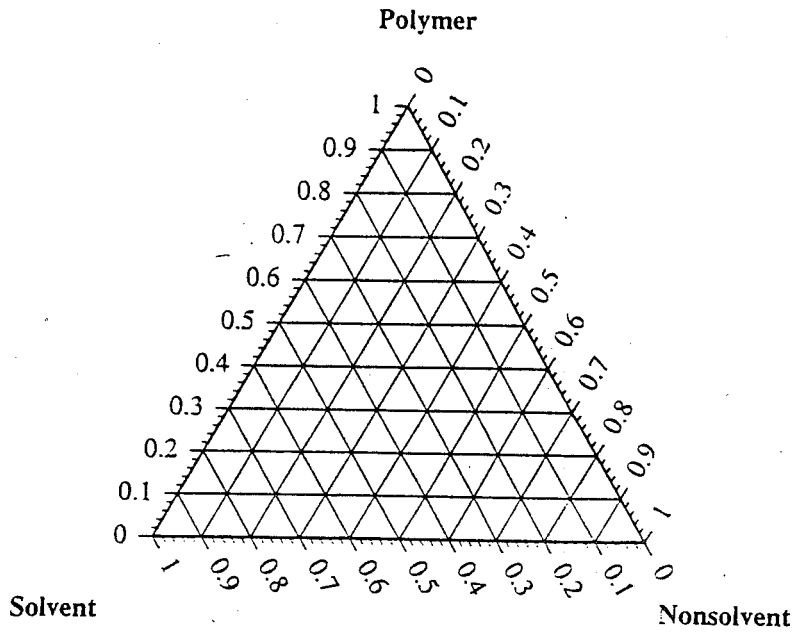
Appendix 1.

Physical properties of various organic solvents;
Molecular weight (M_w); boiling point (B_p); molar volume (V_m); density (ρ); surface tension (γ); dynamic viscosity (η).

	M_w (g/mol)	B_p (°C)	V_m [#] (cm³/mol)	ρ [#] (g/cm³)	γ [§] (mN/m)	η [§] (mPa.s)
water	18.0	100.0	18.1	0.997	71.99	0.890[1])
methanol	32.0	65.2	40.7	0.791	22.07	0.544
ethanol	46.1	78.5	58.7	0.789	21.97	1.074
n-propanol	60.1	97.4	75.2	0.804	23.32	1.945
n-butanol	74.1	117.2	92.0	0.810	24.93	2.554
hexane	86.2	69.0	131.6	0.660	17.89	0.300
heptane	100.2	98.4	147.5	0.684	19.65	0.387
octane	114.3	125.7	163.5	0.703	21.14	0.508
cyclohexane	84.2	80.7	108.8	0.779	24.65	0.894
benzene	78.1	80.1	89.4	0.879	28.22	0.604
toluene	92.2	110.6	106.9	0.867	27.93	0.560
chloroform	119.4	61.7	80.7	1.483	26.67	0.537
1,2 dichloroethane	98.9	83.5	80.1	1.235	31.86	0.779
acetone	58.1	56.2	73.5	0.790	23.46	0.306
tetrahydrofurane	72.1	67	81.1	0.889	26.00	0.456
ethyl acetate	88.1	77.1	97.9	0.900	23.39	0.423
dimethylformamide	73.1	149	77.1	0.948	35.00	0.794

Values are taken from various sources including: Binas, Wolters-Noordhoff, Groningen; Morrison & Boyd, Organic Chemistry, Allyn and Bacon, Boston, 1966; Handbook of Chemistry and Physics, CRC Press, 76th Edition, 1995-1996.

\# at 20°C

§ at 25°C

1) at 20°C: η_{water} = 1.0 mPa.s

Appendix 2.

Antoine constants of various organic solvents[§]

	Bp (°C)	A	B	C
acetone	55.9	6.24204	1210.59	229.664
1-butanol	117.2	6.96290	1558.19	196.881
chloroform	60.9	6.07955	1170.97	226.232
cyclohexane	80.1	5.97636	1206.47	223.136
1,2-dichloroethane	78.9	6.15020	1271.25	222.927
dimethylformamide	220.0	6.23340	1537.78	210.390
ethanol	78.5	7.23710	1592.86	226.184
ethyl acetate	76.9	6.22669	1244.95	217.881
hexane	68.9	6.00266	1171.53	224.366
heptane	98.9	6.01876	1264.37	216.640
methanol	65.2	7.20587	1582.27	239.726
octane	125.6	6.05632	1358.80	209.855
1-propanol	97.4	6.86906	1437.69	198.463
toluene	110.6	6.07577	1342.31	219.187
tetrahydrofurane	55.3	6.12005	1202.29	226.254
water	100.0	7.19621	1730.63	233.426

[§] Values taken from J. Gmehling, and B. Kolbe, Thermodynamik, Thieme verlag, Stuttgart, 1988

Antoine equation :

$$\log p° = A - \frac{B}{T + C}$$

$p°$ in kPa and T in °C

Answers to exercises: Solved problems

Chapter I

1 The retention is given by

$$R = \frac{c_{sucr,feed} - c_{sucr,perm}}{c_{sucr,feed}} = 1 - \frac{c_{sucr,perm}}{c_{sucr,feed}} = 1 - \frac{150}{30,000} = 0.995$$

or R = 99.5 %.

The selectivity factor $\alpha_{sucr/water}$ is given by

$$\alpha_{s/w} = \frac{c_{sucr,perm} / c_{water,perm}}{c_{sucr,feed} / c_{water,feed}} = \frac{150/999,850}{3/97} = 4.85 \; 10^{-3} \text{ or } \alpha_{w/s} = 206$$

For liquid mixtures, consisting of a solvent and a solute it is more convenient to express the selectivity in terms of the retention R towards the solute, because the solvent molecules pass freely through the membrane. $\alpha_{w/s} = 206$ is not a good way to indicate the retention of a solute.

2. The retention is given by

$$R = 1 - \frac{c_{O_2,perm}}{c_{O_2,feed}} = 1 - \frac{25}{80} = 0.6875$$

or R = 68.75%

The selectivity factor $\alpha_{O2/N2}$ is given by

$$\alpha_{O_2/N_2} = \frac{75/25}{20/80} = 12$$

The performance of a dense membrane in which components are not retained but permeate with different velocities, such as in gas separation, is better expressed by the selectivity factor than by the retention.

Chapter II

1. In many gas separation applications very high pressures are employed, up to or more than 100 bar. It is important to know whether the Tg is changing under these conditions.
Upon increasing the pressure the volume of a polymer reduces in general. Since the free volume will decrease as well it is expected that the glass transition temperature increases. The fractional free volume is given by

$$v_{f,T} = v_{f,Tg} + \Delta\alpha (T - T_g)$$

The compressibility κ is defined as

$$\kappa = -\frac{1}{V}\left(\frac{\partial V}{\partial P}\right)_T$$

At constant temperature (T_g at $p = 1$ bar) the fractional free volume at pressure p is given by

$$v_{f,P} = v_{f,P=1} + \alpha_f (T - T_g) - \kappa_f P$$

(In fact the 'standard' glass transition should be taken here at zero pressure but in general glass transitions are always taken at 1 bar ($=$ 1 atmosphere) pressure). Under special conditions,

$$v_{f,P} = v_{f,P=1} \Rightarrow \alpha_f (T - T_g) = \kappa_f P$$

Differentiating with respect to pressure results in

$$\left(\frac{\partial T_p}{\partial P}\right)_{v_f} = \frac{\kappa_f}{\alpha_f} = \frac{1.5 \ 10^{-5}}{4.8 \ 10^{-4}} = 0.031 \ °C/bar$$

This implies that at a pressure of 100 bar the T_g has been increased with 3.1 °C to Tg = 103.1 °C. It is clear from this that pressure is not an important factor in plasticisation (see for more details, Sperling, L.H., Introduction to Physical Polymer Science, John Wiley, 1986.

Chapter III

1.
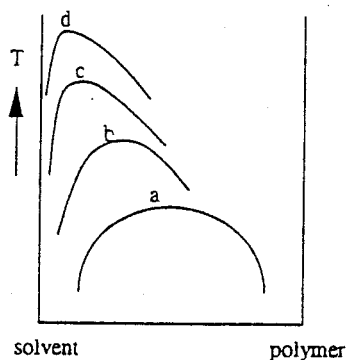
solvent   polymer

Binary system : solvent (1) and polymer (2)
The critical point is characterised by :

$$\frac{\partial^2 \Delta G_m}{\partial \phi_2^2} = \frac{\partial \Delta \mu_1}{\partial \phi_2} = 0 \qquad \text{and}$$

$$\frac{\partial^3 \Delta G_m}{\partial \phi_2^3} = \frac{\partial^2 \Delta \mu_1}{\partial \phi_2^2} = 0$$

The solvent activity can given as a function of the polymer volume fraction

$$\ln a_1 = \frac{\Delta \mu_1}{RT} = \ln(1 - \phi_2) + \left(1 - \frac{V_1}{V_2}\right)\phi_2 + \chi \phi_2^2 \quad \Rightarrow$$

$$\frac{\partial \Delta \mu_1}{\partial \phi_2} = -\frac{1}{1 - \phi_{2,c}} + 1 - \frac{V_1}{V_2} + 2\chi \phi_{2,c} = 0 \quad \Rightarrow \quad (*)$$

$$\frac{\partial^2 \Delta \mu_1}{\partial \phi_2^2} = -\frac{1}{(1 - \phi_{2,c})^2} + 2\chi = 0 \quad \Rightarrow \quad 2\chi = \frac{1}{(1 - \phi_{2,c})^2} = \frac{1}{(\phi_{1,c})^2}$$

Substitution into (*) gives

$$-\frac{1}{\phi_{1,c}} + 1 - \frac{V_1}{V_2} + \frac{1 - \phi_{1,c}}{\phi_{1,c}^2} = 0$$

with $\frac{V_1}{V_2} = \frac{1}{n} \quad \Rightarrow \quad -\frac{\phi_{1,c}}{(\phi_{1,c})^2} + 1 - \frac{1}{n} + \frac{1 - \phi_{1,c}}{\phi_{1,c}^2} = 0 \quad \Rightarrow$

$$\left(\frac{1}{n} - 1\right)\phi_{1,c}^2 + 2\phi_{1,c} - 1 = 0$$

This is a quadratic equation in $\phi_{1,c}$ and the solution of this equation is

$$\phi_{1,c} = \frac{-2 \pm \sqrt{4 - 4\left(\frac{1}{n} - 1\right)(-1)}}{2\left(\frac{1}{n} - 1\right)} = \frac{-2 + \sqrt{\frac{4}{n}}}{2\left(\frac{1}{n} - 1\right)} = \frac{2\left(\sqrt{\frac{1}{n}} - 1\right)}{2\left(\frac{1}{n} - 1\right)} = \frac{1}{\left(\sqrt{\frac{1}{n}}\right) + 1}$$

$$\phi_{2,c} = 1 - \phi_{1,c} = \frac{1 + \sqrt{n}}{1 + \sqrt{n}} - \frac{\sqrt{n}}{1 + \sqrt{n}} = \frac{1}{1 + \sqrt{n}}$$

$n = 10 \quad \Rightarrow \phi_{2,c} = 0.24$

$n = 100 \quad \Rightarrow \phi_{2,c} = 0.09$

$n = 1000 \quad \Rightarrow \phi_{2,c} = 0.03$

It is clear that the composition of the critical point is shifted to solvent axis with increasing n (increasing mol. weight).

Chapter IV

1.a The saturation pressure of cyclohexane at 34 °C can be obtained from the Antoine equation.

$$\log p^\circ = A - \frac{B}{T + C}$$

with $A = 5.97636$, $B = 1206.47$, $C = 223.136$ (see appendix 2) and $T = 34$ °C.

$\Rightarrow \log p^\circ = 1.284$ or $p^\circ = 19.25$ kPa = 192.5 mbar.

$p_r = 0.78 \quad \Rightarrow \quad p = 0.78 \times 192.5$ mbar = 150.1 mbar.

b. A sudden increase in oxygen flux which does not increase further upon decreasing the vapour pressure indicates the existence of *one* pore size.

c. From the Kelvin eq. we have

$$r_k = - \frac{2 \gamma V_m}{R T \ln p_r} \quad \Rightarrow$$

$$r_k = - \frac{2 \cdot 20.10^{-3} \ (J/m^2) \cdot 108.8 \cdot 10^{-6} \ (m^3/mol)}{8.31 \ (J/mol \cdot K) \cdot 307 \ (K) \cdot (-0.248)} = 6.9 \ 10^{-9} \ m = 6.9 \ nm$$

The pore radius (r_p) can be obtained now

$$r_p = r_k + t = 6.9 + 0.5 = 7.4 \ nm$$

2. The porosity per cm^2 is $n.\pi.r^2$ where the pore radius is expressed in cm^2.

The flux is given by

$$J = \frac{\varepsilon \ (-) \ r^2 \ (m^2)}{8 \ \eta \ (N \cdot s /m^2) \ \tau \ (-)} \frac{dP \ (N/m^2)}{dx \ (m)}$$

The porosity and the water flux at 1 bar can now be calculated and the values are given in the table.

pore radius(μm)	number of pores	ε (%)	J $(l/m^2.h)$
2.5	$5.0 \ 10^5$	9.8	$1.4 \ 10^6$
0.5	$1.3 \ 10^7$	10.2	$57.6 \ 10^3$
0.1	$3.2 \ 10^8$	10.1	2273
0.025	$4.0 \ 10^9$	7.8	110

Chapter V

1. From the time-lag method the following result is obtained in which p_2, the permeate pressure, is given as a function of time
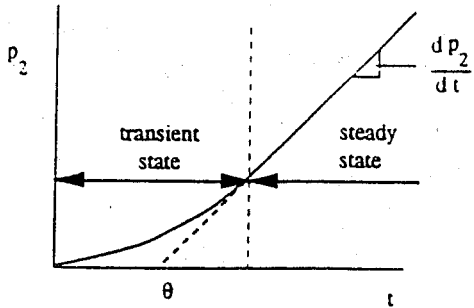
For the steady-state the flux or pressure increase can be given by the following equation

$$p_2 = a.t - b$$

in which

a : slope $= \left(\dfrac{dp_2}{dt}\right)$

b: intercept $= p_1$

extrapolation $p_2 \Rightarrow 0$ gives $t = \theta$
The time-lag θ can now be obtained from

$$\theta = \frac{b}{a} = \frac{p_1}{\left(\dfrac{dp_2}{dt}\right)}$$

The diffusion coefficient is given by

$$D = \frac{\ell^2}{6\theta}$$

p_1 (CO_2) (mmHg)	$d\,p_2/dt$ (mmHg/s)	θ (s)	D (cm²/s)
1000	34.5	29.0	5.2 10⁻⁸
2000	81.6	24.5	6.1 10⁻⁸
3000	130.4	23.0	6.5 10⁻⁸
4000	190.5	21.0	7.1 10⁻⁸
5000	256.4	19.5	7.7 10⁻⁸

From the results it can be seen that the diffusion coefficient is dependent on the concentration of CO_2 in the polymer, D increases with increasing upstream pressure.

b. For helium the diffusion coefficient is constant and the time-lag θ is independent on feed pressure. Consequently, the following curves are obtained;
curve 1 : high upstream pressure
curve 2 : low upstream pressure
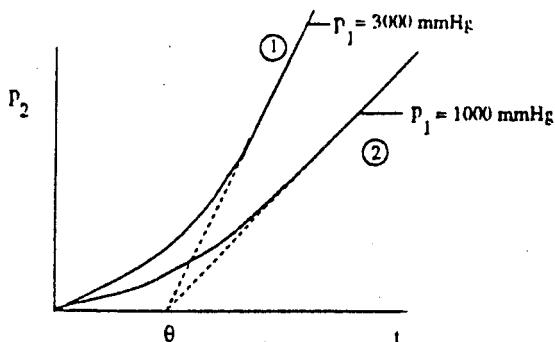
2. The water flux can be obtained by the Hagen-Poissueille equation

$$J = \frac{\varepsilon\ (-)\ r^2\ (m^2)}{8\ \eta\ (N\ .\ s\ /m^2\ )\ \tau\ (-)} \frac{dP\ (N/m^2)}{dx\ (m)}$$

Microfiltration :

$$J = \frac{0.6 * (2.0\ 10^{-7})^2}{8 * 10^{-3} * 1.2} \frac{* 10^5}{10^{-4}} = 2.5\ 10^{-3}\ m/s = 9000\ l/m^2.h$$

Ultrafiltration :

$$J = \frac{0.02 * (2.0\ 10^{-9})^2}{8 * 10^{-3} * 1.2} \frac{* 5\ .\ 10^5}{10^{-4}} = 4.2\ 10^{-6}\ m/s = 15\ l/m^2.h$$

3a. The fractional free volume v_f is calculated by

$$v_f = \frac{V - V_o}{V}$$

where V is the specific volume (= $1/\rho$) and V_o is the volume occupied by the molecules. V_o can be obtained from the Van der Waals volume (V_w):

$V_o = 1.3\ V_w.$

The free volume fraction v_f can be calculated now:

polymer	ρ (g/cm^3)	V (cm^3/g)	V_w (cm^3/mol)	M_w (segm) (g/mol)	V_w (cm^3/g)	V_o (cm^3/g)	v_f[#] (-)	P_{O2} (Barrer)
PE	0.854	1.171	20.46	28.0	0.721	0.950	0.189	15.7
PIB	0.910	1.099	40.90	57.0	0.718	0.933	0.151	2.1
PVDF	1.670	0.599	25.56	64.0	0.399	0.519	0.134	0.39
PVDC	1.780	0.562	38.03	99.0	0.384	0.499	0.112	

[#] The v_f values given in the reference are somewhat different than the one calculated here.

It can be seen from the calculated values that the permeability is related to the fractional free volume or in fact to the reciprocal of the fractional free volume. i.e. the permeability decreases as the fractional free volume decreases.

b. The permeability can be related to the fractional free volume according to

$P = A \exp(-B/v_f)$ where A and B are constants.

Plotting ln P versus $1/v_f$ gives a straight line. From linear regression using the P_{O2} and $1/v_f$ values of PE, PIB, and PVDF) the permeability in PVDC can be estimated $\Rightarrow P_{O2}$ in PVDC = 0.036 Barrer. The value given in the reference is somewhat lower (P_{O2} = 0.0013 Barrer) but since PE, PVDF and PVDC are semi-crystalline this estimate is fairly good.

Chapter VI

1. The osmotic pressure can be calculated by van 't Hoffs law, assuming ideal conditions. This gives the following result for the various solutes:

NaCl :
$$\pi = \frac{2 * 30.10^3 \ (g/m^3) * 8.31 \ (Nm/mol.K) * 298 \ (K)}{58.45 \ (g/mol)} = 2.54 \ 10^6 \ N/m^2 = 25.4 \ bar$$

Albumin:
$$\pi = \frac{30.10^3 \ (g/m^3) * 8.31 \ (Nm/mol.K) * 298 \ (K)}{65000 \ (g/mol)} = 0.01 \ 10^5 \ N/m^2 = 0.01 \ bar$$

Suspension:
$$\pi = \frac{30.10^{12} \ (-/m^3) * 8.31 \ (Nm/mol.K) * 298 \ (K)}{6.02.10^{23} \ (-/mol)} = 1.2 \ 10^{-7} \ N/m^2 = 1.2 \ 10^{-12} \ bar$$

2. The permeability coefficient of 'inert' gases such as hydrogen, helium, nitrogen, methane (characterised by a low critical temperature) are generally not dependent on applied pressure, neither for elastomers nor for many glassy polymers. Hence it can not be deduced from these results whether the material is glassy or an elastomer.

b. Diffusion of a gas through a polymeric membrane is an activated process that can be described by an Arrhenius type of equation:

$$P = P_o \exp\left(\frac{-E_{act}}{R \ T}\right)$$

Hence, $\ln P = \ln Po - E_{act}/RT$ and plotting lnP vs 1/T gives a straight line with a slope: slope = $- E_{act}/R$
Slope = $- 5112 \Rightarrow E_{act} = -$ slope * R = 42.5 kJ/mol.
The system is methane/polyethylene and the values were obtained from Waack et al, Ind.Eng.Chem., 47(1955)2524.
Diffusion coefficient may be described in the same way and it is not so obvious to draw straightforward conclusions from the values. For a given polymer, the activation energy is smaler in the glassy state than in the rubbery state (see e.g. Kumins and Roteman, J.Pol.Sci., 55 (1961) 683 or Koros and Paul, J.Pol.Sci.Polym.Phys.Ed. 16(1978) 2171)

3. The facilitation factor has been defined as

$$F = 1 + \frac{\alpha K'}{1 + K'}$$

The total flux with carrier has been given eq. VI - 88

$$J_A = \frac{D_A}{\ell} c_{A_0} + \frac{D_{AC}}{\ell} \left(\frac{K \bar{c} c_{A_0}}{1 + K c_{A_0}} \right)$$

The first term on the right hand side gives the solute flux without carrier. F can now be calculated

$$F = \frac{\frac{D_A}{\ell} c_{A_0} + \frac{D_{AC}}{\ell} \left(\frac{K \bar{c} c_{A_0}}{1 + K c_{A_0}} \right)}{\frac{D_A}{\ell} c_{A_0}} = 1 + \frac{D_{AC} \bar{c}}{D_A c_{A_0}} \left(\frac{K c_{A_0}}{1 + K c_{A_0}} \right) = 1 + \frac{\alpha K'}{1 + K'}$$

b.
α and K' can now be calculated

$$\alpha = \frac{D_{AC} \bar{c}}{D_A c_{A_0}} = \frac{2.52 \ 10^{-6} \ cm^2/s \ * \ 8.32 \ M}{2.52 \ 10^{-6} \ cm^2/s \ * \ 8.46 \ 10^{-2} \ M} = 98.3$$

$$K' = K . c_{A.0} = 3.74 \ 10^2 \ M^{-1} \ * \ 8.46 \ 10^{-2} \ M = 31.6$$

and

$$F = 1 + \frac{98.3 \ * \ 31.6}{1 + 31.6} = 96.3$$

In this example it is assumed that the diffusion coefficients of the solute and carrier solute complex are equal this in contradiction of the work of Way and Noble. (Maybe this is not such a good example, anyway).

4. The number of fibers can be obtained when the membrane area is known since

$$A = n \ \pi d L$$

in which n = number of fibers, d = fiber diameter and L = module length (It should be clear from the question that the feed is at the shell side of the fiber since only the outside diameter is given. Furthermore, RO hollow fiber modules for seawater desalination are generally of this type.
The membrane area can be obtained from

$$A = q_p / J$$

In which J is the flux and q_p is the permeate flow rate (= 5 m^3/day). J can be calculated if the osmotic pressure is known, since

$$J = L_p (\Delta P - \Delta \pi)$$

The osmotic pressure is 25.4 bar (see solved problem VI.1) $\Rightarrow$

$J = 1.6 \ 10^{-8} \ (m^3/m^2.s.bar) \ (60 - 25.4) \ (bar) = 5.5 . \ 10\text{-}7 \ m^3/m^2.s = 2.0 \ l/m^2.h = 48 \ l/m^2.day$

$A = \dfrac{q_p}{J} = \dfrac{5000 \ (l/day)}{48 \ (l/m^2.day)} = 104.2 \ m^2$

The number of fibers can now be calculated

$A = n \pi d L \Rightarrow n = \dfrac{A}{\pi d L} = \dfrac{104.2 \ m^2}{3.14 * 10^{-4} \ (m) * 1 \ (m)} = 3.3 \ 10^5$

Flux per fiber is

$q_{fiber} = J * A_{fiber} = 48 \ l/m^2.day * 3.14 \ 10^{-4} \ (m^2) = 0.015 \ l/day = 15 \ ml/day$

Chapter VII

1. The concentration polarization modulus can be obtained from eq. VII - 9

$$\dfrac{c_m}{c_b} = \exp\left(\dfrac{J}{k}\right)$$

Here J is known and k can be calculated from the mass transfer correlations. First we need to find out whether the flow is laminar or turbulent.
For $v = 0.5$ m/s we find for the Reynolds number

$$Re = \dfrac{\rho \, v \, d}{\eta} = \dfrac{10^3 \ (kg/m^3) * 0.5 \ (m/s) * 6.10^{-3} \ (m)}{1.2.10^{-3} \ (Pa.s \ or \ kg.m.s/s^2m^2)} = 2500$$

For $v = 4.5$ m/s $\Rightarrow Re = 22500$

For both velocities the flow regime is turbulent and the following equation can be used to determine k

$$k = \dfrac{D}{d_h} * 0.04 * Re^{0.75} * Sc^{0.33}$$

The Schmidt number is

$$Sc = \dfrac{\eta}{\rho D} = \dfrac{1.1 \ 10^{-3} \ (kg/m.s)}{10^3 \ (kg/m^3) * 4.2 \ 10^{-10} \ (m^2/s)} = 2619$$

For $v = 0.5$ m/s the mass transfer coefficient k becomes

$$k = \dfrac{4.2 \ 10^{-10}}{6 \ 10^{-3}} * 0.04 * (2500)^{0.75} * (2619)^{0.33} = 1.3 \ 10^{-5} \ m/s$$

and $v = 4.5$ m/s $\Rightarrow k = 6.9 \ 10^{-5}$ m/s. The conc. pol. modulus can now be calculated. For $v = 0.5$ m/s

$$\frac{c_m}{c_b} = \exp\left(\frac{J}{k}\right) = \exp\left(\frac{9.3\ 10^{-6}}{1.3\ 10^{-5}}\right) = 2.0$$

and for $v = 4.5$ m/s $\Rightarrow c_m/c_b = 1.2$

b. The flux at 10 bar can be calculated by

$$J_v = L_p\ (\Delta P - \Delta \pi)$$

First the water permeability coefficient L_p must be determined. This value is a membrane property and independent on flow velocity. For $v = 0.5$ m/s the osmotic pressure is given by

$$\Delta \pi = a\ c_m^b = 0.05 * 100^{1.1} = 7.9\ \text{bar}$$

for $v = 4.5$ m/s $\Rightarrow \Delta \pi = 4.5$ bar

and

$$L_p = \frac{J}{\Delta P - \Delta \pi} = \frac{38.3\ (l/m^2.h)}{20 - 7.9\ (bar)} = 3.16\ (l/m^2.h.bar)$$

The flux at 10 bar can now be calculated,

$v = 0.5$ m/s $\quad J = 3.16\ (10 - 7.9) = 6.64\ l/m^2.h.bar$
$v = 4.5$ m/s $\quad J = 3.16\ (10 - 4.5) = 17.38\ l/m^2.h.bar$

c.   The concentration polarization modulus will not remain constant. Since the flux is lower at 10 bar the concentration polarization will be lower as well and the assumption is not complete correct.

2.   The flux can be described the following equation in which the total resistance can be considered as two resistances in series, the cake resistance R_c and the membrane resistance R_m.

$$J = \frac{\Delta P}{\eta\ (R_m + R_c)}$$

The membrane resistance can be determined from

$$J = \frac{1}{R_m \cdot \eta} \Delta P \quad \text{or} \quad R_m = \frac{\Delta P}{J \cdot \eta} = \frac{3\ 10^5\ (N/m^2)}{\frac{0.210}{3600}\ (m/s) * 10^{-3}\ (Ns/m^2)} = 5.1\ 10^{12}\ m^{-1}$$

The cake resistance Rc is now the only unknown and can be obtained from the oil-emulsion experiment

$$R_c + R_m = \frac{\Delta P}{\eta \cdot J} = \frac{4.5\ 10^5}{10^{-3} * \frac{0.035}{3600}} = 4.6\ 10^{13}\ m^{-1}$$

or $R_c = 46\ 10^{12} - 5.1\ 10^{12} = 40.9\ 10^{12}\ m^{-1}$

The thickness of the cake can be calculated according to

$$\delta_{cake} = \frac{R_c}{r_c} = \frac{40.9 \; 10^{12} \; (m^{-1})}{1.5 \; 10^{18} \; (m^{-2})} = 27.3 \; 10^{-6} \; m = 27.3 \; \mu m$$

Chapter VIII

1. For counter-current flow in dialysis we can apply eq. VIII-86

$$\frac{\left(c_{f,i}^{in} - c_{f,i}^{out}\right)}{\left(c_{f,i}^{in} - c_{d,i}^{in}\right)} = \frac{1 - \exp\left[-\dfrac{k_{i,ov} \; A}{q_f}\left(1 + \dfrac{q_f}{q_d}\right)\right]}{\dfrac{q_f}{q_d} + 1}$$

Since $q_d \gg q_f \Rightarrow \dfrac{q_d}{q_f} \approx 0$ and $c_{d,i} \approx 0$

Substitution into eq. VIII - 86 gives

$$\frac{\left(c_{f,i}^{in} - c_{f,i}^{out}\right)}{\left(c_{f,i}^{in}\right)} = 1 - \exp\left[-\frac{k_{i,ov} \; A}{q_f}\right]$$

or $\quad 1 - \dfrac{c_{f,i}^{out}}{\left(c_{f,i}^{in}\right)} = 1 - \exp\left[-\dfrac{k_{i,ov} \; A}{q_f}\right]$

giving finally $\quad c_{f,i}^{out} = c_{f,i}^{in} \cdot \exp\left[-\dfrac{k_{i,ov} \; A}{q_f}\right]$

2. The selectivity is given by

$$\alpha_{CO_2/N_2} = \frac{P_{CO_2}}{P_{N_2}} = \frac{81}{5.3} = 15.3$$

while the pressure ratio $\phi = p_h/p_l = 5$

The permeate composition can be obtained from eq. VIII- 23.

$$B = 0.5\left[1 + \frac{5}{14.3} + 5 * 0.2\right] = 1.175$$

and

$$x_{p,CO_2} = 1.175 - \left[(1.175)^2 - \frac{15.3 * 5}{14.3} \; 0.2\right]^{0.5} = 0.60$$

Now from the mass balances the carbon dioxide recovery can be calculated

$$q_f = q_p + q_r \Rightarrow q_r = 10^4 - q_p$$

$x_{f,5362} \cdot q_f = x_{p,CO2} \cdot q_p + x_{r,CO2} \cdot q_r \Rightarrow 0.5 * 10^4 = 0.6 \, q_p + 0.2 * (10^4 - q_p) \Rightarrow$

$q_p = 75(X) \, m^3/h$

The carbon dioxide recovery can now be calculated

$$S_{CO_2} = \frac{0.6 * 7.5 \, 10^3}{0.5 * 10^4} = 0.9$$

The carbon dioxide flux can be calculated according to

$J_{CO_2} = P_{CO_2}/\ell \, (p_h \cdot x_{r,CO2} - p_\ell \cdot x_{p,CO2}) = 81.10^{-10}/10^{-4} [190 * 0.2 - 38 * 0.6] =$

$1.23 \, 10^{-3} \, cm^3 \, (STP)/cm^2.s$

3. The flux is given by

$$J = - \frac{1}{A} \frac{dV}{dt} \quad \text{or} \quad \frac{dV}{dt} = - A \, J$$

integration to time t gives

$$\int_{V_0}^{V_t} dV = - A \, J \int_{t=0}^{t=t} dt$$

or $V_t - V_0 = - A \, J \, t \Rightarrow 100 - 1000 = - (1.5 * 100 * t) \Rightarrow t = 900/150 = 6 \, hours$

4. 　　　A simplified flow diagram is given in the figure below.
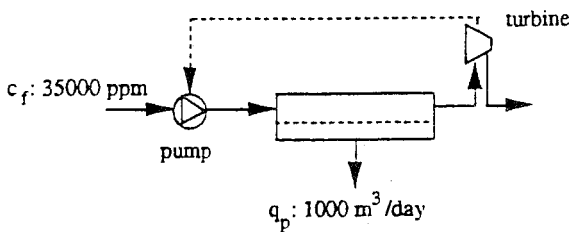
Flow diagram for a 1000 m^3/day single-stage reverse osmosis seawater desalination plant.

The flux is given at 15 bar, 16°C and 1500 ppm NaCl so that the water permeability coefficient A must be calculated under these conditions. The volume flux is given by

$J = A \, (\Delta P - \Delta \pi)$

with

$\Delta\pi = RT\,\Delta c\,n/M = (2402*1.5*1000*2) / 58.5 = 1.23\ 10^5\ Pa = 1.23\ bar$

and

$A = 54.2 / (15 - 1.23) = 3.9\ l\ m^{-2}\ h^{-1}\ bar^{-1}$

The retentate concentration c_r can be calculated using eq. VIII - 23, i.e.

$c_r = c_f\ (1 - S)^{-R}$

while the average permeate concentration c_p may be obtained from eq. VIII - 27, i.e.

$$\bar{c}_p = \frac{c_f}{S}\left[1 - (1 - S)^{1-R}\right]$$

$\Rightarrow$ c_p = 208 ppm and c_r = 49,910 ppm.

indicating that the desired product quality (c_p < 250 ppm) is obtained.

From the retentate and feed concentrations, the average osmotic pressure on the feed side can be calculated:

$\Delta\pi_f = 28.7\ bar$

$\Delta\pi_r = 40.9\ bar$

Using an average osmotic pressure $\Delta\pi = 34.8\ bar$, the flux at 55 bar can now be calculated:

$\Rightarrow$ $J = 79\ l\ m^{-2}\ h^{-1}$

while the module flux is

$\Rightarrow$ $J_{module} = 237\ l\ /\ h = 5.7\ m^3\ /\ day$

This means that 1000 / 5.7 $\approx$ 176 modules with a total membrane area of 528 m^2 are required.

Energy consumption

The energy consumption is mainly determined by the high-pressure feed pump. The flow rate to be pumped is:

$q_f = q_p\ /\ S = 3300\ m^3/day$

$\Rightarrow$ $E_{pump} = \Delta P \cdot q_f\ /\ \eta_{pump} = 323\ 10^3\ J/s = 323\ kW$

Part of this energy is recovered by means of a turbine (the pressure losses that actually occur are not considered here):

$$\Rightarrow E_{turbine} = \Delta P \cdot q_r / \eta_{turbine} = 195 \text{ kW}$$

5.
Single-stage recirculation system
The schematic flow diagram for the single-stage unit is given in the figure below.
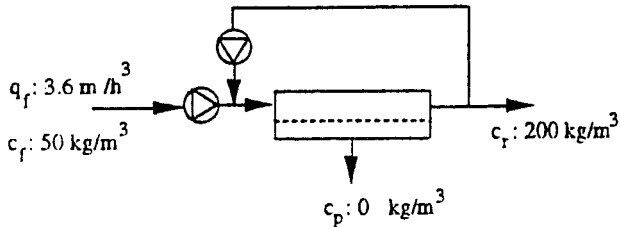
Flow diagram for a single-stage unit.

The required membrane area (A_{area}) can be calculated from

$$A_{area} = q_p / J$$

with the permeate flow rate (q_p) and the retentate flow rate (q_r) being obtained from the volume balance and mass balance.

Mass balance

$$q_f \cdot c_f = q_r \cdot c_r \qquad (c_p = 0)$$

$$\Rightarrow q_r = 0.9 \text{ m}^3/h$$

Volume balance

$$q_f = q_r + q_p$$

$$\Rightarrow q_p = 2.7 \text{ m}^3/h = 75 \ 10^{-4} \text{ m}^3/s$$

We can now calculate k, J and A for various cross-flow velocities (see table).

TABLE. Calculated values of the membrane area A, flux J and mass transfer coefficient k for various cross-flow velocities in a single-stage system

v (m/s)	k 10^5 (m/s)	J 10^5 (m/s)	A_{area} (m²)
1	2.0	0.8	94
2	3.4	1.4	54
3	4.6	1.9	39

Two-stage recirculation system

The flow diagram for the two-stage unit is given in the figure below.

q_f: 36 m³/h
c_f: 50 kg/m³
c_r: 200 kg/m³
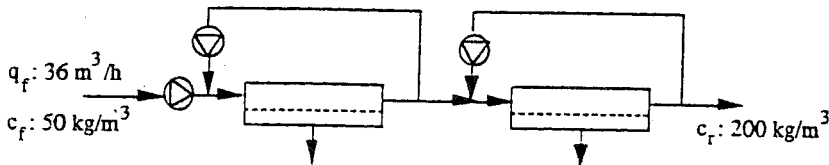
Flow diagram of a two-stage recirculation unit

From this diagram we can write the volume balances as:

$$q_{f,1} = q_{r,1} + q_{p,1}$$

$$q_{f,2} = q_{r,2} + q_{p,2}$$

and since

$$q_{r,1} = q_{f,2} \quad \text{and} \quad c_{r,1} = c_{f,2} , \quad \text{one obtains}$$

$$q_{f,1} = q_{r,2} + q_{p,1} + q_{p,2}$$

$$q_{f,1} \cdot c_{f,1} = q_{r,2} \cdot c_{r,2} \qquad (c_{p,1} = c_{p,2} = 0)$$

$$\Rightarrow q_{r,2} = 0.9 \text{ m}^3/\text{h}$$

If we assume that the permeate flow in both stages is the same, then

$$\Rightarrow q_{p,1} = q_{p,2} = 1.35 \text{ m}^3/\text{h} = 3.75 \cdot 10^{-4} \text{ m}^3/\text{s}$$

$$\Rightarrow q_{r,1} = 2.25 \text{ m}^3/\text{h} \text{ and} \Rightarrow c_{r,1} = 80 \text{ kg/m}^3$$

The required membrane area for the two-stage process is given in table VIII - 8.

Energy consumption.

Some simple calculations will be carried out to estimate the energy consumption for a single-stage and a two-stage process. The type of membrane configuration (or module configuration) is not involved in calculations of the required membrane area. However, the membrane configuration has to be taken into account in calculating the energy consumption. Here we consider tubular membranes with a diameter of 1 cm. The power consumption to maintain a certain cross-flow velocity is then given by:

$$P = (q_r \ \Delta p) / \eta_{eff}$$

where η_{eff} is the pump efficiency and Δp the pressure drop over the tubes. The latter is given by (see e.g. Beek, W.J., and Muttzall, K.M.K., Mass transport phenomena, John Wiley, 1977):

$$\Delta p = 4f \ (L/d_h) \ 0.5 \ \rho \ v^2$$

where d_h, the hydraulic diameter, is for a tube simply its diameter d. The friction factor in the turbulent region can be obtained from the Blasius relationship (see reference above):

$$4f = 0.316 \ Re^{-0.25}$$

with the Reynolds number being given by

$$Re = \rho \ v \ d / \eta$$

The recirculation flow q_r is given by

$$q_r = A_d \ v$$

where A_d is the cross-sectional area of the tube. Because there is not a single (very long) tube but a number of parallel tubes (n), then

$$q_r = n \ (\pi/4) \ d^2 \ v$$

and the membrane area is equal to

$$A_{area} = n \ \pi \ d \ L$$

Combination of all these equations gives the power consumption as:

$$P = 0.06 \ Re^{-0.25} \ A \ \rho \ v^3 / \eta_{eff}$$

(Note that the energy consumption is related to the third power of the velocity, $P \approx f \ v^3$, (in fact to $v^{2.75}$) where f is a friction factor). The membrane area and power consumption are listed in table below for both the single-stage and the two-stage process.

TABLE. Membrane area and power consumption for the single-stage and two-stage process

v (m/s)	Re. 10^{-3}	single-stage process		two-stage process	
		A_{area} (m²)	P (kW)	A_{area} (m²)	P (kW)
1	15	94	0.5	60	0.3
2	30	54	2.0	36	1.3
3	45	39	4.5	27	2.9

This example shows that both the membrane area required and the power consumption are lower for the two-stage process. On the other hand, the capital cost will be higher for the two-stage process. Furthermore, by increasing the cross-flow velocity from 1 to 3 m/s, the membrane area is reduced by more than a factor of two, whereas the energy consumption increases by one order of magnitude. These data can be used to calculate the actual process costs, where power consumption and membrane area are important parameters.

6.   A very interesting application of air separation is the production of oxygen-enriched air as well as nitrogen-enriched air. Most of the oxygen and nitrogen produced nowadays is obtained via cryogenic techniques, but membrane processes (and also pressure swing adsorption) show very good prospects especially for small applications.

A major application for oxygen-enriched air is for enhancing combustion. Other applications are in the medical and biotechnological field. Nitrogen-enriched air is used as an inert gas for blanketing flammable liquids. Another application is as a sealant gas to prevent the oxidation of foods (fruits, vegetables, etc.).

The process design and membrane choice are different for both applications as will be shown by the following examples. The driving force across the membranes can be established either by pressurising the feed or applying a vacuum on the permeate side.

Oxygen enrichment in a single stage process

Oxygen with an enrichment of 25 - 40 % is generally of interest for enhanced combustion. To obtain concentrations of this order a proper membrane must be chosen on the basis of selectivity and permeation rate. Another factor of interest is the pressure ratio across the membrane.

Since the cost of air is negligible, the process will be carried out with low recoveries (or, in other words, the composition does not change on the feed side, $x_f \approx x_r$) using a vacuum pump on the permeate side. The figure below shows a simplified flow scheme.
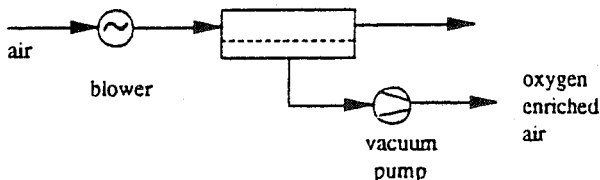
Process scheme for oxygen enriched air.

It is assumed that the process operates at very low recoveries, i.e. at constant feed composition, x_f = x_r. The relevant data are summarised in the table below.

It can be calculated from the selectivity that the membranes selected are capable of producing 30% oxygen-enriched air. In fact a permeate concentration of 33% is obtained which means that the pressure ratio can be reduced (saving power requirement) or air can be added as a diluent.

TABLE   Relevant data necessary for the calculations

oxygen feed conc.	x_f : 0.21
oxygen permeate conc.	x_p : 0.3
selectivity	α_{O_2/N_2} : 2.2
permeate flow rate	q_p : 10 m^3/h
oxygen permeability	P_{O_2} : 600 Barrer
membrane thickness	ℓ : 1 μm
upstream pressure	P_h : 1 bar
downstream pressure	P_ℓ : 0.2 bar

A flow diagram of this single-stage membrane process is given in the figure below

x_f: 0.21 O_2

x_p: 0.30 O_2 q_p : 10 m^3 / h
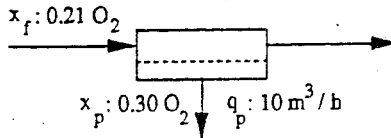
Single-stage membrane process for oxygen enrichment.

The oxygen flux can be calculated

$$J_{O_2} = (P_{O_2} / \ell) [P_h \cdot x_f - P_\ell \cdot x_p]$$

$$\Rightarrow P_{O_2} / \ell = 1.63 \ m^3(STP) \ m^{-2} \ h^{-1} \ bar^{-1}$$

$$\Rightarrow J_{O_2} = 0.235 \ m^3 \ m^{-2} \ h^{-1}$$

$$\Rightarrow q_{O_2} = q_p * 0.33 = 3.3 \ m^3/h$$

which means that a membrane area of about 14 m^2 is required:
-    when the thickness of the silicone rubber layer is reduced from 1 μm to 0.1 μm, then the membrane area reduces to $\approx$ 1.4 m^2.

- when a more selective membrane of lower permeability is used, the pressure ratio can be decreased or air can be added as a diluent to obtain 30% oxygen-enriched air. However, high permeabilities are preferred in the system design with a vacuum pump.

Energy consumption

The energy consumption is determined by the power consumption of the vacuum pump and the blower. The power requirement (assuming isothermal compression or expansion) can be calculated using the following equation:

$$E = \frac{n\,RT}{\eta}\,\ln\frac{p_h}{p_l}$$

where η is the pump efficiency, n the number of moles to be pumped per second and p_h/p_l the pressure ratio. It is assumed that the blower efficiency is 60%, the vacuum pump efficiency 50% and the pressure ratio across the blower $p_h/p_\ell = 1.05$, while the feed flow rate may be estimate as q_f: 200 m^3/h (q_f / q_p = 20). The power consumption of vacuum pump and blower at 25°C can now be calculated, i.e.

vacuum pump: $\Rightarrow P = 988$ J/s ≈ 1.0 kW

blower : $\Rightarrow P = 599$ J/s $= 0.6$ kW

7

Another application of air separation is nitrogen-enriched air with 95 - 99.9% N$_2$ being the range of interest since the minimum nitrogen concentration for blanketing is about 95%. In contrast to oxygen-enrichment, nitrogen-enrichment systems (where the retentate stream is the product) operate with pressure applied on the feed side as shown in the figure below.

air   compressor   nitrogen enriched air
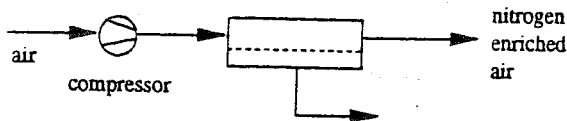
Flow scheme for the production of nitrogen-enriched air.

The membranes used in this application have a higher selectivity than those used for oxygen enrichment. A flow diagram is depicted in the figure below, where the mole fractions of oxygen are given.

x_f : 0.21 O$_2$ x_r : 0.05 O$_2$ q_r : 10 m^3/ h
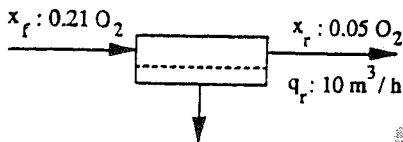
Flow diagram for the production of nitrogen-enriched air.

The equations given in section VIII - 12 cannot be applied directly because the difference between the oxygen feed composition and the retentate composition is too large ($x_r/x_f < 0.5$). Hence the calculations must be performed in steps. This example employs a two step calculation, i.e.

1st step: 21% $O_2 \Rightarrow$ 10% O_2
2nd step: 10% $O_2 \Rightarrow$ 5% O_2
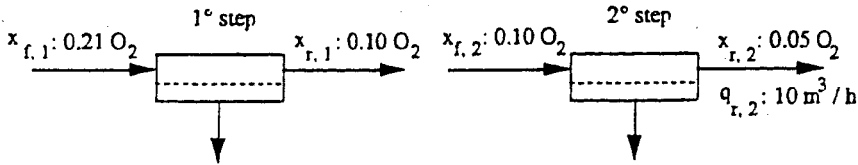
Two-step calculation for a nitrogen enrichment system.

The retentate flow rate in step 1 is the inlet flow rate of step 2 ($x_{r,1} = x_{f,2}$ and $q_{r,1} = q_{f,2}$). Step 2 will be first considered since $q_{r,2}$ is known.

Step 2:
The log mean average oxygen feed concentration in step 2 is:

$\Rightarrow x_2 = 0.072$

and the oxygen permeate concentration $x_{p,2}$ can be calculated from eq. VIII - 41.

$\Rightarrow x_{p,2} = 0.20$

The feed and permeate flow rates can be determined from the material balance equations and consequently the membrane area can be calculated.

$q_{f,2} = q_{p,2} + 10$

$0.1 * q_{f,2} = 0.20 * q_{p,2} + 10 * 0.05$

$\Rightarrow q_{f,2} = 15 \ m^3/h$ and $q_{p,2} = 5 \ m^3/h$

$J_{O2} = (P_{O2} / \ell) [\ p_h \cdot x_2 - p_\ell \cdot x_{p,2} \ ]$

$\Rightarrow P_{O2}/\ell = 0.137 \ m^3(STP) \ m^{-2} \ h^{-1} \ bar^{-1}$

$\Rightarrow J_{O2} = 0.071 \ m^3 \ m^{-2} \ h^{-1}$

$$\Rightarrow q_{O2} = q_p * 0.20 = 1 \ m^3/h$$

This means that a membrane area $A_2 = 14 \ m^2$ is required in step 2.

step 1:

$$q_{f,1} = q_{f,2} = 15 \ m^3/h$$

The log mean average oxygen feed concentration in step 1 is

$$\Rightarrow x_1 = 0.144$$

and the oxygen permeate concentration $x_{p,1}$ can be calculated from eq. VIII - 41 as:

$$\Rightarrow x_{p,1} = 0.36$$

Then

$$q_{f,1} = q_{p,1} + 15$$

$$0.21 * q_{f,1} = 0.36 * q_{p,1} + 0.1 * 15$$

$$\Rightarrow q_{f,1} = 25 \ m^3/h \ \text{and} \ q_{p,1} = 10 \ m^3/h$$

$$\Rightarrow J_{O2} = 0.148 \ m^3 \ m^{-2} \ h^{-1}$$

$$\Rightarrow q_{O2} = q_p * 0.36 = 3.6 \ m^3/h$$

This means that a membrane area $A_1 = 24 \ m^2$ is required. Hence, the total membrane area required is $A_{total} = A_1 + A_2 = 38 \ m^2$.

This example demonstrates that it is also possible to have two product streams, an oxygen-enriched stream in the first step and a nitrogen-enriched stream in the second step. This is shown schematically in the figure below.
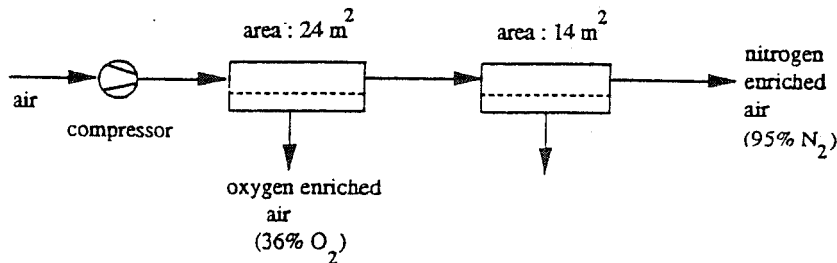
Separation of air into two product streams, i.e. an oxygen-enriched stream and a nitrogen-enriched stream.

Energy consumption

The energy consumption is determined by the power requirement of the compressor. The latter can
be calculated using the same equation as that for the vacuum pump. The efficiency of the
compressor is assumed to be 70%.

$$q_{f,1} = 25 \text{ m}^3/\text{h} \implies n = 0.284 \text{ mol/s}$$

$$\implies P = 2313 \text{ J/s} \approx 2.3 \text{ kW}$$

Answers to exercises: Unsolved problems

Chapter I

1. 6.90×10^3 N/m^2; 4.72×10^{-4} m^3/s; 2.74×10^{-4} m^3(STP).m/m^2.h.Pa; 1.18×10^3 m^3(STP)/h; 280 kJ/m^3; 0.43 J/mol.K; 10^{-3} Pa.s; 2.046×10^3 (J/m^3)$^{0.5}$

2. mol.fractions; $x_{toluene} = 1.0$ and $x_{PPO} = 4.8 \times 10^{-5}$
   vol.fraction; $\phi_{toluene} = 0.96$ and $\phi_{PPO} = 0.04$

3. membrane A : 0.6 l/m^2.h.bar (typically reverse osmosis)
   membrane B : 16.7 l/m^2.h.bar (typically ultrafiltration)

4. 4.37 l/m^2.h.bar

6. 234 l/m^2.h.bar

7. 137 m^3 (STP)/m^2.h.bar
   1.68×10^{-5} mol/m^2.s.Pa

9. water : 0.185 l/m^2.h
   ethanol : 0.035 l/m^2.h

Chapter II

1a. PMA, $T_g = 279$ K; PMMA, $T_g = 387$ K; Due to methyl group that reduces rotational freedom.

b. PPMA, $T_g = 370$ K; PEMA, $T_g = 338$ K; PPMA, $T_g = 308$ K; P-nBMA, $T_g = 293$ K; P-nHMA, $T_g = 268$ K; P-nOMA, $T_g = 253$ K; P-nDMA, $T_g = 208$ K.

7. $M_n = 50,500$ g/mol ; $M_w = 99,010$ g/mol

Chapter III

5c. $\gamma_1 = 1.044$; $\gamma_2 = 1.036$

d. $\chi = 0.15$

7. $\chi = 0.44$

8. $\chi = 1.3$

9. $g_{12} = 0.29$; $g_{12} = 0.23$; $g_{12} = 0.20$

12. $g_{12} = 1.87$; $g_{12} = 1.43$; $g_{12} = 1.08$

13. $\chi = 2.9$; $\chi = 2.4$; $\chi = 2.0$; $\chi = 1.6$
    $\Delta = 10.5$; $\Delta = 8.4$; $\Delta = 7.0$; $\Delta = 6.1$

Chapter IV

1a. no

b. 3.64 bar at $\theta = 0°$

c. $\approx 6\%$

d. no, bubble point too high

2. 31.4%

3c. 105.7 l/m^2.h

d. 89%

4a. $r_p = 1.34$ nm

5. weight fraction : 0.50 ; volume fraction : 0.47

7. $7.4 < r_p < 370$ nm

8. r_p (μm)   R% (without adsorpuon)   R% (with adsorpuon)

    0.05   26   88

    0.1   8   14

9a. $\approx 12\%$

 b. 16.7%

13. - 94 mV

Chapter V

3.   Water: $D_{N2} = 1.15 \ 10^{-9}$ m²/s (exp. value = 1.9); SR: $D_{N2} = 2.8 \ 10^{-9}$ m²/s ; PI : $D_{N2} = 1.5 \ 10^{-12}$ m²/s

7. $\phi = 0.02$: $D_i = 0.96 \ D_T$

     $\phi = 0.5$: $D_i = 0.25 \ D_T$

8b. $\gamma = 115$

10. $\tau = 1.3$

11. $\varepsilon = 0.1$, $\Delta x_{av} = 0.206$ μm; $\varepsilon = 0.01$, $\Delta x_{av} = 0.259$ μm; $\varepsilon = 0.1$, $\Delta x_{av} = 0.502$ μm;

13. 1 bar : $p_{O2} = 0.2$ bar and $\mu_{O2} = - 65.1$ kJ/mol; 100 bar : $p_{O2} = 20$ bar and $\mu_{O2} = - 53.7$ kJ/mol;

14. $\mu°_{H2O}$ (1,298) = - 306.6 kJ/mol; $\mu°_{H2O}$ (10,298) = - 306.2 kJ/mol; $\mu°_{H2O}$ (1,363) = - 311.7 kJ/mol;

15. $S_{He} = 0.014$ cm³/cm³.bar; $S_{N2} = 0.052$ cm³/cm³.bar; $S_{Ar} = 0.10$ cm³/cm³.bar; $S_{He} = 0.20$ cm³/cm³.bar; $S_{CO2} = 1.2$ cm³/cm³.bar;

16. $E_{N2} = 47.1$ kJ/mol; $E_{C2H6} = 48.3$ kJ/mol.

17. $\sigma_{glucose} = 0.63$; $\sigma_{sucrose} = 0.63$; $\sigma_{triose} = 0.63$;

18. $L_p = 2.9 \ 10^{-6}$ cm/bar.s; $\sigma = 0.86$; $\omega = 6.5 \ 10^{-9}$ mol/cm².s.bar

19. $c_{CO2} = 11.0$ cm³(STP)/cm³ atl bar; $c_{CO2} = 42.0$ cm³(STP)/cm³ at 8 bar.

20. $a = 0.3 \Rightarrow S_{tri} = 1.8$ cm³(STP)/cm³.cmHg; $a = 0.9 \Rightarrow S_{tri} = 4.6$ cm³(STP)/cm³.cmHg;

21. left: Na⁺ = $5.15 \ 10^{-3}$ M; Cl⁻ = $0.15 \ 10^{-3}$ M; right: Na⁺ = $0.85 \ 10^{-3}$ M; Cl⁻ = $0.85 \ 10^{-3}$ M;

22. $c_s^m/c_s = 0.05$ (NaCl); $c_s^m/c_s = 0.01$ (Na$_2$SO$_4$); $c_s^m/c_s = 0.32$ (CaCl$_2$);

Chapter VI

1.   4.95 bar; 83.3 bar

2    $J = 60$ l/m².h

4.   3% NaCl : P = 1.6 W/m²; 15% NaCl : P = 40.4 W/m²;

5. $B_{NaCl} = 0.23$ g/m².s ; $B_{Na2SO4} = 9.7 \ 10^{-3}$ g/m².s;

7. $J_v = 22.9$ l/m².h; R = 99.4 %; $c_p = 0.23$ g/l; $J_s = 1.4 \ 10^{-7}$ g/cm².s

8.   R = 97.8%

11. $\phi = 10^{-4}$: $y_{VOC} = 50$ mol% ($\alpha = 200$); $y_{VOC} = 72$ ($\alpha = 500$)

     $\phi = 0.2$: $y_{VOC} = 2.5$ mol% (independent on α)

12. $J_{H2O} = 2.2 \ 10^{-3}$ cm³(STP)/cm².s

13a. $\alpha = 20$; $J_{O2} = 0.12$ cm³/cm².s

 d. double-layer : $J_{O2} = 3.6 \ 10^{-2}$ cm³/cm².s ; triple-layer : $J_{O2} = 2.8 \ 10^{-2}$ cm³/cm².s

 e. triple-layer : $\alpha = 6.4$

14a $\Delta p_{O2} = 147$ mbar

 b $J_{O2} = 2.2 \ 10^{-2}$ cm³(STP)/cm².min

 c. A = 1.16 m²

 d $q_{CO2} = 102$ cm³(STP)/min; not enough

15. $J_{O2} = 3.65 \ 10^{-5} \ cm^3(STP)/cm^2.s$; $J_{N2} = 5.47 \ 10^{-5} \ cm^3(STP)/cm^2.s$

16b. $J_{H2O} = 6.7 \ 10^{-5} \ cm^3(STP)/cm^2.s$

17. $t = 169$ days

19. $P_{H2O} = 1.1 \ 10^{-10} \ mol.m/m^2.s.Pa$; $P_{H2O} = 1.3 \ 10^{-7} \ cm^3(STP). \ cm/cm^2.s.cmHg$ (= 1300 Barrer)

20b. $P = 2.5 \ 10^{-7} \ (cm^3(STP).cm/cm^2.s.cmHg)$ at 1%; $P = 4.8 \ 10^{-7} \ (cm^3(STP).cm/cm^2.s.cmHg)$ at 2%;
     $P = 1.1 \ 10^{-6} \ (cm^3(STP).cm/cm^2.s.cmHg)$ at 3%; $P = 1.4 \ 10^{-6} \ (cm^3(STP).cm/cm^2.s.cmHg)$ at 4%;
     $P = 1.7 \ 10^{-6} \ (cm^3(STP).cm/cm^2.s.cmHg)$ at 5%;

21. $\gamma = 37.2$

22. $\alpha = 25.3$; $J_{tol} = 15.9 \ g/m^2.h$

23b. 192 hours

24a. $P = 1.83 \ 10^{-6} \ m/s$; $J = 6.4 \ 10^{-5} \ mol/m^2.s$

25. $\approx 98\%$

26a. $J_{NaClO4} = 9.9 \ 10^{-13} \ mol/cm^2.s$; $J_{KClO4} = 1.2 \ 10^{-12} \ mol/cm^2.s$

  b. $J_{NaClO4} = 1.1 \ 10^{-13} \ mol/cm^2.s$; $J_{KClO4} = 9.6 \ 10^{-11} \ mol/cm^2.s$

  c. $F_{NaClO4} = 0.11$; $F_{KClO4} = 80$

28. $J_{urea} = 1.7 \ g/m^2.h$; contribution bl layer $\approx 28\%$

29. $K = 1.0$

31. $J_{H2O}(50) = 0.15 \ l/m^2.h$; $J_{H2O}(90) = 1.0 \ l/m^2.h$;

32. $I = 49.8 \ A$; $E = 199.2 \ V$

33a. $\iota_{lim} = 15.4 \ mA/cm^2$

34. $t = 9.2$ hours

35. $emf = 1.22 \ V$

Chapter VII

1. $t = 96$ hours; $t = 29$ hours

2. $q_p = 6.8 \ l/h$; $\Delta p = 0.8$ bar

3a. $J_v = 103 \ l/m^2.hr$

  b. $r_{bl}/c_{bl} = 3.5 \ 10^{15} \ m/kg$

  c. $c_{bl} = 250 \ kg/m^3$

4a. BSA: $r_{bl} = 4.3 \ 10^{19} \ m^{-2}$; Suspension : $r_{bl} = 9.2 \ 10^{13} \ m^{-2}$

  b. $J_{susp}/J_{BSA} = 4.7 \ 10^5$

5. $c_g = 26.4 \ wt\% = 264 \ g/l$

6a. $k_{exp} = 1.8 \ 10^{-6} \ m/s$; $k_{theor} = 1.0 \ 10^{-6} \ m/s$;

7. $A = 0.47 \ m^2$; $Re = 1178$; $k = 1.5 \ 10^{-8} \ m/s$

8. pressure drop Δp (Pa)

d (m) \ v (m/s)	0.5	1.0	5.0
10^{-2}	$1.6 \ 10^2$	$3.2 \ 10^2$	$1.6 \ 10^3$
$2.0 \ 10^{-3}$	$4.0 \ 10^3$	$8.0 \ 10^3$	$4.0 \ 10^4$
10^{-4}	$16 \ 10^5$	$32 \ 10^5$	$16 \ 10^6$

Reynolds number (Re)

v (m/s)	0.5	1.0	5.0
d (m)			
10^{-2}	$5 \ 10^3$	10^4	$5 \ 10^3$
$2.0 \ 10^{-3}$	10^3	$2 \ 10^3$	10^4
10^{-4}	50	100	500

9c. $R_m = 3.6 \ 10^{11}$ m^{-1}

9f. $R_m = 4.0 \ 10^{11}$ m^{-1}

10. $c_m = 217$ g/l

11.   sheet flow : $\Delta p = 0.6$ bar (without spacer); $\Delta p = 1.8$ bar (with spacer)

       tortuous path: $\Delta p = 1.5$ bar (without spacer); $\Delta p = 7.0$ bar (with spacer)

12. $c_p = 90$ ppm

14. $J = 118$ l/m^2.h

15. $t = 35$ hours

16. $t = 10.7$ hours

17. $c_m/c_b = 1.5$; $R_{obs} = 91$ %

18a.   Contribution membrane resistance $R_m \approx 4$%

   b. $l_{gel} = 14.2$ µm

   c. $J = 10$ l/m^2.h ; $l_{gel} = 17.2$ µm

19. $\Delta T = 6.8$ °C

20.   25°C: $\Delta P = 0.3$ bar; 45°C: $\Delta P = 0.2$ bar

21.   dead-end: $k = 8.2 \ 10^{-6}$ m/s; cross-flow : $k = 6.8 \ 10^{-6}$ m/s

22a. $k = 5.7 \ 10^{-6}$ m/s

   b. Rint = 98.6%; 99.3%; 98.4% and 98.2 % .

   c. $J = 40.2$ l/m^2.h: 37.3 l/m^2.h: 31.6 l/m^2.h: 28.7 l/m^2.h;

Chapter VIII

1.   R = 97.8%; α = 0.021; S = 0.8; VR = 5

2.   36,300 m^2/m^3

3.   36 modules

4.   31%; 33% ; 38%: 46% ; 57%

5.   33%; 40% ; 46%: 52% ; 54%; 57%;

6a.   case 6

   b. case 3 and 6

   c. $S_{methane} = 0.95$

   d. $P_{separation \ process} = 30.6$ kW; $P_{combustion} = 300$ kW

7b.   A = 123 m^2

   f. P = 8.2 kW

8.   A = 6.0 m^2 (v = 0.5 m/s); A = 3.5 m^2 (v = 1 m/s); A = 1.0 m^2 (v = 5 m/s);

9a. V_w = 485 kg

   b. V_w = 485 kg

   c. R = 90% $\Rightarrow \delta$ = 0.38; R = 99% $\Rightarrow \delta$ = 0.05

10b.   cases 1 and 2

c.   case 1: $J_{tol} = 0.7$ m^3/m^2.h and A = 26 m^2; case 2: $J_{tol} = 1.4$ m^3/m^2.h and A = 13 m^2;

11a. $p_h/p_\ell = 10 \Rightarrow x_{p.tol} = 5$ vol%; $p_h/p_\ell = 100 \Rightarrow x_{p.tol} = 29$ vol%; $p_h/p_\ell = 1000 \Rightarrow x_{p.tol} = 48$ vol%;

c.   no improvement

12a. S = 0.4

b.   312 ppm NaCl

c.   A = 26.0 m^2

13a. A = 8.6 m^2

b.   A = 25.1 m^2

15.   A = 4.2 m^2; P = 675 J.

16.   15 bars: A = 2164 m^2 and E = 32 kWh; 30 bars: A = 734 m^2 and E = 64 kWh;

17b. T = 6.3 °C

c.   A = 100 cm^2

18.   A = 118 m^2

19 a. $J_{osm} = 27$ l/h

b.   A = 0.2 m^2

c.   Recovery HNO$_3$ = 82%

20.   case I : 0.9 kW; (case 2 and case 3 require 1.5 kW and 1.3 kW, respectively)

21.   S = 0.4

22.   417 min.

23a. S = 0.65

b.   S = 0.31

24.   complete mixing: $c_p = 0.125$ g/l; cross-flow: $c_p = 0.05$ g/l

25.   t = 9 hours

26.   complete mixing: $c_p = 1.3$ g/l; cross-flow: $c_p = 0.28$ g/l

27.   A = 51.8 m^2

28.   MF: $w_{min} = 10^{-13}$ kJ/kg; UF: $w_{min} = 10^{-3}$ kJ/kg; NF: $w_{min} = 0.25$ kJ/kg; RO: $w_{min} = 2.5$ kJ/kg; Evaporation: $w_{min} = 2256$ kJ/kg;

29. $x_{p.A} = 0.604$; S = 0.71; A = 2.7 10^4 m^2

30. $c_{p.butanol} = 42.1\%$

LIST OF SYMBOLS

Symbol	Description	Units
a	activity	(-)
A	surface area	(m^2)
A	water permeability coefficient	$(m^3/m^2.s.bar)$
b	friction factor	(-)
B	constant	(-)
B	solute permeability coefficient	(m/s)
c_i	concentration of i	(kg/m^3)
c	amount of sorbed gas per amount of polymer	$(m^3(STP)/m^3)$
c'	geometrical parameter	(-)
c_b	concentration in the bulk	(kg/m^3)
c'_H	Langmuir capacity constant	$(m^3(STP)/m^3)$
c	concentration	(kg/m^3)
c	average concentration	(kg/m^3)
d_p	pore diameter	(m)
D_{ij}	diffusion coefficient of i in j	(m^2/s)
D_i	diffusivity of i in polymer fixed frame	(m^2/s)
D_T	thermodynamic diffusion coefficient	(m^2/s)
E	activation energy	(J/mole)
E	electrochemical potential	(V)
E_{don}	Donnan potential	(V)
f	fraction free volume	(-)
f_{ij}	friction coefficient	$(J.s/m^2)$
F	Faraday constant	(C/equiv)
F_i	driving force	(N)
g	concentration dependent interaction parameter	(-)
G_m	Free energy of mixing	(J/mole)
H_m	Enthalpy of mixing	(J/mole)
i	current density	$(C/cm^2.s)$
J_i	flux of component i	(m/s)
J_v	volume flux	(m/s)
k	mass transfer coefficient	(m/s)
k	Planck constant	(J.s)
k	rate constants	(1/s)
k_D	Henry's law solubility coefficient	$(m^3(STP)/m^3.atm)$
k_n	constant	(m^2)

l	thickness	(m)
L_{ij}	phenomenological coefficient	(kg.s/m)
L_p	water permeability coefficient	$(g/s.bar.m^2)$
m	mobility	(mol.m/N.s)
M_w	molecular weight	(kg/kmol)
M_t	mass	(kg)
n	number of moles	(-)
n	exponent	(-)
n_k	number of pores	(-)
N_{av}	Avogadro's number	(1/mole)
r or r_p	pore radius	(m)
p	vapour pressure	(Pa)
p^o	saturation vapour pressure	(Pa)
P	(hydraulic) pressure	(Pa)
P_A	permeability constant of the pure component A	$(m^3/m^2s.Pa.m)$
q	differential heat of adsorption	(J/mole)
q	flow rate	(m^3/s)
R	gas constant	(J/mole.K)
R	resistance	$(cm^2.s.bar/cm^3)$
R	retention	(-)
Re	Reynolds number	(-)
R_{ij}	friction coefficients	$(J.s/m^2)$
r	(pore) radius	(m)
r_k	Kelvin radius	(m)
r_c	specific cake resistance	( )
S_m	Entropy of mixing	(J/mole.K)
S	Surface area	(m^2/g)
S	solubility coefficient	$(m^3/m^3.Pa)$
S	Recovery	(-)
Sc	Schmidt number	(-)
t	time	(s)
T	temperature	(K)
T_g	glass-rubber transition temperature	(K)
u_i	velocity of i in a membrane	(m/s)
v_A	average molecular velocity	(m/s)
v_i	partial specific volume	(m^3/kg)
v_f	fractional free volume	(-)
V	molar volume	$(m^3/mole)$

VR	Volume reduction	(-)
x_i	(molar) fraction	(-)
X	driving force	(N/mole)

Greek symbols:

α	selectivity	(-)
α	coefficient of thermal expansion	(K^{-1})
δ	thickness of the boundary layer	(m)
ε	porosity	(-)
η	viscosity	(Pa.s)
μ	chemical potential	(J/kg)
λ	mean free path of (gas)molecules	(m)
ρ	density	(kg/m^3)
τ	tortuosity	(-)
γ	activity coefficient	(-)
$\gamma^{\pm}$	mean ionic activity coefficient	(-)
γ	surface tension	(N/m)
γ	exponential factor	(-)
ϕ_i	volume fraction of component i	(-)
π	osmotic pressure	(Pa)
σ	reflection coefficient	(-)
χ	Flory - Huggins' interaction parameter	(-)
θ	time lag	(s)
θ	contact angle	(-)
ω	permeability coefficient	(m/s)
Ψ_c	fraction crystalline polymer	(-)

subscripts and superscripts:

b	bulk
bl	boundary layer
f	feed
i	component i
g	gel
h	high (high pressure side; feed side)
l	low (low pressure side; permeate side)
m	membrane
p	permeate
p	polymer

r	retentate
s	solvent
w	water
v	volume
1	nonsolvent
2	solvent
3	polymer
ave	average
sorp	sorption
obs	observed
int	intrinsic

INDEX

D

E

F

G

H